13 Analysis and Design of Slabs

13.1 TYPES OF SLABS

In reinforced concrete construction, slabs are used to provide flat, useful surfaces. A reinforced concrete slab is a broad, flat plate, usually horizontal, with top and bottom surfaces parallel or nearly so. It may be supported by reinforced concrete beams (and is usually cast monolithically with such beams), by masonry or reinforced concrete walls, by structural steel members, directly by columns, or continuously by the ground.

Slabs may be supported on two opposite sides only, as shown in Fig. 13.1*a*, in which case the structural action of the slab is essentially *one-way*, the loads being carried by the slab in the direction perpendicular to the supporting beams. There may be beams on all four sides, as shown in Fig. 13.1*b*, so that *two-way* slab action is obtained. Intermediate beams, as shown in Fig. 13.1*c*, may be provided. If the ratio of length to width of one slab panel is larger than about 2, most of the load is carried in the short direction to the supporting beams and one-way action is obtained in effect, even though supports are provided on all sides.

Concrete slabs in some cases may be carried directly by columns, as shown in Fig. 13.1*d*, without the use of beams or girders. Such slabs are described as *flat plates* and are commonly used where spans are not large and loads not particularly heavy. *Flat slab* construction, shown in Fig. 13.1*e*, is also beamless but incorporates a thickened slab region in the vicinity of the column and often employs flared column tops. Both are devices to reduce stresses due to shear and negative bending around the columns. They are referred to as *drop panels* and *column capitals*, respectively. Closely related to the flat plate slab is the two-way joist, also known as a *grid* or *waffle slab*, shown in Fig. 13.1*f*. To reduce the dead load of solid-slab construction, voids are formed in a rectilinear pattern through use of metal or fiberglass form inserts. A two-way ribbed construction results. Usually inserts are omitted near the columns, so a solid slab is formed to resist moments and shears better in these areas.

In addition to the column-supported types of construction shown in Fig. 13.1, many slabs are supported continuously on the ground, as for highways, airport runways, and warehouse floors. In such cases, a well-compacted layer of crushed stone or gravel is usually provided to ensure uniform support and to allow for proper subgrade drainage.†

Reinforcing steel for slabs is primarily parallel to the slab surfaces. Straight bar reinforcement is generally used, although in continuous slabs bottom bars are sometimes bent up to serve as negative reinforcement over the supports. Welded wire reinforcement

† Design guidance for slabs-on-ground, including the effects of deformation of both the slab and the subgrade, can be found in *Design of Slabs-on-Ground* reported by ACI Committee 360 (Ref. 13.1).

FIGURE 13.1
Types of structural slabs.

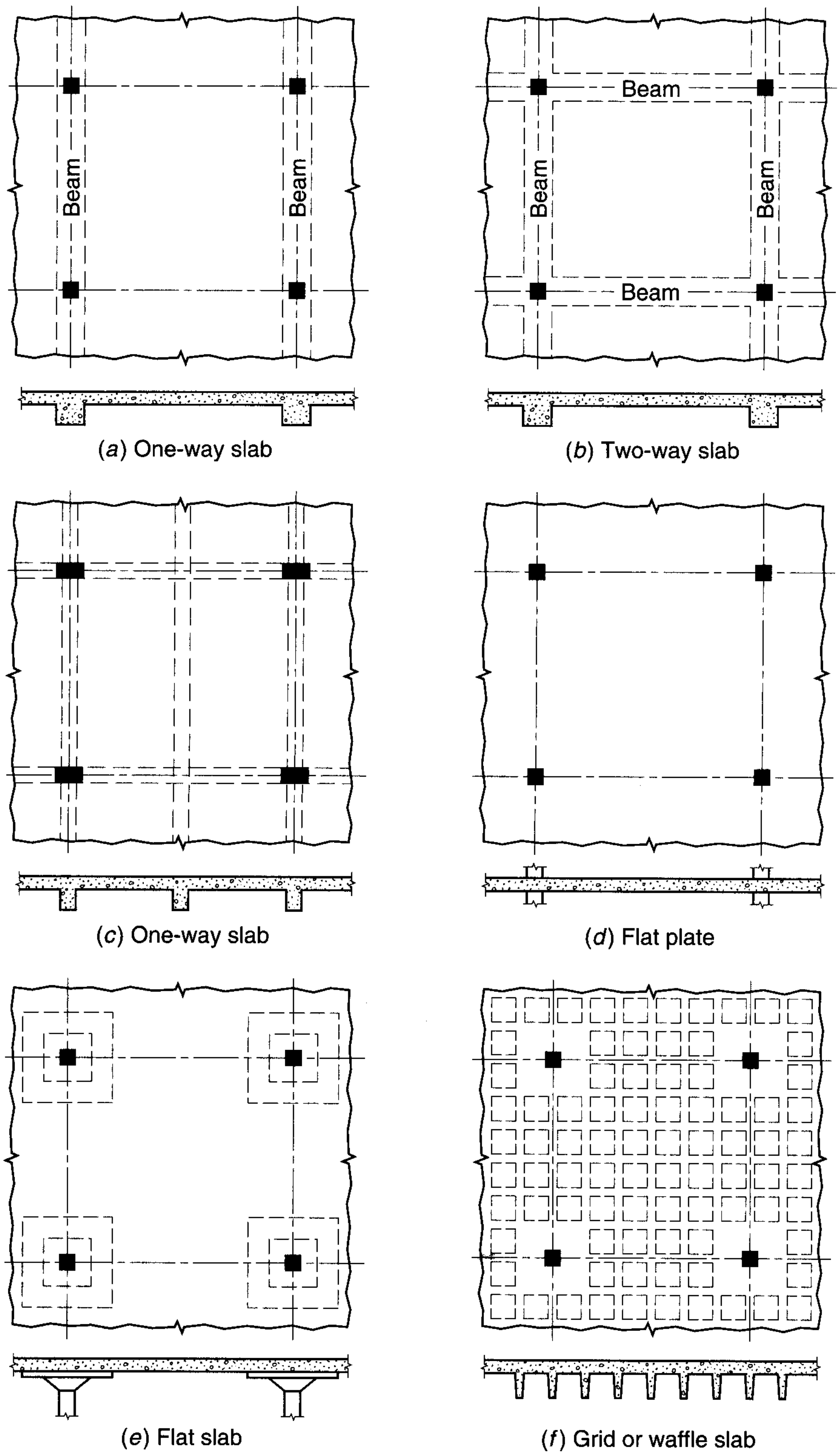

is commonly employed for slabs on the ground. Bar mats are available for the heavier reinforcement sometimes needed in highway slabs and airport runways. Slabs may also be prestressed using high tensile strength strands.

Reinforced concrete slabs of the types shown in Fig. 13.1 are usually designed for loads assumed to be uniformly distributed over one entire slab panel, bounded by supporting beams or column centerlines. Minor concentrated loads can be accommodated through two-way action of the reinforcement (two-way flexural steel for two-way slab systems or one-way flexural steel plus lateral distribution steel for one-way systems). Heavy concentrated loads generally require supporting beams.

One-way and two-way edge-supported slabs, such as shown in Fig. 13.1*a*, *b*, and *c*, will be discussed in Sections 13.2 to 13.4. Two-way beamless systems, such as shown in Fig. 13.1*d*, *e*, and *f*, as well as two-way edge-supported slabs (Fig. 13.1*b*), will be treated in Sections 13.5 to 13.13. Special methods based on limit analysis at the overload state, applicable to all types of slabs, will be presented in Chapters 14 and 15.

13.2 DESIGN OF ONE-WAY SLABS

The structural action of a one-way slab may be visualized in terms of the deformed shape of the loaded surface. Figure 13.2 shows a rectangular slab, simply supported along its two opposite long edges and free of any support along the two opposite short edges. If a uniformly distributed load is applied to the surface, the deflected shape will be as shown by the solid lines. Curvatures, and consequently bending moments, are the same in all strips s spanning in the short direction between supported edges, whereas there is no curvature, hence no bending moment, in the long strips l parallel to the supported edges. The surface is approximately cylindrical.

For purposes of analysis and design, a unit strip of such a slab cut out at right angles to the supporting beams, as shown in Fig. 13.3, may be considered as a rectangular beam of unit width, with a depth h equal to the thickness of the slab and a span l_a equal to the distance between supported edges. This strip can then be analyzed by the methods that were used for rectangular beams, the bending moment being computed for the strip of unit width. The load per unit area on the slab becomes the load per unit length on the slab strip. Since all of the load on the slab must be transmitted to the two supporting beams, it follows that all of the reinforcement should be placed at right

FIGURE 13.2
Deflected shape of uniformly loaded one-way slab.

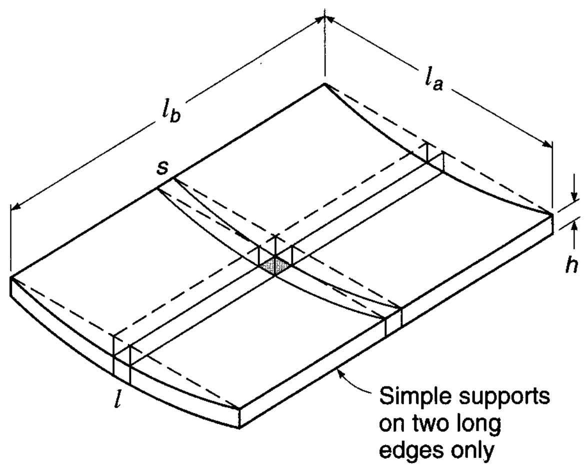

FIGURE 13.3
Unit strip basis for flexural design.

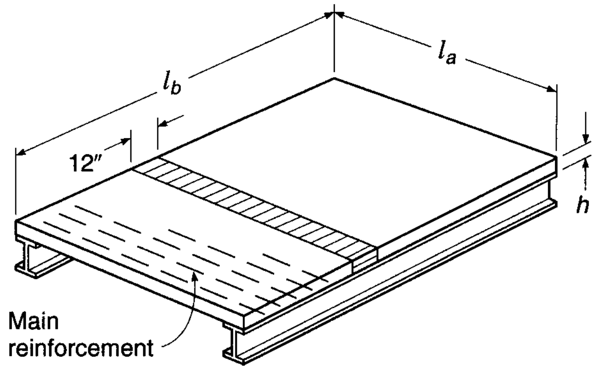

angles to these beams, with the exception of any bars that may be placed in the other direction to control shrinkage and temperature cracking. A one-way slab, thus, consists of a set of rectangular beams side by side.

This simplified analysis, which assumes Poisson's ratio to be zero, is slightly conservative. Actually, flexural compression in the concrete in the direction of l_a will result in lateral expansion in the direction of l_b unless the compressed concrete is restrained. In a one-way slab, this lateral expansion is resisted by adjacent slab strips, which tend to expand also. The result is a slight strengthening and stiffening in the span direction, but this effect is small and can be disregarded.

The reinforcement ratio for a slab can be determined by dividing the area of one bar by the area of concrete between two successive bars, the latter area being the product of the depth to the center of the bars and the distance between them, center to center. The reinforcement ratio can also be determined by dividing the average area of steel per foot of width by the effective area of concrete in a 1 ft strip. The average area of steel per foot of width is equal to the area of one bar times the average number of bars in a 1 ft strip (12 divided by the spacing in inches), and the effective area of concrete in a 1 ft (or 12 in.) strip is equal to 12 times the effective depth d.

To illustrate the latter method of obtaining the reinforcement ratio ρ, assume a 5 in. slab with an effective depth of 4 in., with No. 4 (No. 13) bars spaced $4\frac{1}{2}$ in. center to center. The average number of bars in a 12 in. strip of slab is $12/4.5 = 2\frac{2}{3}$ bars, and the average steel area in a 12 in. strip is $2\frac{2}{3} \times 0.20 = 0.533$ in^2. Hence $\rho = 0.533/(12 \times 4) = 0.0111$. By the other method,

$$\rho = \frac{0.20}{4.5 \times 4} = 0.0111$$

The spacing of bars that is necessary to furnish a given area of steel per foot of width is obtained by dividing the number of bars required to furnish this area into 12. For example, to furnish an average area of 0.46 in^2/ft, with No. 4 (No. 13) bars, requires $0.46 \div 0.20 = 2.3$ bars per foot; the bars must be spaced not more than $12/2.3 = 5.2$ in. center to center. The determination of slab steel areas for various combinations of bars and spacings is facilitated by Table A.3 of Appendix A.

Factored moments and shears in one-way slabs can be found either by elastic analysis or through the use of the same coefficients as used for beams (see Chapter 12). If the slab rests freely on its supports, the span length may be taken equal to the clear span plus the depth of the slab but need not exceed the distance between centers of supports, according to ACI Code 8.9.1. In general, center-to-center distances should be used in continuous slab analysis, but a reduction is allowed in negative moments to

TABLE 13.1
Minimum thickness h of nonprestressed one-way slabs

Simply supported	$l/20$
One end continuous	$l/24$
Both ends continuous	$l/28$
Cantilever	$l/10$

account for support width as discussed in Chapter 12. For slabs with clear spans not more than 10 ft that are built integrally with their supports, ACI Code 8.9.4 permits analysis as a continuous slab on knife edge supports with spans equal to the clear spans and the width of the beams otherwise neglected. If moment and shear coefficients are used, computations should be based on clear spans.

One-way slabs are normally designed with tensile reinforcement ratios well below the maximum practical value of $\rho_{0.005}$. Typical reinforcement ratios range from about 0.004 to 0.008. This is partially for reasons of economy, because the saving in steel associated with increasing the effective depth more than compensates for the cost of the additional concrete, and partially because very thin slabs with high reinforcement ratios would be likely to permit large deflections. Thus, flexural design may start with selecting a relatively low reinforcement ratio, say about $0.3\rho_{0.005}$, setting $M_u = \phi M_n$ in Eq. (3.38), and solving for the required effective depth d, given that $b = 12$ in. for the unit strip. Alternatively, Table A.5 or Graph A.1 of Appendix A may be used. Table A.9 is also useful. The required steel area per 12 in. strip $A_s = \rho bd$ is then easily found.

ACI Code 9.5.2 specifies the minimum thickness in Table 13.1 for nonprestressed slabs of normalweight concrete ($w_c = 145$ pcf) using Grade 60 reinforcement, provided that the slab is not supporting or attached to construction that is likely to be damaged by large deflections. Lesser thicknesses may be used if calculation of deflections indicates no adverse effects. For concretes having unit weight w_c in the range from 90 to 115 pcf, the tabulated values should be multiplied by $1.65 - 0.005w_c$, but not less than 1.09. For reinforcement having a yield stress f_y other than 60,000 psi, the tabulated values should be multiplied by $0.4 + f_y/100{,}000$. Slab deflections may be calculated, if required, by the same methods as for beams (see Section 6.7).

Shear will seldom control the design of one-way slabs, particularly if low tensile reinforcement ratios are used. It will be found that the shear capacity of the concrete ϕV_c will, almost without exception, be well above the required shear strength V_u at factored loads.

The total slab thickness h is usually rounded to the next higher $\frac{1}{4}$ in. for slabs up to 6 in. thickness, and to the next higher $\frac{1}{2}$ in. for thicker slabs. Best economy is often achieved when the slab thickness is selected to match nominal lumber dimensions. The concrete protection below the reinforcement should follow the requirements of ACI Code 7.7.1, calling for $\frac{3}{4}$ in. below the bottom of the steel (see Fig. 3.13*b*). In a typical slab, 1 in. below the center of the steel may be assumed. The lateral spacing of the bars, except those used only to control shrinkage and temperature cracks (see Section 13.3), should not exceed 3 times the thickness h or 18 in., whichever is less, according to ACI Code 7.6.5. Generally, bar size should be selected so that the actual spacing is not less than about 1.5 times the slab thickness, to avoid excessive cost for bar fabrication and handling. Also, to reduce cost, straight bars are usually used for slab reinforcement, cut off where permitted as described for beams in Section 5.10.

13.3 TEMPERATURE AND SHRINKAGE REINFORCEMENT

Concrete shrinks as it dries out, as was pointed out in Section 2.11. It is advisable to minimize such shrinkage by using concretes with the smallest possible amounts of water and cement compatible with other requirements, such as strength and workability, and by thorough moist-curing of sufficient duration. However, no matter what precautions are taken, a certain amount of shrinkage is usually unavoidable. If a slab of moderate dimensions rests freely on its supports, it can contract to accommodate the shortening of its length produced by shrinkage. Usually, however, slabs and other members are joined rigidly to other parts of the structure and cannot contract freely. This results in tension stresses known as *shrinkage stresses*. A decrease in temperature relative to that at which the slab was cast, particularly in outdoor structures such as bridges, may have an effect similar to shrinkage. That is, the slab tends to contract and if restrained from doing so becomes subject to tensile stresses.

Since concrete is weak in tension, these temperature and shrinkage stresses are likely to result in cracking. Cracks of this nature are not detrimental, provided their size is limited to what are known as *hairline cracks*. This can be achieved by placing reinforcement in the slab to counteract contraction and distribute the cracks uniformly. As the concrete tends to shrink, such reinforcement resists the contraction and consequently becomes subject to compression. The total shrinkage in a slab so reinforced is less than that in one without reinforcement; in addition, whatever cracks do occur will be of smaller width and more evenly distributed by virtue of the reinforcement.

In one-way slabs, the reinforcement provided for resisting the bending moments has the desired effect of reducing shrinkage and distributing cracks. However, as contraction takes place equally in all directions, it is necessary to provide special reinforcement for shrinkage and temperature contraction in the direction perpendicular to the main reinforcement. This added steel is known as *temperature* or *shrinkage reinforcement*, or *distribution steel.*

Reinforcement for shrinkage and temperature stresses normal to the principal reinforcement should be provided in a structural slab in which the principal reinforcement extends in one direction only. ACI Code 7.12.2 specifies the minimum ratios of reinforcement area to *gross concrete area* (i.e., based on the total depth of the slab) shown in Table 13.2, but in no case may such reinforcing bars be placed farther apart than 5 times the slab thickness or more than 18 in. In no case is the reinforcement ratio to be less than 0.0014.

The steel required by the ACI Code for shrinkage and temperature crack control also represents the minimum permissible reinforcement in the span direction of one-way slabs; the usual minimums for flexural steel do not apply.

TABLE 13.2
Minimum ratios of temperature and shrinkage reinforcement in slabs based on gross concrete area

Slabs where Grade 40 or 50 deformed bars are used	0.0020
Slabs where Grade 60 deformed bars or welded wire fabric (smooth or deformed) is used	0.0018
Slabs where reinforcement with yield strength exceeding 60,000 psi measured at yield strain of 0.35 percent is used	$\dfrac{0.0018 \times 60{,}000}{f_y}$

EXAMPLE 13.1

One-way slab design. A reinforced concrete slab is built integrally with its supports and consists of two equal spans, each with a clear span of 15 ft. The service live load is 100 psf, and 4000 psi concrete is specified for use with steel with a yield stress equal to 60,000 psi. Design the slab, following the provisions of the ACI Code.

Solution. The thickness of the slab is first estimated, based on the minimum thickness from Table 13.1: $l/28 = 15 \times 12/28 = 6.43$ in. A trial thickness of 6.50 in. will be used, for which the weight is $150 \times 6.50/12 = 81$ psf. The specified live load and computed dead load are multiplied by the ACI load factors:

$$\begin{aligned} \text{Dead load} &= 81 \times 1.2 = 97 \text{ psf} \\ \text{Live load} &= 100 \times 1.6 = \underline{160 \text{ psf}} \\ \text{Total} &= 257 \text{ psf} \end{aligned}$$

For this case, factored moments at critical sections may be found using the ACI moment coefficients (see Table 12.1):

$$\begin{aligned} &\text{At interior support:} && -M = \tfrac{1}{9} \times 0.257 \times 15^2 = 6.43 \text{ ft-kips} \\ &\text{At midspan:} && +M = \tfrac{1}{14} \times 0.257 \times 15^2 = 4.13 \text{ ft-kips} \\ &\text{At exterior support:} && -M = \tfrac{1}{24} \times 0.257 \times 15^2 = 2.41 \text{ ft-kips} \end{aligned}$$

The maximum practical reinforcement ratio is, according to Eq. (3.30*d*),

$$\rho_{0.005} = (0.85^2)\frac{4}{60}\frac{0.003}{0.003 + 0.005} = 0.0181$$

If this value of ρ were actually used, the minimum required effective depth, controlled by negative moment at the interior support, would be found from Eq. (3.38) to be

$$\begin{aligned} d^2 &= \frac{M_u}{\phi\rho f_y b(1 - 0.59\rho f_y/f'_c)} \\ &= \frac{6.43 \times 12}{0.90 \times 0.0181 \times 60 \times 12[1 - 0.59 \times 0.0181 \times (60/4)]} = 7.83 \text{ in}^2 \\ d &= 2.80 \text{ in.}^\dagger \end{aligned}$$

This is less than the effective depth of $6.50 - 1.00 = 5.50$ in. resulting from application of Code restrictions, and the latter figure will be adopted. At the interior support, if the stress-block depth $a = 1.00$ in., the area of steel required per foot of width in the top of the slab is [Eq. (3.37)]

$$A_s = \frac{M_u}{\phi f_y(d - a/2)} = \frac{6.43 \times 12}{0.90 \times 60 \times (5.50 - 1.00/2)} = 0.29 \text{ in}^2$$

Checking the assumed depth a by Eq. (3.32), one gets

$$a = \frac{A_s f_y}{0.85 f'_c b} = \frac{0.29 \times 60}{0.85 \times 4 \times 12} = 0.43 \text{ in.}$$

A second trial will be made with $a = 0.43$ in. Then

$$A_s = \frac{6.43 \times 12}{0.90 \times 60 \times (5.50 - 0.43/2)} = 0.27 \text{ in}^2$$

for which $a = 0.43 \times 0.27/0.29 = 0.40$ in. No further revision is necessary. At other critical-moment sections, it will be satisfactory to use the same lever arm to determine steel areas, and

† The depth is more easily found using Graph A.1 of Appendix A. For $\rho = \rho_{0.005}$, $M_u/\phi bd^2 = 913$, from which $d = 2.80$ in. Table A.5*a* may also be used.

At midspan: $$A_s = \frac{4.13 \times 12}{0.90 \times 60 \times (5.50 - 0.40/2)} = 0.17 \text{ in}^2$$

At exterior support: $$A_s = \frac{2.41 \times 12}{0.90 \times 60 \times (5.50 - 0.40/2)} = 0.10 \text{ in}^2$$

The minimum reinforcement is that required for control of shrinkage and temperature cracking. This is

$$A_s = 0.0018 \times 12 \times 6.50 = 0.14 \text{ in}^2$$

per 12 in. strip. This requires a small increase in the amount of steel used at the exterior support.

The factored shear force at a distance d from the face of the interior support is

$$V_u = 1.15 \times \frac{257 \times 15}{2} - 257 \times \frac{5.50}{12} = 2100 \text{ lb}$$

By Eq. (4.12*b*), the nominal shear strength of the concrete slab is

$$V_n = V_c = 2\lambda\sqrt{f_c'}\,bd = 2 \times 1\sqrt{4000} \times 12 \times 5.50 = 8350 \text{ lb}$$

Thus, the design strength of the concrete slab $\phi V_c = 0.75 \times 8350 = 6260$ lb is well above the required strength in shear of $V_u = 2100$.

The required tensile steel areas may be provided in a variety of ways, but whatever the selection, due consideration must be given to the actual placing of the steel during construction. The arrangement should be such that the steel can be placed rapidly with the minimum of labor costs even though some excess steel is necessary to achieve this end.

Two possible arrangements are shown in Fig. 13.4. In Fig. 13.4*a*, bent bars are used, while in Fig. 13.4*b* all bars are straight.

FIGURE 13.4
One-way slab design example.

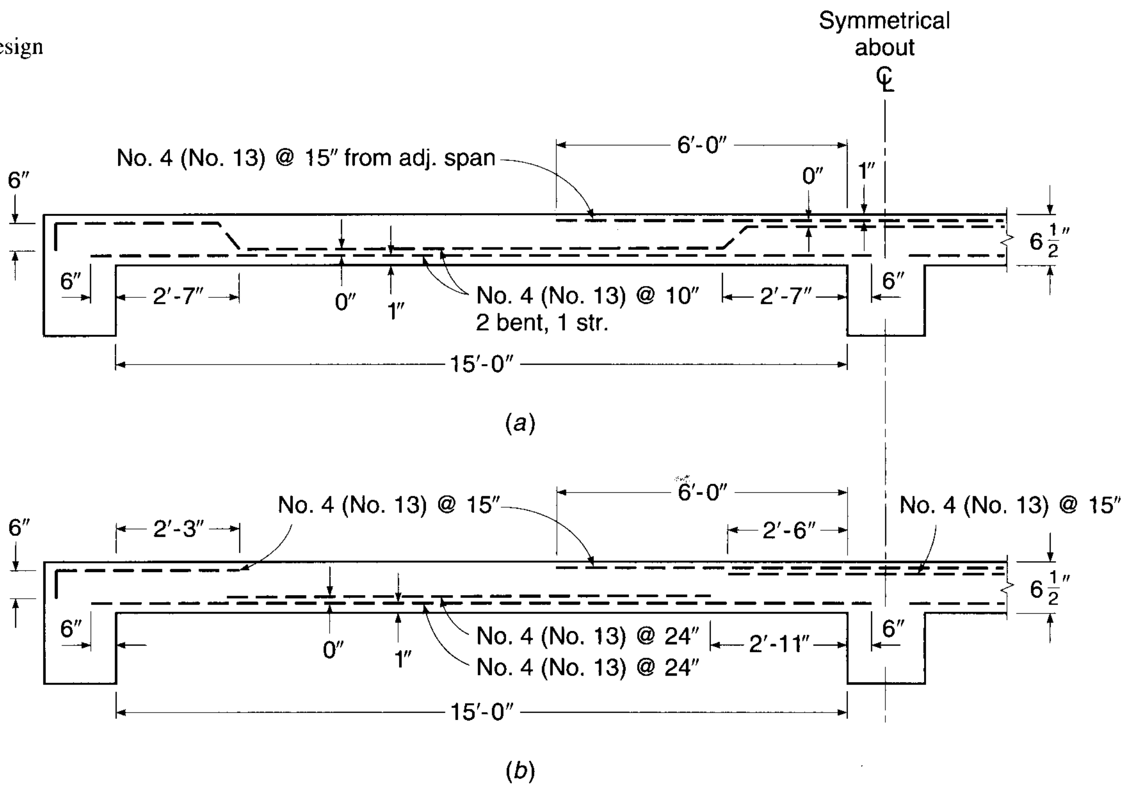

In the arrangement of Fig. 13.4*a*, No. 4 (No. 13) bars at 10 in. furnish 0.24 in^2 of steel at midspan, slightly more than required. If two-thirds of these bars are bent upward for negative reinforcement over the interior support, the average spacing of such bent bars at the interior support will be $(10 + 20)/2 = 15$ in. Since an identical pattern of bars is bent upward from the other side of the support, the effective spacing of the No. 4 (No. 13) bars over the interior support is $7\frac{1}{2}$ in. This pattern satisfies the required steel area of 0.27 in^2 per foot width of slab over the support. The bars bent at the interior support will also be bent upward for negative reinforcement at the exterior support, providing reinforcement equivalent to No. 4 (No. 13) bars at 15 in., or 0.16 in^2 of steel.

Note that it is not necessary to achieve uniform spacing of reinforcement in slabs, and that the steel provided can be calculated safely on the basis of average spacing, as in the example. Care should be taken to satisfy requirements for both minimum and maximum spacing of principal reinforcement, however.

The locations of bend and cutoff points shown in Fig. 13.4*a* were obtained using Graph A.3 of Appendix A, as explained in Section 5.10 and Table A.10 (see also Fig. 5.19).

The arrangement shown in Fig. 13.4*b* uses only straight bars. Although it is satisfactory according to the ACI Code (since the shear stress does not exceed two-thirds of that permitted), cutting off the shorter positive and negative bars as shown leads to an undesirable condition at the ends of those bars, where there will be concentrations of stress in the concrete. The design would be improved if the negative bars were cut off 3 ft from the face of the interior support rather than 2 ft 6 in. as shown, and if the positive steel were cut off at 2 ft 2 in. rather than at 2 ft 11 in. This would result in an overlap of approximately $2d$ of the cut positive and negative bars. Figure 5.20*a* suggests a somewhat simpler arrangement that would also prove satisfactory.

The required area of steel to be placed normal to the main reinforcement for purposes of temperature and shrinkage crack control is 0.14 in^2. This will be provided by No. 4 (No. 13) bars at 16 in. spacing, placed directly on top of the main reinforcement in the positive-moment region and below the main steel in the negative-moment zone.

13.4 BEHAVIOR OF TWO-WAY EDGE-SUPPORTED SLABS

The slabs discussed in Sections 13.2 and 13.3 deform under load into an approximately cylindrical surface. The main structural action is one-way in such cases, in the direction normal to supports on two opposite edges of a rectangular panel. In many cases, however, rectangular slabs are of such proportions and are supported in such a way that two-way action results. When loaded, such slabs bend into a dished surface rather than a cylindrical one. This means that at any point the slab is curved in both principal directions, and since bending moments are proportional to curvatures, moments also exist in both directions. To resist these moments, the slab must be reinforced in both directions, by at least two layers of bars perpendicular, respectively, to two pairs of edges. The slab must be designed to take a proportionate share of the load in each direction.

Types of reinforced concrete construction that are characterized by two-way action include slabs supported by walls or beams on all sides (Fig. 13.1*b*), flat plates (Fig. 13.1*d*), flat slabs (Fig. 13.1*e*), and waffle slabs (Fig. 13.1*f*).

The simplest type of two-way slab action is that represented by Fig. 13.1*b*, where the slab, or slab panel, is supported along its four edges by relatively deep, stiff, monolithic concrete beams or by walls or steel girders. If the concrete edge beams are shallow or are omitted altogether, as they are for flat plates and flat slabs, deformation of the floor system along the column lines significantly alters the distribution of

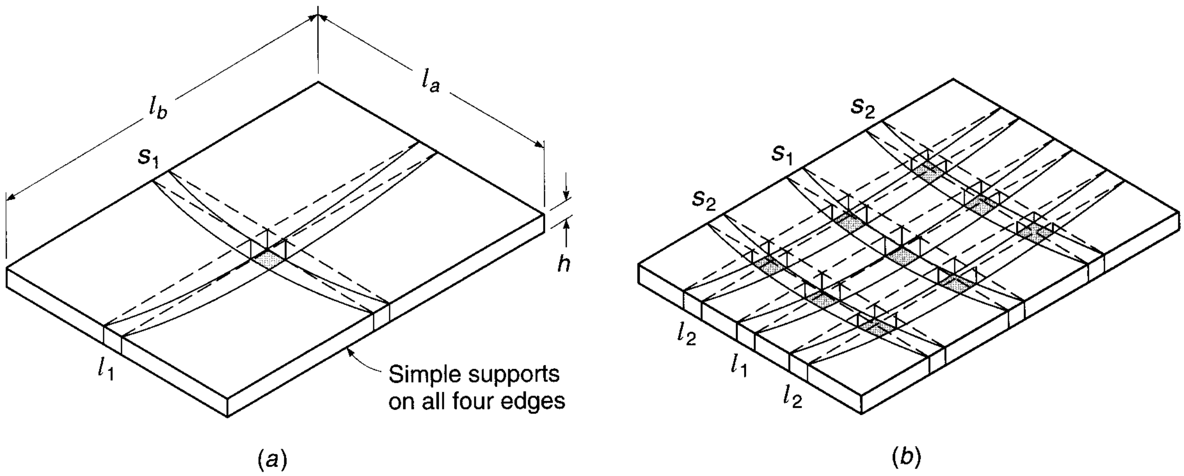

FIGURE 13.5
Two-way slab on simple edge supports: (*a*) bending of center strips of slab; (*b*) grid model of slab.

moments in the slab panel itself (Ref. 13.2). Two-way systems of this type are considered separately, beginning in Section 13.5. The present discussion pertains to the former type, in which edge supports are stiff enough to be considered unyielding.

Such a slab is shown in Fig. 13.5*a*. To visualize its flexural performance, it is convenient to think of it as consisting of two sets of parallel strips, in each of the two directions, intersecting each other. Evidently, part of the load is carried by one set and transmitted to one pair of edge supports, and the remainder by the other.

Figure 13.5*a* shows the two center strips of a rectangular plate with short span l_a and long span l_b. If the uniform load is q per square foot of slab, each of the two strips acts approximately as a simple beam, uniformly loaded by its share of q. Because these imaginary strips actually are part of the same monolithic slab, their deflections at the intersection point must be the same. Equating the center deflections of the short and long strips gives

$$\frac{5q_a l_a^4}{384EI} = \frac{5q_b l_b^4}{384EI} \tag{a}$$

where q_a is the share of the load q carried in the short direction and q_b is the share of the load q carried in the long direction. Consequently,

$$\frac{q_a}{q_b} = \frac{l_b^4}{l_a^4} \tag{b}$$

One sees that the larger share of the load is carried in the short direction, the ratio of the two portions of the total load being inversely proportional to the fourth power of the ratio of the spans.

This result is approximate because the actual behavior of a slab is more complex than that of the two intersecting strips. An understanding of the behavior of the slab itself can be gained from Fig. 13.5*b*, which shows a slab model consisting of two sets of three strips each. It is seen that the two central strips s_1 and l_1 bend in a manner similar to that shown in Fig. 13.5*a*. The outer strips s_2 and l_2, however, are not only bent but also twisted. Consider, for instance, one of the intersections of s_2 with l_2. It is seen that at the intersection the exterior edge of strip l_2 is at a higher elevation than the interior edge, while at the nearby end of strip l_2 both edges are at the same elevation; the strip is twisted. This twisting results in torsional stresses and torsional moments that are seen to be most pronounced near the corners. Consequently, the total load on the slab is carried not only by the bending moments in two directions but also by the twisting moments. For this reason, bending moments in elastic slabs are smaller than would be computed for sets of unconnected strips loaded by q_a and q_b. For instance, for a simply supported square slab, $q_a = q_b = q/2$. If only bending were present, the maximum moment in each strip would be

$$\frac{(q/2)l^2}{8} = 0.0625ql^2 \tag{c}$$

The exact theory of bending of elastic plates shows that actually the maximum moment in such a square slab is only $0.048ql^2$, so that in this case the twisting moments relieve the bending moments by about 25 percent.

The largest moment occurs where the curvature is sharpest. Figure 13.5*b* shows this to be the case at midspan of the short strip s_1. Suppose the load is increased until this location is overstressed, so that the steel at the middle of strip s_1 is yielding. If the strip were an isolated beam, it would now fail. Considering the slab as a whole, however, one sees that no immediate failure will occur. The neighboring strips (those parallel as well as those perpendicular to s_1), being actually monolithic with it, will take over any additional load that strip s_1 can no longer carry until they, in turn, start yielding. This inelastic redistribution will continue until in a rather large area in the central portion of the slab all the steel in both directions is yielding. Only then will the entire slab fail. From this reasoning, which is confirmed by tests, it follows that slabs need not be designed for the absolute maximum moment in each of the two directions (such as $0.048ql^2$ in the example given in the previous paragraph), but only for a smaller average moment in each of the two directions in the central portion of the slab. For instance, one of the several analytical methods in general use permits a square slab to be designed for a moment of $0.036ql^2$. By comparison with the actual elastic maximum moment $0.048ql^2$, it is seen that, owing to inelastic redistribution, a moment reduction of 25 percent is provided.

The largest moment in the slab occurs at midspan of the short strip s_1 of Fig. 13.5*b*. It is evident that the curvature, and hence the moment, in the short strip s_2 is less than at the corresponding location of strip s_1. Consequently, a variation of short-span moment occurs in the long direction of the span. This variation is shown qualitatively in Fig. 13.6. The short-span moment diagram in Fig. 13.6*a* is valid only along the center strip at 1-1. Elsewhere, the maximum-moment value is less, as shown. Other moment ordinates are reduced proportionately. Similarly, the long-span moment diagram in Fig. 13.6 applies only at the longitudinal centerline of the slab; elsewhere, ordinates are reduced according to the variation shown. These variations in maximum moment across the width and length of a rectangular slab are accounted for in an approximate way in most practical design methods by designing for a reduced moment in the outer quarters of the slab span in each direction.

It should be noted that only slabs with side ratios less than about 2 need be treated as two-way slabs. From Eq. (*b*) above, it is seen that for a slab of this proportion, the share of the load carried in the long direction is only on the order of one-sixteenth of that in the short direction. Such a slab acts almost as if it were spanning in the short direction only. Consequently, rectangular slab panels with an aspect ratio of 2 or more may be reinforced for one-way action, with the main steel perpendicular to the long edges.

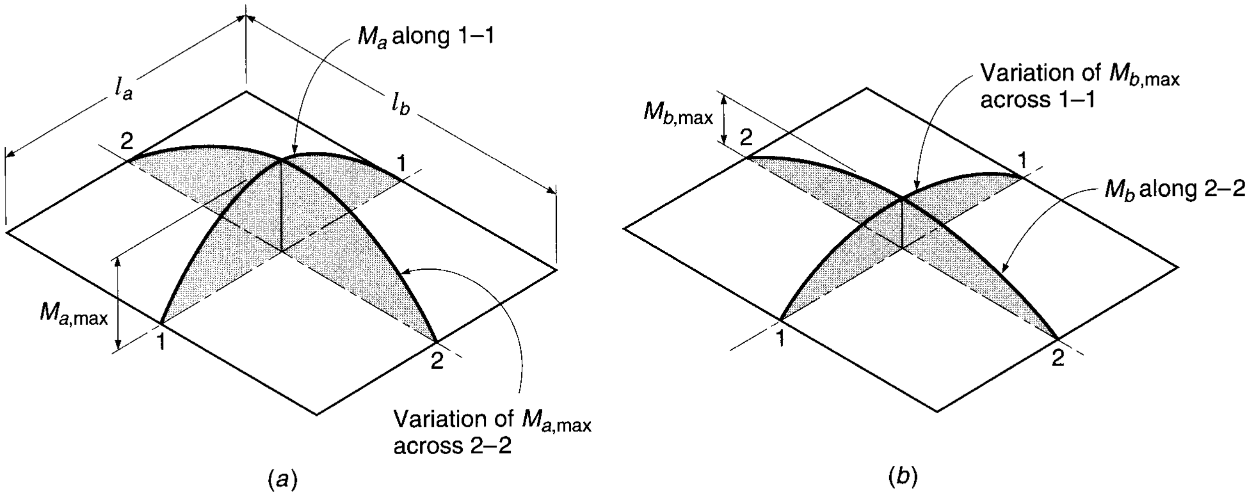

FIGURE 13.6
Moments and moment variations in a uniformly loaded slab with simple supports on four sides.

Consistent with the assumptions of the analysis of two-way edge-supported slabs, the main flexural reinforcement is placed in an orthogonal pattern, with reinforcing bars parallel and perpendicular to the supported edges. As the positive steel is placed in two layers, the effective depth d for the upper layer is smaller than that for the lower layer by one bar diameter. Because the moments in the long direction are the smaller ones, it is economical to place the steel in that direction on top of the bars in the short direction. The stacking problem does not exist for negative reinforcement perpendicular to the supporting edge beams except at the corners, where moments are small.

Either straight bars, cut off where they are no longer required, or bent bars may be used for two-way slabs, but economy of bar fabrication and placement will generally favor all straight bars. The precise locations of inflection points (or lines of inflection) are not easily determined, because they depend upon the side ratio, the ratio of live to dead load, and continuity conditions at the edges. The standard cutoff and bend points for beams, summarized in Fig. 5.21, may be used for edge-supported slabs as well.

According to ACI Code 13.3.1, the minimum reinforcement in each direction for two-way slabs is that required for shrinkage and temperature crack control, as given in Table 13.2. For two-way systems, the spacing of flexural reinforcement at critical sections must not exceed 2 times the slab thickness h.

The twisting moments discussed earlier are usually of consequence only at exterior corners of a two-way slab system, where they tend to crack the slab at the bottom along the panel diagonal, and at the top perpendicular to the panel diagonal. Special reinforcement should be provided at exterior corners in both the bottom and top of the slab, for a distance in each direction from the corner equal to one-fifth the longer span of the corner panel, as shown in Fig. 13.7. The reinforcement at the top of the slab should be parallel to the diagonal from the corner, while that at the bottom should be perpendicular to the diagonal. Alternatively, either layer of steel may be placed in two bands parallel to the sides of the slab. The positive and negative reinforcement, in any case, should be of a size and spacing equivalent to

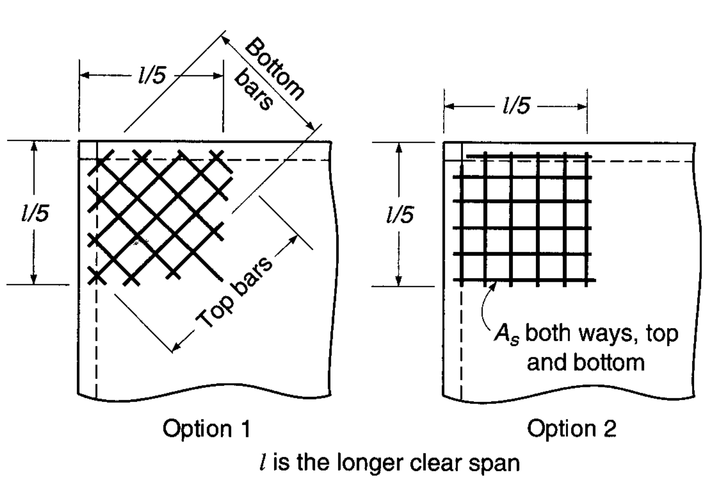

FIGURE 13.7
Special reinforcement at exterior corners of a beam-supported two-way slab.

that required for the maximum positive moment (per foot of width) in the panel, according to ACI Code 13.3.6.

13.5 TWO-WAY COLUMN-SUPPORTED SLABS

When two-way slabs are supported by relatively shallow, flexible beams (Fig. 13.1*b*), or if column-line beams are omitted altogether, as for flat plates (Fig. 13.1*d*), flat slabs (Fig. 13.1*e*), or two-way joist systems (Fig. 13.1*f*), then a number of new considerations are introduced. Figure 13.8*a* shows a portion of a floor system in which a rectangular slab panel is supported by relatively shallow beams on four sides. The beams, in turn, are carried by columns at the intersection of their centerlines. If a surface load q is applied, that load is shared between imaginary slab strips l_a in the short direction and l_b in the long direction, as described in Section 13.4. The portion of the load that is carried by the long strips l_b is delivered to the beams B1 spanning in the short direction of the panel. The portion carried by the beams B1 plus that carried directly in the short direction by the slab strips l_a sums up to 100 percent of the load applied to the panel. Similarly, the short-direction slab strips l_a deliver a part of the load to long-direction beams B2. That load, plus the load carried directly in the long direction by the slab, includes 100 percent of the applied load. It is clearly a requirement of statics that, for column-supported construction, *100 percent of the applied load must be carried in each direction*, jointly by the slab and its supporting beams (Ref. 13.3).

A similar situation is obtained in the flat plate floor shown in Fig. 13.8*b*. In this case beams are omitted. However, broad strips of the slab centered on the column lines in each direction serve the same function as the beams of Fig. 13.8*a*; for this case, also, the full load must be carried in each direction. The presence of drop panels or column capitals (Fig. 13.1*e*) in the double-hatched zone near the columns does not modify this requirement of statics.

Figure 13.9*a* shows a flat plate floor supported by columns at *A, B, C,* and *D*. Figure 13.9*b* shows the moment diagram for the direction of span l_1. In this direction, the slab may be considered as a broad, flat beam of width l_2. Accordingly, the load per foot of span is ql_2. In any span of a continuous beam, the sum of the midspan positive

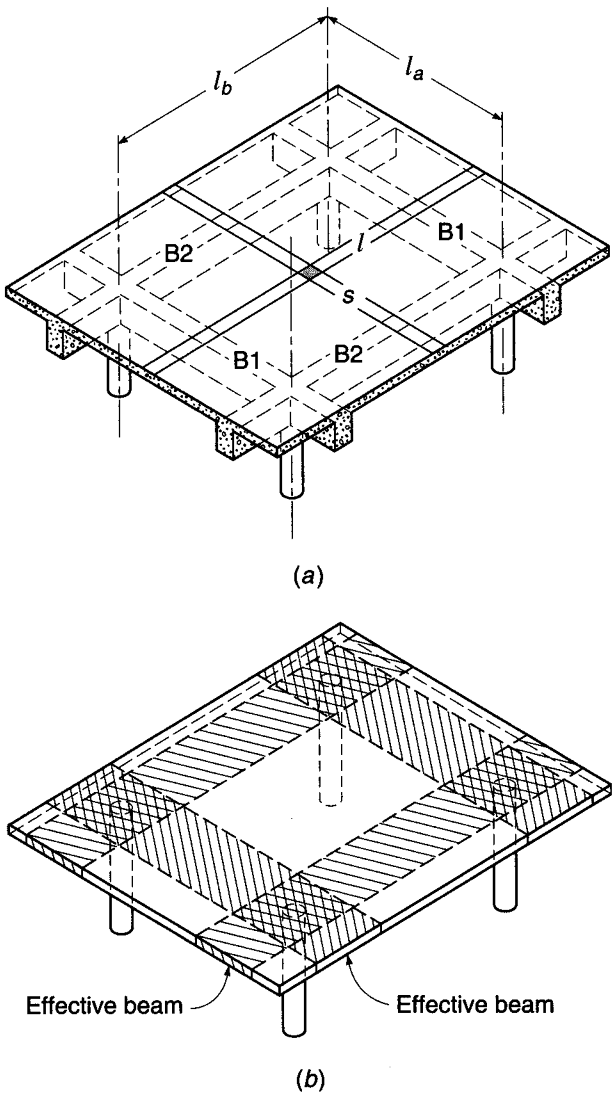

FIGURE 13.8
Column-supported two-way slabs: (*a*) two-way slab with beams; (*b*) two-way slab without beams.

moment and the average of the negative moments at adjacent supports is equal to the midspan positive moment of a corresponding simply supported beam. In terms of the slab, this requirement of statics may be written

$$\tfrac{1}{2}(M_{ab} + M_{cd}) + M_{ef} = \tfrac{1}{8}ql_2l_1^2 \tag{a}$$

A similar requirement exists in the perpendicular direction, leading to the relation

$$\tfrac{1}{2}(M_{ac} + M_{bd}) + M_{gh} = \tfrac{1}{8}ql_1l_2^2 \tag{b}$$

These results disclose nothing about the relative magnitudes of the support moments and span moments. The proportion of the total static moment that exists at each critical section can be found from an elastic analysis that considers the relative span lengths in adjacent panels, the loading pattern, and the relative stiffness of the

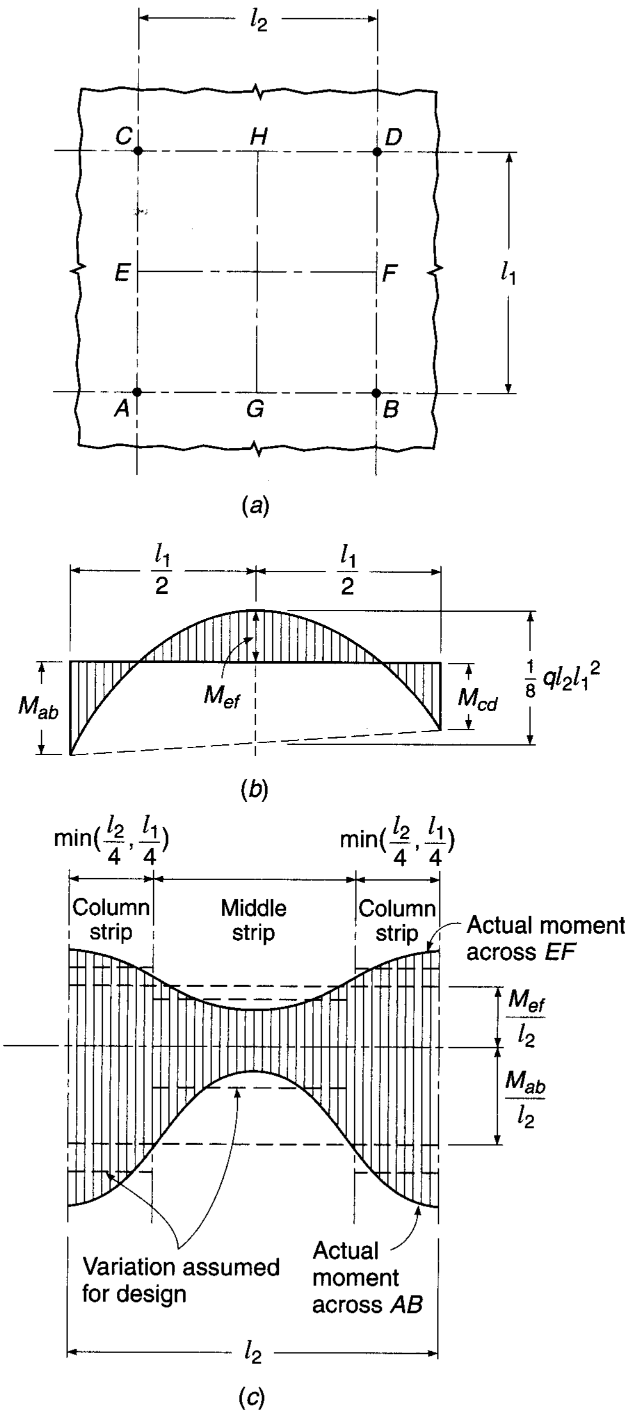

FIGURE 13.9
Moment variation in column-supported two-way slabs: (*a*) critical-moment sections; (*b*) moment variation along a span; (*c*) moment variation across the width of critical sections.

supporting beams, if any, and that of the columns. Alternatively, empirical methods that have been found to be reliable under restricted conditions may be adopted.

The moments across the width of critical sections such as *AB* or *EF* are not constant but vary as shown qualitatively in Fig. 13.9*c*. The exact variation depends on the presence or absence of beams on the column lines, the existence of drop panels

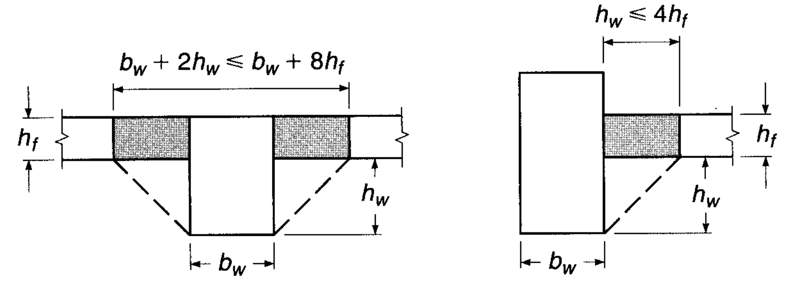

(*a*) Symmetric slab (*b*) Single side slab

FIGURE 13.10
Portion of slab to be included with beam.

and column capitals, as well as on the intensity of the load. For design purposes, it is convenient to divide each panel as shown in Fig. 13.9*c* into column strips, having a width of one-fourth the panel width, on each side of the column centerlines, and middle strips in the one-half panel width between two column strips. Moments may be considered constant within the bounds of a middle strip or column strip, as shown, unless beams are present on the column lines. In the latter case, while the beam must have the same curvature as the adjacent slab strip, the beam moment will be larger in proportion to its greater stiffness, producing a discontinuity in the moment-variation curve at the lateral face of the beam. Since the total moment must be the same as before, according to statics, the slab moments must be correspondingly less.

Chapter 13 of the ACI Code deals in a unified way with all such two-way systems. Its provisions apply to slabs supported by beams and to flat slabs and flat plates, as well as to two-way joist slabs. While permitting design "by any procedure satisfying the conditions of equilibrium and geometrical compatibility," specific reference is made to two alternative approaches: a semiempirical *direct design method* and an approximate elastic analysis known as the *equivalent frame method.*

In either case, a typical panel is divided, for purposes of design, into *column strips* and *middle strips.* A column strip is defined as a strip of slab having a width on each side of the column centerline equal to one-fourth the smaller of the panel dimensions l_1 and l_2. Such a strip includes column-line beams, if present. A middle strip is a design strip bounded by two column strips. In all cases, l_1 is defined as the span in the direction of the moment analysis and l_2 as the span in the lateral direction measured center to center of the support. In the case of monolithic construction, beams are defined to include that part of the slab on each side of the beam extending a distance equal to the projection of the beam above or below the slab h_w (whichever is greater) but not greater than 4 times the slab thickness (see Fig. 13.10).

13.6 DIRECT DESIGN METHOD FOR COLUMN-SUPPORTED SLABS

Moments in two-way slabs can be found using the semiempirical direct design method, subject to the following restrictions:

1. There must be a minimum of three continuous spans in each direction.
2. The panels must be rectangular, with the ratio of the longer to the shorter spans within a panel not greater than 2.
3. The successive span lengths in each direction must not differ by more than one-third of the longer span.

4. Columns may be offset a maximum of 10 percent of the span in the direction of the offset from either axis between centerlines of successive columns.
5. Loads must be due to gravity only, and the unfactored live load must not exceed 2 times the unfactored dead load.
6. If beams are used on the column lines, the relative stiffness of the beams in the two perpendicular directions, given by the ratio $\alpha_{f1} l_2^2 / \alpha_{f2} l_1^2$, must be between 0.2 and 5.0 (see definitions below).

a. Total Static Moment at Factored Loads

For purposes of calculating the total static moment M_o in a panel, the clear span l_n in the direction of moments is used. The *clear span* is defined to extend from face to face of the columns, capitals, brackets, or walls but is not to be less than $0.65l_1$. The total factored moment in a span, for a strip bounded laterally by the centerline of the panel on each side of the centerline of supports, is

$$M_o = \frac{q_u l_2 l_n^2}{8} \tag{13.1}$$

b. Assignment of Moments to Critical Sections

For interior spans, the total static moment is apportioned between the critical positive and negative bending sections according to the following ratios:

$$\text{Negative factored moment: Neg } M_u = 0.65M_o \tag{13.2}$$

$$\text{Positive factored moment: Pos } M_u = 0.35M_o \tag{13.3}$$

as illustrated by Fig. 13.11. The critical section for negative bending is taken at the face of rectangular supports, or at the face of an equivalent square support having the same cross-sectional area as a round support.

In the case of end spans, the apportionment of the total static moment among the three critical moment sections (interior negative, positive, and exterior negative, as illustrated by Fig. 13.11) depends upon the flexural restraint provided for the slab by the exterior column or the exterior wall, as the case may be, and depends also upon

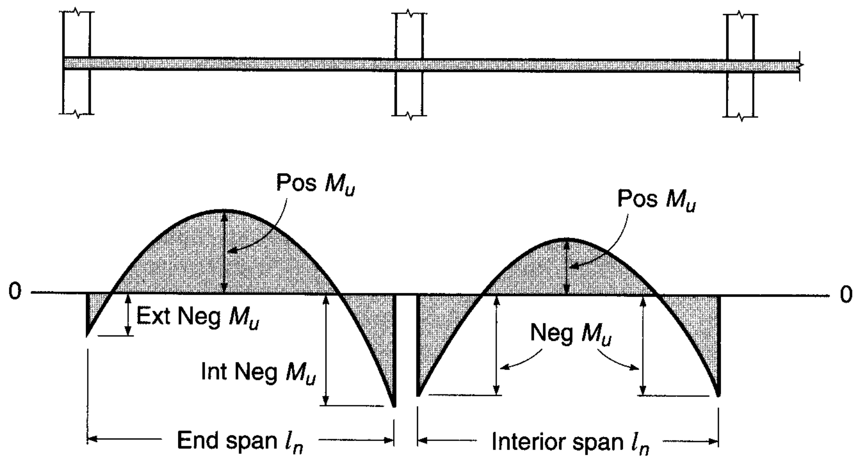

FIGURE 13.11
Distribution of total static moment M_o to critical sections for positive and negative bending.

the presence or absence of beams on the column lines. ACI Code 13.6.3 specifies five alternative sets of moment distribution coefficients for end spans, as shown in Table 13.3 and illustrated in Fig. 13.12.

TABLE 13.3
Distribution factors applied to static moment M_o for positive and negative moments in end span

	(a)	(b)	(c)	(d)	(e)
			Slab without Beams between Interior Supports		
	Exterior Edge Unrestrained	Slab with Beams between All Supports	Without Edge Beam	With Edge Beam	Exterior Edge Fully Restrained
Interior negative moment	0.75	0.70	0.70	0.70	0.65
Positive moment	0.63	0.57	0.52	0.50	0.35
Exterior negative moment	0	0.16	0.26	0.30	0.65

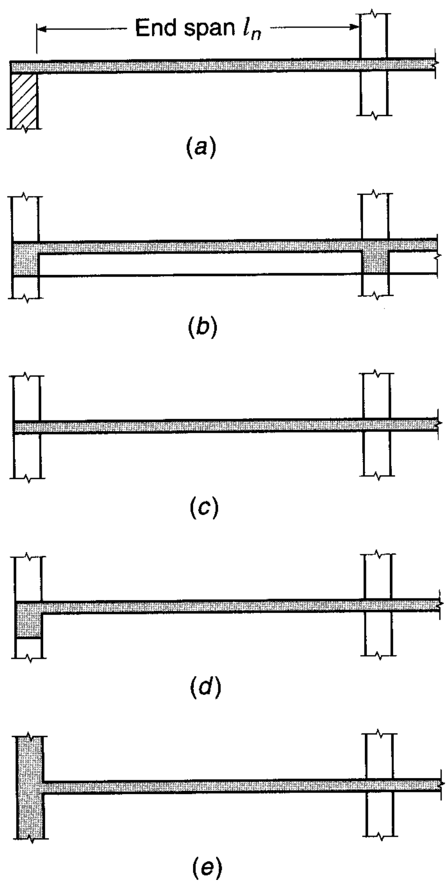

FIGURE 13.12
Conditions of edge restraint considered in distributing total static moment M_o to critical sections in an end span: (*a*) exterior edge unrestrained, e.g., supported by a masonry wall; (*b*) slab with beams between all supports; (*c*) slab without beams, i.e., flat plate; (*d*) slab without beams between interior supports but with edge beam; (*e*) exterior edge fully restrained, e.g., by monolithic concrete wall.

In case *a*, the exterior edge has no moment restraint, such as would be the condition with a masonry wall, which provides vertical support but no rotational restraint. Case *b* represents a two-way slab with beams on all sides of the panels. Case *c* is a flat plate, with no beams at all, while case *d* is a flat plate in which a beam is provided along the exterior edge. Finally, case *e* represents a fully restrained edge, such as that obtained if the slab is monolithic with a very stiff reinforced concrete wall. The appropriate coefficients for each case are given in Table 13.3 and are based on three-dimensional elastic analysis modified to some extent in the light of tests and practical experience (Refs. 13.4 to 13.11).

At interior supports, negative moments may differ for spans framing into the common support. In such a case, the slab should be designed to resist the larger of the two moments, unless a special analysis based on relative stiffnesses is made to distribute the unbalanced moment (see Chapter 12). Edge beams if they are used, or the edge of the slab if they are not, must be designed to resist in torsion their share of the exterior negative moment indicated by Table 13.3 (see Chapter 7).

c. Lateral Distribution of Moments

Having distributed the moment M_o to the positive and negative-moment sections as just described, the designer still must distribute these design moments across the width of the critical sections. For design purposes, as discussed in Section 13.5, it is convenient to consider the moments constant within the bounds of a middle strip or column strip unless there is a beam present on the column line. In the latter case, because of its greater stiffness, the beam will tend to take a larger share of the column-strip moment than the adjacent slab. The distribution of total negative or positive moment between slab middle strips, slab column strips, and beams depends upon the ratio l_2/l_1, the relative stiffness of the beam and the slab, and the degree of torsional restraint provided by the edge beam.

A convenient parameter defining the relative stiffness of the beam and slab spanning in either direction is

$$\alpha_f = \frac{E_{cb}I_b}{E_{cs}I_s} \tag{13.4}$$

in which E_{cb} and E_{cs} are the moduli of elasticity of the beam and slab concrete (usually the same) and I_b and I_s are the moments of inertia of the effective beam and the slab. Subscripted parameters α_{f1} and α_{f2} are used to identify α computed for the directions of l_1 and l_2, respectively.

The flexural stiffnesses of the beam and slab may be based on the gross concrete section, neglecting reinforcement and possible cracking, and variations due to column capitals and drop panels may be neglected. For the beam, if present, I_b is based on the effective cross section defined as in Fig. 13.10. For the slab, I_s is taken equal to $bh^3/12$, where b in this case is the width between panel centerlines on each side of the beam.

The relative restraint provided by the torsional resistance of the effective transverse edge beam is reflected by the parameter β_t, defined as

$$\beta_t = \frac{E_{cb}C}{2E_{cs}I_s} \tag{13.5}$$

where I_s, as before, is calculated for the slab spanning in direction l_1 and having width bounded by panel centerlines in the l_2 direction. The constant C pertains to the torsional rigidity of the effective transverse beam, which is defined according to ACI Code 13.7.5 as the largest of the following:

1. A portion of the slab having a width equal to that of the column, bracket, or capital in the direction in which moments are taken
2. The portion of the slab specified in 1 plus that part of any transverse beam above and below the slab
3. The transverse beam defined as in Fig. 13.10

The constant C is calculated by dividing the section into its component rectangles, each having smaller dimension x and larger dimension y, and summing the contributions of all the parts by means of the equation

$$C = \sum \left(1 - 0.63\frac{x}{y}\right)\frac{x^3y}{3} \tag{13.6}$$

The subdivision can be done in such a way as to maximize C.

With these parameters defined, ACI Code 13.6.4 distributes the negative and positive moments between column strips and middle strips, assigning to the column strips the percentages of positive and negative moments shown in Table 13.4. Linear interpolations are to be made between the values shown.

Implementation of these provisions is facilitated by the interpolation charts of Graph A.4 of Appendix A. Interior negative and positive-moment percentages can be read directly from the charts for known values of l_2/l_1 and $\alpha_{f1}l_2/l_1$. For exterior negative moment, the parameter β_t requires an additional interpolation, facilitated by the auxiliary diagram on the right side of the charts. To illustrate its use for

TABLE 13.4
Column-strip moment, percent of total moment at critical section

		l_2/l_1		
		0.5	**1.0**	**2.0**
Interior negative moment				
$\alpha_{f1}l_2/l_1 = 0$		75	75	75
$\alpha_{f1}l_2/l_1 \geq 1.0$		90	75	45
Exterior negative moment				
$\alpha_{f1}l_2/l_1 = 0$	$\beta_t = 0$	100	100	100
	$\beta_t \geq 2.5$	75	75	75
$\alpha_{f1}l_2/l_1 \geq 1.0$	$\beta_t = 0$	100	100	100
	$\beta_t \geq 2.5$	90	75	45
Positive moment				
$\alpha_{f1}l_2/l_1 = 0$		60	60	60
$\alpha_{f1}l_2/l_1 \geq 1.0$		90	75	45

$l_2/l_1 = 1.55$ and $\alpha_{f1}l_2/l_1 = 0.6$, the dotted line indicates moment percentages of 100 for $\beta_t = 0$ and 65 for $\beta_t = 2.5$. Projecting to the right as indicated by the arrow to find the appropriate vertical scale of 2.5 divisions for an intermediate value of β_t, say 1.0, then upward and finally to the left, one reads the corresponding percentage of 86 on the main chart.

The column-line beam spanning in the direction l_1 is to be proportioned to resist 85 percent of the column-strip moment if $\alpha_{f1}l_2/l_1$ is equal to or greater than 1.0. For values between 1 and 0, the proportion to be resisted by the beam may be obtained by linear interpolation. Concentrated or linear loads applied directly to such a beam should be accounted for separately.

The portion of the moment not resisted by the column strip is proportionately assigned to the adjacent half-middle strips. Each middle strip is designed to resist the sum of the moments assigned to its two half-middle strips. A middle strip adjacent and parallel to a wall is designed for twice the moment assigned to the half-middle strip corresponding to the first row of interior supports.

d. Shear in Slab Systems with Beams

Special attention must be given to providing the proper resistance to shear, as well as to moment, when designing by the direct method. According to ACI Code 13.6.8, beams with $\alpha_{f1}l_2/l_1 \geq 1.0$ must be proportioned to resist the shear caused by loads on a tributary area defined as shown in Fig. 13.13. For values of $\alpha_{f1}l_2/l_1$ between 1 and 0, the proportion of load carried by beam shear is found by linear interpolation. The remaining fraction of the load on the shaded area is assumed to be transmitted directly by the slab to the columns at the four corners of the panel, and the shear stress in the slab computed accordingly (see Section 13.10).

FIGURE 13.13
Tributary areas for shear calculation.

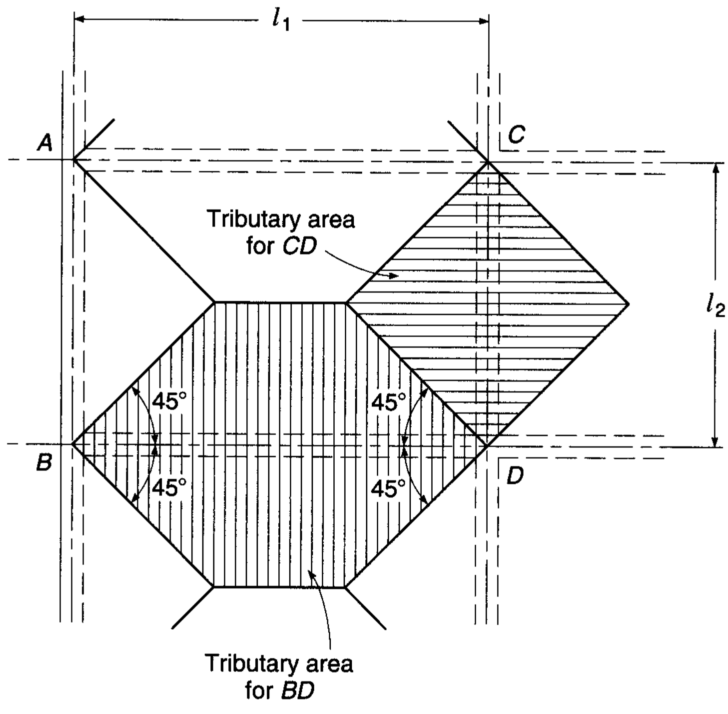

e. Design of Columns

Columns in two-way construction must be designed to resist the moments found from analysis of the slab-beam system. The column supporting an edge beam must provide a resisting moment equal to the moment applied from the edge of the slab (see Table 13.4). At interior locations, slab negative moments are found, assuming that dead and full live loads act. For the column design, a more severe loading results from partial removal of the live load. Accordingly, ACI Code 13.6.9 requires that interior columns resist a moment

$$M_u = 0.07\left[(q_{Du} + 0.5q_{Lu})l_2 l_n^2 - q'_{Du} l'_2 (l'_n)^2\right] \tag{13.7}$$

In Eq. (13.7), q_{Du} and q_{Lu} are, respectively, the factored dead and live loads per unit area. The primed quantities refer to the shorter of the two adjacent spans (assumed to carry dead load only), and the unprimed quantities refer to the longer span (assumed to carry dead load and half live load). In all cases, the moment is distributed to the upper and lower columns in proportion to their relative flexural stiffness.

13.7 FLEXURAL REINFORCEMENT FOR COLUMN-SUPPORTED SLABS

Consistent with the assumptions made in analysis, flexural reinforcement in two-way slab systems is placed in an orthogonal grid, with bars parallel to the sides of the panels. Bar diameters and spacings may be found as described in Section 13.2. Straight bars are generally used throughout, although in some cases positive-moment steel is bent up where no longer needed, to provide for part or all of the negative requirement. To provide for local concentrated loads, as well as to ensure that tensile cracks are narrow and well distributed, a maximum bar spacing at critical sections of 2 times the total slab thickness is specified by ACI Code 13.3.2 for two-way slabs. At least the minimum steel required for temperature and shrinkage crack control (see Section 13.3) must be provided. For protection of the steel against damage from fire or corrosion, at least $\frac{3}{4}$ in. concrete cover must be maintained.

Because of the stacking that results when bars are placed in perpendicular layers, the inner steel will have an effective depth 1 bar diameter less than the outer steel. For flat plates and flat slabs, the stacking problem relates to middle-strip positive steel and column-strip negative bars. In two-way slabs with beams on the column lines, stacking occurs for the middle-strip positive steel, and in the column strips is important mainly for the column-line beams, because slab moments are usually very small in the region where column strips intersect.

In the discussion of the stacking problem for two-way slabs supported by walls or stiff edge beams, in Section 13.4 it was pointed out that, because curvatures and moments in the short direction are greater than in the long direction of a rectangular panel, short-direction bars are normally placed closer to the top or bottom surface of the slab, with the larger effective depth d, and long-direction bars are placed inside these, with the smaller d. For two-way beamless flat plates, or slabs with relatively flexible edge beams, things are not so simple.

Consider a rectangular interior panel of a flat plate floor. If the slab column strips provided unyielding supports for the middle strips spanning in the perpendicular direction, the short-direction middle-strip curvatures and moments would be the larger. In fact, the column strips deflect downward under load, and this softening of the effective support greatly reduces curvatures and moments in the supported middle strip.

For the entire panel, including both middle strips and column strips in each direction, the moments in the long direction will be larger than those in the short direction, as is easily confirmed by calculating the static moment M_o in each direction for a rectangular panel. Noting that the apportioning of M_o first to negative and positive-moment sections, and then laterally to column and middle strips, is done by applying exactly the same ratios in each direction to the corresponding section, it is clear that the middle-strip positive moments (for example) are larger in the long direction than the short direction, exactly the opposite of the situation for the slab with stiff edge beams. In the column strips, positive and negative moments are larger in the long than in the short direction. On this basis, the designer is led to place the long-direction negative and positive bars, in both middle and column strips, closer to the top or bottom surface of the slab, respectively, with the larger effective depth.

If column-line beams are added, and if their stiffness is progressively increased for comparative purposes, it will be found that the short-direction slab moments gradually become dominant, although the long-direction beams carry larger moments than the short-direction beams. This will be clear from a careful study of Table 13.4.

The situation is further complicated by the influence of the ratio of short to long side dimensions of a panel, and by the influence of varying conditions of edge restraint (e.g., corner vs. typical exterior vs. interior panel). The best guide in specifying steel placement order in areas where stacking occurs is the relative magnitudes of design moments obtained from analysis for a particular case, with maximum d provided for the bars resisting the largest moment. No firm rules can be given. For square slab panels, many designers calculate the required steel area based on the average effective depth, thus obtaining the same bar size and spacing in each direction. This is slightly conservative for the outer layer and slightly unconservative for the inner steel. Redistribution of loads and moments before failure would provide for the resulting differences in capacities in the two directions.

Reinforcement cutoff points could be calculated from moment envelopes if available; however, when the direct design method is used, moment envelopes and lines of inflection are not found explicitly. In such a case (and often when the equivalent frame method of Section 13.9 is used as well), standard bar cutoff points from Fig. 13.14 are used, as recommended in the ACI Code.

ACI Code 13.3.8.5 requires that all bottom bars within the column strip in each direction be continuous or spliced with Class B splices (see Section 5.13a) or mechanical or welded splices located as shown in Fig. 13.14. At least two of the column strip bars in each direction must pass within the column core and must be anchored at exterior supports. The continuous column strip bottom steel is intended to provide some residual ability to carry load to adjacent supports by catenary action if a single support should be damaged or destroyed. The two continuous bars through the column can be considered to be "integrity steel" and are provided to give the slab some residual capacity following a single punching shear failure.

The need for special reinforcement at the exterior corners of two-way beam-supported slabs was described in Section 13.4, and typical corner reinforcement is shown in Fig. 13.7. According to ACI Code 13.3.6, such reinforcement is required for slabs with beams between supporting columns if the value of α_f given by Eq. (13.3) is greater than 1.0.

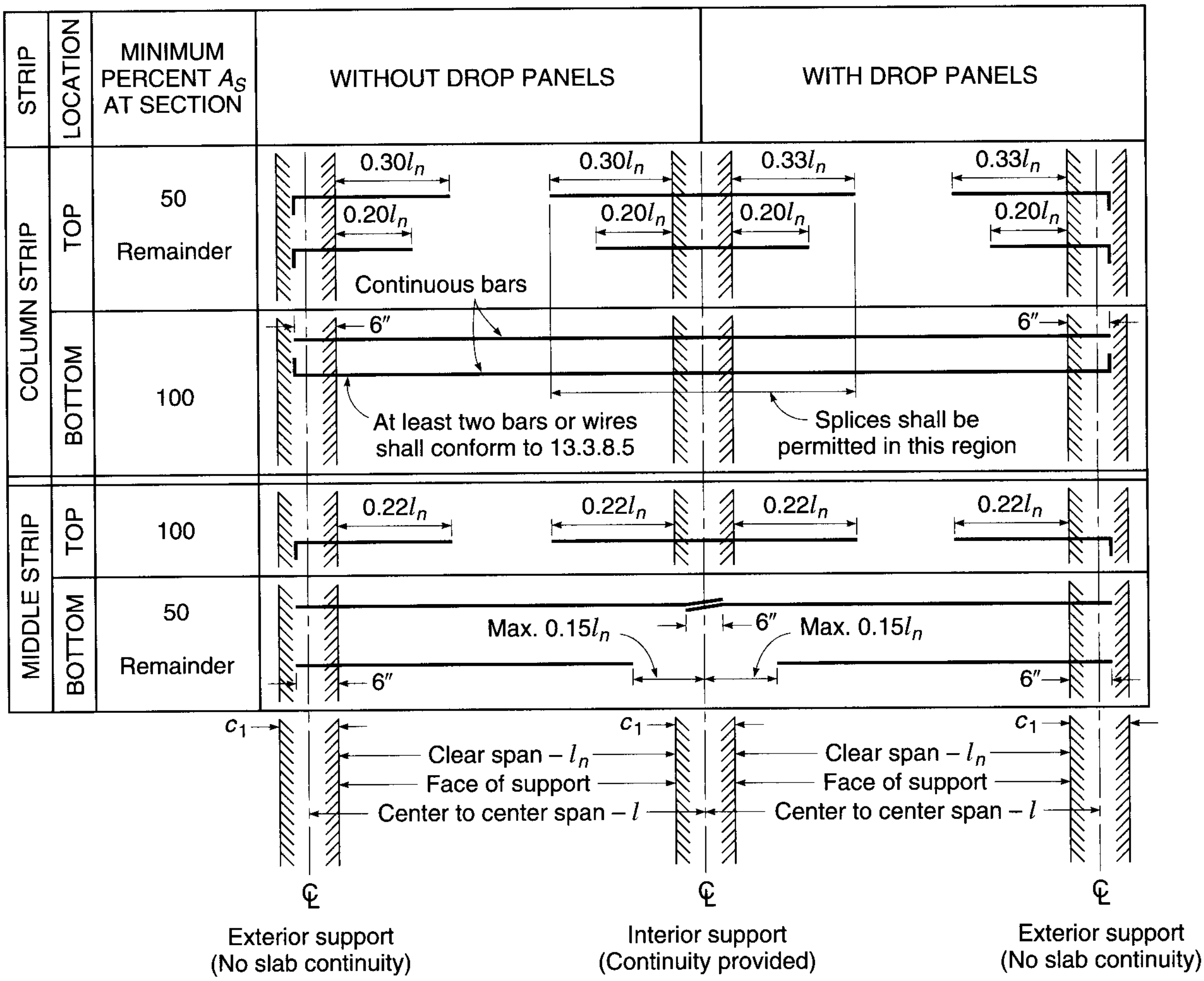

FIGURE 13.14
Minimum length of slab reinforcement in a slab without beams.

13.8 DEPTH LIMITATIONS OF THE ACI CODE

To ensure that slab deflections in service will not be troublesome, the best approach is to compute deflections for the total load or load component of interest and to compare the computed deflections with limiting values. Methods have been developed that are both simple and acceptably accurate for predicting deflections of two-way slabs. A method for calculating the deflection of two-way column-supported slabs will be found in Section 13.13.

Alternatively, deflection control can be achieved indirectly by adhering to more or less arbitrary limitations on minimum slab thickness, limitations developed from review of test data and study of the observed deflections of actual structures. As a result of efforts to improve the accuracy and generality of the limiting equations, they have become increasingly complex.

TABLE 13.5
Minimum thickness of slabs without interior beams

Yield Stress f_y, psi	Without Drop Panels: Exterior Panels: Without Edge Beams	Without Drop Panels: Exterior Panels: With Edge Beams[a]	Without Drop Panels: Interior Panels	With Drop Panels: Exterior Panels: Without Edge Beams	With Drop Panels: Exterior Panels: With Edge Beams[a]	With Drop Panels: Interior Panels
40,000	$l_n/33$	$l_n/36$	$l_n/36$	$l_n/36$	$l_n/40$	$l_n/40$
60,000	$l_n/30$	$l_n/33$	$l_n/33$	$l_n/33$	$l_n/36$	$l_n/36$
75,000	$l_n/28$	$l_n/31$	$l_n/31$	$l_n/31$	$l_n/34$	$l_n/34$

[a] Slabs with beams along exterior edges. The value of α_f for the edge beam shall not be less than 0.8.

ACI Code 9.5.3 establishes minimum thicknesses for two-way construction designed according to the methods of ACI Code Chapter 13, i.e., for slabs designed by either the equivalent frame method or the direct design method. Simplified criteria are included pertaining to slabs without interior beams (flat plates and flat slabs with or without edge beams), while more complicated limit equations are to be applied to slabs with beams spanning between the supports on all sides. In both cases, minimum thicknesses less than the specified value may be used if calculated deflections are within Code-specified limits, as quoted in Table 6.2.

a. Slabs without Interior Beams

The minimum thickness of two-way slabs without interior beams, according to ACI Code 9.5.3.2, must not be less than provided by Table 13.5. Edge beams, often provided even for two-way slabs otherwise without beams to improve moment and shear transfer at the exterior supports, permit a reduction in minimum thickness of about 10 percent in exterior panels. In all cases, the minimum thickness of slabs without interior beams must not be less than the following:

For slabs without drop panels	5 in.
For slabs with drop panels	4 in.

b. Slabs with Beams on All Sides

The parameter used to define the relative stiffness of the beam and slab spanning in either direction is α_f, calculated from Eq. (13.4) of Section 13.6c. Then α_{fm} is defined as the average value of α_f for all beams on the edges of a given panel. According to ACI Code 9.5.3.3, for α_{fm} equal to or less than 0.2, the minimum thicknesses of Table 13.5 shall apply.

For α_{fm} greater than 0.2 but not greater than 2.0, the slab thickness must not be less than

$$h = \frac{l_n(0.8 + f_y/200{,}000)}{36 + 5\beta(\alpha_{fm} - 0.2)} \tag{13.8a}$$

and not less than 5.0 in.

For α_{fm} greater than 2.0, the thickness must not be less than

$$h = \frac{l_n(0.8 + f_y/200{,}000)}{36 + 9\beta} \tag{13.8b}$$

and not less than 3.5 in.,

where l_n = clear span in long direction, in.
α_{fm} = average value of α_f for all beams on edges of a panel [see Eq. (13.4)]
β = ratio of clear span in long direction to clear span in short direction

At discontinuous edges, an edge beam must be provided with a stiffness ratio α_f not less than 0.8; otherwise the minimum thickness provided by Eq. (13.8*a*) or (13.8*b*) must be increased by at least 10 percent in the panel with the discontinuous edge.

In all cases, slab thickness less than the stated minimum may be used if it can be shown by computation that deflections will not exceed the limit values of Table 6.2.

Equations (13.8*a*) and (13.8*b*) can be restated in the general form

$$h = \frac{l_n(0.8 + f_y/200{,}000)}{F} \tag{13.8c}$$

where F is the value of the denominator in each case. Figure 13.15 shows the value of F as a function of α_{fm}, for comparative purposes, for three panel aspect ratios β:

1. Square panel, with $\beta = 1.0$
2. Rectangular panel, with $\beta = 1.5$
3. Rectangular panel, with $\beta = 2.0$, the upper limit of applicability of Eqs. (13.8*a*) and (13.8*b*)

Note that, for α_{fm} less than 0.2, column-line beams have little effect, and minimum thickness is given by Table 13.5. For stiff, relatively deep edge beams, with α_{fm} of 2 or greater, Eq. (13.8*b*) governs. Equation (13.8*a*) provides a transition for slabs with shallow column-line beams having α_{fm} in the range from 0.2 to 2.0.

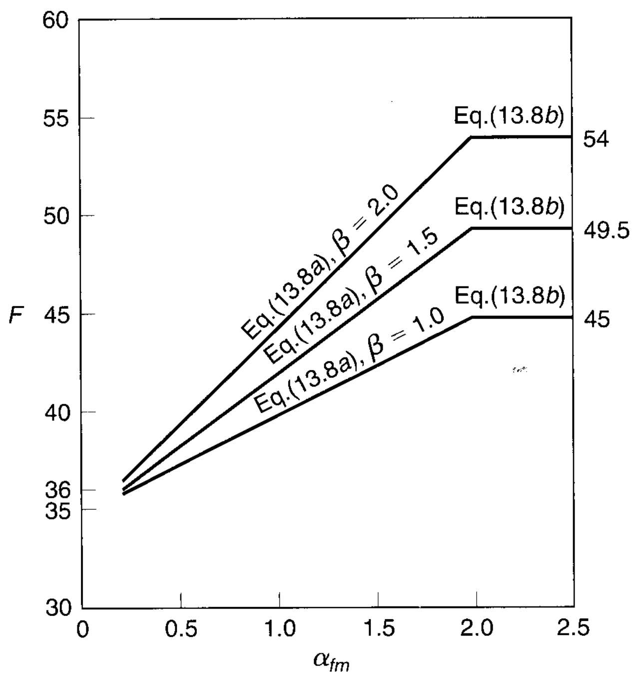

FIGURE 13.15
Parameter F governing minimum thickness of two-way slabs; minimum thickness $h = l_n(0.8 + f_y/200{,}000)/F$.

EXAMPLE 13.2 **Design of two-way slab with edge beams.**† A two-way reinforced concrete building floor system is composed of slab panels measuring 20 × 25 ft in plan, supported by shallow column-line beams cast monolithically with the slab, as shown in Fig. 13.16. Using concrete with $f_c' = 4000$ psi and steel with $f_y = 60{,}000$ psi, design a typical exterior panel to carry a service live load of 144 psf in addition to the self-weight of the floor.

SOLUTION. The floor system satisfies all limitations stated in Section 13.6, and the ACI direct design method will be used. For illustrative purposes, only a typical exterior panel, as shown in Fig. 13.16, will be designed. The depth limitations of Section 13.8 will be used as a guide to the desirable slab thickness. To use Eqs. (13.8*a*) and (13.8*b*), a trial value of $h = 7$ will be introduced, and beam dimensions 14 × 20 in. will be assumed, as shown in Fig. 13.16. The effective flange projection beyond the face of the beam webs is the lesser of $4h_f$ or h_w, and in the present case is 13 in. The moment of inertia of the T beams will be estimated as multiples of that of the rectangular portion as follows:

For the edge beams: $I = \frac{1}{12} \times 14 \times 20^3 \times 1.5 = 14{,}000 \text{ in}^4$

For the interior beams: $I = \frac{1}{12} \times 14 \times 20^3 \times 2 = 18{,}700 \text{ in}^4$

FIGURE 13.16
Two-way slab floor with beams on column lines:
(*a*) partial floor plan;
(*b*) section *X*-*X* (section *Y*-*Y* similar).

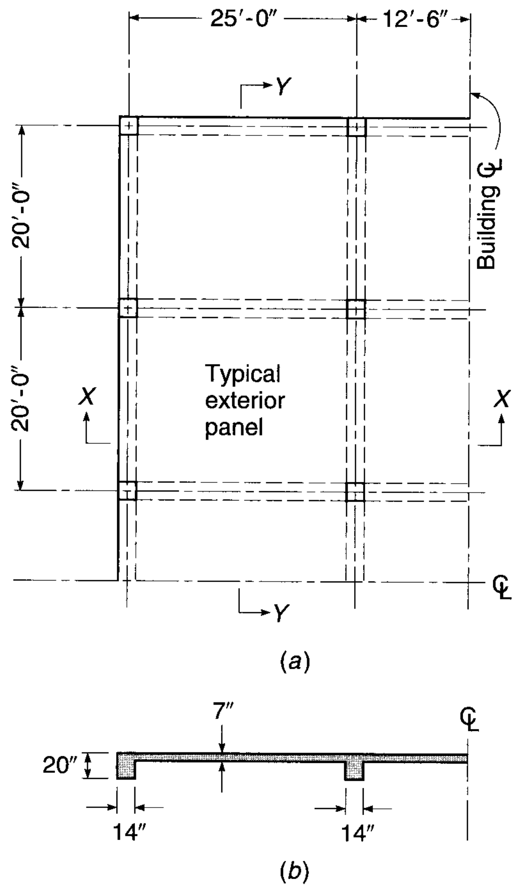

† The design of a two-way slab without beams, i.e., a flat plate floor system, which may also be done by the direct design method if the restrictions of Section 13.6 are met, will be illustrated by an example in Section 13.7.

For the slab strips:

For the 13.1 ft edge width: $I = \frac{1}{12} \times 13.1 \times 12 \times 7^3 = 4500 \text{ in}^4$
For the 20 ft width: $I = \frac{1}{12} \times 20 \times 12 \times 7^3 = 6900 \text{ in}^4$
For the 25 ft width: $I = \frac{1}{12} \times 25 \times 12 \times 7^3 = 8600 \text{ in}^4$

Thus, for the edge beam $\alpha_f = 14{,}000/4500 = 3.1$, for the two 25 ft long beams $\alpha_f = 18{,}700/6900 = 2.7$, and for the 20 ft long beam $\alpha_f = 18{,}700/8600 = 2.2$, producing an average value $\alpha_{fm} = 2.7$. The ratio of long to short clear spans is $\beta = 23.8/18.8 = 1.27$. Then the minimum thickness is not to be less than that given by Eq. (13.8*b*):

$$h = \frac{286(0.8 + 60/200)}{36 + 9 \times 1.27} = 6.63 \text{ in.}$$

The 3.5 in. limitation of Section 13.8 clearly does not control in this case, and the 7 in. depth tentatively adopted will provide the basis of further calculation.

For a 7 in. slab, the dead load is $\frac{7}{12} \times 150 = 88$ psf. Applying the usual load factors to obtain design load gives

$$q = 1.2 \times 88 + 1.6 \times 144 = 336 \text{ psf}$$

For the *short-span direction*, for the slab-beam strip centered on the interior column line, the total static design moment is

$$M_o = \tfrac{1}{8} \times 0.336 \times 25 \times 18.8^2 = 371 \text{ ft-kips}$$

This is distributed as follows:

$$\text{Negative design moment} = 371 \times 0.65 = 241 \text{ ft-kips}$$
$$\text{Positive design moment} = 371 \times 0.35 = 130 \text{ ft-kips}$$

The column strip has a width of $2 \times 20/4 = 10$ ft. With $l_2/l_1 = 25/20 = 1.25$ and $\alpha_{f1}l_2/l_1 = 2.2 \times 25/20 = 2.75$, Graph A.4 of Appendix A indicates that 68 percent of the negative moment, or 163 ft-kips, is taken by the column strip, of which 85 percent, or 139 ft-kips, is taken by the beam and 24 ft-kips by the slab. The remaining 78 ft-kips is allotted to the slab middle strip. Graph A.4 also indicates that 68 percent of the positive moment, or 88 ft-kips, is taken by the column strip, of which 85 percent, or 75 ft-kips, is assigned to the beam and 13 ft-kips to the slab. The remaining 42 ft-kips is taken by the slab middle strip.

A similar analysis is performed for the slab-beam strip at the edge of the building, based on a total static design moment of

$$M_o = \tfrac{1}{8} \times 0.336 \times 13.1 \times 18.8^2 = 194 \text{ ft-kips}$$

of which 65 percent is assigned to the negative and 35 percent to the positive bending sections as before. In this case, $\alpha_{f1}l_2/l_1 = 3.1 \times 25/20 = 3.9$. The distribution factor for column-strip moment, from Graph A.4, is 68 percent for positive and negative moments as before, and again 85 percent of the column-strip moments is assigned to the beams.

In summary, the short-direction moments, in ft-kips, are as follows:

	Beam Moment	Column-Strip Slab Moment	Middle-Strip Slab Moment
Interior slab-beam strip—20 ft span			
Negative	139	24	78
Positive	75	13	42
Exterior slab-beam strip—20 ft span			
Negative	73	13	40
Positive	39	7	22

The total static design moment in the *long direction* of the exterior panel is

$$M_o = \tfrac{1}{8} \times 0.336 \times 20 \times 23.8^2 = 476 \text{ ft-kips}$$

This will be apportioned to the negative and positive moment sections according to Table 13.3, and distributed laterally across the width of critical moment sections with the aid of Graph A.4. The moment ratios to be applied to obtain exterior negative, positive, and interior negative moments are, respectively, 0.16, 0.57, and 0.70. The torsional constant for the edge beam is found from Eq. (13.6) for a 14 × 20 in. rectangular shape with a 7 × 13 in. projecting flange:

$$C = \left(1 - 0.63 \times \frac{14}{20}\right) \frac{14^3 \times 20}{3} + \left(1 - 0.63 \times \frac{7}{13}\right) \frac{7^3 \times 13}{3} = 11{,}210$$

With $l_2/l_1 = 0.80$, $\alpha_{f1} l_2/l_1 = 2.7 \times 20/25 = 2.2$, and from Eq. (13.5), $\beta_t = 11{,}210/(2 \times 6900) = 0.81$, Graph A.4 indicates that the column strip will take 93 percent of the exterior negative moment, 81 percent of the positive moment, and 81 percent of the interior negative moment. As before, the column-line beam will account for 85 percent of the column-strip moment. The results of applying these moment ratios are as follows:

	Beam Moment	Column-Strip Slab Moment	Middle-Strip Slab Moment
Exterior negative—25 ft span	60	11	5
Positive—25 ft span	187	33	51
Interior negative—25 ft span	229	40	63

It is convenient to tabulate the design of the slab reinforcement, as shown in Table 13.6. In the 25 ft direction, the two half-column strips may be combined for purposes of calculation into one strip of 106 in. width. In the 20 ft direction, the exterior half-column strip and the interior half-column strip will normally differ and are treated separately. Factored moments from the previous distributions are summarized in column 3 of the table.

The short-direction positive steel will be placed first, followed by the long-direction positive bars. If $\frac{3}{4}$ in. clear distance below the steel is allowed and use of No. 4 (No. 13) bars is anticipated, the effective depth in the short direction will be 6 in., while that in the long direction will be 5.5 in. A similar situation occurs for the top steel.

After calculating the design moment per foot strip of slab (column 6), find the minimum effective slab depth required for flexure. For the material strengths to be used, the maximum practical reinforcement ratio is $\rho_{0.005} = 0.0181$. For this ratio,

$$d^2 = \frac{M_u}{\phi \rho f_y b(1 - 0.59 \rho f_y/f'_c)}$$

$$= \frac{M_u}{0.90 \times 0.0181 \times 60{,}000 \times 12(1 - 0.59 \times 0.0181 \times 60/4)} = \frac{M_u}{9850}$$

Hence $d = \sqrt{M_u/9850}$. Thus, the following minimum effective depths are needed:

In 25 ft direction: $$d = \sqrt{6.30 \times \frac{12{,}000}{9850}} = 2.77 \text{ in.}$$

In 20 ft direction: $$d = \sqrt{5.20 \times \frac{12{,}000}{9850}} = 2.52 \text{ in.}$$

both well below the depth dictated by deflection requirements. An underreinforced slab results. The required reinforcement ratios (column 7) are conveniently found from Table A.5 with $R = M_u/\phi bd^2$ or from Table A.9. Note that a minimum steel area equal to 0.0018 times the gross concrete area must be provided for control of temperature and shrinkage cracking. For a 12 in. slab strip, the corresponding area is $0.0018 \times 7 \times 12 = 0.151$ in^2. Expressed in terms of minimum reinforcement ratio for actual effective depths, this gives

TABLE 13.6
Design of slab reinforcement

(1)	(2) Location	(3) M_u, ft-kips	(4) b, in.	(5) d, in.	(6) $M_u \times 12/b$, ft-kips/ft	(7) ρ	(8) A_s, in^2	(9) Number of No. 4 (No. 13) Bars
25 ft span Two half-column strips	Exterior negative	11	106	5.5	1.25	0.0023[a]	1.34	7
	Positive	33	106	5.5	3.74	0.0023	1.34	7
	Interior negative	40	106	5.5	4.53	0.0029	1.69	9
Middle strip	Exterior negative	5	120	5.5	0.50	0.0023[a]	1.52	9[b]
	Positive	51	120	5.5	5.10	0.0033	2.18	11
	Interior negative	63	120	5.5	6.30	0.0041	2.71	14
20 ft span Exterior half-column strip	Negative	13	53	6	2.94	0.0021[a]	0.67	4
	Positive	7	53	6	1.58	0.0021[a]	0.67	4
Middle strip	Negative	78	180	6	5.20	0.0028	3.03	16
	Positive	42	180	6	2.80	0.0021[a]	2.27	13[b]
Interior half-column strip	Negative	12	53	6	2.71	0.0021[a]	0.67	4
	Positive	6.5	53	6	1.47	0.0021[a]	0.67	4

[a] Reinforcement ratio controlled by shrinkage and temperature requirements.
[b] Number of bars controlled by maximum spacing requirements.

In 25 ft direction: $$\rho_{\min} = \frac{0.151}{5.5 \times 12} = 0.0023$$

In 20 ft direction: $$\rho_{\min} = \frac{0.151}{6 \times 12} = 0.0021$$

This requirement controls at the locations indicated in Table 13.6.

The total steel area in each band is easily found from the reinforcement ratio and is given in column 8. Finally, with the aid of Table A.2, the required number of bars is obtained. Note that in two locations, the number of bars used is dictated by the maximum spacing requirement of $2 \times 7 = 14$ in.

The shear capacity of the slab is checked on the basis of the tributary areas shown in Fig. 13.13. At a distance d from the face of the long beam,

$$V_u = 0.336\left(10 - \frac{14}{2 \times 12} - \frac{6}{12}\right) = 3.00 \text{ kips}$$

The design shear strength of the slab is

$$\phi V_c = 0.75 \times 2\sqrt{4000} \times 12 \times \frac{6}{1000}$$

$$= 6.83 \text{ kips}$$

well above the shear applied at factored loads.

Each beam must be designed for its share of the total static moment, as found in the above calculations, as well as the moment due to its own weight; this moment may be distributed to positive and negative bending sections, using the same ratios used for the static moments due to slab loads. Beam shear design should be based on the loads from the tributary areas shown in Fig. 13.13. Since no new concepts would be introduced, the design of the beams will not be presented here.

Since $0.85 \times 93 = 79$ percent of the exterior negative moment in the long direction is carried directly to the column by the column-line beam in this example, torsional stresses in the spandrel beam are very low and may be disregarded. In other circumstances, the spandrel beams would be designed for torsion following the methods of Chapter 7.

13.9 EQUIVALENT FRAME METHOD

a. Basis of Analysis

The direct design method for two-way slabs described in Section 13.6 is useful if each of the six restrictions on geometry and load is satisfied by the proposed structure. Otherwise, a more general method is needed. One such method, proposed by Peabody in 1948 (Ref. 13.12), was incorporated in subsequent editions of the ACI Code as *design by elastic analysis*. The method was greatly expanded and refined based on research in the 1960s (Refs. 13.13 and 13.14), and it appears in Chapter 13 of the current ACI Code as the *equivalent frame method*.

It will be evident that the equivalent frame method was derived with the assumption that the analysis would be done using the moment distribution method (see Chapter 12). If analysis is done by computer using a standard frame analysis program, special modeling devices are necessary. This point will be discussed further in Section 13.9e.

By the equivalent frame method, the structure is divided, for analysis, into continuous frames centered on the column lines and extending both longitudinally and transversely, as shown by the shaded strips in Fig. 13.17. Each frame is composed of a row of columns and a broad continuous beam. The beam, or slab beam, includes the portion of the slab bounded by panel centerlines on either side of the columns, together with column-line beams or drop panels, if used. For vertical loading, each floor with its columns may be analyzed separately, with the columns assumed to be fixed at the floors above and below. In calculating bending moment at a support, it is convenient and sufficiently accurate to assume that the continuous frame is completely fixed at the support two panels removed from the given support, provided the frame continues past that point.

b. Moment of Inertia of Slab Beam

Moments of inertia used for analysis may be based on the concrete cross section, neglecting reinforcement, but variations in cross section along the member axis should be accounted for.

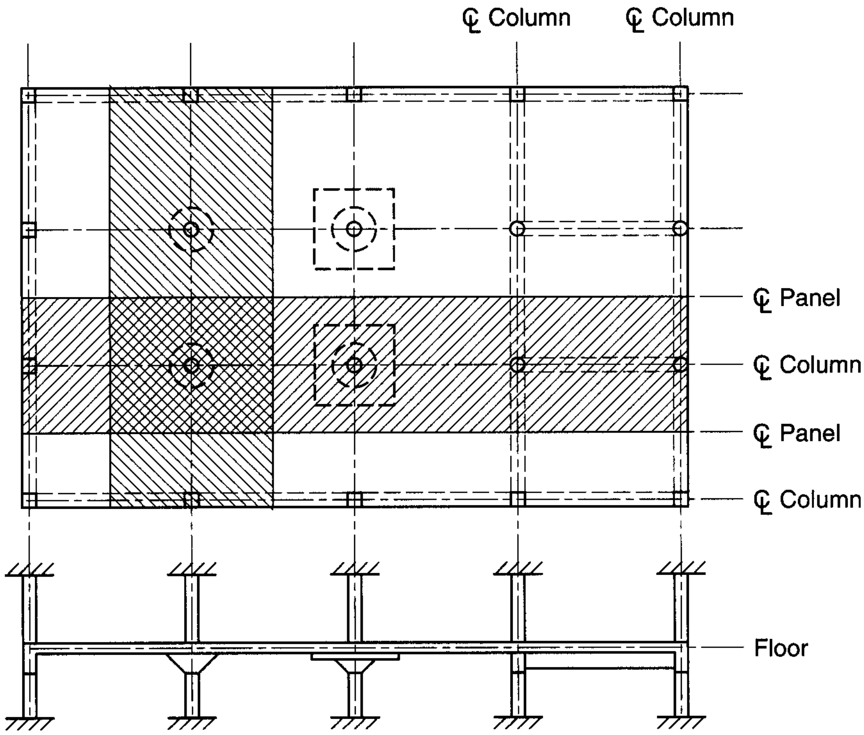

FIGURE 13.17
Building idealization for equivalent frame analysis.

For the beam strips, the first change from the midspan moment of inertia normally occurs at the edge of drop panels, if they are used. The next occurs at the edge of the column or column capital. While the stiffness of the slab strip could be considered infinite within the bounds of the column or capital, at locations close to the panel centerlines (at each edge of the slab strip), the stiffness is much less. According to ACI Code 13.7.3, from the center of the column to the face of the column or capital, the moment of inertia of the slab is taken equal to the value at the face of the column or capital, divided by the quantity $(1 - c_2/l_2)^2$, where c_2 and l_2 are the size of the column or capital and the panel width, respectively, both measured transverse to the direction in which moments are being determined.

Accounting for these changes in moments of inertia results in a member, for analysis, in which the moment of inertia varies in a stepwise manner. The stiffness factors, carryover factors, and uniform-load fixed-end moment factors needed for moment distribution analysis (see Chapter 12) are given in Table A.13*a* of Appendix A for a slab without drop panels and in Table A.13*b* for a slab with drop panels with a depth equal to 1.25 times the slab depth and a total length equal to one-third the span length.

c. The Equivalent Column

In the equivalent frame method of analysis, the columns are considered to be attached to the continuous slab beam by torsional members that are transverse to the direction of the span for which moments are being found; the torsional member extends to the panel centerlines bounding each side of the slab beam under study. Torsional deformation of these transverse supporting members reduces the effective flexural stiffness provided by

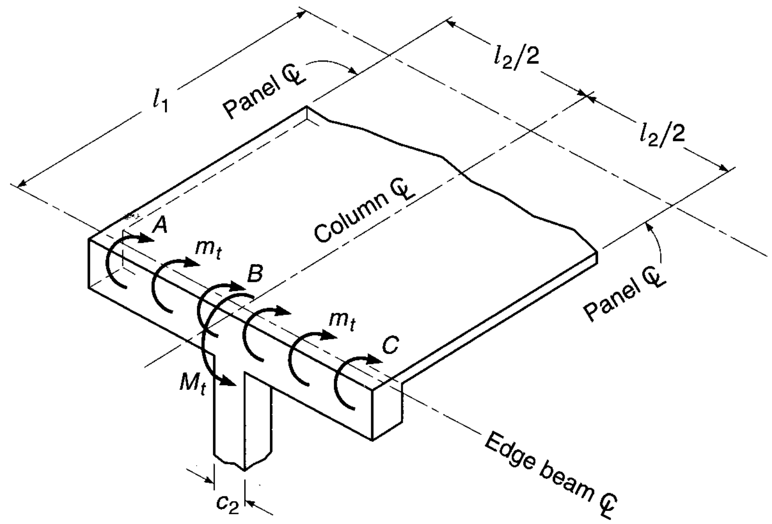

FIGURE 13.18
Torsion at a transverse supporting member illustrating the basis of the equivalent column.

the actual column at the support. This effect is accounted for in the analysis by use of what is termed an *equivalent column* having stiffness less than that of the actual column.

The action of a column and the transverse torsional member is easily explained with reference to Fig. 13.18, which shows, for illustration, the column and transverse beam at the exterior support of a continuous slab-beam strip. From Fig. 13.18, it is clear that the rotational restraint provided at the end of the slab spanning in the direction l_1 is influenced not only by the flexural stiffness of the column but also by the torsional stiffness of the edge beam AC. With distributed torque m_t applied by the slab and resisting torque M_t provided by the column, the edge-beam sections at A and C will rotate to a greater degree than the section at B, owing to torsional deformation of the edge beam. To allow for this effect, the actual column and beam are replaced by an equivalent column, so defined that the total flexibility (inverse of stiffness) of the equivalent column is the sum of the flexibilities of the actual column and beam. Thus,

$$\frac{1}{K_{ec}} = \frac{1}{\Sigma K_c} + \frac{1}{K_t} \tag{13.9}$$

where K_{ec} = flexural stiffness of equivalent column
K_c = flexural stiffness of actual column
K_t = torsional stiffness of edge beam

all expressed in terms of moment per unit rotation. In computing K_c, the moment of inertia of the actual column is assumed to be infinite from the top of the slab to the bottom of the slab beam, and I_g is based on the gross concrete section elsewhere along the length. Stiffness factors for such a case are given in Table A.13*c*.

The effective cross section of the transverse torsional member, which may or may not include a beam web projecting below the slab, as shown in Fig. 13.18, is the same as defined earlier in Section 13.6c. The torsional constant C is calculated by Eq. (13.6) based on the effective cross section so determined. The torsional stiffness K_t can then be calculated by the expression

$$K_t = \sum \frac{9E_{cs}C}{l_2(1 - c_2/l_2)^3} \tag{13.10}$$

where E_{cs} = modulus of elasticity of slab concrete
c_2 = size of rectangular column, capital, or bracket in direction l_2
C = cross-sectional constant [see Eq. (13.6)]

The summation applies to the typical case in which there are slab beams (with or without edge beams) on both sides of the column. The length l_2 is measured center to center of the supports and thus may have different values in each of the summation terms in Eq. (13.10), if the transverse spans are unequal.

If a panel contains a beam parallel to the direction in which moments are being determined, the value of K_t obtained from Eq. (13.10) leads to values of K_{ec} that are too low. Accordingly, in such cases, the value of K_t found by Eq. (13.10) should be multiplied by the ratio of the moment of inertia of the slab with such a beam to the moment of inertia of the slab without it.

The concept of the equivalent column, illustrated with respect to an exterior column, is employed at *all* supporting columns for each continuous slab beam, according to the equivalent frame method.

d. Moment Analysis

With the effective stiffness of the slab-beam strip and the supports found as described, the analysis of the equivalent frame can proceed by moment distribution (see Chapter 12).

In keeping with the requirements of statics (see Section 13.5), equivalent beam strips in each direction must each carry 100 percent of the load. If the unfactored live load does not exceed three-quarters of the unfactored dead load, maximum moment may be assumed to occur at all critical sections when the full factored live load (plus factored dead load) is on the entire slab, according to ACI Code 13.7.6. Otherwise pattern loadings must be used to maximize positive and negative moments. Maximum positive moment is calculated with three-quarters factored live load on the panel and on alternate panels, while maximum negative moment at a support is calculated with three-quarters factored live load on the adjacent panels only. Use of three-quarters live load rather than the full value recognizes that maximum positive and negative moments cannot occur simultaneously (since they are found from different loadings) and that redistribution of moments to less highly stressed sections will take place before failure of the structure occurs. Factored moments must not be taken less than those corresponding to full factored live load on all panels, however.

Negative moments obtained from that analysis apply at the centerlines of supports. Since the support is not a knife edge but a rather broad band of slab spanning in the transverse direction, some reduction in the negative design moment is proper (see also Section 12.5a). At interior supports, the critical section for negative bending, in both column and middle strips, may be taken at the face of the supporting column or capital, but in no case at a distance greater than $0.175l_1$ from the center of the column, according to ACI Code 13.7.7. To avoid excessive reduction of negative moment at the exterior supports (where the distance to the point of inflection is small) for the case where columns are provided with capitals, the critical section for negative bending in the direction perpendicular to an edge should be taken at a distance from the face of support not greater than one-half the projection of the capital beyond the face of the support.

With positive and negative design moments obtained as just described, it still remains to distribute these moments across the widths of the critical sections. For design purposes, the total strip width is divided into column strip and adjacent half-middle strips, defined previously in Section 13.5, and moments are assumed constant within the bounds of each. The distribution of moments to column and middle strips is done using the same percentages given in connection with the direct design method. These are summarized in Table 13.4 and by the interpolation charts of Graph A.4 of Appendix A.

The distribution of moments and shears to column-line beams, if present, is in accordance with the procedures of the direct design method also. Restriction 6 of Section 13.6, pertaining to the relative stiffness of column-line beams in the two directions, applies here also if these distribution ratios are used.

EXAMPLE 13.3

Design of flat plate floor by equivalent frame method. An office building is planned using a flat plate floor system with the column layout as shown in Fig. 13.19. No beams, drop panels, or column capitals are permitted. Specified live load is 100 psf, and dead load will include the weight of the slab plus an allowance of 20 psf for finish floor plus suspended loads. The columns will be 18 in. square, and the floor-to-floor height of the structure will be 12 ft. Design the interior panel C, using material strengths f_y = 60,000 psi and f'_c = 4000 psi. Straight-bar reinforcement will be used.

Solution. Minimum thickness h for a flat plate, according to the ACI Code, may be found from Table 13.5.† For the present example, the minimum h for the exterior panel is

$$h = \frac{20.5 \times 12}{30} = 8.20 \text{ in.}$$

FIGURE 13.19
Two-way flat plate floor.

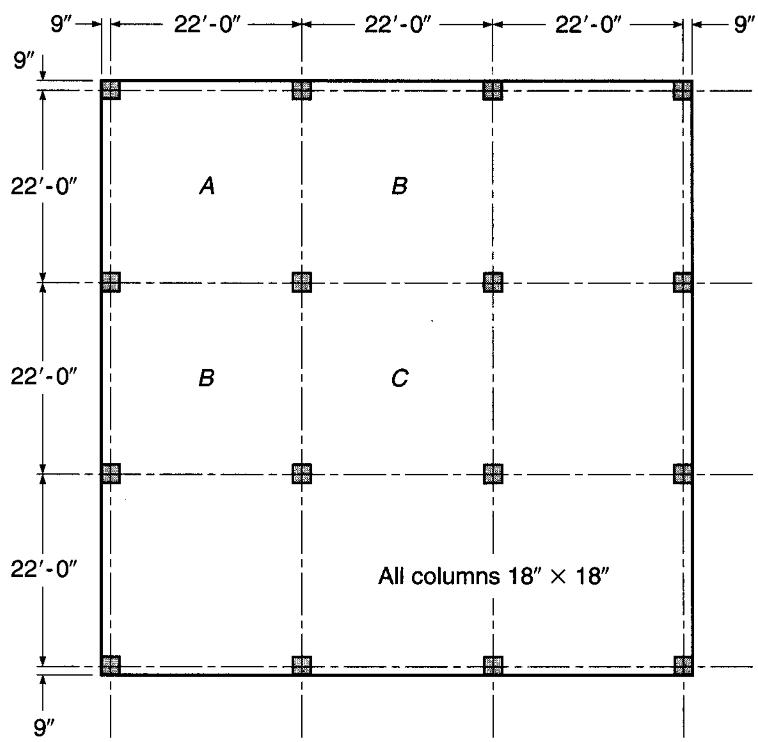

† In many flat plate floors, the minimum slab thickness is controlled by requirements for shear transfer at the supporting columns, and h is determined either to avoid supplementary shear reinforcement or to limit the excess shear to a reasonable margin above that which can be carried by the concrete. Design for shear in flat plates and flat slabs will be treated in Section 13.10.

This will be rounded upward for practical reasons, with calculations based on a trial thickness of 8.5 in. for all panels. Thus the dead load of the slab is $150 \times 8.5/12 = 106$ psf, to which the superimposed dead load of 20 psf must be added. The factored design loads are

$$1.2q_d = 1.2(106 + 20) = 151 \text{ psf}$$

$$1.6q_l = 1.6 \times 100 = 160 \text{ psf}$$

The structure is identical in each direction, permitting the design for one direction to be used for both (an average effective depth to the tensile steel will be used in the calculations). While the restrictions of Section 13.6 are met and the direct design method of analysis is permissible, the equivalent frame method will be adopted to demonstrate its features. Moments will be found by the method of moment distribution.

For flat plate structures, it is usually acceptable to calculate stiffnesses as if all members were prismatic, neglecting the increase in stiffness within the joint region, as it generally has negligible effect on design moments and shears. Then, for the slab spans,

$$K_s = \frac{4E_cI_c}{l}$$

$$= \frac{4E_c(264 \times 8.5^3)}{12 \times 264} = 205E_c$$

and the column stiffnesses are

$$K_c = \frac{4E_c(18 \times 18^3)}{12 \times 144} = 243E_c$$

Calculation of the equivalent column stiffness requires consideration of the torsional deformation of the transverse strip of slab that functions as the supporting beam. Applying the criteria of the ACI Code establishes that the effective torsional member has width 18 in. and depth 8.5 in. For this section, the torsional constant C from Eq. (13.5) is

$$C = \left(1 - 0.63 \times \frac{8.5}{18}\right)8.5^3 \times \frac{18}{3} = 2590 \text{ in}^4$$

and the torsional stiffness, from Eq. (13.10), is

$$K_t = \frac{9E_c \times 2590}{264(1 - 1.5/22)^3} = 109E_c$$

From Eq. (13.9), accounting for two columns and two torsional members at each joint,

$$\frac{1}{K_{ec}} = \frac{1}{2 \times 243E_c} + \frac{1}{2 \times 109E_c}$$

from which $K_{ec} = 151E_c$. Distribution factors at each joint are then calculated in the usual way.

For the present example, the ratio of service live load to dead load is $100/126 = 0.79$, and because this exceeds 0.75, according to ACI Code 13.7.6 maximum positive and negative moments must be found based on pattern loadings, with full factored dead load in place and three-quarters factored live load positioned to cause the maximum effect. In addition, the design moments must not be less than those produced by full factored live and dead loads on all panels. Thus three load cases must be considered: (*a*) full factored dead and live load, 311 psf, on all panels; (*b*) factored dead load of 151 psf on all spans plus three-quarters factored live load, 120 psf, on panel *C*; and (*c*) full factored dead load on all spans and three-quarters live load on first and second spans. Fixed-end moments and final moments obtained from moment distribution are summarized in Table 13.7. The results indicate that load case *a* controls the slab design in the support region, while load case *b* controls at the midspan of panel *C*. Moment diagrams for the two controlling cases are shown in Fig. 13.20*a*. According to the ACI Code the critical section at interior supports may be taken at the face of supports, but not greater than $0.175l_1$ from the column centerline. The former criterion controls here, and the negative design

TABLE 13.7
Moments in flat plate floor, ft-kips

Panel	B		C		B	
Joint	**1**	**2**	**2**	**3**	**3**	**4**
(*a*) 311 psf all panels						
Fixed-end moments	+276	−276	+276	−276	+276	−276
Final moments	+125	−323	+295	−295	+323	−125
Span moment in *C*			119			
(*b*) 151 psf panels *B* and 271 psf panel *C*						
Fixed-end moments	+134	−134	+240	−240	+134	−134
Final moments	+50	−200	+224	−224	+200	−50
Span moment in *C*			137			
(*c*) 271 psf panels *B* (left) and *C* and 151 psf panel *B* (right)						
Fixed-end moments	+240	−240	+240	−240	+134	−134
Final moments	+107	−290	+274	−207	+191	−52
Span moment in *C*			120			

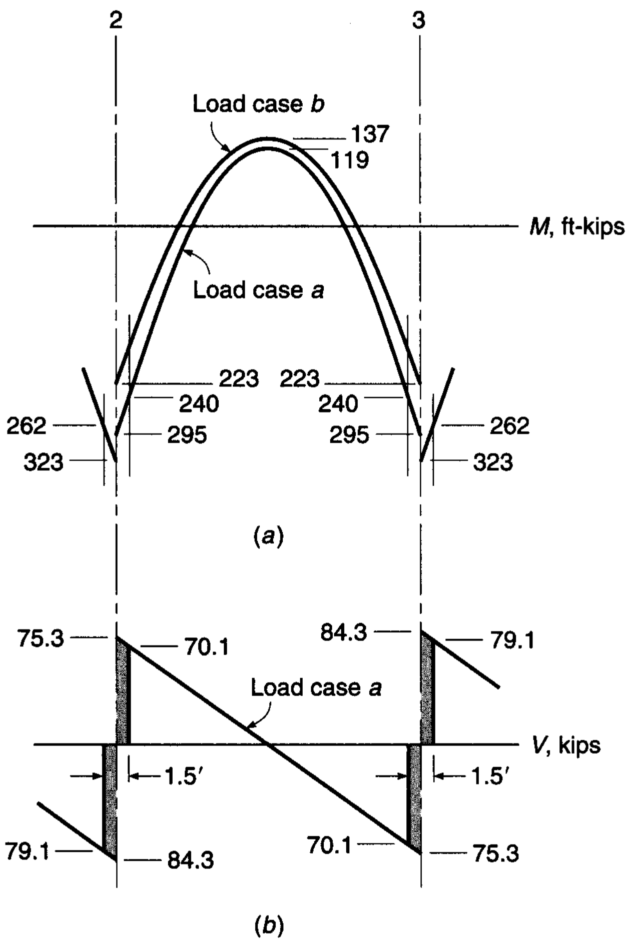

FIGURE 13.20
Design moments and shears for flat plate floor interior panel *C*: (*a*) moments; (*b*) shears.

TABLE 13.8
Design of flat plate reinforcement

(1)	(2) Location	(3) M_u, ft-kips	(4) b, in.	(5) d, in.	(6) $M_u \times 12/b$, ft-kips/ft	(7) ρ	(8) A_s, in^2	(9) Number and Size of Bars
Column strip	Negative	196	132	7	17.82	0.0075	6.65	16 No. 6 (No. 19)
	Positive	82	132	7	7.45	0.0029	2.68	9 No. 5 (No. 16)
Two half-middle strips	Negative	66	132	7	6.00	0.0023	2.13	8 No. 5 (No. 16)[a]
	Positive	55	132	7	5.00	0.0020	1.85	8 No. 5 (No. 16)[a]

[a] Number of bars controlled by maximum spacing requirement.

moment is calculated by subtracting the area under the shear diagram between the centerline and face of support, for load case *a*, from the negative moment at the support centerline. The shear diagram for load case *a* is given in Fig. 13.20*b*, with the adjusted design moments shown in Fig. 13.20*a*.

Because the effective depth for all panels will be the same, and because the negative steel for panel *C* will continue through the support region to become the negative steel for panels *B*, the larger negative moment found for the panels *B* will control. Accordingly, the design negative moment is 262 ft-kips and the design positive moment is 137 ft-kips.†

Moments will be distributed laterally across the slab width according to Table 13.4, which indicates that 75 percent of the negative moment will be assigned to the column strip and 60 percent of the positive moment assigned to the column strip. The design of the slab reinforcement is summarized in Table 13.8.

Other important aspects of the design of flat plates include design for punching shear at the columns, which may require supplementary shear reinforcement, and transfer of unbalanced moments to the columns, which may require additional flexural bars in the negative bending region of the column strips or adjustment of spacing of negative steel. These considerations are of special importance at exterior columns and corner columns, such as shown in Fig. 13.19. Shear and moment transfer at the columns will be discussed in Sections 13.10 and 13.11, respectively.

e. Equivalent Frame Analysis by Computer

It is clear that the equivalent frame method, as described in the ACI Code and the ACI Code Commentary, is oriented toward analysis using the method of moment distribution. Presently, most offices make use of computers, and frame analysis is done using general-purpose programs based on the direct stiffness method. Plane frame analysis programs can be used for slab analysis based on the concepts of the equivalent frame method, but the frame must be specially modeled. Variable moments of inertia along the axis of slab-beams and columns require nodal points (continuous joints) between sections where I is to be considered constant (i.e., in the slab at the junction of slab and drop panel, drop panel and capital, and in the

† When slab systems that meet the restrictions of the direct design method are designed by the equivalent frame method, according to ACI Code 13.7.7 the resulting design moments may be reduced proportionately so that the sum of the positive and average negative moments in a span is no greater than M_o calculated for the direct design method according to Eq. (13.1). There is no theoretical basis for this. The reduction is less than 5 percent in the present example, and it will not be included in the design calculations.

columns at the bottom of the capitals). In addition, it is necessary to compute K_{ec} for each column and then to compute the equivalent value of the moment of inertia for the column.

Alternately, a three-dimensional frame analysis may be used, in which the torsional properties of the transverse supporting beams may be included directly. A third option is to make use of specially written computer programs, the most widely used being pcaSlab, developed by the Portland Cement Association (Skokie, Illinois).

13.10 SHEAR DESIGN IN FLAT PLATES AND FLAT SLABS

When two-way slabs are supported directly by columns, as in flat slabs and flat plates, or when slabs carry concentrated loads, as in footings, shear near the columns is of critical importance. Tests of flat plate structures indicate that, in most practical cases, the capacity is governed by shear (Ref. 13.15).

a. Slabs without Special Shear Reinforcement

Two kinds of shear may be critical in the design of flat slabs, flat plates, or footings. The first is the familiar beam-type shear leading to diagonal tension failure. Applicable particularly to long narrow slabs or footings, this analysis considers the slab to act as a wide beam, spanning between supports provided by the perpendicular column strips. A potential diagonal crack extends in a plane across the entire width l_2 of the slab. The critical section is taken a distance d from the face of the column or capital. As for beams, the design shear strength ϕV_c must be at least equal to the required strength V_u at factored loads. The nominal shear strength V_c should be calculated by either Eq. (4.12a) or Eq. (4.12b), with b_w equal to the panel width l_2 in this case.

Alternatively, failure may occur by *punching shear*, with the potential diagonal crack following the surface of a truncated cone or pyramid around the column, capital, or drop panel, as shown in Fig. 13.21a. The failure surface extends from the bottom of the slab, at the support, diagonally upward to the top surface. The angle of inclination with the horizontal θ (see Fig. 13.21b) depends upon the nature and amount of reinforcement in the slab. It may range between about 20 and 45°. The

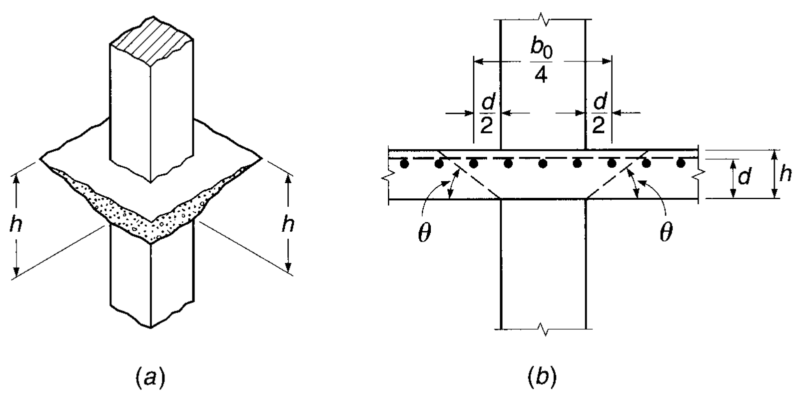

FIGURE 13.21
Failure surface defined by punching shear.

critical section for shear is taken perpendicular to the plane of the slab and a distance $d/2$ from the periphery of the support, as shown. The shear force V_u to be resisted can be calculated as the total factored load on the area bounded by panel centerlines around the column less the load applied within the area defined by the critical shear perimeter, unless significant moments must be transferred from the slab to the column (see Section 13.11).

At such a section, in addition to the shearing stresses and horizontal compressive stresses due to negative bending moment, vertical or somewhat inclined compressive stress is present, owing to the reaction of the column. The simultaneous presence of vertical and horizontal compression increases the shear strength of the concrete. For slabs supported by columns having a ratio of long to short sides not greater than 2, tests indicate that the nominal shear strength may be taken equal to

$$V_c = 4\lambda\sqrt{f'_c}b_o d \tag{13.11a}$$

according to ACI Code 11.11.2, where b_o = the perimeter along the critical section, and λ is the lightweight concrete factor (see Section 4.5*a*).

However, for slabs supported by very rectangular columns, the shear strength predicted by Eq. (13.11*a*) has been found to be unconservative. According to tests reported in Ref. 13.16, the value of V_c approaches $2\lambda\sqrt{f'_c}b_o d$ as β, the ratio of long to short sides of the column, becomes very large. Reflecting these test data, ACI Code 11.11.2 states further that V_c in punching shear shall not be taken greater than

$$V_c = \left(2 + \frac{4}{\beta}\right)\lambda\sqrt{f'_c}b_o d \tag{13.11b}$$

The variation of the shear strength coefficient, as governed by Eqs. (13.11*a*) and (13.11*b*), is shown in Fig. 13.22 as a function of β.

Further tests, reported in Ref. 13.17, have shown that the shear strength V_c decreases as the ratio of critical perimeter to slab depth b_o/d increases. Accordingly, ACI Code 11.11.2 states that V_c in punching shear must not be taken greater than

$$V_c = \left(\frac{\alpha_s d}{b_o} + 2\right)\lambda\sqrt{f'_c}b_o d \tag{13.11c}$$

where α_s is 40 for interior columns, 30 for edge columns, and 20 for corner columns, i.e., columns having critical sections with 4, 3, or 2 sides, respectively.

FIGURE 13.22
Shear strength coefficient for flat plates as a function of ratio β of long side to short side of support.

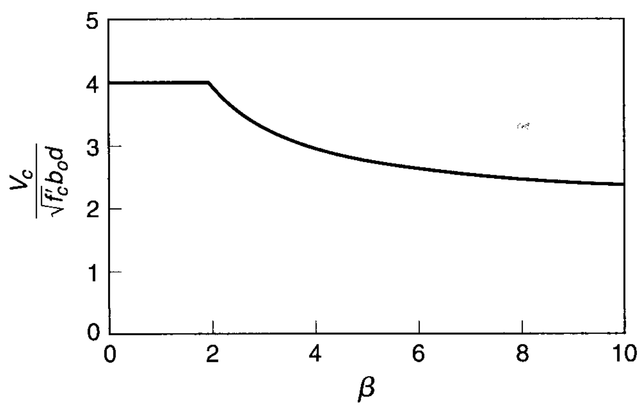

FIGURE 13.23
Punching shear for columns of irregular shape.

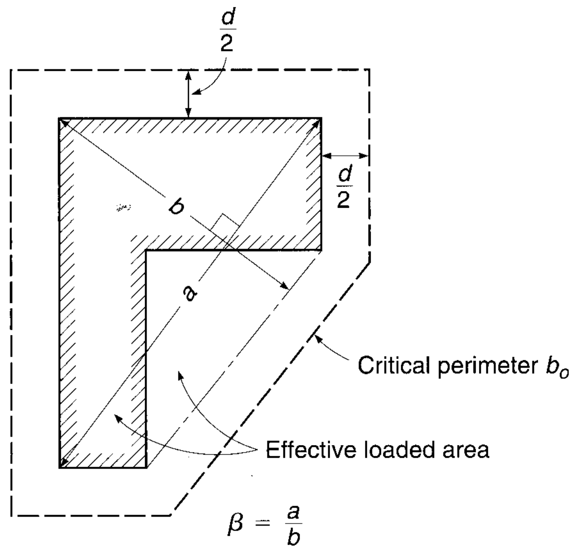

Thus, according to the ACI Code, the punching shear strength of slabs and footings is to be taken as the smallest of the values of V_c given by Eqs. (13.11*a*), (13.11*b*), and (13.11*c*). The design strength is taken as ϕV_c as usual, where $\phi = 0.75$ for shear. The basic requirement is then $V_u \leq \phi V_c$.

For columns with nonrectangular cross sections the ACI Code indicates that the perimeter b_o must be of minimum length, but need not approach closer than $d/2$ to the perimeter of the reaction area. The manner of defining the critical perimeter b_o and the ratio β for such irregular support configurations is illustrated in Fig. 13.23.

b. Types of Shear Reinforcement

Special shear reinforcement is often used at the supports for flat plates, and sometimes for flat slabs as well. It may take several forms. A few common types are shown in Fig. 13.24.

The *shearheads* shown in Fig. 13.24*a* and *c* consist of standard structural steel shapes embedded in the slab and projecting beyond the column. They serve to increase the effective perimeter b_o of the critical section for shear. In addition, they may contribute to the negative bending resistance of the slab. The reinforcement shown in Fig. 13.24*a* is particularly suited for use with concrete columns. It consists of short lengths of I or wide-flange beams, cut and welded at the crossing point so that the arms are continuous through the column. Normal negative slab reinforcement passes over the top of the structural steel, while bottom bars are stopped short of the shearhead. Column bars pass vertically at the corners of the column. The effectiveness of this type of shearhead has been documented by tests by Corley and Hawkins (Ref. 13.18). The channel frame in Fig. 13.24*c* is very similar in its action, but is adapted for use with steel columns. The bent-bar arrangement in Fig. 13.24*b* is suited for use with concrete columns. The bars are usually bent at 45° across the potential diagonal tension crack, and extend along the bottom of the slab a distance sufficient to develop their strength by bond. The flanged collar in Fig. 13.24*d* is designed mainly for use with lift-slab construction (see Chapter 18). It consists of a flat bottom plate with vertical stiffening ribs. It may incorporate sockets for lifting rods, and usually is

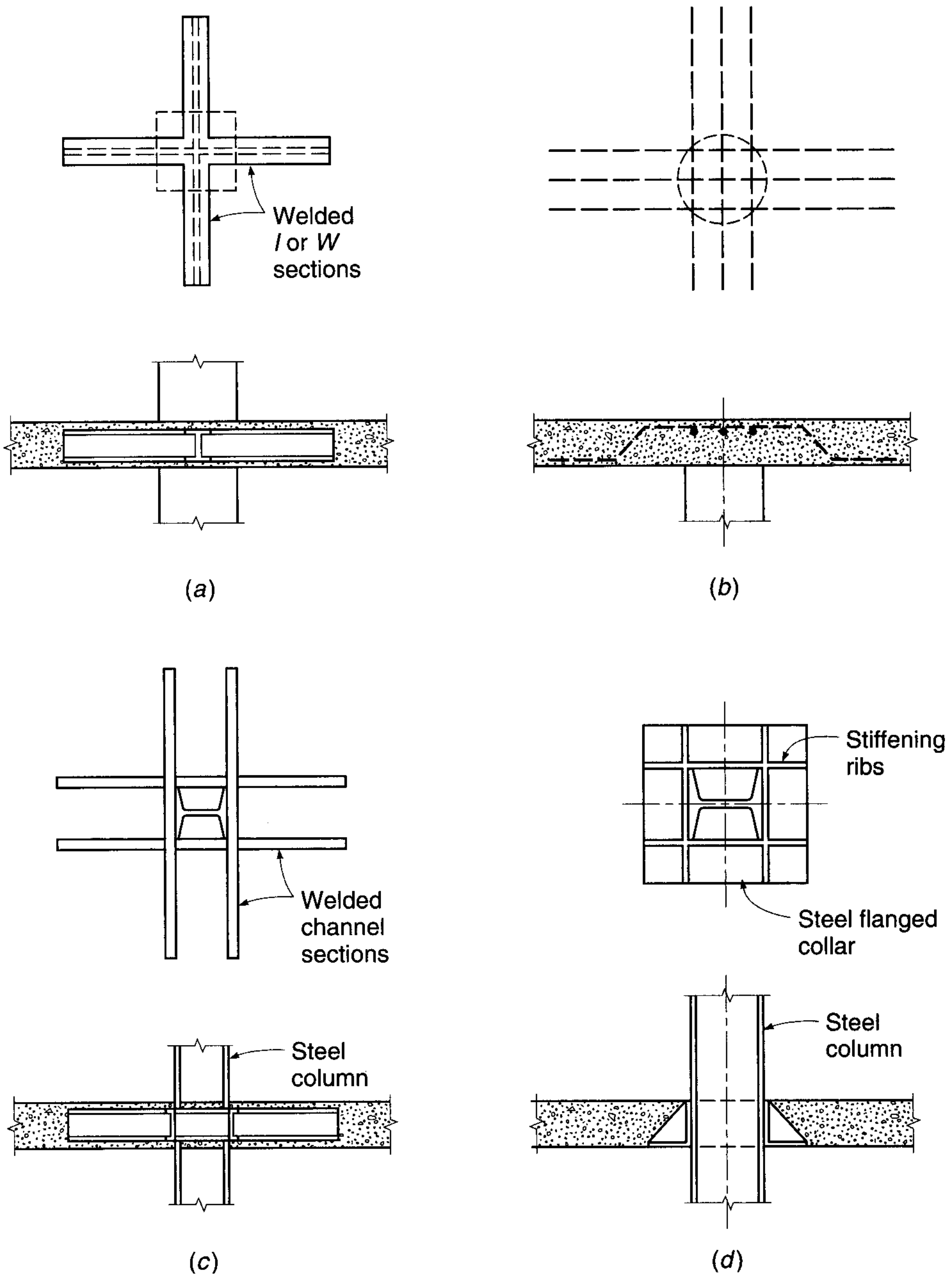

FIGURE 13.24
Shear reinforcement for flat plates (*continued on next page*).

used in conjunction with shear pads welded directly to the column surfaces below the collar to transfer the vertical reaction.

Another type of shear reinforcement is illustrated in Fig. 13.24*e*, where vertical stirrups have been used in conjunction with supplementary horizontal bars radiating outward in two perpendicular directions from the support, to form what are termed *integral beams* contained entirely within the slab thickness. These beams act in the same general way as the shearheads shown in Fig. 13.24*a* and *c*. Adequate anchorage of the stirrups is difficult in slabs thinner than about 10 in. ACI Code 11.11.3 requires the slab effective depth d to be at least 6 in., but not less than 16 times the diameter of

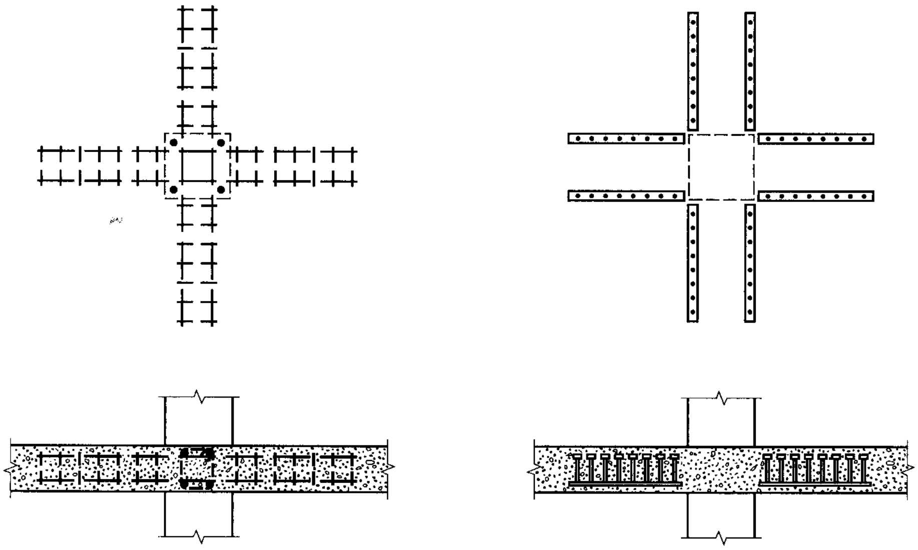

FIGURE 13.24
(continued)

(*e*) (*f*)

the shear reinforcement. In all cases, closed hoop stirrups should be used, with a large-diameter horizontal bar at each bend point, and the stirrups must be terminated with a standard hook (Ref. 13.19).

Headed shear stud reinforcement, shown in Fig. 13.24*f*, is governed by ACI Code 11.11.5. This consists of large-head studs welded to steel strips. The strips are supported on wire chairs during construction to maintain the required concrete cover to the bottom of the slab below the strip, and the usual cover is maintained over the top of the head. Because of the positive anchorage provided by the stud head and the steel strip, these devices are more effective, according to tests, than either the bent-bar or integral beam reinforcement (Refs. 13.20 and 13.21). In addition, they can be placed more easily, with less interference with other reinforcement, than other types of shear steel.

c. Design of Bent-Bar Reinforcement

If shear reinforcement in the form of bars is used (Fig. 13.24*b*), the limit value of nominal shear strength V_n, calculated at the critical section $d/2$ from the support face, may be increased to $6\sqrt{f_c'}\,b_o d$ according to ACI Code 11.11.3. The shear resistance of the concrete V_c is reduced to $2\lambda\sqrt{f_c'}\,b_o d$, and reinforcement must provide for the excess shear above ϕV_c. The total bar area A_v crossing the critical section at slope angle α is easily obtained by equating the vertical component of the steel force to the excess shear force to be accommodated:

$$\phi A_v f_y \sin\alpha = V_u - \phi V_c$$

Where inclined shear reinforcement is all bent at the same distance from a support, $V_s = A_v f_y \sin\alpha$ is not to exceed $3\sqrt{f_c'}\,b_o d$, according to ACI Code 11.4.7. The required area of reinforcement for shear is found by transposing the preceding equation:

$$A_v = \frac{V_u - \phi V_c}{\phi f_y \sin\alpha} \tag{13.12}$$

Successive sections at increasing distances from the support must be investigated and reinforcement provided where V_u exceeds ϕV_c as given by Eq. (13.11).† Only the center three-quarters of the inclined portion of the bent bars can be considered effective in resisting shear, and full development length must be provided past the location of peak stress in the steel, which is assumed to be at slab middepth $d/2$.

EXAMPLE 13.4 **Design of bar reinforcement for punching shear.** A flat plate floor has thickness $h = 7\frac{1}{2}$ in. and is supported by 18 in. square columns spaced 20 ft on centers each way. The floor will carry a total factored load of 300 psf. Check the adequacy of the slab in resisting punching shear at a typical interior column, and provide shear reinforcement, if needed, using bent bars similar to Fig. 13.24*b*. An average effective depth $d = 6$ in. may be used. Material strengths are $f_y = 60{,}000$ psi and $f'_c = 4000$ psi.

Solution. The first critical section for punching shear is a distance $d/2 = 3$ in. from the column face, providing a shear perimeter $b_o = 24 \times 4 = 96$ in. Based on the tributary area of loaded floor, the factored shear is

$$V_u = 300(20^2 - 2^2) = 118{,}800 \text{ lb}$$

and if no shear reinforcement is used, the design strength of the slab, controlled by Eq. (13.11*a*), is

$$\phi V_c = 0.75 \times 4\sqrt{4000} \times 96 \times 6 = 109{,}300 \text{ lb}$$

confirming that shear reinforcement is required. Bars bent at 45° will be used in two directions, as shown in Fig. 13.25. When shear strength is provided by a combination of reinforcement and concrete, the concrete contribution is reduced to

$$\phi V_c = 0.75 \times 2\sqrt{4000} \times 96 \times 6 = 54{,}600 \text{ lb}$$

and so the shear V_s to be resisted by the reinforcement is

$$V_s = \frac{V_u - \phi V_c}{\phi} = \frac{118{,}800 - 54{,}600}{0.75} = 85{,}600 \text{ lb}$$

This is below the maximum permissible value of $3\sqrt{4000} \times 96 \times 6 = 109{,}300$ lb. The required bar area is then found from Eq. (13.12) to be

$$A_v = \frac{85{,}600}{60{,}000 \times 0.707} = 2.02 \text{ in}^2$$

A total of four bars will be used (two in each direction), and with eight legs crossing the critical section, the necessary area per bar is $2.02/8 = 0.25$ in^2. No. 5 (No. 16) bars will be used as shown in Fig. 13.25. The upper limit of $V_n = 6\sqrt{f'_c}\, b_o d$ is automatically satisfied in this case, given the more stringent limit on V_s.

† ACI Code 11.11.3 and ACI Commentary 11.11.3 are ambiguous regarding the value of V_c to be used for flat plate slabs beyond the region where shear reinforcement is required. In general, for slabs where shear reinforcement is not required, V_c is calculated from Eqs. (13.11*a*) to (13.11*c*), with V_c in most cases equal to $4\lambda\sqrt{f'_c}\, b_o d$. When shear reinforcement is provided, the limiting shear may be increased to a maximum of $6\sqrt{f'_c} b_o d$; however, the shear reinforcement must be designed to carry all shear in excess of ϕV_c with $V_c = 2\lambda\sqrt{f'_c}\, b_o d$. This seems to imply that the reduction in V_c to one-half its normal value applies only where there is a sharing of the force between concrete and steel reinforcement and that, in the region where shear reinforcement is *not* required, the full concrete contribution of $4\lambda\sqrt{f'_c}\, b_o d$ can be used. The examples that follow have been prepared on that basis. The alternative interpretation is that if shear reinforcement is required at the column, then the concrete contribution is reduced to $2\lambda\sqrt{f'_c}\, b_o d$ throughout the slab. This more conservative interpretation could be adopted in many cases without significant cost increase, because of the rapid increase in V_c with increasing distance from the column resulting from the increase in concrete shear perimeter b_o, as well as the reduction in net shear force V_u.

FIGURE 13.25
Bar reinforcement for punching shear in flat plate slab.

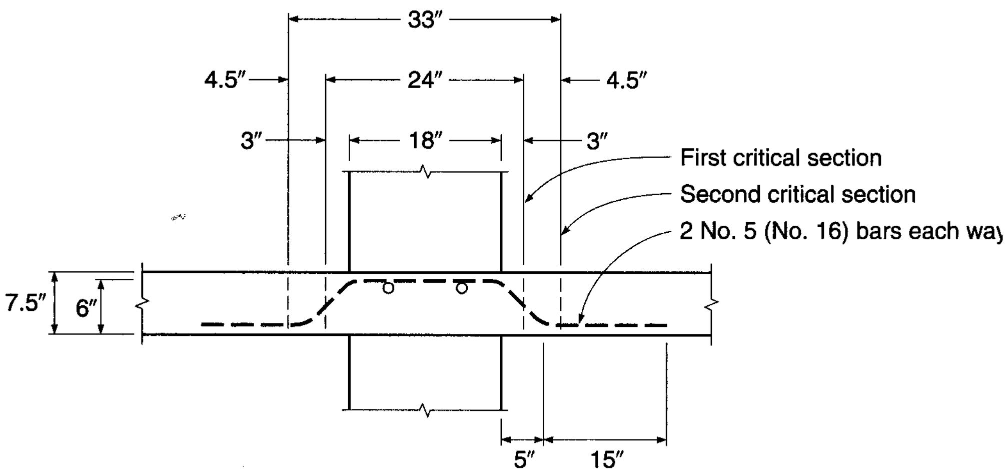

With bars bent at 45° and effective through the center three-fourths of the inclined length, the next critical section is approximately $\frac{3}{4}$ times the effective depth, or 4.5 in., past the first, as shown, giving a shear perimeter of $33 \times 4 = 132$ in. The factored shear at that critical section is

$$V_u = 300(20^2 - 2.75^2) = 117{,}700 \text{ lb}$$

and the design capacity of the concrete is

$$\phi V_c = 0.75 \times 4 \times 1\sqrt{4000} \times 132 \times 6 = 150{,}300 \text{ lb}$$

confirming that no additional bent bars are needed. The No. 5 (No. 16) bars will be extended along the bottom of the slab the full development length of 15 in., as shown in Fig. 13.25.

d. Design of Integral Beams with Vertical Stirrups

The bent-bar shear reinforcement cages of Section 13.10c may lead to troublesome congestion of reinforcement in the column-slab joint region. Shear reinforcement using vertical stirrups in *integral beams,* as shown in Fig. 13.24*e,* avoids much of this difficulty.

The first critical section for shear design in the slab is taken at $d/2$ from the column face, as usual, and the stirrups, if needed, are extended outward from the column in four directions for the typical interior case (three or two directions for exterior or corner columns, respectively), until the concrete alone can carry the shear, with $V_c = 4\lambda\sqrt{f'_c}b_o d$ at the second critical section.† Within the region adjacent to the column, where shear resistance is provided by a combination of concrete and steel, the nominal shear strength V_n must not exceed $6\sqrt{f'_c}b_o d$, according to ACI Code 11.11.3. In this region, the concrete contribution is reduced to $V_c = 2\lambda\sqrt{f'_c}b_o d$. The second critical section crosses each integral beam at a distance $d/2$ measured outward from the last stirrup and is located so that its perimeter b_o is a minimum (i.e., for the typical case, defined by 45° lines between the integral beams). The required spacing of the vertical stirrups s is found using Eq. (4.14*a*), but must not exceed $d/2$, with the first

† Neither the ACI Code nor the ACI Commentary makes clear whether Eqs. (13.11*b*) and (13.11*c*) are to be applied at successive critical sections past the first, immediately adjacent to the column. The research on which these equations were based considered only the first critical section at the column. Except in extreme cases, the aspect ratio of the column, in Eq. (13.11*b*), seems less relevant with increasing distance from the column; however, the b_o/d ratio, in Eq. (13.11*c*), may be influential, and that equation might conservatively be applied.

line of stirrups not more than $d/2$ from the column face. The spacing of the stirrup legs (measured parallel to the face of the column) in the first line of shear reinforcement must not exceed $2d$.

The problem of anchorage of the shear reinforcement in shallow flat plates is critical, and closed hoop stirrups, terminating in standard hooks, always should be provided with interior corner bars to improve pullout resistance.

EXAMPLE 13.5

Design of an integral beam with vertical stirrups. The flat plate slab with 7.5 in. total thickness and 6 in. effective depth shown in Fig. 13.26 is carried by 12 in. square columns 15 ft on centers in each direction. A factored load of 120 kips must be transmitted from the slab to a typical interior column. Concrete and steel strengths used are, respectively, $f'_c = 4000$ psi and $f_y = 60{,}000$ psi. Determine if shear reinforcement is required for the slab; and if so, design integral beams with stirrups to carry the excess shear.

Solution. The design shear strength of the concrete alone at the critical section $d/2$ from the face of the column, by the controlling Eq. (13.11*a*), is

$$\phi V_c = 0.75 \times 4 \times 1\sqrt{4000} \times 72 \times 6 = 82.0 \text{ kips}$$

This is less than $V_u = 120$ kips, indicating that shear reinforcement is required. The effective depth $d = 6$ in. just satisfies the minimum allowed to use stirrup reinforcement, as described in Section 13.10b. In this case, the maximum design strength allowed by the ACI Code is

$$\phi V_n = 0.75 \times 6\sqrt{4000} \times 72 \times 6 = 122.9 \text{ kips}$$

FIGURE 13.26
Vertical stirrup shear reinforcement for slab in Example 13.5.

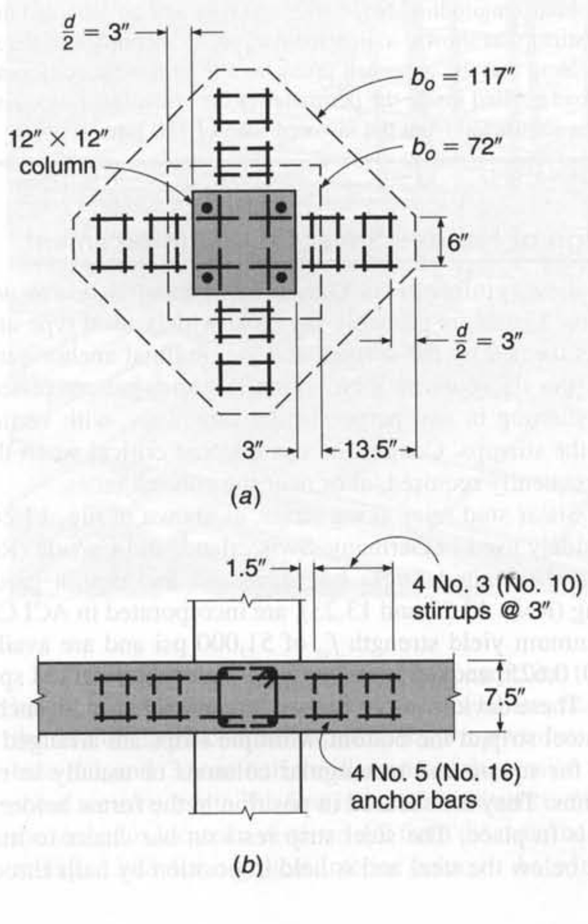

satisfactorily above the actual V_u. When shear is resisted by combined action of concrete and bar reinforcement, the concrete contribution is reduced to

$$\phi V_c = 0.75 \times 2\sqrt{4000} \times 72 \times 6 = 41.0 \text{ kips}$$

The No. 3 (No. 10) vertical closed hoop stirrups will be used since d must be $\geq$ 16 times the stirrup diameter ($d/16 = \frac{3}{8}$ in.) and arranged along four integral beams as shown in Fig. 13.26. Thus, the A_v provided is $4 \times 2 \times 0.11 = 0.88$ in^2 at the first critical section, a distance $d/2$ from the column face, and the required spacing can be found from Eq. (4.14a):

$$s = \frac{\phi A_v f_y d}{V_u - \phi V_c} = \frac{0.75 \times 0.88 \times 60 \times 6}{120 - 41.0} = 3.01 \text{ in.}$$

However, the maximum spacing of $d/2 = 3$ in. controls here, and No. 3 (No. 10) stirrups at a constant spacing of 3 in. will be used. In other cases, stirrup spacing might be increased with distance from the column, as excess shear is less, although this would complicate placement of the reinforcement and generally save little steel.

The required perimeter of the second critical section, at which the concrete alone can carry the shear, is found from the controlling Eq. (13.11a) as follows:

$$\phi V_c = 0.75 \times 4\sqrt{4000} \times b_o \times 6 = 120{,}000 \text{ lb}$$

from which the minimum perimeter $b_o = 105.4$ in. Using this value of b_o in Eq. (13.11e) gives $\phi V_c = 121{,}500$ lb; thus, Eq. (13.11a) governs. It is easily confirmed that $b_o = 105.4$ in. requires a minimum projection of the critical section past the face of the column of 11.39 in. Four stirrups at a constant 3 in. spacing will be sufficient, the first placed at $s/2 = 1.5$ in. $\leq d/2 = 3$ in. from the column face, as indicated in Fig. 13.26. This provides a perimeter b_o at the second critical section of $(16.5\sqrt{2} + 6) \times 4 = 117$ in., exceeding the requirement.

Four longitudinal No. 5 (No. 16) bars will be provided inside the corners of each closed hoop stirrup, as shown, to provide for proper anchorage of the shear reinforcement.

Note that the approach taken here is somewhat conservative because the portion of the slab load applied inside the perimeter of the critical section does not act on that section and can thus be subtracted from the factored load of 120 kips.

e. Design of Headed Shear Stud Reinforcement

Slab shear reinforcement consisting of integral beams with stirrups, as described in Section 13.10d, is probably the most widely used type at present. However, the cage that is formed by the stirrups and longitudinal anchor bars may be difficult to install. Also, the slab-column joint region is somewhat congested, with top and bottom slab steel running in two perpendicular directions, with vertical bars in the column, and with the stirrups. Congestion can become critical when the slab has openings, which are frequently required, at or near the column faces.

Shear stud reinforcing strips, as shown in Fig. 13.24f and in Fig. 13.27a and b, are widely used in Germany, Switzerland, and Canada (Refs. 13.20 and 13.21). Their use in the United States has increased and design guidelines, based on extensive testing (Refs. 13.22 and 13.23), are incorporated in ACI Code 11.11.5. The studs have a minimum yield strength f_{yt} of 51,000 psi and are available in diameters of 0.375, 0.500, 0.625, and 0.750 in., in accordance with ASTM specification A1044.

These devices are composed of vertical bars with anchor heads at their top, welded to a steel strip at the bottom. Multiple strips are arranged in two perpendicular directions for square and rectangular columns or usually in radial directions for circular columns. They are secured in position in the forms before the top and bottom flexural steel is in place. The steel strip rests on bar chairs to maintain the needed concrete cover below the steel and is held in position by nails through holes in the strip.

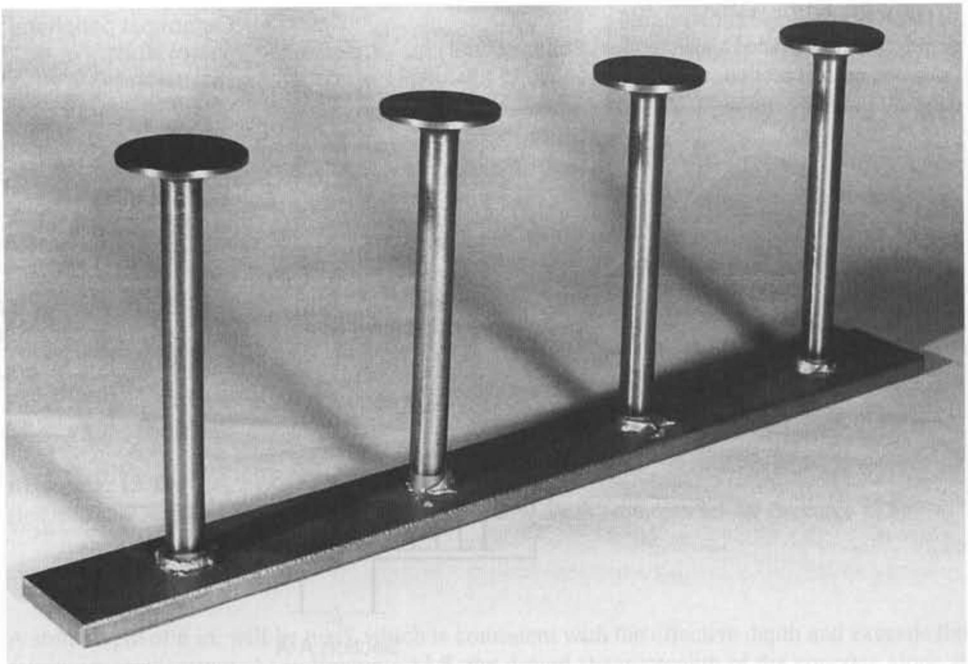

FIGURE 13.27*a*
Shear stud reinforcement for concrete slabs: shear stud assembly. (*Courtesy of Amin Ghali and Walter H. Dilger.*)

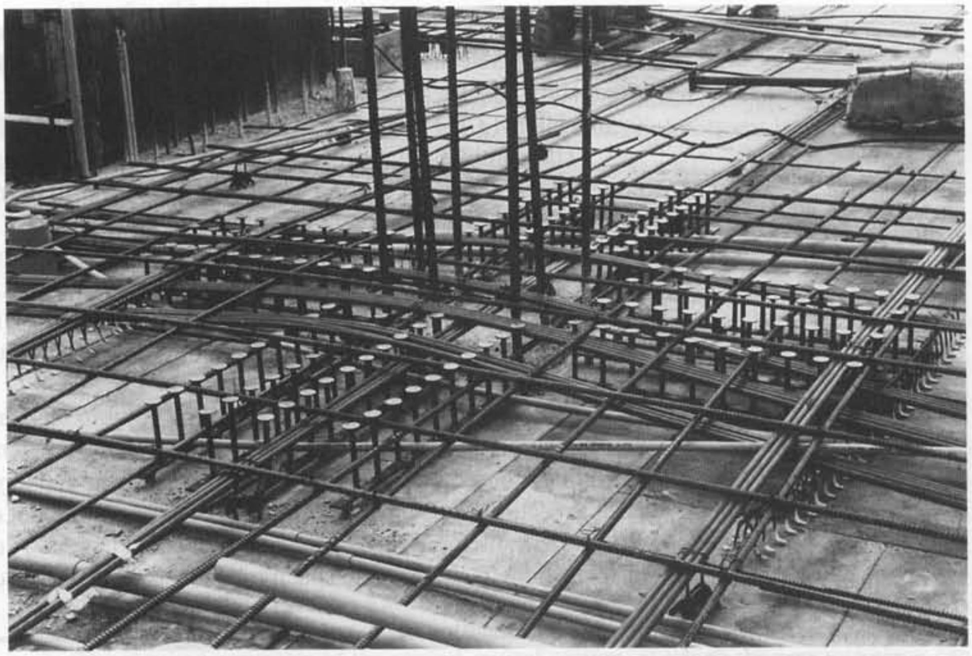

FIGURE 13.27*b*
Shear stud reinforcements for concrete slabs: shear reinforcement installed in forms for prestressed concrete slab. (*Courtesy of Amin Ghali and Walter H. Dilger.*)

Headed shear studs are placed perpendicular to the plane of the slab. The overall height of the shear stud assembly may not be less than the thickness of the member less the sum of (1) the concrete cover over the top reinforcement, (2) the concrete cover on the base rail, and (3) one-half the diameter of the tension flexural reinforcement. Two critical shear sections exist. The first is located a distance $d/2$ from the face of the column, and the second is located a distance $d/2$ from the outermost peripheral line of studs, as shown in Fig. 13.28 for a typical interior column. As with the integral beams with vertical

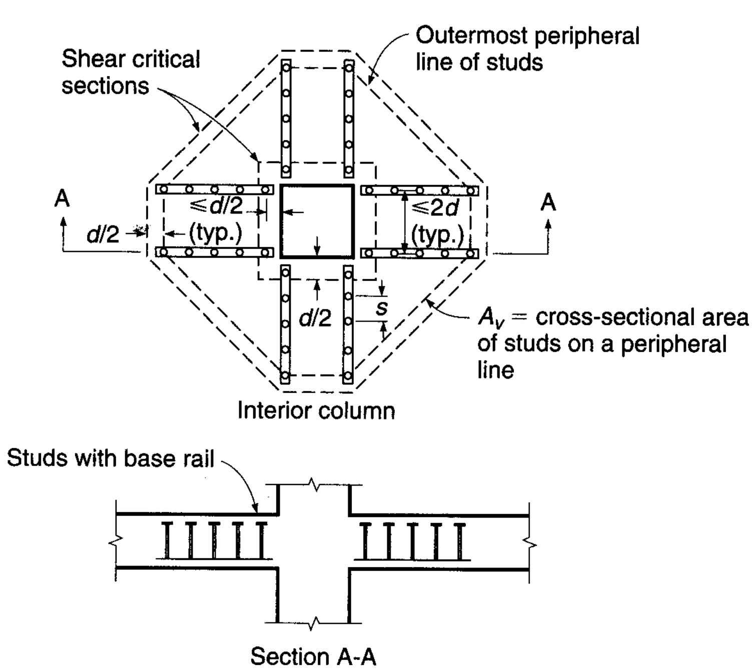

FIGURE 13.28
Arrangement of headed shear studs and critical sections for a typical interior column.

stirrups described in Section 13.10d, the studs are extended outward from the column until the concrete alone can carry the shear; but in the case of slabs reinforced with headed shear studs, the shear stress due to the factored shear force and any unbalanced moment (see Section 13.11) may not exceed $2\phi\lambda\sqrt{f_c'}$ on the second critical section.

The nominal shear capacity of the headed shear stud assembly V_n is the sum of the concrete contribution V_c and the shear stud contribution V_s. In the region adjacent to the column, the concrete contribution V_c is reduced to $3\lambda\sqrt{f_c'}b_od$, and the total nominal capacity V_n may not exceed $8\sqrt{f_c'}b_od$. The shear stud contribution is $A_vf_{yt}d/s$, where A_v is the area of the studs on a peripheral line and s is the spacing between the peripheral lines, as shown in Fig. 13.28. The value of the shear stud contribution, expressed as a stress on the critical section as A_vf_{yt}/b_os, must be at least $2\sqrt{f_c'}$ in accordance with ACI Code 11.11.5.

The spacing of the studs between the column face and the first peripheral line of studs should not exceed $d/2$, and the spacing of the concentric peripheral lines of studs s should be based on the combined effects of shear and any unbalanced moment on the critical section adjacent to the column face and should not exceed $0.75d$ when the shear stress due to factored loads is less than or equal to $6\phi\sqrt{f_c'}$ or $0.5d$ when the shear stress exceeds $6\phi\sqrt{f_c'}$. Lastly, the spacing between the shear stud rails should not exceed $2d$.

EXAMPLE 13.6

Design of headed stud reinforcement. Repeat Example 13.5, using headed stud reinforcement. The No. 5 (No. 16) bars will be used as negative flexural reinforcement. The yield strength is f_{yt} = 51,000 psi for studs.

Solution. The minimum height of the shear stud assembly equals the thickness of the slab less the cover over the rail, the cover over the reinforcement, and one-half the reinforcement bar diameter. Thus, from Fig 13.29*b* the minimum height is

$$7.5 - 0.75 - 0.75 - 0.5 \times 0.625 = 5.68 \text{ in.}$$

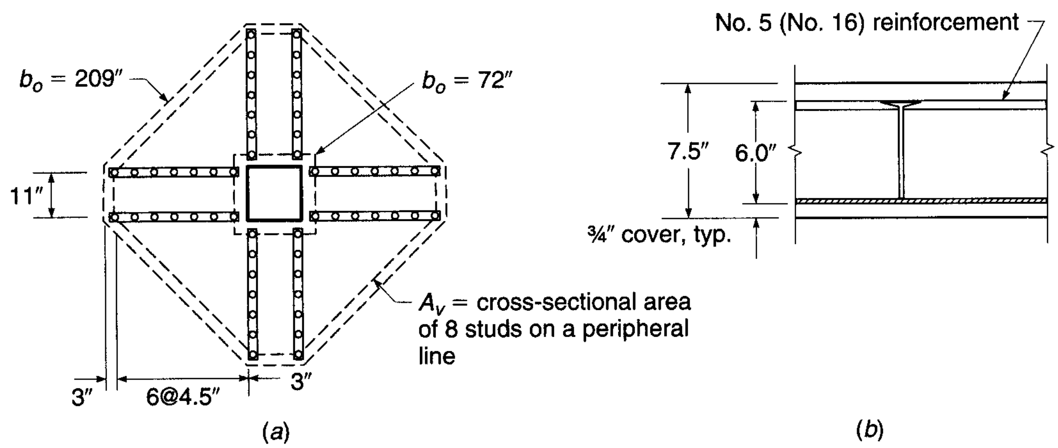

FIGURE 13.29
Headed shear stud arrangement and detail of structural depth requirements for Example 13.6.

A stud height of 6 in. will be used, which is consistent with the effective depth and exceeds the minimum requirement. As in Example 13.5, the design shear strength of the concrete alone at the critical section from the face of the column based on an effective depth of 6 in., by the controlling Eq. (13.11*a*), is

$$\phi V_c = 0.75 \times 4 \times 1\sqrt{4000} \times 72 \times 6 = 82.0 \text{ kips}$$

which is less than $V_u = 120$ kips, indicating that shear reinforcement is required. The maximum design strength allowed by the ACI Code when headed stud reinforcement is used is

$$\phi V_n = 0.75 \times 8\sqrt{4000} \times 72 \times 6 = 163.9 \text{ kips}$$

which is satisfactorily above the actual V_u. The maximum concrete strength allowed by ACI in conjunction with headed shear studs is

$$\phi V_c = 0.75 \times 3 \times 1\sqrt{4000} \times 72 \times 6 = 61.5 \text{ kips}$$

The maximum spacing between the stud rails must be less than $2d$, so two lines of studs are needed for a 12 in. square column; a center-to-center spacing of 11 in. will be used. The shear stress in the slab at the first critical section is approximately $4.4\sqrt{f'_c}$, which is below $\phi 6\sqrt{f'_c} = 4.5\sqrt{f'_c}$, giving a maximum stud spacing of $0.75d$. A spacing of 4.5 in., equal to the maximum, is selected. The area of the studs is found from Eq. (4.14*a*):

$$A_v = \frac{(V_u - \phi V_c)s}{\phi f_{yt} d} = \frac{(120 - 61.5) \times 4.5}{0.75 \times 51 \times 6} = 1.15 \text{ in}^2$$

A peripheral line of studs contains 8 studs, requiring a cross-sectional area of 0.14 in^2 per stud, so 0.500 in. diameter studs with a cross-sectional area of 0.20 in^2 per stud are selected.

The required perimeter of the second critical section, at which the concrete alone can carry the shear, is based on a maximum shear stress of $2\phi\lambda\sqrt{f'_c}$. Thus,

$$\phi V_c = 0.75 \times 2 \times 1\sqrt{4000} \times b_o \times 6 = 120{,}000 \text{ lb}$$

from which the minimum perimeter $b_o = 211$ in. The first stud is placed at $d/2$ or 3 in. from the column face. Six studs at a spacing of 4.5 in. provide a minimum perimeter of 209 in., as shown in Fig. 13.29*a*, which is considered satisfactory since the load applied inside the perimeter of the outer critical section has not been discounted.

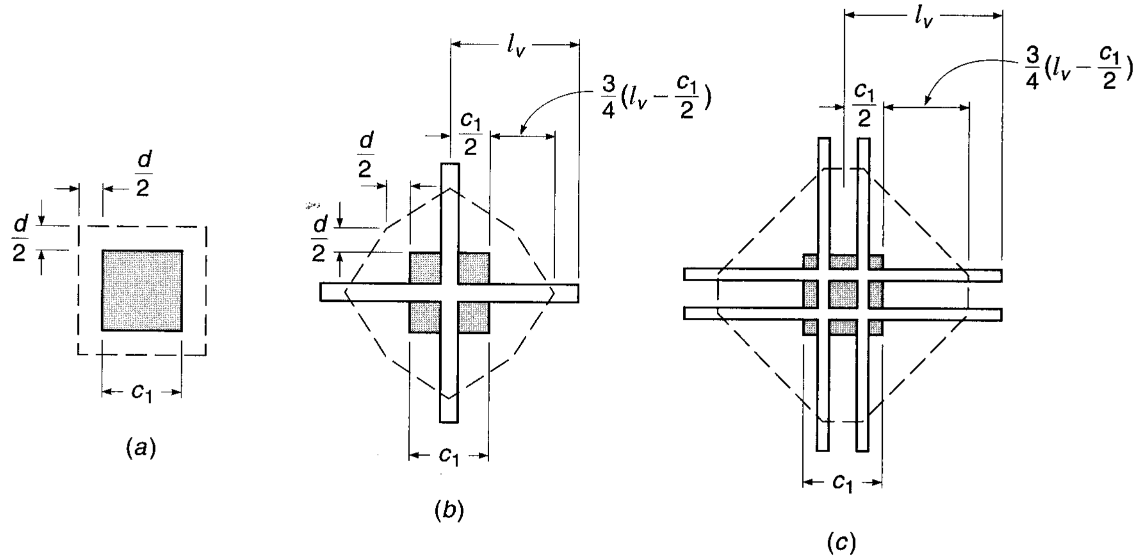

FIGURE 13.30
Critical sections for shear for flat plates: (*a*) no shearhead; (*b*) small shearhead; (*c*) large shearhead.

f. Design of Shearhead Reinforcement

If embedded structural steel shapes are used, as shown in Fig. 13.24*a* and *c*, the limiting value of V_n may be increased to $7\sqrt{f'_c}b_od$. As with the techniques described in Sections 13.10c, d, and e, such a shearhead, provided it is sufficiently stiff and strong, has the effect of moving the critical section out away from the column, as shown in Fig. 13.30. According to ACI Code 11.11.4, this critical section crosses each arm of the shearhead at a distance equal to three-quarters of the projection beyond the face of the support, and is defined so that the perimeter is a minimum. It need not approach closer than $d/2$ to the face of the support.

Moving the critical section out in this way provides the double benefit of increasing the effective perimeter b_o and decreasing the total shear force for which the slab must be designed. The nominal shear V_n at the new critical section must not be taken greater than $4\sqrt{f'_c}b_od$, according to ACI Code 11.11.4.

Tests reported in Ref. 13.18 indicate that throughout most of the length of a shearhead arm the shear is constant, and, further, that the part of the total shear carried by the shearhead arm is proportional to α_v, its relative flexural stiffness, compared with that of the surrounding concrete section:

$$\alpha_v = \frac{E_s I_s}{E_c I_c} \tag{13.13}$$

The concrete section is taken with an effective width of $c_2 + d$, where c_2 is the width of the support measured perpendicular to the arm direction. Properties are calculated for the cracked, transformed section, including the shearhead. The observation that shear is essentially constant, at least up to the diagonal cracking load, implies that the reaction is concentrated largely at the end of the arm. Thus, if the total shear at the support is V and if the shearhead has n identical arms (generally $n = 4$ for shearheads at interior columns), the constant shear force in each arm is equal to $\alpha_v V/n$.

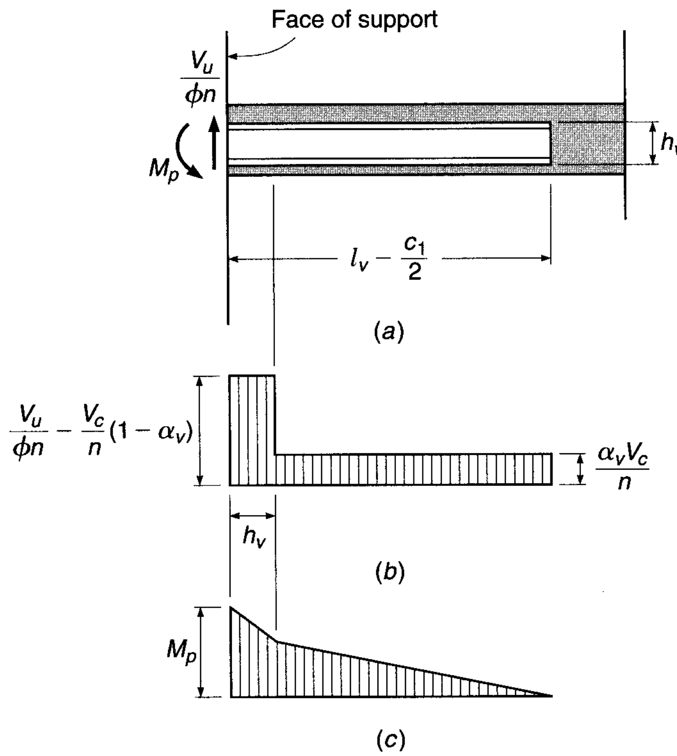

FIGURE 13.31
Stress resultants in shearhead arm: (*a*) shearhead arm; (*b*) shear; (*c*) moment.

If the load is increased past that which causes diagonal cracking immediately around the column, tests indicate that the increased shear above the cracking shear V_c is carried mostly by the steel shearhead, and that the shear force in the projecting arm within a distance from the column face equal to h_v, the depth of the arm, assumes a nearly constant value greater than $\alpha_v V/n$. This increased value is very nearly equal to the total shear per arm $V_u/\phi n$ minus the shear carried by the partially cracked concrete. The latter term is equal to $(V_c/n)(1 - \alpha_v)$; hence, the idealized shear diagram shown in Fig. 13.31*b* is obtained.

The moment diagram of Fig. 13.31*c* is obtained by integration of the shear diagram. If V_c is equal to $V_n/2 = V_u/2\phi$, as tests indicate for shearheads of common proportions, it is easily confirmed that the plastic moment M_p at the face of the support, for which the shearhead arm must be proportioned, is

$$M_p = \frac{V_u}{2\phi n}\left[h_v + \alpha_v\left(l_v - \frac{c_1}{2}\right)\right] \tag{13.14}$$

in which $\phi = 0.90$, the capacity reduction factor for tension-controlled members.

According to ACI Code 11.11.4, the value of α_v must be at least equal to 0.15; more flexible shearheads have proved ineffective. The compression flange must not be more than $0.3d$ from the bottom surface of the slab, and the steel shapes used must not be deeper than 70 times the web thickness.

For flexural design of the slab, moments found at the support centerline by the equivalent frame method are reduced to moments at the support face, assumed to be the critical section for moment. By the direct design method, support-face moments are calculated directly through the use of the clear-span distance. If shearheads are used, they have the effect of reducing the design moment in the column strips still further by increasing the effective support width. This reduction is proportional to the share of the load carried by the shearhead and to its size, and can be estimated conservatively (see Fig. 13.31*b* and *c*) by the expression

$$M_v = \frac{\phi \alpha_v V_u}{2n}\left(l_v - \frac{c_1}{2}\right) \tag{13.15}$$

where $\phi = 0.90$. According to ACI Code 11.11.4, the reduction may not be greater than 30 percent of the total design moment for the slab column strip, or greater than the change in column-strip moment over the distance l_v, or greater than M_p given by Eq. (13.14).

Limited test information pertaining to shearheads at a slab edge indicates that behavior may be substantially different due to torsional and other effects. If shearheads are to be used at an edge or corner column, special attention must be given to anchorage of the embedded steel within the column. The use of edge beams or a cantilevered slab edge may be preferred.

EXAMPLE 13.7 **Design of shearhead reinforcement.** A flat plate slab $7\frac{1}{2}$ in. thick is supported by 10 in. square columns and is reinforced for negative bending with No. 5 (No. 16) bars 5 in. on centers in each direction, with an average effective depth *d* of 6 in. The concrete strength f'_c is 3000 psi. The slab must transfer a factored shear V_u of 107,000 lb to the column. What special slab reinforcement is required, if any, at the column to transfer the factored shear?

Solution. The nominal shear strength at the critical section $d/2$ from the face of the column is found from Eq. (13.11*a*) to be

$$V_c = 4\sqrt{3000} \times 64 \times 6 = 84.1 \text{ kips}$$

and $\phi V_c = 0.75 \times 84.1 = 63.1$ kips. This is less than $V_u = 107$ kips, indicating that shear reinforcement is necessary. A shearhead similar to Fig. 13.24*a* will be used, fabricated from I-beam sections with $f_y = 50$ ksi. Maintaining $\frac{3}{4}$ in. clearance below such steel, bar clearance at the top of the slab permits use of an I beam with a $4\frac{5}{8}$ in. depth; a nominal 4 in. section will be used. With such reinforcement, the upper limit of shear V_n on the critical section is $7\sqrt{3000}\,(64 \times 6) = 147$ kips, and $\phi V_n = 0.75 \times 147 = 110$ kips, above the value of V_u to be resisted. The required perimeter b_o can be found by setting $V_u = \phi V_c$, where V_c is given by Eq. (13.11*a*):

$$b_o = \frac{V_u}{4\phi\sqrt{f'_c}\,d} = \frac{107{,}000}{4 \times 0.75\sqrt{3000} \times 6} = 109 \text{ in.}$$

(Note that the actual shear force to be transferred at the critical section is slightly less than 107 kips because a part of the floor load is within the effective perimeter b_o; however, the difference is small except for very large shearheads.) The required projecting length l_v of the shearhead arm is found from geometry, with b_o expressed in terms of l_v.

$$b_o = 4\sqrt{2}\left[\frac{c_1}{2} + \frac{3}{4}\left(l_v - \frac{c_1}{2}\right)\right] = 109 \text{ in.}$$

from which $l_v = 24.0$ in. To determine the required plastic section modulus for the shear arm, it is necessary to assume a trial value of the relative stiffness α_v. After selecting 0.25 for trial, the required moment capacity is found from Eq. (13.14):

$$M_p = \frac{107{,}000}{8 \times 0.90}[4 + 0.25(24.0 - 5)] = 130{,}000 \text{ in-lb}$$

A standard I beam S4 × 7.7, with yield stress of 50 ksi, provides 176,000 in-lb resistance and will tentatively be adopted. The E_sI_s value provided by the beam is 174×10^6 in^2-lb. The effective

FIGURE 13.32
Effective section of slab.

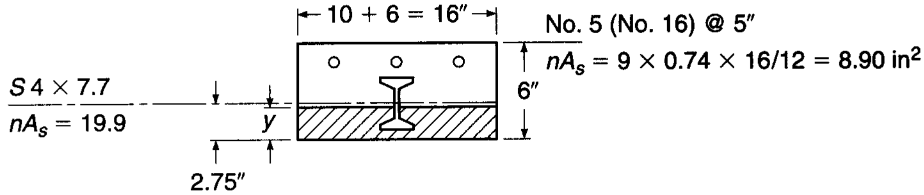

cross section of the slab strip is shown in Fig. 13.32. Taking moments of the composite cracked section about the bottom surface to locate the neutral axis gives

$$y = \frac{8.90 \times 6 + 19.9 \times 2.75 + 8y^2}{8.90 + 19.9 + 16y}$$

from which $y = 2.29$ in. The moment of inertia of the composite section is

$$I_c = \tfrac{1}{3} \times 16 \times 2.29^3 + 8.90 \times 3.71^2 + 6 \times 9 + 19.9 \times 0.46^2 = 244 \text{ in}^4$$

the flexural stiffness of the effective composite slab strip is

$$E_c I_c = 3.1 \times 10^6 \times 244 = 756 \times 10^6 \text{ in}^2\text{-lb}$$

and, from Eq. (13.13),

$$\alpha_v = \frac{174}{756} = 0.23$$

This is greater than the specified minimum of 0.15 and close to the 0.25 value assumed earlier. The revised value of M_p is

$$M_p = \frac{107{,}000}{8 \times 0.90}[4 + 0.23(24.0 - 5)] = 124{,}400 \text{ in-lb}$$

The 4 in. beam is adequate. The calculated length l_v of 24.0 in. will be retained. The reduction in column-strip moment in the slab may be based on this actual length. From Eq. (13.15),

$$M_v = \frac{0.90 \times 0.23 \times 107{,}000}{8}(24 - 5) = 52{,}600 \text{ in-lb}$$

This value is less than M_p, as required by specification, and must also be less than 30 percent of the design negative moment in the column strip and less than the change in the column-strip moment in the distance l_v.

13.11 TRANSFER OF MOMENTS AT COLUMNS

The analysis for punching shear in flat plates and flat slabs presented in Section 13.10 assumed that the shear force V_u was resisted by shearing stresses uniformly distributed around the perimeter b_o of the critical section, a distance $d/2$ from the face of the supporting column. The nominal shear strength V_c was given by Eqs. (13.11*a*), (13.11*b*), and (13.11*c*).

If significant moments are to be transferred from the slab to the columns, as would result from unbalanced gravity loads on either side of a column or from horizontal loading due to wind or seismic effects, the shear stress on the critical section is no longer uniformly distributed.

FIGURE 13.33
Transfer of moment from slab to column: (*a*) forces resulting from vertical load and unbalanced moment; (*b*) critical section for an interior column; (*c*) shear stress distribution for an interior column; (*d*) critical section for an edge column; (*e*) shear stress distribution for an edge column.

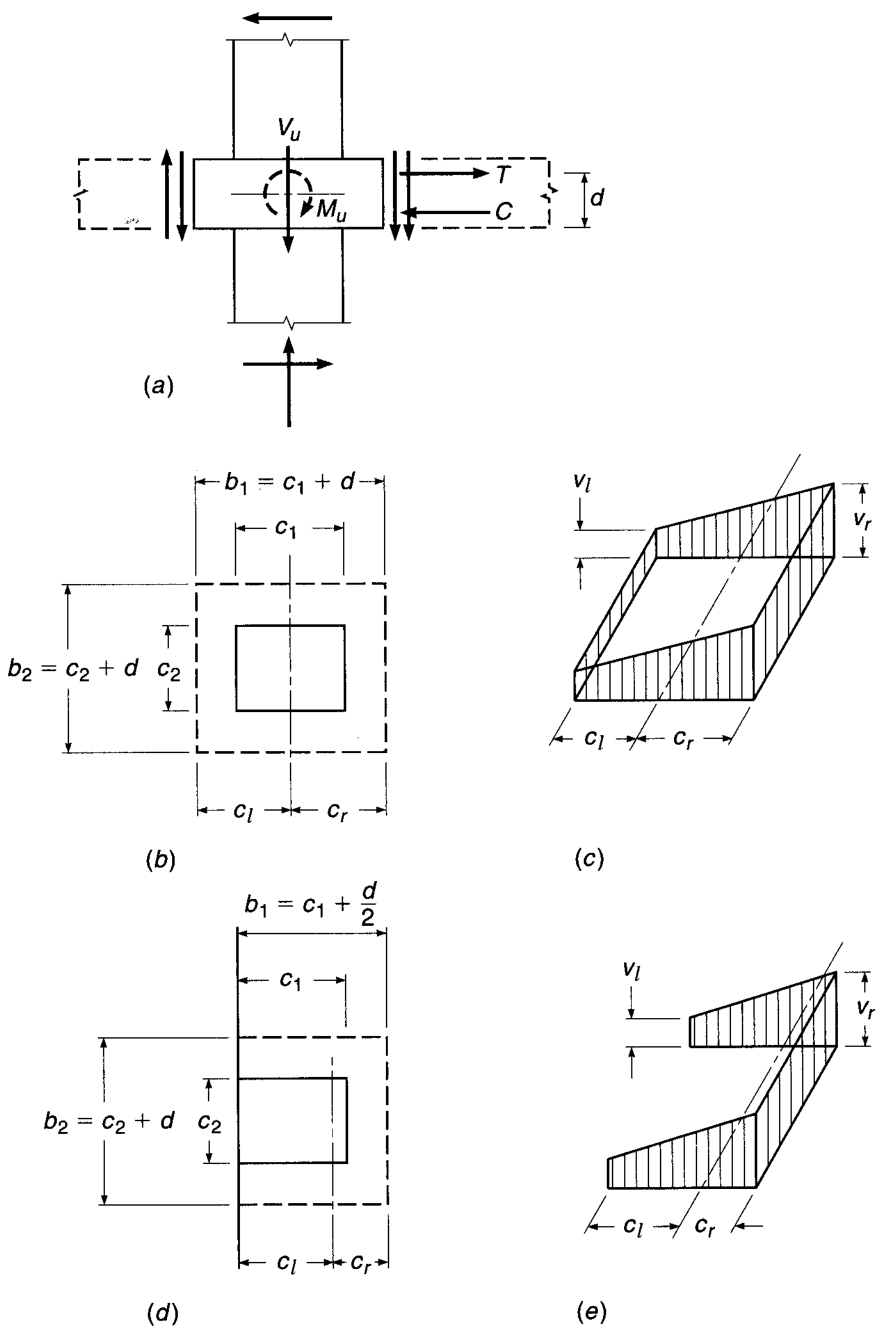

The situation can be modeled as shown in Fig. 13.33*a*. Here V_u represents the total vertical reaction to be transferred to the column, and M_u represents the unbalanced moment to be transferred, both at factored loads. The vertical force V_u causes shear stress distributed more or less uniformly around the perimeter of the critical section as assumed earlier, represented by the inner pair of vertical arrows, acting downward. The unbalanced moment M_u causes additional loading on the joint, represented by the outer pair of vertical arrows, which add to the shear stresses otherwise present on the right side, in the sketch, and subtract on the left side.

Tests indicate that for square columns about 60 percent of the unbalanced moment is transferred by flexure (forces T and C in Fig. 13.33a) and about 40 percent by shear stresses on the faces of the critical section (Ref. 13.24). For rectangular columns, it is reasonable to suppose that the portion transferred by flexure increases as the width of the critical section that resists the moment increases, i.e., as $c_2 + d$ becomes larger relative to $c_1 + d$ in Fig. 13.33b. According to ACI Code 13.5.3, the moment considered to be transferred by flexure is

$$M_{ub} = \gamma_f M_u \tag{13.16a}$$

where

$$\gamma_f = \frac{1}{1 + \frac{2}{3}\sqrt{b_1/b_2}} \tag{13.16b}$$

and b_1 = width of critical section for shear measured in direction of span for which moments are determined

b_2 = width of critical section for shear measured in direction perpendicular to b_1

The value of γ_f may be modified if certain conditions are met: For unbalanced moments about an axis parallel to the edge of exterior supports, γ_f may be increased to 1.0, provided that the factored shear V_u at the edge support does not exceed $0.75\phi V_c$ or at a corner support does not exceed $0.5\phi V_c$. For unbalanced moments at interior supports and about an axis perpendicular to the edge at exterior supports, γ_f may be increased up to 1.25 times the value in Eq. (13.16b), provided that $V_u \le 0.4\phi V_c$. In all of these cases, the net tensile strain ϵ_t calculated for the section within 1.5h on either side of the column or column capital must be at least 0.010.

The moment assumed to be transferred by shear, by ACI Code 11.11.7, is

$$M_{ub} = (1 - \gamma_f)M_u = \gamma_v M_u \tag{13.16c}$$

It is seen that for a square column Eqs. (13.16a), (13.16b), and (13.16c) indicate that 60 percent of the unbalanced moment is transferred by flexure and 40 percent by shear, in accordance with the available data. If b_2 is very large relative to b_1, nearly all of the moment is transferred by flexure.

The moment M_{ub} can be accommodated by concentrating a suitable fraction of the slab column-strip reinforcement near the column. According to ACI Code 13.5.3, this steel must be placed within a width between lines 1.5h on each side of the column or capital, where h is the total thickness of the slab or drop panel.

The moment M_{uv}, together with the vertical reaction delivered to the column, causes shear stresses assumed to vary linearly with distance from the centroid of the critical section, as indicated for an interior column by Fig. 13.33c. The stresses can be calculated from

$$v_l = \frac{V_u}{A_c} - \frac{M_{uv}c_l}{J_c} \tag{13.17a}$$

$$v_r = \frac{V_u}{A_c} + \frac{M_{uv}c_r}{J_c} \tag{13.17b}$$

where A_c = area of critical section = $2d[(c_1 + d) + (c_2 + d)]$

c_l, c_r = distances from centroid of critical section to left and right faces of section, respectively

J_c = property of critical section analogous to polar moment of inertia

For an interior column, the quantity J_c is

$$J_c = \frac{2d(c_1 + d)^3}{12} + \frac{2(c_1 + d)d^3}{12} + 2d(c_2 + d)\left(\frac{c_1 + d}{2}\right)^2 \tag{13.18}$$

Note the implication, in the use of the parameter J_c in the form of a polar moment of inertia, that shear stresses indicated on the near and far faces of the critical section in Fig. 13.33*c* have horizontal as well as vertical components.

According to ACI Code 11.11.7, the maximum shear stress calculated by Eq. (13.17) must not exceed ϕv_n. For slabs without shear reinforcement, $\phi v_n = \phi V_c/b_o d$, where V_c is the smallest value given by Eqs. (13.11*a*), (13.11*b*), or (13.11*c*). For slabs with shear reinforcement other than shearheads, $\phi v_n = \phi(V_c + V_s)/b_o d$, where V_c and V_s are as established in Section 13.10c, d, or e. Where shearhead reinforcement (see Section 13.10f) is used, the sum of the shear stresses due to vertical load on the second critical section, near the end of the shearhead arms, and the shear stresses resulting from moment transfer about the centroid of the first critical section $d/2$ from the support faces must not exceed $4\phi\lambda\sqrt{f'_c}$. In support of the last calculation, ACI Commentary 11.11.7.3 notes that tests indicate the first critical section is appropriate for calculation of stresses caused by transfer of moments even when shearheads are used. Even though the critical sections for direct shear transfer and shear due to moment transfer differ, they coincide or are in close proximity at the column corners where failures initiate, and it is conservative to take the maximum shear as the sum of the two components.

Equations similar to those above can be derived for the edge columns shown in Fig. 13.33*d* and *e* or for a corner column. Although the centroidal distances c_l and c_r are equal for the interior column, this is not true for the edge column of Fig. 13.33*d* or for a corner column.

According to ACI Code 13.6.3.6, when the direct design method is used, the moment to be transferred between the slab and an edge column by shear is to be taken equal to $0.30M_o$, where M_o is found from Eq. (13.1). This is intended to compensate for assigning a high proportion of the static moment to the positive and interior negative moment regions according to Table 13.3, and to ensure that adequate shear strength is provided between the slab and the edge column, where unbalanced moment is high and the critical section width is reduced.

The application of moment to a column from a slab or beam introduces shear to the column also, as is clear from Fig. 13.33*a*. This shear must be considered in the design of lateral column reinforcement.

As pointed out in Section 13.10, most flat plate structures, if they are overloaded, fail in the region close to the column, where large shear and bending forces must be transferred. There has been much research aimed at developing improved design details for this region. The design engineer should consult Refs. 13.24 through 13.26 for additional specific information.

13.12 OPENINGS IN SLABS

Almost invariably, slab systems must include openings. These may be of substantial size, as required by stairways and elevator shafts, or they may be of smaller dimensions, such as those needed to accommodate heating, plumbing, and ventilating risers; floor and roof drains; and access hatches.

Relatively small openings usually are not detrimental in *beam-supported slabs.* As a general rule, the equivalent of the interrupted reinforcement should be added at the sides of the opening. Additional diagonal bars should be included at the corners to control the cracking that will almost inevitably occur there. The importance of small openings in *slabs supported directly by columns* (flat slabs and flat plates) depends upon the location of the opening with respect to the columns. From a structural point of view, they are best located away from the columns, preferably in the area common to the slab middle strips. Unfortunately, architectural and functional considerations usually cause them to be located close to the columns. In this case, the reduction in effective shear perimeter is the major concern, because such floors are usually shear-critical.

According to ACI Code 11.11.6, if the opening is close to the column (within 10 slab thicknesses or within the column strips), then that part of b_o included within the radial lines projecting from the opening to the centroid of the column should be considered ineffective. This is shown in Fig. 13.34, along with the effect of free edges on the perimeter of the critical section. If shearheads (see Section 13.10f) are used under such circumstances, the reduction in width of the critical section is found in the same way, except that only one-half the perimeter included within the radial lines need be deducted.

With regard to flexural requirements, the total amount of steel required by calculation must be provided regardless of openings. Any steel interrupted by holes should be matched with an equivalent amount of supplementary reinforcement on either side, properly lapped to transfer stress by bond. Concrete compression area to provide the required strength must be maintained; usually this would be restrictive only

FIGURE 13.34
Effect of openings and free edges on the determination of the perimeter of the critical section for shear b_o.

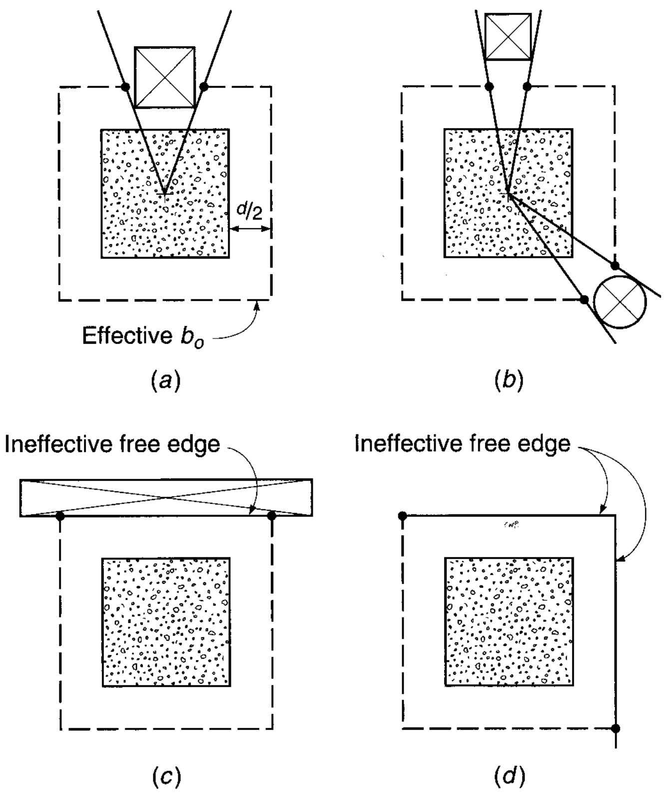

near the columns. According to ACI Code 13.4.2, openings of any size may be located in the area common to intersecting middle strips. In the area common to intersecting column strips, not more than one-eighth of the width of the column strip in either span can be interrupted by openings. In the area common to one middle strip and one column strip, not more than one-quarter of the reinforcement in either strip may be interrupted by the opening.

ACI Code 13.4.1 permits openings of *any* size if it can be shown by analysis that the strength of the slab is at least equal to that required and that all serviceability conditions, i.e., cracking and deflection limits, are met. The *strip method* of analysis and design for openings in slabs, by which specially reinforced integral beams, or *strong bands*, of depth equal to the slab depth are used to frame the openings, will be described in detail in Chapter 15. Very large openings should preferably be framed by beams or slab bands of increased depth to restore, as nearly as possible, the continuity of the slab. The beams must be designed to carry a portion of the floor load, in addition to loads applied directly by partition walls, elevator support beams, or stair slabs.

13.13 DEFLECTION CALCULATIONS

The deflection of a uniformly loaded flat plate, flat slab, or two-way slab supported by beams on column lines can be calculated by an equivalent frame method that corresponds with the method for moment analysis described in Section 13.9 (Ref. 13.27). The definition of column and middle strips, the longitudinal and transverse moment distribution coefficients, and many other details are the same as for the moment analysis. Following the calculation of deflections by this means, they can be compared directly with limiting values like those of Table 6.2, which are applicable to slabs as well as to beams, according to the ACI Code.

A slab region bounded by column centerlines is shown in Fig. 13.35. While no column-line beams, drop panels, or column capitals are shown, the presence of any of these introduces no fundamental complication.

The deflection calculation considers the deformation of such a typical region in one direction at a time, after which the contributions from each direction are added to obtain the total deflection at any point of interest.

In reference to Fig. 13.35*a*, the slab is considered to act as a broad, shallow beam of width equal to the panel dimension l_y and having the span l_x. Initially the slab is considered to rest on unyielding support lines at $x = 0$ and $x = l_x$. Because of variation of moment as well as flexural stiffness across the width of the slab, not all unit strips in the X direction will deform identically. Typically the slab curvature in the middle-strip region will be less than that in the region of the column strips because the middle-strip moments are less. The result is as indicated in Fig. 13.35*a*.

Next the slab is analyzed for bending in the Y direction (Fig. 13.35*b*). Once again the effect of transverse variation of bending moment and flexural rigidity is seen.

The actual deformed shape of the panel is represented in Fig. 13.35*c*. The midpanel deflection is the sum of the midspan deflection of the column strip in one direction and that of the middle strip in the other direction; i.e.,

$$\Delta_{\max} = \Delta_{cx} + \Delta_{my} \tag{13.19a}$$

or

$$\Delta_{\max} = \Delta_{cy} + \Delta_{mx} \tag{13.19b}$$

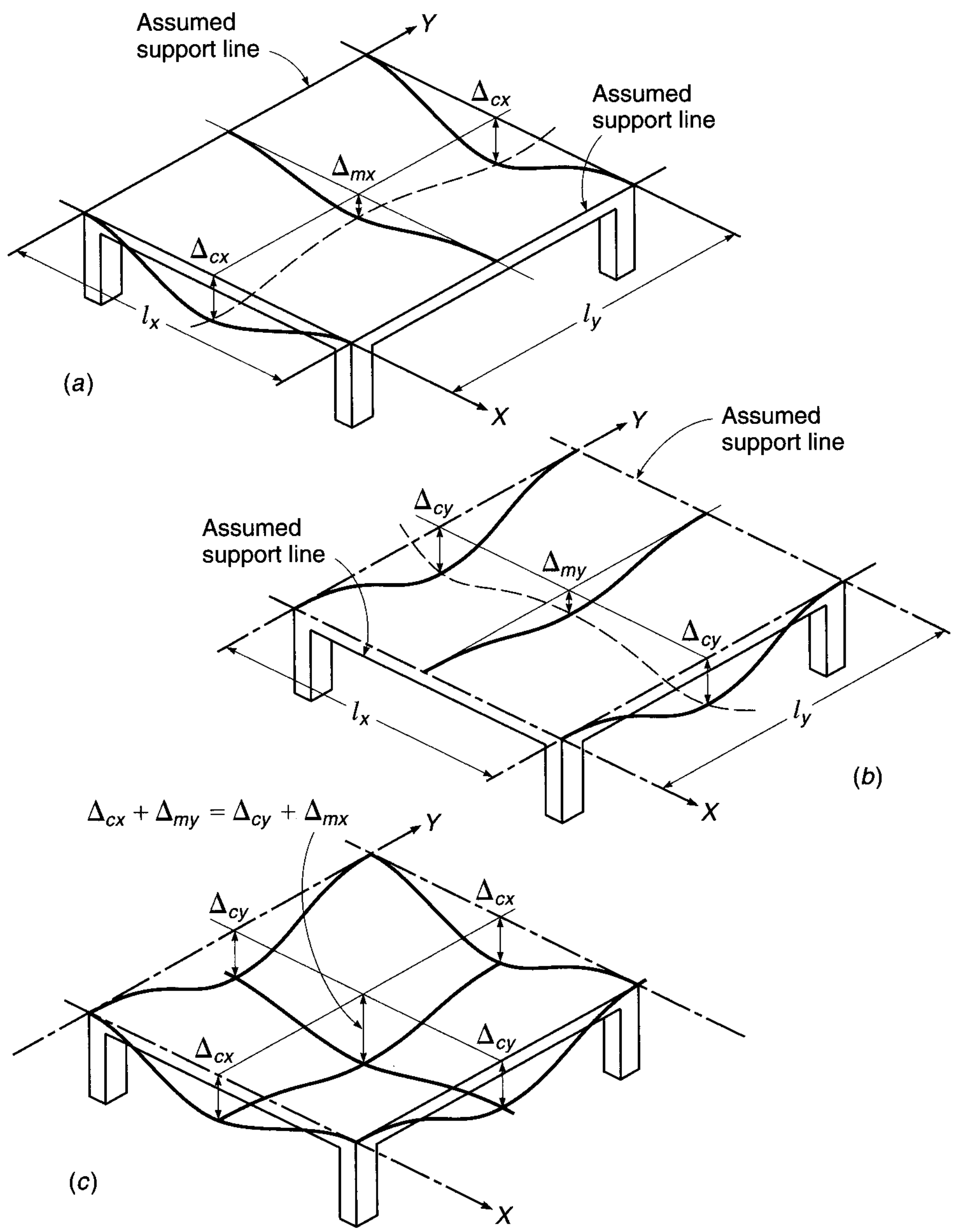

FIGURE 13.35
Basis of equivalent frame method for deflection analysis: (*a*) *X* direction bending; (*b*) *Y* direction bending; (*c*) combined bending.

In calculations of the deformation of the slab panel in either direction, it is convenient first to assume that it deforms into a cylindrical surface, as it would if the bending moment at all sections were uniformly distributed across the panel width and if lateral bending of the panel were suppressed. The supports are considered to be fully fixed against both rotation and vertical displacement at this stage. Thus, a *reference deflection* is computed:

$$\Delta_{f,\mathrm{ref}} = \frac{wl^4}{384E_cI_{\mathrm{frame}}} \tag{13.20}$$

FIGURE 13.36
Effective cross sections for deflection calculations: (*a*) full-width frame; (*b*) column strip; (*c*) middle strips.

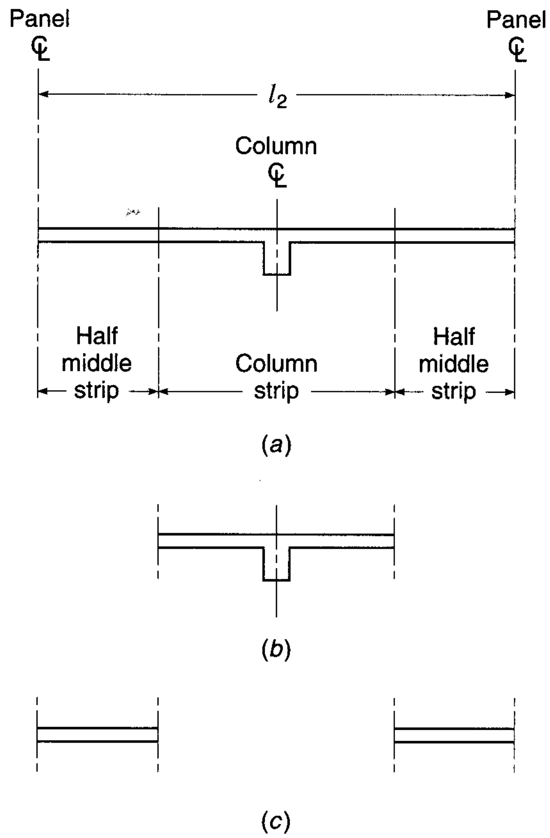

where w is the load per foot along the span of length l and I_{frame} is the moment of inertia of the full-width panel (Fig. 13.36*a*) including the contribution of the column-line beam or drop panels and column capitals if present.

The effect of the actual moment variation across the width of the panel and the variation of stiffness due to beams, variable slab depth, etc., are accounted for by multiplying the reference deflection by the ratio of M/EI for the respective strips to that of the full-width frame:

$$\Delta_{f,\text{col}} = \Delta_{f,\text{ref}} \frac{M_{\text{col}}}{M_{\text{frame}}} \frac{E_c I_{\text{frame}}}{E_c I_{\text{col}}} \tag{13.21a}$$

$$\Delta_{f,\text{mid}} = \Delta_{f,\text{ref}} \frac{M_{\text{mid}}}{M_{\text{frame}}} \frac{E_c I_{\text{frame}}}{E_c I_{\text{mid}}} \tag{13.21b}$$

The subscripts relate the deflection Δ, the bending moment M, or the moment of inertia I to the full-width frame, column strip, or middle strip, as shown in Fig. 13.36*a*, *b*, and *c*, respectively.

The moment ratios $M_{\text{col}}/M_{\text{frame}}$ and $M_{\text{mid}}/M_{\text{frame}}$ are identical to the lateral moment distribution factors already found for the flexural analysis (see Table 13.4). A minor complication results from the fact that the lateral distribution of bending moments, according to the ACI Code, is not the same at the negative and positive-moment sections. However, it appears consistent with the degree of accuracy usually required, as well as consistent with deflection methods endorsed elsewhere in the ACI Code, to use a simple average of lateral distribution coefficients for the negative and positive portions of each strip.

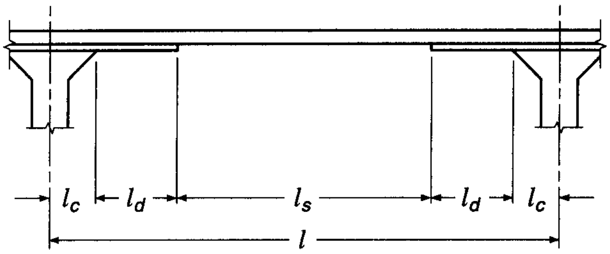

FIGURE 13.37
Flat slab span with variable moment of inertia.

The presence of drop panels or column capitals in the column strip of a flat slab floor requires consideration of the variation of the moment of inertia in the span direction (see Fig. 13.37). It is suggested in Ref. 13.28 that a weighted average moment of inertia be used in such cases:

$$I_{av} = 2\frac{l_c}{l}I_c + 2\frac{l_d}{l}I_d + \frac{l_s}{l}I_s \tag{13.22}$$

where I_c = moment of inertia of slab including both drop panel and capital
I_d = moment of inertia of slab with drop panel only
I_s = moment of inertia of slab alone

Span distances are defined in Fig. 13.37.

Next it is necessary to correct for the rotations of the equivalent frame at the supports, which until now were considered fully fixed. If the ends of the columns are considered fixed at the floor above and floor below, as usual for frame analysis, the rotation of the column at the floor divided by the stiffness of the equivalent column is

$$\theta = \frac{M_{net}}{K_{ec}} \tag{13.23}$$

where θ = angle change, radians
M_{net} = difference in floor moments to left and right of column
K_{ec} = stiffness of equivalent column (see Section 13.9c)

In some cases, the connection between the floor slab and column transmits negligible moment, as for lift slabs; thus $K_{ec} = 0$. The flexural analysis will indicate that the net moment is zero. The support rotation can be found in such cases by applying the moment-area theorems, taking moments of the M/EI area about the far end of the span and dividing by the span length.

Once the rotation at each end is known, the associated midspan deflection of the equivalent frame can be calculated. It is easily confirmed that the midspan deflection of a member experiencing an end rotation of θ rad, the far end being fixed, is

$$\Delta_\theta = \frac{\theta l}{8} \tag{13.24}$$

Thus the total deflection at midspan of the column strip or middle strip is the sum of the three parts

$$\Delta_{col} = \Delta_{f,col} + \Delta_{\theta l} + \Delta_{\theta r} \tag{13.25a}$$

$$\Delta_{mid} = \Delta_{f,mid} + \Delta_{\theta l} + \Delta_{\theta r} \tag{13.25b}$$

where the subscripts l and r refer to the left and right ends of the span, respectively.

The calculations described are repeated for the equivalent frame in the second direction of the structure, and the total deflection at midpanel is obtained by summing the column-strip deflection in one direction and the middle-strip deflection in the other, as indicated by Eqs. (13.19).

The midpanel deflection should be the same whether calculated by Eq. (13.19*a*) or Eq. (13.19*b*). Actually, a difference will usually be obtained because of the approximate nature of the calculations. For very rectangular panels, the main contribution to midpanel deflection is that of the long-direction column strip. Consequently, the midpanel deflection is best found by summing the deflections of the long-direction column strip and the short-direction middle strip. However, for exterior panels, the important contribution is from the column strips perpendicular to the discontinuous edge, even though the long side of the panel may be parallel to that edge.

In slabs, as in beams, the effect of concrete cracking is to reduce the flexural stiffness. According to ACI Code 9.5.3, the effective moment of inertia given by Eq. (6.8) is applicable to slabs as well as beams, although other values may be used if results are in reasonable agreement with tests. In most cases, two-way slabs will be essentially uncracked at service loads, and it is satisfactory to base deflection calculations on the uncracked moment of inertia I_g (see Ref. 13.27 for comparison with tests). In Ref. 13.29, Branson suggests the following refinements: (1) for slabs without beams, use I_g for all dead load deflections; for dead plus live load deflections, use I_g for middle strips and I_e for column strips; (2) for slabs with beams, use I_g for all dead load deflections; for dead plus live load deflections, use I_g for column strips and I_e for middle strips. For continuous spans, I_e can be based on the midspan positive moment without serious error.

The deflections calculated using the procedure described are short-term deflections. Long-term slab deflections can be calculated by multiplying the short-term deflections by the factor λ_Δ of Eq. (6.11), as for beams. Because compression steel is seldom used in slabs, a multiplier of 2.0 results. Test evidence and experience with actual structures indicate that this may seriously underestimate long-term slab deflections, and multipliers for long-term deflection from 2.5 to 4.0 have been recommended (Refs. 13.29 to 13.31). A multiplier of 3.0 gives acceptable results in most cases.

It should be recognized that the prediction of slab deflections, both initial elastic and long-term, is complicated by the many uncertainties associated with actual building construction. Loading history, particularly during construction, has a profound effect on final deflections (Ref. 13.32). Construction loads can equal or exceed the service live load. Such loads may include the weight of stacked building material and usually include the weight of slabs above the one cast earlier, applied through shoring and reshoring to the lower slab. Because construction loads are applied to immature concrete in the slabs, the immediate elastic deflections are large, and, upon removal of the construction loads, elastic recovery is less than the initial elastic deflection because E_c increases with age. Cracking resulting from construction loading does not disappear with removal of the temporary load and may result in live load deflections greater than expected. Creep during construction loading may be greater than expected because of the early age of the concrete when loaded. Shrinkage deflections of thin slabs are often of the same order of magnitude as the elastic deflections, and some cases must be calculated separately.

It is important to recognize that both initial and time-dependent slab deflections are subject to a high degree of variability. Calculated deflections are an estimate, at best, and considerable deviation from calculated values is to be expected in actual structures.

EXAMPLE 13.8 **Calculation of deflections.** Find the deflections at the center of the typical exterior panel of the two-way floor designed in Example 13.2 due to dead and live loads. The live load may be considered a short-term load and will be distributed uniformly over all panels. The floor will support nonstructural elements that are likely to be damaged by large deflections. Take $E_c = 3.6 \times 10^6$ psi.

Solution. The elastic deflection due to the self-weight of 88 psf will be found, after which the additional long-term dead load deflection can be found by applying the factor $\lambda = 3.0$, and the short-term live load deflection due to 144 psf by direct proportion.

The effective concrete cross sections, upon which moment of inertia calculations will be based, are shown in Fig. 13.38 for the full-width frame, the column strip, and the middle strips, for the short-span and long-span directions. Note that the width of the column strip in both directions is based on the shorter panel span, according to the ACI Code. The values of moment of inertia are as follows:

	Short Direction	Long Direction
I_{frame}	27,900 in^4	25,800 in^4
I_{col}	21,000 in^4	21,000 in^4
I_{mid}	5,150 in^4	3,430 in^4

First calculating the deflections of the floor in the *short-span direction* of the panel, from Eq. (13.20) the reference deflection is

$$\Delta_{f,\text{ref}} = \frac{88 \times 25(20 \times 12)^4}{12 \times 384 \times 3.6 \times 10^6 \times 27{,}900} = 0.016 \text{ in.}$$

(Note that the centerline span distance is used here, although clear span was used in the moment analysis to approximate the moment reduction due to support width, according to ACI Code procedures.) From the moment analysis in the short-span direction, it was concluded that

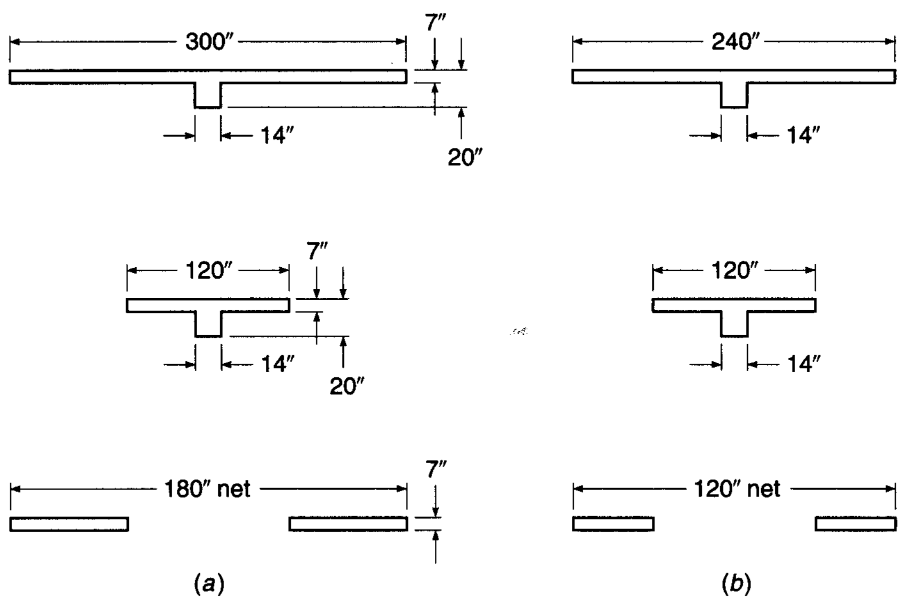

FIGURE 13.38
Cross-sectional dimensions for deflection example: (*a*) short-span direction frame, column strip, and middle strip; (*b*) long-span direction frame, column strip, and middle strip.

68 percent of the moment at both negative and positive sections was taken by the column strip and 32 percent by the middle strips. Accordingly, from Eqs. (13.21*a*) and (13.21*b*),

$$\Delta_{f,\mathrm{col}} = 0.016 \times 0.68 \times \frac{27{,}900}{21{,}000} = 0.014 \text{ in.}$$

$$\Delta_{f,\mathrm{mid}} = 0.016 \times 0.32 \times \frac{27{,}900}{5150} = 0.028 \text{ in.}$$

For the panel under investigation, which is fully continuous over both supports in the short direction, it may be assumed that support rotations are negligible; consequently, $\Delta_{\theta \ell}$ and $\Delta_{\theta r} = 0$, and from Eqs. (13.25*a*) and (13.25*b*),

$$\Delta_{\mathrm{col}} = 0.014 \text{ in.}$$

$$\Delta_{\mathrm{mid}} = 0.028 \text{ in.}$$

Now calculating the deformations in the *long direction* of the panel gives the reference deflection

$$\Delta_{f,\mathrm{ref}} = \frac{88 \times 20(25 \times 12)^4}{12 \times 384 \times 3.6 \times 10^6 \times 25{,}800} = 0.033 \text{ in.}$$

From the moment analysis it was found that the column strip would take 93 percent of the exterior negative moment, 81 percent of the positive moment, and 81 percent of the interior negative moment. Thus the average lateral distribution factor for the column strip is

$$\left(\frac{0.93 + 0.81}{2} + 0.81\right)\frac{1}{2} = 0.84$$

or 84 percent, while the middle strips are assigned 16 percent. Then from Eqs. (13.21*a*) and (13.21*b*),

$$\Delta_{f,\mathrm{col}} = 0.033 \times 0.84 \times \frac{25{,}800}{21{,}000} = 0.034 \text{ in.}$$

$$\Delta_{f,\mathrm{mid}} = 0.033 \times 0.16 \times \frac{25{,}800}{3430} = 0.040 \text{ in.}$$

While rotation at the interior column may be considered negligible, rotation at the exterior column cannot. For the dead load of the slab, the full static moment is

$$M_o = \tfrac{1}{8} \times 0.088 \times 20 \times 25^2 = 137.5 \text{ ft-kips}$$

It was found that 16 percent of the static moment, or 22.0 ft-kips, should be assigned to the exterior support section. The resulting rotation is found from Eq. (13.23). It is easily confirmed that the stiffness of the equivalent column (see Section 13.9c) is $169 \times 3.6 \times 10^6$ in-lb/rad; hence

$$\theta = \frac{22{,}000 \times 12}{169 \times 3.6 \times 10^6} = 0.00043 \text{ rad}$$

From Eq. (13.24), the corresponding midpanel deflection component is

$$\Delta_{\theta l} = \frac{0.00043 \times 25 \times 12}{8} = 0.016 \text{ in.}$$

Thus, from Eqs. (13.25*a*) and (13.25*b*), the deflections of the column and middle strips in the long direction are

$$\Delta_{\mathrm{col}} = 0.034 + 0.016 = 0.050 \text{ in.}$$

$$\Delta_{\mathrm{mid}} = 0.040 + 0.016 = 0.056 \text{ in.}$$

and from Eq. (13.19*a*) the short-term midpanel deflection due to self-weight is

$$\Delta_{max} = 0.050 + 0.028 = 0.078 \text{ in.}$$

The long-term deflection due to dead load is $3.0 \times 0.078 = 0.234$ in., and the short-term live load deflection is $0.078 \times 144/88 = 0.128$.

The ACI limiting value for the present case is found to be 1/480 times the span, or $20 \times 12/480 = 0.500$ in., based on the sum of the long-time deflection due to sustained load and the immediate deflection due to live load. The sum of these deflection components in the present case is

$$\Delta_{max} = 0.234 + 0.128 = 0.362 \text{ in.}$$

well below the permissible value.

13.14 ANALYSIS FOR HORIZONTAL LOADS

Either the direct design method or the equivalent frame method, described in the preceding sections of this chapter, may be used for the analysis of two-way slab systems for gravity loads, according to ACI Code 13.5.1. However, the ACI Code provisions are not meant to apply to the analysis of buildings subject to lateral loads, such as loads caused by wind or earthquake. For lateral load analysis, the designer may select any method that is shown to satisfy equilibrium and geometric compatibility, and to give results that are in reasonable agreement with available test data. The results of the lateral load analysis may then be combined with those from the vertical load analysis, according to ACI Code 13.5.1.

Plane frame analysis, with the building assumed to consist of parallel frames each bounded laterally by the panel centerlines on either side of the column lines, has often been used in analyzing unbraced buildings for horizontal loads, as well as vertical. For vertical load analysis by the equivalent frame method, a single floor is usually studied as a substructure with attached columns assumed fully fixed at the floors above and below, but for horizontal frame analysis the equivalent frame includes all floors and columns, extending from the bottom to the top of the structure.

The main difficulty in equivalent frame analysis for horizontal loads lies in modeling the stiffness of the region at the beam-column (or slab-beam-column) connections. Transfer of forces in this region involves bending, torsion, shear, and axial load, and is further complicated by the effects of concrete cracking in reducing stiffness, and reinforcement in increasing it. Frame moments are greatly influenced by horizontal displacements at the floors, and a conservatively low value of stiffness should be used to ensure that a reasonable estimate of drift is included in the analysis.

While a completely satisfactory basis for modeling the beam-column joint stiffness has not been developed, at least two methods have been used in practice (Ref. 13.33). The first is based on an equivalent beam width αl_2, less than the actual width, to reduce the stiffness of the slab for purposes of analysis. Figure 13.39*a* shows a plate fixed at the far edge and supported by a column of width c_2 at the near side. If a rotation θ is imposed at the column, the plate rotation along the axis A will vary as shown by Fig. 13.39*a*, from θ at the column to smaller values away from the column. An equivalent width factor α is obtained from the requirement that the stiffness of a prismatic beam of width αl_2 must equal the stiffness of the plate of width l_2. This equality is obtained if the areas under the two rotation diagrams of Fig. 13.39*b* are equal. Thus the frame analysis is based on a reduced slab (or slab-beam) stiffness found using αl_2

FIGURE 13.39
Equivalent beam width for horizontal load analysis.

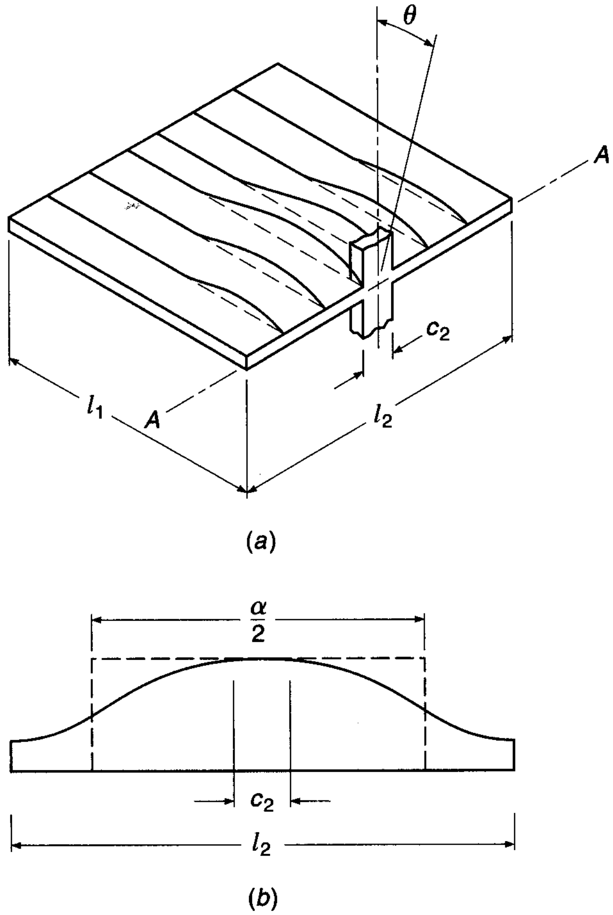

rather than l_2. Comparative studies indicate that, for flat plate floors, a value for α between 0.25 and 0.50 may be used (Ref. 13.33).

Alternatively, the beam-column stiffness can be modeled based on a transverse torsional member corresponding to that used in deriving the stiffness of the equivalent column for the vertical load analysis of two-way slabs by the equivalent frame method (see Section 13.9c). Rotational stiffness of the joint is a function of the flexural stiffness of the columns framing into the joint from above and below and the torsional stiffness of the transverse strip of slab or slab beam at the column. The equivalent column stiffness is found from Eq. (13.9) and the torsional stiffness from Eq. (13.10), as before.

Finally, for frames in which two-way systems act as primary members resisting lateral loads, ACI Code 13.3.8 requires that the lengths of reinforcement be determined by analysis because the lengths shown in Fig. 13.14 may not be adequate. The values in Fig. 13.14, however, are retained as minimum values.

REFERENCES

13.1. ACI Committee 360, *Design of Slabs-on-Ground* (ACI 360R-06), American Concrete Institute, Farmington Hills, MI, 2006.
13.2. W. L. Gamble, "Moments in Beam-Supported Slabs," *J. ACI*, vol. 69, no. 3, 1972, pp. 149–157.

13.3. J. R. Nichols, "Statical Limitations upon the Steel Requirement in Reinforced Concrete Flat Slab Floors," *Trans. ASCE*, vol. 77, 1914, pp. 1670–1736.
13.4. D. S. Hatcher, M. A. Sozen, and C. P. Siess, "Test of a Reinforced Concrete Flat Plate," *J. Struct. Div.*, ASCE, vol. 91, no. ST5, 1965, pp. 205–231.
13.5. S. A. Guralnick and R. W. LaFraugh, "Laboratory Study of a Forty-Five Foot Square Flat Plate Structure," *J. ACI*, vol. 60, no. 9, 1963, pp. 1107–1185.
13.6. D. S. Hatcher, M. A. Sozen, and C. P. Siess, "Test of a Reinforced Concrete Flat Slab," *J. Struct. Div.*, ASCE, vol. 95, no. ST6, 1969, pp. 1051–1072.
13.7. J. O. Jirsa, M. A. Sozen, and C. P. Siess, "Test of a Flat Slab Reinforced with Welded Wire Fabric," *J. Struct. Div.*, ASCE, vol. 92, no. ST3, 1966, pp. 199–224.
13.8. W. L. Gamble, M. A. Sozen, and C. P. Siess, "Tests of a Two-Way Reinforced Concrete Floor Slab," *J. Struct. Div.*, ASCE, vol. 95, no. ST6, 1969, pp. 1073–1096.
13.9. M. D. Vanderbilt, M. A. Sozen, and C. P. Siess, "Test of a Modified Reinforced Concrete Two-Way Slab," *J. Struct. Div.*, ASCE, vol. 95, no. ST6, 1969, pp. 1097–1116.
13.10. W. L. Gamble, "Moments in Beam-Supported Slabs," *J. ACI*, vol. 69, no. 3, 1972, pp. 149–157.
13.11. J. O. Jirsa, M. A. Sozen, and C. P. Siess, "Pattern Loadings on Reinforced Concrete Floor Slabs," *J. Struct. Div.*, ASCE, vol. 95, no. ST6, 1969, pp. 1117–1137.
13.12. D. Peabody, Jr., "Continuous Frame Analysis of Flat Slabs," *J. Boston Society Civ. Eng.*, January 1948.
13.13. W. G. Corley, M. A. Sozen, and C. P. Siess, "The Equivalent Frame Method for Reinforced Concrete Slabs," Univ. Ill. Dept. Civ. Eng. Struct. Res. Series 218, June 1961.
13.14. W. G. Corley and J. O. Jirsa, "Equivalent Frame Analysis for Slab Design," *J. ACI*, vol. 67, no. 11, 1970, pp. 875–884.
13.15. ASCE-ACI Task Committee 426, "The Shear Strength of Reinforced Concrete Members—Slabs," *J. Struct. Div.*, ASCE, vol. 100, no. ST8, 1974, pp. 1543–1591.
13.16. N. M. Hawkins, H. B. Fallsen, and R. C. Hinojosa, "Influence of Column Rectangularity on the Behavior of Flat Plate Structures," in *Cracking, Deflection, and Ultimate Load of Concrete Slab Systems*, ACI Publication SP-30, 1971, p. 127.
13.17. M. D. Vanderbilt, "Shear Strength of Continuous Plates," *J. Struct. Div.*, ASCE, vol. 98, no. ST5, 1972, pp. 961–973.
13.18. W. G. Corley and N. M. Hawkins, "Shearhead Reinforcement for Slabs," *J. ACI*, vol. 65, no. 10, 1968, pp. 811–824.
13.19. N. W. Hawkins, D. Mitchell, and S. N. Hanna, "Effects of Shear Reinforcement on the Reversed Cyclic Loading Behavior of Flat Plate Structures," *Can. J. Civ. Eng.*, vol. 2, no. 4, 1975, pp. 572–582.
13.20. A. Ghali, "An Efficient Solution to Punching of Slabs," *Concr. Intl.*, vol. 11, no. 6, 1989, pp. 50–54.
13.21. A. A. Elgabry and A. Ghali, "Design of Stud-Shear Reinforcement for Slabs," *ACI Struct. J.*, vol. 87, no. 3, 1990, pp. 350–361.
13.22. A. S. Mokhtar, A. Ghali, and W. Dilger, "Stud Shear Reinforcement for Flat Concrete Plates," *J. ACI*, vol. 82, no. 5, 1985, pp. 676–683.
13.23. A. A. Elgabry and A. Ghali, "Tests on Concrete Slab-Column Connections with Stud Shear Reinforcement Subjected to Shear-Moment Transfer," *ACI Struct. J.*, vol. 84, no. 5, 1987, pp. 433–442.
13.24. N. M. Hawkins, A. Bao, and J. Yamazaki, "Moment Transfer from Concrete Slabs to Columns," *ACI Struct. J.*, vol. 86, no. 6, 1989, pp. 705–716.
13.25. "Recommendations for Design of Slab-Column Connections in Monolithic Reinforced Concrete Structures," reported by ACI-ASCE Committee 352, *ACI Struct. J.*, vol. 85, no. 6, 1988, pp. 675–696.
13.26. J. P. Moehle, M. E. Kreger, and R. Leon, "Background to Recommendations for Design of Reinforced Concrete Slab-Column Connections," *ACI Struct. J.*, vol. 85, no. 6, 1988, pp. 636–644.
13.27. A. H. Nilson and D. B. Walters, "Deflection of Two-Way Floor Systems by the Equivalent Frame Method," *J. ACI*, vol. 72, no. 5, May 1975, pp. 210–218.
13.28. E. S. Hoffman, D. P. Gustafson, and A. J. Gouwens, *Structural Design Guide to the ACI Building Code*, 4th ed., Kluwer Academic Publishers, Boston, 1998.
13.29. D. E. Branson, *Deformation of Concrete Structures*, McGraw-Hill, New York, 1977.
13.30. P. J. Taylor and J. L. Heiman, "Long-Term Deflection of Reinforced Concrete Flat Slabs and Plates," *J. ACI*, vol. 74, no. 11, 1977, pp. 556–561.
13.31. C. J. Graham and A. Scanlon, "Long-Time Multipliers for Estimating Two-Way Slab Deflections," *J. ACI*, vol. 83, no. 6, 1986, pp. 899–908.
13.32. N. J. Gardner and A. Scanlon, "Long-Term Deflections of Two-Way Slabs," *Concr. Intl.*, vol. 12, no. 1, 1990, pp. 63–67.
13.33. M. D. Vanderbilt and W. G. Corley, "Frame Analysis of Concrete Buildings," *Concr. Intl.*, vol. 5, no. 12, 1983, pp. 33–43.

PROBLEMS

13.1. A footbridge is to be built, consisting of a one-way solid slab spanning 16 ft between masonry abutments, as shown in Fig. P13.1. A service live load of 100 psf must be carried. In addition, a 2000 lb concentrated load, assumed to be uniformly distributed across the bridge width, may act at any location on the span. A 2 in. asphalt wearing surface will be used, weighing 20 psf. Precast concrete curbs are attached so as to be nonstructural. Prepare a design for the slab, using material strengths $f_y = 60{,}000$ psi and $f_c' = 4000$ psi, and summarize your results in the form of a sketch showing all concrete dimensions and reinforcement.

FIGURE P13.1

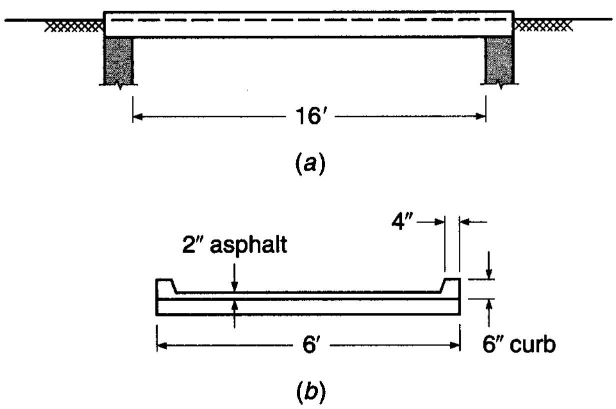

13.2. A reinforced concrete building floor system consists of a continuous one-way slab built monolithically with its supporting beams, as shown in cross section in Fig. P13.2. Service live load will be 125 psf. Dead loads include a 10 psf allowance for nonstructural lightweight concrete floor fill and surface, and a 10 psf allowance for suspended loads, plus the self-weight of the floor. Using ACI coefficients from Chapter 12, calculate the design moments and shears and design the slab, using a maximum tensile reinforcement ratio of 0.006. Use all straight bar reinforcement. One-half of the positive-moment bars will be discontinued where no longer required; the other half will be continued into the supporting beams as specified by the ACI Code. All negative steel will be discontinued at the same distance from the support face in each case. Summarize your design with a sketch showing concrete dimensions, and size, spacing, and cutoff points for all reinforcement. Material strengths are f_y = 60,000 psi and f_c' = 3000 psi.

FIGURE P13.2

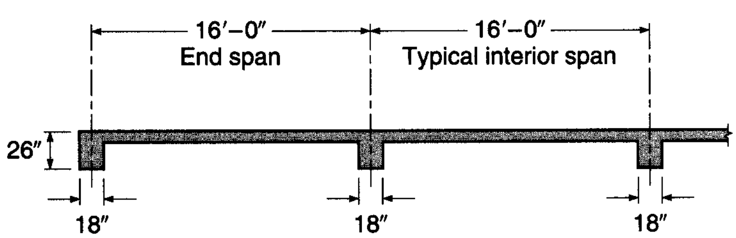

13.3. For the one-way slab floor in Problem 13.2, calculate the immediate and long-term deflection due to dead loads. Assume that all dead loads are applied when the construction shoring is removed. Also determine the deflection due to application of the full-service live load. Assuming that sensitive equipment will be installed 6 months after the shoring is removed, calculate the relevant deflection components and compare the total with maximum values recommended in the ACI Code.

13.4. A monolithic reinforced concrete floor consists of rectangular bays measuring 21 × 26 ft, as shown in Fig. P13.4. The floor is designed to carry a service live load of 125 psf uniformly distributed over its surface in addition to its own weight, using a concrete strength of 5000 psi and reinforcement having f_y = 60,000 psi. Design a typical interior panel using the ACI direct design method of Sections 13.6 through 13.8.

FIGURE P13.4

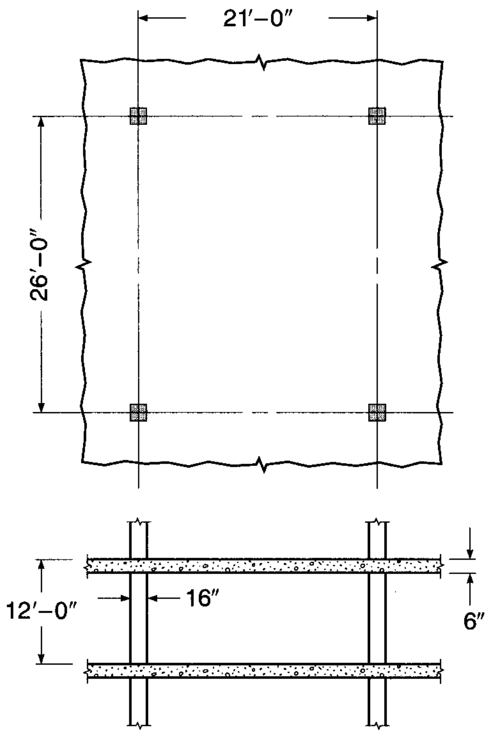

13.5. Redesign the typical exterior panel of the floor of Example 13.2 as a part of a flat plate structure, with no beams between interior columns but with beams provided along the outside edge to stiffen the slab. No drop panels or column capitals are permitted, but shear reinforcement similar to Fig. 13.24*b* may be incorporated if necessary. Column size is 20 × 20 in., and the floor-to-floor height is 12 ft. Use either the direct design method or the equivalent frame method. Summarize your design by means of a sketch showing plan and typical cross sections.

13.6. For the four-story structure shown in Figure P13.6, (*a*) select the slab thickness, (*b*) design the highlighted floor slab panel using the equivalent frame method,

FIGURE P13.6

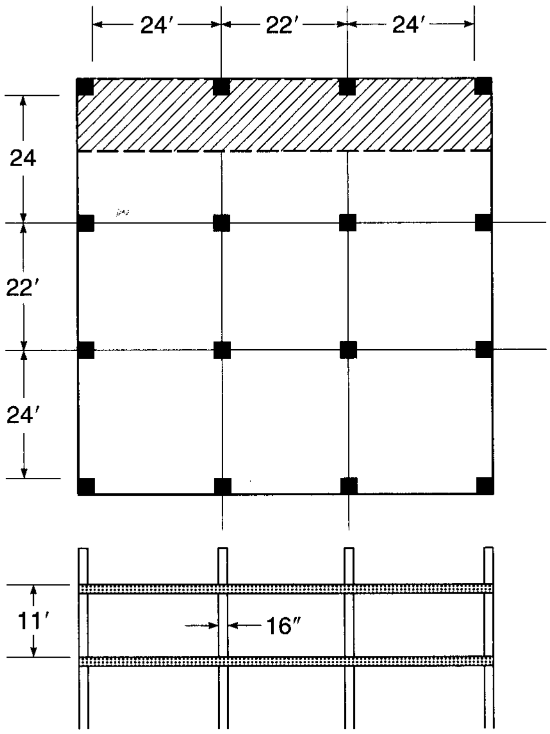

(c) prepare sketches of the steel layout, and (d) comment on your selection of the original thickness and what effect using shear studs might have on the design. Material strengths are $f_y = 60{,}000$ psi and $f'_c = 4000$ psi. Building loads are the superimposed dead load of 30 psf and live load of 50 psf.

13.7. A multistory commercial building is to be designed as a flat plate system with floors of uniform thickness having no beams or drop panels. Columns are laid out on a uniform 20 ft spacing in each direction and have a 16 in. square section and a vertical dimension 10 ft from floor to floor. Specified service live load is 100 psf including partition allowance. Using the direct design method, design a typical interior panel, determining the required floor thickness, size and spacing of reinforcing bars, and bar details including cutoff points. To simplify construction, the reinforcement in each direction will be the same; use an average effective depth in the calculations. Use all straight bars. For moderate spans such as this, it has been determined that supplementary shear reinforcement would not be economical, although column capitals may be used if needed. Thus, slab thickness may be based on Eqs. (13.11a), (13.11b), and (13.11c); or column capital dimensions can be selected using those equations if slab thickness is based on the equations in Section 13.8. Material strengths are $f_y = 60{,}000$ psi and $f'_c = 4000$ psi.

13.8. Prepare alternative designs for shear reinforcement at the supports of the slab described in Example 13.7, (a) using bent-bar reinforcement similar to Fig. 13.24b, (b) using integral beams with vertical stirrups similar to Fig. 13.24e, and (c) using headed shear stud reinforcement similar to Fig. 13.24f.

13.9. Prepare an alternative design for shear reinforcement at the supports of the slab described in Example 13.4, using a shearhead similar to Fig. 13.24a.

As an alternative to shear reinforcement of any kind, calculate the smallest acceptable dimensions for a 45° column capital (see Fig. 13.1*e*) that would permit the concrete slab to resist the entire shear force. Drop panels are not permitted.

13.10. Figure P13.10 shows a flat plate floor designed to carry a factored load of 325 psf. The total slab thickness $h = 7\frac{1}{2}$ in. and the average effective depth $d = 6$ in. Material strengths are $f_y = 60{,}000$ psi and $f'_c = 4000$ psi. The design for punching shear at a typical interior column B2 provided the basis for Example 13.4. To provide a full perimeter b_o at the exterior column B1, the slab is cantilevered past the columns as shown. A total shear force $V_u = 105$ kips must be transmitted to the column, along with a bending moment $M_u =$ 120 ft-kips about an axis parallel to the edge of the slab. Check for punching shear at column B1 and, if ACI Code restrictions are not met, suggest appropriate modifications in the proposed design. Edge beams are not permitted.

FIGURE P13.10

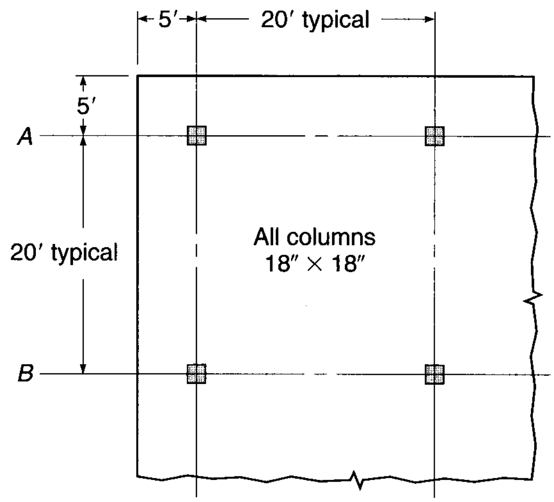

13.11. For the flat plate floor in Example 13.3, find the following deflection components at the center of panel *C*: (*a*) immediate deflection due to total dead load; (*b*) additional dead load deflection after a long period of time, due to total dead load; (*c*) immediate deflection due to three-quarters full live load. The moment of inertia of the cross concrete sections I_g may be used for all calculations. It may be assumed that maximum deflection will be obtained for the same loading pattern that would produce maximum positive moment in the panel. Check predicted deflection against ACI limitations, assuming that nonstructural attached elements would be damaged by excessive deflections.

13.12. A parking garage is to be designed using a two-way flat slab on the column lines, as shown in Fig. P13.12. A live load of 100 psf is specified. Find the required slab thickness, using a reinforcement ratio of approximately 0.005, and design the reinforcement for a typical corner panel *A*, edge panel *B*, and interior panel *C*. Check shear capacity. Detail the reinforcement, showing size, spacing, and length. All straight bars will be used. Material strengths will be $f_y = 60{,}000$ psi and $f'_c = 5000$ psi. Specify the design method selected and comment on your results.

FIGURE P13.12

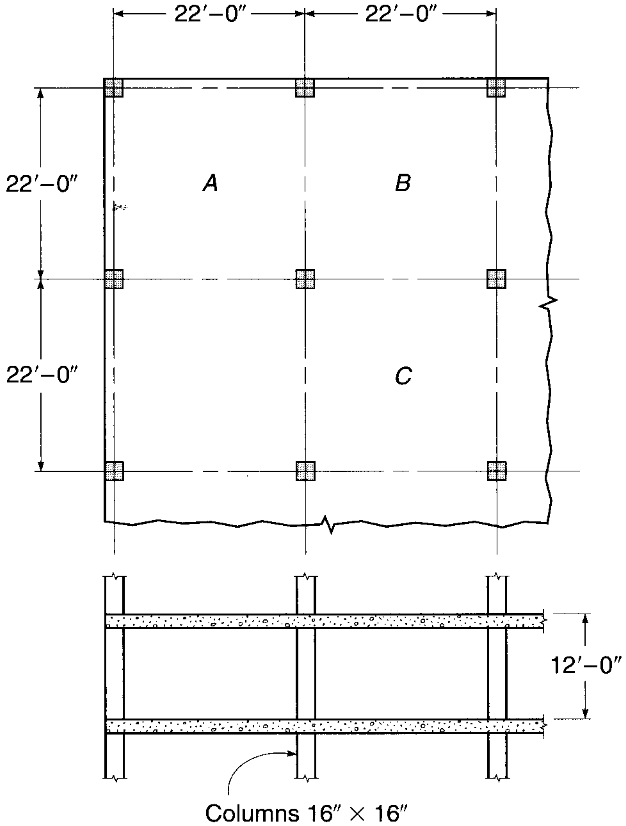

13.13. For the typical interior panel C of the parking garage in Problem 13.12, (a) compute the immediate and long-term deflections due to dead load and (b) compute the deflection due to the full-service live load. Compare with ACI Code maximum permissible values, given that there are no elements attached that would be damaged by large deflections.

14 Yield Line Analysis for Slabs

14.1 INTRODUCTION

Most concrete slabs are designed for moments found by the methods described in Chapter 13. These methods are based essentially upon elastic theory. On the other hand, reinforcement for slabs is calculated by strength methods that account for the actual inelastic behavior of members at the factored load stage. A corresponding contradiction exists in the process by which beams and frames are analyzed and designed, as was discussed in Section 12.9, and the concept of limit, or plastic, analysis of reinforced concrete was introduced. Limit analysis not only eliminates the inconsistency of combining elastic analysis with inelastic design, but also accounts for the reserve strength characteristic of most reinforced concrete structures and permits, within limits, an arbitrary readjustment of moments found by elastic analysis to arrive at design moments that permit more practical reinforcing arrangements.

For slabs, there is still another good reason for interest in limit analysis. The elasticity-based methods of Chapter 13 are restricted in important ways. Slab panels must be square or rectangular. They must be supported along two opposite sides (one-way slabs), two pairs of opposite sides (two-way edge-supported slabs), or by a fairly regular array of columns (flat plates and related forms). Loads must be uniformly distributed, at least within the bounds of any single panel. There can be no large openings. But in practice, many slabs do not meet these restrictions. Answers are needed, for example, for round or triangular slabs, slabs with large openings, slabs supported on two or three edges only, and slabs carrying concentrated loads. Limit analysis provides a powerful and versatile tool for treating such problems.

It was evident from the discussion of Section 12.9 that full plastic analysis of a continuous reinforced concrete beam or frame would be tedious and time-consuming because of the need to calculate the rotation requirement at all plastic hinges and to check rotation capacity at each hinge to ensure that it is adequate. Consequently, for beams and frames, the very simplified approach to plastic moment redistribution of ACI Code 8.4 is used. However, for slabs, which typically have tensile reinforcement ratios much below the balanced value and consequently have large rotation capacity, it can be safely assumed that the necessary ductility is present. Practical methods for the plastic analysis of slabs are thus possible and have been developed. *Yield line theory*, presented in this chapter, is one of these. Although the ACI Code contains no specific provisions for limit or plastic analysis of slabs, ACI Code 1.4 permits use of "any system of design or construction," the adequacy of which has been shown by successful use, analysis, or tests, and ACI Commentary 13.5.1 refers specifically to yield line analysis as an acceptable approach.

Yield line analysis for slabs was first proposed by Ingerslev (Ref. 14.1) and was greatly extended by Johansen (Refs. 14.2 and 14.3). Early publications were mainly in Danish, and it was not until Hognestad's English language summary (Ref. 14.4) of Johansen's work that the method received wide attention. Since that time, a number of important publications on the method have appeared (Refs. 14.5 through 14.15). A particularly useful and comprehensive treatment will be found in Ref. 14.15.

The *plastic hinge* was introduced in Section 12.9 as a location along a member in a continuous beam or frame at which, upon overloading, there would be large inelastic rotation at essentially a constant resisting moment. For slabs, the corresponding mechanism is the *yield line*. For the overloaded slab, the resisting moment per unit length measured along a yield line is constant as inelastic rotation occurs; the yield line serves as an axis of rotation for the slab segment.

Figure 14.1*a* shows a simply supported, uniformly loaded reinforced concrete slab. It will be assumed to be underreinforced (as are almost all slabs), with $\rho < \rho_{0.005}$. The elastic moment diagram is shown in Fig. 14.1*b*. As the load is increased, when the applied moment becomes equal to the flexural capacity of the slab cross section, the tensile steel starts to yield along the transverse line of maximum moment.

Upon yielding, the curvature of the slab at the yielding section increases sharply, and deflection increases disproportionately. The elastic curvatures along the slab span are small compared with the curvature resulting from plastic deformation at the yield line, and it is acceptable to consider that the slab segments between the yield line and supports remain rigid, with all the curvature occurring at the yield line, as shown in Fig. 14.1*c*. The "hinge" that forms at the yield line rotates with essentially constant resistance, according to the relation shown earlier in Fig. 12.13*a*. The resistance per unit width of slab is the nominal flexural strength of the slab; that is, $m_p = m_n$, where m_n is calculated by the usual equations. For design purposes, m_p would be taken equal to ϕm_n, with ϕ typically equal to 0.90, since ρ is well below $\rho_{0.005}$ for most slabs.

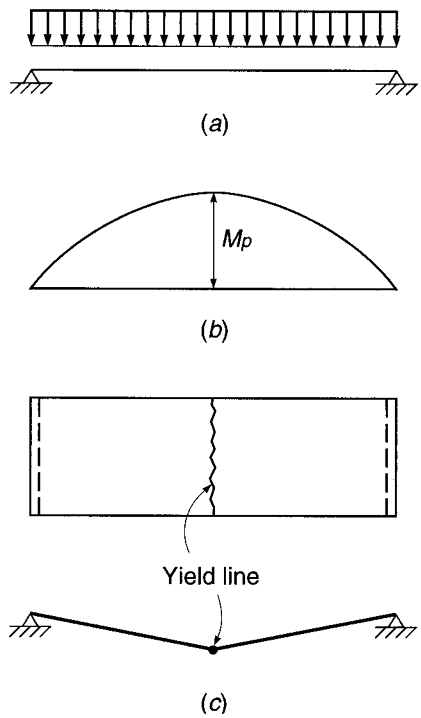

FIGURE 14.1
Simply supported, uniformly loaded one-way slab.

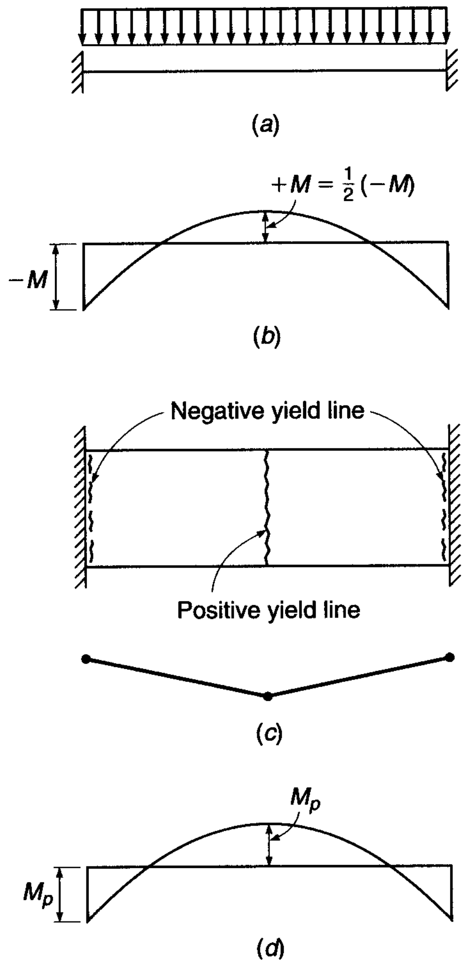

FIGURE 14.2
Fixed-end, uniformly loaded one-way slab.

For a statically determinate slab like that in Fig. 14.1, the formation of one yield line results in collapse. A "mechanism" forms; i.e., the segments of the slab between the hinge and the supports are able to move without an increase in load. Indeterminate structures, however, can usually sustain their loads without collapse even after the formation of one or more yield lines. When it is loaded uniformly, the fixed-fixed slab in Fig. 14.2*a*, assumed here to be equally reinforced for positive and negative moments, will have an elastic distribution of moments, as shown in Fig. 14.2*b*. As the load is gradually increased, the more highly stressed sections at the support start yielding. Rotations occur at the support line hinges, but restraining moments of constant value m_p continue to act. The load can be increased further, until the moment at midspan becomes equal to the moment capacity there, and a third yield line forms, as shown in Fig. 14.2*c*. The slab is now a mechanism, large deflections occur, and collapse takes place.

The moment diagram just before failure is shown in Fig. 14.2*d*. Note that the ratio of elastic positive to negative moments of 1:2 no longer holds. Due to inelastic deformation, the ratio of these moments just before collapse is 1:1 for this particular structure. Redistribution of moments was discussed earlier in Section 12.9, and it was pointed out that the moment ratios at the collapse stage depend upon the reinforcement provided, not upon the results of elastic analysis.

14.2 UPPER AND LOWER BOUND THEOREMS

Plastic analysis methods such as the yield line theory derive from the general theory of structural plasticity, which states that the collapse load of a structure lies between two limits, an upper bound and a lower bound of the true collapse load. These limits can be found by well-established methods. A full solution by the theory of plasticity would attempt to make the lower and upper bounds converge to a single correct solution.

The lower bound theorem and the upper bound theorem, when applied to slabs, can be stated as follows:

> **Lower bound theorem:** If, for a given external load, it is possible to find a distribution of moments that satisfies equilibrium requirements, with the moment not exceeding the yield moment at any location, and if the boundary conditions are satisfied, then the given load is a lower bound of the true carrying capacity.

> **Upper bound theorem:** If, for a small increment of displacement, the internal work done by the slab, assuming that the moment at every plastic hinge is equal to the yield moment and that boundary conditions are satisfied, is equal to the external work done by the given load for that same small increment of displacement, then that load is an upper bound of the true carrying capacity.

If the lower bound conditions are satisfied, the slab can certainly carry the given load, although a higher load may be carried if internal redistributions of moment occur. If the upper bound conditions are satisfied, a load greater than the given load will certainly cause failure, although a lower load may produce collapse if the selected failure mechanism is incorrect in any sense.

In practice, in the plastic analysis of structures, one works with either the lower bound theorem or the upper bound theorem, not both, and precautions are taken to ensure that the predicted failure load at least closely approaches the correct value.

The yield line method of analysis for slabs is an upper bound method, and consequently, the failure load calculated for a slab with known flexural resistances may be higher than the true value. This is certainly a concern, as the designer would naturally prefer to be correct, or at least on the safe side. However, procedures can be incorporated in yield line analysis to help ensure that the calculated capacity is correct. Such procedures will be illustrated by the examples in Sections 14.4 and 14.5.

14.3 RULES FOR YIELD LINES

The location and orientation of the yield line were evident for the simple slab in Fig. 14.1. Similarly, the yield lines were easily established for the one-way indeterminate slab in Fig. 14.2. For other cases, it is helpful to have a set of guidelines for drawing yield lines and locating axes of rotation. When a slab is on the verge of collapse because of the existence of a sufficient number of real or plastic hinges to form a mechanism, axes of rotation will be located along the lines of support or over point supports such as columns. The slab segments can be considered to rotate as rigid bodies in space about these axes of rotation. The yield line between any two adjacent slab segments is a straight line, being the intersection of two essentially plane surfaces. Because the yield line (as a line of intersection of two planes) contains all points common to these two planes, it must contain the point of intersection (if any) of the two axes of rotation, which is also common to the two planes. That is, the yield line (or yield line extended) must pass through the point of intersection of the axes of rotation of the two adjacent slab segments.

The terms *positive yield line* and *negative yield line* are used to distinguish between those associated with tension at the bottom and tension at the top of the slab, respectively.

Guidelines for establishing axes of rotation and yield lines are summarized as follows:

1. Yield lines are straight lines because they represent the intersection of two planes.
2. Yield lines represent axes of rotation.
3. The supported edges of the slab will also establish axes of rotation. If the edge is fixed, a negative yield line may form, providing constant resistance to rotation. If the edge is simply supported, the axis of rotation provides zero restraint.
4. An axis of rotation will pass over any column support. Its orientation depends on other considerations.
5. Yield lines form under concentrated loads, radiating outward from the point of application.
6. A yield line between two slab segments must pass through the point of intersection of the axes of rotation of the adjacent slab segments.

In Fig. 14.3, which shows a slab simply supported along its four sides, rotation of slab segments A and B is about ab and cd, respectively. The yield line ef between these two segments is a straight line passing through f, the point of intersection of the axes of rotation.

Illustrations are given in Fig. 14.4 of the application of the guidelines to the establishment of yield line locations and failure mechanisms for a number of slabs with various support conditions. Figure 14.4*a* shows a slab continuous over parallel supports. Axes of rotation are situated along the supports (negative yield lines) and near midspan, parallel to the supports (positive yield line). The particular location of the positive yield line in this case and the other cases in Fig. 14.4 depends upon the distribution of loading and the reinforcement of the slab. Methods for determining its location will be discussed later.

For the continuous slab on nonparallel supports, shown in Fig. 14.4*b*, the midspan yield line (extended) must pass through the intersection of the axes of rotation over the supports. In Fig. 14.4*c* there are axes of rotation over all four simple supports. Positive yield lines form along the lines of intersection of the rotating segments of the slab. A rectangular two-way slab on simple supports is shown in Fig. 14.4*d*. The diagonal yield lines must pass through the corners, while the central yield line is

FIGURE 14.3
Two-way slab with simply supported edges.

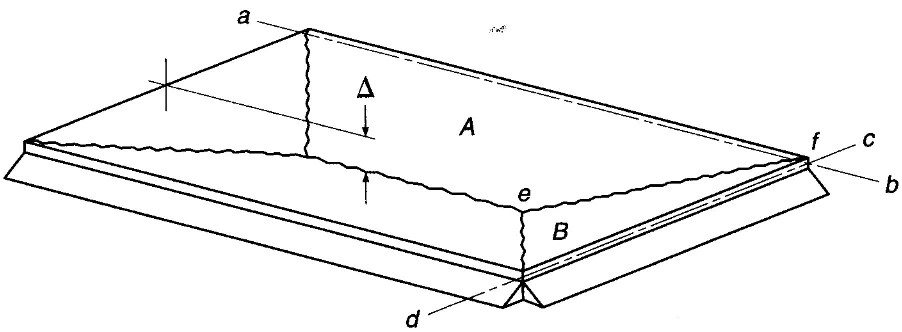

FIGURE 14.4
Typical yield line patterns.

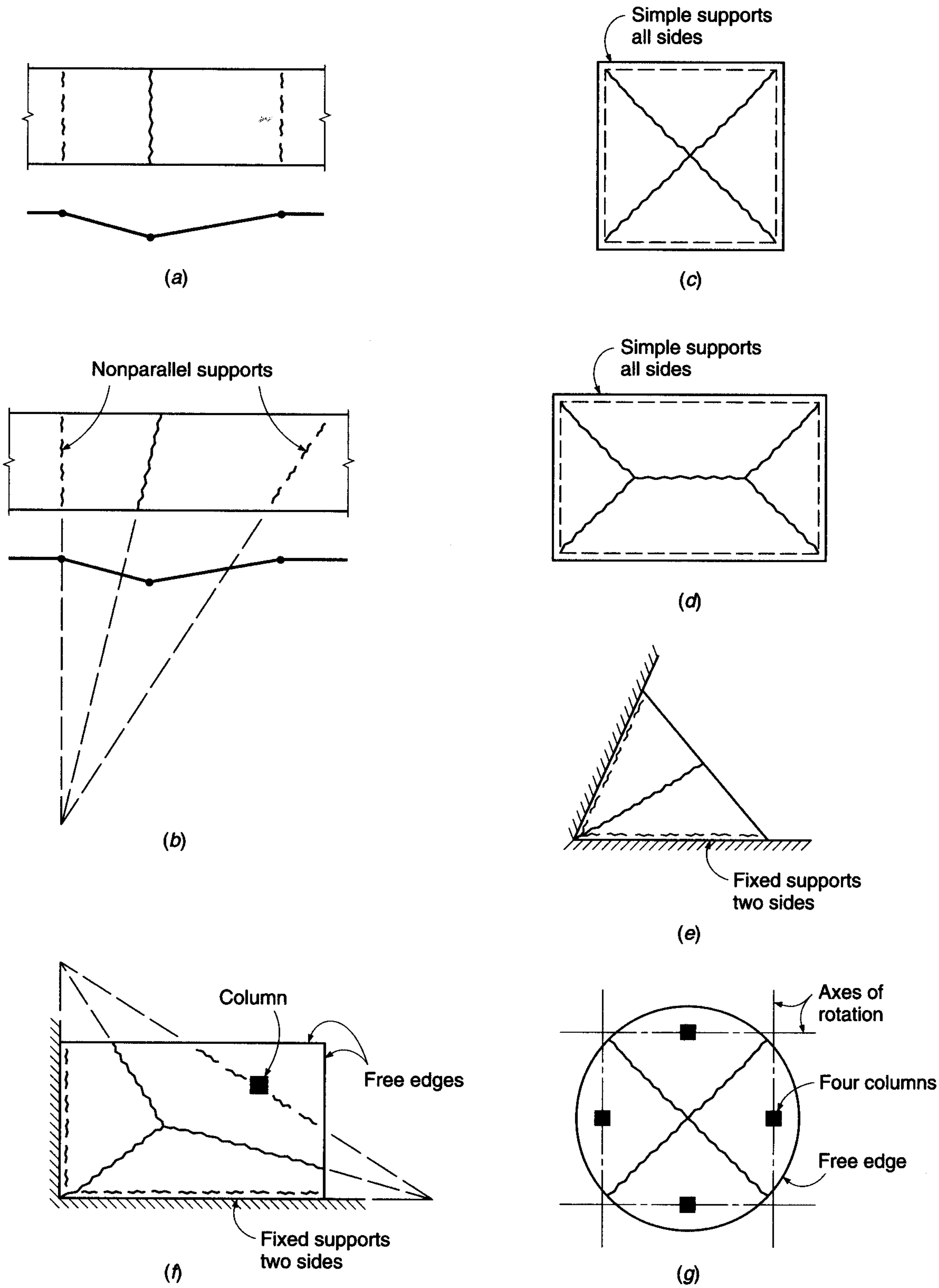

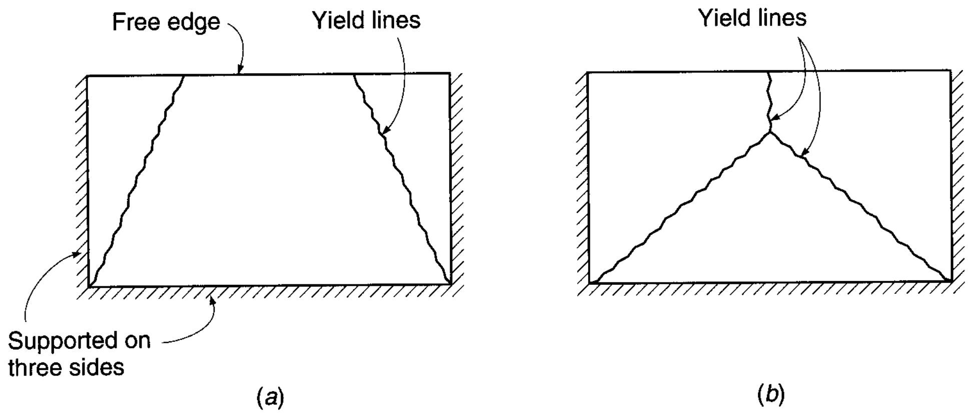

FIGURE 14.5
Alternative mechanisms for a slab supported on three sides.

parallel to the two long sides (axes of rotation along opposite supports intersect at infinity in this case).

With this background, the reader should have no difficulty in applying the guidelines to the slabs in Fig. 14.4*e* to *g* to confirm the general pattern of yield lines shown. Many other examples will be found in Refs. 14.1 to 14.15.

Once the general pattern of yielding and rotation has been established by applying the guidelines just stated, the specific location and orientation of the axes of rotation and the failure load for the slab can be established by either of two methods. The first will be referred to as the *method of segment equilibrium* and will be presented in Section 14.4. It requires consideration of the equilibrium of the individual slab segments forming the collapse mechanism and leads to a set of simultaneous equations permitting solution for the unknown geometric parameters and for the relation between load capacity and resisting moments. The second, the *method of virtual work*, will be described in Section 14.5. This method is based on equating the internal work done at the plastic hinges with the external work done by the loads as the predefined failure mechanism is given a small virtual displacement.

It should be emphasized that *either method of yield line analysis is an upper bound approach* in the sense that the true collapse load will never be higher, but may be lower, than the load predicted. For either method, the solution has two essential parts: (1) establishing the correct failure pattern and (2) finding the geometric parameters that define the exact location and orientation of the yield lines and solving for the relation between applied load and resisting moments. Either method can be developed in such a way as to lead to the correct solution for the mechanism chosen for study, but the true failure load will be found only if the correct mechanism has been selected.

For example, the rectangular slab in Fig. 14.5, supported along only three sides and free along the fourth, may fail by either of the two mechanisms shown. An analysis based on yield pattern *a* may indicate a slab capacity higher than one based on pattern *b*, or vice versa. It is necessary to investigate *all possible mechanisms* for any slab to confirm that the correct solution, giving the lowest failure load, has been found.†

† The importance of this point was underscored by Professor Arne Hillerborg, of Lund Institute of Technology, Sweden, in a letter to the editor of the ACI publication *Concr. Intl*, vol. 13, no. 5, 1991. Professor Hillerborg noted that, in reality, there are two additional yield line patterns for a slab such as shown in Fig. 14.5. For a particular set of dimensions and reinforcement, both of these gave a lower failure load than did the mechanism shown in Fig. 14.5*a*.

The method of segment equilibrium should not be confused with a true equilibrium method such as the strip method described in Chapter 15. A true equilibrium method is a lower bound method of analysis; i.e., it will always give a *lower bound* of the true capacity of the slab.

14.4 ANALYSIS BY SEGMENT EQUILIBRIUM

Once the general pattern of yielding and rotation has been established by applying the guidelines of Section 14.3, the location and orientation of axes of rotation and the failure load for the slab can be established based on the equilibrium of the various segments of the slab. Each segment, studied as a free body, must be in equilibrium under the action of the applied loads, the moments along the yield lines, and the reactions or shear along the support lines. Because the yield moments are principal moments, twisting moments are zero along the yield lines, and in most cases the shearing forces are also zero. Only the unit moment m generally is considered in writing equilibrium equations.

EXAMPLE 14.1

Segment equilibrium analysis of one-way slab. The method will be demonstrated first with respect to the one-way, uniformly loaded, continuous slab of Fig. 14.6*a*. The slab has a 10 ft span and is reinforced to provide a resistance to positive bending $\phi m_n = 5.0$ ft-kips/ft through the span. In addition, negative steel over the supports provides moment capacities of 5.0 ft-kips/ft at A and 7.5 ft-kips/ft at C. Determine the load capacity of the slab.

Solution. The number of equilibrium equations required will depend upon the number of unknowns. One unknown is always the relation between the resisting moments of the slab and the load. Other unknowns are needed to define the locations of yield lines. In the present instance, one additional equation will suffice to define the distance of the yield line from the

FIGURE 14.6
Analysis of a one-way slab by segment equilibrium equations.

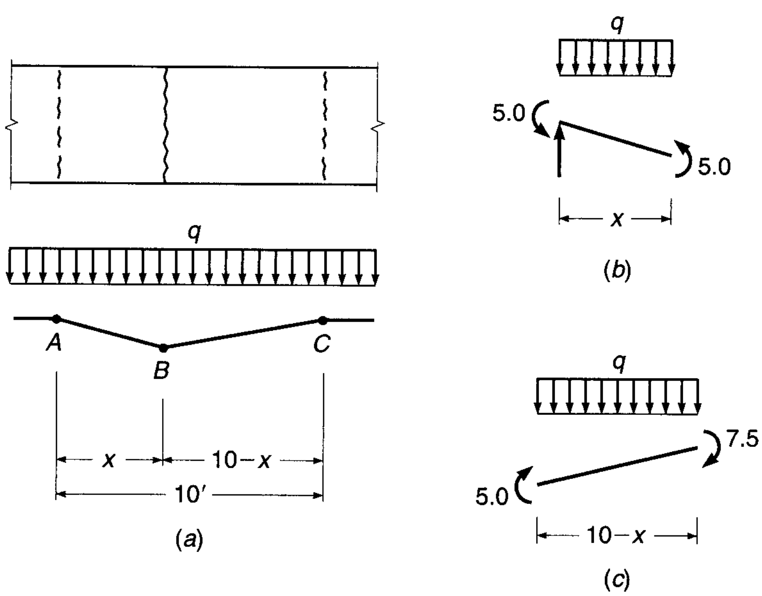

supports. Taking the left segment of the slab as a free body and writing the equation for moment equilibrium about the left support line (see Fig. 14.6*b*) lead to

$$\frac{qx^2}{2} - 10.0 = 0 \tag{a}$$

Similarly, for the right slab segment,

$$\frac{q}{2}(10 - x)^2 - 12.5 = 0 \tag{b}$$

Solving Eqs. (*a*) and (*b*) simultaneously for w and x results in

$$q = 0.89 \text{ kip/ft}^2 \qquad x = 4.75 \text{ ft}$$

If a slab is reinforced in orthogonal directions so that the resisting moment is the same in these two directions, the moment capacity of the slab will be the same along any other line, regardless of direction. Such a slab is said to be *isotropically* reinforced. If, however, the strengths are different in two perpendicular directions, the slab is called *orthogonally anisotropic*, or simply *orthotropic*. Only isotropic slabs will be discussed in this section. Orthotropic reinforcement, which is very common in practice, will be discussed in Section 14.6.

It is convenient in yield line analysis to represent moments with vectors. The standard convention, in which the moment acts in a clockwise direction when viewed along the vector arrow, will be followed. Treatment of moments as vector quantities will be illustrated by the following example:

EXAMPLE 14.2 **Segment equilibrium analysis of square slab.** A square slab is simply supported along all sides and is to be isotropically reinforced. Determine the resisting moment $m = \phi m_n$ per linear foot required just to sustain a uniformly distributed factored load of q psf.

SOLUTION. Conditions of symmetry indicate the yield line pattern shown in Fig. 14.7*a*. Considering the moment equilibrium of any one of the identical slab segments about its support (see Fig. 14.7*b*), one obtains

$$\frac{qL^2}{4}\frac{L}{6} - 2\frac{mL}{\sqrt{2}}\frac{1}{\sqrt{2}} = 0$$

$$m = \frac{qL^2}{24}$$

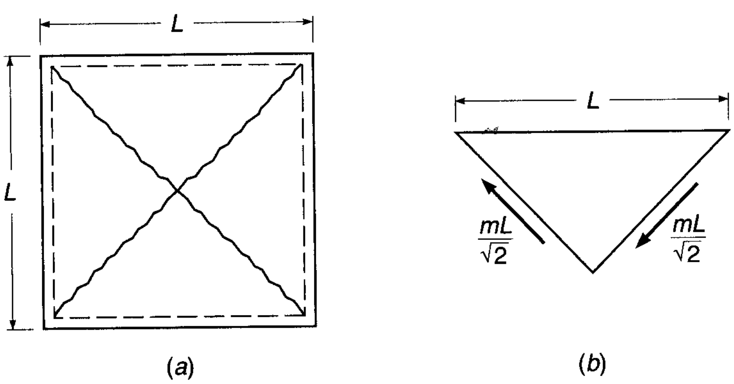

FIGURE 14.7
Analysis of a square two-way slab by segment equilibrium equations.

In both examples just given, the resisting moment was constant along any particular yield line; i.e., the reinforcing bars were of constant diameter and equally spaced along a given yield line. On the other hand, it will be recalled that, by the elastic methods of slab analysis presented in Chapter 13, reinforcing bars generally have a different spacing and may be of different diameter in middle strips compared with column or edge strips. A slab designed by elastic methods, leading to such variations, can easily be analyzed for strength by the yield line method. It is merely necessary to subdivide a yield line into its component parts, within any one of which the resisting moment per unit length of hinge is constant. Either the equilibrium equations of this section or the work equations of Section 14.5 can be modified in this way.

14.5 ANALYSIS BY VIRTUAL WORK

Alternative to the method of Section 14.4 is a method of analysis using the principle of virtual work. Since the moments and loads are in equilibrium when the yield line pattern has formed, an infinitesimal increase in load will cause the structure to deflect further. The external work done by the loads to cause a small arbitrary virtual deflection must equal the internal work done as the slab rotates at the yield lines to accommodate this deflection. The slab is therefore given a virtual displacement, and the corresponding rotations at the various yield lines can be calculated. By equating internal and external work, the relation between the applied loads and the resisting moments of the slab is obtained. Elastic rotations and deflections are not considered when writing the work equations, as they are very small compared with the plastic deformations.

a. External Work Done by Loads

An external load acting on a slab segment, as a small virtual displacement is imposed, does work equal to the product of its constant magnitude and the distance through which the point of application of the load moves. If the load is distributed over a length or an area, rather than concentrated, the work can be calculated as the product of the total load and the displacement of the point of application of its resultant.

Figure 14.8 illustrates the basis for external work calculation for several types of loads. If a square slab carrying a single concentrated load at its center (Fig. 14.8*a*) is given a virtual displacement defined by a unit value under the load, the external work is

$$W_e = P \times 1 \qquad (a)$$

If the slab shown in Fig. 14.8*b*, supported along three sides and free along the fourth, is loaded with a line load w per unit length along the free edge, and if that edge is given a virtual displacement having unit value along the central part, the external work is

$$W_e = (2wa) \times \frac{1}{2} + wb = w(a + b) \qquad (b)$$

When a distributed load q per unit area acts on a triangular segment defined by a hinge and yield lines, such as Fig. 14.8*c*,

$$W_e = \frac{qab}{2} \times \frac{1}{3} = \frac{qab}{6} \qquad (c)$$

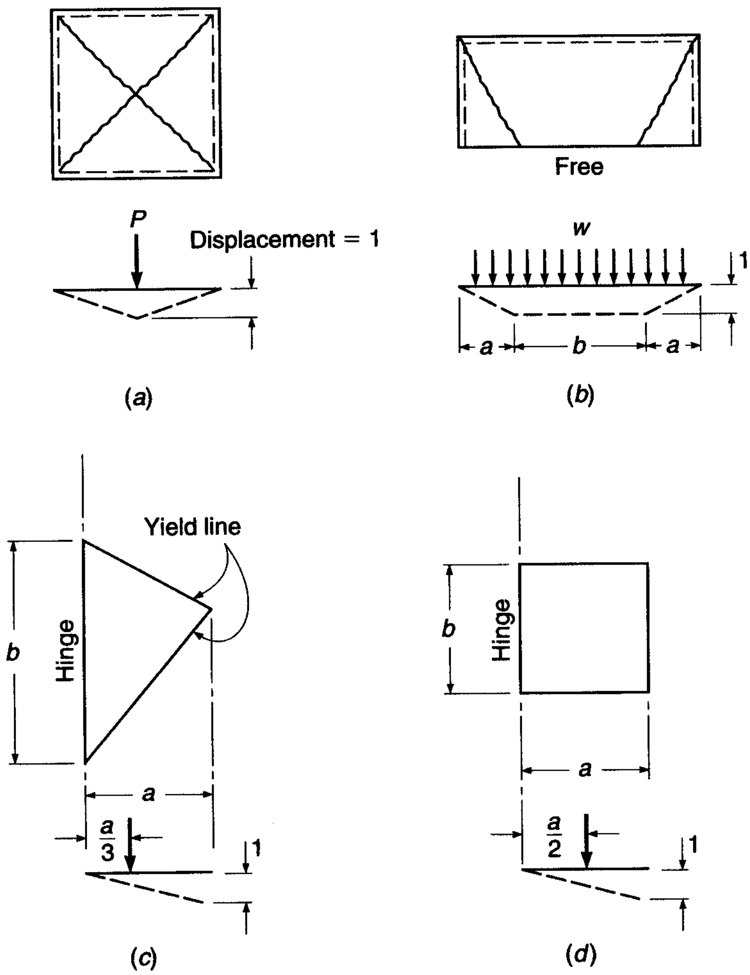

FIGURE 14.8
External work basis for various types of loads.

while for the rectangular slab segment shown in Fig. 14.8*d*, carrying a distributed load q per unit area, the external work is

$$W_e = \frac{qab}{2} \tag{d}$$

More complicated trapezoidal shapes may always be subdivided into component triangles and rectangles. The total external work is then calculated by summing the work done by loads on the individual parts of the failure mechanism, with all displacements keyed to a unit value assigned somewhere in the system. There is no difficulty in combining the work done by concentrated loads, line loads, and distributed loads, if these act in combination.

b. Internal Work Done by Resisting Moments

The internal work done during the assigned virtual displacement is found by summing the products of yield moment m per unit length of hinge times the plastic rotation θ at the respective yield lines, consistent with the virtual displacement. If the resisting moment m is constant along a yield line of length l, and if a rotation θ is experienced, the internal work is

$$W_i = ml\theta \tag{e}$$

If the resisting moment varies, as would be the case if bar size or spacing were not constant along the yield line, the yield line is divided into n segments, within each one of which the moment is constant. The internal work is then

$$W_i = (m_1 l_1 + m_2 l_2 + \cdots + m_n l_n)\theta \tag{f}$$

For the entire system, the total internal work done is the sum of the contributions from all yield lines. In all cases, the internal work contributed is positive, regardless of the sign of m, because the rotation is in the same direction as the moment. External work, on the other hand, may be either positive or negative, depending on the direction of the displacement of the point of application of the force resultant.

EXAMPLE 14.3

Virtual work analysis of one-way slab. Determine the load capacity of the one-way uniformly loaded continuous slab shown in Fig. 14.9, using the method of virtual work. The resisting moments of the slab are 5.0, 5.0, and 7.5 ft-kips/ft at A, B, and C, respectively.

SOLUTION. A unit deflection is given to the slab at B. Then the external work done by the load is the sum of the loads times their displacements and is equal to

$$\frac{qx}{2} + \frac{q}{2}(10 - x)$$

The rotations at the hinges are calculated in terms of the unit deflection (Fig. 14.9) and are

$$\theta_A = \theta_{B1} = \frac{1}{x} \qquad \theta_{B2} = \theta_C = \frac{1}{10 - x}$$

The internal work is the sum of the moments times their corresponding rotation angles:

$$5 \times \frac{1}{x} \times 2 + 5 \times \frac{1}{10 - x} + 7.5 \times \frac{1}{10 - x}$$

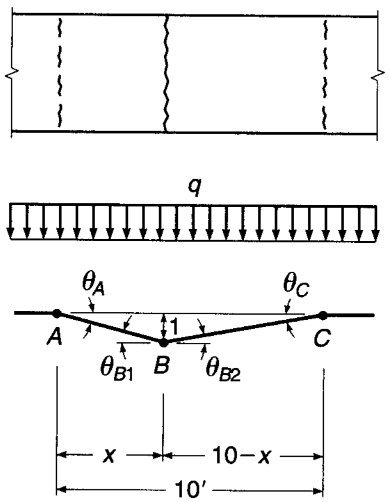

FIGURE 14.9
Virtual work analysis of one-way slab.

Equating the external and internal work gives

$$\frac{qx}{2} + 5q - \frac{qx}{2} = \frac{10}{x} + \frac{5}{10-x} + \frac{7.5}{10-x}$$

$$5q = \frac{10}{x} + \frac{25}{2(10-x)}$$

$$q = \frac{2}{x} + \frac{5}{2(10-x)}$$

To determine the minimum value of w, this expression is differentiated with respect to x and set equal to zero:

$$\frac{dq}{dx} = -\frac{2}{x^2} + \frac{5}{2(10-x)^2} = 0$$

from which

$$x = 4.75 \text{ ft}$$

Substituting this value in the preceding expression for w, one obtains

$$q = 0.89 \text{ kips/ft}^2$$

as before.

In many cases, particularly those with yield lines established by several unknown dimensions (such as Fig. 14.4f), direct solution by virtual work would become quite tedious. The ordinary derivatives in Example 14.3 would be replaced by several partial derivatives, producing a set of equations to be solved simultaneously. In such cases it is often more convenient to select an arbitrary succession of possible yield line locations, solve the resulting mechanisms for the unknown load (or unknown moment), and determine the correct minimum load (or maximum moment) by trial.

EXAMPLE 14.4 **Virtual work analysis of rectangular slab.** The two-way slab shown in Fig. 14.10 is simply supported on all four sides and carries a uniformly distributed load of q psf. Determine the required moment resistance for the slab, which is to be isotropically reinforced.

Solution. Positive yield lines will form in the pattern shown in Fig. 14.10a, with the dimension a unknown. The correct dimension a will be such as to maximize the moment resistance required to support the load q. The values of a and m will be found by trial.

In Fig. 14.10a the length of the diagonal yield line is $\sqrt{25 + a^2}$. From similar triangles,

$$b = 5\frac{\sqrt{25 + a^2}}{a} \qquad c = a\frac{\sqrt{25 + a^2}}{5}$$

Then the rotation of the plastic hinge at the diagonal yield line corresponding to a unit deflection at the center of the slab (see Fig. 14.10b) is

$$\theta_1 = \frac{1}{b} + \frac{1}{c} = \frac{a}{5\sqrt{25 + a^2}} + \frac{5}{a\sqrt{25 + a^2}} = \frac{1}{\sqrt{25 + a^2}}\left(\frac{a}{5} + \frac{5}{a}\right)$$

The rotation of the yield line parallel to the long edges of the slab (see Fig. 14.10c) is

$$\theta_2 = \frac{1}{5} + \frac{1}{5} = 0.40$$

FIGURE 14.10
Virtual work analysis for rectangular two-way slab.

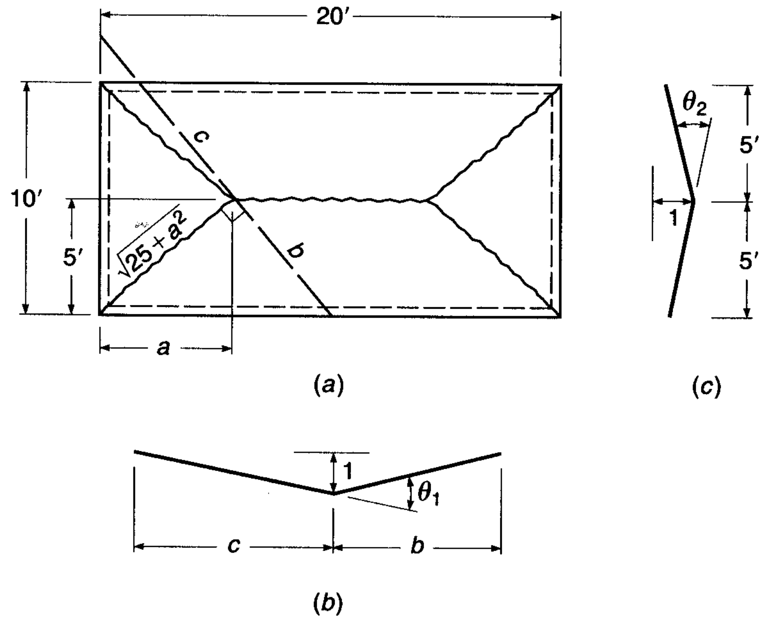

For a first trial, let $a = 6$ ft. Then the length of the diagonal yield line is

$$\sqrt{25 + 36} = 7.81 \text{ ft}$$

The rotation at the diagonal yield line is

$$\theta_1 = \frac{1}{7.81}\left(\frac{6}{5} + \frac{5}{6}\right) = 0.261$$

At the central yield line, it is $\theta_2 = 0.40$. The internal work done as the incremental deflection is applied is

$$W_i = (m \times 7.81 \times 0.261 \times 4) + (m \times 8 \times 0.40) = 11.36m$$

The external work done during the same deflection is

$$W_e = (10 \times 6 \times \tfrac{1}{2}q \times \tfrac{1}{3} \times 2) + (8 \times 5q \times \tfrac{1}{2} \times 2) + (12 \times 5 \times \tfrac{1}{2}q \times \tfrac{1}{3} \times 2) = 80q$$

Equating W_i and W_e, one obtains

$$m = \frac{80q}{11.36} = 7.05q$$

Successive trials for different values of a result in the following data:

a	W_i	W_e	m
6.0	11.36m	80.0q	7.05q
6.5	11.08m	78.4q	7.08q
7.0	10.87m	76.6q	7.04q
7.5	10.69m	75.0q	7.02q

It is evident that the yield line pattern defined by $a = 6.5$ ft is critical. The required resisting moment for the given slab is 7.08q.

14.6 ORTHOTROPIC REINFORCEMENT AND SKEWED YIELD LINES

Generally slab reinforcement is placed orthogonally, i.e., in two perpendicular directions. The same reinforcement is often provided in each direction, but the effective depths will be different. In many practical cases, economical designs are obtained using reinforcement having different bar areas or different spacings in each direction. In such cases, the slab will have different moment capacities in the two orthogonal directions and is said to be orthogonally anisotropic, or simply orthotropic.

Often yield lines will form at an angle with the directions established by the reinforcement; this was so in many of the examples considered earlier. For yield line analysis, it is necessary to calculate the resisting moment, per unit length, along such skewed yield lines. This requires calculation of the contribution to resistance from each of the two sets of bars.

Figure 14.11*a* shows an orthogonal grid of reinforcement, with angle α between the yield line and the X direction bars. Bars in the X direction are at spacing v and have moment resistance m_y per unit length about the Y axis, while bars in the Y direction are at spacing u and have moment resistance m_x per unit length about the X axis. The resisting moment per unit length for the bars in the Y and X directions will be determined separately, with reference to Fig. 14.11*b* and *c*, respectively.

For the Y direction bars, the resisting moment *per bar* about the X axis is $m_x u$, and the component of that resistance about the α axis is $m_x u \cos \alpha$. The resisting moment per unit length along the α axis provided by the Y direction bars is therefore

$$m_{\alpha y} = \frac{m_x u \cos \alpha}{u/\cos \alpha} = m_x \cos^2 \alpha \tag{a}$$

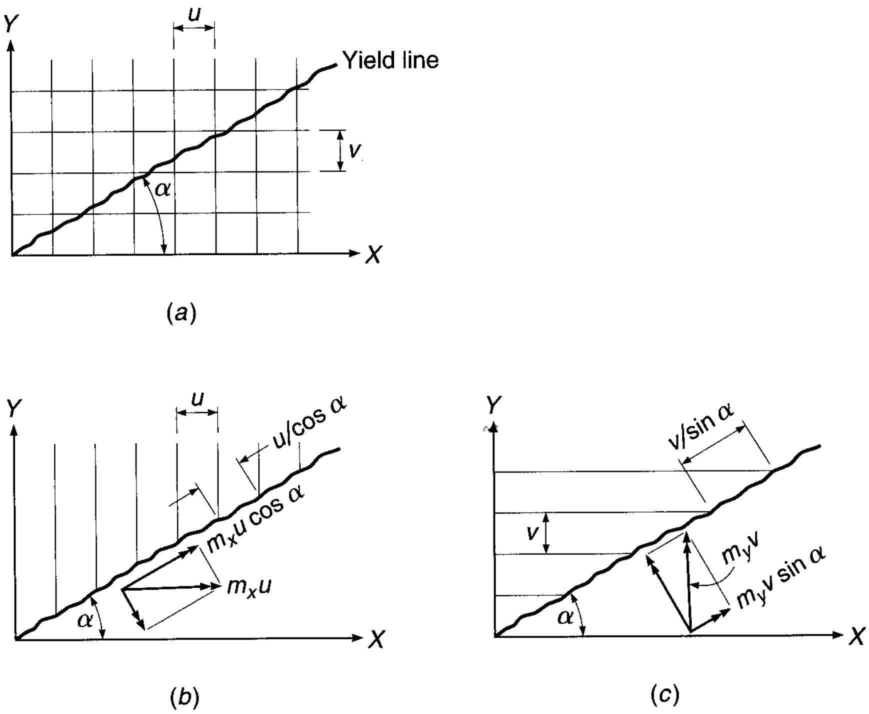

FIGURE 14.11
Yield line skewed with orthotropic reinforcement: (*a*) orthogonal grid and yield line; (*b*) Y direction bars; (*c*) X direction bars.

For the bars in the X direction, the resisting moment per bar about the Y axis is $m_y v$, and the component of that resistance about the α axis is $m_y v \sin \alpha$. Thus the resisting moment per unit length along the α axis provided by the X direction bars is

$$m_{\alpha x} = \frac{m_y v \sin \alpha}{v/\sin \alpha} = m_y \sin^2 \alpha \qquad (b)$$

Thus, for the combined sets of bars, the resisting moment per unit length measured along the α axis is given by the sum of the resistances from Eqs. (a) and (b):

$$m_\alpha = m_x \cos^2 \alpha + m_y \sin^2 \alpha \qquad (14.1)$$

For the special case where $m_x = m_y = m$, with the same reinforcement provided in each direction,

$$m_\alpha = m(\cos^2 \alpha + \sin^2 \alpha) = m \qquad (14.2)$$

The slab is said to be *isotropically reinforced*, with the same resistance per unit length regardless of the orientation of the yield line.

The analysis just presented neglects any consideration of strain compatibility along the yield line, and assumes that the displacements at the level of the steel during yielding, which are essentially perpendicular to the yield line, are sufficient to produce yielding in both sets of bars. This is reasonably in accordance with test data, except for values of α close to 0 to 90°. For such cases, it would be conservative to neglect the contribution of the bars nearly parallel to the yield line.

It has been shown that the analysis of an orthotropic slab can be simplified to that of a related isotropic slab, referred to as the *affine slab*, provided that the ratio of negative to positive reinforcement areas is the same in both directions. The horizontal dimensions and slab loads must be modified to permit this transformation. Details will be found in Refs. 14.1 to 14.5.

EXAMPLE 14.5 **Resisting moment along a skewed yield line.** The balcony slab in Fig. 14.12 has fixed supports along two adjacent sides and is unsupported along the third side. It is reinforced for positive bending with No. 5 (No. 16) bars at 10 in. spacing and 5.5 in. effective depth, parallel

FIGURE 14.12
Skewed yield line example.

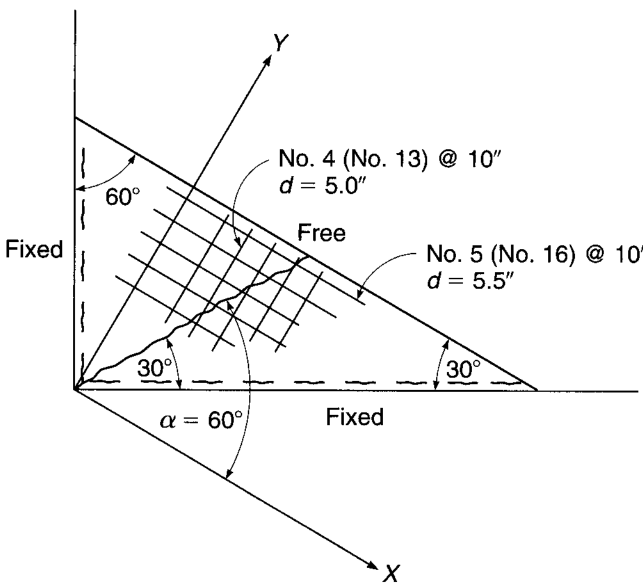

to the free edge, and No. 4 (No. 13) bars at 10 in. spacing and 5.0 in. effective depth perpendicular to that edge. Concrete strength and steel yield stress are 4000 psi and 60,000 psi, respectively. One possible failure mechanism includes a positive yield line at 30° with the long edge, as shown. Find the total resisting moment along the positive yield line provided by the two sets of bars.

Solution. It is easily confirmed that the resisting moment about the X axis provided by the Y direction bars is $m_x = 5.21$ ft-kips/ft, and the resisting moment about the Y axis provided by the X direction bars is $m_y = 8.70$ ft-kips/ft (both with $\phi = 0.90$ included). The yield line makes an angle of 60° with the X axis bars. With $\cos\alpha = 0.500$ and $\sin\alpha = 0.866$, from Eq. (14.1) the resisting moment along the α axis is

$$m_\alpha = 5.21 \times 0.500^2 + 8.70 \times 0.866^2 = 7.83 \text{ ft-kips/ft}$$

14.7 SPECIAL CONDITIONS AT EDGES AND CORNERS

Certain simplifications were made in defining yield line patterns in some of the preceding examples, in the vicinity of edges and corners. In some cases, such as Fig. 14.4*b* and *f*, positive yield lines were shown intersecting an edge at an angle. Actually, at a free or simply supported edge, both bending and twisting moments should theoretically be zero. The principal stress directions are parallel and perpendicular to the edge, and consequently the yield lines should enter an edge perpendicular to it. Tests confirm that this is the case, but the yield lines generally turn only quite close to the edge, the distance t in Fig. 14.13 being small compared to the dimensions of the slab (Ref. 14.4).

Referring to Fig. 14.13, the actual yield line of *a* can be simplified by extending the yield line in a straight line to the edge, as in *b*, if a pair of concentrated shearing forces m_t is introduced at the corners of the slab segments. The force m_t acting downward at the acute corner (circled cross) and the force m_t acting upward at the obtuse corner (circled dot) together are the static equivalent of twisting moments and shearing forces near the edge. It is shown in Ref. 14.4 that the magnitude of the fictitious shearing forces m_t is given by the expression

$$m_t = m \cot\alpha \tag{14.3}$$

where m is the resisting moment per unit length along the yield line and α is the acute angle between the simplified yield line and the edge of the slab.

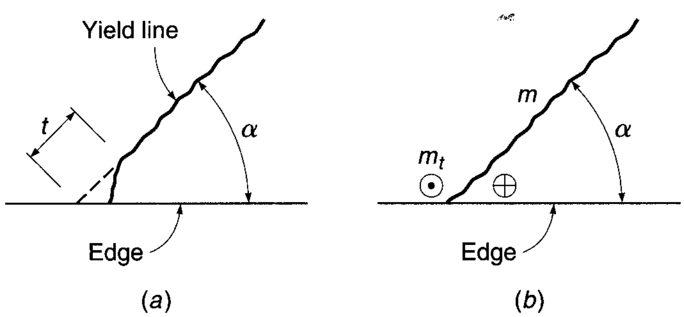

FIGURE 14.13
Conditions at edge of slab:
(*a*) actual yield line;
(*b*) simplified yield line.

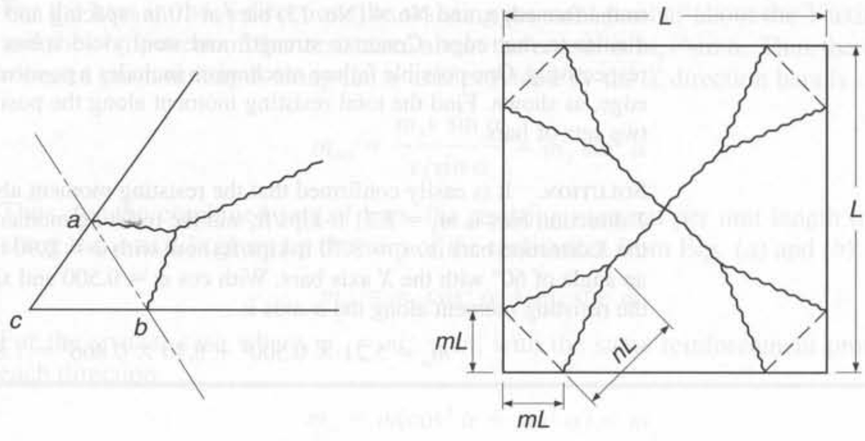

FIGURE 14.14
Corner conditions.

It should be noted that while the fictitious forces enter the solution by the equilibrium method, the virtual work solution is not affected because the net work done by the pair of equal and opposite forces moving through the identical virtual displacement is zero.

Also, in the preceding examples, it was assumed that yield lines enter the corners between the two intersecting sides. An alternative possibility is that the yield line forks before it reaches the corner, forming what is known as a *corner lever*, shown in Fig. 14.14*a*.

If the corner is not held down, the triangular element *abc* will pivot about the axis *ab* and lift off the supports. The development of such a corner lever is clearly shown in Fig. 14.15. The photograph shows a model reinforced concrete slab that was tested under uniformly distributed load. The edges were simply supported and were

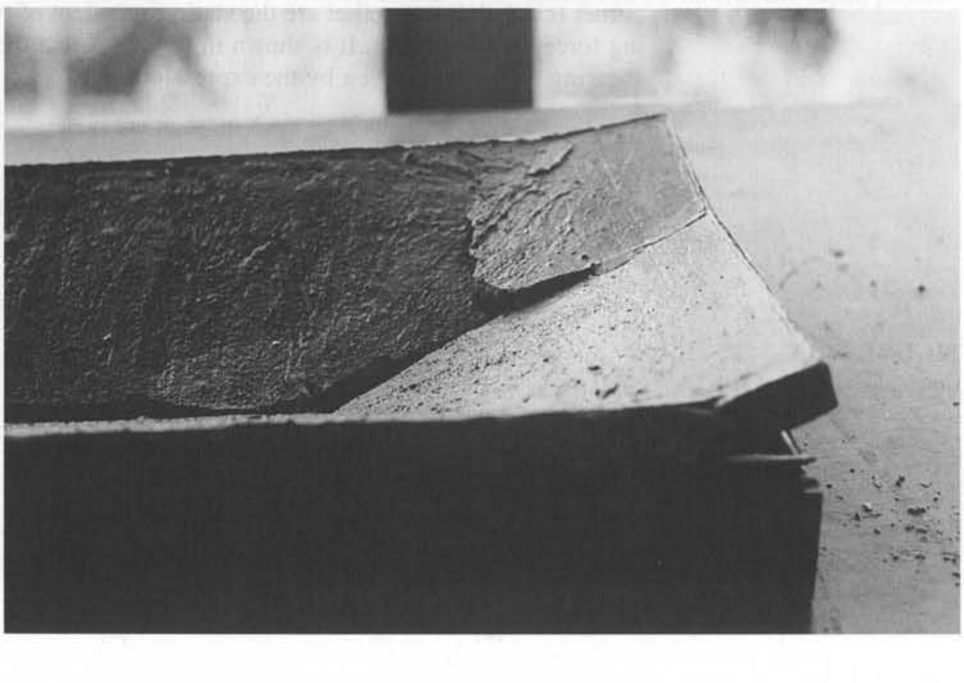

FIGURE 14.15
Development of corner levers in a simply supported, uniformly loaded slab.

not restrained against upward movement. If the corner is held down, a similar situation occurs, except that the line *ab* becomes a yield line. If cracking at the corners of such a slab is to be controlled, top steel more or less perpendicular to the line *ab* must be provided. The direction taken by the positive yield lines near the corner indicates the desirability of supplementary bottom-slab reinforcement at the corners, placed approximately parallel to the line *ab* (see Section 13.4).

Although yield line patterns with corner levers are generally more critical than those without, they are often neglected in yield line analysis. The analysis becomes considerably more complicated if the possibility of corner levers is introduced, and the error made by neglecting them is usually small.

To illustrate, the uniformly loaded square slab of Example 14.2, when analyzed for the assumed yield pattern shown in Fig. 14.7, required a moment capacity of $qL^2/24$. The actual yield line pattern at failure is probably as shown in Fig. 14.14*b*. Since two additional parameters *m* and *n* have necessarily been introduced to define the yield line pattern, a total of three equations of equilibrium is now necessary. These equations are obtained by summing moments and vertical forces on the segments of the slab. Such an analysis results in a required resisting moment of $qL^2/22$, an increase of about 9 percent compared with the results of an analysis neglecting corner levers. The influence of such corner effects may be considerably larger when the corner angle is less than 90°.

14.8 FAN PATTERNS AT CONCENTRATED LOADS

If a concentrated load acts on a reinforced concrete slab at an interior location, away from any edge or corner, a negative yield line will form in a more or less circular pattern, as in Fig. 14.16*a*, with positive yield lines radiating outward from the load point.

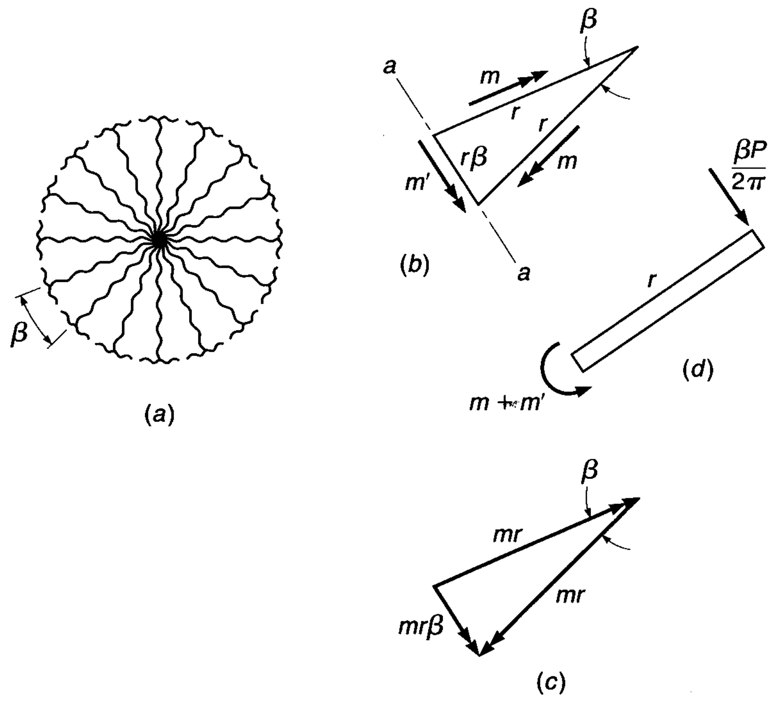

FIGURE 14.16
Yield fan geometry at concentrated load: (*a*) yield fan; (*b*) moment vectors acting on fan segment; (*c*) resultant of positive-moment vectors; (*d*) edge view of fan segment.

If the positive resisting moment per unit length is m and the negative resisting moment m', the moments per unit length acting along the edges of a single element of the fan, having a central angle β and radius r, are as shown in Fig. 14.16b. For small values of the angle β, the arc along the negative yield line can be represented as a straight line of length $r\beta$.

Figure 14.16c shows the moment resultant obtained by vector addition of the positive moments mr acting along the radial edges of the fan segment. The vector sum is equal to $mr\beta$, acting along the length $r\beta$, and the resultant positive moment, per unit length, is therefore m. This acts in the same direction as the negative moment m', as shown in Fig. 14.16d. Figure 14.16d also shows the fractional part of the total load P that acts on the fan segment.

Taking moments about the axis $a - a$ gives

$$(m + m')r\beta - \frac{\beta Pr}{2\pi} = 0$$

from which

$$P = 2\pi(m + m') \tag{14.4}$$

The collapse load P is seen to be independent of the fan radius r. Thus, with only a concentrated load acting, a complete fan of any radius could form with no change in collapse load.

It follows that Eq. (14.4) also gives the collapse load for a fixed-edge slab of any shape, carrying only a concentrated load P. The only necessary condition is that the boundary must be capable of a restraining moment equal to m' at all points. Finally, Eq. (14.4) is useful in establishing whether flexural failure will occur before a punching shear failure under a concentrated load.

Other load cases of practical interest, including a concentrated load near or at a free edge, and a concentrated corner load, are treated in Ref. 14.5. Loads distributed over small areas and load combinations are discussed in Ref. 14.12.

14.9 LIMITATIONS OF YIELD LINE THEORY

The usefulness of yield line theory should be apparent from the preceding sections. In general, elastic solutions are available only for restricted conditions, usually uniformly loaded rectangular slabs and slab systems. They do not account for the effects of inelastic action, except empirically. By yield line analysis, a rational determination of flexural strength may be had for slabs of any shape, supported in a variety of ways, with concentrated loads as well as distributed and partially distributed loads. The effects of holes of any size can be included. It is thus seen to be a powerful analytical tool for the structural engineer.

On the other hand, as an upper bound method, it will predict a collapse load that may be greater than the true collapse load. The actual capacity will be less than predicted if the selected mechanism is not the controlling one or if the specific locations of yield lines are not exactly correct. Most engineers would prefer an approach that would be in error, if at all, on the safe side. In this respect, the strip method of Chapter 15 is distinctly superior.

Beyond this, it should be evident that yield line theory provides, in essence, a method for determining the capacity of trial designs, arrived at by some other means, rather than for determining the amount and spacing of reinforcement. It is not, strictly speaking, a design method. To illustrate, yield line theory provides no inducement for the designer to place steel at anything other than a uniform lateral spacing along a yield line. It is necessary to consider the results of elastic analysis of a flat plate, for example, to recognize that reinforcement in that case should be placed in strong bands across the columns.

In applying yield line analysis to slabs, it must be remembered that the analysis is predicated upon available rotation capacity at the yield lines. If the slab reinforcement happens to correspond closely to the elastic distribution of moments in the slab, little rotation is required. If, on the other hand, there is a marked difference, it is possible that the required rotation will exceed the available rotation capacity, in which case the slab will fail prematurely. However, in general, because slabs are typically rather lightly reinforced, they will have adequate rotation capacity to attain the collapse loads predicted by yield line analysis.

It should also be borne in mind that the yield line analysis focuses entirely on the flexural capacity of the slab. It is presumed that earlier failure will not occur due to shear or torsion and that cracking and deflections at service load will not be excessive. ACI Code 13.5.1 calls attention specifically to the need to meet "all serviceability conditions, including limits on deflections," and ACI Commentary 13.5.1 calls attention to the need for "evaluation of the stress conditions around the supports in relation to shear and torsion as well as flexure."

REFERENCES

14.1. A. Ingerslev, "The Strength of Rectangular Slabs," *J. Inst. Struct. Eng.*, London, vol. 1, no. 1, 1923, pp. 3–14.
14.2. K. W. Johansen, *Brutlinieteorier*, Jul. Gjellerups Forlag, Copenhagen, 1943 (see also *Yield Line Theory*, English translation, Cement and Concrete Association, London, 1962).
14.3. K. W. Johansen, *Pladeformler*, 2nd ed., Polyteknisk Forening, Copenhagen, 1949 (see also *Yield Line Formulae for Slabs*, English translation, Cement and Concrete Association, London, 1972).
14.4. E. Hognestad, "Yield Line Theory for the Ultimate Flexural Strength of Reinforced Concrete Slabs," *J. ACI*, vol. 24, no. 7, 1953, pp. 637–656.
14.5. L. L. Jones and R. H. Wood, *Yield Line Analysis of Slabs*, American Elsevier, New York, 1967.
14.6. R. Taylor, D. R. H. Maher, and B. Hayes, "Effect of the Arrangement of Reinforcement on the Behavior of Reinforced Concrete Slabs," *Mag. Concr. Res.*, vol. 18, no. 55, 1966, pp. 85–94.
14.7. R. Lenschow and M. A. Sozen, "A Yield Criterion for Reinforced Concrete Slabs," *J. ACI*, vol. 64, no. 5, 1967, pp. 266–273.
14.8. S. H. Simmonds and A. Ghali, "Yield Line Design of Slabs," *J. Struct. Div.*, ASCE, vol. 102, no. ST1, 1976, pp. 109–123.
14.9. K. H. Chu and R. B. Singh, "Yield Analysis of Balcony Floor Slabs," *J. ACI*, vol. 63, no. 5, 1966, pp. 571–586.
14.10. E. C. Demsky and D. S. Hatcher, "Yield Line Analysis of Slabs Supported on Three Sides," *J. ACI*, vol. 66, no. 9, 1969, pp. 741–744.
14.11. A. Zaslavsky and C. H. Avraham, "Yield Line Design of Rectangular Reinforced Concrete Balconies," *J. ACI*, vol. 67, no. 1, 1970, pp. 53–56.
14.12. H. Gesund, "Limit Design of Slabs for Concentrated Loads," *J. Struct. Div.*, ASCE, vol. 107, no. ST9, 1981, pp. 1839–1856.
14.13. A. Zaslavsky, "Yield Line Analysis of Rectangular Slabs with Central Openings," *J. ACI*, vol. 64, no. 12, 1967, pp. 838–844.
14.14. S. Islam and R. Park, "Yield Line Analysis of Two-Way Reinforced Concrete Slabs with Openings," *J. Inst. Struct. Eng.*, vol. 49, no. 6, 1971, pp. 269–276.
14.15. R. Park and W. L. Gamble, *Reinforced Concrete Slabs*, 2nd ed., John Wiley & Sons, New York, 1999.

PROBLEMS

14.1. A square slab measuring 10 ft on each side is simply supported on three sides and unsupported along the fourth. It is reinforced for positive bending with an isotropic mat of steel providing resistance ϕm_n of 7000 ft-lb/ft in each of the two principal directions. Determine the uniformly distributed load that would cause flexural failure, using the method of virtual work.

14.2. The triangular slab shown in Fig. P14.2 has fixed supports along the two perpendicular edges and is free of any support along the diagonal edge. Negative reinforcement perpendicular to the supported edges provides design strength $\phi m_n = 4$ ft-kips/ft. The slab is reinforced for positive bending by an orthogonal grid providing resistance $\phi m_n = 2.67$ ft-kips/ft in all directions. Find the total factored load w_u that will produce flexural failure. A virtual work solution is suggested.

FIGURE P14.2

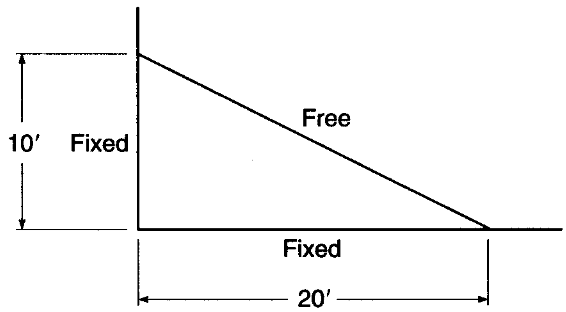

14.3. The one-way reinforced concrete slab shown in Fig. P14.3 spans 20 ft. It is simply supported at its left edge, fully fixed at its right edge, and free of support along the two long sides. Reinforcement provides design strength $\phi m_n =$ 5 ft-kips/ft in positive bending and $\phi m_n = 7.5$ ft-kips/ft in negative bending at the right edge. Using the equilibrium method, find the factored load q_u uniformly distributed over the surface that would cause flexural failure.

FIGURE P14.3

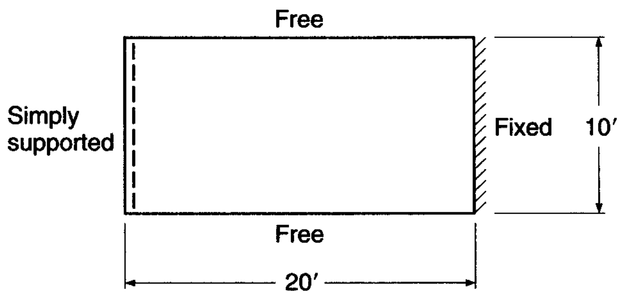

14.4. Solve Problem 14.3 using the method of virtual work.

14.5. The triangular slab shown in Fig. P14.5 is to serve as weather protection over a loading dock. Support conditions are essentially fixed along AB and BC, and AC is a free edge. In addition to self-weight, a superimposed dead load of 15 psf and service live load of 40 psf must be provided for. Material strengths are $f'_c = 4000$ psi and $f_y = 60{,}000$ psi. Using yield line analysis, find the required slab thickness h and find the reinforcement required at critical sections. Neglect corner pivots. Use a maximum reinforcement ratio of 0.005. Select bar sizes and spacings, and provide a sketch summarizing important aspects of the design. Make an approximate, conservative check of safety against shear failure for the design. Also include a conservative estimate of the deflection near the center of edge AC due to a full live load.

FIGURE P14.5

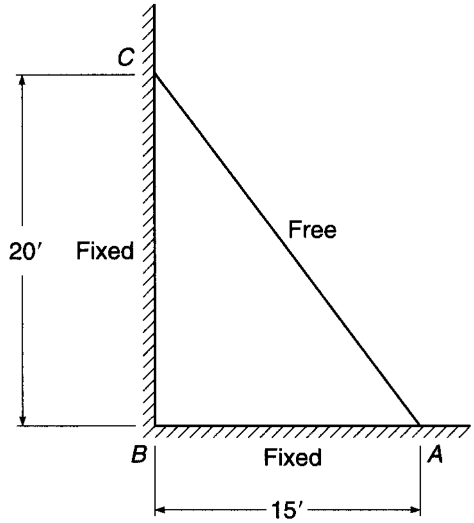

14.6. The square concrete slab shown in Fig. P14.6 is supported by monolithic concrete walls providing full vertical and rotational restraint along two adjacent edges, and by a 6 in. diameter steel pipe column, near the outer corner, that offers negligible rotational restraint. It is reinforced for positive bending by an orthogonal grid of bars parallel to the walls, providing design moment capacity $\phi m_n = 6.5$ ft-kips/ft in all directions. Negative reinforcement perpendicular to the walls and negative bars at the outer corner parallel to the slab diagonal provide $\phi m_n = 8.9$ ft-kips/ft. Neglecting corner pivots, find the total factored uniformly distributed load q_u that will initiate flexural failure. Solution by the method of virtual work is recommended, with collapse geometry established by successive trials. Yield line lengths and perpendicular distances are most easily found graphically. Include a check of the shear capacity of the slab, using approximate methods. The steel column is capped with a 12 × 12 in. plate providing bearing.

FIGURE P14.6

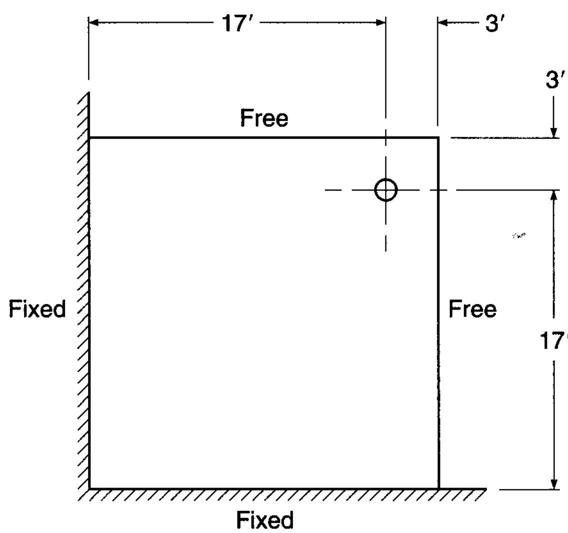

14.7. The square slab shown in Fig. P14.7 is supported by, and is monolithic with, a reinforced concrete wall along the edge *CD* that provides full fixity, and also is supported by a masonry wall along *AB* that provides a simply supported line. It is to carry a factored load q_u = 300 psf including its self-weight. Assuming a uniform 6 in. slab thickness, find the required reinforcement. Include a sketch summarizing details of your design, indicating placement and length of all reinforcing bars. Also check the shear capacity of the structure, making whatever assumptions appear reasonable and necessary. Use f'_c = 4000 psi and f_y = 60,000 psi.

FIGURE P14.7

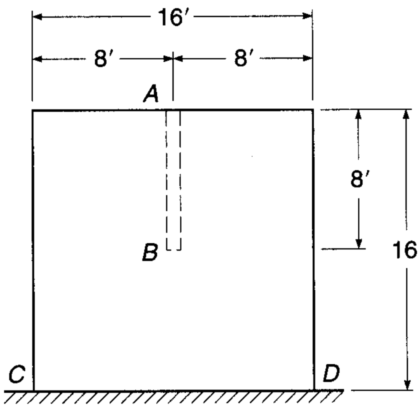

14.8. The slab of Fig. P14.8 is supported by three fixed edges but has no support along one long side. It has a uniform thickness of 7 in., resulting in effective depths in the long direction of 6.0 in. and in the short direction of 5.5 in. Bottom reinforcement consists of No. 4 (No. 13) bars at 14 in. centers in each direction, continued to the supports and the free edge. Top negative steel along the supported edges consists of No. 4 (No. 13) bars at 12 in. on centers, except that in a 2 ft wide "strong band" parallel and adjacent to the free edge, four No. 5 (No. 16) bars are used. All negative bars extend past the points of inflection, as required by ACI Code. Material strengths are f'_c = 4000 psi and f_y = 60,000 psi. Using the yield line method, determine the factored load q_u that can be carried.

FIGURE P14.8

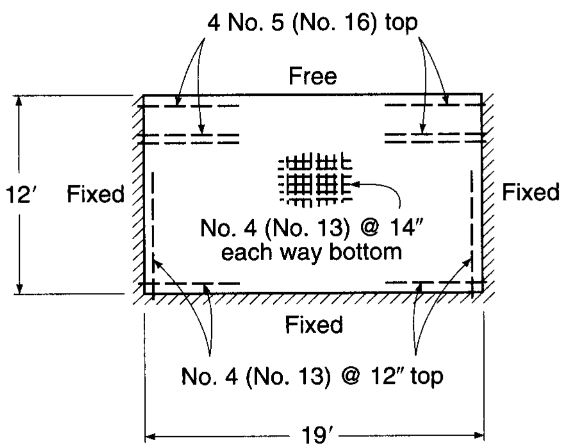

14.9. Using virtual work and yield line theory, compute the flexural collapse load of the one-way slab in Example 13.1. Assume that all straight bars are used, according to Fig. 13.4*b*. Compare the calculated collapse load with the original factored design load, and comment on differences.

14.10. Using virtual work and yield line theory, compute the flexural collapse load of the two-way column-supported flat plate of Example 13.3. To simplify the calculations, assume that all positive moment bars are carried to the edges of the panels, not cut off in the span. Consider all possible failure mechanisms, including a circular fan around the column. Neglect corner effects. Compare the calculated collapse load with the original factored design load and comment on differences.

15 Strip Method for Slabs

15.1 INTRODUCTION

In Section 14.2, the upper and lower bound theorems of the theory of plasticity were presented, and it was pointed out that the yield line method of slab analysis was an *upper bound approach* to determining the flexural strength of slabs. An upper bound analysis, if in error, will be so on the unsafe side. The actual carrying capacity will be less than, or at best equal to, the capacity predicted, which is certainly a cause for concern in design. Also, when applying the yield line method, it is necessary to assume that the distribution of reinforcement is known over the whole slab. It follows that the yield line approach is a tool to *analyze* the capacity of a given slab and can be used for *design* only in an iterative sense, for calculating the capacities of trial designs with varying reinforcement until a satisfactory arrangement is found.

These circumstances motivated Hillerborg to develop what is known as the *strip method* for slab design, his first results being published in Swedish in 1956 (Ref. 15.1). In contrast to yield line analysis, the strip method is a *lower bound approach*, based on satisfaction of equilibrium requirements everywhere in the slab. By the strip method (sometimes referred to as the *equilibrium theory*), a moment field is first determined that fulfills equilibrium requirements, after which the reinforcement in the slab at each point is designed for this moment field. If a distribution of moments can be found that satisfies both equilibrium and boundary conditions for a given external loading, and if the yield moment capacity of the slab is nowhere exceeded, then the given external loading will represent a lower bound of the true carrying capacity.

The strip method gives results on the safe side, which is certainly preferable in practice, and differences from the true carrying capacity will never impair safety. The strip method is a *design* method, by which the needed reinforcement can be calculated. It encourages the designer to vary the reinforcement in a logical way, leading to an economical arrangement of steel, as well as a safe design. It is generally simple to use, even for slabs with holes or irregular boundaries.

In his original work in 1956, Hillerborg set forth the basic principles for edge-supported slabs and introduced the expression *strip method* (Ref. 15.1). He later expanded the method to include the practical design of slabs on columns and L-shaped slabs (Refs. 15.2 and 15.3). The first treatment of the subject in English was by Crawford (Ref. 15.4). In 1964, Blakey translated the earlier Hillerborg work into English (Ref. 15.5). Important contributions, particularly regarding continuity conditions, have been made by Kemp (Refs. 15.6 and 15.7) and Wood and Armer (Refs. 15.8, 15.9, and 15.10). Load tests of slabs designed by the strip method were carried out by Armer (Ref. 15.11) and confirmed that the method produces safe and satisfactory designs. In 1975, Hillerborg produced Ref. 15.12 "for the practical designer, helping him in the simplest possible way to produce safe designs for most of the slabs that he will meet in practice, including slabs that are irregular in plan or that carry unevenly distributed loads." Subsequently, he published a paper in which he summarized what has become known as the *advanced strip method*, pertaining to the design of slabs supported on columns, reentrant corners, or interior walls (Ref. 15.13). Useful summaries of both the simple and advanced strip methods will be found in Refs. 15.14 and 15.15.

The strip method is appealing not only because it is safe, economical, and versatile over a broad range of applications, but also because it formalizes procedures followed instinctively by competent designers in placing reinforcement in the best possible position. In contrast with the yield line method, which provides no inducement to vary bar spacing, the strip method encourages the use of strong bands of steel where needed, such as around openings or over columns, improving economy and reducing the likelihood of excessive cracking or large deflections under service loading.

15.2 BASIC PRINCIPLES

The governing equilibrium equation for a small slab element having sides dx and dy is

$$\frac{\partial^2 m_x}{\partial x^2} + \frac{\partial^2 m_y}{\partial y^2} - 2\frac{\partial^2 m_{xy}}{\partial x \partial y} = -q \tag{15.1}$$

where q = external load per unit area
m_x, m_y = bending moments per unit width in X and Y directions, respectively
m_{xy} = twisting moment (Ref. 15.16)

According to the lower bound theorem, any combination of m_x, m_y, and m_{xy} that satisfies the equilibrium equation at all points in the slab and that meets boundary conditions is a valid solution, provided that the reinforcement is placed to carry these moments.

The basis for the simple strip method is that the torsional moment is chosen equal to zero; no load is assumed to be resisted by the twisting strength of the slab. Therefore, if the reinforcement is parallel to the axes in a rectilinear coordinate system,

$$m_{xy} = 0$$

The equilibrium equation then reduces to

$$\frac{\partial^2 m_x}{\partial x^2} + \frac{\partial^2 m_y}{\partial y^2} = -q \tag{15.2}$$

This equation can be split conveniently into two parts, representing twistless beam strip action

$$\frac{\partial^2 m_x}{\partial x^2} = -kq \tag{15.3a}$$

and

$$\frac{\partial^2 m_y}{\partial y^2} = -(1 - k)q \tag{15.3b}$$

where the proportion of load taken by the strips is k in the X direction and $1 - k$ in the Y direction. In many regions in slabs, the value of k will be either 0 or 1. With $k = 0$, all of the load is dispersed by strips in the Y direction; with $k = 1$, all of the load is carried in the X direction. In other regions, it may be reasonable to assume that the load is divided equally in the two directions (i.e., $k = 0.5$).

15.3 CHOICE OF LOAD DISTRIBUTION

Theoretically, the load q can be divided arbitrarily between the X and Y directions. Different divisions will, of course, lead to different patterns of reinforcement, and not all will be equally appropriate. The desired goal is to arrive at an arrangement of steel that is safe and economical and that will avoid problems at the service load level associated with excessive cracking or deflections. In general, the designer may be guided by knowledge of the general distribution of elastic moments.

To see an example of the strip method and to illustrate the choices open to the designer, consider the square, simply supported slab shown in Fig. 15.1, with side length a and a uniformly distributed factored load q per unit area.

The simplest load distribution is obtained by setting $k = 0.5$ over the entire slab, as shown in Fig. 15.1. The load on all strips in each direction is then $q/2$, as illustrated by the load dispersion arrows of Fig. 15.1a. This gives maximum moments

$$m_x = m_y = \frac{qa^2}{16} \tag{15.4}$$

over the whole slab, as shown in Fig. 15.1c, with a uniform lateral distribution across the width of the critical section, as in Fig. 15.1d.

FIGURE 15.1
Square slab with load shared equally in two directions.

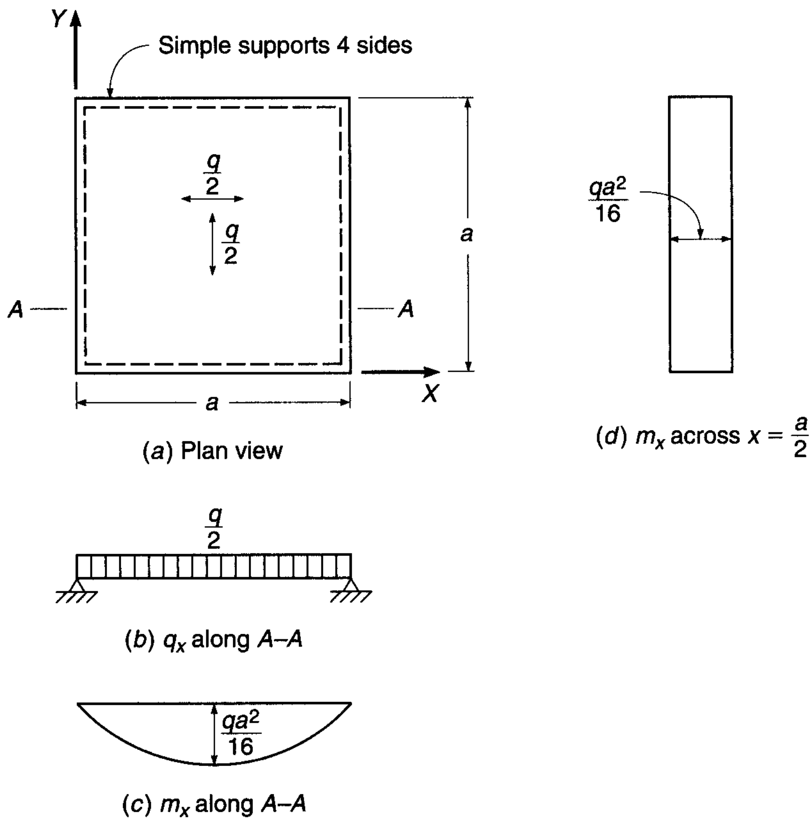

FIGURE 15.2
Square slab with load dispersion lines following diagonals.

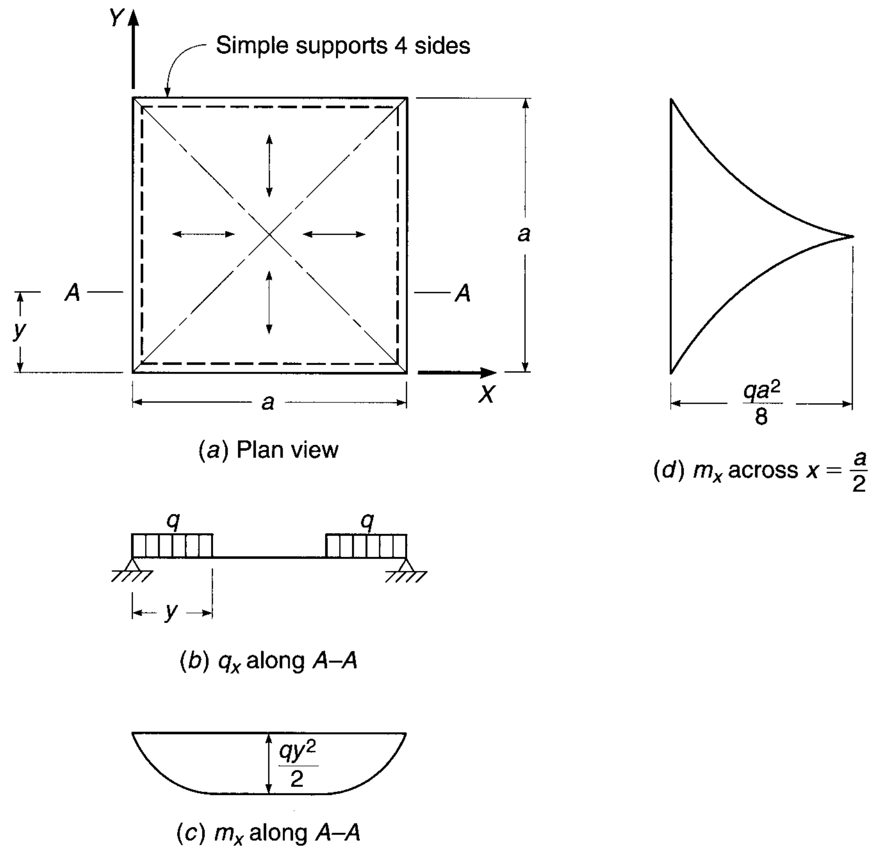

This would not represent an economical or serviceable solution because it is recognized that curvatures, hence moments, must be greater in the strips near the middle of the slab than near the edges in the direction parallel to the edge (see Fig. 13.5). If the slab were reinforced according to this solution, extensive redistribution of moments would be required, certainly accompanied by much cracking in the highly stressed regions near the middle of the slab.

An alternative, more reasonable distribution is shown in Fig. 15.2. Here the regions of different load dispersion, separated by the dash-dotted "discontinuity lines," follow the diagonals, and all of the load on any region is carried in the direction giving the shortest distance to the nearest support. The solution proceeds, giving k values of either 0 or 1, depending on the region, with load transmitted in the directions indicated by the arrows of Fig. 15.2a. For a strip A–A at a distance $y \leq a/2$ from the X axis, the moment is

$$m_x = \frac{qy^2}{2} \tag{15.5}$$

The load acting on a strip A–A is shown in Fig. 15.2b, and the resulting diagram of moment m_x is given in Fig. 15.2c. The lateral variation of m_x across the width of the slab is as shown in Fig. 15.2d.

The lateral distribution of moments shown in Fig. 15.2d would theoretically require a continuously variable bar spacing, obviously an impracticality. One way of using the distribution in Fig. 15.2, which is considerably more economical than that in Fig. 15.1, would be to reinforce for the *average* moment over a certain width, approximating the actual lateral variation shown in Fig. 15.2*d* in a stepwise manner. Hillerborg notes that this is not strictly in accordance with the equilibrium theory and that the design is no longer certainly on the safe side, but other conservative assumptions, e.g., neglect of membrane strength in the slab and neglect of strain hardening of the reinforcement, would surely compensate for the slight reduction in safety margin.

A third alternative distribution is shown in Fig. 15.3. Here the division is made so that the load is carried to the nearest support, as before, but load near the diagonals has been divided, with one-half taken in each direction. Thus, k is given values of 0 or 1

FIGURE 15.3
Square slab with load near diagonals shared equally in two directions.

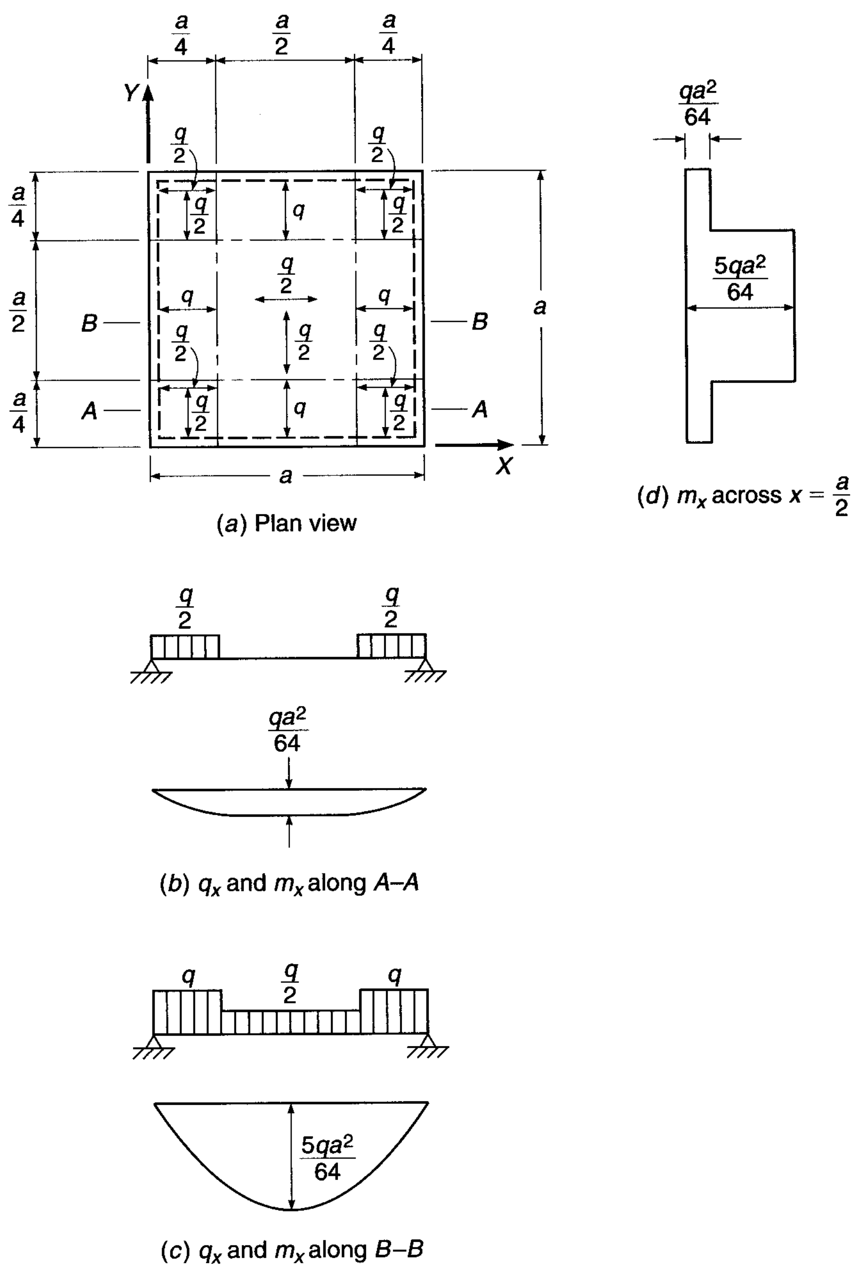

(a) Plan view

(d) m_x across $x = \frac{a}{2}$

(b) q_x and m_x along A–A

(c) q_x and m_x along B–B

along the middle edges and a value of 0.5 in the corners and center of the slab, with load dispersion in the directions indicated by the arrows shown in Fig. 15.3*a*. Two different strip loadings are now identified. For an X direction strip along section A–A, the maximum moment is

$$m_x = \frac{q}{2} \times \frac{a}{4} \times \frac{a}{8} = \frac{qa^2}{64} \tag{15.6a}$$

and for a strip along section B–B, the maximum moment is

$$m_x = q \times \frac{a}{4} \times \frac{a}{8} + \frac{q}{2} \times \frac{a}{4} \times \frac{3a}{8} = \frac{5qa^2}{64} \tag{15.6b}$$

The variation of m_x along the line $x = a/2$ is shown in Fig. 15.3*d*. This design leads to a practical arrangement of reinforcement, one with constant spacing through the center strip of width $a/2$ and a wider spacing through the outer strips, where the elastic curvatures and moments are known to be less. The averaging of moments necessitated in the second solution is avoided here, and the third solution is fully consistent with the equilibrium theory.

Comparing the three solutions just presented shows that the first would be unsatisfactory, as noted earlier, because it would require great redistribution of moments to achieve, possibly accompanied by excessive cracking and large deflections. The second, with discontinuity lines following the slab diagonals, has the advantage that the reinforcement more nearly matches the elastic distribution of moments, but it either leads to an impractical reinforcing pattern or requires an averaging of moments in bands that involves a deviation from strict equilibrium theory. The third solution, with discontinuity lines parallel to the edges, does not require moment averaging and leads to a practical reinforcing arrangement, so it will often be preferred.

The three examples also illustrate the simple way in which moments in the slab can be found by the strip method, based on familiar beam analysis. It is important to note, too, that the load on the supporting beams is easily found because it can be computed from the end reactions of the slab beam strips in all cases. This information is not available from solutions such as those obtained by the yield line theory.

15.4 RECTANGULAR SLABS

With rectangular slabs, it is reasonable to assume that, throughout most of the area, the load will be carried in the short direction, consistent with elastic theory (see Section 13.4). In addition, it is important to take into account the fact that because of their length, longitudinal reinforcing bars will be more expensive than transverse bars of the same size and spacing. For a uniformly loaded rectangular slab on simple supports, Hillerborg presents one possible division, as shown in Fig. 15.4, with discontinuity lines originating from the slab corners at an angle depending on the ratio of short to long sides of the slab. All of the load in each region is assumed to be carried in the directions indicated by the arrows.

Instead of the solution of Fig. 15.4, which requires continuously varying reinforcement to be strictly correct, Hillerborg suggests that the load can be distributed as shown in Fig. 15.5, with discontinuity lines parallel to the sides of the slab. For such cases, it is reasonable to take edge bands of width equal to one-fourth the short span dimension. Here the load in the corners is divided equally in the X and Y directions as shown, while elsewhere all of the load is carried in the direction indicated by the arrows.

FIGURE 15.4
Rectangular slab with discontinuity lines originating at the corners.

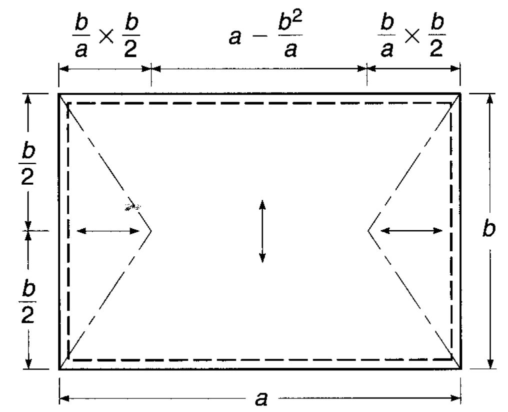

FIGURE 15.5
Discontinuity lines parallel to the sides for a rectangular slab.

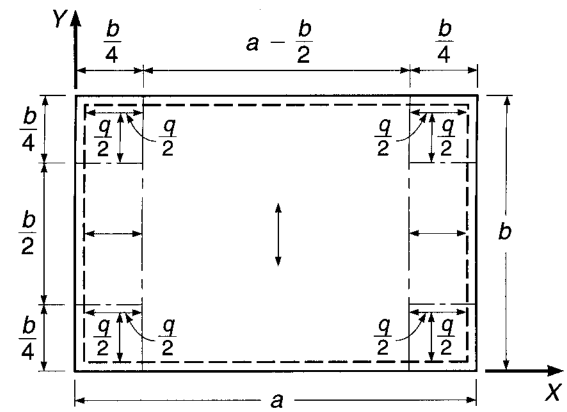

The second, preferred arrangement, shown in Fig. 15.5, gives slab moments as follows:

In the X direction:

Side strips:
$$m_x = \frac{q}{2} \times \frac{b}{4} \times \frac{b}{8} = \frac{qb^2}{64} \tag{15.7a}$$

Middle strips:
$$m_x = q \times \frac{b}{4} \times \frac{b}{8} = \frac{qb^2}{32} \tag{15.7b}$$

In the Y direction:

Side strips:
$$m_y = \frac{qb^2}{64} \tag{15.8a}$$

Middle strips:
$$m_y = \frac{qb^2}{8} \tag{15.8b}$$

This distribution, requiring no averaging of moments across band widths, is always on the safe side and is both simple and economical.

15.5 FIXED EDGES AND CONTINUITY

Designing by the strip method has been shown to provide a large amount of flexibility in assigning load to various regions of slabs. This same flexibility extends to the assignment of moments between negative and positive bending sections of slabs that are fixed or continuous over their supported edges. Some attention should be paid to elastic moment ratios to avoid problems with cracking and deflection at service loads. However, the redistribution that can be achieved in slabs, which are typically rather lightly reinforced and, thus, have large plastic rotation capacities when overloaded, permits considerable arbitrary readjustment of the ratio of negative to positive moments in a strip.

This is illustrated by Fig. 15.6, which shows a slab strip carrying loads only near the supports and unloaded in the central region, such as often occurs in designing by the strip method. It is convenient if the unloaded region is subject to a constant moment (and zero shear), because this simplifies the selection of positive reinforcement. The sum of the absolute values of positive span moment and negative end moment at the left or right end, shown as m_l and m_r in Fig. 15.6, depends only on the conditions at the respective end and is numerically equal to the negative moment if the strip carries the load as a cantilever. Thus, in determining moments for design, one calculates the "cantilever" moments, selects the span moment, and determines the corresponding support moments. Hillerborg notes that, as a general rule for fixed edges, the support moment should be about 1.5 to 2.5 times the span moment in the same strip. Higher values should be chosen for longitudinal strips that are largely unloaded, and in such cases a ratio of support to span moment of 3 to 4 may be used. However, little will be gained by using such a high ratio if the positive moment steel is controlled by minimum requirements of the ACI Code.

For slab strips with one end fixed and one end simply supported, the dual goals of constant moment in the unloaded central region and a suitable ratio of negative to positive moments govern the location to be chosen for the discontinuity lines. Figure 15.7*a* shows a uniformly loaded rectangular slab having two adjacent edges fixed and the other two edges simply supported. Note that although the middle strips have the same width as those of Fig. 15.5, the discontinuity lines are shifted to account for the greater stiffness of the strips with fixed ends. Their location is defined by a coefficient α, with a value clearly less than 0.5 for the slab shown, its exact value yet to be determined. It will be seen that the selection of α relates directly to the ratio of negative to positive moments in the strips.

The moment curve of Fig. 15.7*b* is chosen so that moment is constant over the unloaded part, i.e., shearing force is zero. With constant moment, the positive steel can be fully stressed over most of the strip. The maximum positive moment in the X direction middle strip is then

$$m_{xf} = \frac{\alpha q b}{2} \times \frac{\alpha b}{4} = \alpha^2 \frac{q b^2}{8} \tag{15.9}$$

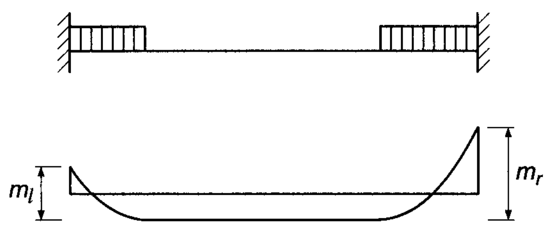

FIGURE 15.6
Slab strip with central region unloaded.

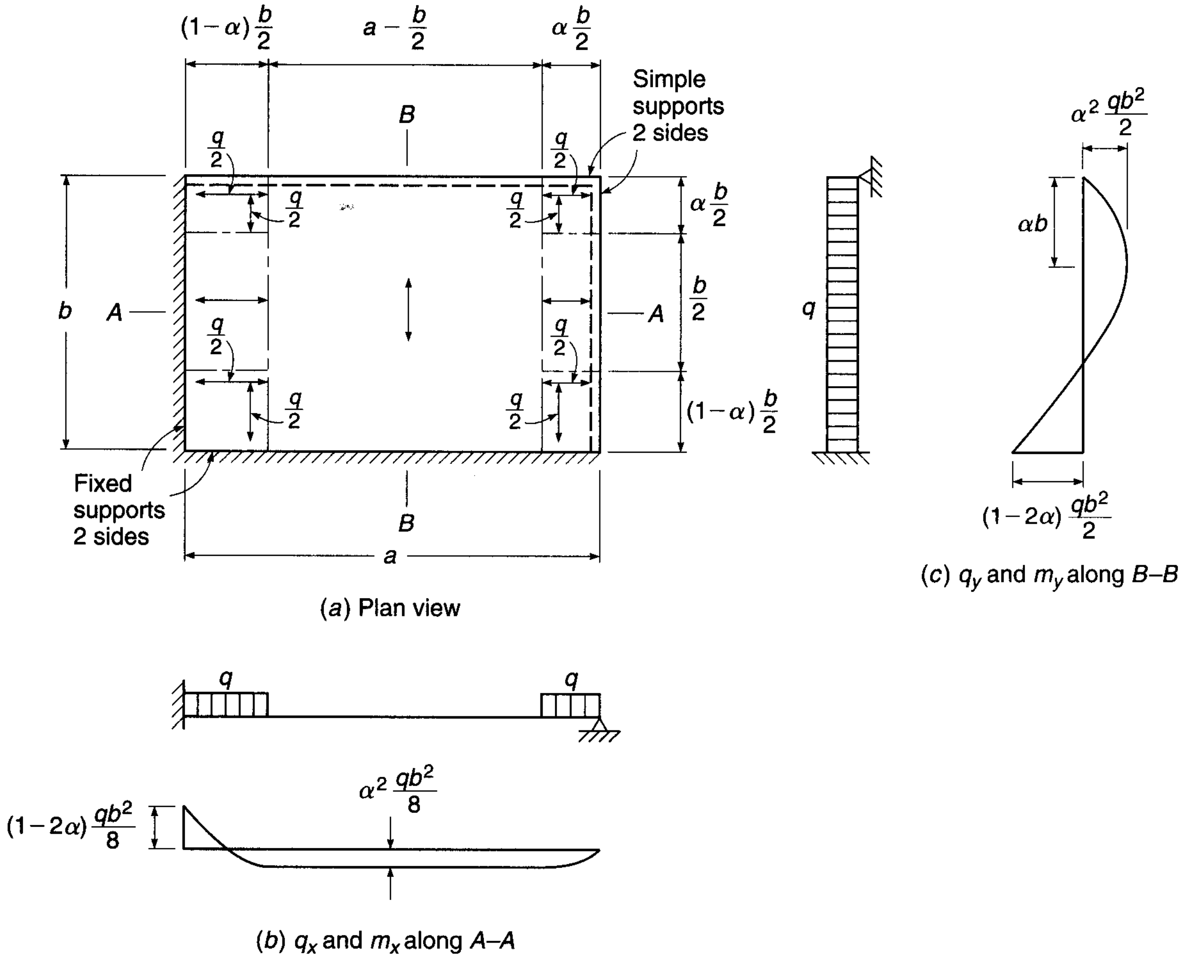

FIGURE 15.7
Rectangular slab with two edges fixed and two edges simply supported.

The cantilever moment at the left support is

$$m_x = (1-\alpha)\frac{qb}{2}(1-\alpha)\frac{b}{4} = (1-\alpha)^2\frac{qb^2}{8} \tag{15.10}$$

and so the negative moment at the left support is

$$m_{xs} = (1-\alpha)^2\frac{qb^2}{8} - \alpha^2\frac{qb^2}{8} = (1-2\alpha)\frac{qb^2}{8} \tag{15.11}$$

For reference, the ratio of negative to positive moments in the X direction middle strip is

$$\frac{m_{xs}}{m_{xf}} = \frac{1-2\alpha}{\alpha^2} \tag{15.12}$$

The moments in the X direction edge strips are one-half of those in the middle strips because the load is one-half as great.

It is reasonable to choose the same ratio between support and span moments in the Y direction as in the X direction. Accordingly, the distance from the right support,

Fig. 15.7*c*, to the maximum positive moment section is chosen as αb. It follows that the maximum positive moment is

$$m_{yf} = \alpha q b \times \frac{\alpha b}{2} = \alpha^2 \frac{qb^2}{2} \tag{15.13}$$

Applying the same methods as used for the *X* direction shows that the negative support moment in the *Y* direction middle strips is

$$m_{ys} = (1 - 2\alpha)\frac{qb^2}{2} \tag{15.14}$$

It is easily confirmed that the moments in the *Y* direction edge strips are just one-eighth of those in the *Y* direction middle strip.

With the above expressions, all of the moments in the slab can be found once a suitable value for α is chosen. From Eq. (15.12), it can be confirmed that values of α from 0.35 to 0.39 give corresponding ratios of negative to positive moments from 2.45 to 1.45, the range recommended by Hillerborg. For example, if it is decided that support moments are to be twice the span moments, the value of α should be 0.366, and the negative and positive moments in the central strip in the *Y* direction are, respectively, $0.134qb^2$ and $0.067qb^2$. In the middle strip in the *X* direction, moments are one-fourth those values; and in the edge strips in both directions, they are one-eighth of those values.

EXAMPLE 15.1 **Rectangular slab with fixed edges.** Figure 15.8 shows a typical interior panel of a slab floor in which support is provided by beams on all column lines. Normally proportioned beams will be stiff enough, both flexurally and torsionally, that the slab can be assumed fully restrained on all sides. Clear spans for the slab, face to face of beams, are 25 and 20 ft, as shown. The floor must carry a service live load of 150 psf, using concrete with $f_c' = 3000$ psi and steel with $f_y = 60{,}000$ psi. Find the moments at all critical sections, and determine the required slab thickness and reinforcement.

SOLUTION. The minimum slab thickness required by the ACI Code can be found from Eq. (13.8*b*), with $l_n = 25$ ft and $\beta = 1.25$:

$$h = \frac{25 \times 12(0.8 + 60/200)}{36 + 9 \times 1.25} = 6.98 \text{ in.}$$

A total thickness of 7 in. will be selected, for which $q_d = 150 \times 7/12 = 87.5$ psf. Applying the load factors of 1.2 and 1.6 to dead load and live load, respectively, determines that the total factored load for design is 340 psf. For strip analysis, discontinuity lines will be selected as shown in Fig. 15.8, with edge strips of width $b/4 = 20/4 = 5$ ft. In the corners, the load is divided equally in the two directions; elsewhere, 100 percent of the load is assigned to the direction indicated by the arrows. A ratio of support moment to span moment of 2.0 will be used. Calculation of moments then proceeds as follows:

X direction middle strip:

Cantilever: $$m_x = \frac{qb^2}{32} = 340 \times \frac{400}{32} = 4250 \text{ ft-lb/ft}$$

Negative: $$m_{xs} = 4250 \times \frac{2}{3} = 2833$$

Positive: $$m_{xf} = 4250 \times \frac{1}{3} = 1417$$

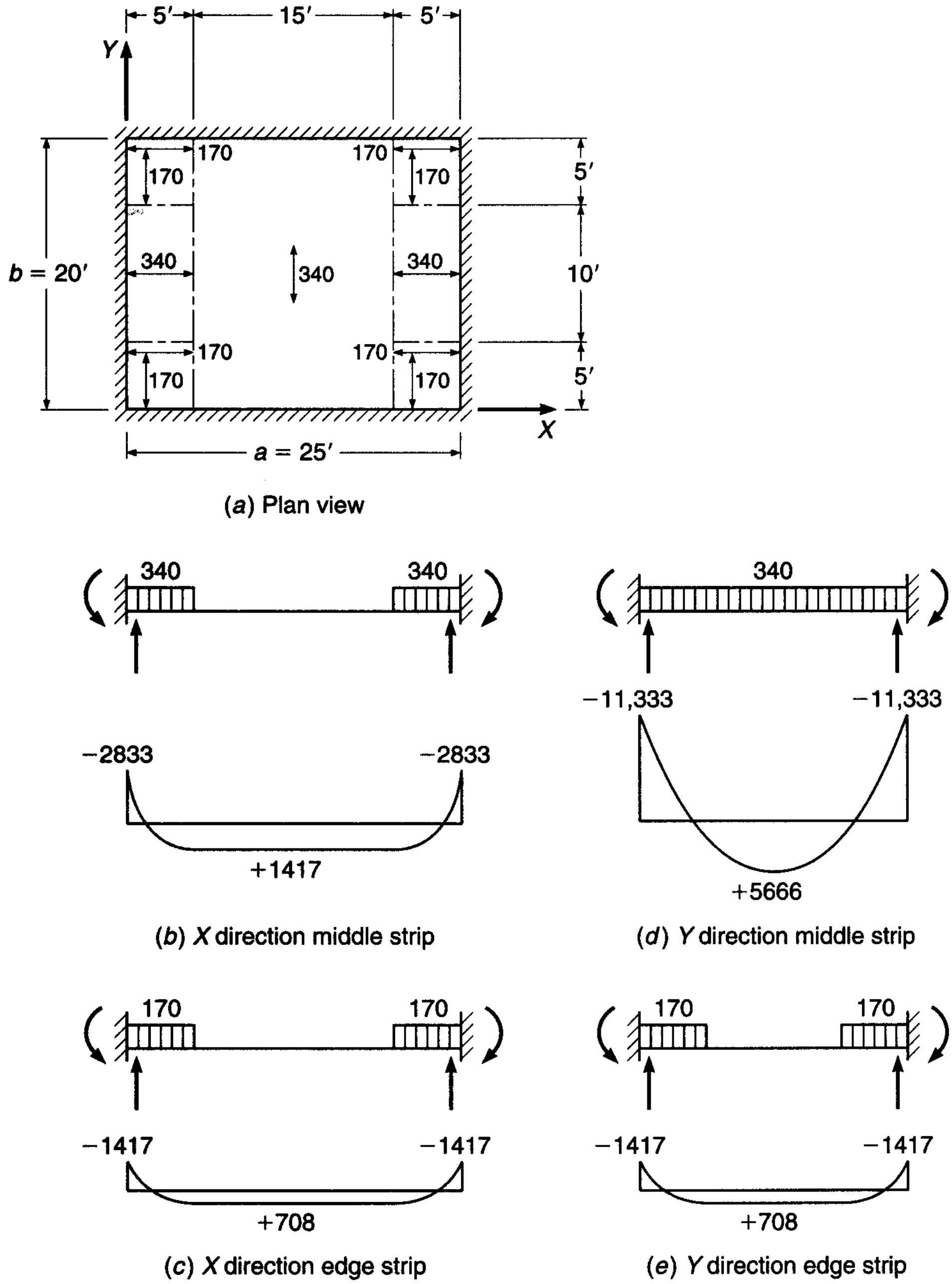

FIGURE 15.8
Design example: two-way slab with fixed edges.

X direction edge strips:

Cantilever: $$m_x = \frac{qb^2}{64} = 340 \times \frac{400}{64} = 2125 \text{ ft-lb/ft}$$

Negative: $$m_{xs} = 2125 \times \frac{2}{3} = 1417$$

Positive: $$m_{xf} = 2125 \times \frac{1}{3} = 708$$

Y direction middle strip:

Cantilever: $$m_y = \frac{qb^2}{8} = 340 \times \frac{400}{8} = 17{,}000 \text{ ft-lb/ft}$$

Negative: $$m_{ys} = 17{,}000 \times \frac{2}{3} = 11{,}333$$

Positive: $$m_{yf} = 17{,}000 \times \frac{1}{3} = 5666$$

Y direction edge strips:

Cantilever: $$m_y = \frac{qb^2}{64} = 340 \times \frac{400}{64} = 2125 \text{ ft-lb/ft}$$

Negative: $$m_{ys} = 2125 \times \frac{2}{3} = 1417$$

Positive: $$m_{yf} = 2125 \times \frac{1}{3} = 708$$

Strip loads and moment diagrams are as shown in Fig. 15.8. According to ACI Code 7.12, the minimum steel required for shrinkage and temperature crack control is $0.0018 \times 7 \times 12 = 0.151 \text{ in}^2/\text{ft}$ strip. With a total depth of 7 in., with $\frac{3}{4}$ in. concrete cover, and with estimated bar diameters of $\frac{1}{2}$ in., the effective depth of the slab in the short direction will be 6 in., and in the long direction, 5.5 in. Accordingly, the flexural reinforcement ratio provided by the minimum steel acting at the smaller effective depth is

$$\rho_{\min} = \frac{0.151}{5.5 \times 12} = 0.0023$$

From Table A.5a of Appendix A, $R = 134$, and the flexural design strength is

$$\phi m_n = \phi R b d^2 = \frac{0.90 \times 134 \times 12 \times 5.5^2}{12} = 3648 \text{ ft-lb/ft}$$

Comparing this with the required moment resistance shows that the minimum steel will be adequate in the X direction in both middle and edge strips and in the Y direction edge strips. No. 3 (No. 10) bars at 9 in. spacing will provide the needed area. In the Y direction middle strip, for negative bending,

$$R = \frac{m_u}{\phi b d^2} = \frac{11{,}333 \times 12}{0.90 \times 12 \times 6^2} = 350$$

and from Table A.5a, the required reinforcement ratio is 0.0069. The required steel is then

$$A_s = 0.0063 \times 12 \times 6 = 0.45 \text{ in}^2/\text{ft}$$

This will be provided with No. 5 (No. 16) bars at 8 in. on centers. For positive bending,

$$R = \frac{5666 \times 12}{0.90 \times 12 \times 6^2} = 175$$

for which $\rho = 0.0030$, and the required positive steel area per strip is

$$A_s = 0.0030 \times 12 \times 6 = 0.22 \text{ in}^2/\text{ft}$$

to be provided by No. 4 (No. 13) bars on 10 in. centers. Note that all bar spacings are less than $2h = 2 \times 7 = 14$ in., as required by the Code, and that the reinforcement ratios are well below the value for a tension-controlled section of 0.0135.

Negative bar cutoff points can easily be calculated from the moment diagrams. For the X direction middle strip, the point of inflection a distance x from the left edge is found as follows:

$$1700x - 2833 - 340\left(\frac{x^2}{2}\right) = 0$$

$$x = 2.11 \text{ ft}$$

According to the Code, the negative bars must be continued at least d or $12d_b$ beyond that point, requiring a 6 in. extension in this case. Thus, the negative bars will be cut off 2.11 + 0.50 = 2.61 ft, say 2 ft 8 in., from the face of support. The same result is obtained for the X direction edge strips and the Y direction edge strips. For the Y direction middle strip, the distance y = 4.23 ft from face of support to inflection point is found in a similar manner. In this case, with No. 5 (No. 10) bars used, the required extension is 7.5 in., giving a total length past the face of supports of 4.23 + 0.63 = 4.86 ft or 4 ft 11 in. All positive bars will be carried 6 in. into the face of the supporting beams.

15.6 UNSUPPORTED EDGES

The slabs considered in the preceding sections, together with the supporting beams, could also have been designed by the methods of Chapter 13. The real power of the strip method becomes evident when dealing with nonstandard problems, such as slabs with an unsupported edge, slabs with holes, or slabs with reentrant corners (L-shaped slabs).

For a slab with one edge unsupported, for example, a reasonable basis for analysis by the simple strip method is that a strip along the unsupported edge takes a greater load per unit area than the actual unit load acting, i.e., that the strip along the unsupported edge acts as a support for the strips at right angles. Such strips have been referred to by Wood and Armer as *strong bands* (Ref. 15.8). A strong band is, in effect, an integral beam, usually having the same total depth as the remainder of the slab but containing a concentration of reinforcement. The strip may be made deeper than the rest of the slab to increase its carrying capacity, but this will not usually be necessary.

Figure 15.9*a* shows a rectangular slab carrying a uniformly distributed factored load q per unit area, with fixed edges along three sides and no support along one short side. Discontinuity lines are chosen as shown. The load on a unit middle strip in the X direction, shown in Fig. 15.9*b*, includes the downward load q in the region adjacent to the fixed left edge and the upward reaction kq in the region adjacent to the free edge. Summing moments about the left end, with moments positive clockwise and with the unknown support moment denoted m_{xs}, gives

$$m_{xs} + \frac{qb^2}{32} - \frac{kqb}{4}\left(a - \frac{b}{8}\right) = 0$$

from which

$$k = \frac{1 + 32m_{xs}/qb^2}{8(a/b) - 1} \tag{15.15}$$

Thus, k can be calculated after the support moment is selected.

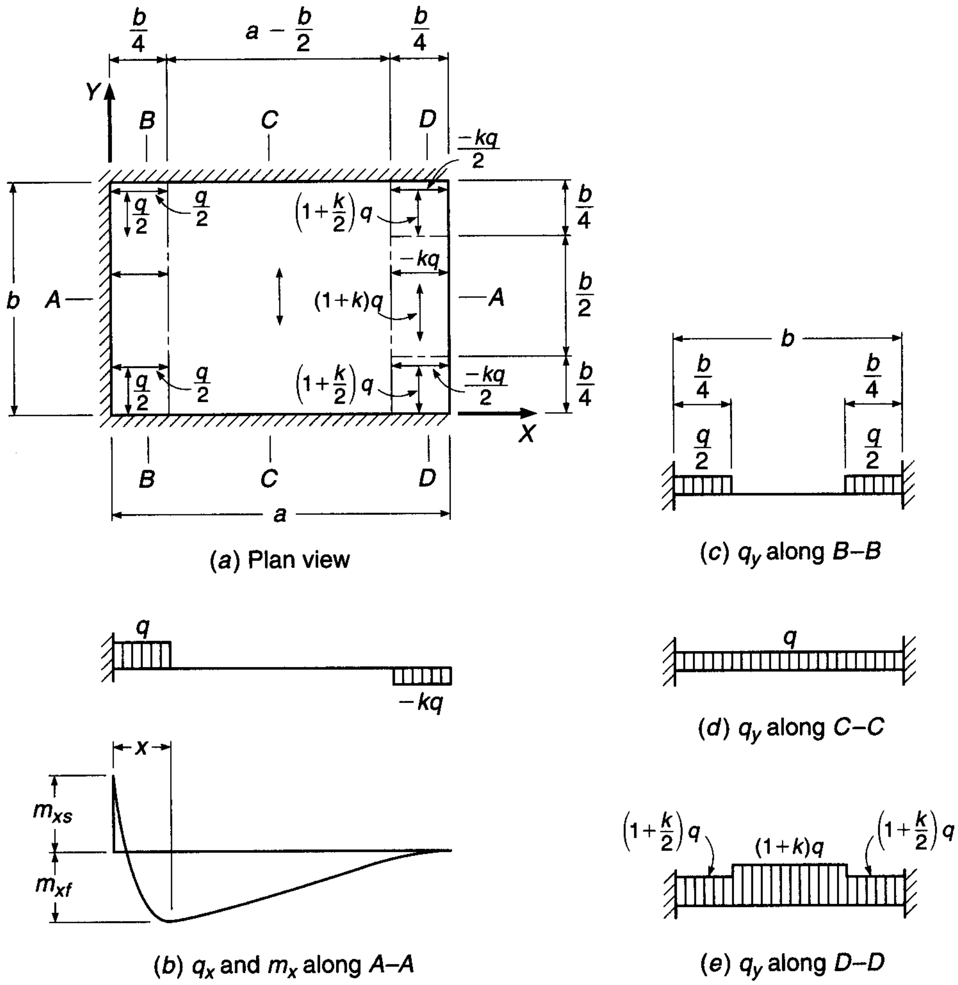

FIGURE 15.9
Slab with free edge along short side.

The appropriate value of m_{xs} to be used in Eq. (15.15) will depend on the shape of the slab. If a is large relative to b, the strong band in the Y direction at the edge will be relatively stiff, and the moment at the left support in the X direction strips will approach the elastic value for a propped cantilever. If the slab is nearly square, the deflection of the strong band will tend to increase the support moment; a value about one-half the free cantilever moment might be selected (Ref. 15.14).

Once m_{xs} is selected and k is known, it is easily shown that the maximum span moment occurs when

$$x = (1 - k)\frac{b}{4}$$

It has a value

$$m_{xf} = \frac{kqb^2}{32}\left(\frac{8a}{b} - 3 + k\right) \tag{15.16}$$

The moments in the X direction edge strips are one-half of those in the middle strip. In the Y direction middle strip, Fig. 15.9d, the cantilever moment is $qb^2/8$. Adopting a ratio of support to span moment of 2 results in support and span moments, respectively, of

$$m_{ys} = \frac{qb^2}{12} \tag{15.17a}$$

$$m_{yf} = \frac{qb^2}{24} \tag{15.17b}$$

Moments in the Y direction strip adjacent to the fixed edge, Fig. 15.9c, will be one-eighth of those values. In the Y direction strip along the free edge, Fig. 15.9e, moments can, with slight conservatism, be made equal to $(1 + k)$ times those in the Y direction middle strip.

If the unsupported edge is in the long-span direction, then a significant fraction of the load in the slab central region will be carried in the direction perpendicular to the long edges, and the simple distribution shown in Fig. 15.10a is more suitable. A strong band along the free edge serves as an integral edge beam, with width βb normally chosen as low as possible considering limitations on tensile reinforcement ratio in the strong band.

For a Y direction strip, with moments positive clockwise,

$$m_{ys} + \frac{1}{2} k_1 q(1 - \beta)^2 b^2 - k_2 q \beta b^2 (1 - \beta/2) = 0$$

FIGURE 15.10
Slab with free edge in long-span direction.

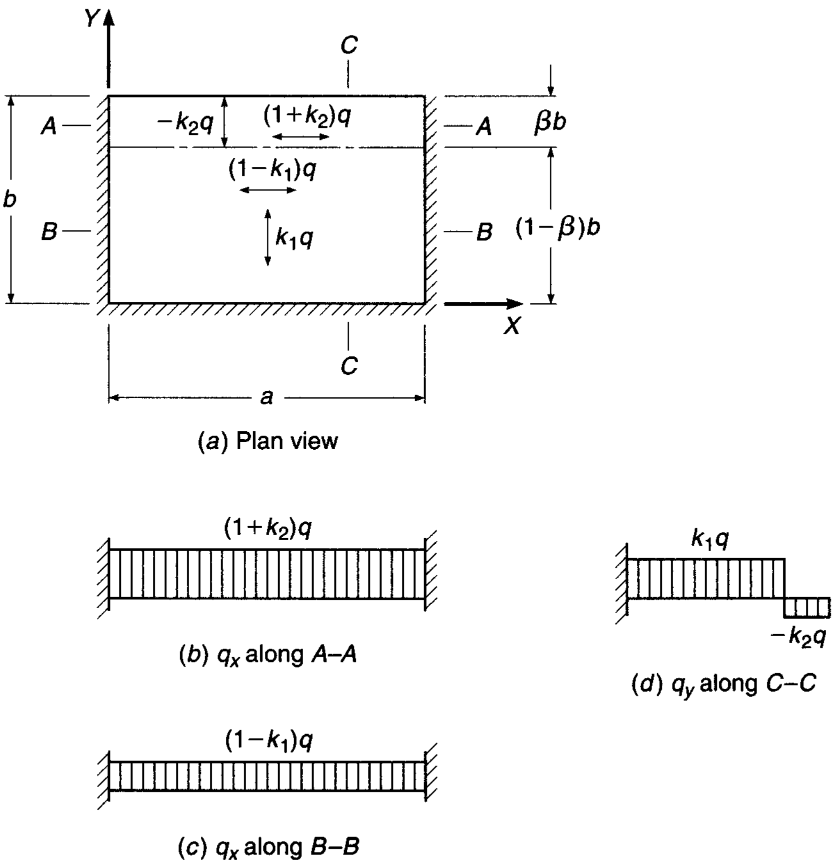

from which

$$k_2 = \frac{k_1(1-\beta)^2 + 2m_{ys}/qb^2}{\beta(2-\beta)} \tag{15.18}$$

The value of k_1 may be selected so as to make use of the minimum steel in the X direction required by ACI Code 7.12. In choosing m_{ys} to be used in Eq. (15.18) for calculating k_2, one should again recognize that the deflection of the strong band along the free edge will tend to increase the Y direction moment at the supported edge above the propped cantilever value based on zero deflection. A value for m_{ys} of about one-half the free cantilever moment may be appropriate in typical cases. A high ratio of a/b will permit greater deflection of the free edge through the central region, tending to increase the support moment, and a low ratio will restrict deflection, reducing the support moment.

EXAMPLE 15.2 **Rectangular slab with long edge unsupported.** The 12 × 19 ft slab shown in Fig. 15.11*a*, with three fixed edges and one long edge unsupported, must carry a uniformly distributed service live load of 125 psf; f'_c = 4000 psi, and f_y = 60,000 psi. Select an appropriate slab thickness, determine all factored moments in the slab, and select reinforcing bars and spacings for the slab.

SOLUTION. The minimum thickness requirements of the ACI Code do not really apply to the type of slab considered here. However, Table 13.5, which controls for beamless flat plates, can be applied conservatively because although the present slab is beamless along the free edge, it has infinitely stiff supports on the other three edges. From that table, with l_n = 19 ft,

$$h = \frac{19 \times 12}{33} = 6.91 \text{ in.}$$

A total thickness of 7 in. will be selected. The slab dead load is $150 \times \frac{7}{12} = 88$ psf, and the total factored design load is $1.2 \times 88 + 1.6 \times 125 = 306$ psf.

A strong band 2 ft wide will be provided for support along the free edge. In the main slab, a value $k_1 = 0.45$ will be selected, resulting in a slab load in the Y direction of $0.45 \times 306 = 138$ psf and in the X direction of $0.55 \times 306 = 168$ psf.

First, with regard to the Y direction slab strips, the negative moment at the supported edge will be chosen as one-half the free cantilever value, which in turn will be approximated based on 138 psf over an 11 ft distance from the support face to the center of the strong band. The restraining moment is thus

$$m_{ys} = \frac{1}{2} \times \frac{138 \times 11^2}{2} = 4175 \text{ ft-lb/ft}$$

Then, from Eq. (15.18)

$$k_2 = \frac{0.45(5/6)^2 - 2 \times 4175/(306 \times 144)}{(1/6)(2-1/6)} = 0.403$$

Thus, an uplift of $0.403 \times 306 = 123$ psf will be provided for the Y direction strips by the strong band, as shown in Fig. 15.11*d*. For this loading, the negative moment at the left support is

$$m_{ys} = 138 \times \frac{10^2}{2} - 123 \times 2 \times 11 = 4194 \text{ ft-lb/ft}$$

The difference from the original value of 4175 ft-lb/ft is caused by numerical rounding of the load terms. The statically consistent value of 4194 ft-lb/ft will be used for design. The maximum positive moment in the Y direction strips will be located at the point of zero shear.

FIGURE 15.11
Design example: slab with long edge unsupported.

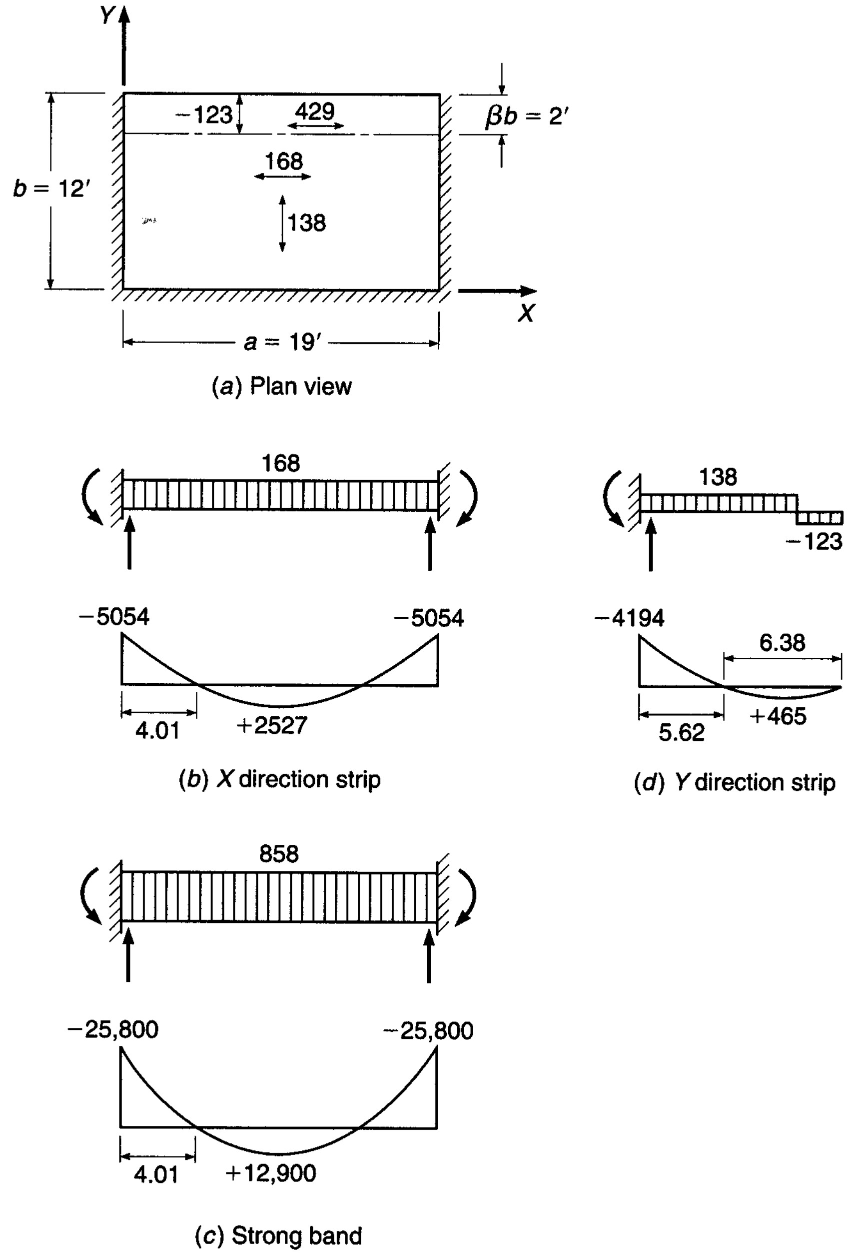

With y_1 as the distance of that point from the free edge to the zero shear location, and with reference to Fig. 15.11*d*,

$$123 \times 2 - 138(y_1 - 2) = 0$$

from which $y_1 = 3.78$ ft. The maximum positive moment, found at that location, is

$$m_{yf} = 123 \times 2(3.78 - 1) - 138 \times \frac{1.78^2}{2} = 465 \text{ ft-lb/ft}$$

For later reference in cutting off bars, the point of inflection is located a distance y_2 from the free edge:

$$123 \times 2(y_2 - 1) - \frac{138}{2}(y_2 - 2)^2 = 0$$

FIGURE 15.11
(*Continued*)

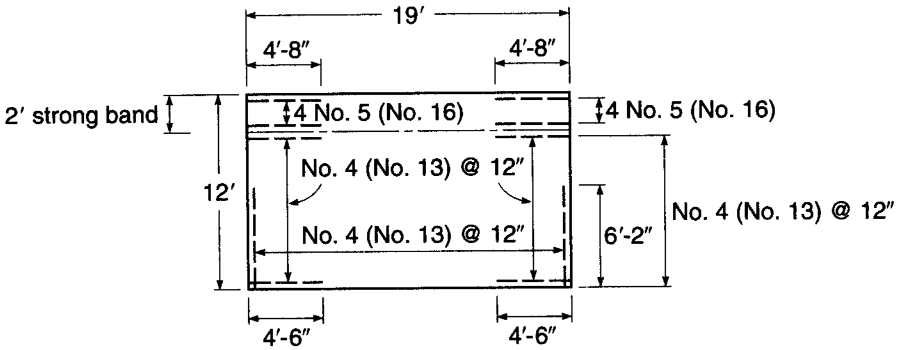

(*e*) Top bars

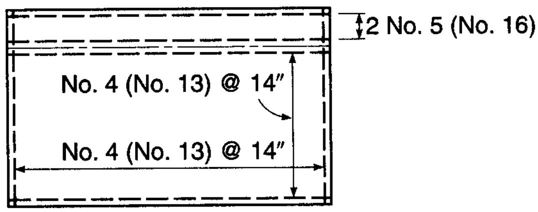

(*f*) Bottom bars

resulting in $y_2 = 6.38$ ft.

For the X direction slab strips, the cantilever moment is

Cantilever: $$m_x = \frac{168 \times 19^2}{8} = 7581 \text{ ft-lb/ft}$$

A ratio of negative to positive moments of 2.0 will be chosen here, resulting in negative and positive moments, respectively, of

Negative: $$m_{xs} = 7581 \times \frac{2}{3} = 5054 \text{ ft-lb/ft}$$

Positive: $$m_{xf} = 7581 \times \frac{1}{3} = 2527 \text{ ft-lb/ft}$$

as shown in Fig. 15.11*b*.

The unit load on the strong band in the X direction is

$$(1 + k_2)q = (1 + 0.403) \times 306 = 429 \text{ psf}$$

so for the 2 ft wide band the load per foot is $2 \times 429 = 858$ psf, as indicated in Fig. 15.11*c*. The cantilever, negative, and positive strong band moments are, respectively,

Cantilever: $$M_x = 858 \times 19^2/8 = 38{,}700 \text{ ft-lb}$$

Negative: $$M_{xs} = 38{,}700 \times \frac{2}{3} = 25{,}800 \text{ ft-lb}$$

Positive: $$M_{xf} = 38{,}700 \times \frac{1}{3} = 12{,}900 \text{ ft-lb}$$

With a negative moment of $-25{,}800$ ft-lb and a support reaction of $858 \times \frac{19}{2} = 8151$ lb, the point of inflection in the strong band is found as follows:

$$-25{,}800 + 8151x - \frac{858x^2}{2} = 0$$

giving $x = 4.01$ ft. The inflection point in the X direction slab strips will be at the same location.

In designing the slab steel in the X direction, one notes that the minimum steel required by the ACI Code is $0.0018 \times 7 \times 12 = 0.15$ in²/ft. The effective slab depth in the X direction, assuming $\frac{1}{2}$ in. diameter bars with $\frac{3}{4}$ in. cover, is $7.0 - 1.0 = 6.0$ in. The corresponding flexural reinforcement ratio in the X direction is $\rho = 0.15/(12 \times 6) = 0.0021$. From Table A.5a, $R = 124$, and the design strength is

$$\phi m_n = \phi R b d^2 = \frac{0.90 \times 124 \times 12 \times 6^2}{12} = 4018 \text{ ft-lb/ft}$$

It is seen that the minimum slab steel required by the Code will provide for the positive bending moment of 2527 ft-lb/ft. The requirement of 0.15 in²/ft could be met by No. 3 (No. 10) bars at 9 in. spacing, but to reduce placement costs, No. 4 (No. 13) bars at the maximum permitted spacing of $2h = 14$ in. will be selected, providing 0.17 in²/ft. The X direction negative moment of 5054 ft-lb/ft requires

$$R = \frac{m_u}{\phi b d^2} = \frac{5054 \times 12}{0.90 \times 12 \times 6^2} = 156$$

and Table A.5a indicates that the required $\rho = 0.0027$. Thus, the negative bar requirement is $A_s = 0.0027 \times 12 \times 6 = 0.19$ in²/ft. This will be provided by No. 4 (No. 13) bars at 12 in. spacing, continued $4.01 \times 12 + 6 = 54$ in., or 4 ft 6 in., from the support face.

In the Y direction, the effective depth will be one bar diameter less than in the X direction, or 5.5 in. Thus, the flexural reinforcement ratio provided by the shrinkage and temperature steel is $\rho = 0.15/(12 \times 5.5) = 0.0023$. This results in $R = 135$, so the design strength is

$$\phi m_n = \frac{0.90 \times 135 \times 12 \times 5.5^2}{12} = 3675 \text{ ft-lb/ft}$$

well above the requirement for positive bending of 473 ft-lb/ft. No. 4 (No. 13) bars at 14 in. will be satisfactory for positive steel in this direction also. For the negative moment of 4194 ft-lb/ft,

$$R = \frac{4194 \times 12}{0.90 \times 12 \times 5.5^2} = 154$$

and from Table A.5a, the required $\rho = 0.0027$. The corresponding steel requirement is $0.0027 \times 12 \times 5.5 = 0.18$ in²/ft. No. 4 (No. 13) bars at 12 in. will be used, and they will be extended $5.62 \times 12 + 6 = 74$ in., or 6 ft 2 in., past the support face.

In the strong band, the positive moment of 13,100 ft-lb requires

$$R = \frac{12{,}900 \times 12}{0.90 \times 24 \times 6^2} = 199$$

The corresponding reinforcement ratio is 0.0034, and the required bar area is $0.0034 \times 24 \times 6 = 0.49$ in². This can be provided by two No. 5 (No. 16) bars. For the negative moment of 26,200 ft-lb,

$$R = \frac{25{,}800 \times 12}{0.90 \times 24 \times 6^2} = 398$$

resulting in $\rho = 0.0070$, and required steel equal to $0.0070 \times 24 \times 6 = 1.01$ in². Four No. 5 (No. 16) bars, providing an area of 1.23 in², will be used, and they will be cut off $4.01 \times 12 + 7.5 = 56$ in., or 4 ft 8 in., from the support face.

The final arrangement of bar reinforcement is shown in Fig. 15.11*e* and *f*. Negative bar cutoff locations are as indicated, and development by embedded lengths into the supports will be provided. All positive bars in the slab and strong band will be carried 6 in. into the support faces.

A design problem commonly met in practice is that of a slab supported along three edges and unsupported along the fourth, with a distributed load that increases linearly from zero along the free edge to a maximum at the opposite supported edge. Examples include the wall of a rectangular tank subjected to liquid pressure and earth-retaining walls with buttresses or counterforts (see Section 17.1).

Figure 15.12 shows such a slab, with load of intensity q_0 at the long, supported edge, reducing to zero at the free edge. In the main part of the slab, a constant load $k_2 q_0$ is carried in the X direction, as shown in Fig. 15.12*c*; thus, a constant load $k_2 q_0$ is deducted from the linear varying load in the Y direction, as shown in Fig. 15.12*d*. Along the free edge, a strong band of width βb is provided, carrying a load $k_1 q_0$, as in Fig. 15.12*a*, and so providing an uplift load equal to that amount at the end of the Y direction strip in Fig. 15.12*d*. The choice of k_1 and k_2 depends on the ratio of a/b. If this ratio is high, k_2 should be chosen with regard to the minimum slab reinforcement required by the ACI Code. The value of k_1 is then calculated by statics, based on a selected value of the restraining moment at the fixed edge, say one-half of the free cantilever value. In many cases it will be convenient to let k_1 equal k_2. Then it is the support moment that follows from statics. The value of β is selected as low as possible considering the upper limit on tensile reinforcement ratio in the strong band imposed by the Code for beams. The strong band is designed for a load of intensity $k_1 q_0$ distributed uniformly over its width βb.

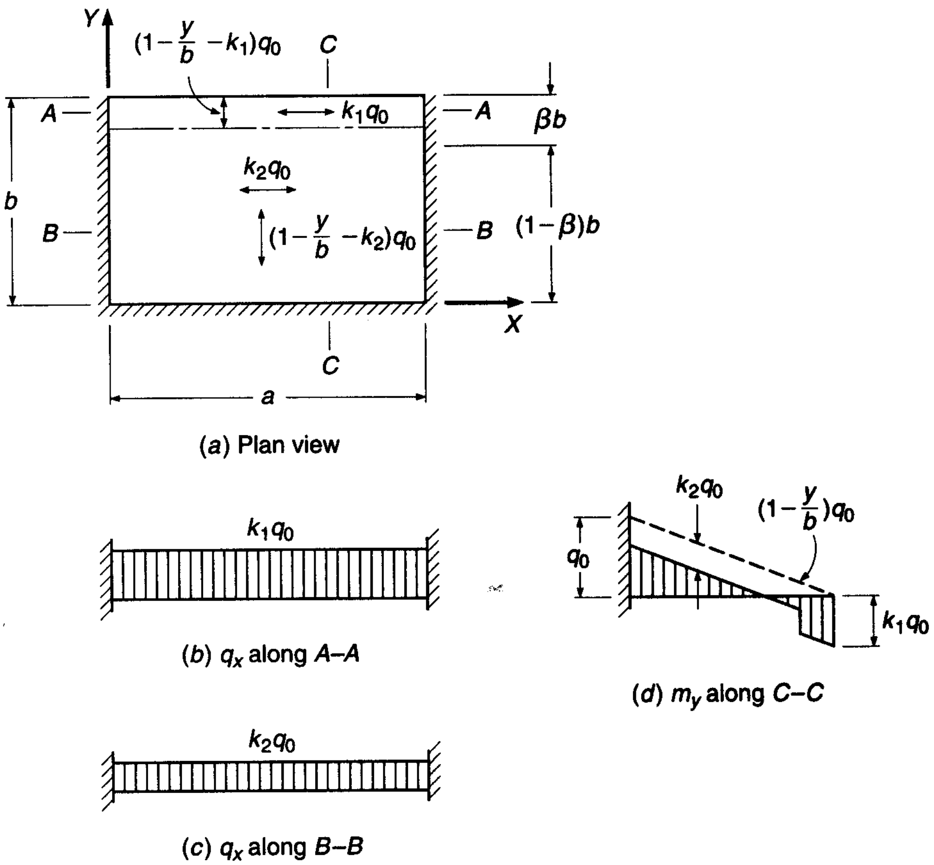

FIGURE 15.12
Slab with one free edge and linearly varying load.

15.7 SLABS WITH HOLES

Slabs with small openings can usually be designed as if there were no openings, replacing the interrupted steel with bands of reinforcing bars of equivalent area on either side of the opening in each direction (see Section 13.12). Slabs with larger openings must be treated more rigorously. The strip method offers a rational and safe basis for design in such cases. Integral load-carrying beams are provided along the edges of the opening, usually having the same depth as the remainder of the slab but with extra reinforcement, to pick up the load from the affected regions and transmit it to the supports. In general, these integral beams should be chosen so as to carry the loads most directly to the supported edges of the slab. The width of the strong bands should be selected so that the reinforcement ratios ρ are at or below the value required to produce a tension-controlled member (i.e., $\epsilon_t \geq 0.005$ and $\phi = 0.90$). Doing so will ensure ductile behavior of the slab.

Use of the strip method for analysis and design of a slab with a large central hole will be illustrated by the following example.

EXAMPLE 15.3 **Rectangular slab with central opening.** Figure 15.13*a* shows a 16 × 28 ft slab with fixed supports along all four sides. A central opening 4 × 8 ft must be accommodated. Estimated slab thickness, from Eq. (13.8*b*), is 7 in. The slab is to carry a uniformly distributed factored load of 300 psf, including self-weight. Devise an appropriate system of strong bands to reinforce the opening, and determine moments to be resisted at all critical sections of the slab.

SOLUTION. The basic pattern of discontinuity lines and load dispersion will be selected according to Fig. 15.5. Edge strips are defined having width $\frac{16}{4} = 4$ ft. In the corners, the load is equally divided in the two directions. In the central region, 100 percent of the load is assigned to the Y direction, while along the central part of the short edges, 100 percent of the load is carried in the X direction. Moments for this "basic case" without the hole will be calculated and later used as a guide in selecting moments for the actual slab with hole. A ratio of support to

FIGURE 15.13
Design example: slab with central hole.

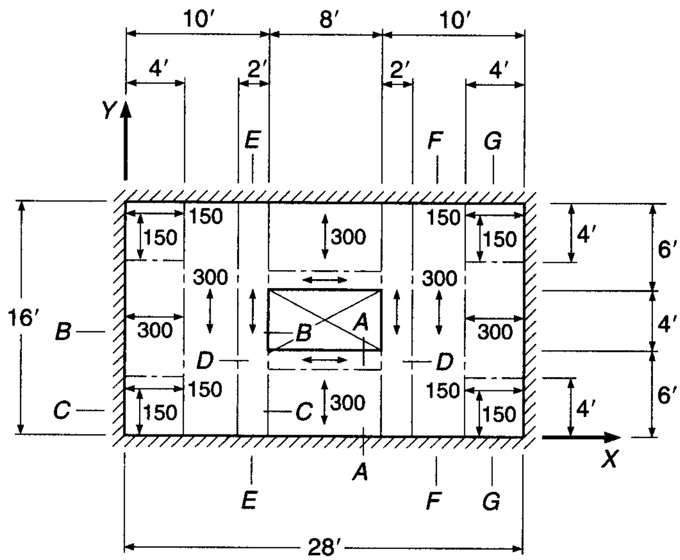

(*a*) Plan view

span moments of 2.0 will be used generally, as for the previous examples. Moments for the slab, neglecting the hole, would then be as follows:

X direction middle strips:

Cantilever: $$m_x = \frac{qb^2}{32} = 300 \times \frac{16^2}{32} = 2400 \text{ ft-lb/ft}$$

Negative: $$m_{xs} = 2400 \times \frac{2}{3} = 1600$$

Positive: $$m_{xf} = 2400 \times \frac{1}{3} = 800$$

X direction edge-strip moments are one-half of the middle-strip moments.

Y direction middle strips:

Cantilever: $$m_y = \frac{qb^2}{8} = 300 \times \frac{16^2}{8} = 9600 \text{ ft-lb/ft}$$

Negative: $$m_{ys} = 9600 \times \frac{2}{3} = 6400$$

Positive: $$m_{yf} = 9600 \times \frac{1}{3} = 3200$$

Y direction edge-strip moments are one-half of the middle-strip moments.

Because of the hole, certain strips lack support at one end. To support them, 1 ft wide strong bands will be provided in the X direction at the long edges of the hole and 2 ft wide strong bands in the Y direction on each side of the hole. The Y direction bands will provide for the reactions of the X direction bands. With the distribution of loads shown in Fig. 15.13*a*, strip reactions and moments are found as follows:

Strip *A–A*
It may at first be assumed that propped cantilever action is obtained, with the restraint moment along the slab edge taken as 6400 ft-lb/ft, the same as for the basic case. Summing moments about the left end of the loaded strip then results in

$$q_1 = \frac{300 \times 6 \times 3 - 6400}{1 \times 5.5} = -182 \text{ psf}$$

The negative value indicates that the cantilever strips are serving as supports for strip *D–D*, and in turn for the strong bands in the Y direction, which is hardly a reasonable assumption. Instead, a discontinuity line will be assumed 5 ft from the support, as shown in Fig. 15.13*b*, terminating the cantilever and leaving the 1 ft strip *D–D* along the edge of the opening in the X direction to carry its own load. It follows that the support moment in the cantilever strip is

Negative: $$m_{ys} = 300 \times 5 \times 2.5 = 3750 \text{ ft-lb/ft}$$

Strip *B–B*
The restraint moment at the supported edge will be taken to be the same as the basic case, i.e., 1600 ft-lb/ft. Summing moments about the left end of the strip of Fig. 15.13*c* then results in an uplift reaction at the right end, to be provided by strip *E–E*, of

$$q_2 = \frac{300 \times 4 \times 2 - 1600}{2 \times 9} = 44 \text{ psf}$$

FIGURE 15.13
(*Continued*)

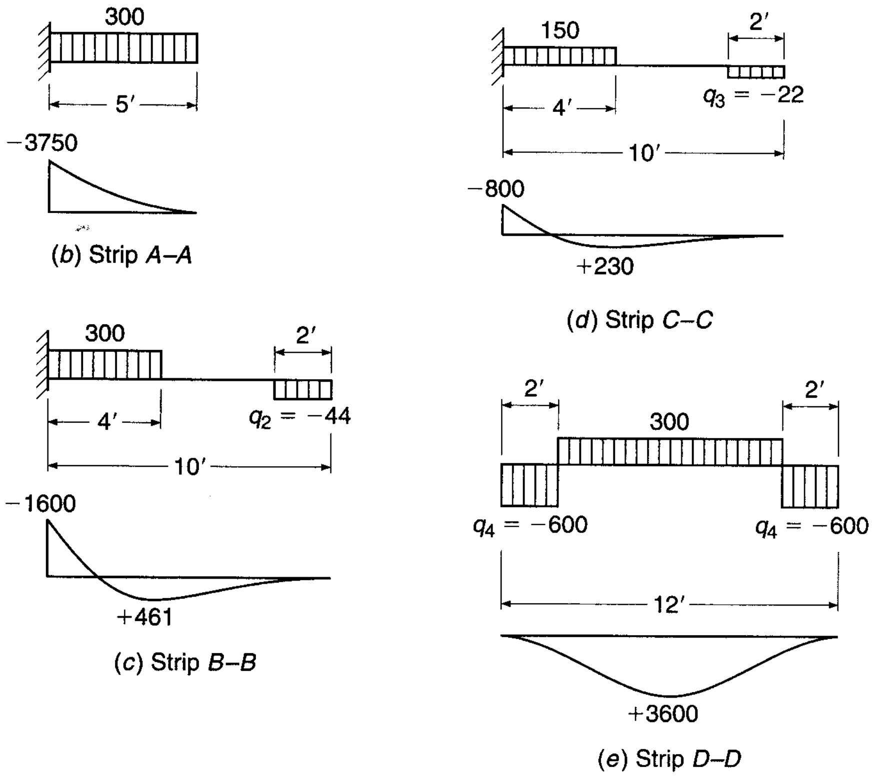

The left reaction is easily found to be 1112 lb, and the point of zero shear is 3.70 ft from the left support. The maximum positive moment, at that point, is

Positive: $$m_{xf} = 1112 \times 3.70 - 1600 - 300\,\frac{3.70^2}{2} = 461 \text{ ft-lb/ft}$$

Strip *C–C*
Negative and positive moments and the reaction to be provided by strip *E–E*, as shown in Fig. 15.13*d*, are all one-half the corresponding values for strip *B–B*.

Strip *D–D*
The 1 ft wide strip carries 300 psf in the *X* direction with reactions provided by the strong bands *E–E*, as shown in Fig. 15.13*e*. The maximum positive moment is

$$m_{xf} = 600 \times 2 \times 5 - 300 \times 4 \times 2 = 3600 \text{ ft-lb/ft}$$

Strip *E–E*
In reference to Fig. 15.13*f*, the strong bands in the *Y* direction carry the directly applied load of 300 psf plus the 44 psf load from strip *B–B*, the 22 psf load from strip *C–C*, and the 600 psf end reaction from strip *D–D*. For strip *E–E* the cantilever, negative, and positive moments are

Cantilever: $$m_y = 300 \times 8 \times 4 + 22 \times 4 \times 2 + 44 \times 4 \times 6 + 600 \times 1 \times 5.5$$
$$= 14{,}132 \text{ ft-lb/ft}$$

Negative: $$m_{ys} = 14{,}132 \times \frac{2}{3} = 9421$$

Positive: $$m_{yf} = 14{,}132 \times \frac{1}{3} = 4711$$

FIGURE 15.13
(Continued)

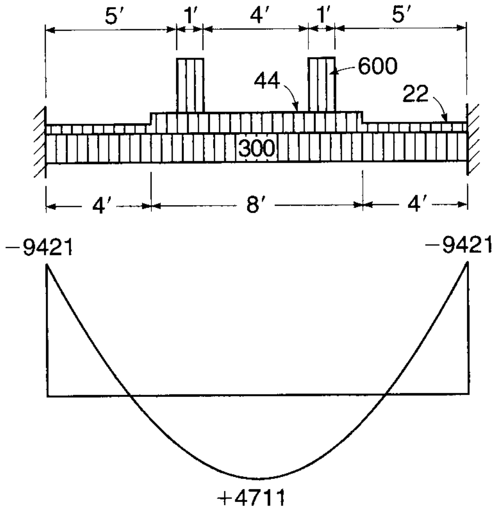

(*f*) Strip *E–E*

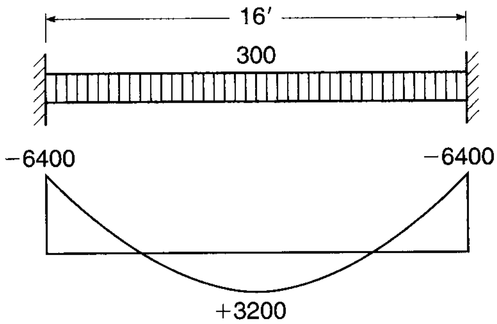

(*g*) Strip *F–F*

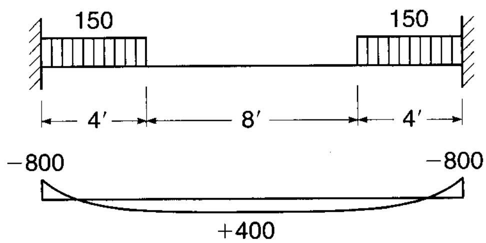

(*h*) Strip *G–G*

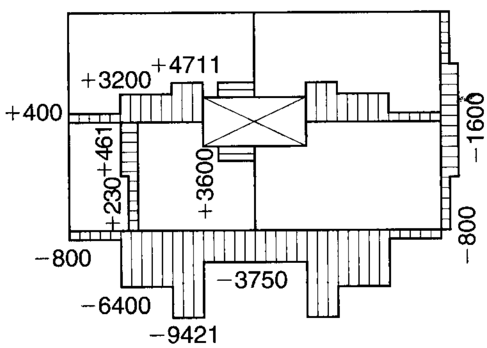

(*i*) Factored moments – symmetrical about both axes

It should be emphasized that the loads shown are psf and would be multiplied by 2 to obtain loads per foot acting on the strong bands. Correspondingly, the moments just obtained are per foot width and must be multiplied by 2 to give the support and span moments for the 2 ft wide strong band.

Strip *F–F*

The moments for the Y direction middle strip of the basic case may be used without change; thus, in Fig. 15.13*g*,

Negative: $m_{ys} = 6400$ ft-lb/ft

Positive: $m_{yf} = 3200$

Strip *G–G*

Moments for the Y direction edge strips of the basic case are used without change, resulting in

Negative: $m_{ys} = 800$ ft-lb/ft

Positive: $m_{yf} = 400$

as shown in Fig. 15.13*h*.

The final distribution of moments across the negative and positive critical sections of the slab is shown in Fig. 15.13*i*. The selection of reinforcing bars and determination of cutoff points would follow the same methods as presented in Examples 15.1 and 15.2 and will not be given here. Reinforcing bar ratios needed in the strong bands are well below the maximum permitted for the 7 in. slab depth.

It should be noted that strips *B–B*, *C–C*, and *D–D* have been designed as if they were simply supported at the strong band *E–E*. To avoid undesirably wide cracks where these strips pass over the strong band, nominal negative reinforcement should be added in this region. Positive bars should be extended fully into the strong bands.

15.8 ADVANCED STRIP METHOD

The simple strip method described in the earlier sections of this chapter is not directly suitable for the design of slabs supported by columns (e.g., flat plates) or slabs supported at reentrant corners.† For such cases, Hillerborg introduced the advanced strip method (Refs. 15.2, 15.5, 15.12, and 15.13).

Fundamental to the advanced strip method is the corner-supported element, such as that shown shaded in Fig. 15.14*a*. The corner-supported element is a rectangular region of the slab with the following properties:

1. The edges are parallel to the reinforcement directions.
2. It carries a uniform load q per unit area.
3. It is supported at only one corner.
4. No shear forces act along the edges.
5. No twisting moments act along the edges.
6. All bending moments acting along an edge have the same sign or are zero.
7. The bending moments along the edges are the factored moments used to design the reinforcing bars.

† However, Wood and Armer, in Ref. 15.8, suggest that beamless slabs with column supports can be solved by the simple strip method through the use of strong bands between columns or between columns and exterior walls.

FIGURE 15.14
Slab with central supporting column.

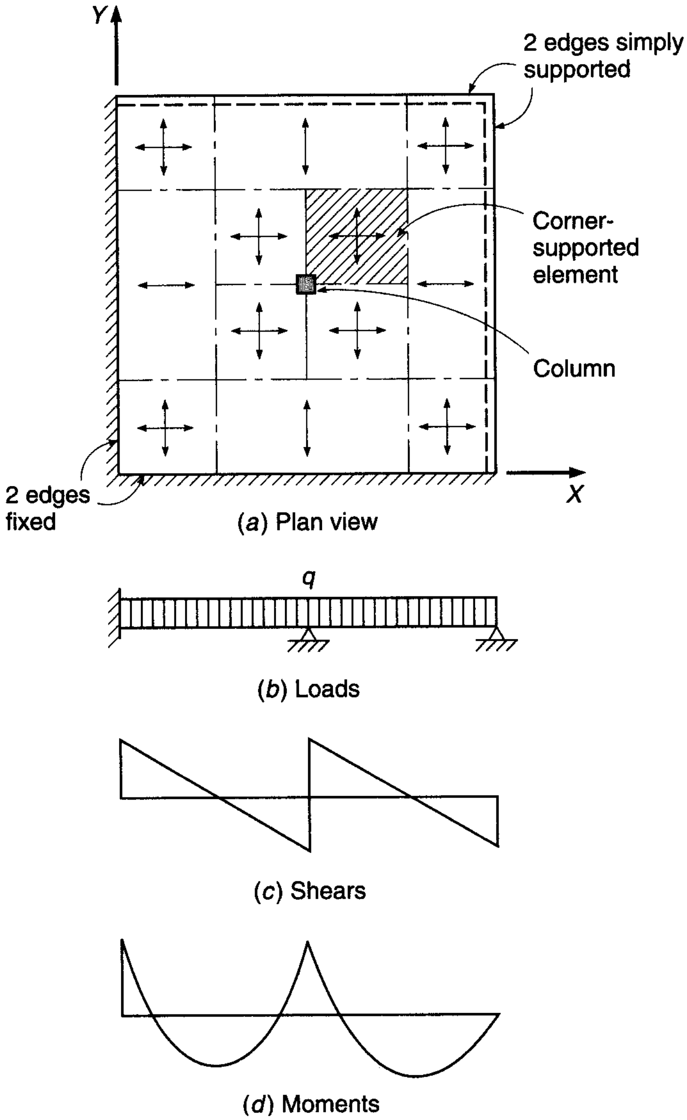

A uniformly loaded strip in the X direction, shown in Fig. 15.14*b*, will thus have shear and moment diagrams as shown in Fig. 15.14*c* and *d*, respectively. Maximum moments are located at the lines of zero shear. The outer edges of the corner-supported element are defined at the lines of zero shear in both the X and Y directions.

A typical corner-supported element, with an assumed distribution of moments along the edges, is shown in Fig. 15.15. It will be assumed that the bending moment is constant along each half of each edge. The vertical reaction is found by summing vertical forces:

$$R = qab \tag{15.19}$$

and moment equilibrium about the Y axis gives

$$m_{xfm} - m_{xsm} = \frac{qa^2}{2} \tag{15.20}$$

FIGURE 15.15
Corner-supported element.

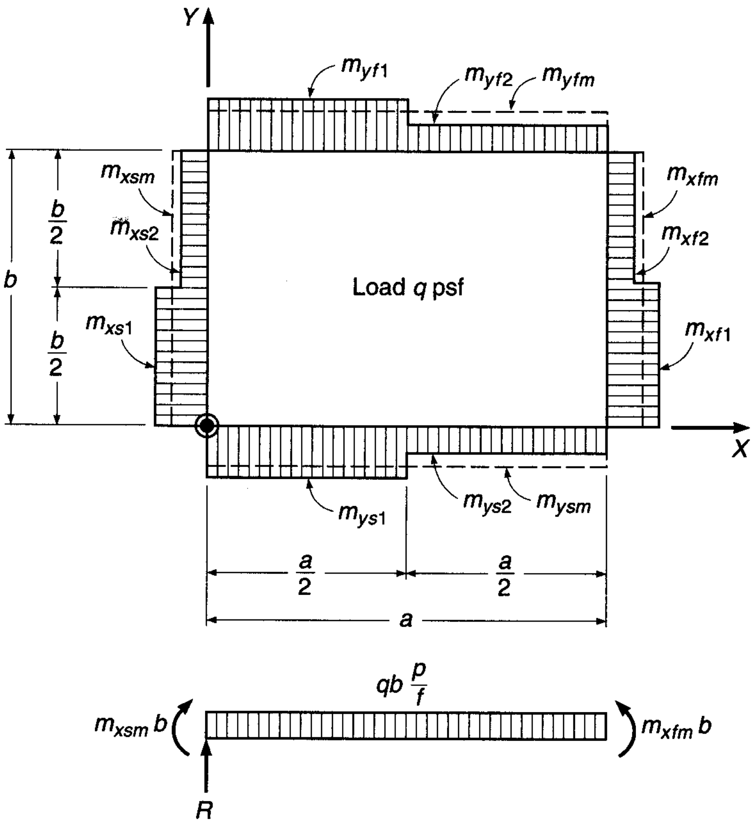

where m_{xfm} and m_{xsm} are the mean span and support moments per unit width, and the beam sign convention is followed. Similarly,

$$m_{yfm} - m_{ysm} = \frac{qb^2}{2} \tag{15.21}$$

The last two equations are identical with the condition for a corresponding part of a simple strip—Eq. (15.20) spanning in the X direction and Eq. (15.21) in the Y direction—supported at the axis and carrying the load qb or qa per foot. So if the corner-supported element forms a part of a strip, that part should carry 100 percent of the load q in each direction. (This requirement was discussed earlier in Chapter 13 and is simply a requirement of static equilibrium.)

The distribution of moments within the boundaries of a corner-supported element is complex. With the load on the element carried by a single vertical reaction at one corner, strong twisting moments must be present within the element; this contrasts with the assumptions of the simple strip method used previously.

The moment field within a corner-supported element and its edge moments have been explored in great detail in Ref. 15.12. It is essential that the edge moments, given in Fig. 15.15, are used to design the reinforcing bars (i.e., that nowhere within the element will a bar be subjected to a greater moment than at the edges). To meet this requirement, a limitation must be put on the moment distribution along the edges. Based on his studies (Ref. 15.12), Hillerborg has recommended the following restriction on edge moments:

$$m_{xf2} - m_{xs2} = \alpha\,\frac{qa^2}{2} \tag{15.22a}$$

with

$$0.25 \le \alpha \le 0.7 \tag{15.22b}$$

where m_{xf2} and m_{xs2} are the positive and negative X direction moments, respectively, in the outer half of the element, as shown in Fig. 15.15. The corresponding restriction applies in the Y direction. He notes further that for most practical applications, the edge moment distribution shown in Fig. 15.16 is appropriate, with

$$m_{xf1} = m_{xf2} = m_{xfm} \tag{15.23}$$

$$m_{xs2} = 0 \tag{15.24a}$$

$$m_{xs1} = 2m_{xsm} \tag{15.24b}$$

(Alternatively, it is suggested in Ref. 15.14 that negative support moments across the column line be taken at $1.5m_{xsm}$ in the half-element width by the column and at $0.5m_{xsm}$ in the remaining outside half-element width.) Positive reinforcement in the span should be carried through the whole corner-supported element. The negative reinforcement corresponding to $m_{xs1} - m_{xs2}$ in Fig. 15.15 must be extended at least $0.6a$ from the support. The remaining negative steel, if any, should be carried through the whole corner-supported element. The corresponding restrictions apply in the Y direction.

In practical applications, corner-supported elements are combined with each other and with parts of one-way strips, as shown in Fig. 15.14, to form a system of strips. In this system, each strip carries the total load q, as discussed earlier. In laying out the elements and strips, the concentrated corner support for the element may be assumed to be at the center of the supporting column, as shown in Fig. 15.14, unless supports are of significant size. In that case, the corner support may be taken at the corner of the column, and an ordinary simple strip may be included that spans between the column faces, along the edge of the corner-supported elements. Note in the figure that the corner regions of the slab are not included in the main strips that

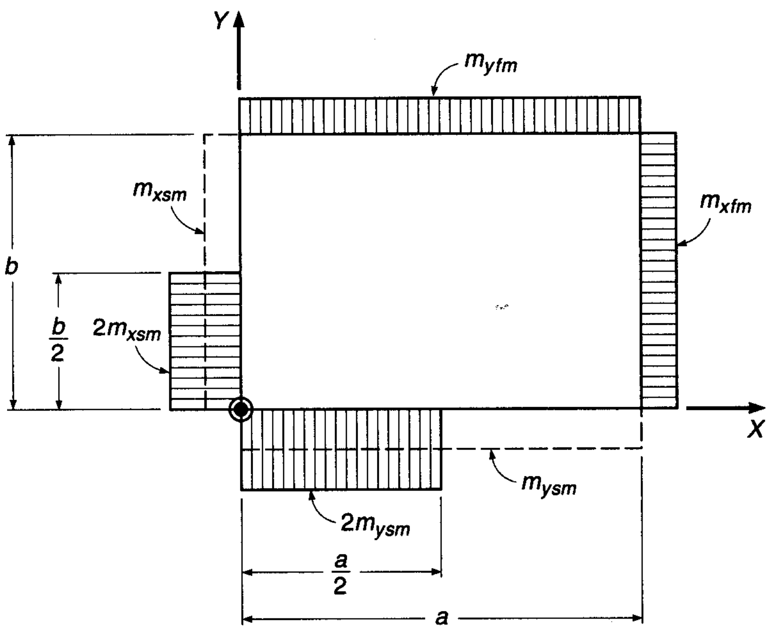

FIGURE 15.16
Recommended distribution of moments for typical corner-supported element.

include the corner-supported elements. These may safely be designed for one-third of the corresponding moments in the main strips (Ref. 15.13).

EXAMPLE 15.4 **Edge-supported flat plate with central column.** Figure 15.17*a* illustrates a flat plate with overall dimensions 34 × 34 ft, with fixed supports along the left and lower edges in the sketch, hinged supports at the right and upper edges, and a single central column 16 in. square. It must carry a service live load of 40 psf over its entire surface plus its own weight and an additional superimposed dead load of 7 psf. Find the moments at all critical sections, and determine the required slab thickness and reinforcement. Material strengths are specified at $f_y = 60{,}000$ psi and $f'_c = 4000$ psi.

SOLUTION. A trial slab depth will be chosen based on Table 13.5, which governs for flat plates. It will be conservative for the present case, where continuous support is provided along the outer edges.

$$h = \frac{17 \times 12}{33} = 6.18 \text{ in.}$$

A thickness of 6.5 in. will be selected tentatively, for which the self-weight is $150 \times 6.5/12 = 81$ psf. The total factored load to be carried is thus

$$q_u = 1.2(81 + 7) + 1.6 \times 40 = 170 \text{ psf}$$

The average strip moments in the X direction in the central region caused by the load of 170 psf are found by elastic theory and are shown in Fig. 15.17*c*. The analysis in the Y direction is identical. The points of zero shear (and maximum moments) are located 9.11 ft to the left of the column and 10.32 ft to the right, as indicated. These dimensions determine the size of the four corner-supported elements.

Moments in the slab are then determined according to the preceding recommendations. At the fixed edge along the left side of the main strips, the moment m_{xs} is simply the moment

FIGURE 15.17
Design example: edge-supported flat plate with central column.

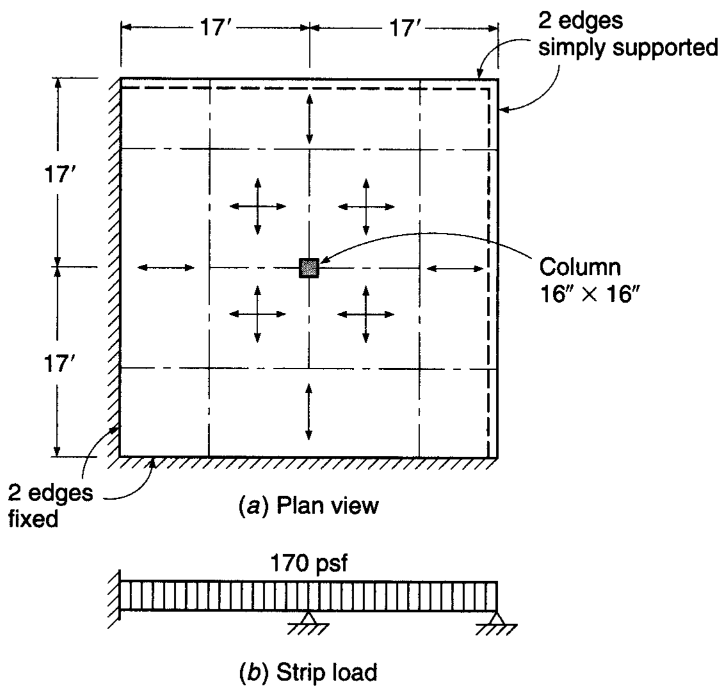

FIGURE 15.17
(*Continued*)

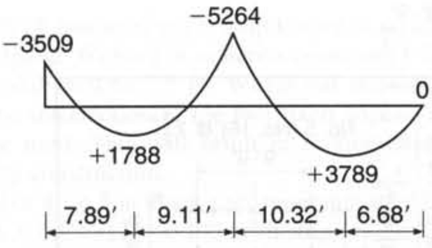

(*c*) Moments m_x, ft-lb/ft

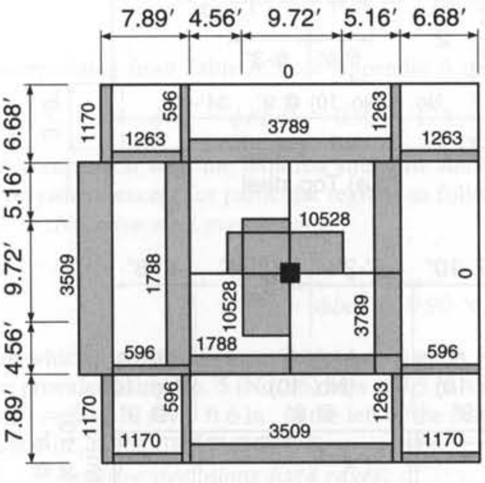

(*d*) Factored moments per 1 foot strip

per foot strip from the elastic analysis, 3509 ft-lb/ft. At the left edge of the corner-supported element in the left span,

$$m_{xf1} = m_{xf2} = m_{xfm} = 1788 \text{ ft-lb/ft}$$

Along the centerline of the slab, over the column, following the recommendations shown in Fig. 15.16,

$$m_{xs2} = 0$$
$$m_{xs1} = 2m_{xsm} = 10{,}528 \text{ ft-lb/ft}$$

At the right edge of the corner-supported element in the right span,

$$m_{xf1} = m_{xf2} = m_{xfm} = 3789 \text{ ft-lb/ft}$$

At the outer, hinge-supported edge, all moments are zero. Make a check of the α values, using Eq. (15.22*b*), and note from Eq. (15.20) that $qa^2/2 = m_{xfm} - m_{xsm}$. Thus, in the left span,

$$\alpha = \frac{m_{xf2} - m_{xs2}}{qa^2/2} = \frac{1788 - 0}{1788 + 5264} = 0.25$$

and in the right span,

$$\alpha = \frac{3789 - 0}{3789 + 5264} = 0.42$$

Because both values are within the range of 0.25 to 0.75, the proposed distribution of moments is satisfactory. If the first value had been below the lower limit of 0.25, the negative moment in the column half-strip might have been reduced from 10,528 ft-lb/ft, and the negative moment

FIGURE 15.17
(Continued)

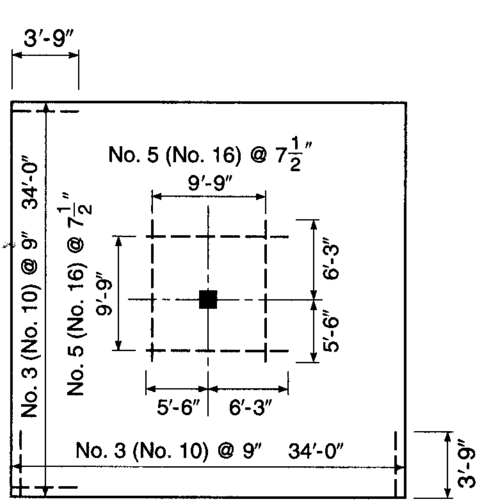

(*e*) Top steel

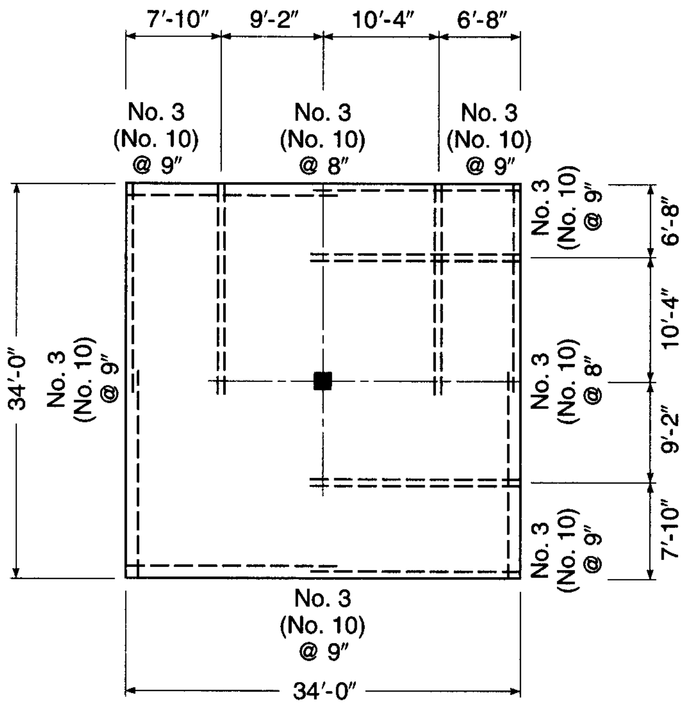

(*f*) Bottom steel

in the adjacent half-strip might have been increased above the 0 value used. Alternatively, the total negative moment over the column might have been somewhat decreased, with a corresponding increase in span moments.

Moments in the Y direction correspond throughout, and all results are summarized in Fig. 15.17*d*. Moments in the strips adjacent to the supported edges are set equal to one-third of those in the adjacent main strips.

With moments per ft strip known at all critical sections, the required reinforcement is easily found. With a $\frac{3}{4}$ in. concrete cover and $\frac{1}{2}$ in. bar diameter, in general the effective depth of the slab will be 5.5 in. Where bar stacking occurs—i.e., over the central column and near the intersection of the two fixed edges—an average effective depth equal to 5.25 in. will be used. This will result in reinforcement identical in the two directions and will simplify construction.

For the 6.5 in. thick slab, minimum steel for shrinkage and temperature crack control is $0.0018 \times 6.5 \times 12 = 0.140$ in^2/ft strip, which will be provided by No. 3 (No. 10) bars at 9 in. spacing. The corresponding flexural reinforcement ratio is

$$\rho_{\min} = \frac{0.140}{5.5 \times 12} = 0.0021$$

Interpolating from Table A.5a of Appendix A makes $R = 124$, and the design strength is

$$\phi m_n = \phi R b d^2 = 0.90 \times 124 \times 12 \times 5.5^2/12 = 3376 \text{ ft-lb/ft}$$

In comparison with the required strengths summarized in Fig. 15.17*d*, this will be adequate everywhere except for particular regions as follows:

Negative steel over column:

$$R = \frac{m_u}{\phi b d^2} = \frac{10{,}528 \times 12}{0.90 \times 12 \times 5.25^2} = 424$$

for which $\rho = 0.0076$ (from Table A.5a), and $A_s = 0.0076 \times 12 \times 5.25 = 0.48$ in^2/ft. This will be provided using No. 5 (No. 16) bars at 7.5 in. spacing. They will be continued a distance $0.6 \times 9.11 = 5.47$ ft, say 5 ft 6 in., to the left of the column centerline, and $0.6 \times 10.32 = 6.19$ ft, say 6 ft 3 in., to the right.

Negative steel along fixed edges:

$$R = \frac{3509 \times 12}{0.90 \times 12 \times 5.50^2} = 129$$

for which $\rho = 0.0022$ and $A_s = 0.0022 \times 12 \times 5.5 = 0.15$ in^2/ft. No. 3 (No. 10) bars at 9 in. spacing will be adequate. The point of inflection for the slab in this region is easily found to be 3.30 ft from the fixed edge. The negative bars will be extended 5.5 in. beyond that point, resulting in a cutoff 45 in., or 3 ft 9 in., from the support face.

Positive steel in outer spans:

$$R = \frac{3789 \times 12}{0.90 \times 12 \times 5.50^2} = 139$$

resulting in $\rho = 0.0024$ and $A_s = 0.0024 \times 12 \times 5.5 = 0.16$ in^2/ft. No. 3 (No. 10) bars at 8 in. spacing will be used. In all cases, the maximum spacing of $2h = 13$ in. is satisfied. That maximum would preclude the economical use of larger-diameter bars.

Bar size and spacing and cutoff points for the top and bottom steel are summarized in Fig. 15.17*e* and *f*, respectively.

Finally, the load carried by the central column is

$$P = 170 \times 19.43 \times 19.43 = 64{,}200 \text{ lb}$$

Investigating punching shear at a critical section taken $d/2$ from the face of the 16 in. column, with reference to Eq. (13.11*a*) and with $b_o = 4 \times (16.00 + 5.25) = 85$ in., gives

$$\phi V_c = 4\phi\sqrt{f'_c}\, b_o d = 4 \times 0.75\sqrt{4000} \times 85 \times 5.25 = 84{,}700 \text{ lb}$$

This is well above the applied shear of 64,200 lb, confirming that the slab thickness is adequate and that no shear reinforcement is required.

15.9 COMPARISONS OF METHODS FOR SLAB ANALYSIS AND DESIGN

The conventional methods of slab analysis and design, as described in Chapter 13 and as treated in Chapter 13 of the ACI Code, are limited to applications in which slab panels are supported on opposite sides or on all four sides by beams or walls or to the case of flat plates and related forms supported by a relatively regular array of columns. In all cases, slab panels must be square or rectangular, loads must be uniformly distributed within each panel, and slabs must be free of significant holes.

Both the yield line theory and the strip method offer the designer rational methods for slab analysis and design over a much broader range, including the following:

1. Boundaries of any shape, including rectangular, triangular, circular, and L-shaped boundaries with reentrant corners
2. Supported or unsupported edges, skewed supports, column supports, or various combinations of these conditions
3. Uniformly distributed loads, loads distributed over partial panel areas, linear varying distributed loads, line loads, and concentrated loads
4. Slabs with significant holes

The most important difference between the strip method and the yield line method is the fact that the strip method produces results that are always on the safe side, but yield line analysis may result in unsafe designs. A slab designed by the strip method may possibly carry a higher load than estimated, through internal force redistributions, before collapse; a slab analyzed by yield line procedures may fail at a lower load than anticipated if an incorrect mechanism has been selected as the basis or if the defining dimensions are incorrect.

Beyond this, it should be realized that the strip method is a tool for *design*, by which the slab thickness and reinforcing bar size and distribution may be selected to resist the specified loads. In contrast, the yield line theory offers only a means for *analyzing the capacity of a given slab*, with known reinforcement. According to the yield line approach, the design process is actually a matter of reviewing the capacities of a number of trial designs and alternative reinforcing patterns. All possible yield line patterns must be investigated and specific dimensions varied to be sure that the correct solution has been found. Except for simple cases, this is likely to be a time-consuming process.

Neither the strip method nor the yield line approach provides any information regarding cracking or deflections at service load. Both focus attention strictly on flexural strength. However, by the strip method, if care is taken at least to approximate the elastic distribution of moments, little difficulty should be experienced with excessive cracking. The methods for deflection prediction presented in Section 13.13 can, without difficulty, be adapted for use with the strip method, because the concepts are fully compatible.

With regard to economy of reinforcement, it might be supposed that use of the strip method, which always leads to designs on the safe side, might result in more expensive structures than the yield line theory. Comparisons, however, indicate that in most cases this is not so (Refs. 15.8 and 15.12). Through proper use of the strip method, reinforcing bars are placed in a nonuniform way in the slab (e.g., in strong bands around openings) where they are used to best effect; yield line methods, on the other hand, often lead to uniform bar spacings, which may mean that individual bars are used inefficiently.

Many tests have been conducted on slabs designed by the strip method (Ref. 15.11; also, see the summary in Ref. 15.12). These tests included square slabs, rectangular slabs, slabs with both fixed and simply supported edges, slabs supported directly by columns, and slabs with large openings. The conclusions drawn determine that the strip method provides for safe design with respect to nominal strength and that at service load, behavior with respect to cracking and deflections is generally satisfactory. The method has been widely and successfully used in the Scandinavian countries since the 1960s.

References

15.1. A. Hillerborg, "Equilibrium Theory for Reinforced Concrete Slabs" (in Swedish), *Betong*, vol. 41, no. 4, 1956, pp. 171–182.

15.2. A. Hillerborg, *Strip Method for Slabs on Columns, L-Shaped Plates, Etc.* (in Swedish), Svenska Riksbyggen, Stockholm, 1959.

15.3. A. Hillerborg, "A Plastic Theory for the Design of Reinforced Concrete Slabs," *Proc. Sixth Congr.*, International Association for Bridge and Structural Engineering, Stockholm, 1960.

15.4. R. E. Crawford, *Limit Design of Reinforced Concrete Slabs*, thesis submitted to University of Illinois for the degree of Ph.D., Urbana, IL, 1962.

15.5. F. A. Blakey, *Strip Method for Slabs on Columns, L-Shaped Plates, Etc.* (translation of Ref. 15.2), Commonwealth Scientific and Industrial Research Organization, Melbourne, 1964.

15.6. K. O. Kemp, "A Lower Bound Solution to the Collapse of an Orthotropically Reinforced Slab on Simple Supports," *Mag. Concr. Res.*, vol. 14, no. 41, 1962, pp. 79–84.

15.7. K. O. Kemp, "Continuity Conditions in the Strip Method of Slab Design," *Proc. Inst. Civ. Eng.*, vol. 45, 1970, p. 283 (supplement paper 7268s).

15.8. R. H. Wood and G. S. T. Armer, "The Theory of the Strip Method for the Design of Slabs," *Proc. Inst. Civ. Eng.*, vol. 41, 1968, pp. 285–311.

15.9. R. H. Wood, "The Reinforcement of Slabs in Accordance with a Predetermined Field of Moments," *Concrete*, vol. 2, no. 2, 1968, pp. 69–76.

15.10. G. S. T. Armer, "The Strip Method: A New Approach to the Design of Slabs," *Concrete*, vol. 2, no. 9, 1968, pp. 358–363.

15.11. G. S. T. Armer, "Ultimate Load Tests of Slabs Designed by the Strip Method," *Proc. Inst. Civ. Eng.*, vol. 41, 1968, pp. 313–331.

15.12. A. Hillerborg, *Strip Method of Design*, Viewpoint Publications, Cement and Concrete Association, Wexham Springs, Slough, England, 1975.

15.13. A. Hillerborg, "The Advanced Strip Method—a Simple Design Tool," *Mag. Concr. Res.*, vol. 34, no. 121, 1982, pp. 175–181.

15.14. R. Park and W. L. Gamble, *Reinforced Concrete Slabs*, 2nd ed. (Chapter 6), John Wiley, New York, 2000, pp. 232–302.

15.15. A. Hillerborg, *Strip Method Design Handbook*, E & FN Spon/Chapman & Hill, London, 1996.

15.16. S. Timoshenko and S. Woinowsky-Krieger, *Theory of Plates and Shells*, 2nd ed., McGraw-Hill, New York, 1959.

Problems

Note: For all the following problems, use material strengths f_y = 60,000 psi and f'_c = 4000 psi. All ACI Code requirements for minimum steel, maximum spacings, bar cutoff, and special corner reinforcement are applicable.

15.1. The square slab of Fig. P15.1 is simply supported by masonry walls along all four sides. It is to carry a service live load of 100 psf in addition to its self-weight. Specify a suitable load distribution; determine moments at all controlling sections; and select the slab thickness, reinforcing bars, and spacing.

FIGURE P15.1

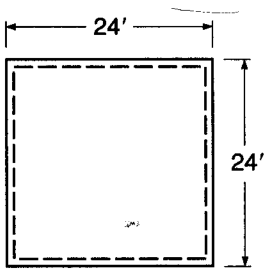

15.2. The rectangular slab shown in Fig. P15.2 is a typical interior panel of a large floor system having beams on all column lines. Columns and beams are sufficiently stiff that the slab can be considered fully restrained along all sides. A live load of 100 psf and a superimposed dead load of 30 psf must be carried in addition to the slab self-weight. Determine the required slab thickness, and specify all reinforcing bars and spacings. Cutoff points for negative bars should be specified; all positive steel may be carried into the supporting beams. Take support moments to be 2 times the span moments in the strips.

FIGURE P15.2

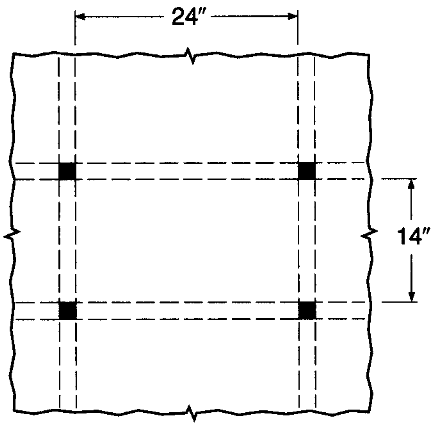

15.3. The slab of Fig. P15.3 may be considered fully fixed along three edges, but it is without support along the fourth, long side. It must carry a uniformly distributed live load of 80 psf plus an external dead load of 40 psf. Specify a suitable slab depth, and determine reinforcement and cutoff points.

FIGURE P15.3

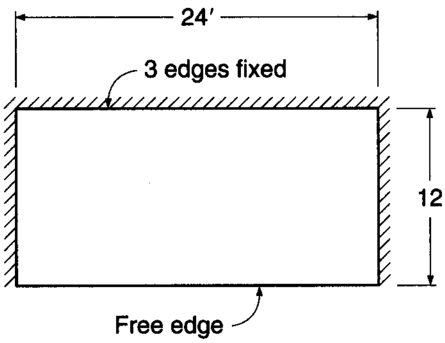

15.4. Figure P15.4 shows a counterfort retaining wall (see Section 17.9) consisting of a base slab and a main vertical wall of constant thickness retaining the earth. Counterfort walls spaced at 19 ft on centers along the wall provide additional

FIGURE P15.4

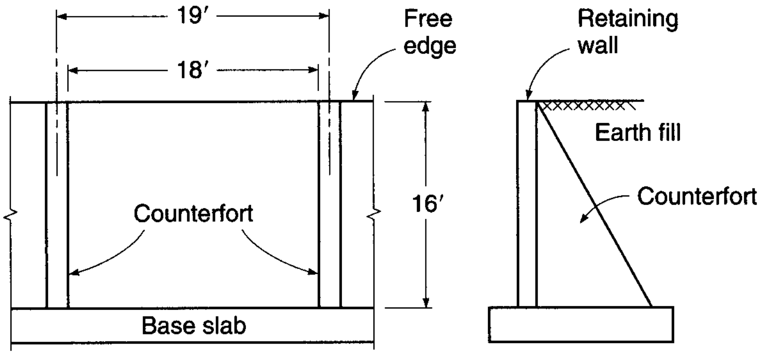

support for the main slab. Each section of the main wall, which is 16 ft high and 18 ft long, may be considered fully fixed at its base and also along its two vertical sides (because of full continuity and identical loadings on all such panels). The top of the main wall is without support. The horizontal earth pressure varies from 0 at the top of the wall to 587 psf at the top of the base slab. Determine a suitable thickness for the main wall, and select reinforcing bars and spacing.

15.5. The triangular slab shown in Fig. P15.5, providing cover over a loading dock, is fully fixed along two adjacent sides and free of support along the diagonal edge. A uniform snow load of 60 psf is anticipated. Dead load of 10 psf will act, in addition to self-weight. Determine the required slab depth and specify all reinforcement. (*Hint:* The main bottom reinforcement should be parallel to the free edge, and the negative reinforcement should be perpendicular to the supported edges.)

FIGURE P15.5

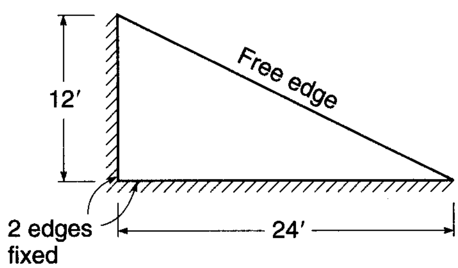

15.6. Figure P15.6 shows a rectangular slab with a large opening near one corner. It is simply supported along one long side and the adjacent short side, and the two

FIGURE P15.6

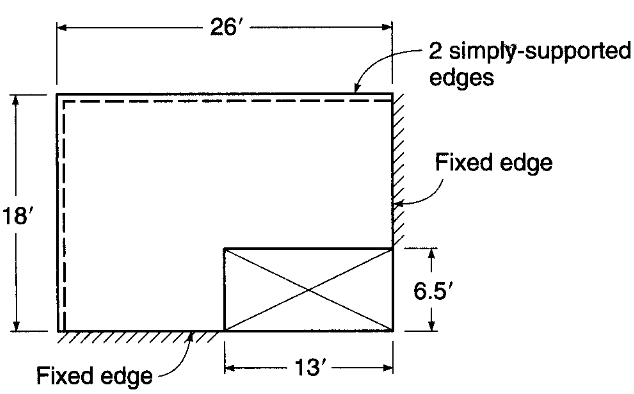

edges adjacent to the opening are fully fixed. A factored load of 250 psf must be carried. Find the required slab thickness, and specify all reinforcement.

15.7. The roof deck slab of Fig. P15.7 is intended to carry a total factored load, including self-weight, of 165 psf. It will have fixed supports along the two long sides and one short side, but the fourth edge must be free of any support. Two 16 in. square columns will be located as shown.

(*a*) Determine an acceptable slab thickness.
(*b*) Select appropriate load dispersion lines.
(*c*) Determine moments at all critical sections.
(*d*) Specify bar sizes, spacings, and cutoff points.
(*e*) Check controlling sections in the slab for shear strength.

FIGURE P15.7

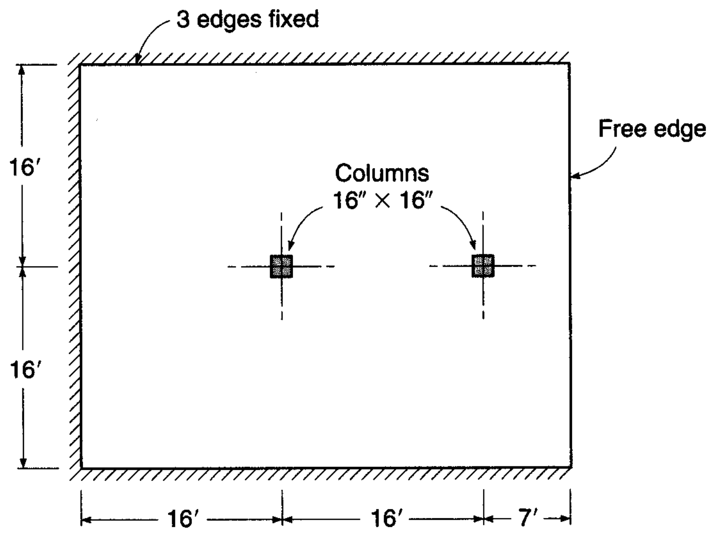

16 Footings and Foundations

16.1 TYPES AND FUNCTIONS

The substructure, or foundation, is the part of a structure that is usually placed below the surface of the ground and that transmits the load to the underlying soil or rock. All soils compress noticeably when loaded and cause the supported structure to settle. The two essential requirements in the design of foundations are that the total settlement of the structure be limited to a tolerably small amount and that differential settlement of the various parts of the structure be eliminated as nearly as possible. With respect to possible structural damage, the elimination of differential settlement, i.e., different amounts of settlement within the same structure, is even more important than limitations on uniform overall settlement.

To limit settlements as indicated, it is necessary (1) to transmit the load of the structure to a soil stratum of sufficient strength and (2) to spread the load over a sufficiently large area of that stratum to minimize bearing pressure. If adequate soil is not found immediately below the structure, it becomes necessary to use deep foundations such as piles or caissons to transmit the load to deeper, firmer layers. If satisfactory soil directly underlies the structure, it is merely necessary to spread the load, by footings or other means. Such substructures are known as *spread* foundations, and it is mainly this type that will be discussed. Information on the more special types of deep foundations can be found in texts on foundation engineering, e.g., Refs. 16.1 to 16.4.

16.2 SPREAD FOOTINGS

Spread footings can be classified as wall and column footings. The horizontal outlines of the most common types are given in Fig. 16.1. A wall footing is simply a strip of reinforced concrete, wider than the wall, that distributes its pressure. Single-column footings are usually square, sometimes rectangular, and represent the simplest and most economical type. Their use under exterior columns meets with difficulties if property rights prevent the use of footings projecting beyond the exterior walls. In this case, combined footings or strap footings are used that enable one to design a footing that will not project beyond the wall column. Combined footings under two or more columns are also used under closely spaced, heavily loaded interior columns where single footings, if they were provided, would completely or nearly merge.

Such individual or combined column footings are the most frequently used types of spread foundations on soils of reasonable bearing capacity. If the soil is weak and/or column loads are great, the required footing areas become so large as to be uneconomical. In this case, unless a deep foundation is called for by soil conditions, a mat

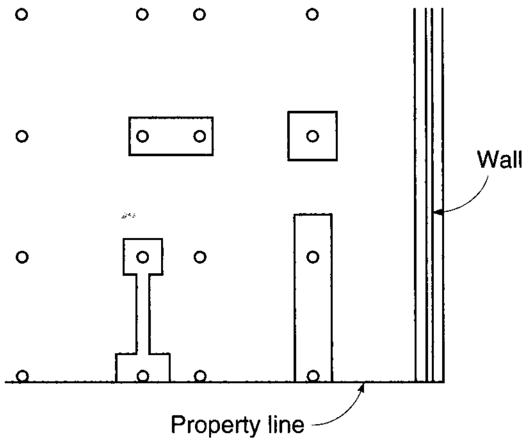

FIGURE 16.1
Types of spread footing.

or raft foundation is resorted to. This consists of a solid reinforced concrete slab that extends under the entire building and, consequently, distributes the load of the structure over the maximum available area. Such a foundation, in view of its own rigidity, also minimizes differential settlement. It consists, in its simplest form, of a concrete slab reinforced in both directions. A form that provides more rigidity consists of an inverted girder floor. Girders are located in the column lines in each direction, and the slab is provided with two-way reinforcement, spanning between girders. Inverted flat slabs, with capitals at the bottoms of the columns, are also used for mat foundations.

16.3 DESIGN FACTORS

In ordinary construction, the load on a wall or column is transmitted vertically to the footing, which in turn is supported by the upward pressure of the soil on which it rests. If the load is symmetrical with respect to the bearing area, the bearing pressure is assumed to be uniformly distributed (Fig. 16.2*a*). It is known that this is only approximately true. Under footings resting on coarse-grained soils, the pressure is larger at the center of the footing and decreases toward the perimeter (Fig. 16.2*b*). This is so because the individual grains in such soils are somewhat mobile, so that the soil located close to the perimeter can shift very slightly outward in the direction of lower soil stresses. In contrast, in clay soils pressures are higher near the edge than at the center of the footing, since in such soils the load produces a shear resistance around the perimeter that adds to the upward pressure (Fig. 16.2*c*). It is customary to disregard these nonuniformities (1) because their numerical amount is uncertain and highly

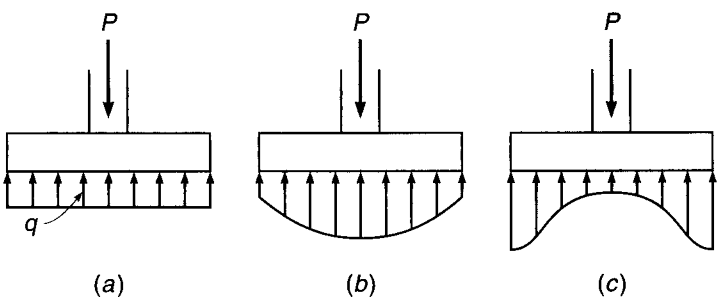

FIGURE 16.2
Bearing pressure distribution: (*a*) as assumed; (*b*) actual, for granular soils; (*c*) actual, for cohesive soils.

variable, depending on types of soil, and (2) because their influence on the magnitudes of bending moments and shearing forces in the footing is relatively small.

On compressible soils, footings should be loaded concentrically to avoid tilting, which will result if bearing pressures are significantly larger under one side of the footing than under the opposite side. This means that single footings should be placed concentrically under the columns and wall footings concentrically under the walls and that, for combined footings, the centroid of the footing area should coincide with the resultant of the column loads. Eccentrically loaded footings can be used on highly compacted soils and on rock. It follows that one should count on rotational restraint of the column by a single footing only when such favorable soil conditions are present and when the footing is designed for both the column load and the restraining moment. Even then, less than full fixity should be assumed, except for footings on rock.

The accurate determination of stresses in foundation elements of all kinds is difficult, partly because of the uncertainties in determining the actual distribution of upward pressures but also because the structural elements themselves represent relatively massive blocks or thick slabs subject to heavy concentrated loads from the structure above. Design procedures for single-column footings are based largely on the results of experimental investigations by Talbot (Ref. 16.5) and Richart (Ref. 16.6). These tests and the recommendations resulting from them have been reevaluated in the light of more recent research, particularly that focusing on shear and diagonal tension (Refs. 16.7 to 16.9). Combined footings and mat foundations also can be designed by simplified methods, although increasing use is made of more sophisticated tools, such as finite element analysis and strut-and-tie models (Ref. 16.10).

16.4 LOADS, BEARING PRESSURES, AND FOOTING SIZE

Footing sizes are determined for *unfactored* service loads and *allowable* soil pressures, in contrast to the strength design of reinforced concrete members, which uses factored loads and factored nominal strengths. This is because, for footing design, safety is provided by overall safety factors, in contrast to the separate load and strength reduction factors used to dimension members.

Allowable bearing pressures are established from principles of soil mechanics, on the basis of load tests and other experimental determinations (see, for example, Refs. 16.1 to 16.4). Allowable bearing pressures q_a under service loads are usually based on a safety factor of 2.5 to 3.0 against exceeding the bearing capacity of the particular soil and to keep settlements within tolerable limits. Many local building codes contain allowable bearing pressures for the types of soils and soil conditions found in the particular locality.

For concentrically loaded footings, the required area is determined from

$$A_{\text{req}} = \frac{D + L}{q_a} \tag{16.1}$$

In addition, most building codes, including the *International Building Code* (IBC) (Ref. 16.11), which is used throughout the United States, permit a 33 percent increase in the allowable pressure when the effects of wind W or earthquake E are included, if specific loading combinations are used for foundation design. For example,

$$A_{\text{req}} = \frac{D + L + \omega W}{1.33 q_a} \quad \text{or} \quad A_{\text{req}} = \frac{D + L + S + E/1.4}{1.33 q_a} \tag{16.2}$$

where $\omega = 1.3$ if the wind load is calculated based on ASCE/SEI 7 (Ref. 16.12) and 1.0 otherwise, and the 1.4 factor that divides E recognizes that a load factor of 1.0 is used for earthquake loads in strength design.

The required footing area A_{req} is the larger of those determined by Eqs. (16.1) and (16.2). The loads in the numerators of Eqs. (16.1) and (16.2) must be calculated at the level of the base of the footing, i.e., at the contact plane between soil and footing. This means that the weight of the footing and surcharge (i.e., fill and possible liquid pressure on top of the footing) must be included. Wind loads and other lateral loads cause a tendency to overturn. In checking for overturning of a foundation, only those live loads that contribute to overturning should be included, and dead loads that stabilize against overturning should be multiplied by 0.9. A safety factor of at least 1.5 should be maintained against overturning, unless otherwise specified by the local building code (Ref. 16.8).

A footing is eccentrically loaded if the supported column is not concentric with the footing area or if the column transmits at its juncture with the footing not only a vertical load but also a bending moment. In either case, the load effects at the footing base can be represented by the vertical load P and a bending moment M. The resulting bearing pressures are again assumed to be linearly distributed. As long as the resulting eccentricity $e = M/P$ does not exceed the kern distance k of the footing area, the usual flexure formula

$$q_{\substack{max \\ min}} = \frac{P}{A} \pm \frac{Mc}{I} \tag{16.3}$$

permits the determination of the bearing pressures at the two extreme edges, as shown in Fig. 16.3a. The footing area is found by trial and error from the condition $q_{max} \leq q_a$. If the eccentricity falls outside the kern, Eq. (16.3) gives a negative value (tension) for q along one edge of the footing. Because no tension can be transmitted at the contact area between soil and footing, Eq. (16.3) is no longer valid and bearing pressures are distributed as shown in Fig. 16.3b. For rectangular footings of size $l \times b$, the maximum pressure can be found from

$$q_{max} = \frac{2P}{3bm} \tag{16.4}$$

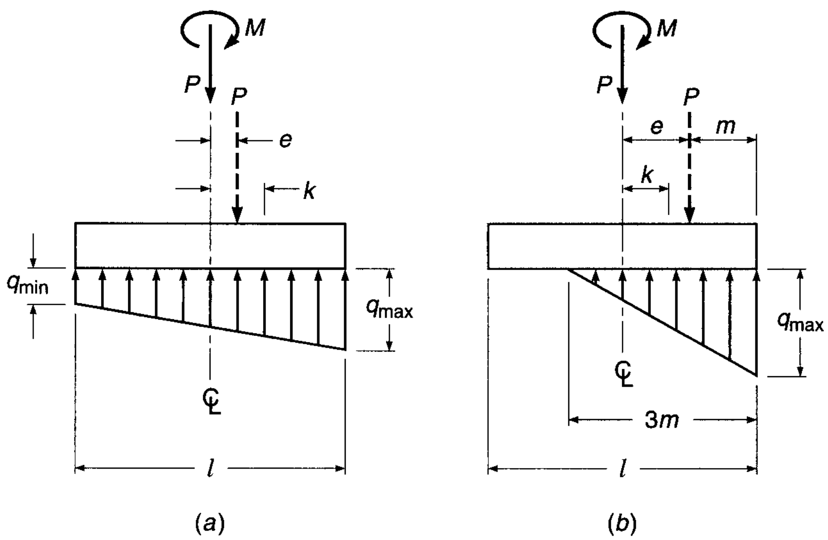

FIGURE 16.3
Assumed bearing pressures under eccentrically loaded footing.

which, again, must be no larger than the allowable pressure q_a. For nonrectangular footing areas of various configurations, kern distances and other aids for calculating bearing pressures can be found in Refs. 16.1 and 16.8 and elsewhere.

Once the required footing area has been determined, the footing must then be designed to develop the necessary strength to resist all moments, shears, and other internal actions caused by the applied loads. For this purpose, the load factors of ACI Code 9.2 apply to footings as to all other structural components. Correspondingly, for strength design, the footing is dimensioned for the effects of the load combinations in Table 1.2. The most common is

$$U = 1.2D + 1.6L$$

or if wind effects are to be included,

$$U = 1.2D + 1.6W + 1.0L + 0.5L_r$$

In seismic zones, earthquake forces E must be considered according to Table 1.2. The requirement that

$$U = 0.9D + 1.6W$$

will hardly ever govern the strength design of a footing, but will affect overturning and stability. Lateral earth pressure H and fluid pressure F must be included if present.

These factored loads must be counteracted and equilibrated by corresponding bearing pressures in the soil. Consequently, once the footing area is determined, the bearing pressures are recalculated for the factored loads for purposes of strength computations. These are fictitious pressures that are needed only to determine the factored loads for use in design. To distinguish them from the actual pressures q under service loads, the soil pressures that equilibrate the factored loads U will be designated q_u.

16.5 WALL FOOTINGS

The simple principles of beam action apply to wall footings with only minor modifications. Figure 16.4 shows a wall footing with the forces acting on it. If bending moments were computed from these forces, the maximum moment would be found to occur at the middle of the width. Actually, the very large rigidity of the wall modifies this situation, and the tests cited in Section 16.3 show that, for footings under concrete walls, it is satisfactory to compute the moment at the face of the wall (section 1-1). Tension cracks in these tests formed at the locations shown in Fig. 16.4, i.e., under the face of the wall rather than in the middle. For footings supporting masonry walls, the maximum moment is computed midway between the middle and the face of the wall, because masonry is generally less rigid than concrete. The maximum bending moment in footings under concrete walls is therefore given by

$$M_u = \frac{1}{8} q_u (b - a)^2 \tag{16.5}$$

For determining shear stresses, the vertical shear force is computed on section 2-2, located, as in beams, at a distance d from the face of the wall. Thus,

$$V_u = q_u \left(\frac{b - a}{2} - d \right) \tag{16.6}$$

The calculation of development length is based on the section of maximum moment, i.e., section 1-1.

FIGURE 16.4
Wall footing.

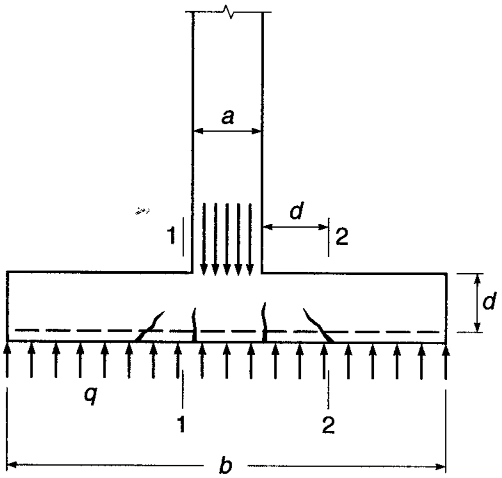

EXAMPLE 16.1 **Design of wall footing.** A 16 in. concrete wall supports a dead load $D = 14$ kips/ft and a live load $L = 10$ kips/ft. The allowable bearing pressure is $q_a = 4.5$ kips/ft^2 at the level of the bottom of the footing, which is 4 ft below grade. Design a footing for this wall using 4000 psi concrete and Grade 60 steel.

Solution. With a 12 in. thick footing, the footing weight per square foot is 150 psf, and the weight of the 3 ft fill on top of the footing is $3 \times 100 = 300$ psf. Consequently, the portion of the allowable bearing pressure that is available or effective for carrying the wall load is

$$q_e = 4500 - (150 + 300) = 4050 \text{ psf}$$

The required width of the footing is therefore $b = 24{,}000/4050 = 5.93$ ft. A 6 ft wide footing will be assumed.

The bearing pressure for strength design of the footing, caused by the factored loads, is

$$q_u = \frac{1.2 \times 14 + 1.6 \times 10}{6} \times 10^3 = 5470 \text{ psf}$$

From this, the factored moment at the face of the wall, section 1-1, for strength design is

$$M_u = \frac{1}{8} \times 5470(6 - 1.33)^2 \times 12 = 178{,}900 \text{ in-lb/ft}$$

and assuming $d = 9$ in., the shear at section 2-2 is

$$V_u = 5470\left[\frac{1}{2}(6 - 1.33) - \frac{9}{12}\right] = 8670 \text{ lb/ft}$$

Shear usually governs the depth of footings, particularly since the use of shear reinforcements in footings is generally avoided as uneconomical. The design shear strength per foot [see Eq. (4.12b)] is

$$\phi V_c = \phi(2\lambda\sqrt{f_c'}\,bd) = 0.75(2 \times 1\sqrt{4000} \times 12d) = 1138d \text{ lb/ft}$$

from which

$$d = \frac{8670}{1138} = 7.6 \text{ in.}$$

Since ACI Code 7.7.1 calls for a 3 in. clear cover on bars, a 12 in. thick footing will be selected, giving $d = 8.5$ in. This is sufficiently close to the assumed values, and the calculations need not be revised.

To determine the required steel area, $M_u/\phi bd^2 = 178{,}900/(0.90 \times 12 \times 8.5^2) = 229$ is used to enter Graph A.1b of Appendix A. For this value, the curve 60/4 gives the reinforcement ratio $\rho = 0.0038$. The required steel area is then $A_s = 0.0038 \times 8.5 \times 12 = 0.39$ in^2/ft. No. 5 (No. 16), $9\frac{1}{2}$ in. on centers, furnish $A_s = 0.39$ in^2/ft. The required development length according to Table A.10 of Appendix A is 24 in. This length is to be furnished from section 1-1 outward. The length of each bar, if end cover is 3 in., is $72 - 6 = 66$ in., and the actual development length from section 1-1 to the nearby end is $\frac{1}{2}(66 - 16) = 25$ in., which is more than the required development length.

Longitudinal shrinkage and temperature reinforcement, according to ACI Code 7.12, must be at least $0.0018 \times 12 \times 12 = 0.26$ in^2/ft. No. 5 (No. 16) bars on 12 in. centers will furnish 0.31 in^2/ft.

16.6 COLUMN FOOTINGS

In plan, single-column footings are usually square. Rectangular footings are used if space restrictions dictate this choice or if the supported columns have a strongly elongated rectangular cross section. In the simplest form, they consist of a single slab (Fig. 16.5*a*). Another type is that shown in Fig. 16.5*b*, where a pedestal or cap is interposed between the column and the footing slab; the pedestal provides for a more favorable transfer of load and in many cases is required to provide the necessary development length for dowels. This form is also known as a *stepped* footing. All parts of a stepped footing must be cast at one time to provide monolithic action. Sometimes sloped footings like those shown in Fig. 16.5*c* are used. They require less concrete than stepped footings, but the additional labor necessary to produce the sloping surfaces (formwork, etc.) usually makes stepped footings more economical. In general, single-slab footings (Fig. 16.5*a*) are most economical for thicknesses up to 3 ft.

Single-column footings can be represented as cantilevers projecting out from the column in both directions and loaded upward by the soil pressure. Corresponding tension stresses are caused in both of these directions at the bottom surface. Such footings are, therefore, reinforced by two layers of steel, perpendicular to each other and parallel to the edges.

The required bearing area is obtained by dividing the total load, including the weight of the footing, by the selected bearing pressure. Weights of footings, at this stage, must be estimated and usually amount to 4 to 8 percent of the column load, the former value applying to the stronger types of soils.

In computing bending moments and shears, only the upward pressure q_u that is caused by the factored column loads is considered. The weight of the footing proper

FIGURE 16.5
Types of single-column footings.

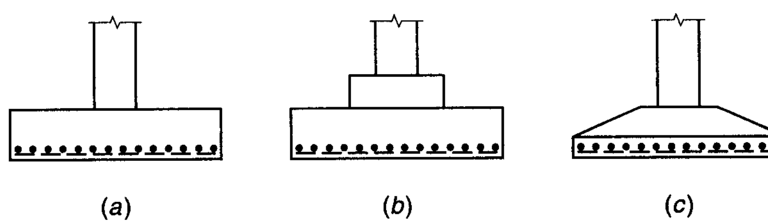

does not cause moments or shears, just as no moments or shears are present in a book lying flat on a table.

a. Shear

Once the required footing area A_{req} has been established from the allowable bearing pressure q_a and the most unfavorable combination of service loads, including weight of footing and overlying fill (and such surcharge as may be present), the thickness h of the footing must be determined. In single footings, the effective depth d is mostly governed by shear. Since such footings are subject to two-way action, i.e., bending in both major directions, their performance in shear is much like that of flat slabs in the vicinity of columns (see Section 13.10). However, in contrast to two-way floor and roof slabs, it is generally not economical in footings to use shear reinforcement. For this reason, only the design of footings in which all shear is carried by the concrete will be discussed here. For the rare cases where the thickness is restricted so that shear reinforcement must be used, the information in Section 13.10 about slabs applies also to footings.

Two different types of shear strength are distinguished in footings: two-way, or punching, shear and one-way, or beam, shear.

A column supported by the slab shown in Fig. 16.6 tends to punch through that slab because of the shear stresses that act in the footing around the perimeter of the column. At the same time, the concentrated compressive stresses from the column spread out into the footing so that the concrete adjacent to the column is in vertical or slightly inclined compression, in addition to shear. As a consequence, if failure occurs, the fracture takes the form of the truncated pyramid shown in Fig. 16.6 (or of a truncated cone for a round column), with sides sloping outward at an angle approaching 45°. The average shear stress in the concrete that fails in this manner can be taken as that acting on vertical planes laid through the footing around the column on a perimeter a distance $d/2$ from the faces of the column (vertical section through $abcd$ in Fig. 16.7). The concrete subject to this shear stress v_{u1} is also in vertical compression from the stresses spreading out from the column, and in horizontal compression in both major directions because of the biaxial bending moments in the footing. This triaxiality of stress increases

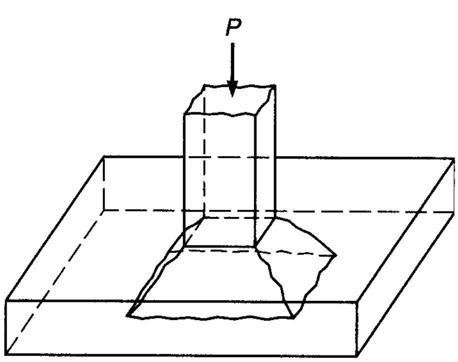

FIGURE 16.6
Punching-shear failure in single footing.

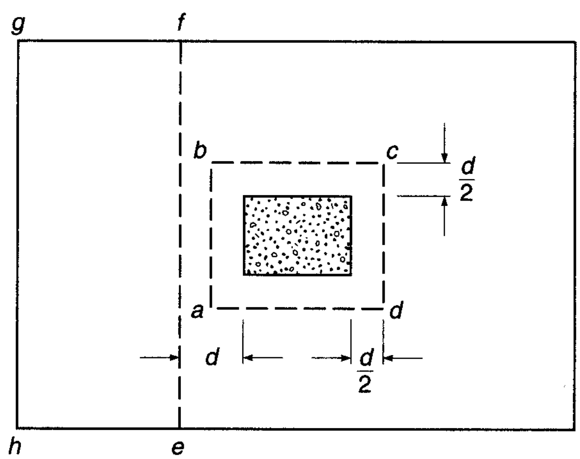

FIGURE 16.7
Critical sections for shear.

the shear strength of the concrete. Tests of footings and of flat slabs have shown, correspondingly, that for punching-type failures the shear stress computed on the critical perimeter area is larger than in one-way action (e.g., beams).

As discussed in Section 13.10, the ACI Code equations (13.11*a,b,c*) give the nominal punching-shear strength on this perimeter:

$$V_c = 4\lambda\sqrt{f'_c}\, b_o d \tag{16.7a}$$

except for columns of elongated cross section, for which

$$V_c = \left(2 + \frac{4}{\beta}\right)\lambda\sqrt{f'_c}\, b_o d \tag{16.7b}$$

For cases in which the ratio of critical perimeter to slab depth b_o/d is very large,

$$V_c = \left(\frac{\alpha_s d}{b_o} + 2\right)\lambda\sqrt{f'_c}\, b_o d \tag{16.7c}$$

where b_o is the perimeter *abcd* in Fig. 16.7; $\beta = a/b$ is the ratio of the long to short sides of the column cross section; and α_s is 40 for interior loading, 30 for edge loading, and 20 for corner loading of a footing. The punching-shear strength of the footing is to be taken as the smallest of the values given by Eqs. (16.7*a*), (16.7*b*), and (16.7*c*); and the design strength is ϕV_c, as usual, where $\phi = 0.75$ for shear.

The application of Eqs. (16.7) to punching shear in footings under columns with other than a rectangular cross section is shown in Fig. 13.23. For such situations, ACI Code 11.11.1 indicates that the perimeter b_o must be of minimum length but need not approach closer than $d/2$ to the perimeter of the actual loaded area. The manner of defining a and b for such irregular loaded areas is also shown in Fig. 13.23. If a moment is transferred from the column to the footing, the criteria discussed in Section 13.11 for the transfer of moment by bending and shear at slab-column connections must be satisfied.

Shear failures can also occur, as in beams or one-way slabs, at a section a distance d from the face of the column, such as section *ef* of Fig. 16.7. Just as in beams and one-way slabs, the nominal shear strength is given by Eq. (4.12*a*), that is,

$$V_c = \left(1.9\lambda\sqrt{f'_c} + 2500\rho\frac{V_u d}{M_u}\right)bd \le 3.5\lambda\sqrt{f'_c}\, bd \tag{16.8a}$$

where b = width of footing at distance d from face of column
= *ef* in Fig. 16.7
V_u = total factored shear force on that section
= q_u times footing area outside that section (area *efgh* in Fig. 16.7)
M_u = moment of V_u about *ef*

In footing design, the simpler and somewhat more conservative Eq. (4.12*b*) is generally used, i.e.,

$$V_c = 2\lambda\sqrt{f'_c}\, bd \tag{16.8b}$$

The required depth of footing d is then calculated from the usual equation

$$V_u \le \phi V_c \tag{16.9}$$

applied separately in connection with Eqs. (16.7) and (16.8). For Eq. (16.7), $V_u = V_{u1}$ is the total upward pressure caused by q_u on the area outside the perimeter *abcd* in Fig. 16.7. For Eq. (16.8), $V_u = V_{u2}$ is the total upward pressure on the area *efgh* outside the section *ef* in Fig. 16.7. The required depth is then the larger of those calculated from either Eq. (16.7) or (16.8). For shear, $\phi = 0.75$.

Although the lightweight concrete factor λ appears in Eqs. (16.7) and (16.8), normalweight concrete ($\lambda = 1$) is almost universally used in foundations.

b. Bearing: Transfer of Forces at Base of Column

When a column rests on a footing or pedestal, it transfers its load to only a part of the total area of the supporting member. The adjacent footing concrete provides lateral support to the directly loaded part of the concrete. This causes triaxial compressive stresses that increase the strength of the concrete that is loaded directly under the column. Based on tests, ACI Code 10.14.1 provides that when the supporting area is wider than the loaded area on all sides, the design bearing strength is

$$\phi P_n = \phi(0.85 f_c' A_1)\sqrt{\frac{A_2}{A_1}} \le \phi(0.85 f_c' A_1) \times 2 \qquad (16.10)$$

For bearing on concrete, $\phi = 0.65$, f_c' is the specified compressive strength of the footing concrete, which frequently is less than that of the column, and A_1 is the loaded area. A_2 is the area of the lower base of the largest frustum of a pyramid, cone, or tapered wedge contained wholly within the support and having for its upper base the loaded area and having side slopes of 1 vertical to 2 horizontal. The meaning of this definition of A_2 may be clarified by Fig. 16.8. For the somewhat unusual case shown, where the top of the support is stepped, a step that is deeper or closer to the loaded area than that shown may result in reduction in the value of A_2. A footing for which the top surface is sloped away from the loaded area more steeply than 1 to 2 will result in a value of A_2 equal to A_1. In most usual cases, for which the top of the footing is flat and the sides are vertical, A_2 is simply the maximum area of the portion of the supporting surface that is geometrically similar to, and concentric with, the loaded area.

FIGURE 16.8
Definition of areas A_1 and A_2.

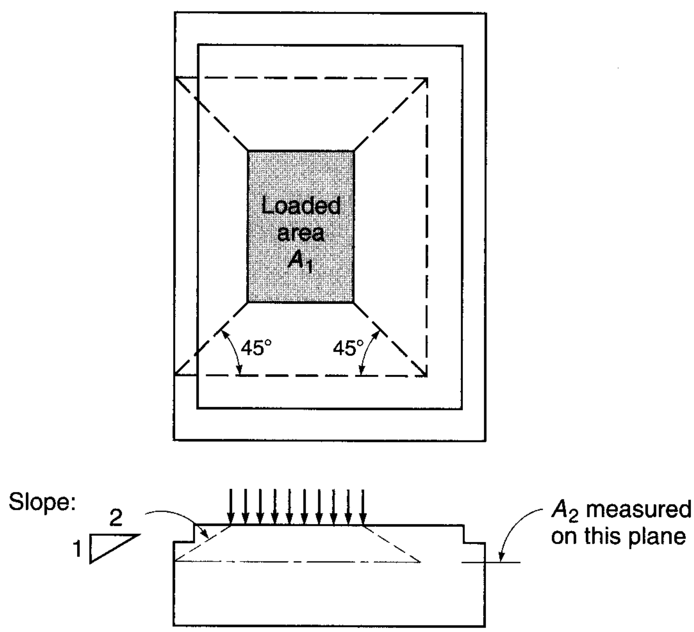

All axial forces and bending moments that act at the bottom section of a column must be transferred to the footing at the bearing surface by compression in the concrete and by reinforcement. With respect to the reinforcement, this may be done either by extending the column bars into the footing or by providing dowels that are embedded in the footing and project above it. In the latter case, the column bars merely rest on the footing and in most cases are tied to dowels. This results in a simpler construction procedure than extending the column bars into the footing. To ensure the integrity of the junction between column and footing, ACI Code 15.8.2 requires that the minimum area of reinforcement that crosses the bearing surface (dowels or column bars) be 0.005 times the gross area of the supported column. The length of the dowels or bars of diameter d_b must be sufficient on both sides of the bearing surface to provide the required development length for compression bars (see Section 5.8), that is, $l_{dc} \geq 0.02 f_y d_b / \sqrt{f'_c}$ and $\geq 0.0003 f_y d_b$. In addition, if dowels are used, the lapped length must be at least that required for a lap splice in compression (see Section 5.11b); i.e., the length of lap must not be less than the usual development length in compression and must not be less than $0.0005 f_y d_b$. Where bars of different sizes are lap-spliced, the splice length should be the larger of the development length of the larger bar or the splice length of the smaller bar, according to the ACI Code.

The two largest bar sizes, Nos. 14 (No. 43) and 18 (No. 57), are frequently used in columns with large axial forces. Under normal circumstances, the ACI Code specifically prohibits the lap splicing of these bars because tests have shown that welded splices or other positive connections are necessary to develop these heavy bars fully. A specific exception, however, is made for dowels for Nos. 14 (No. 43) and 18 (No. 57) column bars. Relying on long-standing successful use, ACI Code 12.16.2 permits these heavy bars to be spliced to dowels of lesser diameter [i.e., No. 11 (No. 36) or smaller], provided that the dowels have a development length into the column corresponding to that of the column bar [i.e., Nos. 14 or 18 (Nos. 43 or 57), as the case may be] and into the footing as prescribed for the particular dowel size [i.e., No. 11 (No. 36) or smaller, as the case may be].

c. Bending Moments, Reinforcement, and Bond

If a vertical section is passed through a footing, the bending moment that is caused in the section by the net upward soil pressure (i.e., factored column load divided by bearing area) is obtained from simple statics. Figure 16.9 shows such a section *cd* located along the face of the column. The bending moment about *cd* is that caused by the upward pressure q_u on the area to one side of the section, i.e., the area *abcd*. The reinforcement perpendicular to that section, i.e., the bars running in the long direction, is calculated from this bending moment. Likewise, the moment about section *ef* is caused by the pressure q_u on the area *befg*, and the reinforcement in the short direction, i.e., perpendicular to *ef*, is calculated for this bending moment. In footings that support reinforced concrete columns, the critical section *cd* or *ef* for bending is located at the face of the column, as shown in Fig. 16.10*a*, according to ACI Code 15.4.2.

In footings supporting masonry columns, the critical section *cd* or *ef* is located halfway between the centerline and the face of the column, as shown in Fig. 16.10*b*; and in footings supporting steel columns, the critical section *cd* or *ef* is located halfway between the face of the steel column and the edge of the steel base plate, as shown in Fig. 16.10*c*.

In footings with *pedestals*, the width resisting compression in sections *cd* and *ef* is that of the pedestal; the corresponding depth is the sum of the thickness of pedestal

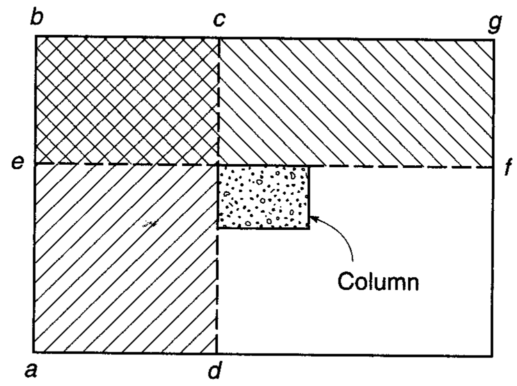

FIGURE 16.9
Critical sections for bending and bond.

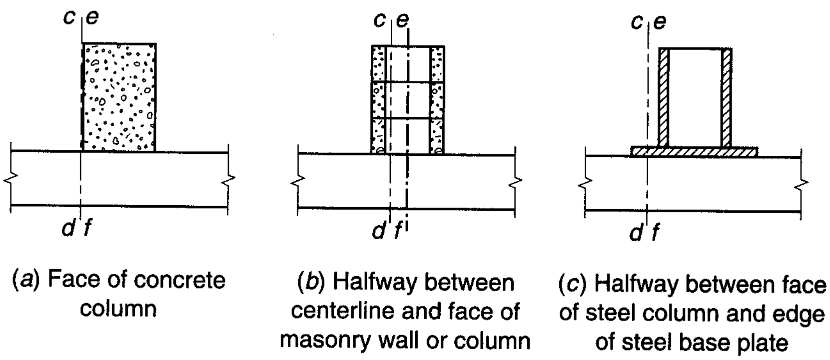

FIGURE 16.10
Critical sections *cd* or *ef* for concrete, masonry, and steel columns.

and footing. Further sections parallel to *cd* and *ef* are passed at the edge of the pedestal, and the moments are determined in the same manner, to check the strength at locations in which the depth is that of the footing only.

For footings with relatively small pedestals, the latter are often discounted in moment and shear computation, and bending is checked at the face of the column, with width and depth equal to that of the footing proper.

In *square footings*, the reinforcement is uniformly distributed over the width of the footing in each of the two layers; i.e., the spacing of the bars is constant. The moments for which the two layers are designed are the same. However, the effective depth d for the upper layer is less by 1 bar diameter than that of the lower layer. Consequently, the required A_s is larger for the upper layer. Instead of using different spacings or different bar diameters in each of the two layers, it is customary to determine A_s based on average depth and to use the same arrangement of reinforcement for both layers.

In *rectangular footings*, the reinforcement *in the long direction* is again uniformly distributed over the pertinent (shorter) width. In locating the bars in the short direction, one has to consider that the support provided to the footing by the column is concentrated near the middle. Consequently, the curvature of the footing is sharpest, i.e., the moment per foot largest, immediately under the column, and it decreases in the long direction with increasing distance from the column. For this reason, a larger steel area per longitudinal foot is needed in the central portion than near the far ends of the footing. ACI Code 15.4.4, therefore, provides the following:

> For reinforcement in the short direction, a portion of the total reinforcement $\gamma_s A_s$ shall be distributed uniformly over a band width (centered on the centerline of the column or pedestal) equal to the length of the short side of the footing. The remainder of the

reinforcement required in the short direction $(1 - \gamma_s)A_s$ shall be distributed uniformly outside the center band width of the footing

$$\gamma_s = \frac{\text{reinforcement in band width}}{\text{total reinforcement in short direction}} = \frac{2}{\beta + 1} \tag{16.11}$$

where β is the ratio of the long side to the short side of the footing.

According to the ACI Code 10.5.4, the usual minimum flexural reinforcement ratios of Section 3.4e need not be applied to either slabs or footings. Instead, the minimum steel requirements for shrinkage and temperature crack control for structural slabs are to be imposed, as given in Table 13.2. The maximum spacing of bars in the direction of the span is reduced to the lesser of 3 times the footing thickness h and 18 in., rather than $5h$ as is normal for shrinkage and temperature steel. These requirements for minimum steel and maximum spacing are to be applied to mat foundations as well as individual footings.

Earlier editions of the ACI Code, through 1989, were somewhat ambiguous as to whether or not minimum steel requirements for flexural members were to be applied to slabs and footings. For slabs, the argument was presented that an overload would be distributed laterally and that a sudden failure is therefore less likely than for beams; therefore the usual requirement could be relaxed. Although that reasoning may apply to highly indeterminate building floors, the possibility for redistribution in a footing is much more limited. Because of this, and because of the importance of a footing to the safety of the structure, many engineers apply the minimum flexural reinforcement ratio of Eq. (3.41) to footings as well as beams. This seems prudent, and the following design examples use the more conservative minimum flexural steel requirements of Eq. (3.41).

The critical sections for development length of footing bars are the same as those for bending. Development length may also have to be checked at all vertical planes in which changes of section or of reinforcement occur, as at the edges of pedestals or where part of the reinforcement may be terminated.

EXAMPLE 16.2 **Design of a square footing.** A column 18 in. square, with $f_c' = 4$ ksi, reinforced with eight No. 8 (No. 25) bars of $f_y = 60$ ksi, supports a dead load of 225 kips and a live load of 175 kips. The soil (fill) has a unit weight of 100 pcf. The allowable soil pressure q_a is 5 kips/ft^2. Design a square footing with base 5 ft below grade, using $f_c' = 4$ ksi and $f_y = 60$ ksi.

SOLUTION. Since the space between the bottom of the footing and the surface will be occupied partly by concrete and partly by soil (fill), an average unit weight of 125 pcf will be assumed. The pressure of this material at the 5 ft depth is $5 \times 125 = 625$ psf, leaving a bearing pressure of $q_e = 5000 - 625 = 4375$ psf available to carry the column service load. Hence, the required footing area $A_{\text{req}} = (225 + 175)/4.375 = 91.5$ ft^2. A base 9 ft 6 in. square is selected, furnishing a footing area of 90.3 ft^2, which differs from the required area by about 1 percent.

For strength design, the upward pressure caused by the factored column loads is $q_u = (1.2 \times 225 + 1.6 \times 175)/9.5^2 = 6.10$ kips/ft^2.

The footing depth in square footings is usually determined based on two-way or punching shear on the critical perimeter *abcd* in Fig. 16.11. Trial calculations suggest $d = 19$ in. Hence, the length of the critical perimeter is

$$b_o = 4(18 + d) = 148 \text{ in.}$$

The shear force acting on this perimeter, being equal to the total upward pressure minus that acting within the perimeter *abcd*, is

$$V_{u1} = 6.10\left[9.5^2 - \left(\frac{37}{12}\right)^2\right] = 492 \text{ kips}$$

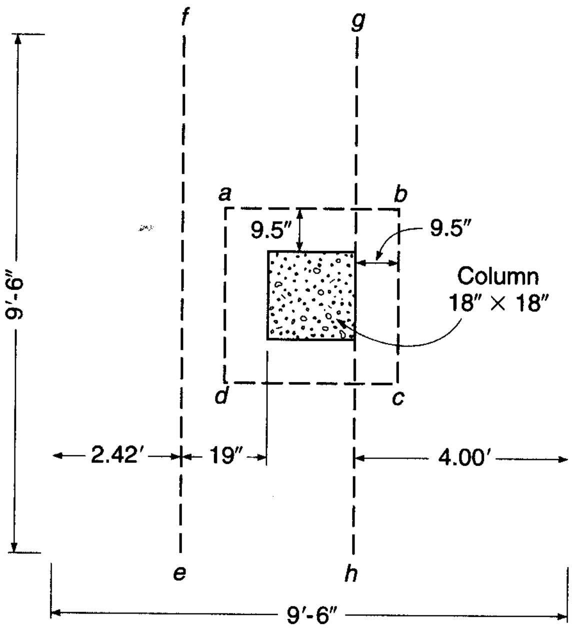

FIGURE 16.11
Critical sections for Example 16.2.

The corresponding nominal shear strength [Eq. (13.11*a*)] is

$$V_c = 4 \times 1\sqrt{4000} \times 148 \times \frac{19}{1000} = 711 \text{ kips}$$

and

$$\phi V_c = 0.75 \times 711 = 534 \text{ kips}$$

Since the design strength exceeds the factored shear V_{u1}, the depth $d = 19$ in. is adequate for punching shear. The selected value $d = 19$ in. will now be checked for one-way or beam shear on section *ef*. The factored shear force acting on that section is

$$V_{u2} = 6.10 \times 2.42 \times 9.5 = 140 \text{ kips}$$

and the nominal shear strength is

$$V_c = 2 \times 1\sqrt{4000} \times 9.5 \times 12 \times \frac{19}{1000} = 274 \text{ kips}$$

The design shear strength $0.75 \times 274 = 205$ kips is larger than the factored shear V_{u2}, so that $d = 19$ in. is also adequate for one-way shear.

The bending moment on section *gh* of Fig. 16.11 is

$$M_u = 6.10 \times 9.5\left(\frac{4.0^2}{2}\right)12 = 5560 \text{ in-kips}$$

Because the depth required for shear is greatly in excess of that required for bending, the reinforcement ratio will be low and the corresponding depth of the rectangular stress block small. If $a = 2$ in., the required steel area is

$$A_s = \frac{5560}{0.90 \times 60(19 - 1)} = 5.72 \text{ in}^2$$

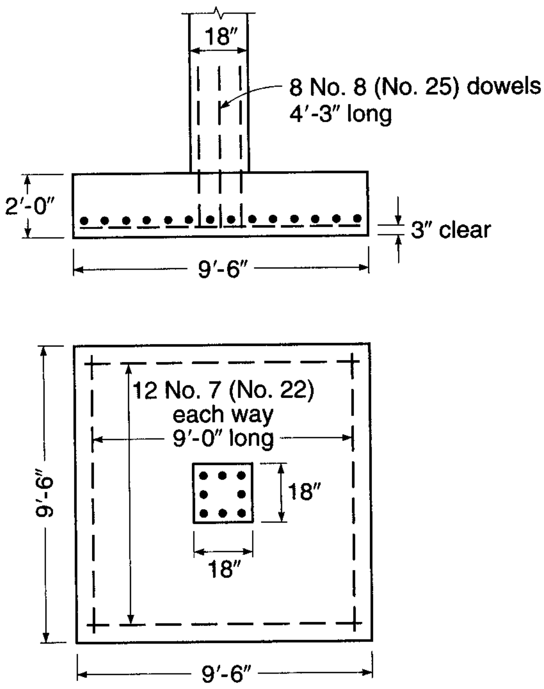

FIGURE 16.12
Footing in Example 16.2.

Checking the minimum reinforcement ratio using Eq. (3.41) results in

$$A_{s,\min} = \frac{3\sqrt{4000}}{60{,}000} \times 114 \times 19 = 6.85 \text{ in}^2$$

but not less than

$$A_{s,\min} = \frac{200}{60{,}000} \times 114 \times 19 = 7.22 \text{ in}^2$$

The controlling value of 7.22 in^2 is larger than the 5.72 in^2 calculated for bending. Twelve No. 7 (No. 22) bars furnishing 7.20 in^2 will be used in each direction. The required development length beyond section *gh* is found from Table A.10 to be 41 in., which is more than adequately met by the actual length of bars beyond section *gh*, namely, $48 - 3 = 45$ in.

Checking for transfer of forces at the base of the column shows that the footing concrete, which has the same f_c' as the column concrete and for which the strength is enhanced according to Eq. (16.10), is clearly capable of carrying that part of the column load transmitted by the column concrete. The force in the column carried by the steel will be transmitted to the footing using dowels to match the column bars. These must extend into the footing the full development length in compression, which is found from Table A.11 of Appendix A to be 19 in. for No. 8 (No. 25) bars. This is accommodated in a footing with $d = 19$ in. Above the top surface of the footing, the No. 8 (No. 25) dowels must extend into the column that same development length, but not less than the requirement for a lapped splice in compression (see Section 5.13b). The minimum lap splice length for the No. 8 (No. 25) bars is $0.0005 \times 1.0 \times 60{,}000 = 30$ in., which is seen to control here. Thus the bars will be carried 30 in. into the column, requiring a total dowel length of 49 in. This will be rounded upward for practical reasons to 4.25 ft, as shown in Fig. 16.12. It is easily confirmed that the minimum dowel steel requirement of $0.005 \times 18 \times 18 = 1.62$ in^2 does not control here.

For concrete in contact with ground, a minimum cover of 3 in. is required for corrosion protection. With $d = 19$ in., measured from the top of the footing to the center of the upper layer of bars, the total thickness of the footing that is required to provide 3 in. clear cover for the lower steel layer is

$$h = 19 + 1.5 \times 1 + 3 = 23.5 \text{ in.}$$

The footing, with 24 in. thickness, is shown in Fig. 16.12.

16.7 COMBINED FOOTINGS

Spread footings that support more than one column or wall are known as *combined footings*. They can be divided into two categories: those that support two columns and those that support more than two (generally large numbers of) columns.

Examples of the first type, i.e., two-column footings, are shown in Fig. 16.1. In buildings where the allowable soil pressure is large enough for single footings to be adequate for most columns, two-column footings are seen to become necessary in two situations: (1) if columns are so close to the property line that single-column footings cannot be made without projecting beyond that line, and (2) if some adjacent columns are so close to each other that their footings would merge. Both situations are shown in Fig. 16.1.

When the bearing capacity of the subsoil is low so that large bearing areas become necessary, individual footings are replaced by *continuous strip footings* that support more than two columns and usually all columns in a row. Sometimes such strips are arranged in both directions, in which case a *grid foundation* is obtained, as shown in Fig. 16.13. Strip footings can be made to develop a much larger bearing area much more economically than can be done by single footings because the individual strips represent continuous beams whose moments are much smaller than the cantilever moments in large single footings that project far out from the column in all four directions.

FIGURE 16.13
Grid foundation.

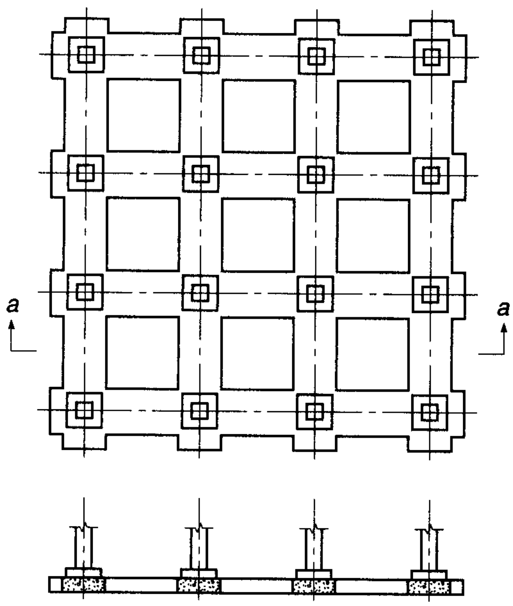

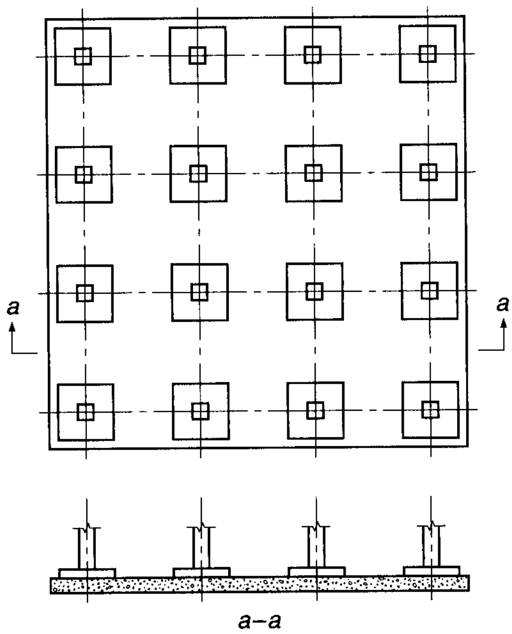

FIGURE 16.14
Mat foundation.

In many cases, the strips are made to merge, resulting in a mat foundation, as shown in Fig. 16.14. That is, the foundation consists of a solid reinforced concrete slab under the entire building. In structural action, such a mat is very similar to a flat slab or a flat plate, upside down, i.e., loaded upward by the bearing pressure and downward by the concentrated column reactions. The mat foundation evidently develops the maximum available bearing area under the building. If the soil's capacity is so low that even this large bearing area is insufficient, some form of deep foundation, such as piles or caissons, must be used. These are discussed in texts on foundation design and fall outside the scope of the present volume.

Mat foundations may be designed with the column pedestals, as shown in Figs. 16.13 and 16.14, or without them, depending on whether they are necessary for shear strength and the development length of dowels.

Apart from developing large bearing areas, another advantage of strip and mat foundations is that their continuity and rigidity help in reducing differential settlements of individual columns relative to each other, which may otherwise be caused by local variations in the quality of subsoil, or other causes. For this purpose, continuous foundations are frequently used in situations where the superstructure or the type of occupancy provides unusual sensitivity to differential settlement.

Much useful and important design information pertaining to combined footings and mats is found in Refs. 16.10 and 16.13.

16.8 TWO-COLUMN FOOTINGS

It is desirable to design combined footings so that the centroid of the footing area coincides with the resultant of the two column loads. This produces uniform bearing pressure over the entire area and forestalls a tendency for the footings to tilt. In plan, such footings are rectangular, trapezoidal, or T-shaped, the details of the shape being arranged to produce coincidence of centroid and resultant. The simple relationships

FIGURE 16.15
Two-column footing.
(*Adapted from Ref. 16.8.*)

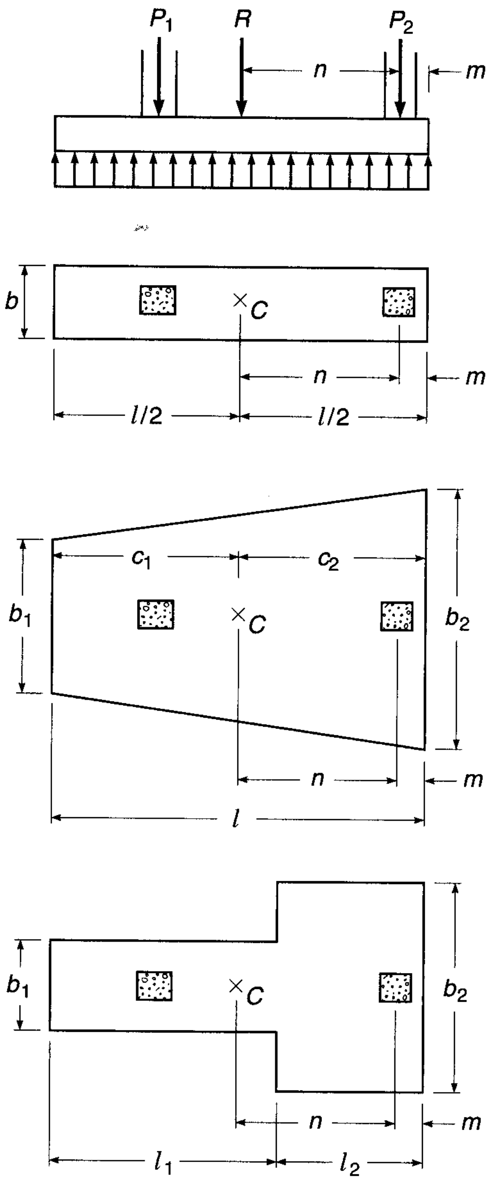

$$l = 2(m+n)$$
$$b = \frac{R}{q_e l}$$

$$\frac{b_2}{b_1} = \frac{3(n+m) - l}{2l - 3(n+m)}$$
$$(b_1+b_2) = \frac{2R}{q_e l}$$
$$c_1 = \frac{l(b_1+2b_2)}{3(b_1+b_2)}$$
$$c_2 = \frac{l(2b_1+b_2)}{3(b_1+b_2)}$$

$$b_1 = \frac{R}{q_e} = \left[\frac{2(n+m) - l_2}{l_1(l_1+l_2)}\right]$$
$$b_2 = \frac{R}{l_2 q_e} - \frac{l_1 b_1}{l_2}$$
$$l_1 b_1 + l_2 b_2 = \frac{R}{q_e}$$

shown in Fig. 16.15 facilitate the determination of the shape of the bearing area (from Ref. 16.8). In general, the distances m and n are given, the former being the distance from the center of the exterior column to the property line and the latter the distance from that column to the resultant of both column loads.

Another expedient that is used if a single footing cannot be centered under an exterior column is to place the exterior column footing eccentrically and to connect it with the nearest interior column footing by a beam or strap. This strap, being counterweighted by the interior column load, resists the tilting tendency of the eccentric exterior footing and equalizes the pressure under it. Such foundations are known as *strap, cantilever*, or *connected footings*.

The two examples that follow demonstrate some of the peculiarities of the design of two-column footings.

EXAMPLE 16.3 **Design of a combined footing supporting one exterior and one interior column.** An exterior 24 × 18 in. column with D = 170 kips, L = 130 kips, and an interior 24 × 24 in. column with D = 250 kips, L = 200 kips are to be supported on a combined rectangular footing whose outer end cannot protrude beyond the outer face of the exterior column (see Fig. 16.1). The distance center to center of columns is 18 ft 0 in., and the allowable bearing pressure of the soil is 6000 psf. The bottom of the footing is 6 ft below grade, and a surcharge of 100 psf is specified on the surface. Design the footing for f'_c = 3000 psi and f_y = 60,000 psi.

Solution. The space between the bottom of the footing and the surface will be occupied partly by concrete (footing, concrete floor) and partly by backfill. An average unit weight of 125 pcf can be assumed. Hence, the effective portion of the allowable bearing pressure that is available for carrying the column loads is $q_e = q_a$ − (weight of fill and concrete + surcharge) = 6000 − (6 × 125 + 100) = 5150 psf. Then the required area A_{req} = sum of column loads/q_e = 750/5.15 = 145.5 ft^2. The resultant of the column loads is located from the center of the exterior column a distance 450 × 18/750 = 10.8 ft. Hence, the length of the footing must be 2(10.8 + 0.75) = 23.1 ft. A length of 23 ft 3 in. is selected. The required width is then 145.5/23.25 = 6.3 ft. A width of 6 ft 6 in. is selected (see Fig. 16.16).

Longitudinally, the footing represents a beam, loaded from below, spanning between columns and cantilevering beyond the interior column. Since this beam is considerably wider than the columns, the column loads are distributed crosswise by transverse beams, one under each column. In the present relatively narrow and long footing, it will be found that the required minimum depth for the transverse beams is smaller than is required for the footing in the longitudinal direction. These "beams," therefore, are not really distinct members but merely represent transverse strips in the main body of the footing, reinforced so that they are capable of resisting the transverse bending moments and the corresponding shears. It then

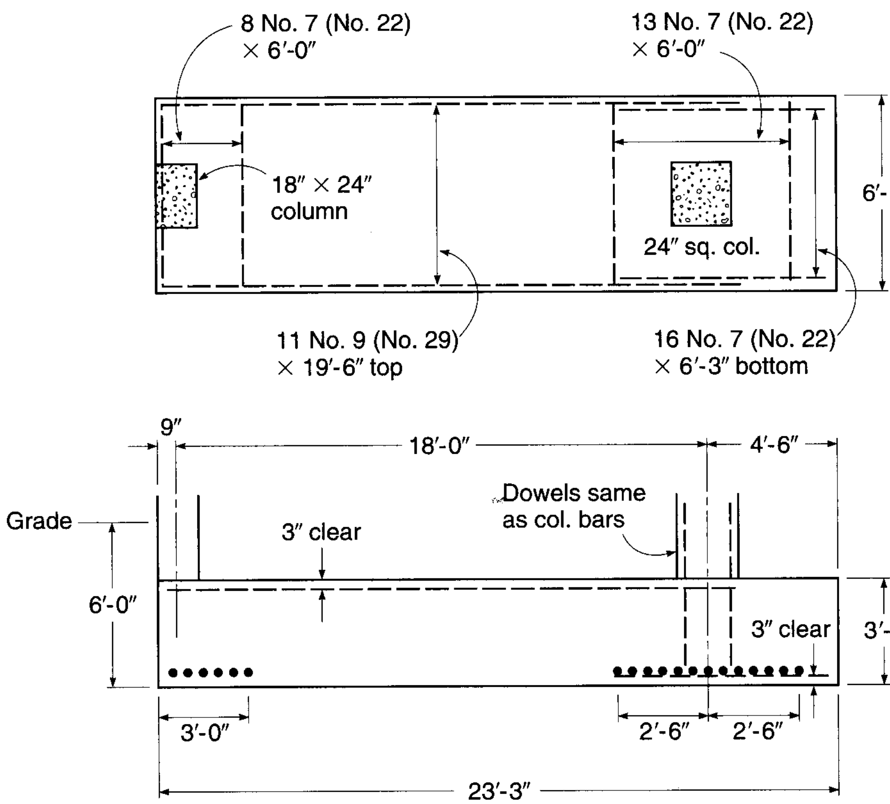

FIGURE 16.16
Combined footing in Example 16.3.

becomes necessary to decide how large the effective width of this transverse beam can be assumed to be. Obviously, the strip directly under the column does not deflect independently and is strengthened by the adjacent parts of the footing. The effective width of the transverse beams is therefore evidently larger than that of the column. In the absence of definite rules for this case, or of research results on which to base such rules, the authors recommend conservatively that the load be assumed to spread outward from the column into the footing at a slope of 2 vertical to 1 horizontal. This means that the effective width of the transverse beam is assumed to be equal to the width of the column plus $d/2$ on either side of the column, d being the effective depth of the footing.

Strength design in longitudinal direction
The net upward pressure caused by the factored column loads is

$$q_u = \frac{1.2(170 + 250) + 1.6(130 + 200)}{23.25 \times 6.5} = 6.83 \text{ kips/ft}^2$$

Then the net upward pressure per linear foot in the longitudinal direction is $6.83 \times 6.5 = 44.4$ kips/ft. The maximum negative moment between the columns occurs at the section of zero shear. Let x be the distance from the outer edge of the exterior column to this section. Then (see Fig. 16.17)

$$V_u = 44{,}400x - 412{,}000 = 0$$

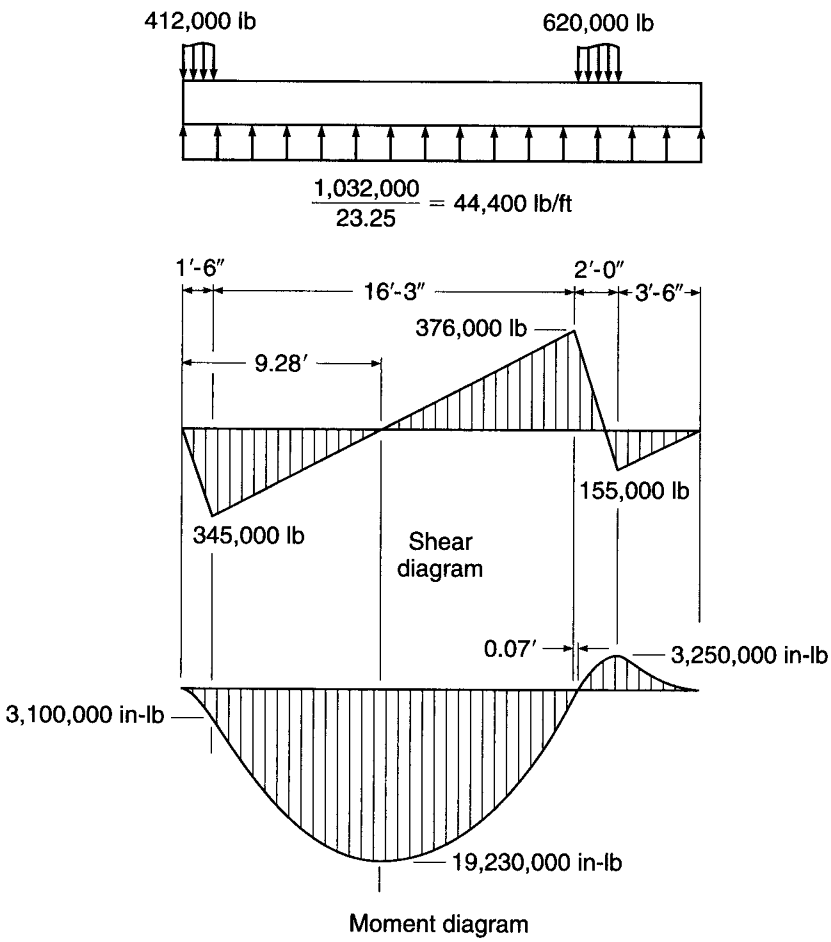

FIGURE 16.17
Moment and shear diagrams for footing in Example 16.3.

results in $x = 9.28$ ft. The moment at this section is

$$M_u = \left[44{,}400\frac{9.28^2}{2} - 412{,}000(9.28 - 0.75)\right]12 = -19{,}230{,}000 \text{ in-lb}$$

The moment at the right edge of the interior column is

$$M_u = 44{,}400\left(\frac{3.5^2}{2}\right)12 = 3{,}260{,}000 \text{ in-lb}$$

and the details of the moment diagram are as shown in Fig. 16.17. Try $d = 37.5$ in.

From the shear diagram in Fig. 16.17, it is seen that the critical section for flexural shear occurs at a distance d to the left of the left face of the interior column. At that point, the factored shear is

$$V_u = 376{,}000 - \frac{37.5}{12}(44{,}400) = 237{,}000 \text{ lb}$$

and the design shear strength

$$\phi V_c = 0.75 \times 2 \times 1\sqrt{3000} \times 78 \times 37.5 = 240{,}000 \text{ lb} > V_u$$

indicating that $d = 37.5$ in. is adequate.

Additionally, as in single footings, punching shear should be checked on a perimeter section a distance $d/2$ around the column, on which the nominal shear stress $v_c = 4 \times 1\sqrt{3000} = 220$ psi. Of the two columns, the exterior one with a three-sided perimeter a distance $d/2$ from the column is more critical in regard to this punching shear. The perimeter is

$$b_o = 2\left(1.5 + \frac{37.5/12}{2}\right) + \left(2.0 + \frac{37.5}{12}\right) = 11.25 \text{ ft}$$

and the shear force, being the column load minus the soil pressure within the perimeter, is

$$V_u = 412{,}000 - 3.06 \times 5.12(6830) = 305{,}000 \text{ lb}$$

On the other hand, the design shear strength on the perimeter section is

$$\phi V_c = 0.75 \times 220 \times 11.25 \times 12 \times 37.5 = 835{,}000 \text{ lb}$$

considerably larger than the factored shear V_u.

With $d = 37.5$ in., and with 3.5 in. cover from the center of the bars to the top surface of the footing, the total thickness is 41 in.

To determine the required steel area, $M_u/\phi bd^2 = 19{,}230{,}000/(0.9 \times 78 \times 37.5^2) = 195$ is used to enter Graph A.1b of Appendix A. For this value, the curve 60/3 gives the reinforcement ratio $\rho = 0.0035$. The required steel area is $A_s = 0.0035 \times 37.5 \times 78 = 10.3$ in^2. Eleven No. 9 (No. 29) bars furnish 11.00 in^2. The required development length is found to be 6.7 ft. From Fig. 16.17, the distance from the point of maximum moment to the nearer left end of the bars is seen to be $9.30 - \frac{3}{12} = 9.05$ ft, much larger than the required minimum development length. The selected reinforcement is therefore adequate for both bending and bond.

For the portion of the longitudinal beam that cantilevers beyond the interior column, the minimum required steel area controls. Here,

$$A_{s,\min} = \frac{3\sqrt{3000}}{60{,}000} \times 78 \times 37.5 = 8.01 \text{ in}^2$$

but not less than

$$A_{s,\min} = \frac{200}{60{,}000} \times 78 \times 37.5 = 9.75 \text{ in}^2$$

Sixteen No. 7 (No. 22) bars with $A_s = 9.62$ in^2 are selected; their development length is computed and for bottom bars is found satisfactory.

Design of transverse beam under interior column

The width of the transverse beam under the interior column can now be established as previously suggested and is $24 + 2(d/2) = 24 + 2 \times 18.75 = 61.5$ in. The net upward load per linear foot of the transverse beam is 620,000/6.5 = 95,400 lb/ft. The moment at the edge of the interior column is

$$M_u = 95{,}400\left(\frac{2.25^2}{2}\right)12 = 2{,}900{,}000 \text{ in-lb}$$

Since the transverse bars are placed on top of the longitudinal bars (see Fig. 16.16), the actual value of d furnished is $37.5 - 1.0 = 36.5$ in. The minimum required steel area controls; i.e.,

$$A_s = \frac{200}{60{,}000}\, 61.5 \times 36.5 = 7.48 \text{ in}^2$$

Thirteen No. 7 (No. 22) bars are selected and placed within the 61.5 in. effective width of the transverse beam.

Punching shear at the perimeter a distance $d/2$ from the column has been checked before. The critical section for regular flexural shear, at a distance d from the face of the column, lies beyond the edge of the footing, and therefore no further check on shear is needed.

The design of the transverse beam under the exterior column is the same as the design of that under the interior column, except that the effective width is 36.75 in. The details of the calculations are not shown. It can be easily checked that eight No. 7 (No. 22) bars, placed within the 36.75 in. effective width, satisfy all requirements. Design details are shown in Fig. 16.16.

EXAMPLE 16.4 **Design of a strap footing.** In a strap or connected footing, the exterior footing is placed eccentrically under its column so that it does not project beyond the property line. Such an eccentric position would result in a strongly uneven distribution of bearing pressure, which could lead to tilting of the footing. To counteract this eccentricity, the footing is connected by a beam or strap to the nearest interior footing.

Both footings are so proportioned that under service load the pressure under each of them is uniform and the same under both footings. To achieve this, it is necessary, as in other combined footings, that the centroid of the combined area for the two footings coincide with the resultant of the column loads. The resulting forces are shown schematically in Fig. 16.18. They consist of the loads P_e and P_i of the exterior and interior columns, respectively, and of the net upward pressure q, which is uniform and equal under both footings. The resultants R_e and R_i of these upward pressures are also shown. Since the interior footing is concentric with the interior column, R_i and P_i are collinear. This is not the case for the exterior forces R_e and P_e where the resulting couple just balances the effect of the eccentricity of the column relative to the center

FIGURE 16.18
Forces and reactions on the strap footing in Example 16.4.

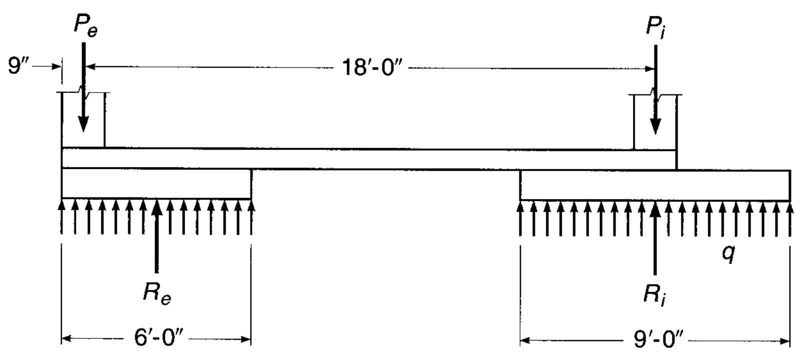

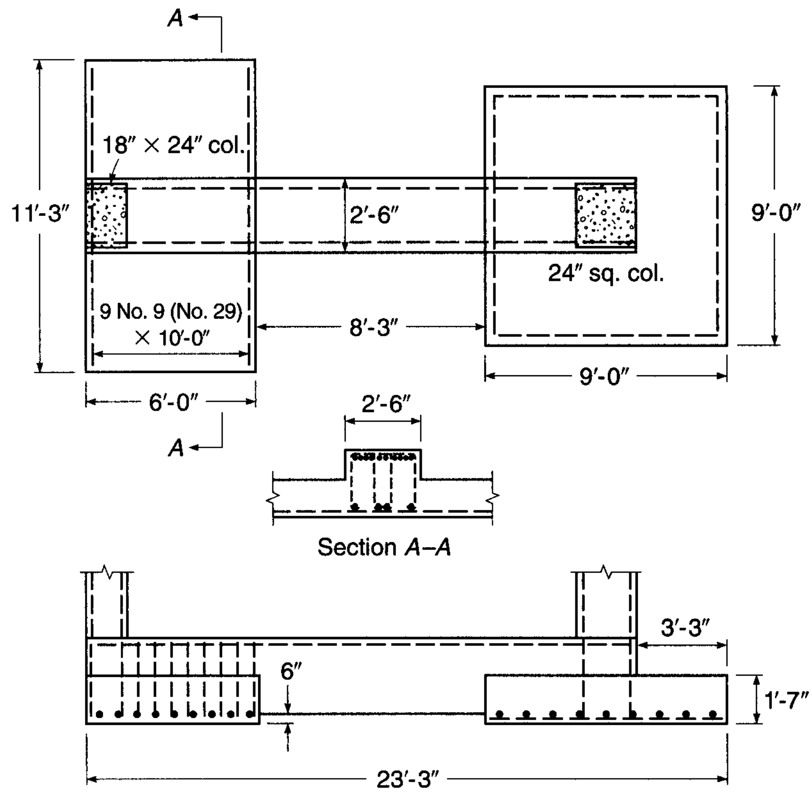

FIGURE 16.19
Strap footing in Example 16.4.

of the footing. The strap proper is generally constructed so that it will not bear on the soil. This can be achieved by providing formwork not only for the sides but also for the bottom face and by withdrawing it before backfilling.

To illustrate this design, the columns in Example 16.3 will now be supported on a strap footing. Its general shape, plus dimensions as determined only subsequently by calculations, is seen in Fig. 16.19. With an allowable bearing pressure of $q_a = 6.0$ kips/ft^2 and a depth of 6 ft to the bottom of the footing as before, the bearing pressure available for carrying the external loads applied to the footing is $q_e = 5.15$ kips/ft^2, as in Example 16.3. These external loads, for the strap footing, consist of the column loads and of the weight plus fill and surcharge of that part of the strap that is located between the footings. (The portion of the strap located directly on top of the footing displaces a corresponding amount of fill and therefore is already accounted for in the determination of the available bearing pressure q.) If the bottom of the strap is 6 in. above the bottom of the footings to prevent bearing on soil, the total depth to grade is 5.5 ft. If the strap width is estimated to be 2.5 ft, its estimated weight plus fill and surcharge is $2.5 \times 5.5 \times 0.125 + 0.100 \times 2.5 = 2$ kips/ft. If the gap between footings is estimated to be 8 ft, the total weight of the strap is 16 kips. Hence, for purposes of determining the required footing area, 8 kips will be added to the dead load of each column. The required total area of both footings is then $(750 + 16)/5.15 = 149$ ft^2. The distance of the resultant of the two column loads plus the strap load from the axis of the exterior column, with sufficient accuracy, is $458 \times 18/766 = 10.75$ ft, or 11.50 ft from the outer edge, almost identical to that calculated for Example 16.3. Trial calculations show that a rectangular footing 6 ft 0 in. × 11 ft 3 in. under the exterior column and a square footing 9 × 9 ft under the interior column have a combined area of 149 ft^2 and a distance from the outer edge to the centroid of the combined areas of $(6 \times 11.25 \times 3 + 9 \times 9 \times 18.75) \div 149 = 11.55$ ft, which is almost exactly equal to the previously calculated distance to the resultant of the external forces.

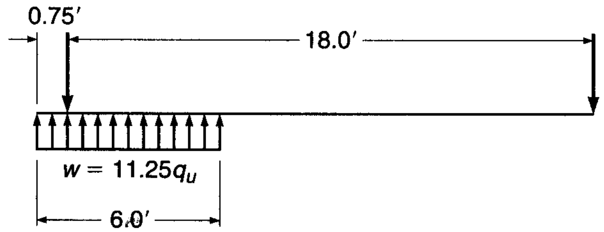

FIGURE 16.20
Forces acting on strap in Example 16.4.

For *strength calculations*, the bearing pressure caused by the factored external loads, including that of the strap with its fill and surcharge, is

$$q_u = \frac{1.2(170 + 250 + 16) + 1.6(130 + 200)}{149} = 7.06 \text{ kips/ft}^2$$

Design of footings
The exterior footing performs exactly like a wall footing with a length of 6 ft. Even though the column is located at its edge, the balancing action of the strap results in uniform bearing pressure, the downward load being transmitted to the footing uniformly by the strap. Hence, the design is carried out exactly as it is for a wall footing (see Section 16.5).

The interior footing, even though it merges in part with the strap, can safely be designed as an independent, square single-column footing (see Section 16.6). The main difference is that, because of the presence of the strap, punching shear cannot occur along the truncated pyramid surface shown in Fig. 16.6. For this reason, two-way or punching shear, according to Eq. (16.7), should be checked along a perimeter section located at a distance $d/2$ outward from the longitudinal edges of the strap and from the free face of the column, d being the effective depth of the footing. Flexural or one-way shear, as usual, is checked at a section a distance d from the face of the column.

Design of strap
Even though the strap is in fact monolithic with the interior footing, the effect on the strap of the soil pressure under this footing can safely be neglected because the footing has been designed to withstand the entire upward pressure as if the strap were absent. In contrast, because the exterior footing has been designed as a wall footing that receives its load from the strap, the upward pressure from the wall footing becomes a load that must be resisted by the strap. With this simplification of the actually somewhat more complex situation, the strap represents a single-span beam loaded upward by the bearing pressure under the exterior footing and supported by downward reactions at the centerlines of the two columns (Fig. 16.20). A width of 30 in. is selected. For a column width of 24 in., this permits beam and column bars to be placed without interference where the two members meet and allows the column forms to be supported on the top surface of the strap. The maximum moment, as determined by equating the shear force to zero, occurs close to the inner edge of the exterior footing. Shear forces are large in the vicinity of the exterior column. Stirrup design is completed using a strut-and-tie model. The footing is drawn approximately to scale in Fig. 16.19, which also shows the general arrangement of the reinforcement in the footings and the strap.

16.9 STRIP, GRID, AND MAT FOUNDATIONS

As mentioned in Section 16.7, continuous foundations are often used to support heavily loaded columns, especially when a structure is located on relatively weak or uneven soil. The foundation may consist of a *continuous strip footing* supporting all columns in a given row, or of two sets of such strip footings intersecting at right angles so that they form one continuous *grid foundation* (Fig. 16.13). For even larger loads or weaker soils, the strips are made to merge, resulting in a *mat foundation* (Fig. 16.14).

For the design of such continuous foundations, it is essential that reasonably realistic assumptions be made regarding the distribution of bearing pressures that act as upward loads on the foundation. For compressible soils, it can be assumed, as a first approximation, that the deformation or settlement of the soil at a given location and the bearing pressure at that location are proportional to each other. If columns are spaced at moderate distances and if the strip, grid, or mat foundation is quite rigid, the settlements in all portions of the foundation will be substantially the same. This means that the bearing pressure, also known as *subgrade reaction*, will be the same, provided that the centroid of the foundation coincides with the resultant of the loads. If they do not coincide, then for such rigid foundations the subgrade reaction can be assumed to vary linearly. Bearing pressures can be calculated based on statics, as discussed for single footings (see Fig. 16.3). In this case, all loads, the downward column loads as well as the upward-bearing pressures, are known. Hence, moments and shear forces in the foundation can be found by statics alone. Once these are determined, the design of strip and grid foundations is similar to that of inverted continuous beams, and that of mat foundations to that of inverted flat slabs or plates.

On the other hand, if the foundation is relatively flexible and the column spacing large, settlements will no longer be uniform or linear. For one thing, the more heavily loaded columns will cause larger settlements, and thereby larger subgrade reactions, than the lighter ones. Also, since the continuous strip or slab midway between columns will deflect upward relative to the nearby columns, the soil settlement, and thereby the subgrade reaction, will be smaller midway between columns than directly at the columns. This is shown schematically for a strip footing in Fig. 16.21; the subgrade reaction can no longer be assumed to be uniform. Mat foundations likewise require

FIGURE 16.21
Strip footing. (*Adapted from Ref. 16.8.*)

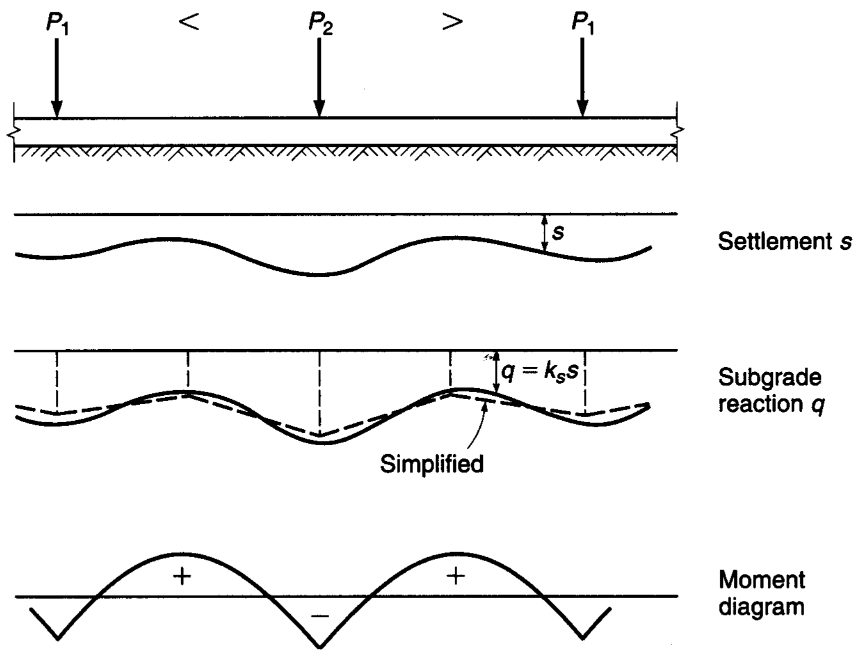

different approaches, depending on whether they can be assumed to be rigid when calculating the soil reaction.

Criteria have been established as a measure of the relative stiffness of the structure versus the stiffness of the soil (Refs. 16.10 and 16.13). If the relative stiffness is low, the foundation should be designed as a flexible member with a nonlinear upward reaction from the soil. For strip footings, a reasonably accurate but fairly complex analysis can be done using the theory of beams on elastic foundations (Ref. 16.14). Kramrisch (Ref. 16.8) has suggested simplified procedures, based on the assumption that contact pressures vary linearly between load points, as shown in Fig. 16.21.

For nonrigid mat foundations, great advances in analysis have been made using finite element methods, which can account specifically for the stiffnesses of both the structure and the soil. There are a large number of commercially available programs (e.g., pcaMats, Portland Cement Association, Skokie, Illinois) based on the finite element method, permitting quick modeling and analysis of combined footings, strip footings, and mat foundations.

16.10 PILE CAPS

If the bearing capacity of the upper soil layers is insufficient for a spread foundation, but firmer strata are available at greater depth, piles are used to transfer the loads to these deeper strata. Piles are generally arranged in groups or clusters, one under each column. The group is capped by a spread footing or cap that distributes the column load to all piles in the group. These pile caps are in most ways very similar to footings on soil, except for two features. For one, reactions on caps act as concentrated loads at the individual piles, rather than as distributed pressures. For another, if the total of all pile reactions in a cluster is divided by the area of the footing to obtain an equivalent uniform pressure (for purposes of comparison only), it is found that this equivalent pressure is considerably higher in pile caps than for spread footings. This means that moments, and particularly shears, are also correspondingly larger, which requires greater footing depths than for a spread footing of similar horizontal dimensions. To spread the load evenly to all piles, it is in any event advisable to provide ample rigidity, i.e., depth, for pile caps.

Allowable bearing capacities of piles R_a are obtained from soil exploration, pile-driving energy, and test loadings, and their determination is not within the scope of the present book (see Refs. 16.1 to 16.4). As in spread footings, the effective portion of R_a available to resist the unfactored column loads is the allowable pile reaction less the weight of footing, backfill, and surcharge per pile. That is,

$$R_e = R_a - W_f \tag{16.12}$$

where W_f is the total weight of footing, fill, and surcharge divided by the number of piles.

Once the available or effective pile reaction R_e is determined, the number of piles in a concentrically loaded cluster is the integer next larger than

$$n = \frac{D + L}{R_e}$$

As far as the effects of wind, earthquake moments at the foot of the columns, and safety against overturning are concerned, design considerations are the same as described in

Section 16.4 for spread footings. These effects generally produce an eccentrically loaded pile cluster in which different piles carry different loads. The number and location of piles in such a cluster are determined by successive approximations based on the requirement that the load on the most heavily loaded pile not exceed the allowable pile reaction R_a. With a linear distribution of pile loads due to bending, the maximum pile reaction is

$$R_{\max} = \frac{P}{n} + \frac{M}{I_{pg}/c} \tag{16.13}$$

where P is the maximum load (including weight of cap, backfill, etc.) and M the moment to be resisted by the pile group, both referred to the bottom of the cap; I_{pg} is the moment of inertia of the entire pile group about the centroidal axis about which bending occurs; and c is the distance from that axis to the extreme pile. $I_{pg} = \Sigma_1^n(1 \times y_i^2)$; i.e., it is the moment of inertia of n piles, each counting as one unit and located a distance y_i from the described centroidal axis.

Piles are generally arranged in tight patterns, which minimizes the cost of the caps, but they cannot be placed closer than conditions of driving and of undisturbed carrying capacity will permit. A spacing of about 3 times the butt (top) diameter of the pile but no less than 2 ft 6 in. is customary. Commonly, piles with allowable reactions of 30 to 70 tons are spaced at 3 ft 0 in. (Ref. 16.8).

The *design* of footings on piles is similar to that of single-column footings. One approach is to design the cap for the pile reactions calculated for the factored column loads. For a concentrically loaded cluster, this would give $R_u = (1.2D + 1.6L)/n$. However, since the number of piles was taken as the next-larger integral according to Eq. (16.13), determining R_u in this manner can lead to a design where the strength of the cap is less than the capacity of the pile group. It is therefore recommended that the pile reaction for strength design be taken as

$$R_u = R_e \times \text{average load factor} \tag{16.14}$$

where the average load factor $= (1.2D + 1.6L)/(D + L)$. In this manner, the cap is designed to be capable of developing the full allowable capacity of the pile group. Details of a typical pile cap are shown in Fig. 16.22.

As in single-column spread footings, the depth of the pile cap is usually governed by shear. ACI Code 15.5.3 specifies that when the distance between the axis of a pile and the axis of a column is more than 2 times the distance from the top of the pile cap and the top of the pile, shear design must follow the procedures for flat slabs and footings, as described in Section 16.6a. For closer spacings between piles and columns, the Code specifies either the use of the procedures described in Section 16.6a or the use of a three-dimensional strut-and-tie model (ACI Code Appendix A) based on the principles described in Chapter 10. In the latter case, the struts must be designed as bottle-shaped without transverse reinforcement (Table 10.1) because of the difficulty of providing such reinforcement in a pile cap. The use of strut-and-tie models to design pile caps is discussed in Ref. 16.15.

When the procedures for flat slabs and footings are used, both punching or two-way shear and flexural or one-way shear need to be considered. The critical sections are the same as given in Section 16.6a. The difference is that shear in caps is caused by concentrated pile reactions rather than by distributed bearing pressures. This poses the question of how to calculate shear if the critical section intersects the circumference of one or more piles. For this case ACI Code 15.5.4 accounts for the fact that a

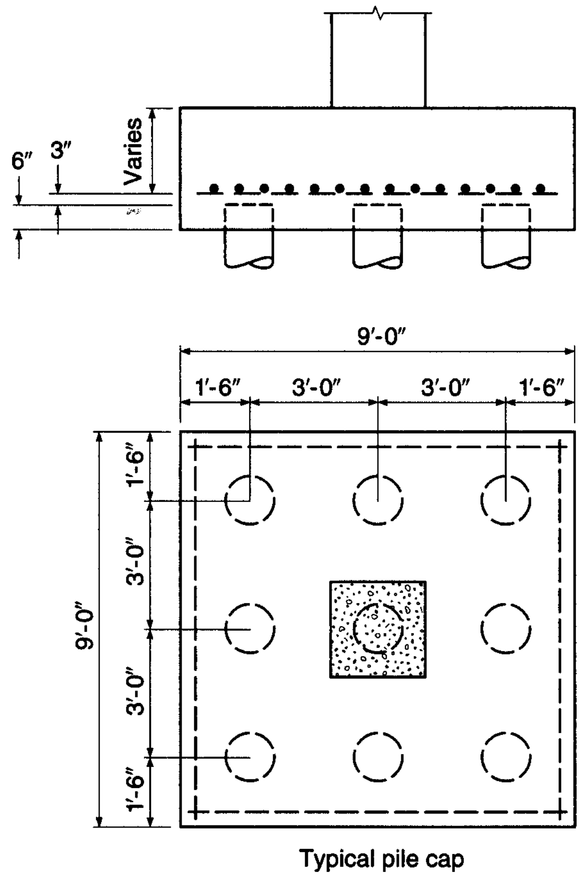

FIGURE 16.22
Typical single-column footing on piles (pile cap).

pile reaction is not really a point load, but is distributed over the pile-bearing area. Correspondingly, for piles with diameters d_{pile}, it stipulates as follows:

> Computation of shear on any section through a footing on piles shall be in accordance with the following:
>
> (*a*) The entire reaction from any pile whose center is located $d_{\text{pile}}/2$ or more outside this section shall be considered as producing shear on that section.
>
> (*b*) The reaction from any pile whose center is located $d_{\text{pile}}/2$ or more inside the section shall be considered as producing no shear on that section.
>
> (*c*) For intermediate positions of the pile center, the portion of the pile reaction to be considered as producing shear on the section shall be based on straight-line interpolation between the full value at $d_{\text{pile}}/2$ outside the section and zero at $d_{\text{pile}}/2$ inside the section.

In addition to checking two-way and one-way shear, as just discussed, punching shear must also be investigated for the individual pile. Particularly in caps on a small number of heavily loaded piles, it is this possibility of a pile punching upward through the cap that may govern the required depth. The critical perimeter for this action, again, is located at a distance $d/2$ outside the upper edge of the pile. However, for relatively deep caps and closely spaced piles, critical perimeters around adjacent piles may overlap. In this case, fracture, if any, would undoubtedly occur along an

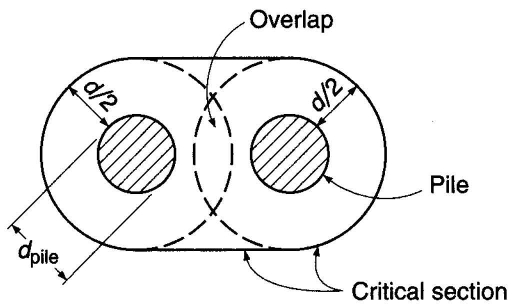

FIGURE 16.23
Critical section for punching shear with closely spaced piles.

outward-slanting surface around both adjacent piles. For such situations the critical perimeter is so located that its length is a minimum, as shown for two adjacent piles in Fig. 16.23.

REFERENCES

16.1. R. B. Peck, W. E. Hanson, and T. H. Thornburn, *Foundation Engineering*, 2nd ed., John Wiley & Sons, New York, 1974.
16.2. K. Terzaghi, R. B. Peck, and G. Mesri, *Soil Mechanics in Engineering Practice*, 3rd ed., John Wiley & Sons, New York, 1996.
16.3. J. E. Bowles, *Foundation Analysis and Design*, 5th ed., McGraw-Hill, New York, 1996.
16.4. H.-Y. Fang, *Foundation Engineering Handbook*, 2nd ed., Van Nostrand Reinhold, New York, 1991.
16.5. A. N. Talbot, "Reinforced Concrete Wall Footings and Column Footings," *Univ. Ill. Eng. Exp. Stn. Bull.* 67, 1913.
16.6. F. E. Richart, "Reinforced Concrete Wall and Column Footings," *J. ACI*, vol. 45, 1948, pp. 97 and 237.
16.7. E. Hognestad, "Shearing Strength of Reinforced Column Footings," *J. ACI*, vol. 50, 1953, p. 189.
16.8. F. Kramrisch, "Footings," chap. 5 in M. Fintel (ed.), *Handbook of Concrete Engineering*, 2nd ed., Van Nostrand Reinhold, New York, 1985.
16.9. ASCE–ACI Committee 426, "The Shear Strength of Reinforced Concrete Members—Slabs," *J. Struct. Div.*, ASCE, vol. 100, no. ST8, 1974, pp. 1543–1591.
16.10. ACI Committee 336, *Suggested Analysis and Design Procedures for Combined Footings and Mats* (Reapproved 2002), ACI 326.2R-88, American Concrete Institute, Farmington Hills, MI, 2002.
16.11. *International Building Code*, International Code Council, Washington, DC, 2006.
16.12. *Minimum Design Loads for Buildings and Other Structures*, ASCE /SEI 7-05, American Society of Civil Engineers, Reston, VA, 2005.
16.13. *Design and Performance of Mat Foundations—State of the Art Review*, SP-152, American Concrete Institute, Detroit, MI, 1995.
16.14. M. Hetenyi, *Beams on Elastic Foundations*, Univ. of Michigan Press, Ann Arbor, 1946.
16.15. P. Adebar, D. Kuchma, and M. P. Collins, "Strut-and-Tie Models for the Design of Pile Caps—An Experimental Study," *ACI Struct. J.*, vol. 87, no. 1, 1990, pp. 81–92.

PROBLEMS

16.1. A continuous strip footing is to be located concentrically under a 12 in. wall that delivers service loads $D = 25{,}000$ lb/ft and $L = 15{,}000$ lb/ft to the top of the footing. The bottom of the footing will be 4 ft below the final ground surface. The soil has a density of 120 pcf and allowable bearing capacity of 8000 psf. Material strengths are $f_c' = 3000$ psi and $f_y = 60{,}000$ psi. Find (*a*) the required width of the footing, (*b*) the required effective and total depths, based on shear, and (*c*) the required flexural steel area.

16.2. An interior column for a tall concrete structure carries total service loads $D = 500$ kips and $L = 514$ kips. The column is 22×22 in. in cross section and is reinforced with 12 No. 11 (No. 36) bars centered 3 in. from the column faces (equal number of bars each face). For the column, $f'_c = 4000$ psi and $f_y = 60{,}000$ psi. The column will be supported on a square footing, with the bottom of the footing 6 ft below grade. Design the footing, determining all concrete dimensions and amount and placement of all reinforcement, including length and placement of dowel steel. No shear reinforcement is permitted. The allowable soil bearing pressure is 8000 psf. Material strengths for the footing are $f'_c = 3000$ psi and $f_y = 60{,}000$ psi.

16.3. Design a single-column footing (including dowels) to support an 11 in. square column reinforced with eight No. 9 (No. 29) bars centered 2.5 in. from the column faces (equal number of bars on each face). The unfactored axial dead load = 135 kips, and the unfactored axial live load = 125 kips. For the column, $f'_c = 4000$ psi and $f_y = 60{,}000$ psi. The base of the footing will be 3 ft below grade. The allowable soil bearing pressure is 3000 lb/ft^2. Material strengths for the footing are $f'_c = 3000$ psi and $f_y = 60{,}000$ psi.

16.4. Two interior columns for a high-rise concrete structure are spaced 15 ft apart, and each carries service loads $D = 500$ kips and $L = 514$ kips. The columns are to be 22 in. square in cross section, and will each be reinforced with 12 No. 11 (No. 36) bars centered 3 in. from the column faces, with an equal number of bars at each face. For the columns, $f'_c = 4000$ psi and $f_y = 60{,}000$ psi. The columns will be supported on a rectangular combined footing with a long-side dimension twice that of the short side. The allowable soil bearing pressure is 8000 psf. The bottom of the footing will be 6 ft below grade. Design the footing for these columns, using $f'_c = 3000$ psi and $f_y = 60{,}000$ psi. Specify all reinforcement, including length and placement of footing bars and dowel steel.

16.5. A pile cap is to be designed to distribute a concentric force from a single column to a nine-pile group, with geometry as shown in Fig. 16.22. The cap will carry calculated dead and service live loads of 280 and 570 kips, respectively, from a 19 in. square concrete column reinforced with six No. 14 (No. 43) bars. The permissible load per pile at service load is 100 kips, and the pile diameter is 16 in. Find the required effective and total depths of the pile cap and the required reinforcement. Check all relevant aspects of the design, including the development length for the reinforcement and transfer of forces at the base of the column. Material strengths for the column are $f'_c = 4000$ psi and $f_y = 60{,}000$ psi, and for the pile cap are $f'_c = 3000$ psi and $f_y = 60{,}000$ psi.

16.6. Complete the design of the strap footing in Example 16.4 and determine all dimensions and reinforcement. Compare the total volume of concrete in the strap footing in Example 16.4 with that of the rectangular combined footing in Example 16.3. It will be found that the strap footing is significantly more economical in terms of material (although forming would be more costly). This economy of material would increase with increasing distance between the columns.

17 Retaining Walls

17.1 FUNCTION AND TYPES OF RETAINING WALLS

Retaining walls are used to hold back masses of earth or other loose material where conditions make it impossible to let those masses assume their natural slopes. Such conditions occur when the width of an excavation, cut, or embankment is restricted by conditions of ownership, use of the structure, or economy. For example, in railway or highway construction the width of the right of way is fixed, and the cut or embankment must be contained within that width. Similarly, the basement walls of buildings must be located within the property and must retain the soil surrounding the basement.

Freestanding retaining walls, as distinct from those that form parts of structures, such as basement walls, are of various types, the most common of which are shown in Fig. 17.1. The gravity wall (Fig. 17.1*a*) retains the earth entirely by its own weight and generally contains no reinforcement. The reinforced concrete cantilever wall (Fig. 17.1*b*) consists of the vertical arm that retains the earth and is held in position by a footing or base slab. In this case, the weight of the fill on top of the heel, in addition to the weight of the wall, contributes to the stability of the structure. Since the arm represents a vertical cantilever, its required thickness increases rapidly with increasing height. To reduce the bending moments in vertical walls of great height, counterforts are used spaced at distances from each other equal to or slightly larger than one-half of the height (Fig. 17.1*c*). Property rights or other restrictions sometimes make it necessary to place the wall at the forward edge of the base slab, i.e., to omit the toe. Whenever it is possible, toe extensions of one-third to one-fourth of the width of the base provide a more economical solution.

Which of the three types of walls is appropriate in a given case depends on a variety of conditions, such as local availability and price of construction materials and property rights. In general, gravity walls are economical only for relatively low walls, possibly up to about 10 ft. Cantilever walls are economical for heights from 10 to 20 ft, while counterforts are used for greater heights.

17.2 EARTH PRESSURE

In terms of physical behavior, soils and other granular masses occupy a position intermediate between liquids and solids. If sand is poured from a dump truck, it flows, but, unlike a frictionless liquid, it will not assume a horizontal surface. It maintains itself in a stable heap with sides reaching an *angle of repose*, the tangent of which is roughly equal to the coefficient of intergranular friction. If a pit is dug in clay soil, its sides can

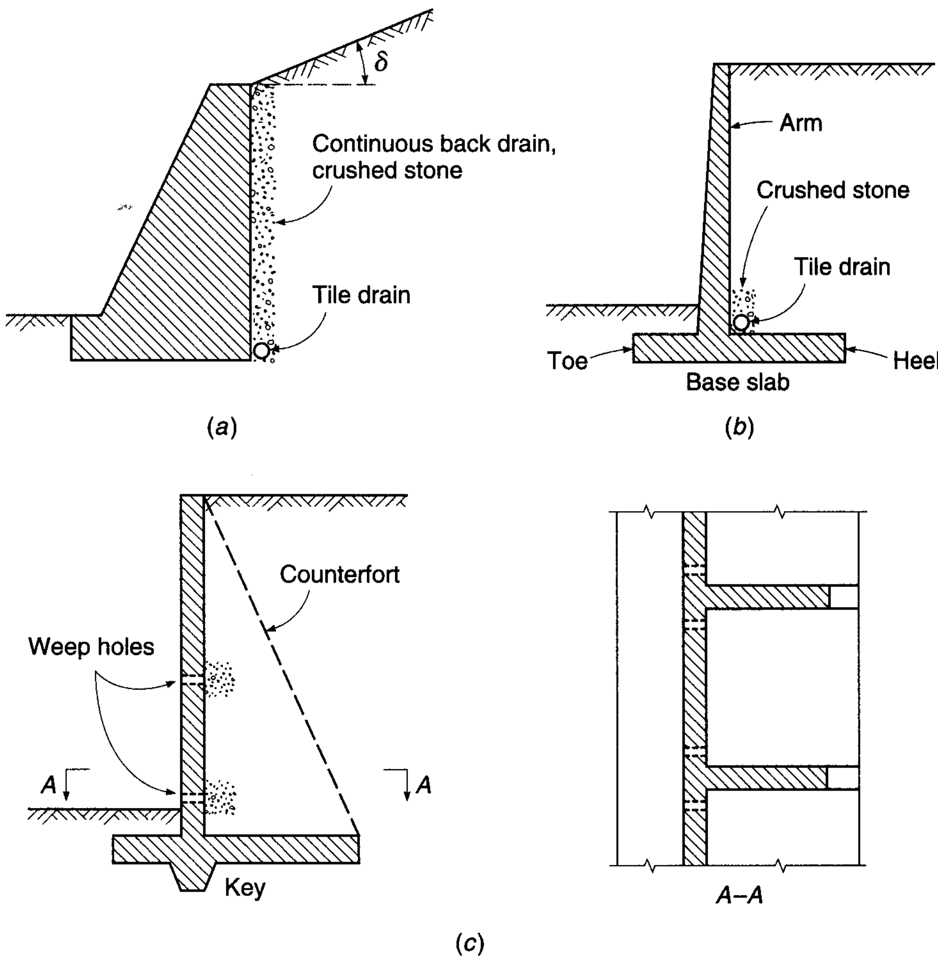

FIGURE 17.1
Types of retaining walls and back drains: (*a*) gravity wall; (*b*) cantilever wall; (*c*) counterfort wall.

usually be made vertical over considerable depths without support; i.e., the clay will behave as a solid and will retain the shape it is given. If, however, the pit is flooded, the sides will give way, and in many cases the saturated clay will be converted nearly into a true liquid. The clay is capable of maintaining its shape by means of its internal cohesion, but flooding reduces that cohesion greatly, often to zero.

If a wall is built in contact with a solid, such as a rock face, no pressure is exerted on it. If, on the other hand, a wall retains a liquid, as in a reservoir, it is subject at any level to the hydrostatic pressure $w_w h$, where w_w is the unit weight of the liquid and h is the distance from the surface. If a vertical wall retains soil, the earth pressure similarly increases proportionally to the depth, but its magnitude is

$$p_h = K_0 wh \tag{17.1}$$

where w is the unit weight of the soil and K_0 is a constant known as the *coefficient of earth pressure at rest*. The value of K_0 depends not only on the nature of the backfill but also on the method of depositing and compacting it. It has been determined experimentally that, for uncompacted noncohesive soils such as sands and gravels, K_0 ranges between 0.4 and 0.5, while it may be as high as 0.8 for the same soils in a highly compacted state (Refs. 17.1 through 17.3). For cohesive soils, K_0 may be on the order of 0.7 to 1.0. Clean sands and gravels are considered superior to all other soils

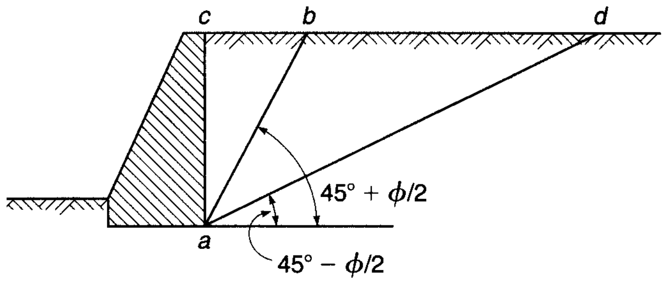

FIGURE 17.2
Basis of active and passive earth pressure determination.

because they are free-draining and are not susceptible to frost action and because they do not become less stable with the passage of time. For this reason, noncohesive backfills are usually specified.

Usually, walls move slightly under the action of the earth pressure. Since walls are constructed of elastic material, they deflect under the action of the pressure, and because they generally rest on compressible soils, they tilt and shift away from the fill. (For this reason, the wall is often constructed with a slight batter toward the fill on the exposed face so that, if and when such tilting takes place, the tilt does not appear evident to the observer.) Even if this movement at the top of the wall is only a fraction of a percent of the wall height ($\frac{1}{2}$ to $\frac{1}{10}$ percent according to Ref. 17.2), the rest pressure is materially decreased by it.

If the wall moves away from the fill, a sliding plane *ab* (Fig. 17.2) forms in the soil mass, and the wedge *abc*, sliding along that plane, exerts pressure against the wall. Here the angle ϕ is known as the *angle of internal friction*; i.e., its tangent is equal to the coefficient of intergranular friction, which can be determined by appropriate laboratory tests. The corresponding pressure is known as the *active earth pressure*. If, on the other hand, the wall is pushed against the fill, a sliding plane *ad* is formed, and the wedge *acd* is pushed upward by the wall along that plane. The pressure that this larger wedge exerts against the wall is known as the *passive earth pressure*. (This latter case will also occur at the left face of the gravity wall in Fig. 17.1*a* when this wall yields slightly to the left under the pressure of the fill.)

The magnitude of these pressures has been analyzed by Rankine, Coulomb, and others. If the soil surface makes an angle δ with the horizontal (Fig. 17.1*a*), then, according to Rankine, the *coefficient for active earth pressure* is

$$K_a = \cos\delta \frac{\cos\delta - \sqrt{\cos^2\delta - \cos^2\phi}}{\cos\delta + \sqrt{\cos^2\delta - \cos^2\phi}} \tag{17.2}$$

and the *coefficient for passive pressure* is

$$K_p = \cos\delta \frac{\cos\delta + \sqrt{\cos^2\delta - \cos^2\phi}}{\cos\delta - \sqrt{\cos^2\delta - \cos^2\phi}} \tag{17.3}$$

K_a and K_p replace K_0 in Eq. (17.1) to determine soil pressure p_h under active and passive conditions, respectively.

For the frequent case of a horizontal surface, that is, $\delta = 0$ (Fig. 17.2), for active pressure,

$$K_{ah} = \frac{1 - \sin\phi}{1 + \sin\phi} \tag{17.4}$$

and for passive pressure,

$$K_{ph} = \frac{1 + \sin\phi}{1 - \sin\phi} \tag{17.5}$$

Rankine's theory is valid only for noncohesive soils such as sand and gravel but, with corresponding adjustments, can also be used successfully for cohesive clay soils.

From Eqs. (17.1) through (17.5), it is seen that the earth pressure at a given depth h depends on the inclination of the surface δ, the unit weight w, and the angle of friction ϕ. The first two of these are easily determined, while little agreement has yet been reached as to the proper values of ϕ. For the ideal case of a dry, noncohesive fill, ϕ could be determined by laboratory tests and then used in the formulas. This is impossible for clays, only part of whose resistance is furnished by intergranular friction, while the rest is due to internal cohesion. For this reason, their actual ϕ values are often increased by an arbitrary amount to account implicitly for the added cohesion. However, this is often unsafe since, as was shown by the example of the flooded pit, cohesion may vanish almost completely due to saturation and inundation.

In addition, fills behind retaining walls are rarely uniform, and, what is more important, they are rarely dry. Proper drainage of the fill is vitally important to reduce pressures (see Section 17.6), but even in a well-drained fill, the pressure will temporarily increase during heavy storms or sudden thaws. This is so because even though the drainage may successfully remove the water as fast as it appears, its movement through the fill toward the drains causes additional pressure (seepage pressure). In addition, frost action and other influences may temporarily increase its value over that of the theoretical active pressure. Many walls that were designed without regard to these factors have failed, been displaced, or cracked.

It is good practice, therefore, to select conservative values for ϕ, considerably smaller than the actual test values, in all cases except where extraordinary and usually expensive precautions are taken to keep the fill dry under all conditions. An example of recommended earth pressure values, which are quite conservative, though based on extensive research and practical experience, can be found in Ref. 17.2. Less conservative values are often used in practical designs, but these should be employed (1) with caution in view of the fact that occasional trouble has been encountered with walls so designed and (2) preferably with the advice of a geotechnical engineer.

Table 17.1 gives representative values for w and ϕ often used in engineering practice. (Note that the ϕ values do not account for probable additional pressures due to porewater, seepage, frost, etc.) The table also contains values for the coefficient of

TABLE 17.1
Unit weights w, effective angles of internal friction ϕ, and coefficients of friction with concrete f

Soil	Unit Weight w, pcf	ϕ, deg	f
1. Sand or gravel without fine particles, highly permeable	110–120	33–40	0.5–0.6
2. Sand or gravel with silt mixture, low permeability	120–130	25–35	0.4–0.5
3. Silty sand, sand and gravel with high clay content	110–120	23–30	0.3–0.4
4. Medium or stiff clay	100–120	25–35[a]	0.2–0.4
5. Soft clay, silt	90–110	20–25[a]	0.2–0.3

[a] For saturated conditions, ϕ for clays and silts may be close to zero.

friction f between concrete and various soils. The values of ϕ for soils 3 through 5 may be quite unconservative; under saturated conditions, clays and silts may become entirely liquid (that is, $\phi = 0$). Soils of type 1 or 2 should be used as backfill for retaining walls wherever possible.

17.3 EARTH PRESSURE FOR COMMON CONDITIONS OF LOADING

In computing earth pressures on walls, three common conditions of loading are most often met: (1) horizontal surface of fill at the top of the wall, (2) inclined surface of fill sloping up and back from the top of the wall, and (3) horizontal surface of fill carrying a uniformly distributed additional load (surcharge), such as from goods in a storage yard or traffic on a road.

The increase in pressure caused by uniform surcharge s (case 3) is computed by converting its load into an equivalent, imaginary height of earth h' above the top of the wall such that

$$h' = \frac{s}{w} \tag{17.6}$$

and measuring the depth to a given point on the wall from this imaginary surface. This amounts to replacing h with $h + h'$ in Eq. (17.1).

The distributions of pressure for cases 1 to 3 are shown in Fig. 17.3. The total earth thrust P per linear foot of wall is equal to the area under the pressure distribution figure, and its line of action passes through the centroid of the pressure. Figure 17.3 gives information, computed in this manner, on magnitude, point of action, and direction of P for these three cases.

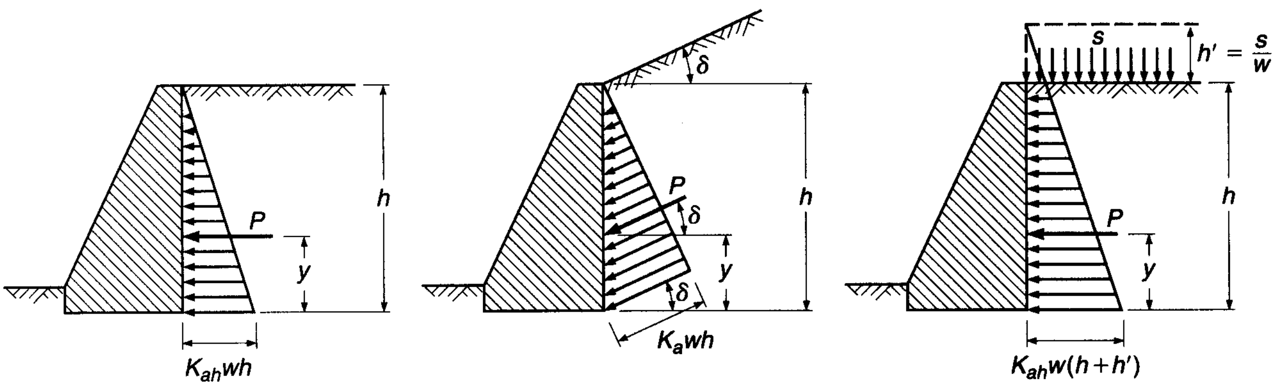

$y = \frac{h}{3}$

$P = \frac{1}{2}K_{ah}wh^2$

(a)

$y = \frac{h}{3}$ $P = \frac{1}{2}K_a wh^2$

For $\delta = \phi$, $K_a = \cos\phi$

(b)

$y = \frac{h^2 + 3hh'}{3(h + 2h')}$

$P = \frac{1}{2}K_{ah}wh(h + 2h')$

(c)

FIGURE 17.3
Earth pressures for (*a*) horizontal surface; (*b*) sloping surface; (*c*) horizontal surface with surcharge *s*.

Occasionally retaining walls must be built for conditions in which the groundwater level is above the base of the wall, either permanently or seasonally. In that case, the pressure of the soil *above* groundwater is determined as usual. The part of the wall *below* groundwater is subject to the sum of the water pressure and the earth pressure. The former is equal to the full hydrostatic pressure $p_w = w_w h_w$, where w_w and h_w are, respectively, the unit weight of water and the distance from the groundwater level to the point on the wall. The additional pressure of the soil below the groundwater level is computed from Eq. (17.1), where, however, for the portion of the soil below water, w is replaced with $w - w_w$, while h, as usual, is measured from the soil surface. That is, for submerged soil, buoyancy reduces the effective weight in the indicated manner. Pressures of this magnitude, which are considerably larger than those of drained soil, will also occur temporarily after heavy rainstorms or thaws in walls without provision for drainage, or if drains have become clogged.

The seeming simplicity of the determination of earth pressure, as indicated here, should not lull the designer into a false sense of security and certainty. No theory is more accurate than the assumptions on which it is based. Actual soil pressures are affected by irregularities of soil properties, porewater and drainage conditions, and climatic and other factors that cannot be expressed in formulas. This situation, on the one hand, indicates that involved refinements of theoretical earth pressure determinations, as sometimes attempted, are of little practical value. On the other hand, the design of a retaining wall is seldom a routine procedure, since the local conditions that affect pressures and safety vary from one locality to another.

17.4 EXTERNAL STABILITY

A wall may fail in two different ways: (1) its individual parts may not be strong enough to resist the acting forces, such as when a vertical cantilever wall is cracked by the earth pressure acting on it; and (2) the wall as a whole may be bodily displaced by the earth pressure, without breaking up internally. To design against the first possibility requires the determination of the necessary dimensions, thicknesses, and reinforcement to resist the moments and shears; this procedure, then, is in no way different from that of determining required dimensions and reinforcement of other types of concrete structures. The usual load factors and strength reduction factors of the ACI Code may be applied (see Section 17.5).

To safeguard the wall against bodily displacements, i.e., to ensure its external stability, requires special consideration. Consistent with current practice in geotechnical engineering, the stability investigation is based on actual earth pressures (as nearly as they may be determined) and on computed or estimated service dead and live loads, all without load factors. Computed bearing pressures are compared with allowable values, and overall factors of safety evaluated by comparing resisting forces to maximum loads acting under service conditions.

A wall, such as that in Fig. 17.4, together with the soil mass *ijkl* that rests on the base slab, may be bodily displaced by the earth thrust P that acts on the plane *ak* by *sliding* along the plane *ab*. Such sliding is resisted by the friction between the soil and footing along the same plane. To forestall motion, the forces that resist sliding must exceed those that tend to produce sliding; a factor of safety of 1.5 is generally assumed satisfactory in this connection.

In Fig. 17.4, the force that tends to produce sliding is the horizontal component P_h of the total earth thrust P. The resisting friction force is fR_v, where f is the coefficient of friction between the concrete and soil (see Table 17.1) and R_v is the vertical

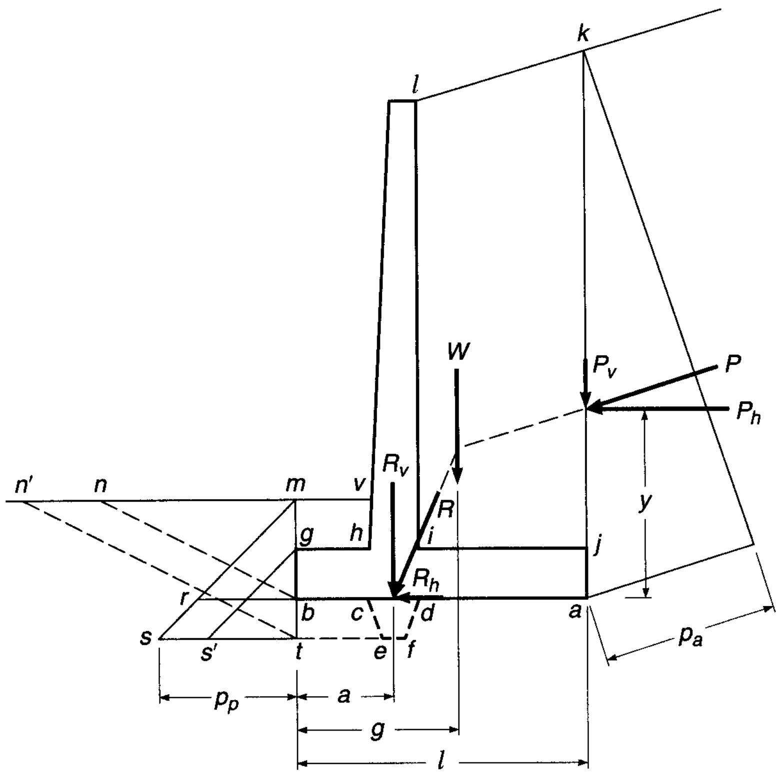

FIGURE 17.4
External stability of a cantilever wall.

component of the total resultant R; that is, $R_v = W + P_v$ (W = weight of wall plus soil resting on the footing, P_v = vertical component of P). Hence, to provide sufficient safety,

$$f(W + P_v) \geq 1.5P_h \tag{17.7}$$

Actually, for the wall to slide to the left, it must push with it the earth *nmb*, which gives rise to the passive earth pressure indicated by the triangle *rmb*. This passive pressure represents a further resisting force that could be added to the left side of Eq. (17.7). However, this should be done only if the proper functioning of this added resistance is ensured. For that purpose, the fill *ghmv* must be placed before the backfill *ijkl* is put in place and must be secure against later removal by scour or other means throughout the lifetime of the wall. If these conditions are not met, it is better not to count on the additional resistance of the passive pressure.

If the required sliding resistance cannot be developed by these means, a key wall *cdef* can be used to increase horizontal resistance. In this case, sliding, if it occurs, takes place along the planes *ad* and *tf*. While along *ad* and *ef*, the friction coefficient f applies, sliding along *te* occurs within the soil mass. The coefficient of friction that applies in this portion is consequently tan ϕ, where the value of ϕ may be taken from the next to last column in Table 17.1. In this situation sliding of the front soil occurs upward along *tn'* so that if the front fill is secure, the corresponding resistance from passive soil pressure is represented by the pressure triangle *stm*. If doubt exists as to the reliability of the fill above the toe, the free surface should more conservatively be assumed at the top level of the footing, in which case the passive pressure is represented by the triangle *s'tg*.

Next, it is necessary to ensure that the pressure under the footing not exceed the *permissible bearing pressure* for the particular soil. Let a (Fig. 17.4) be the distance from the front edge b to the intersection of the resultant with the base plane, and let R_v be the vertical component of R. (This intersection need not be located beneath the vertical arm, as shown, even though an economical wall generally results if it is so located.) Then the base plane ab, 1 ft wide longitudinally, is subject to a normal force R_v and to a moment about the centroid $(l/2 - a)R_v$. When these values are substituted in the usual formula for bending plus axial force

$$q_{\substack{\max \\ \min}} = \frac{N}{A} \pm \frac{Mc}{I} \tag{17.8}$$

it will be found that if the resultant is located within the middle third ($a > l/3$), compression will act throughout the section, and the maximum and minimum pressures can be computed from the equations in Fig. 17.5a. If the resultant is located just at the edge of the middle third ($a = l/3$), the pressure distribution is as shown in Fig. 17.5b, and Eq. (17.8) results in the formula given there.

FIGURE 17.5
Bearing pressures for different locations of resultant.

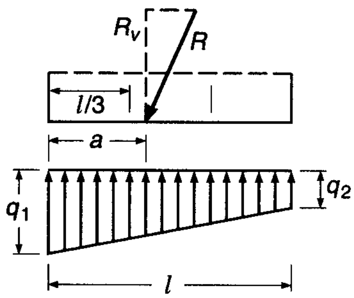

$$q_1 = (4l - 6a)\frac{R_v}{l^2}$$

$$q_2 = (6a - 2l)\frac{R_v}{l^2}$$

$$\text{when } a = \frac{l}{2},\ q_1 = q_2 = \frac{R_v}{l}$$

(a) Resultant in middle third

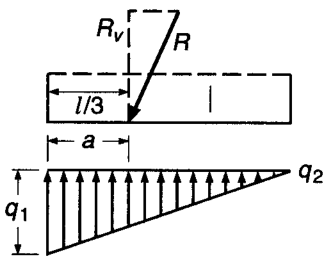

$$q_1 = \frac{2R_v}{l}$$

$$q_2 = 0$$

(b) Resultant at edge of middle third

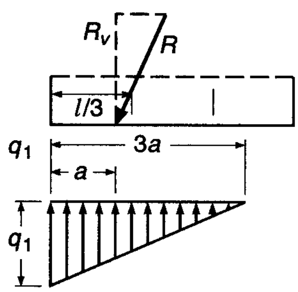

$$q_1 = \frac{2R_v}{3a}$$

(c) Resultant outside middle third

If the resultant were located outside the middle third ($a < l/3$), Eq. (17.8) would indicate tension at and near point a. Obviously, tension cannot be developed between soil and a concrete footing that merely rests on it. Hence, in this case the pressure distribution of Fig. 17.5*c* will develop, which implies a slight lifting off the soil of the rear part of the footing. Equilibrium requires that R_v pass through the centroid of the pressure distribution triangle, from which the formula for q_1 for this case can easily be derived.

It is good practice, in general, to have the resultant located within the middle third. This not only will reduce the magnitude of the maximum bearing pressure but also will prevent too large a nonuniformity of pressure. If the wall is founded on a highly compressible soil, such as certain clays, a pressure distribution as in Fig. 17.5*b* will result in a much larger settlement of the toe than of the heel, with a corresponding tilting of the wall. In a foundation on such a soil, the resultant, therefore, should strike at or very near the center of the footing. If the foundation is on very incompressible soil, such as well-compacted gravel or rock, the resultant can be allowed to fall outside the middle third (Fig. 17.5*c*).

A third mode of failure is the possibility of the wall *overturning* bodily around the front edge b (Fig. 17.4). For this to occur, the overturning moment yP_h about point b would have to be larger than the restoring moment $Wg + P_y l$ in Fig. 17.4, which is the same as saying that the resultant would have to strike outside the edge b. If, as is mostly the case, the resultant strikes within the middle third, adequate safety against overturning exists, and no special check need be made. If the resultant is located outside the middle third, a factor of safety of at least 1.5 should be maintained against overturning; i.e., the restoring moment should be at least 1.5 times the overturning moment.

17.5 BASIS OF STRUCTURAL DESIGN

In the investigation of a retaining wall for external stability, described in Section 17.4, it is the current practice to base the calculations on actual earth pressures, and on computed or estimated service dead and live loads, all with load factors of 1.0 (i.e., without load increase to account for a hypothetical overload condition). Computed soil bearing pressures, for service load conditions, are compared with allowable values set suitably lower than ultimate bearing values. Factors of safety against overturning and sliding are established, based on service load conditions.

On the other hand, the structural design of a retaining wall should be consistent with methods used for all other types of members, and thus should be based on factored loads in recognition of the possibility of an increase above service loading. ACI Code load factors relating to structural design of retaining walls are summarized as follows:

1. If resistance to earth pressure H is included in the design, together with dead loads D and live loads L, the required strength U shall be at least equal to

$$U = 1.2D + 1.6L + 1.6H$$

2. Where D or L reduce the effect of H, the required strength U shall be at least equal to

$$U = 0.9D + 1.6H$$

3. For any combination of D, L, and H, the required strength shall not be less than

$$U = 1.2D + 1.6L$$

While the ACI Code approach to load factor design is logical and relatively easy to apply to members in buildings, its application to structures that are to resist earth pressures is not so easy. Many alternative combinations of factored dead and live loads and lateral pressures are possible. Dead loads such as the weight of the concrete should be multiplied by 0.9 where they reduce design moments, such as for the toe slab of a cantilevered retaining wall, but should be multiplied by 1.2 where they increase moments, such as for the heel slab. The vertical load of the earth over the heel should be multiplied by 1.6. Obviously, no two factored load states could be obtained concurrently. For each combination of factored loads, different reactive soil pressures will be produced under the structure, requiring a new determination of those pressures for each alternative combination. Furthermore, there is no reason to believe that soil pressure would continue to be linearly distributed at the overload stage, or would increase in direct proportion to the load increase; knowledge of soil pressure distributions at incipient failure is incomplete. Necessarily, a somewhat simplified view of load factor design must be adopted in designing retaining walls.

Following the ACI Code, lateral earth pressures are multiplied by a load factor of 1.6. In general, the reactive pressure of the soil under the structure at the factored load stage is taken equal to 1.6 times the soil pressure found for service load conditions in the stability analysis.† For cantilever retaining walls, the calculated dead load of the toe slab, which causes moments acting in the opposite sense to those produced by the upward soil reaction, is multiplied by a factor of 0.9. For the heel slab, the required moment capacity is based on the dead load of the heel slab itself and is multiplied by 1.2, while the downward load of the earth is multiplied by 1.6. Surcharge, if present, is treated as live load with a load factor of 1.6. The upward pressure of the soil under the heel slab is taken equal to zero, recognizing that for the severe overload stage a nonlinear pressure distribution will probably be obtained, with most of the reaction concentrated near the toe. Similar assumptions appear to be reasonable in designing counterfort walls.

In accordance with ACI Code 14.1.2, cantilever retaining walls are designed following the flexural design provisions covered in Chapter 3, with minimum horizontal reinforcement provided in accordance with ACI Code 14.3.3, which stipulates a minimum ratio of

> 0.0020 for deformed bars not larger than No. 5 (No. 16) with a specified yield strength not less than 60,000 psi; or 0.0025 for other deformed bars; or 0.0020 for welded wire reinforcement not larger than W31 or D31.

17.6 DRAINAGE AND OTHER DETAILS

Such failures or damage to retaining walls as have occasionally occurred were due, in most cases, to one of two causes: overloading of the soil under the wall with consequent forward tipping or insufficient drainage of the backfill. In the latter case, hydrostatic pressure from porewater accumulated during or after rainstorms greatly increases the thrust on the wall; in addition, in subfreezing weather, ice pressure of considerable magnitude can develop in such poorly drained soils. The two causes are often interconnected, since large thrusts correspondingly increase the bearing pressure under the footing.

† These reactions are caused by the assumed factored load condition and have no direct relationship to ultimate soil bearing values or pressure distributions.

Allowable bearing pressures should be selected with great care. It is necessary, for this purpose, to investigate not only the type of soil immediately underlying the footing, but also the deeper layers. Unless reliable information is available at the site, subsurface borings should be made to a depth at least equal to the height of the wall. The foundation must be laid below *frost depth*, which amounts to 4 to 5 ft and more in the northern states, to ensure against heaving by the freezing of soils containing moisture.

Drainage can be provided in various ways. *Weep holes* consisting of 6 or 8 in. pipe embedded in the wall, as shown in Fig. 17.1*c*, are usually spaced horizontally at 5 to 10 ft. In addition to the bottom row, additional rows should be provided in walls of substantial height. To facilitate drainage and prevent clogging, 1 ft^3 or more of crushed stone is placed at the rear end of each weeper. Care must be taken that the outflow from the weep holes is carried off safely so as not to seep into and soften the soil underneath the wall. To prevent this, instead of weepers, *longitudinal drains* embedded in crushed stone or gravel can be provided along the rear face of the wall (Fig. 17.1*b*) at one or more levels; the drains discharge at the ends of the wall or at a few intermediate points. The most efficient drainage is provided by a *continuous backdrain* consisting of a layer of gravel or crushed stone covering the entire rear face of the wall (Fig. 17.1*a*), with discharge at the ends. Such drainage is expensive, however, unless appropriate material is cheaply available at the site. Wherever possible, the surface of the fill should be covered with a layer of low permeability and, in the case of a horizontal surface, should be laid with a slight slope away from the wall toward a gutter or other drainage.

In long walls, provision must be made against damage caused by *expansion* or *contraction* from temperate changes and shrinkage. The AASHTO *LRFD Bridge Design Specifications* require that for gravity walls, as well as reinforced concrete walls, expansion joints be placed at intervals of 90 ft or less, and contraction joints at not more than 30 ft (Ref. 17.4). The same specifications provide that, in reinforced concrete walls, temperature reinforcement equal to 0.0018bh in both the vertical and horizontal directions be distributed uniformly on the exposed (including end) surfaces. This AASHTO requirement is expressed as an area of reinforcement per foot on each face equal to

$$A_s \geq \frac{1.30bh}{2(b + h)f_y} \tag{17.9a}$$

$$0.11 \leq A_s \leq 0.60 \text{ in}^2/\text{ft} \tag{17.9b}$$

where b = least width of the component, h = least thickness of the component, and f_y = yield strength of the bars, expressed in ksi, $\leq$ 75 ksi. Similar provisions are found in Ref. 17.5.

17.7 EXAMPLE: DESIGN OF A GRAVITY RETAINING WALL

A gravity wall is to retain a bank 11 ft 6 in. high whose horizontal surface is subject to a live load surcharge of 400 psf. The soil is a sand and gravel mixture with a rather moderate amount of fine, silty particles. It can, therefore, be assumed to be in class 2 of Table 17.1 with the following characteristics: unit weight w = 120 pcf, ϕ = 30° (with adequate drainage to be provided), and base friction coefficient f = 0.5. With sin 30° = 0.5, from Eqs. (17.4) and (17.5), the soil pressure coefficients are K_{ah} = 0.333 and K_{ph} = 3.0. The allowable bearing pressure is assumed to be 8000 psf. This coarse-grained soil has little compressibility, so that the resultant can be allowed to strike near the outer-third point (see Section 17.4). The weight of the concrete is w_c = 150 pcf.

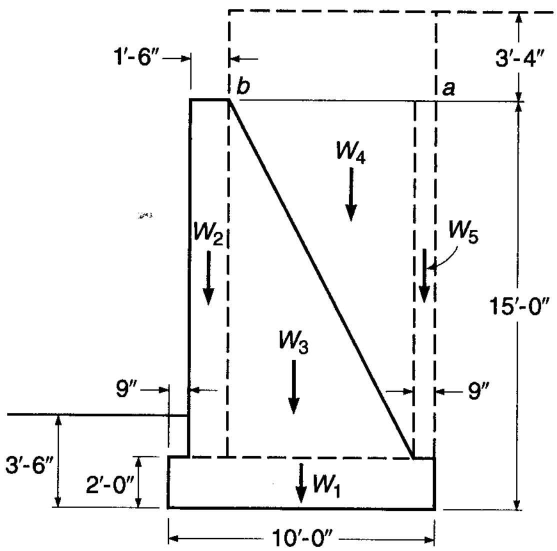

FIGURE 17.6
Gravity retaining wall.

The optimum design of any retaining wall is a matter of successive approximation. Reasonable dimensions are assumed based on experience, and the various conditions of stability are checked for these dimensions. On the basis of a first trial, dimensions are readjusted, and one or two additional trials usually result in a favorable design. In the following, only the final design is analyzed in detail. The final dimensions are shown in Fig. 17.6.

The equivalent height of surcharge is $h' = 400/120 = 3.33$ ft. From Fig. 17.3*c* the total earth thrust is

$$P = \tfrac{1}{2} \times 0.333 \times 120 \times 15 \times 21.67 = 6500 \text{ lb}$$

and its distance from the base is $y = (225 + 150)/(3 \times 21.67) = 5.77$ ft. Hence, the overturning moment $M_o = 6500 \times 5.77 = 37{,}500$ ft-lb. To compute the weight W and its restoring moment M_r about the edge of the toe, individual weights are taken, as shown in Fig. 17.6. With x representing the distance of the line of action of each subweight from the front edge, the following computation results:

Component Weights	W, lb	x, ft	$M_r = xW$, ft-lb
W_1: $10 \times 2 \times 150$	3,000	5.0	15,000
W_2: $1.5 \times 13 \times 150$	2,930	1.5	4,400
W_3: $7/2 \times 13 \times 150$	6,830	4.58	31,300
W_4: $7/2 \times 13 \times 120$	5,460	6.92	37,800
W_5: $0.75 \times 13 \times 120$	1,170	9.63	11,270
Total	19,390		99,770

The distance of the resultant from the front edge is

$$a = \frac{99{,}770 - 37{,}500}{19{,}390} = 3.21 \text{ ft}$$

which is just outside the middle third. The safety factor against overturning, $99{,}770/37{,}500 = 2.66$, is ample. From Fig. 17.5*c* the maximum soil pressure is $q = (2 \times 19{,}390)/(3 \times 3.21) = 4030$ psf.

These computations were made for the case in which the surcharge extends only to the rear edge of the wall, point a of Fig. 17.6. If the surcharge extends forward to point b, the following modifications are obtained:

$$W = 19{,}390 + 400 \times 7.75 = 22{,}490 \text{ lb}$$

$$M_r = 99{,}770 + 400 \times 7.75 \times 6.13 = 118{,}770 \text{ ft-lb}$$

$$a = \frac{118{,}770 - 37{,}500}{22{,}490} = 3.61 \text{ ft}$$

This is inside the middle third, and from Fig. 17.5a, the maximum bearing pressure is

$$q_1 = \frac{(40.0 - 21.7)22{,}490}{100} = 4120 \text{ psf}$$

The situation most conducive to sliding occurs when the surcharge extends only to point a, since additional surcharge between a and b would increase the total weight and the corresponding resisting friction. The friction force is

$$F = 0.5 \times 19{,}390 = 9695 \text{ lb}$$

Additionally, sliding is resisted by the passive earth pressure on the front of the wall. Although the base plane is 3.5 ft below grade, the top layer of soil cannot be relied upon to furnish passive pressure, since it is frequently loosened by roots and the like, or it could be scoured out by cloudbursts. For this reason, the top 1.5 ft will be discounted in computing the passive pressure, which then becomes

$$P_p = \tfrac{1}{2}wh^2K_{ph} = \tfrac{1}{2} \times 120 \times 2^2 \times 3.0 = 720 \text{ lb}$$

The safety factor against sliding, $(9695 + 720)/6500 = 1.6$, is but slightly larger than the required value 1.5, indicating a favorable design. Ignoring the passive pressure gives a safety factor of 1.49, which is very close to the acceptable value.

17.8 EXAMPLE: DESIGN OF A CANTILEVER RETAINING WALL

A cantilever wall is to be designed for the situation of the gravity wall in Section 17.7. Concrete with $f_c' = 4500$ psi and steel with $f_y = 60{,}000$ psi will be used.

a. Preliminary Design

To facilitate computation of weights for checking the stability of the wall, it is advantageous first to ascertain the thickness of the arm and the footing.† For this purpose the thickness of the footing is roughly estimated, and then the required thickness of the arm is determined at its bottom section. With the bottom of the footing at 3.5 ft below grade and an estimated footing thickness of 1.5 ft, the free height of the arm is 13.5 ft. Hence, with respect to the bottom of the arm (see Fig. 17.3c),

$$P = \tfrac{1}{2} \times 0.333 \times 120 \times 13.5 \times 20.16 = 5440 \text{ lb}$$

$$y = \frac{183 + 135}{3 \times 20.16} = 5.25 \text{ ft}$$

$$M_u = 1.6 \times 5440 \times 5.25 = 45{,}700 \text{ ft-lb}$$

† Valuable guidance is provided for the designer in tabulated designs such as those found in Ref. 17.6 and by the sample calculations in Ref. 17.7.

For the given grades of concrete and steel, the maximum practical reinforcement ratio $\rho_{0.005} = 0.0197$. For economy and ease of bar placement, a ratio of about 40 percent of the maximum, or 0.008, will be used. Then from Graph A.1*b* of Appendix A,

$$\frac{M_u}{\phi bd^2} = 430$$

For a unit length of the wall ($b = 12$ in.), with $\phi = 0.90$, the required effective depth is

$$d = \sqrt{\frac{45{,}700 \times 12}{0.90 \times 12 \times 430}} = 10.9 \text{ in.}$$

A protective cover of 2 in. is required for concrete exposed to earth. Thus, estimating the bar diameter to be 1 in., the minimum required thickness of the arm at the base is 13.4 in. This will be increased to 16 in., because the cost of the extra concrete in such structures is usually more than balanced by the simultaneous saving in steel and ease of concrete placement. The arm is then checked for shear at a distance d above the base, or 12.5 ft below the top of the wall:

$$P = \tfrac{1}{2} \times 0.333 \times 120 \times 12.5 \times 19.16 = 4800 \text{ lb}$$

$$V_u = 1.6 \times 4800 = 7680 \text{ lb}$$

$$\begin{aligned}\phi V_c &= \phi 2\lambda\sqrt{f'_c}\,bd \\ &= 0.75 \times 2 \times 1\sqrt{4500} \times 12 \times 13.5 \\ &= 16{,}300 \text{ lb}\end{aligned}$$

confirming that the arm is more than adequate to resist the factored shear force.

The thickness of the base is usually the same as or slightly larger than that at the bottom of the arm. Hence, the estimated 1.5 ft need not be revised. Since the moment in the arm decreases with increasing distance from the base and is zero at the top, the arm thickness at the top will be made 8 in. It is now necessary to assume lengths of heel and toe slabs and to check the stability for these assumed dimensions. Intermediate trials are omitted here, and the final dimensions are shown in Fig. 17.7*a*. Trial computations have shown that safety against sliding can be achieved only by an excessively long heel or by a key. The latter, requiring the smaller concrete volume, has been adopted.

b. Stability Investigation

Weights and moments about the front edge are as follows:

Component Weights	W, lb	x, ft	M_r, ft-lb
W_1: 0.67 × 13.5 × 150	1,360	4.08	5,550
W_2: 0.67 × 0.5 × 13.5 × 150	680	4.67	3,180
W_3: 9.75 × 1.5 × 150	2,190	4.88	10,700
W_4: 1.33 × 1.25 × 150	250	4.42	1,100
W_5: 3.75 × 2 × 120	900	1.88	1,690
W_6: 0.67 × 0.5 × 13.5 × 120	540	4.86	2,620
W_7: 4.67 × 13.5 × 120	7,570	7.42	56,200
Total	13,490		81,040

FIGURE 17.7
Cantilever retaining wall: (*a*) cross section; (*b*) bearing pressure with surcharge to *a*; (*c*) bearing pressure with surcharge to *b*; (*d*) reinforcement; (*e*) moment variation with height.

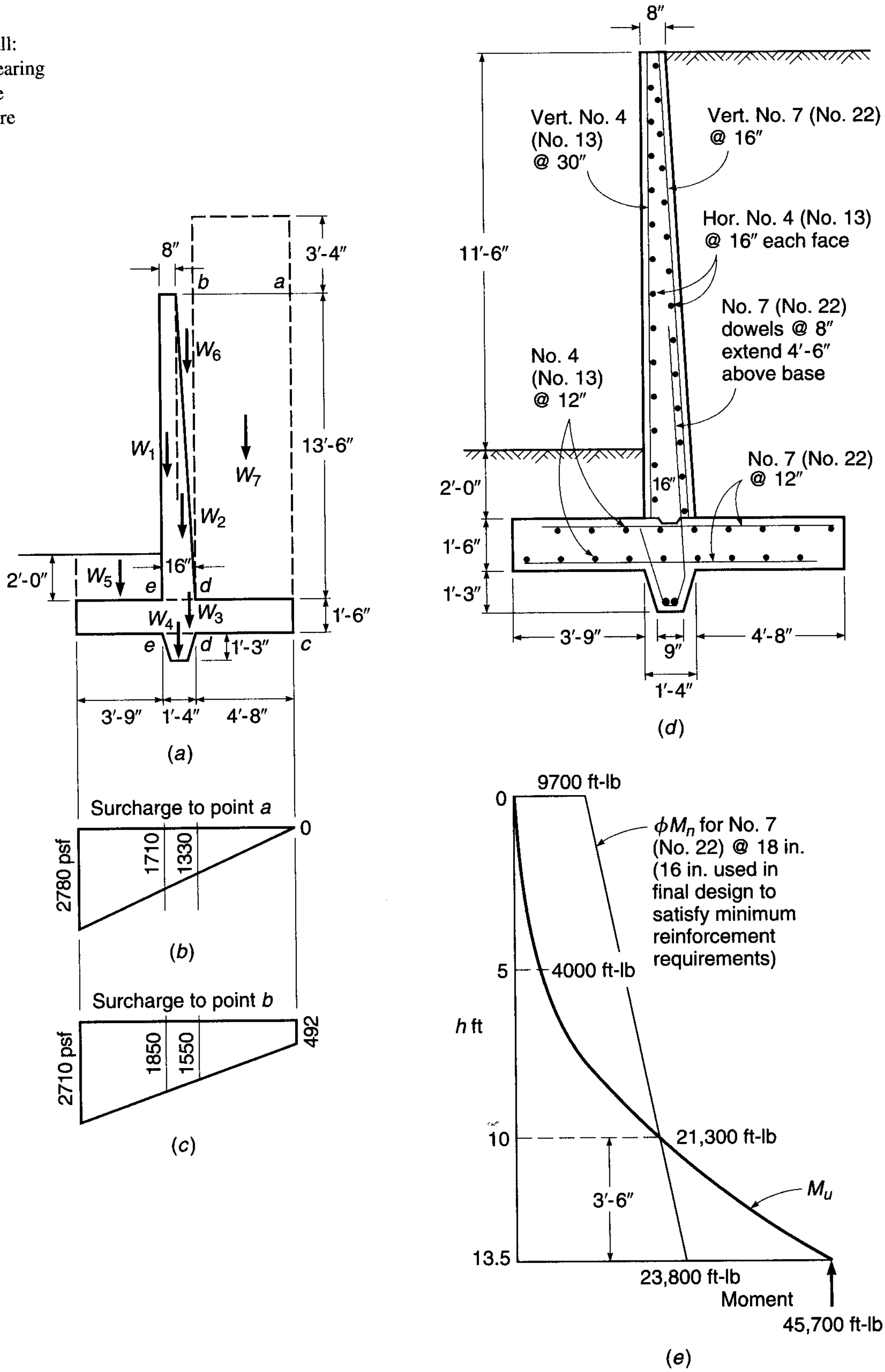

The total soil pressure on the plane *ac* is the same as for the gravity wall designed in Section 17.7; that is, $P = 6500$ lb, and the overturning moment is

$$M_o = 37{,}500 \text{ ft-lb}$$

The distance of the resultant from the front edge is

$$a = \frac{81{,}040 - 37{,}500}{13{,}490} = 3.23 \text{ ft}$$

which locates the resultant barely outside of the middle third. The corresponding maximum soil pressure at the toe, from Fig. 17.5*c*, is

$$q_1 = \frac{2 \times 13{,}470}{3 \times 3.23} = 2780 \text{ psf}$$

The factor of safety against overturning, 81,040/37,500 = 2.16, is ample.

To check the safety against sliding, remember (Section 17.4) that if sliding occurs, it proceeds between concrete and soil along the heel and key (i.e., length *ae* in Fig. 17.4), but takes place within the soil in front of the key (i.e., along length *te* in Fig. 17.4). Consequently, the coefficient of friction that applies for the former length is $f = 0.5$, while for the latter it is equal to the internal soil friction, i.e., $\tan 30° = 0.577$.

The bearing pressure distribution is shown in Fig. 17.7*b*. Since the resultant is at a distance $a = 3.23$ ft from the front, i.e., nearly at the middle third, it is assumed that the bearing pressure becomes zero exactly at the edge of the heel, as shown in Fig. 17.7*b*.

The resisting force is then computed as the sum of the friction forces of the rear and front portion, plus the passive soil pressure in front of the wall. For the latter, as in Section 17.7, the top 1.5 ft layer of soil will be discounted as unreliable. Hence,

Friction, toe:	$(2780 + 1710) \times 0.5 \times 3.75 \times 0.577 = 4860$ lb
Friction, heel and key:	$1710 \times 0.5 \times 6 \times 0.5 = 2570$ lb
Passive earth pressure:	$0.5 \times 120 \times 3.25^2 \times 3.0 = 1900$ lb
Total resistance to sliding:	$= 9330$ lb

The factor of safety against sliding, 9330/6500 = 1.44, is only 4 percent below the recommended value of 1.5 and can be regarded as adequate.

The computations hold for the case in which the surcharge extends from the right to point *a* above the edge of the heel. The other case of load distribution, in which the surcharge is placed over the entire surface of the fill up to point *b*, evidently does not change the earth pressure on the plane *ac*. It does, however, add to the sum of the vertical forces and increases both the restoring moment M_r and the friction along the base. Consequently, the danger of sliding or overturning is greater when the surcharge extends only to *a*, for which situation these two cases have been checked and found adequate. In view of the added vertical load, however, the bearing pressure is largest when the surface is loaded to *b*. For this case,

$$W = 13{,}490 + 400 \times 5.33 = 15{,}600 \text{ lb}$$

$$M_r = 81{,}040 + 400 \times 5.33 \times 7.09 = 96{,}200 \text{ ft-lb}$$

$$a = \frac{96{,}200 - 37{,}500}{15{,}600} = 3.76 \text{ ft}$$

which places the resultant inside the middle third. Hence, from Fig. 17.5*a*,

$$q_1 = (39.0 - 22.5)\frac{15{,}600}{9.75^2} = 2710 \text{ psf}$$

$$q_2 = (22.5 - 19.5)\frac{15{,}600}{9.75^2} = 492 \text{ psf}$$

which is far below the allowable pressure of 8000 psf. The corresponding bearing pressure distribution is shown in Fig. 17.7*c*.

The external stability of the wall has now been ascertained, and it remains to determine the required reinforcement and to check internal resistances.

c. Arm and Key

The moment at the bottom section of the arm has previously been determined as M_u = 45,700 ft-lb, and a wall thickness of 16 in. at the bottom and 8 in. at the top has been selected. With a concrete cover of 2 in. clear, $d = 16.0 - 2.0 - 0.5 = 13.5$ in. Then

$$\frac{M_u}{\phi b d^2} = \frac{45{,}700 \times 12}{0.90 \times 12 \times 13.5^2} = 279$$

Interpolating from Graph A.1*b* of Appendix A, with f_y = 60,000 psi and f_c' = 4500 psi, the required reinforcement ratio ρ is 0.0049 and $A_s = 0.0049 \times 12 \times 13.5 = 0.79$ in²/ft. The required area of steel is provided by No. 7 (No. 22) bars at 9 in. on centers.

The bending moment in the arm decreases rapidly with increasing distance from the bottom. For this reason, only part of the main reinforcement is needed at higher elevations, and alternate bars will be discontinued where no longer needed. To determine the cutoff point, the moment diagram for the arm has been drawn by computing bending moments at two intermediate levels, 10 and 5 ft from the top. These two moments, determined in the same manner as that at the base of the arm, were found to be 21,300 and 4000 ft-lb, respectively. The resisting moment provided by alternate bars, i.e., by No. 7 (No. 22) bars at 18 in. center to center, at the bottom of the arm is

$$\phi M_n = \frac{0.90 \times 0.40 \times 60{,}000}{12}(13.50 - 0.26) = 23{,}800 \text{ ft-lb}$$

At the top, $d = 8.0 - 2.5 = 5.5$ in., and the resisting moment of the same bars is only $\phi M_n = 23{,}800(5.5/13.5) = 9700$ ft-lb. Hence, the straight line drawn in Fig. 17.7*e* indicates the resisting moment provided at any elevation by one-half the number of main bars. The intersection of this line with the moment diagram at a distance of 3 ft 6 in. from the bottom represents the point above which alternate bars are no longer needed. ACI Code 12.10.3 specifies that any bar shall be extended beyond the point at which it is no longer needed to carry flexural stress for a distance equal to d or 12 bar diameters, whichever is greater. In the arm, at a distance of 3 ft 6 in. from the bottom, d = 11.4 in., while 12 bar diameters for No. 7 (No. 22) bars are equal to 10.5 in. Hence, one-half the bars can be discontinued 12 in. above the point where no longer needed, or a distance of 4 ft 6 in. above the base. This exceeds the required development length of 39 in. above the base.

To facilitate construction, the footing is placed first, and a construction joint is provided at the base of the arm, as shown in Fig. 17.7*d*. The main bars of the arm, therefore, end at the top of the base slab, and dowels are placed in the latter to be spliced with them; the integrity of the arm depends entirely on the strength of the splices used for these tension bars. Splicing all tension bars in one section by simple contact splices can easily lead to splitting of the concrete owing to the stress concentrations at the ends of the spliced bars. One way to avoid this difficulty is to weld all splices; this will entail considerable extra cost.

In this particular wall, another way of placing the reinforcing offers a more economical solution. Because alternate bars in the arm can be discontinued at a distance of 4 ft 6 in. above the base, the dowels will be carried up 4 ft 6 in. from the top of the base. These need not be spliced at all, because above that level only alternate No. 7 (No. 22) bars, 18 in. on centers, are needed. These latter bars are placed full length over the entire height of the arm and are spliced at the bottom with alternate shorter dowels. By this means, only 50 percent of the bars needed at the bottom of the arm are spliced; this is not objectionable.

For splices of deformed bars in tension, at sections where the ratio of steel provided to steel required is less than 2 and where no more than 50 percent of the steel is spliced, the ACI Code requires a Class B splice with a length equal to 1.3 times the development length of the bar (see Section 5.13a). The development length of the No. 7 (No. 22) bars for the given material strengths is 39 in., and so the required splice length is $1.3 \times 39 = 50.7$ in., which is less than the 4 ft 6 in. available.

According to the ACI Code, main flexural reinforcement is not to be terminated in a tension zone unless one of three conditions is satisfied: (1) shear at the cutoff point does not exceed two-thirds that permitted, (2) certain excess shear reinforcement is provided, or (3) the continuing reinforcement provides double the area required for flexure at the cutoff point and the factored shear does not exceed three-fourths of the design shear. It is easily confirmed that the shear 4 ft 6 in. above the base is well below two-thirds the value that can be carried by the concrete; thus main bars can be terminated as planned.

Prior to completing the design of the arm, the minimum tensile reinforcement ratio specified by the ACI Code must be checked. The actual ratio provided by the No. 7 (No. 22) bars at 18 in. spacing, with $d = 10.8$ in. just above the cutoff point, is 0.0031, about 10 percent below the minimum value of $3\sqrt{4500}/60{,}000 = 0.0034$. To handle this, the spacing of the No. 7 (No. 22) bars will be reduced to 8 in., giving a spacing of 16 in. above the cutoff. This will increase the amount of steel, but by less than would be needed if the bars were extended to a height where the decreasing value of d allowed the minimum reinforcement ratio to be satisfied. A final ACI Code requirement is that the maximum spacing of the primary flexural reinforcement exceed neither 3 times the wall thickness nor 18 in.; these restrictions are satisfied as well.

Since the dowels had to be extended at least partly into the key to produce the necessary length of embedment, they were bent as shown to provide both reinforcement for the key and anchorage for the arm reinforcement. The exact force that the key must resist is difficult to determine, since probably the major part of the force acting on the portion of the soil in front of the key is transmitted to it through friction along the base of the footing. The relatively strong reinforcement of the key by means of the extended dowels is considered sufficient to prevent separation from the footing.

The sloping sides of the key were provided to facilitate excavation without loosening the adjacent soil. This is necessary to ensure proper functioning of the key.

In addition to the main steel in the stem, reinforcement must be provided in the horizontal direction to control shrinkage and temperature cracking, in accordance with ACI Code 14.3.3. Calculations will be based on the average wall thickness of 12 in. The required steel area is 0.0020 times the gross concrete area. No. 4 (No. 13) bars 16 in. on centers, each face, will be used, as shown in Fig. 17.7*d*. Although not required by the Code for cantilever retaining walls, vertical steel equal to 0.0012 times the gross concrete area will also be provided (to limit horizontal surface cracking), with at least one-half of this value provided on the exposed face, as specified for other walls under ACI Code 14.3.2. No. 4 (No. 13) bars 30 in. on centers will satisfy this requirement.

d. Toe Slab

The toe slab acts as a cantilever projecting outward from the face of the stem. It must resist the upward pressures shown in Fig. 17.7*b* or *c* and the downward load of the toe slab itself, each multiplied by appropriate load factors. The downward load of the earth fill over the toe will be neglected because it is subject to possible erosion or removal. A load factor of 1.6 will be applied to the service load bearing pressures. Comparison of the pressures of Fig. 17.7*b* and *c* indicates that for the toe slab, the more severe loading case results from surcharge to *b*. Because the self-weight of the toe slab tends to reduce design moments and shears, it will be multiplied by a load factor of 0.9. Thus the factored load moment at the outer face of the stem is

$$M_u = 1.6\left(\frac{2710}{2} \times 3.75^2 \times \frac{2}{3} + \frac{1850}{2} \times 3.75^2 \times \frac{1}{3}\right) - 0.9\left(225 \times 3.75^2 \times \frac{1}{2}\right)$$
$$= 25{,}800 \text{ ft-lb}$$

For concrete cast against and permanently exposed to earth, a minimum protective cover for steel of 3 in. is required; if the bar diameter is about 1 in., the effective depth will be $18.0 - 3.0 - 0.5 = 14.5$ in. Thus, for a 12 in. strip of toe slab,

$$\frac{M_u}{\phi b d^2} = \frac{25{,}800 \times 12}{0.90 \times 12 \times 14.5^2} = 136$$

Graph A.1*b* of Appendix A shows that, for this value, the required reinforcement ratio would be below the minimum of $3\sqrt{4500}/60{,}000 = 0.0034$. A somewhat thinner base slab appears possible. However, moments in the heel slab are yet to be investigated, as well as shears in both the toe and heel, and the trial depth of 18 in. will be retained tentatively. The required flexural steel

$$A_s = 0.0034 \times 12 \times 14.5 = 0.59 \text{ in}^2/\text{ft}$$

is provided by No. 7 (No. 22) bars 12 in. on centers. The required length of embedment for these bars past the exterior face of the stem is the full development length of 39 in. Thus, they will be continued 39 in. past the face of the wall, as shown in Fig. 17.7*d*.

Shear will be checked at a distance $d = 1.21$ ft from the face of the stem (2.54 ft from the end of the toe), according to the usual ACI Code procedures. The service load bearing pressure at that location (with reference to Fig. 17.7*c*) is 2130 psf, and the factored load shear is

$$V_u = 1.6(2710 \times \tfrac{1}{2} \times 2.54 + 2130 \times \tfrac{1}{2} \times 2.54) - 0.9(225 \times 2.54)$$
$$= 9320 \text{ lb}$$

The design shear strength of the concrete is

$$\phi V_c = 2 \times 0.75\sqrt{4500} \times 12 \times 14.5 = 17{,}500 \text{ lb}$$

well above the required value V_u.

e. Heel Slab

The heel slab, too, acts as a cantilever, projecting in this case from the back face of the stem and loaded by surcharge, earth fill, and its own weight. The upward reaction of the soil will be neglected here, for reasons given earlier. Applying appropriate load factors, the moment to be resisted is

$$M_u = 1.2 \times 225 \times 4.67^2 \times \tfrac{1}{2} + 1.6(400 \times 4.67^2 \times \tfrac{1}{2} + 1620 \times 4.67^2 \times \tfrac{1}{2})$$
$$= 38{,}200 \text{ ft-lb}$$

Thus,

$$\frac{M_u}{\phi b d^2} = \frac{38{,}200 \times 12}{0.90 \times 12 \times 14.5^2} = 202$$

Interpolating from Graph A.1*b*, the required reinforcement ratio is 0.0035, just above the minimum value of 0.0034. The required steel area will again be provided using No. 7 (No. 22) bars 12 in. on centers, as shown in Fig. 17.7*d*. These bars are classed as top bars, as they have more than 12 in. of concrete below; thus the required length of embedment to the left of the inside face of the stem is $39 \times 1.3 = 51$ in.

According to normal ACI Code procedures, the first critical section for shear would be a distance d from the face of support. However, the justification for this provision of the ACI Code is the presence, in the usual case, of vertical compressive stress near a support which tends to decrease the likelihood of shear failure in that region. However, the cantilevered heel slab is essentially hung from the bottom of the stem by the flexural tensile steel in the stem, and the concrete compression normally found near a support is absent here. Consequently, the critical section for shear in the heel slab will be taken at the back face of the stem. At that location,

$$V_u = 1.2(225 \times 4.67) + 1.6(2020 \times 4.67)$$
$$= 16{,}350 \text{ lb}$$

The design shear strength provided by the concrete is the same as for the toe slab:

$$\phi V_c = 17{,}500 \text{ lb}$$

Because this is only 7 percent in excess of the required value V_u, no reduction in thickness of the base slab, considered earlier, will be made.

The base slab is well below grade and will not be subjected to the extremes of temperature that will be imposed on the stem concrete. Consequently, crack control steel in the direction perpendicular to the main reinforcement is not a major consideration. No. 4 (No. 13) bars 12 in. on centers will be provided, at one face only, placed as shown in Fig. 17.7*d*. These bars serve chiefly as spacers for the main flexural reinforcement.

17.9 COUNTERFORT RETAINING WALLS

The external stability of a counterfort retaining wall is determined in the same manner as in the examples of Sections 17.7 and 17.8. The toe slab represents a cantilever built in along the front face of the wall, loaded upward by the bearing pressure, exactly as in the cantilever wall described in Section 17.8. Reinforcement is provided by bars *a* in Fig. 17.8.

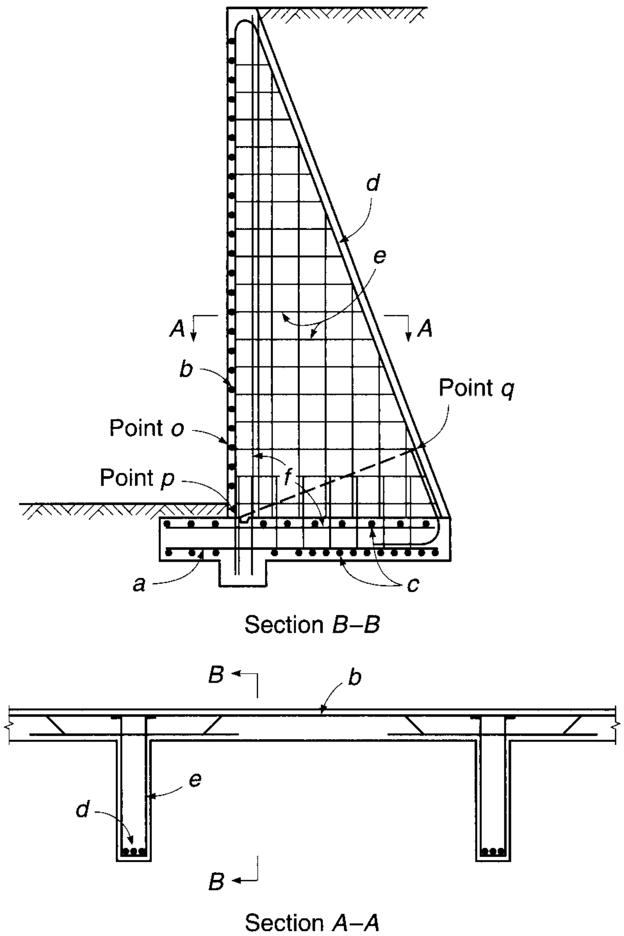

FIGURE 17.8
Details of counterfort retaining wall.

A panel of the vertical wall between two counterforts is a slab acted upon by horizontal earth pressure and supported along three sides, i.e., at the two counterforts and the base slab, while the fourth side, the top edge, is not supported. The earth pressure increases with distance from the free surface. The determination of moments and shears in such a slab supported on three sides and nonuniformly loaded is rather involved. It is customary in the design of such walls to disregard the support of the vertical wall by the base slab and to design it as if it were a continuous slab spanning horizontally between counterforts. This procedure is conservative, because the moments obtained by this approximation are larger than those corresponding to the actual conditions of support, particularly in the lower part of the wall. Hence, for very large installations, significant savings may be achieved by a more accurate analysis. The best computational tool for this is the Hillerborg *strip method*, a plasticity-based theory for design of slabs described in detail in Chapter 15. Alternatively, results of elastic analysis are tabulated for a range of variables in Ref. 17.8.

Slab moments are determined for strips 1 ft wide spanning horizontally, usually for the strip at the bottom of the wall and for three or four equally spaced additional strips at higher elevations. The earth pressure on the different strips decreases with increasing elevation and is determined using Eq. (17.1). Moment values for the bottom strips may be reduced to account for the fact that additional support is provided by the base slab. Horizontal bars *b* (Fig. 17.8) are provided, as required, with increased spacing or decreased diameter corresponding to the smaller moments. Alternate bars are bent to provide for the negative moments in the wall at the counterforts, or additional straight bars are used as negative reinforcement, as shown in Section *A–A* of Fig. 17.8.

The heel slab is supported, as is the wall slab, i.e., by the counterforts and at the wall. It is loaded downward by the weight of the fill resting on it, its own weight, and such surcharge as there may be. This load is partially counteracted by the upward bearing pressure on the underside of the heel. As in the vertical wall, a simplified analysis consists in neglecting the influence of the support along the third side and in determining moments and shears for strips parallel to the wall, each strip representing a continuous beam supported at the counterforts. For a horizontal soil surface, the downward load is constant for the entire heel, whereas the upward load from the bearing pressure is usually smallest at the rear edge and increases frontward. For this reason, the span moments are positive (compression on top) and the support moments negative in the rear portion of the heel. Near the wall, the bearing pressure often exceeds the vertical weights, resulting in a net upward load. The signs of the moments are correspondingly reversed, and steel must be placed accordingly. Bars *c* are provided for these moments.

The counterforts are wedge-shaped cantilevers built in at the bottom in the base slab. They support the wall slab and, therefore, are loaded by the total soil pressure over a length equal to the distance center to center between counterforts. They act as a T beam of which the wall slab is the flange and the counterfort the stem. The maximum bending moment is that of the total earth pressure, taken about the bottom of the wall slab. This moment is held in equilibrium by the force in the bars *d*, and hence, the effective depth for bending is the perpendicular distance *pq* from the center of bars *d* to the center of the bottom section of the wall slab. Since the moment decreases rapidly in the upper parts of the counterfort, part of the bars *d* can be discontinued.

In regard to shear, the authors suggest the horizontal section *oq* as a conservative location for checking adequacy. Modification of the customary shear computation is required for wedge-shaped members (see Section 4.7). Usually concrete alone is sufficient to carry the shear, although bars *e* act as stirrups and can be used for resisting excess shear.

The main purpose of bars *e* is to counteract the pull of the wall slab, and they are thus designed for the full reaction of this slab.

The remaining bars of Fig. 17.8 serve as shrinkage reinforcement, except that bars *f* have an important additional function. It will be recalled that the wall and heel slabs are supported on three sides. Even though they were designed as if supported only by the counterforts, they develop moments where they join. The resulting tension in and near the reentrant corner should be provided for by bars *f*.

The question of reinforcing bar details, always important, is particularly so for corners subject to substantial bending moments, such as are present for both cantilever and counterfort retaining walls. Valuable suggestions are found in Ref. 17.9.

17.10 PRECAST RETAINING WALLS

Largely because of the high cost of forming cast-in-place retaining walls, there has been increasing use in recent years of various forms of precast concrete walls. Sections can be mass produced under controlled factory conditions using standardized forms, with excellent quality control. On-site construction time is greatly reduced, and

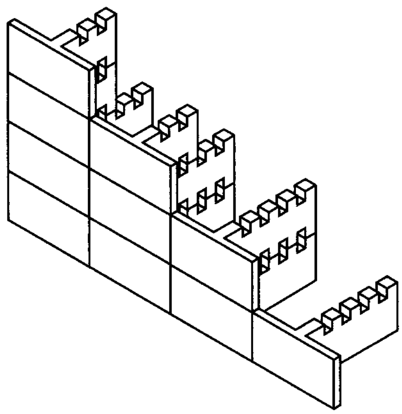

FIGURE 17.9
Precast T-Wall® retaining wall system. *(Courtesy Concrete Systems Inc., Hudson, New Hampshire.)*

generally only a small crew using light equipment is required. Weather becomes much less of a factor in completion of the work than for cast-in-place walls.

One type of precast wall is shown in Fig. 17.9. Precast T sections are used, each 2.5 ft high and 5 ft wide, with T stems varying according to requirements from 4 ft to 20 ft. Individual units are stacked, using shear keys in the space created where teeth of a top and bottom unit come together, at approximately a 6 ft spacing perpendicular to the face of the wall. Calculations for stability against sliding and overturning and for bearing pressures are the same as for cast-in-place cantilever or counterfort walls, with stability provided by the combined weight of the concrete wall and compacted select backfill. Such walls can be constructed with vertical face or battered section, with heights up to 25 ft.

Walls of the type shown have been used for highways, parking lots, commercial and industrial sites, bank stabilization, wing walls, and similar purposes.

References

17.1. R. B. Peck, W. E. Hanson, and T. H. Thornburn, *Foundation Engineering*, 2nd ed., John Wiley & Sons, Inc., New York, 1974.

17.2. K. Terzaghi, R. B. Peck, and G. Mesri, *Soil Mechanics in Engineering Practice*, 3rd ed., John Wiley & Sons, Inc., New York, 1996.

17.3. W. C. Huntington, *Earth Pressures and Retaining Walls*, John Wiley & Sons, Inc., New York, 1957.

17.4. *AASHTO LRFD Bridge Design Specifications*, 4th ed., American Association of State Highway and Transportation Officials (AASHTO), Washington, DC, 2008.

17.5. *Manual for Railway Engineering*, American Railway Engineering and Maintenance of Way Association (AREMA), Landover, MD, 2008.

17.6. *CRSI Design Handbook*, 10th ed., Concrete Reinforcing Steel Institute, Shaumburg, IL, 2008.

17.7. M. Fintel, *Handbook of Concrete Engineering*, 2nd ed., Van Nostrand Reinhold Co., New York, 1985.

17.8. *Rectangular Concrete Tanks*, Publication No. IS003, Portland Cement Association, Skokie, IL, 1998.

17.9. I. H. E. Nilsson and A. Losberg, "Reinforced-Concrete Corners and Joints Subjected to Bending Moment," *J. Struct. Div.*, ASCE, vol. 102, no. ST6, 1976, pp. 1229–1254.

Problems

17.1. A cantilever retaining wall is to be designed with geometry as indicated in Fig. P17.1. Backfill material will be well-drained gravel having unit weight $w = 120$ pcf, internal friction angle $\phi = 33°$, and friction factor against the concrete base $f = 0.55$. Backfill placed in front of the toe will have the same properties and will be well compacted. The final grade behind the wall will be level with the top of the wall, with no surcharge. At the lower level, it will be 3 ft above the top of the base slab. To improve sliding resistance, a key will be used, tentatively projecting to a depth 4 ft below the top of the base slab. (This dimension may be modified if necessary.)

(*a*) Based on a stability investigation, select wall geometry suitable for the specified conditions. For a first trial, place the outer face of the wall $\frac{1}{3}$ the width of the base slab back from the toe.

(*b*) Prepare the complete structural design, specifying size, placement, and cutoff points for all reinforcement. Materials have strengths $f_c' = 4000$ psi and $f_y = 60{,}000$ psi. Allowable soil bearing pressure is 5000 psf.

FIGURE P17.1

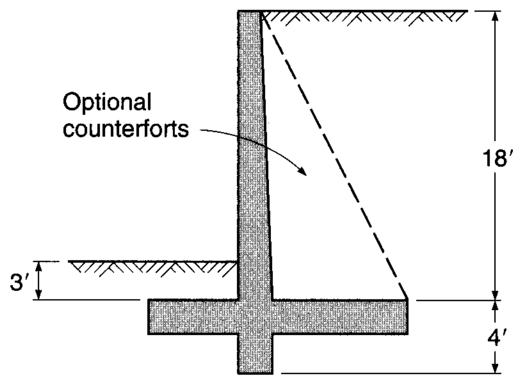

17.2. Redesign the wall of Problem 17.1 as a counterfort retaining wall. Counterforts are tentatively spaced 12 ft on centers, although this may be modified if desirable. Include all reinforcement details, including reinforcement in the counterforts.

18 Concrete Building Systems

18.1 INTRODUCTION

Most of the material in the preceding chapters has pertained to the design of reinforced concrete *structural elements*, e.g., slabs, columns, beams, and footings. These elements are combined in various ways to create *structural systems* for buildings and other construction. An important part of the total responsibility of the structural engineer is to select, from many alternatives, the best structural system for the given conditions. The wise choice of structural system is far more important, in its effect on overall economy and serviceability, than refinements in proportioning the individual members. Close cooperation with the architect in the early stages of a project is essential in developing a structure that not only meets functional and esthetic requirements but exploits to the fullest the special advantages of reinforced concrete, which include the following:

Versatility of form. Usually placed in the structure in the fluid state, the material is readily adaptable to a wide variety of architectural and functional requirements.

Durability. With proper concrete protection of the steel reinforcement, the structure will have long life, even under highly adverse climatic or environmental conditions.

Fire resistance. With proper protection for the reinforcement, a reinforced concrete structure provides the maximum in fire protection.†

Speed of construction. In terms of the entire period, from the date of approval of the contract drawings to the date of completion, a concrete building can often be completed in less time than a steel structure. Although the field erection of a steel building is more rapid, this phase must necessarily be preceded by prefabrication of all parts in the shop.

Cost. In many cases the first cost of a concrete structure is less than that of a comparable steel structure. In almost every case, maintenance costs are less.

Availability of labor and material. It is always possible to make use of local sources of labor, and in many inaccessible areas, a nearby source of good aggregate can be found, so that only the cement and reinforcement need to be brought in from a remote source.

Two record-setting examples of good building design in concrete are shown in Figs. 18.1 and 18.2.

† Code requirements for fire protection are presented in Ref. 18.1.

FIGURE 18.1
View of 311 South Wacker Drive under construction. When completed, it was the world's tallest concrete building, with total height of 946 ft. (*Courtesy of Portland Cement Association.*)

18.2 FLOOR AND ROOF SYSTEMS

The types of concrete floor and roof systems are so numerous as to defy concise classification. In steel construction, the designer usually is limited to using structural shapes that have been standardized in form and size by the relatively few producers in the field. In reinforced concrete, on the other hand, the engineer has almost complete control over the form of the structural parts of a building. In addition, many small producers of reinforced concrete structural elements and accessories can compete profitably in this field, since plant and equipment requirements are not excessive. This has resulted in the development of a wide variety of concrete systems. Only the more common types can be mentioned in this text.

In general, reinforced concrete floor and roof systems can be classified as one-way systems, in which the main reinforcement in each structural element runs in one direction only, and two-way systems, in which the main reinforcement in at least one of the structural elements runs in perpendicular directions. Systems of each type can be identified in the following list:

(a) One-way slab supported by monolithic concrete beams
(b) One-way slab supported by steel beams (shear connectors are used for composite action in the direction of the beam span)

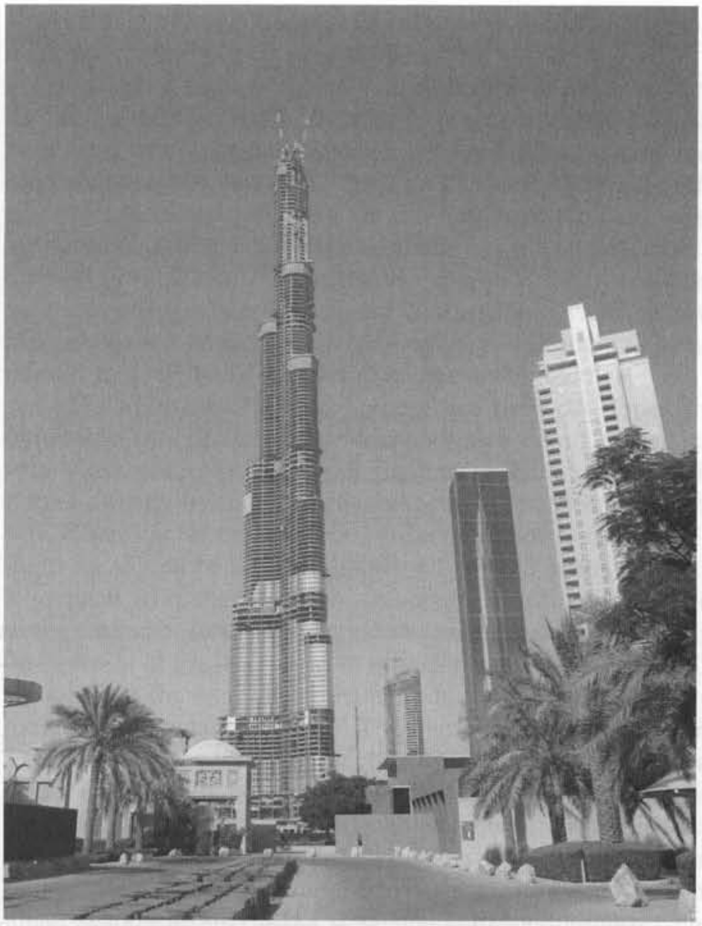

FIGURE 18.2
The Burg Dubai, shown under construction, is the current record holder, not only as the tallest reinforced concrete building, but also as the tallest structure of any type in the world, with a total height in excess of 2100 ft. (*Burg Dubai, designed by and copyright to Skidmore, Owings and Merrill LLP.*)

(c) One-way slab with cold-formed steel decking as form and reinforcement
(d) One-way joist floor (also known as ribbed slab)
(e) Two-way slab supported by edge beams for each panel
(f) Flat slabs, with column capitals or drop panels or both, but without beams
(g) Flat plates, without beams and with no drop panels or column capitals
(h) Two-way joist floors, with or without beams on the column lines

Each of these types will be described briefly in the following sections. Additional information will be found in Refs. 18.2 to 18.4. In addition to the cast-in-place floor and roof systems described in this section, a great variety of precast concrete systems have been devised. Some of these will be described in Section 18.5.

a. Monolithic Beam-and-Girder Floors

A beam-and-girder floor consists of a series of parallel beams supported at their extremities by girders, which in turn frame into concrete columns placed at more or less regular intervals over the entire floor area, as shown in Fig. 18.3. This framework is covered by a one-way reinforced concrete slab, the load from which is transmitted first to the beams and then to the girders and columns. The beams are usually spaced so that they come at the midpoints, at the third points, or at the quarter points of the

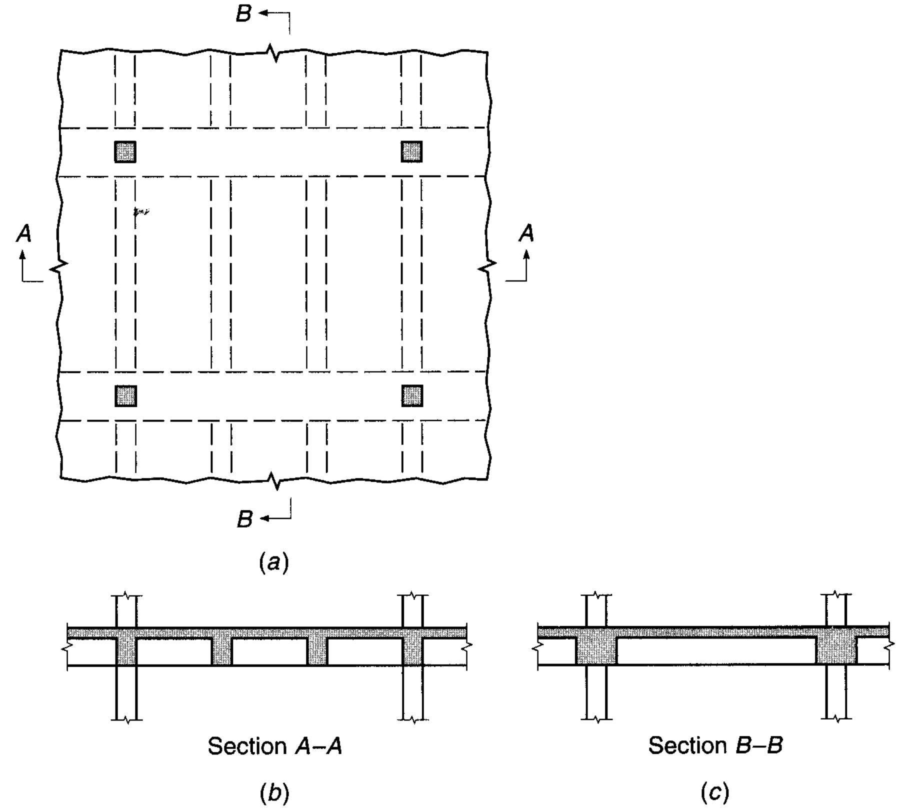

FIGURE 18.3
Framing of beam-and-girder floor: (*a*) plan view; (*b*) section through beams; (*c*) section through girders.

girders. The arrangement of beams and spacing of columns should be determined by economical and practical considerations. These will be affected by the use to which the building is to be put, the size and shape of the ground area, and the load that must be carried. A comparison of a number of trial designs and estimates should be made if the size of the building warrants, and the most satisfactory arrangement selected. If the spans in one direction are not long, say 20 ft or less, the beams may be omitted altogether, and the slab, spanning in one direction, can be carried directly by girders spanning in the perpendicular direction on the column lines. Since the slabs, beams, and girders are built monolithically, the beams and girders are designed as T beams and advantage is taken of continuity.

Beam-and-girder floors are adapted to any loads and to any spans that might be encountered in ordinary building construction. The normal maximum spread in live load values is from 40 to 400 psf, and the normal range in column spacings is from 16 to 32 ft.

The design and detailing of the joints where beams or girders frame into building columns should be given careful consideration, particularly for designs in which substantial horizontal loads are to be resisted by frame action of the building. In this case, the column region, within the depth of the beams framing into it, is subjected to significant horizontal shears as well as to axial and flexural loads. Special horizontal column ties must be included to avoid uncontrolled diagonal cracking and disintegration of the concrete, particularly if the joint is subjected to load reversals. Specific recommendations for the design of beam-column joints are found in Chapter 11 and

Ref. 18.5. Joint design for buildings that resist seismic forces is subject to special ACI Code provisions (see Chapter 20).

In normal beam-and-girder construction, the depth of the beams may be as much as 3 times the web width. Improved economy, however, is achieved by using beams with webs that are generally wider and shallower, coupled with girders that have the same depth as the beams. The resulting girders, more often than not, have webs that are wider than their effective depths. Although the flexural steel in the members is increased because of the reduced effective depth compared with deeper members, the increases in material costs are more than paid for by savings in forming costs (one depth for all members) and easier construction (wider beams are easier to cast than narrow beams). Another key advantage is the reduced construction depth, which permits a reduction in the overall height of the building.

For light loads, a floor system has been developed in which the beams are omitted in one direction, the one-way slab being carried directly by column-line beams that are very broad and shallow, as shown in Fig. 18.4. These beams, supported directly by the columns, become little more than a thickened portion of the slab. This type of construction, in fact, is known as *banded slab construction,* and there are a number of advantages associated with its use, over and above those associated with shallow beam-and-girder construction. In the direction of the slab span, a haunched member is present, in effect, with the maximum effective depth at the location of greatest negative moment, across the support lines. Negative moments are small at the edge of the haunch, but the depth becomes less, and positive slab moments are reduced as well. The increased flexural steel in the beam (slab-band) resulting from the reduced effective depth is often outweighed by savings in the slab steel. Along with reduced construction depth, banded slab construction allows greater flexibility in locating columns, which may be displaced some distance from the centerline of the slab-band without significantly changing the structural action of the floor. Formwork is simplified because of the reduction in the number of framing members. For such systems, special attention should be given to design details at the beam-column joint. Transverse top steel may be required to distribute the column reaction over the width of the slab-band. In addition, punching shear failure is possible; this may be investigated using the same methods presented earlier for flat plates (see Section 13.10).

b. Composite Construction with Steel Beams

One-way reinforced concrete slabs are also frequently used in buildings for which the columns, beams, and girders consist of structural steel. The slab is normally designed for full continuity over the supporting beams, and the usual methods are followed. The spacing of the beams is usually 6 to 8 ft.

To provide composite action, shear connectors are welded to the top of the steel beam and are embedded in the concrete slab, as shown in Fig. 18.5*a*. By preventing longitudinal slip between the slab and steel beam in the direction of the beam axis, the combined member is both stronger and stiffer than if composite action were not developed. Thus, for given loads and deflection limits, smaller and lighter steel beams can be used.

Composite floors may also use encased beams, as shown in Fig. 18.5*b*, offering the advantage of full fireproofing of the steel, but at the cost of more complicated formwork and possible difficulty in placing the concrete around and under the steel member. Such fully encased beams do not require shear connectors as a rule.

FIGURE 18.4
Banded slab floor system.

(*a*) Interior slab band

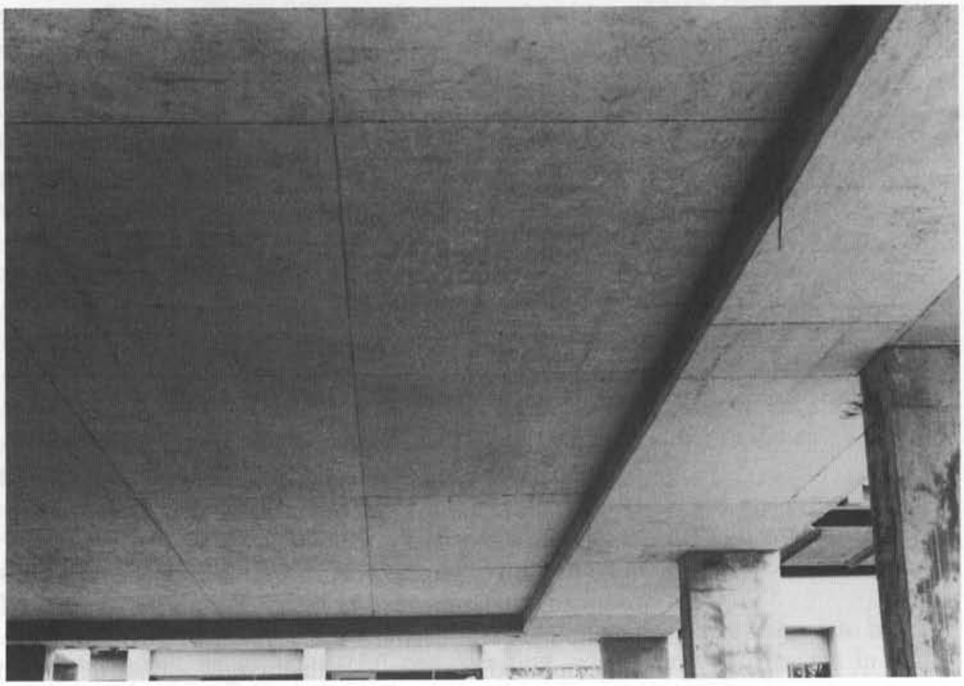

(*b*) Edge band at exterior column

c. Steel Deck Reinforced Composite Slabs

It is nearly standard practice to use stay-in-place light-gage cold-formed steel deck panels in composite floor construction. As shown in Fig. 18.5*c*, the steel deck serves as a stay-in-place form and, with suitable detailing, the slab becomes composite with

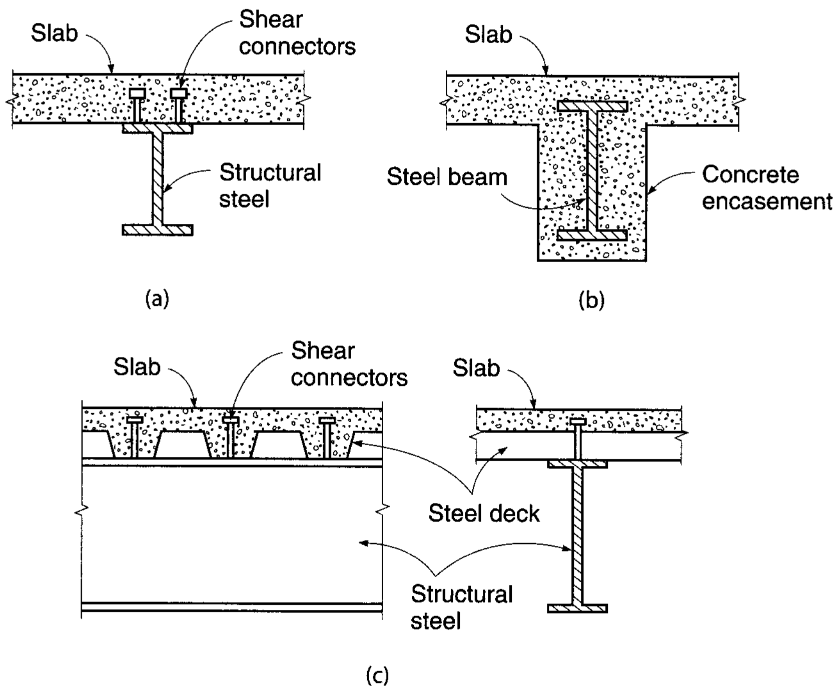

FIGURE 18.5
Composite beam-and-slab floor.

the steel deck, serving as the main tensile flexural steel. Suitable for relatively light floor loading and short spans, composite steel deck reinforced slabs are found in office buildings and apartment buildings, with column-line girders and beams in the perpendicular direction subdividing panels into spans up to about 12 ft. Temporary shoring may be used at the midspan or third point of the panels to avoid excessive stresses and deflections while the concrete is placed, when the steel deck panel alone must carry the load.

d. One-Way Joist Floors

A one-way joist floor consists of a series of small, closely spaced reinforced concrete T beams, framing into monolithically cast concrete girders, which are in turn carried by the building columns. The T beams, called *joists*, are formed by creating void spaces in what otherwise would be a solid slab. Usually these voids are formed using special steel pans, as shown in Fig. 18.6. Concrete is cast between the forms to create ribs, and placed to a depth over the top of the forms so as to create a thin monolithic slab that becomes the T beam flange.

Since the strength of concrete in tension is small and is commonly neglected in design, elimination of much of the tension concrete in a slab by the use of pan forms results in a saving of weight with little change in the structural characteristics of the slab. Ribbed floors are economical for buildings, such as apartment houses, hotels, and hospitals, where the live loads are fairly small and the spans comparatively long. They are not suitable for heavy construction such as in warehouses, printing plants, and heavy manufacturing buildings.

Standard forms for the void spaces between ribs are either 20 or 30 in. wide and 8, 10, 12, 14, 16, or 20 in. deep. They are tapered in cross section, as shown in Fig. 18.7, generally at a slope of 1 to 12, to facilitate removal. Any joist width can be

FIGURE 18.6
Steel forms for one-way joist floor.

obtained by varying the width of the soffit (bottom) form. Tapered end pans are used where it is desired to obtain a wider joist near the end supports, such as may be required for high shear or negative bending moment. After the concrete has hardened, the steel pans are removed for reuse.

According to ACI Code 8.13.2, ribs must not be less than 4 in. wide and may not have a depth greater than 3.5 times the minimum web width. (For easier bar placement and placement of concrete, a minimum web width of 5 in. is desirable.) The clear spacing between ribs (determined by the pan width) must not exceed 30 in. The slab thickness over the top of the pans must not be less than one-twelfth of the clear distance between ribs, nor less than 2 in., according to ACI Code 8.13.6. Table 18.1 gives unit weights, in terms of psf of floor surface, for common combinations of joist width and depth, slab thickness, and form width.

Reinforcement for the joists usually consists of two bars in the positive bending region, with one bar discontinued where no longer needed or bent up to provide

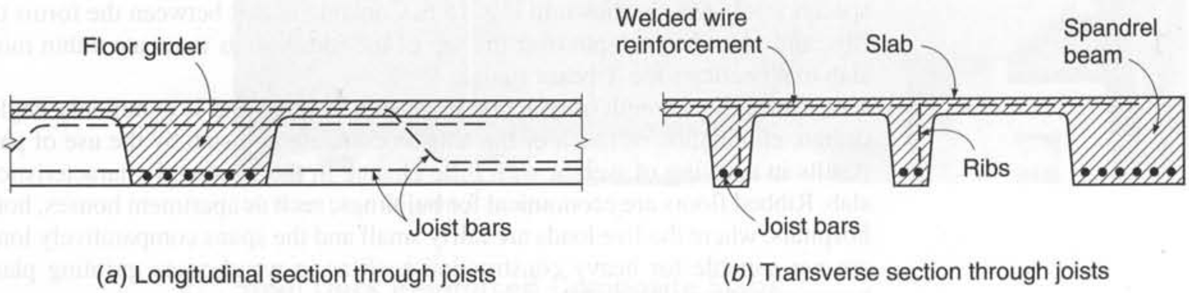

FIGURE 18.7
One-way joist floor cross sections: (*a*) cross section through supporting girder showing ends of joists; (*b*) cross section through typical joists.

TABLE 18.1
Weight of one-way joist floor systems

3 in. Top Slab			$4\frac{1}{2}$ in. Top Slab		
Depth of Pan Form, in.	Width of Joist + Pan Form, in.	Weight, psf	Depth of Pan Form, in.	Width of Joist + Pan Form, in.	Weight, psf
8	5 + 20	60	8	5 + 20	79
8	5 + 30	54	8	5 + 30	72
10	5 + 20	67	10	5 + 20	85
10	5 + 30	58	10	5 + 30	77
12	5 + 20	74	12	5 + 20	92
12	5 + 30	63	12	5 + 30	82
14	5 + 30	68	14	5 + 30	87
14	6 + 30	72	14	6 + 30	91
16	6 + 30	78	16	6 + 30	97
16	7 + 30	83	16	7 + 30	101
20	6 + 30	91	20	6 + 30	109
20	7 + 30	96	20	7 + 30	115

Source: Adapted from Ref. 18.3.

a part of the negative steel requirement over the supporting girders. Straight top bars are added over the support to provide for the negative bending moment. According to ACI Code 7.13.2, at least one bottom bar must be continuous over the support, or at noncontinuous supports, terminated with a standard hook or headed bar, as a measure to improve structural integrity in the event of major structural damage.

ACI Code 7.7.1 permits a reduced concrete cover of $\frac{3}{4}$ in. to be used for joist construction, just as for slabs. The thin slab (top flange) is reinforced mainly for temperature and shrinkage stresses, using welded wire reinforcement or small bars placed at right angles to the joists. The area of this reinforcement is usually 0.18 percent of the gross cross section of the concrete slab.

One-way joists are generally proportioned with the concrete providing all of the shear strength, with no stirrups used. A 10 percent increase in V_c above the value given by Eq. (4.12*a*) or (4.12*b*) is permitted for joist construction, according to ACI Code 8.13.8, based on the possibility of redistribution of local overloads to adjacent joists. Tests have shown that while local redistribution does occur, the shear strength of the full system (all joists acting together) is enhanced by less than 10 percent (Ref. 18.6).

The joists and the supporting girders are placed monolithically. Like the joists, the girders are designed as T beams. The shape of the girder cross section depends on the shape of the end pans that form the joists, as shown in Fig. 18.7*a*. If the girders are deeper than the joists, the thin concrete slab directly over the top of the pans is often neglected in the girder design. The girder width can be adjusted, as needed, by varying the placement of the end pans. The width of the web below the bottom of the joists must be at least 3 in. narrower than the flange (on either side) to allow for pan removal.

A type of one-way joist floor system has evolved known as a *joist-band system* in which the joists are supported by broad girders having the same total depth as the joists, as illustrated in Fig. 18.7. Separate beam forms are eliminated, and the same deck forms the soffit of both the joists and the girders. The simplified formwork, faster construction, level ceiling with no obstructing beams, and reduced overall height of walls, columns, and vertical utilities combine to achieve an overall reduction in cost in most cases.

In one-way joist floors, the thickness of the slab is often controlled by fire resistance requirements. For a rating of 2 hours, for example, the slab must be about $4\frac{1}{2}$ in. thick (Ref. 18.1). If 20 or 30 in. pan forms are used, slab span is small and slab strength is underutilized. This has led to what is known as the *wide module joist system*, or *skip joist system* (Ref. 18.7). Such floors generally have 6 to 8 in. wide ribs that are 5 to 6 ft on centers, with a $4\frac{1}{2}$ in. top slab. These floors not only provide more efficient use of concrete in the slab, but also require less formwork labor. By ACI Code 8.13.4, wide module joist ribs must be designed as ordinary T beams, because the clear spacing between ribs exceeds the 30 in. maximum for joist construction, and the special ACI Code provisions for joists do not apply. Concrete cover for reinforcement is as required for beams, not joists, and the 10 percent increase in V_c does not apply. Often the joists in wide module systems are carried by wide beams on the column lines, the depth of which is the same as that of the joists, to form a joist-band system equivalent to that described earlier.

Useful design information pertaining to one-way joist floors, including extensive load tables, will be found in the *CRSI Design Handbook* (Ref. 18.3). Suggested bar details and typical design drawings are found in the *ACI Detailing Manual* (Ref. 18.4).

e. Two-Way Edge-Supported Slabs

Two-way solid slabs supported by beams on the column lines on all sides of each slab panel have been discussed in detail in Chapter 13. The perimeter beams are usually concrete cast monolithically with the slab, although they may also be structural steel, often encased in concrete for composite action and for improved fire resistance. For monolithic concrete, both the beams and the slabs are designed using the direct design method or the equivalent frame method described in Chapter 13.

Two-way solid slab systems are suitable for intermediate to heavy loads on spans up to about 30 ft. This range corresponds closely to that for beamless slabs with drop panels and column capitals, described in the following section. The latter are often preferred because of the complete elimination of obstructing beams below the slab.

For lighter loads and shorter spans, a two-way solid slab system has evolved in which the column-line beams are wide and shallow, such that a cross section through the floor in either direction resembles the slab-band shown earlier in Fig. 18.4. The result is a two-way slab-band floor that, from below, appears as a paneled ceiling. Advantages are similar to those given earlier for one-way slab-band floors and for joist-band systems.

f. Beamless Flat Slabs with Drop Panels or Column Capitals

By suitably proportioning and reinforcing the slab, it is possible to eliminate supporting beams altogether. The slab is supported directly on the columns. In a rectangular or square region centered on the columns, the slab may be thickened and the column tops flared, as shown in Fig. 18.8. The thickened slab is termed a *drop panel*, and the column flare is referred to as a *column capital*. Both of these serve a double purpose: they increase the shear strength of the floor system in the critical region around the column, and they provide increased effective depth for the flexural steel in the region

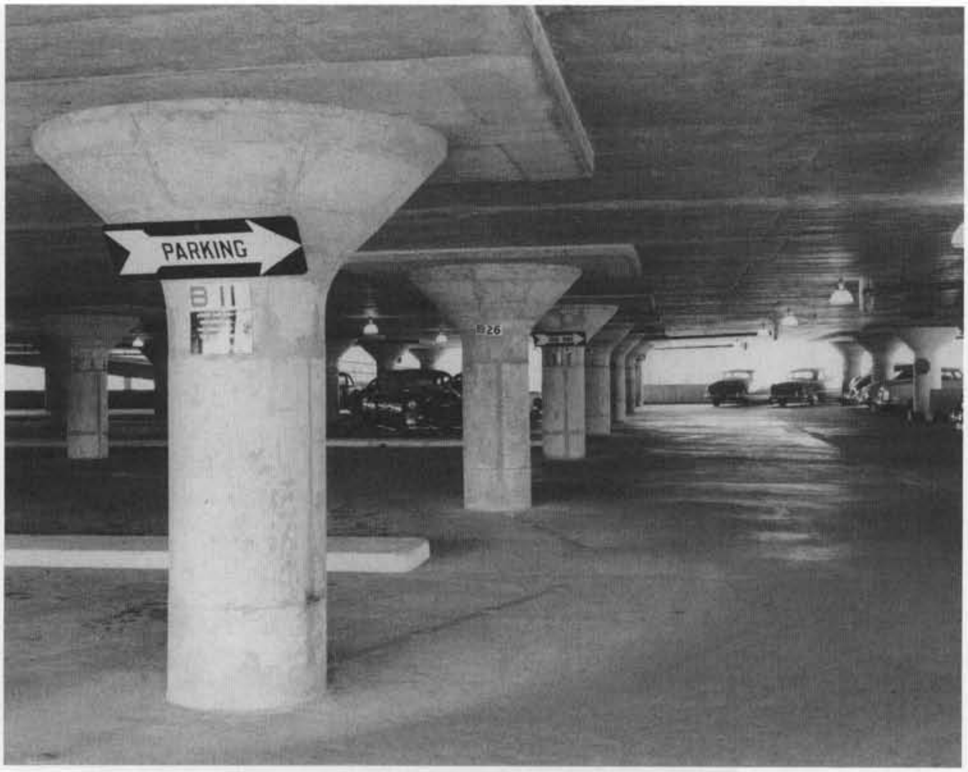

FIGURE 18.8
Flat slab garage floor with both drop panels and column capitals. (*Courtesy of Portland Cement Association.*)

of high negative bending moment over the support. Beamless systems with drop panels or column capitals or both are termed *flat slab systems* (although almost all slabs in structural engineering practice are "flat" in the usual sense of the word), and are differentiated from flat plate systems, with absolutely no projections below the slab, which are described in the following section.

In general, flat slab construction is economical for live loads of 100 psf or more and for spans up to about 30 ft. It is widely used for storage warehouses, parking garages, and below-grade structures carrying heavy earth-fill loads, for example. For lighter loads such as in apartment houses, hotels, and office buildings, flat plates (Section 18.2g) or some form of joist construction (Sections 18.2d and h) will usually prove less expensive. For spans longer than about 30 ft, beams and girders are used because of the greater stiffness of that form of construction.

Flat slabs may be designed by the direct design method or the equivalent frame method, both described in detail in Chapter 13, or the strip method described in Chapter 15.

g. Flat Plate Slabs

A flat plate floor is essentially a flat slab floor with the drop panels and column capitals omitted, so that a floor of uniform thickness is carried directly by prismatic columns. Flat plate floors have been found to be economical and otherwise advantageous for such uses as apartment buildings, as shown in Fig. 18.9, where the spans are moderate (up to about 30 ft) and loads relatively light. Prestressed concrete (Chapter 19) flat plate construction for residential and light commercial buildings has

FIGURE 18.9
Flat plate floor construction. (*Courtesy of Portland Cement Association.*)

spans up to 40 ft. The construction depth for each floor is held to the absolute minimum, with resultant savings in the overall height of the building. The smooth underside of the slab can be painted directly and left exposed for ceiling, or plaster can be applied to the concrete. Minimum construction time and low labor costs result from the very simple formwork.

Certain problems associated with flat plate construction require special attention. Shear stresses near the columns may be very high, requiring the use of special types of slab reinforcement there. The transfer of moments from slab to columns may further increase these shear stresses and requires concentration of negative flexural steel in the region close to the columns. Both these problems are treated in detail in Chapter 13. At the exterior columns, where such shear and moment transfer may cause particular difficulty, the design is much improved by extending the slab past the column in a short cantilever.

Some flat plate buildings are constructed by the lift slab method, shown in Fig. 18.10. A casting bed (often doubling as the ground-floor slab) is placed, steel columns are erected and braced, and at ground level successive slabs, which will later become the upper floors, are cast. A membrane or sprayed parting agent is laid down between successive pours so that each slab can be lifted in its turn, starting with the top. Jacks placed atop the columns are connected to threaded rods extending down the faces of the columns and connecting, in turn, to lifting collars embedded in the slabs, as shown in Fig. 13.24*d*. When a slab is in its final position, shear plates are welded to the column below the lifting collar, or other devices are used to transfer the vertical slab reaction. Lifting collars such as those shown in Fig. 13.24*d*, in addition to providing anchorage for the lifting rods, serve to increase the effective size of the support for the slab and consequently improve the shear strength of the

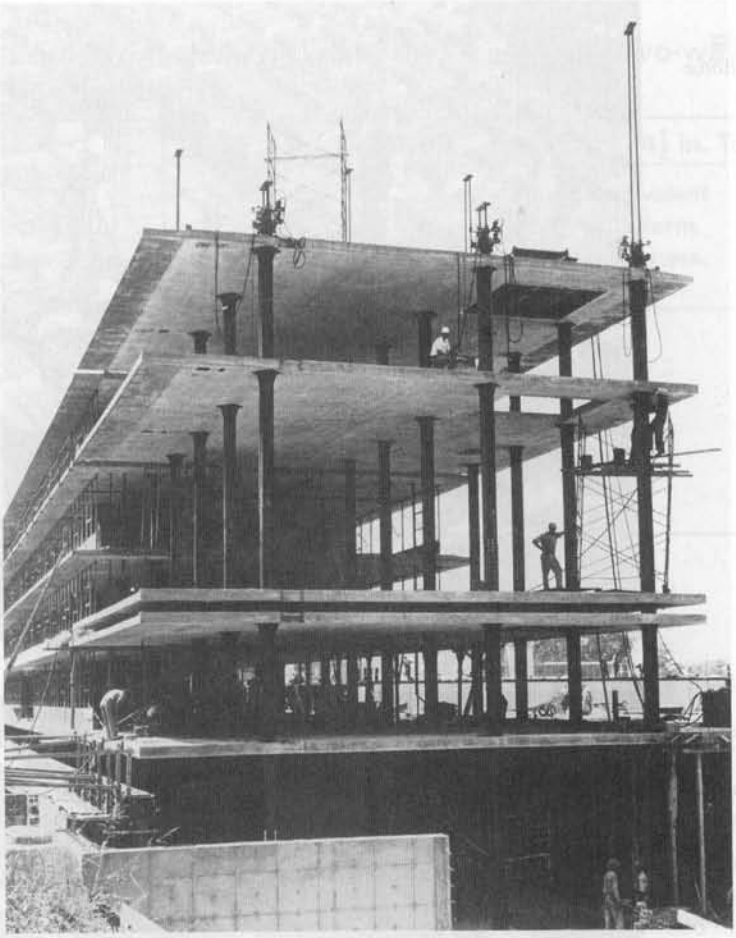

FIGURE 18.10
Lift slab construction used with flat plate floors; student dormitory at Clemson University, South Carolina.

slab. The successful erection of structures using the lift slab method requires precise control of the lifting operation at all times, because even slight differences in level of the support collars may drastically change moments and shears in the slab, possibly leading to reversal of loading. Catastrophic accidents have resulted from failure to observe proper care in lifting or to provide adequate lateral bracing for the columns (Ref. 18.8). As a result of these accidents, this method of construction is used only by specialized contractors.

h. Two-Way Joist Floors

As in one-way floor systems, the dead weight of two-way slabs can be reduced considerably by creating void spaces in what would otherwise be a solid slab. For the most part, the concrete removed is in tension and ineffective, so the lighter floor has virtually the same structural characteristics as the corresponding solid floor. Voids are usually formed using dome-shaped steel pans that are removed for reuse after the slab has hardened. Forms are placed on a plywood platform as shown in Fig. 18.11. Note in the figure that domes have been omitted near the columns to obtain a solid slab in the region of negative bending moment and high shear. The lower flange of each dome contacts that of the adjacent dome, so that the concrete

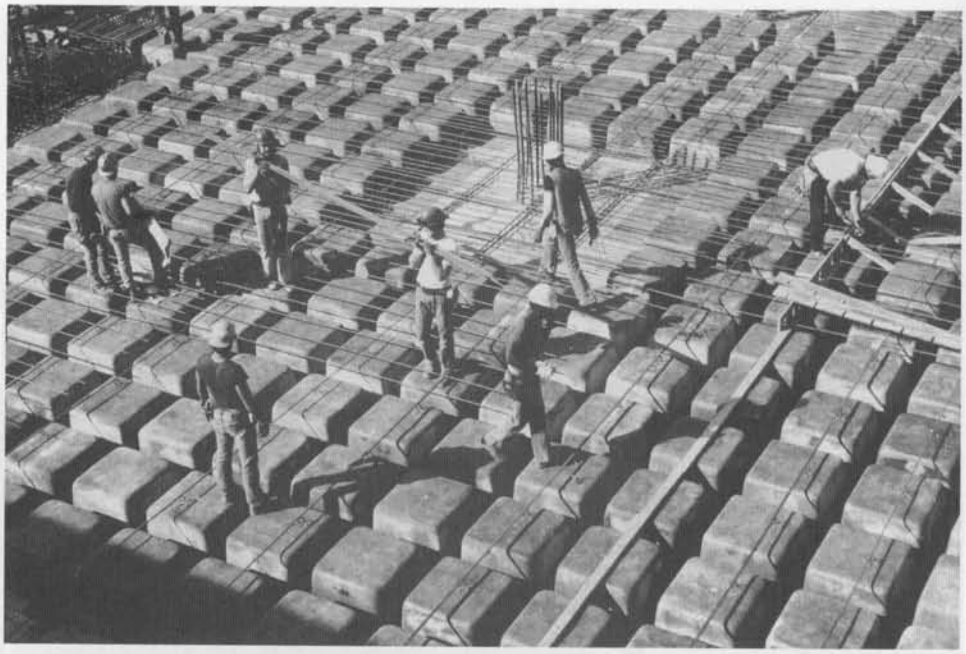

FIGURE 18.11
Two-way joist floor under construction with steel dome forms. (*Courtesy of Ceco Corporation.*)

FIGURE 18.12
Regency House Apartments, San Antonio, with cantilevered two-way joist slab plus integral beams on column lines.

is cast entirely against a metal surface, resulting in an excellent finished appearance of the slab. A wafflelike appearance (these slabs are sometimes called waffle slabs) is imparted to the underside of the slab, which can be featured to architectural advantage, as shown in Fig. 18.12.

TABLE 18.2
Equivalent slab thickness and weight of two-way joist floor systems

Depth of Pan Form, in.	3 in. Top Slab: Equivalent Uniform Thickness, in.	3 in. Top Slab: Weight, psf	$4\frac{1}{2}$ in. Top Slab: Equivalent Uniform Thickness, in.	$4\frac{1}{2}$ in. Top Slab: Weight, psf
36 in. Module (30 in. pans plus 6 in. ribs)				
8	5.7	71	7.2	90
10	6.4	80	7.9	99
12	7.2	90	8.7	109
14	8.0	100	9.5	119
16	8.9	111	10.3	129
20	10.6	132	12.1	151
24 in. Module (19 in. pans plus 5 in. ribs)				
8	6.3	79	7.8	98
10	7.3	91	8.8	110
12	8.2	103	9.8	122
14	9.3	116	10.7	134
16	10.3	129	11.8	148

Source: Adapted from Ref. 18.3.

Two-way joist floors are designed following the usual procedures for two-way solid slab systems, as presented in Chapter 13, with the solid regions at the columns considered as drop panels. Joists in each direction are divided into column strip joists and middle strip joists, the former including all joists that frame into the solid head. Each joist rib usually includes two bars for positive-moment resistance, and one may be discontinued where no longer required. Negative steel is provided by separate straight bars running in each direction over the columns.

In design calculations, the self-weight of two-way joist floors is considered to be uniformly distributed, based on an equivalent slab of uniform thickness having the same volume of concrete as the actual ribbed slab. Equivalent thicknesses and weights are given in Table 18.2 for standard 30 and 19 in. pans of various depths and for either a 3 in. top slab or $4\frac{1}{2}$ in. top slab, based on normalweight concrete (150 lb/ft^3).

18.3 PANEL, CURTAIN, AND BEARING WALLS

As a general rule, the exterior walls of a reinforced concrete building are supported at each floor by the skeleton framework, their only function being to enclose the building. Such walls are called *panel walls*. They may be made of concrete (often precast), concrete block, brick, tile blocks, or insulated metal panels. The latter may be faced with aluminum, stainless steel, or a porcelain-enamel finish over steel, backed by insulating material and an inner surface sheathing. The thickness of each of these types of panel walls will vary according to the material, type of construction, climatological conditions, and the building requirements governing the particular locality in which the construction takes place.

The pressure of the wind is usually the only load that is considered in determining the structural thickness of a wall panel, although in some cases exterior walls are used as diaphragms to transmit forces caused by horizontal loads down to the building foundations.

Curtain walls are similar to panel walls except that they are not supported at each story by the frame of the building, but are self-supporting. However, they are often anchored to the building frame at each floor to provide lateral support.

A *bearing wall* may be defined as one that carries any vertical load in addition to its own weight. Such walls may be constructed of stone masonry, brick, concrete block, or reinforced concrete. Occasional projections or pilasters add to the strength of the wall and are often used at points of load concentration. In small commercial buildings, bearing walls may be used with economy and expediency. In larger commercial and manufacturing buildings, when the element of time is an important factor, the delay necessary for the erection of the bearing wall and the attendant increased cost of construction often dictate the use of some other arrangement.

18.4 SHEAR WALLS

Horizontal forces acting on buildings, e.g., those due to wind or seismic action, can be resisted by different means. Rigid-frame resistance of the structure, augmented by the contribution of ordinary masonry walls and partitions, can provide for wind loads in many cases. However, when heavy horizontal loading is likely, such as would result from an earthquake, reinforced concrete shear walls are used. These may be added solely to resist horizontal forces, or concrete walls enclosing stairways or elevator shafts may also serve as shear walls.

Figure 18.13 shows a building with wind or seismic forces represented by arrows acting on the edge of each floor or roof. The horizontal surfaces act as deep beams to transmit loads to vertical resisting elements *A* and *B*. These shear walls, in turn, act as cantilever beams fixed at their base to carry loads down to the foundation. They are

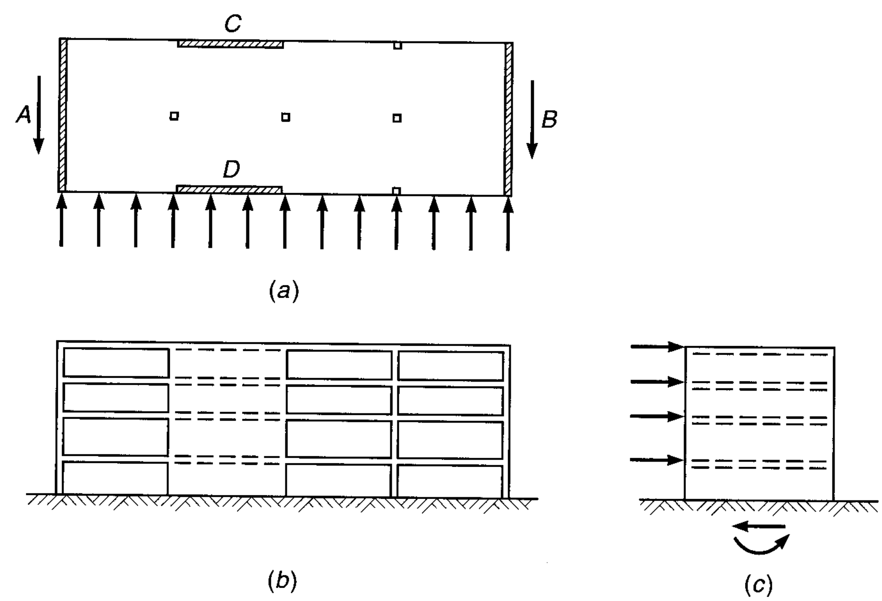

FIGURE 18.13
Building with shear walls subject to horizontal loads: (*a*) typical floor; (*b*) front elevation; (*c*) end elevation.

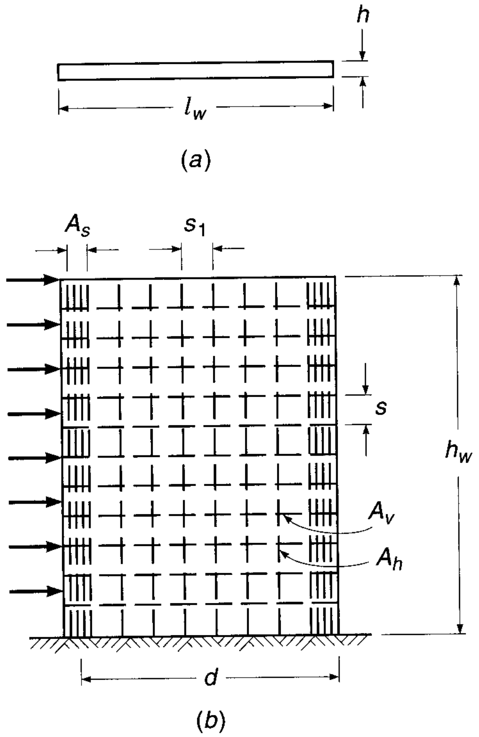

FIGURE 18.14
Geometry and reinforcement of a typical shear wall: (*a*) cross section; (*b*) elevation.

subjected to (1) a variable shear, which reaches a maximum at the base; (2) a bending moment, which tends to cause vertical tension near the loaded edge and compression at the far edge; and (3) a vertical compression due to ordinary gravity loading from the structure. For the building shown, additional shear walls *C* and *D* are provided to resist loads acting in the long direction of the structure.

Shear is apt to be critical for walls with a relatively low ratio of height to length. High shear walls are controlled mainly by flexural requirements.

Figure 18.14 shows a typical shear wall with height h_w, length l_w, and thickness h. It is assumed to be fixed at its base and loaded horizontally along its left edge. Vertical flexural reinforcement of area A_s is provided at the left edge, with its centroid a distance d from the extreme compression face. To allow for reversal of load, identical reinforcement is provided along the right edge. Horizontal shear reinforcement with area A_v at spacing s is provided, as well as vertical shear reinforcement with area A_h at spacing s_1. Such distributed steel is normally placed in two layers, parallel to the faces of the wall.

The design basis for shear walls, according to ACI Code 11.9, is of the same general form as that used for ordinary beams:

$$V_u \leq \phi V_n \tag{18.1}$$

where

$$V_n = V_c + V_s \tag{18.2}$$

Based on tests (Refs. 18.9 and 18.10), an upper limit has been established on the nominal shear strength of walls:

$$V_n \leq 10\lambda\sqrt{f'_c}\, hd \tag{18.3}$$

where λ is the lightweight concrete strength modification factor (see Section 4.5a). In this and all other equations pertaining to the design of shear walls, the distance d is taken equal to $0.8l_w$. A larger value of d, equal to the distance from the extreme compression face to the center of force of all reinforcement in tension, may be used when determined by a strain compatibility analysis.

The value of V_c, the nominal shear strength provided by the concrete, may be based on the usual equations for beams, according to ACI Code 11.9.5. For walls subject to vertical compression,

$$V_c = 2\lambda\sqrt{f'_c}\,hd \tag{18.4}$$

and for walls subject to vertical tension N_u,

$$V_c = 2\left(1 + \frac{N_u}{500A_g}\right)\lambda\sqrt{f'_c}\,hd \tag{18.5}$$

Here, N_u is the factored axial load in pounds, taken negative for tension, and A_g is the gross area of horizontal concrete section in square inches. Alternately, the value of V_c may be based on a more detailed calculation, as the lesser of

$$V_c = 3.3\lambda\sqrt{f'_c}\,hd + \frac{N_u d}{4l_w} \tag{18.6}$$

or

$$V_c = \left[0.6\lambda\sqrt{f'_c} + \frac{l_w(1.25\lambda\sqrt{f'_c} + 0.2N_u/l_w h)}{M_u/V_u - l_w/2}\right]hd \tag{18.7}$$

where N_u is negative for tension as before. Equation (18.6) corresponds to the occurrence of a principal tensile stress of approximately $4\sqrt{f'_c}$ at the centroid of the shear-wall cross section. Equation (18.7) corresponds approximately to the occurrence of a flexural tensile stress of $6\sqrt{f'_c}$ at a section $l_w/2$ above the section being investigated. Thus, the two equations predict, respectively, web-shear cracking and flexure-shear cracking. When the quantity $M_u/V_u - l_w/2$ is negative, Eq. (18.7) is inapplicable. According to the ACI Code, horizontal sections located closer to the wall base than a distance $l_w/2$ or $h_w/2$, whichever is less, may be designed for the same V_c as that computed at a distance $l_w/2$ or $h_w/2$.

When the factored shear force V_u does not exceed $\phi V_c/2$, a wall may be reinforced according to minimum requirements. When V_u exceeds $\phi V_c/2$, reinforcement for shear is to be provided according to the following requirements.

The nominal shear strength V_s provided by the horizontal wall steel is determined on the same basis as for ordinary beams:

$$V_s = \frac{A_v f_y d}{s} \tag{18.8}$$

where A_v = area of horizontal shear reinforcement within vertical distance s, in^2
s = vertical distance between horizontal reinforcement, in.
f_y = yield strength of reinforcement, psi

Substituting Eq. (18.8) into Eq. (18.2), then combining with Eq. (18.1), one obtains the equation for the required area of horizontal shear reinforcement within a distance s:

$$A_v = \frac{(V_u - \phi V_c)s}{\phi f_y d} \tag{18.9}$$

The minimum permitted ratio of horizontal shear steel to gross concrete area of vertical section is

$$\rho_t = 0.0025 \tag{18.10}$$

and the maximum spacing s is not to exceed $l_w/5$, $3h$, or 18 in.

Test results indicate that for low shear walls, vertical distributed reinforcement is needed as well as horizontal reinforcement. Code provisions require vertical steel of area A_h within a spacing s_1, such that the ratio of vertical steel to gross concrete area of horizontal section will be not less than

$$\rho_l = 0.0025 + 0.5\left(2.5 - \frac{h_w}{l_w}\right)(\rho_t - 0.0025) \tag{18.11}$$

nor less than 0.0025. However, the vertical reinforcement ratio need not be greater than the required horizontal reinforcement ratio. The spacing of the vertical bars is not to exceed $l_w/3$, $3h$, or 18 in.

Walls may be subject to flexural tension due to overturning moment, even when the vertical compression from gravity loads is superimposed. In many but not all cases, vertical steel is provided, concentrated near the wall edges, as shown in Fig. 18.14. The required steel area can be found by the usual methods for beams.

The dual function of the floors and roofs in buildings with shear walls should be noted. In addition to resisting gravity loads, they must act as deep beams spanning between shear-resisting elements. Because of their proportions, both shearing and flexural stresses are usually quite low. According to ACI Code 9.2.1, the load factor for live load drops to 1.0 when wind or earthquake effects are combined with the effects of gravity loads. Consequently, floor and roof reinforcement designed for gravity loads can usually serve as reinforcement for horizontal beam action also, with no increase in bar areas.

ACI Code 11.9.1 permits walls with height-to-length ratios not exceeding 2.0 to be designed using strut-and-tie models (Chapter 10). The minimum shear reinforcement criteria of Eqs. (18.9) through (18.11) and the maximum spacing limits for s and s_1 must be satisfied.

There are special considerations and requirements for the design of reinforced concrete walls in structures designed to resist forces associated with seismic motion. These are based on design for energy dissipation in the nonlinear range of response. This subject will be treated separately, in Chapter 20.

18.5 PRECAST CONCRETE FOR BUILDINGS

The earlier sections in this chapter have emphasized cast-in-place reinforced concrete structures. Construction of these structures requires a significant amount of skilled on-site labor. There is, however, another class of concrete construction for which the members are manufactured off site in precasting yards, under factory conditions, and subsequently assembled on site, a process that provides significant advantages in terms of economy and speed of construction.

Precast concrete construction involves the mass production of repetitive and often standardized units: columns, beams, floor and roof elements, and wall panels. On large jobs, precasting yards are sometimes constructed on or adjacent to the site. More frequently, these yards are stationary regional enterprises that supply precast members to sizable areas within reasonable shipping distances, on the order of 200 mi.

Advantages of precast construction include less labor per unit because of mechanized series production; use of unskilled local labor, in contrast to skilled mobile construction labor; shorter construction time because site labor primarily involves only foundation construction and connecting the precast units; better quality control and higher concrete strength that are achievable under factory conditions; and greater independence of construction from weather and season. Disadvantages are the greater cost of transporting precast units, as compared with transporting materials, and the additional technical problems and costs of site connections of precast elements.

Precast construction is used in all major types of structures: industrial buildings, residential and office buildings, halls of sizable span, bridges, stadiums, and prisons. Precast members frequently are prestressed in the casting yard. In the context of the present chapter, it is irrelevant whether a precast member is also prestressed. Discussion is focused on types of precast members and precast structures and on methods of connection; these are essentially independent of whether the desired strength of the member was achieved with ordinary reinforcement or by prestressing. A broader discussion of precast construction, which includes planning, design, materials, manufacturing, handling, construction, and inspection, will be found in Refs. 18.11 and 18.12. ACI Code Chapter 16 is dedicated to precast concrete.

a. Types of Precast Members

A number of types of precast units are in common use. Though most are not formally standardized, they are widely available, with minor local variations. At the same time, the precasting process is sufficiently adaptable for special shapes developed for particular projects to be produced economically, provided that the number of repetitive units is sufficiently large. This is particularly important for exterior wall panels, which permit a wide variety of architectural treatments.

Wall panels are made in a considerable variety of shapes, depending on architectural requirements. The most frequent four shapes are shown in Fig. 18.15. These units are produced in one to four-story-high sections and up to 8 ft in width. They are used either as curtain walls attached to columns and beams or as bearing walls. To improve thermal insulation, sandwich panels are used that consist of an insulation core (e.g., foam glass, glass fiber, or expanded plastic) between two layers of normalweight or lightweight concrete. The two layers must be adequately interconnected through the core to act as one unit. A variety of surface finishes can be produced through the use of special exposed aggregates or of colored cement, sometimes employed in combination. The special design problems that arise in load-bearing wall panels, such as tilt-up construction, are discussed in Ref. 18.13.

Stresses in wall panels are frequently more severe in handling and during erection than in the finished structure, and the design must provide for these temporary conditions. Also, control of cracking is of greater importance in wall panels than in other precast units, for appearance more than for safety. To control cracking, the maximum tensile stress in the concrete, calculated by straight-line theory, should not exceed the modulus of rupture of the particular concrete with an adequate margin of safety. ACI Committee 533 (Ref. 18.14) recommends that tensile stresses for normalweight concrete be limited to $5\sqrt{f_c'}$ under the effects of form removal, handling, transportation, impact, and live load. Maximum tensile stresses equal to 75 and 85 percent of this value are recommended for all-lightweight and sand-lightweight concrete, respectively. A wealth of information on precast wall panels is found in Refs. 18.12 and 18.14.

FIGURE 18.15
Precast concrete wall panels.

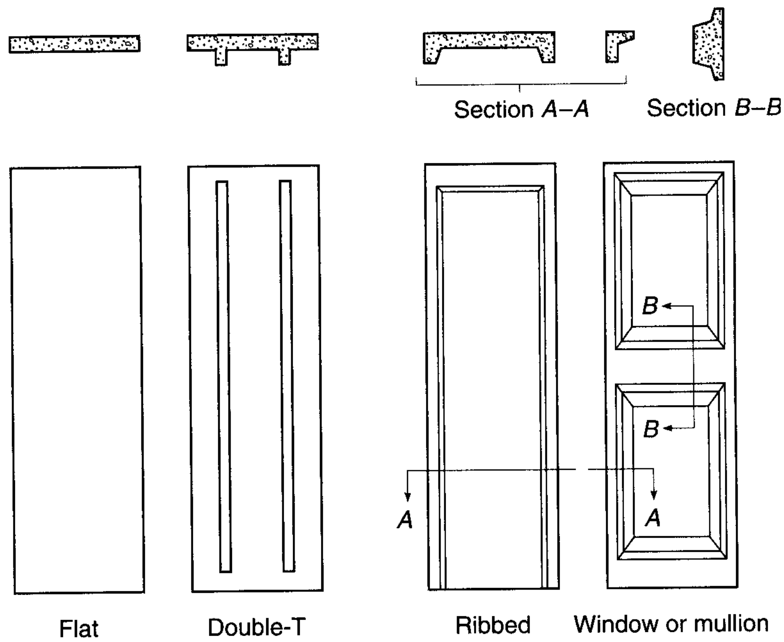

Roof and floor elements are made in a wide variety of shapes adapted to specific conditions, such as span lengths, magnitude of loads, desired fire ratings, and appearance. Figure 18.16 shows typical examples of the most common shapes, arranged in approximate order of increasing span length, even though the spans covered by the various configurations overlap widely.

Flat slabs (Fig. 18.16*a*) are usually 4 in. thick, although they are used as thin as $2\frac{1}{2}$ in. when continuous over several spans, and are produced in widths of 4 to 8 ft and in lengths up to 36 ft. Depending on the magnitude of loads and on deflection limitations, they are used over roof and floor spans ranging from 8 to about

FIGURE 18.16
Precast floor and roof elements.

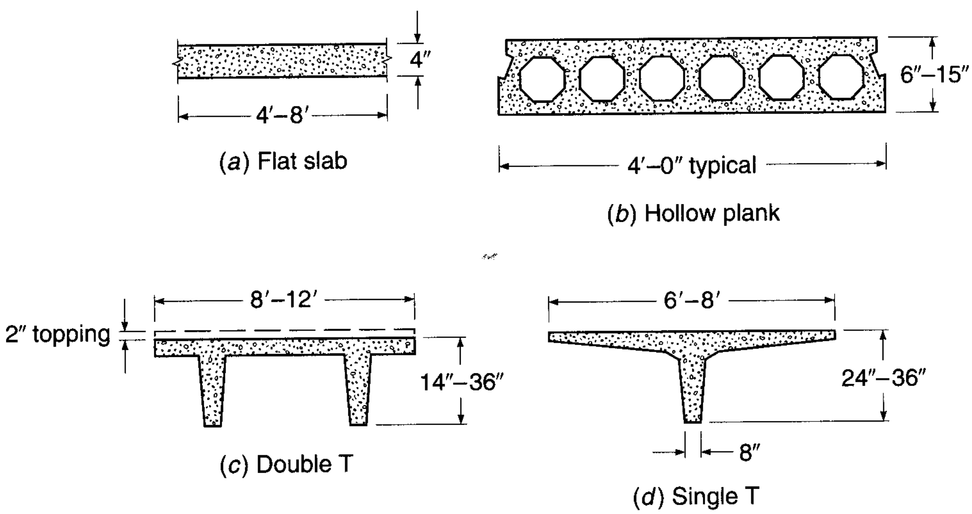

22 ft. For lower weight and better insulation and to cover longer spans, *hollow-core planks* (Fig. 18.16*b*) with a variety of shapes are used. Some of these are made by extrusion in special machines. Depths range from 6 to 15 in., with widths of 3 or 4 ft. Again depending on load and deflection requirements, they are used on roof spans from about 16 to 34 ft and on floor spans from 12 to 26 ft, which can be augmented to about 30 ft if a 2 in. topping is applied to act monolithically with the hollow plank.

For longer spans, *double T* members (Fig. 18.16*c*) are the most widely used shapes. Usual depths are from 14 to 36 in. They are used on roof spans up to 120 ft. When used as floor members, a concrete topping of at least 2 in. is usually applied to act monolithically with the precast members for spans up to about 50 ft, depending on load and deflection requirements. Finally, *single T* members are available in dimensions shown in Fig. 18.16*d*, mostly used for roof spans up to 100 ft and more.

For all of these units, the member itself or its flange constitutes the roof or floor slab. If the floor or roof proper is made of other material (e.g., plywood, gypsum, and plank), it can be supported on *precast joists* in a variety of shapes for spans from about 15 to 60 ft. Reference 18.12 addresses the design of both reinforced and prestressed concrete floor and roof units.

The shape of *precast beams* depends chiefly on the manner of framing. If floor and roof members are supported on top of the beams, these are mostly rectangular in shape (Fig. 18.17*a*). To reduce total depth of floor and roof construction, the tops of beams are often made flush with the top surface of the floor elements. To provide bearing, the beams are then constructed as ledger beams (Fig. 18.17*b*) or L beams (Fig. 18.17*c*). Although these shapes pertain to building construction,

FIGURE 18.17
Precast beams and girders.

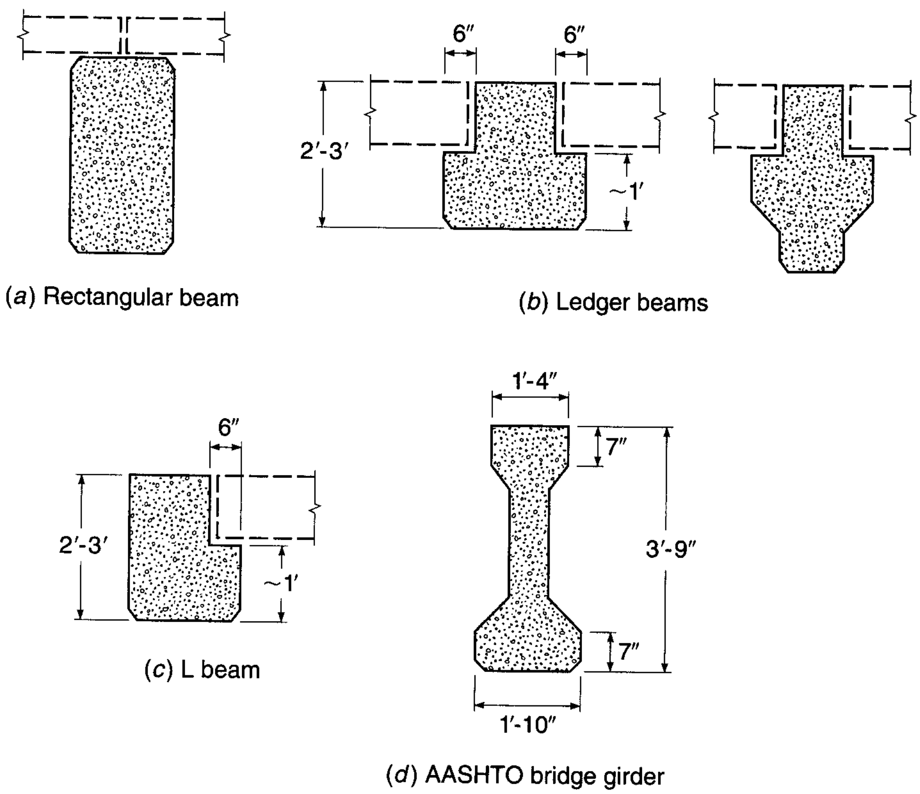

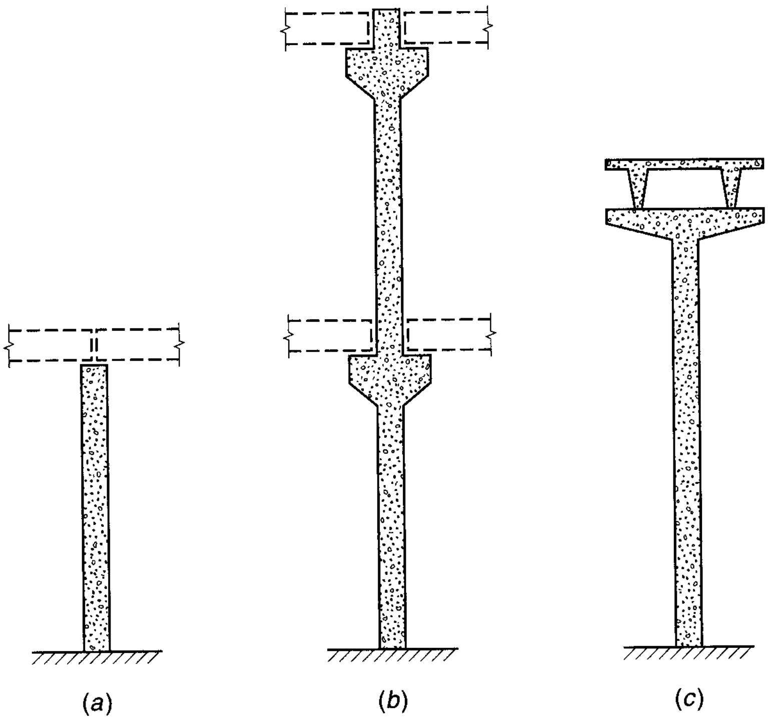

FIGURE 18.18
Precast concrete columns.

precast beams or girders are also frequently used in highway bridges. As an example, Fig. 18.17*d* shows one of the various AASHTO bridge girders, so named because they were developed by the American Association of State Highway and Transportation Officials.

If *precast columns* of single-story height are used so that the beams rest on top of the columns, simple prismatic columns are employed, which are available in sizes from about 12 × 12 to 24 × 24 in. (Fig. 18.18*a*). In this case, the beams are usually made continuous over the columns. Alternatively, in multistory construction, the columns can be made continuous for up to about six stories. In this case, integral brackets are frequently used to provide a bearing for the beams, as shown in Fig. 18.18*b* (see also Section 18.6b). Occasionally, T columns are used for direct support of double T floor members without the use of intermediate beams (Fig. 18.18*c*).

Figures 18.19 to 18.27 illustrate some of the many ways in which precast members have been used. Figure 18.19 shows a floor slab element being placed on precast columns with integral column capitals. The entire building, including elevator and stair shafts, is precast concrete. The photograph in Fig. 18.20 was taken in a precasting yard producing a variety of L, T, and rectangular shapes. Figure 18.21 shows symmetrical precast I beams, such as are used both for buildings and bridges. The projecting stirrup bars along the top flange will provide secure interlock between the precast beams and a cast-in-place slab added later, ensuring composite action. Figure 18.22 shows a multistory parking garage in which three-story precast columns support L-section and inverted T-section girders. The girders, in turn, carry 60 ft span prestressed single T beams, which provide the deck surface.

Figure 18.23 demonstrates that unusual architectural designs can be realized in precast concrete, as in this all-precast administration building. Wall panels are used to

FIGURE 18.19
Precast slab element with precast columns, beams, and lateral framing.

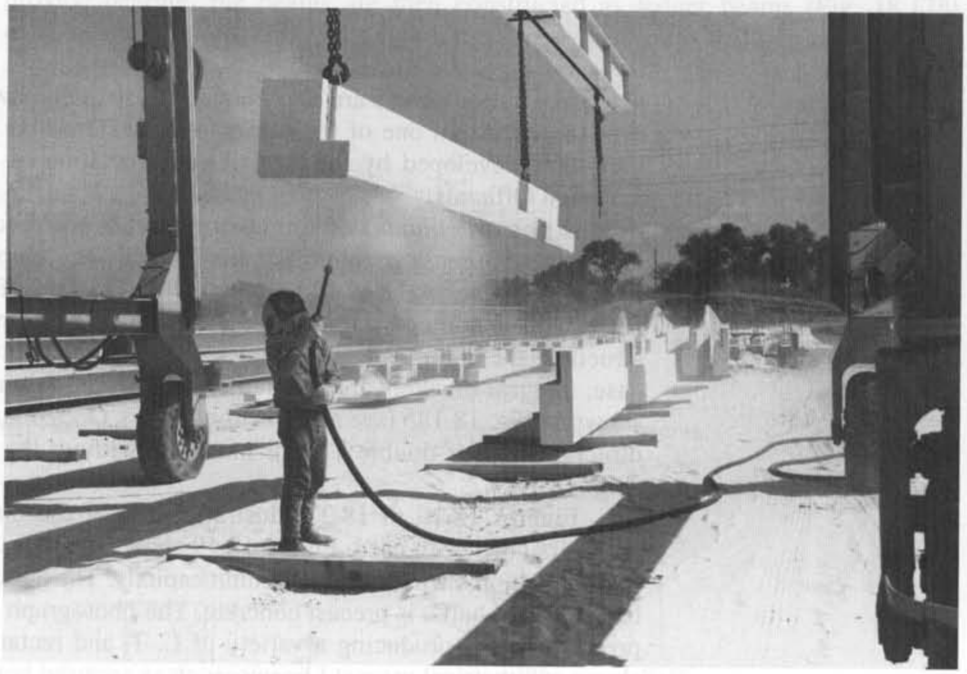

FIGURE 18.20
Sand-blasted architectural finish applied to a precast L beam.

produce a curved facade. Wedge-shaped repetitive floor units span freely from the exterior facade to the interior curved beam and column framework. In the insurance building shown in Fig. 18.24, 44 in. deep precast girders span 99 ft between exterior walls supported on four points each and provide six floors of office space entirely free

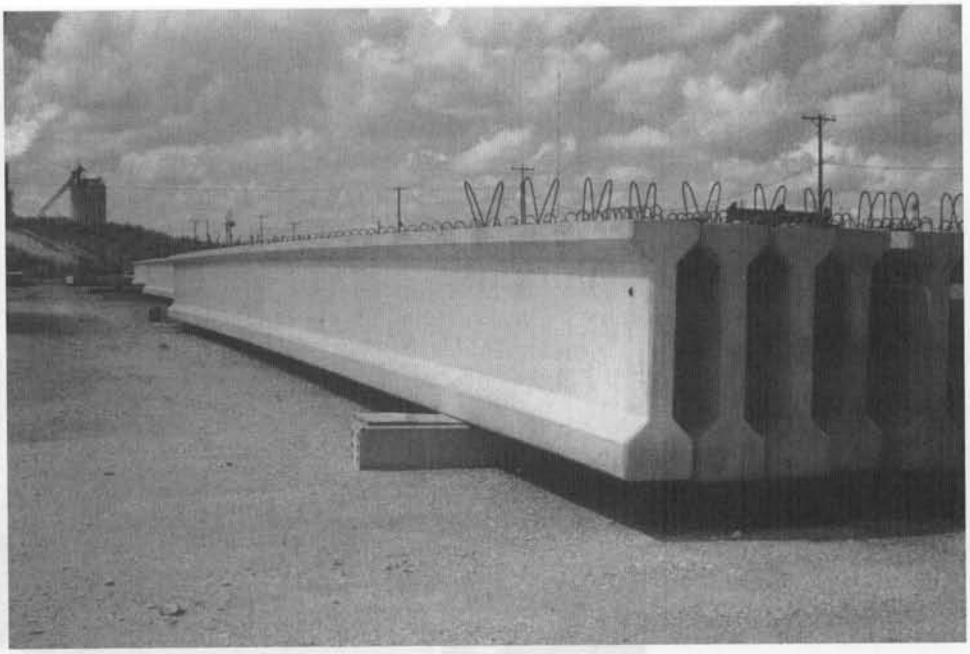

FIGURE 18.21
Precast I beams designed for composite action with a deck slab to be cast in place.

FIGURE 18.22
Precast parking garage at Cornell University.

of interior supports. The convention headquarters of Fig. 18.25 combines cast-in-place frames and floor slabs with precast double T roof beams and precast wall panels of special design. Figure 18.26 shows a 21-story hotel under construction, which, except for the service units, consists entirely of box-shaped, room-sized modules completely prefabricated and stacked on top of each other. Abroad, such precast modules, with

FIGURE 18.23
All precast administration building. (*Courtesy of Portland Cement Association.*)

FIGURE 18.24
Precast girders with 99 ft span and 44 in. depth for a column-free interior. (*Courtesy of Portland Cement Association.*)

FIGURE 18.25
Precast roof and wall panels combined with cast-in-place frames and floor slabs. (*Courtesy of Portland Cement Association.*)

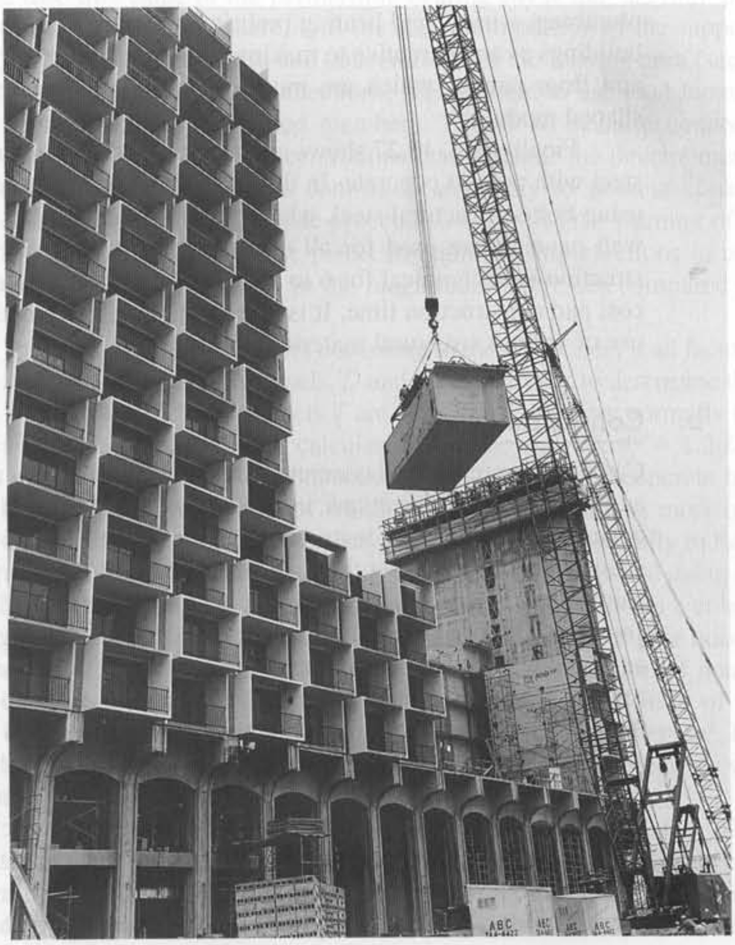

FIGURE 18.26
Precast room-sized modules for a 21-story hotel. (*Courtesy of Portland Cement Association.*)

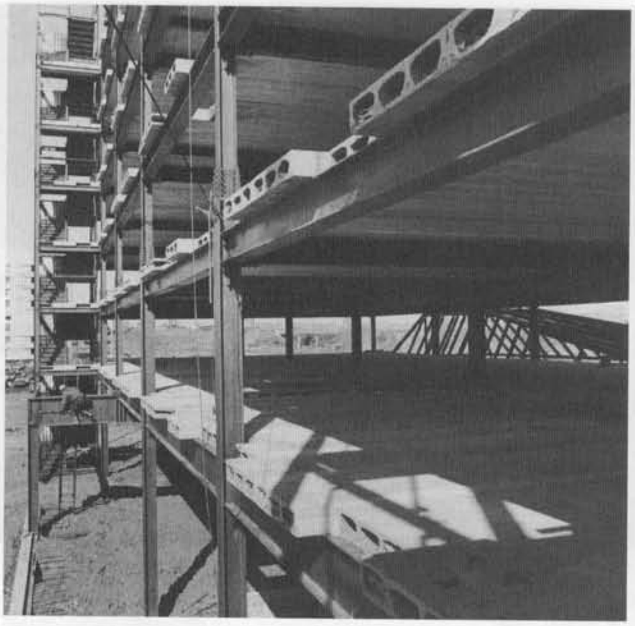

FIGURE 18.27
Steel framing combined with precast concrete floor planks for an 8-story hotel. (*Courtesy of Bethlehem Steel Co.*)

plumbing, wiring, and heating preinstalled, are widely used for multistory apartment buildings as an alternative to making similar apartment structures in precast wall, roof, and floor panels, which are more easily shipped but less easily erected than box-shaped modules.

Finally, Fig. 18.27 shows an example of the frequent combined use of structural steel with precast concrete. In this case, the framing of an eight-story hotel was done using bolted structural steel, while precast concrete floor and roof planks and precast wall panels were used for all other main structural components. This type of construction is economical for 6 to 12-story buildings, where it provides savings in both cost and construction time. It is one example of the increasingly important combined use of various structural materials and methods.

b. Connections

Cast-in-place reinforced concrete structures, by their very nature, tend to be monolithic and continuous. Connections, in the sense of joining two hitherto separate pieces, rarely occur in that type of construction. Precast structures, on the other hand, resemble steel construction in that the final structure consists of large numbers of prefabricated elements that are connected on site to form the finished structure. In both types of construction, such connections can be detailed to transmit gravity forces only, or gravity and horizontal forces, or moments in addition to these forces. In the last case, a continuous structure is obtained much as in cast-in-place construction, and connections that achieve such continuity by appropriate use of special hardware, reinforcing steel, and concrete to transmit all tension, compression, and shear stresses are sometimes called *hard* connections. In contrast, connections that transmit reactions in one direction only, analogous to rockers or rollers in steel structures, but permit a limited amount of motion to relieve other forces, such as horizontal reaction components, are sometimes known as *soft* connections (Ref. 18.15). In almost all precast connections, bearing plates or pads are used to ensure distribution and reasonable uniformity of bearing pressures. Bearing plates are made of steel, while bearing pads are made of materials such as chloroprene, fiber-reinforced polymers, and Teflon. If bearing plates are used, and the plates on two members are suitably joined by welding or other means, a hard connection is obtained in the sense that horizontal, as well as vertical, forces are transmitted. On the other hand, bearing pads transmit gravity loads but can permit sizable horizontal deformations and, thus, relieve horizontal forces.

Precast concrete structures are subject to dimensional changes from creep, shrinkage, and relaxation of prestress in addition to temperature, while in steel structures only temperature changes produce dimensional variations. In the early development of precast construction, there was a tendency to use soft connections extensively to permit these dimensional changes to occur without causing restraint forces in the members, and particularly in the connections. Subsequent experience, however, has shown that the resulting structures possess insufficient stability against lateral forces, such as high wind and, particularly, earthquake effects. Therefore, current practice emphasizes the use of hard connections that provide a high degree of continuity (Refs. 18.12 and 18.16). When designing hard connections, provisions must be made to resist the restraint forces that are caused by the previously described volume changes (Ref. 18.12). Considerable information concerning this and other matters relating to connections is found in Refs. 18.12 and 18.16.

Bearing stresses on plain concrete are limited by ACI Code 10.14.1 to $0.85\phi f_c'$, except when the supporting area is wider on all sides than the loaded area A_1. In such a case this value of the permissible bearing stress may be multiplied by $\sqrt{A_2/A_1}$ but not more than 2.0, where A_2 is the maximum portion of the supporting surface that is geometrically similar to and concentric with the loading area (see Section 16.6b).

In the design of connections, it is prudent to use load factors that exceed those required for the connected members. This is so because connections are generally subject to high stress concentrations that preclude the development of much ductility. In contrast, the members connected are likely to possess considerable ductility if designed by usual ACI Code procedures and will give warning of impending collapse if overloading should take place. In addition, imperfections in connection geometry may cause large changes in the magnitude of stresses compared with those assumed in the design.

In designing members according to the ACI Code, load factors of 1.2 and 1.6 are applied to dead and live loads, D and L respectively, to determine the required strength. When volume change effects T are considered, they are normally treated as dead load, and the factored load U is calculated from the equation $U = 1.2(D + T) + 1.6L$.

A wide variety of connection details for precast concrete building components have evolved, only a few of which will be shown here as more or less representative connections. Many additional possibilities are described fully in Refs. 18.12 and 18.16.

Column base connections are generally accomplished using steel base plates that are anchored into the precast column. Figure 18.28*a* shows a column base detail with projecting base plate. Four anchor bolts are used, with double nuts facilitating erection and leveling of the column. Typically a minimum of 2 in. of nonshrink grout is used between the top of the pier, footing, or wall and the bottom of the steel base plate. Column reinforcement is welded to the top face of the base plate. Tests have confirmed that such column connections can transmit the full moment for which the column is designed, if properly detailed.

An alternative base detail is shown in Fig. 18.28*b*, with the dimensions of the base plate the same as, or slightly smaller than, the outside column dimensions. Anchor bolt pockets are provided, either centered on the column faces as shown or located at the corners. Bolt pockets are grouted after the nuts are tightened. Column

FIGURE 18.28
Column base connections.

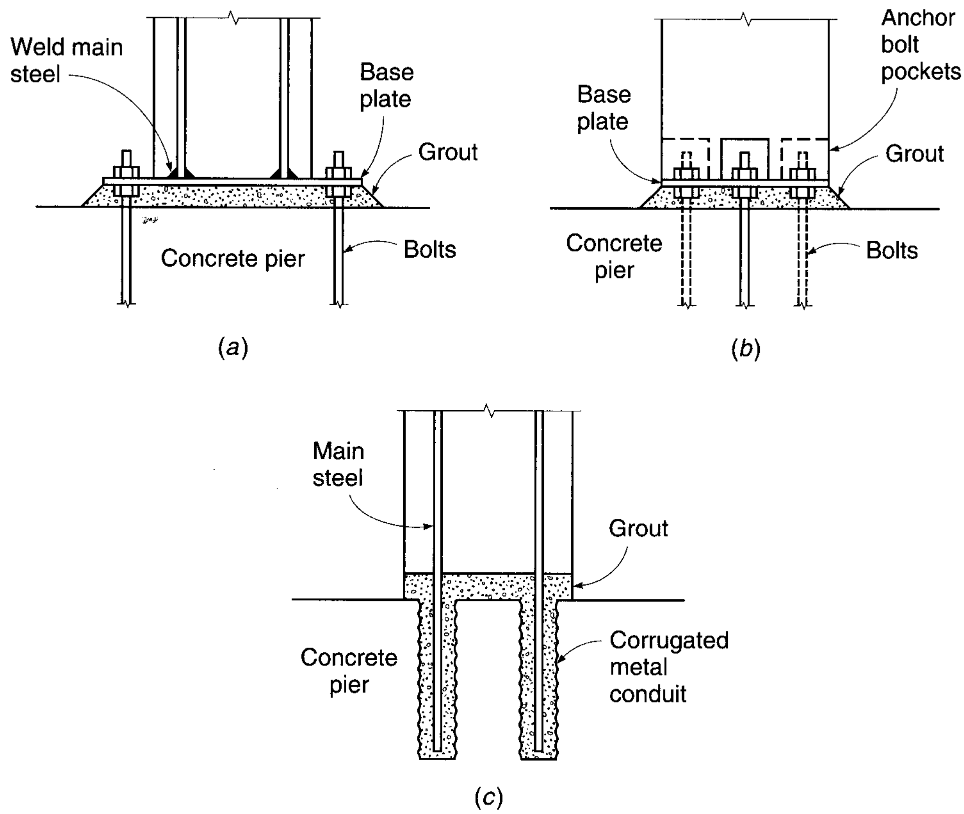

bars, not shown here, would be welded to the top face of the base plate as before. Figure 18.29 shows the base plate detail, similar to Fig. 18.28*b*, that was used for the precast three-story columns in the parking garage shown in Fig. 18.22.

In Fig. 18.28*c*, the main column bars project from the ends of the precast member a sufficient distance to develop their strength by bond. The projecting bars are inserted into grout-filled holes cast in the foundation when it is placed.

In all of the cases shown, confining steel should be provided around the anchor bolts in the form of closed ties. A minimum of four No. 3 (No. 10) ties is recommended, placed on 3 in. centers near the top surface of the pier or wall. Tie reinforcement in the columns should be provided as usual.

Figure 18.30 shows several *beam-to-column* connections. In all cases, rectangular beams are shown, but similar details apply to I or T beams. The figure shows only the basic geometry; and auxiliary reinforcement, anchors, and ties are omitted for the sake of clarity.

Figure 18.30*a* shows a joint detail with a concealed haunch. Well-anchored bearing angles are provided at the column seat and beam end. This type of connection may be used to provide vertical and horizontal reaction components, and with the addition of post-tensioned prestressing, will provide moment resistance as well.

Figure 18.30*b* shows a typical bracket, common for industrial construction where the projecting bracket is not objectionable. The seat angle is welded to reinforcing bars anchored in the column. A steel bearing plate is used at the bottom of the beam and anchored into the concrete.

The embedded steel shape in Fig. 18.30*c* is used when it is necessary to avoid projections beyond the face of the column or below the bottom of the beam. A socket

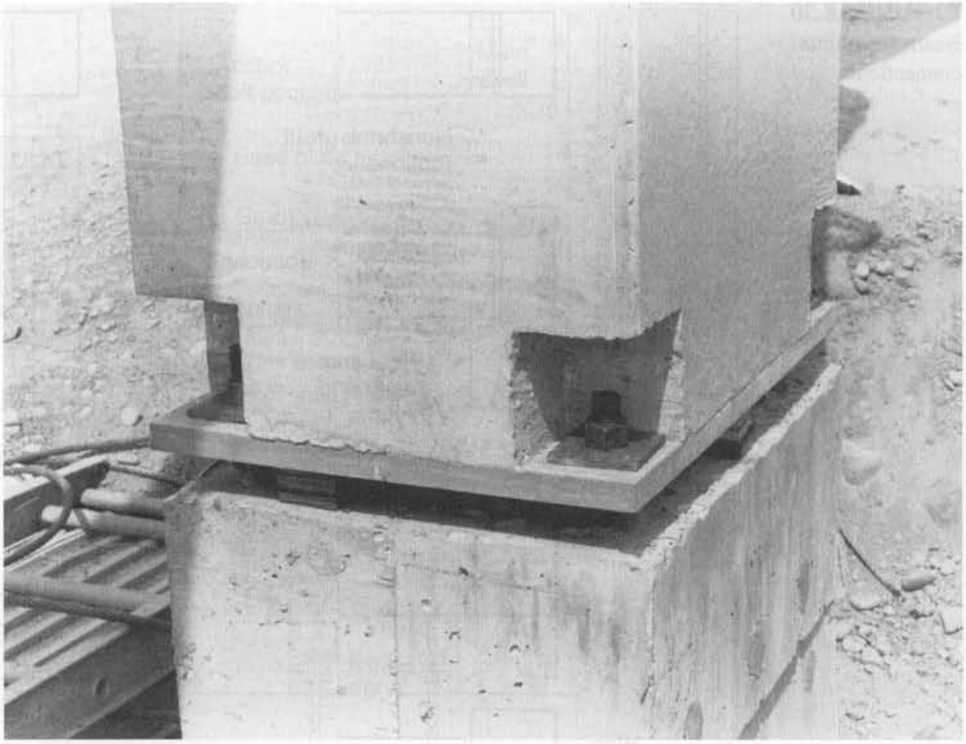

FIGURE 18.29
Detail at base of precast column of Cornell University parking garage shown in Fig. 18.22.

is formed in casting the beam, with steel angle or plate at its top, to receive the beam stub. A steel connection can also be used in place of the bracket shown in Fig. 18.30*b*.

Finally, Fig. 18.30*d* shows a doweled connection with bars projecting from the column into holes formed in the beam ends. These are grouted after the beams are in position. This connection is popular in precast concrete construction but has little flexural capacity (Ref. 18.17).

Figure 18.31 shows several typical *column-to-column* connections. Figure 18.31*a* shows a detail using anchor bolt pockets and a double-nut system for leveling the upper column. Bolts can also be located at the center of the column faces, as shown in Fig. 18.28*b*. The detail shown in Fig. 18.31*b* permits the main steel to be lap-spliced with that in the column below. One of the many possibilities for splicing a column through a continuous beam is shown in Fig. 18.31*c*. Main reinforcing bars in both upper and lower columns should be welded to steel cap and base plates to transfer their load, and anchor bolts should be designed with the same consideration. Closely spaced ties must be provided in the columns and in this case in the beam as well, to transfer the load between columns.

Slab-to-beam connections generally use some variation of the detail shown in Fig. 18.32. Support is provided by an L beam (Fig. 18.32*a*) or an inverted T beam (Fig. 18.32*b*) that is flush with the top of the precast floor planks. The detail shown is sufficient if no mechanical tie is required between the precast parts. Where a positive connection is required, steel plates are set into the top of the members, suitably anchored, and short connecting plates are welded so as to attach the built-in plates.

Basic tools for the design of precast concrete connections are the *shear friction design method* described in detail in Chapter 4 and the *strut-and-tie model* described in Chapter 10. Example 4.6 (Section 4.9) demonstrated the use of the shear-friction

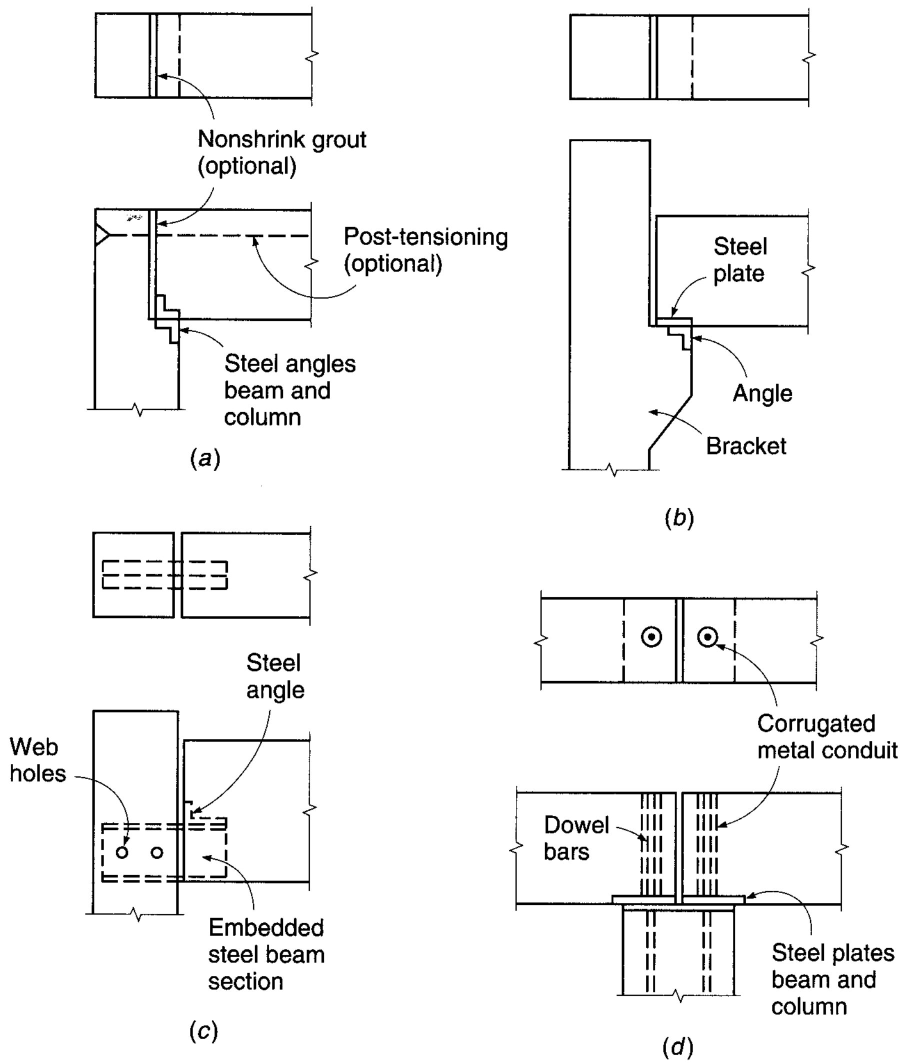

FIGURE 18.30
Beam-to-column connections.

approach to determining the reinforcement for the end-bearing region of a precast concrete girder. The use of both the shear-friction method and a strut-and-tie model for joint behavior was shown in Section 11.7, and Example 11.5 presented the detailed design of a bracket for a precast concrete column. Additional design information pertaining to precast concrete connection design will be found in Refs. 18.12, 18.15, and 18.16.

c. Structural Integrity

Precast concrete structures normally lack the joint continuity and high degree of redundancy characteristic of monolithic, cast-in-place reinforced concrete construction. Progressive collapse in the event of abnormal loading, in which the failure of one element leads to the collapse of another, then another, can produce catastrophic results. For this reason, the structural integrity of precast concrete structures is specifically addressed in ACI Code 16.5. ACI Code 16.5.1 does not permit the use of "soft" connections that rely solely on friction caused by gravity forces. Full moment-resisting

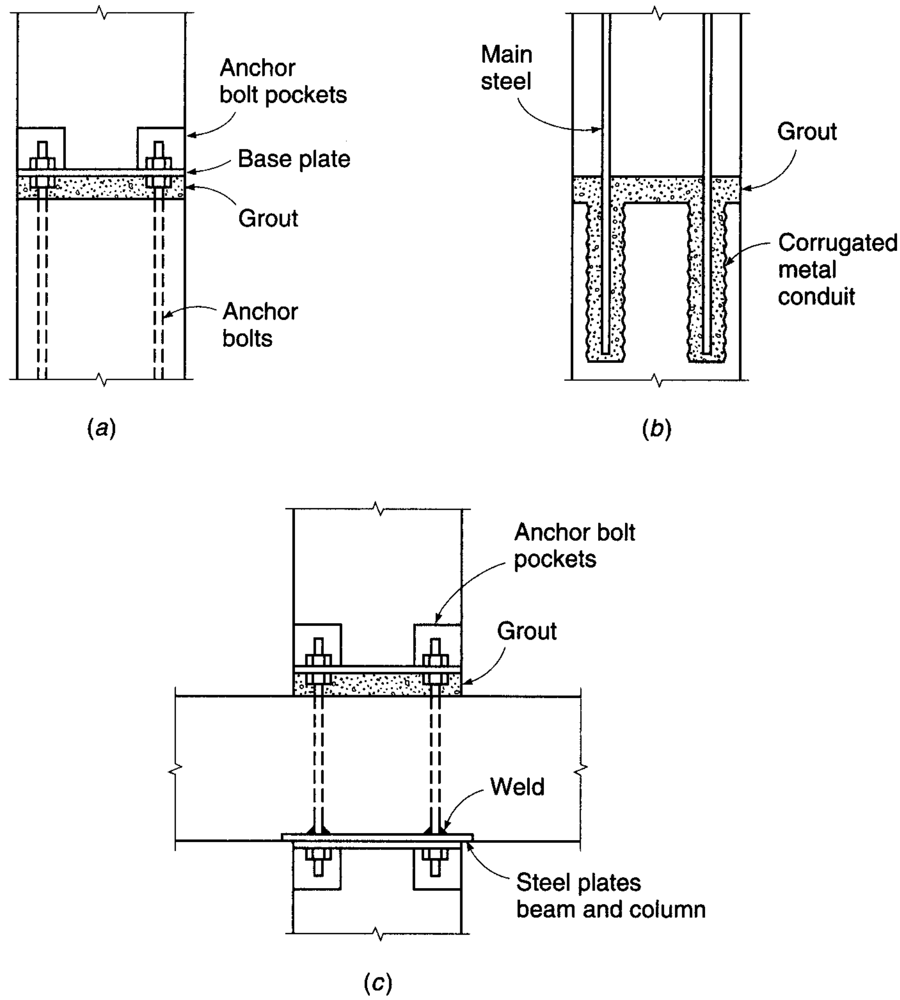

FIGURE 18.31
Column-to-column connections.

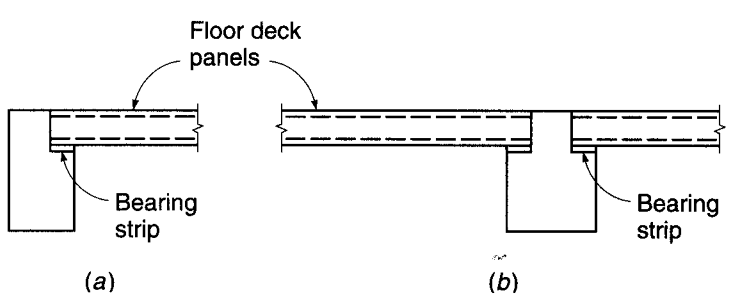

FIGURE 18.32
Slab-to-beam connections.

connections are unusual, but some positive means of connecting members to their supports, with due regard to the need to accommodate dimensional changes associated with creep, shrinkage, and temperature effects, is strongly recommended.

In addition, experience with precast structures has shown that the introduction of special reinforcement in the form of tension ties, though adding little to the cost of construction, can contribute greatly to maintaining structural integrity in the event of extraordinary loading, such as loads caused by extreme winds, earthquake, or explosion. This tension reinforcement is best arranged in a three-dimensional grid, usually on the column lines, tying the floors together vertically and in both horizontal directions. For precast concrete construction, ACI Code 7.13.3 and 16.5.1 require that tension ties be provided in the transverse, longitudinal, and vertical directions of the structure and around its perimeter. Specific details vary widely. Although no specific guidance is offered in either the ACI Code or Commentary regarding steel placement or design forces, valuable suggestions will be found in Refs. 18.11, 18.12, and 18.16.

18.6 ENGINEERING DRAWINGS FOR BUILDINGS

Design information is conveyed to the builder mainly by engineering drawings. Their preparation is therefore a matter of the utmost importance, and they should be carefully checked by the design engineer to ensure that concrete dimensions and reinforcement agree with the calculations.

Engineering drawings for buildings usually consist of a plan view of each floor showing overall dimensions and locating the main structural elements, cross-sectional views through typical members, and beam and slab schedules that give detailed information on the concrete dimensions and reinforcement in tabular form. Sectional views are usually drawn to a larger scale than the plan and serve to locate the steel and establish cutoff and bend points as well as to define the shape of the member. Usually a separate drawing is included that gives, in the form of schedules and cross sections, the details of columns and footings.

The contract documents, including the plans, specifications, and cost estimates, provide detailed descriptions of the material strengths. Additionally, many building officials, particularly in active seismic regions, require a description of the structural framing system, lateral load-resisting system, and design live loads to be included on the structural drawings. Typical concrete design drawings and details will be found in Ref. 18.4.

REFERENCES

18.1. ACI Committee 216, *Code Requirements for Determining Fire Resistance of Concrete and Masonry Construction Assemblies*, ACI 216.1-07, American Concrete Institute, Farmington Hills, MI, 2007.

18.2. E. S. Hoffman, D. P. Gustafson, and A. J. Gouwens, *Structural Design Guide for the ACI Building Code*, Kluwer Academic Publishers, Boston, 1998.

18.3. *CRSI Design Handbook*, 10th ed., Concrete Reinforcing Steel Institute, Schaumburg, IL, 2008.

18.4. *ACI Detailing Manual*, ACI Special Publication SP-66, American Concrete Institute, Farmington Hills, MI, 1994.

18.5. ACI Committee 352, *Recommendations for Design of Beam-Column Joints in Monolithic Reinforced Concrete Structures,* ACI 352R-02, American Concrete Institute, Farmington Hills, MI, 2002.

18.6. S. Ravikumar, D. Darwin, S. L. McCabe, and G. P. Pasley, "Shear Strength of Continuous Lightly Reinforced Concrete Joist Systems," *SM Report* No. 37, University of Kansas Center for Research, Lawrence, March 1994.

18.7. L. E. Svab and R. E. Jurewicz, "Wide Module Concrete Joist Construction," *Concr. Intl.*, vol. 12, no. 11, 1990, pp. 39–42.

18.8. C. F. Scribner and C. G. Culver, "Investigation of the Collapse of L'Ambiance Plaza," *J. Perform. Construct. Facil.* ASCE, vol. 2, no. 2, 1988, pp. 58–79.

18.9. A. E. Cardenas, J. M. Hanson, W. G. Corley, and E. Hognestad, "Design Provisions for Shear Walls," *J. ACI*, vol. 70, no. 3, 1973, pp. 221–230.

18.10. A. E. Cardenas and D. D. Magura, "Strength of High-Rise Shear Walls: Rectangular Cross Section," pp. 119–150 in *Response of Multistory Structures to Lateral Forces*, SP-36, American Concrete Institute, Farmington Hills, MI, 1973.

18.11. ACI Committee 550, "Design Recommendations for Precast Concrete Structures," ACI 550R-96, *Manual of Concrete Practice*, Part 6, American Concrete Institute, Farmington Hills, MI, 2008.
18.12. *PCI Design Handbook*, 6th ed., Precast/Prestressed Concrete Institute, Chicago, 2004.
18.13. K. M. Kripanarayanan and M. Fintel, "Analysis and Design of Slender Tilt-Up Reinforced Concrete Wall Panels," *J. ACI*, vol. 71, no. 1, 1974, pp. 20–28.
18.14. ACI Committee 533, "Guide for Precast Concrete Wall Panels," ACI 533R-93, *Manual of Concrete Practice*, Part 6, American Concrete Institute, Farmington Hills, MI, 2008.
18.15. P. W. Birkland and H. W. Birkland, "Connections in Precast Concrete Construction," *J. ACI*, vol. 63, no. 3, 1966, pp. 345–368.
18.16. PCI Committee on Connection Details, *Design and Typical Details of Connections for Precast and Prestressed Concrete,* MNL-123-88, Precast/Prestressed Concrete Institute, Chicago, 1988.
18.17. C. W. Dolan, J. F. Stanton, and R. G. Anderson, "Moment Resistant Connections and Simple Connections," *J. Precast/Prestressed Concr. Inst.*, vol. 32, no. 2, 1987, pp. 62–74.

19 Prestressed Concrete

19.1 INTRODUCTION

Modern structural engineering tends to progress toward more economical structures through gradually improved methods of design and the use of higher-strength materials. This results in a reduction of cross-sectional dimensions and consequent weight savings. Such developments are particularly important in the field of reinforced concrete, where the dead load represents a substantial part of the total load. Also, in multistory buildings, any saving in depth of members, multiplied by the number of stories, can represent a substantial saving in total height, load on foundations, length of heating and electrical ducts, plumbing risers, and wall and partition surfaces.

Significant savings can be achieved by using high-strength concrete and steel in conjunction with present-day design methods, which permit an accurate appraisal of member strength. However, there are limitations to this development, due mainly to the interrelated problems of cracking and deflection at service loads. The efficient use of high-strength steel is limited by the fact that the amount of cracking (width and number of cracks) is proportional to the strain, and therefore the stress, in the steel. Although a moderate amount of cracking is normally not objectionable in structural concrete, excessive cracking is undesirable in that it exposes the reinforcement to corrosion, it may be visually offensive, and it may trigger a premature failure by diagonal tension. The use of high-strength materials is further limited by deflection considerations, particularly when refined analysis is used. The slender members that result may permit deflections that are functionally or visually unacceptable. This is further aggravated by cracking, which reduces the flexural stiffness of members.

These limiting features of ordinary reinforced concrete have been largely overcome by the development of prestressed concrete. A prestressed concrete member can be defined as one in which there have been introduced internal stresses of such magnitude and distribution that the stresses resulting from the given external loading are counteracted to a desired degree. Concrete is basically a compressive material, with its strength in tension being relatively low. Prestressing applies a precompression to the member that reduces or eliminates undesirable tensile stresses that would otherwise be present. Cracking under service loads can be minimized or even avoided entirely. Deflections may be limited to an acceptable value; in fact, members can be designed to have zero deflection under the combined effects of service load and prestress force. Deflection and crack control, achieved through prestressing, permit the engineer to make use of efficient and economical high-strength steels in the form of strands, wires, or bars, in conjunction with concretes of much higher strength than normal. Thus, prestressing results in the overall improvement in performance of structural concrete used for ordinary loads and spans and extends the range of application far beyond the limits for ordinary reinforced concrete, not only leading to much longer spans than previously thought possible, but also permitting innovative new structural forms to be employed.

19.2 EFFECTS OF PRESTRESSING

There are at least three ways to look at the prestressing of concrete: (a) as a method of achieving *concrete stress control,* by which the concrete is precompressed so that tension normally resulting from the applied loads is reduced or eliminated, (b) as a means for introducing *equivalent loads* on the concrete member so that the effects of the applied loads are counteracted to the desired degree, and (c) as a *special variation of reinforced concrete* in which prestrained high-strength steel is used, usually in conjunction with high-strength concrete. Each of these viewpoints is useful in the analysis and design of prestressed concrete structures, and they will be illustrated in the following paragraphs.

a. Concrete Stress Control by Prestressing

Many important features of prestressed concrete can be demonstrated by simple examples. Consider first the plain, unreinforced concrete beam with a rectangular cross section shown in Fig. 19.1*a*. It carries a single concentrated load at the center of its span. (The self-weight of the member will be neglected here.) As the load W is gradually applied, longitudinal flexural stresses are induced. If the concrete is stressed only within its elastic range, the flexural stress distribution at midspan will be linear, as shown.

At a relatively low load, the tensile stress in the concrete at the bottom of the beam will reach the tensile strength of the concrete f_r, and a crack will form. Because no restraint is provided against upward extension of the crack, the beam will collapse without further increase of load.

Now consider an otherwise identical beam, shown in Fig. 19.1*b*, in which a longitudinal axial force P is introduced prior to the vertical loading. The longitudinal prestressing force will produce a uniform axial compression $f_c = P/A_c$, where A_c is the cross-sectional area of the concrete. The force can be adjusted in magnitude so that when the transverse load Q is applied, the superposition of stresses due to P and Q will result in zero tensile stress at the bottom of the beam as shown. Tensile stress in the concrete may be eliminated in this way or reduced to a specified amount.

It would be more logical to apply the prestressing force near the bottom of the beam, to compensate more effectively for the load-induced tension. A possible design specification, for example, might be to introduce the maximum compression at the bottom of the beam without causing tension at the top, when only the prestressing force acts. It is easily shown that, for a beam with a rectangular cross section, the point of application of the prestressing force should be at the lower third point of the section depth to achieve this. The force P, with the same value as before, but applied with eccentricity $e = h/6$ relative to the concrete centroid, will produce a longitudinal compressive stress distribution varying linearly from zero at the top surface to a maximum of $2f_c = P/A_c + Pec_2/I_c$ at the bottom, where f_c is the concrete stress at the concrete centroid, c_2 is the distance from the concrete centroid to the bottom

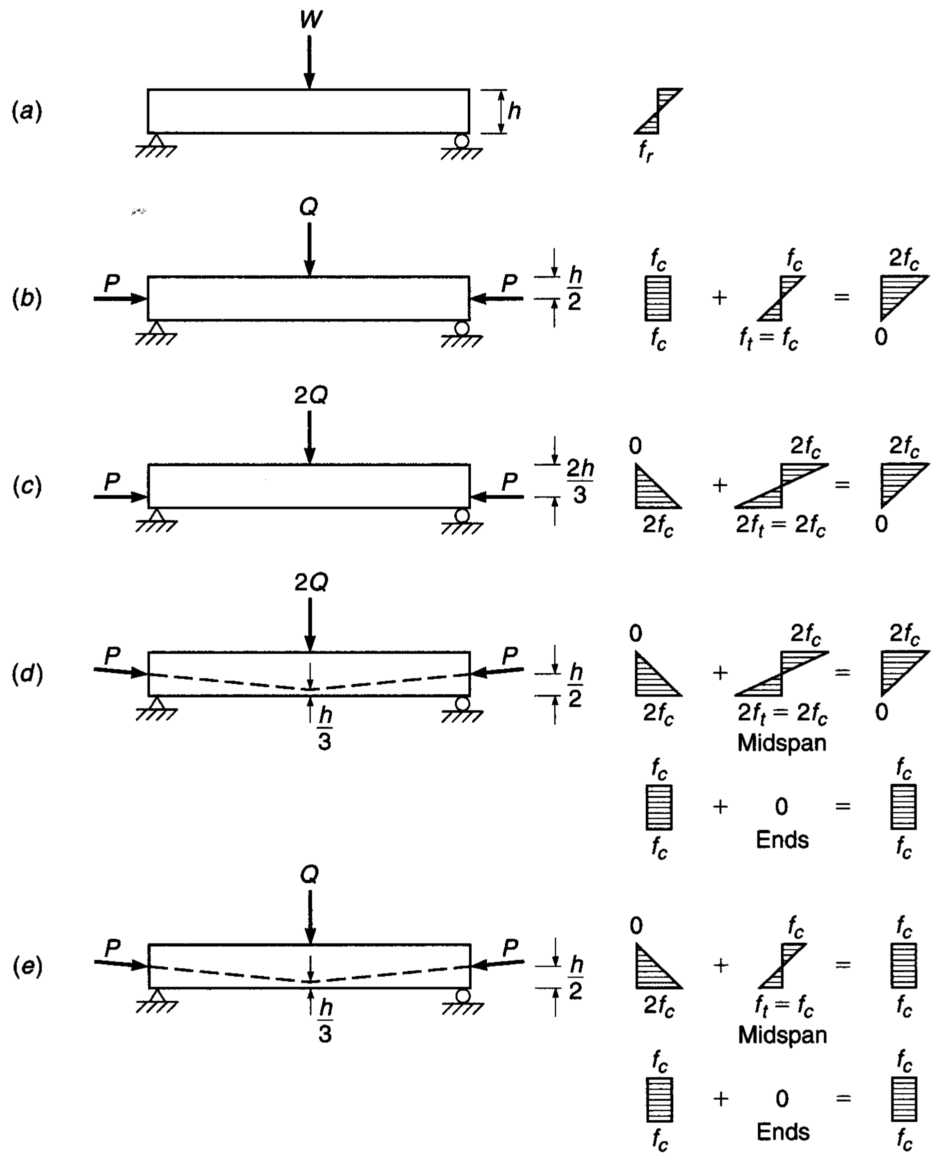

FIGURE 19.1
Alternative schemes for prestressing a rectangular concrete beam: (*a*) plain concrete beam; (*b*) axially prestressed beam; (*c*) eccentrically prestressed beam; (*d*) beam with variable eccentricity; (*e*) balanced load stage for beam with variable eccentricity.

of the beam, and I_c is the moment of inertia of the cross section. This is shown in Fig. 19.1*c*. The stress at the bottom will be exactly twice the value produced before by axial prestressing.

Consequently, the transverse load can now be twice as great as before, or $2Q$, and still cause no tensile stress. In fact, the final stress distribution resulting from the superposition of load and prestressing force in Fig. 19.1*c* is identical to that of Fig. 19.1*b*, with the same prestressing force, although the load is twice as great. The advantage of eccentric prestressing is obvious.

The methods by which concrete members are prestressed will be discussed in Section 19.3. For present purposes, it is sufficient to know that one practical method of prestressing uses high-strength steel tendons passing through a conduit embedded in the concrete beam. The tendon is anchored, under high tension, at both ends of the beam, thereby causing a longitudinal compressive stress in the concrete. The prestress force of Fig. 19.1*b* and *c* could easily have been applied in this way.

A significant improvement can be made, however, by using a prestressing tendon with variable eccentricity with respect to the concrete centroid, as shown in Fig. 19.1*d*. The load $2Q$ produces a bending moment that varies linearly along the span, from zero at the supports to maximum at midspan. Intuitively, one suspects that the best arrangement of prestressing would produce a *countermoment* that acts in the opposite sense to the load-induced moment and that would vary in the same way. This would be achieved by giving the tendon an eccentricity that varies linearly, from zero at the supports to maximum at midspan. This is shown in Fig. 19.1*d*. The stresses at midspan are the same as those in Fig. 19.1*c*, both when the load $2Q$ acts and when it does not. At the supports, where only the prestress force with zero eccentricity acts, a uniform compression stress f_c is obtained as shown.

For each characteristic load distribution, there is a *best tendon profile* that produces a prestress moment diagram that corresponds to that of the applied load. If the prestress countermoment is made exactly equal and opposite to the load-induced moment, the result is a beam that is subject only to uniform axial compressive stress in the concrete all along the span. Such a beam would be free of flexural cracking, and theoretically it would not be deflected up or down when that particular load is in place, compared to its position as originally cast. Such a result would be obtained for a load of $\frac{1}{2} \times 2Q = Q$, as shown in Fig. 19.1*e*, for example.

Some important conclusions can be drawn from these simple examples as follows:

1. Prestressing can control or even eliminate concrete tensile stress for specified loads.
2. Eccentric prestress is usually much more efficient than concentric prestress.
3. Variable eccentricity is usually preferable to constant eccentricity, from the viewpoints of both stress control and deflection control.

b. Equivalent Loads

The effect of a change in the vertical alignment of a prestressing tendon is to produce a vertical force on the concrete beam. That force, together with the prestressing force acting at the ends of the beam through the tendon anchorages, can be looked upon as a system of external loads.

In Fig. 19.2*a*, for example, a tendon that applies force P at the centroid of the concrete section at the ends of a beam and that has a uniform slope at angle θ between the ends and midspan introduces a transverse force $2P \sin \theta$ at the point of change of slope at midspan. At the anchorages, the vertical component of the prestressing force is $P \sin \theta$ and the horizontal component is $P \cos \theta$. The horizontal component is very nearly equal to P for the usual flat slope angles. The moment diagram for the beam of Fig. 19.2*a* is seen to have the same form as that for any center-loaded simple span.

The beam of Fig. 19.2*b*, with a curved tendon, is subject to a vertical upward load from the tendon as well as the forces P at each end. The exact distribution of the load depends on the profile of the tendon. A tendon with a parabolic profile, for example, will produce a uniformly distributed load. In this case, the moment diagram will be parabolic, as it is for a uniformly loaded simple span.

If a straight tendon is used with constant eccentricity, as shown in Fig. 19.2*c*, there are no vertical forces on the concrete, but the beam is subject to a moment Pe at each end, as well as the axial force P, and a diagram of constant moment results.

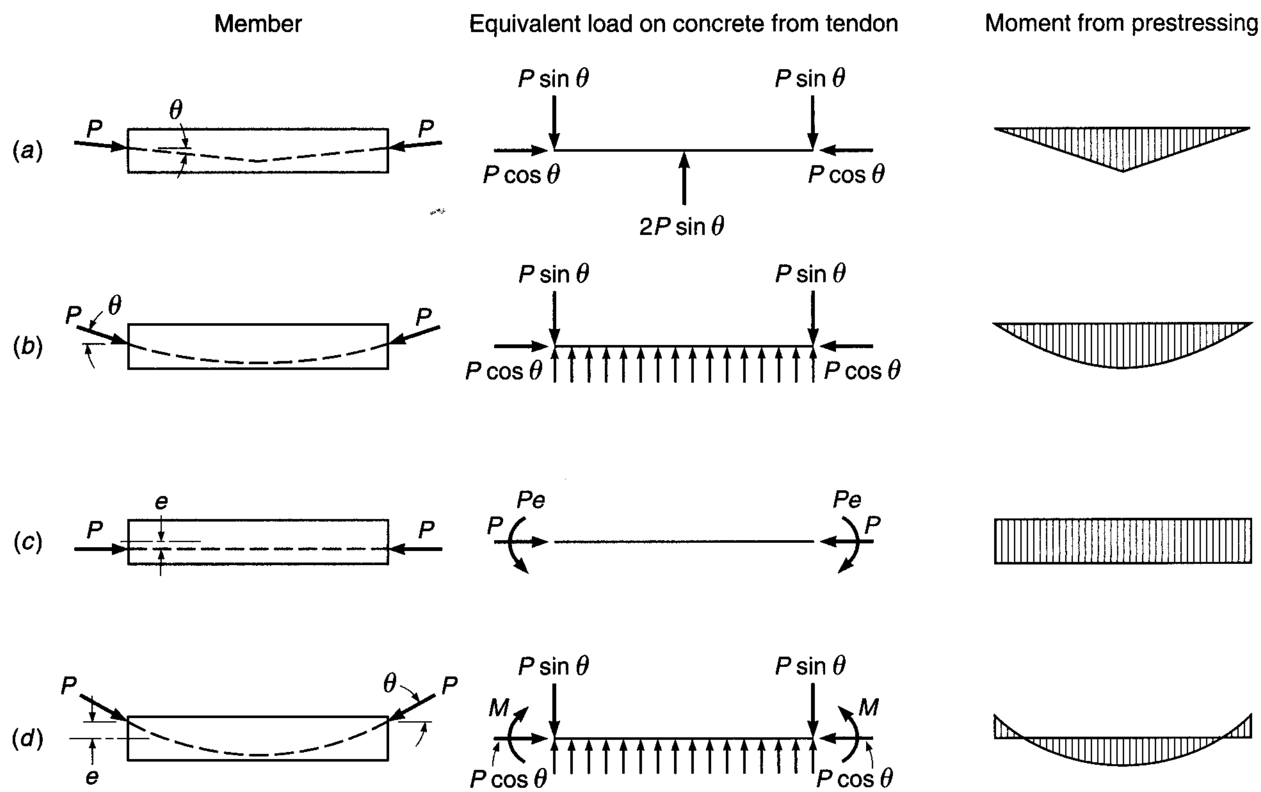

FIGURE 19.2
Equivalent loads and moments produced by prestressing tendons.

The end moment must also be accounted for in the beam shown in Fig. 19.2*d*, in which a parabolic tendon is used that does not pass through the concrete centroid at the ends of the span. In this case, a uniformly distributed upward load plus end anchorage forces are produced, as shown in Fig. 19.2*b*, but in addition, the end moments $M = Pe \cos \theta$ must be accounted for.

It may be evident that for any arrangement of applied loads, a tendon profile can be selected so that the equivalent loads acting on the beam from the tendon are just equal and opposite to the applied loads. The result would be a state of pure compressive stress in the concrete, as discussed in somewhat different terms in reference to stress control and Fig. 19.1*e*. An advantage of the equivalent load concept is that it leads the designer to select what is probably the best tendon profile for a particular loading.

c. Prestressed Concrete as a Variation of Reinforced Concrete

In the descriptions of the effects of prestressing in Sections 19.2a and b, it was implied that the prestress force remained constant as the vertical load was introduced, that the concrete responded elastically, and that no concrete cracking occurred. These conditions may prevail up to about the service load level, but if the loads should be increased much beyond that, flexural tensile stresses will eventually exceed the modulus of rupture and cracks will form. Loads, however, can usually be increased much beyond the cracking load in well-designed prestressed beams, and

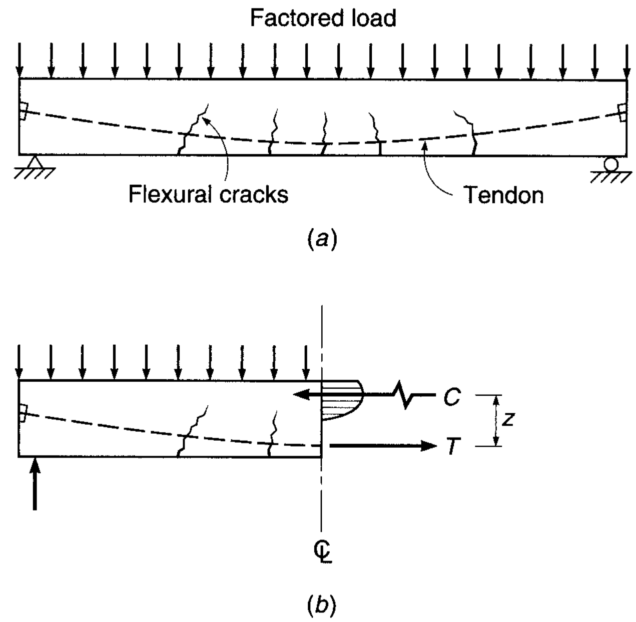

FIGURE 19.3
Prestressed concrete beam at load near flexural failure: (*a*) beam with factored load applied; (*b*) equilibrium of forces on left half of beam.

depending on the level of prestress, the beam response at service load may vary from uncracked, to minor cracking, to fully cracked, as occurs for an ordinary reinforced concrete beam.

Eventually both the steel and concrete at the cracked section will be stressed into the inelastic range. The condition at incipient failure is shown in Fig. 19.3, which shows a beam carrying a *factored load* equal to some multiple of the expected service load. The beam undoubtedly would be in a partially cracked state; a possible pattern of flexural cracking is shown in Fig. 19.3*a*.

At the maximum moment section, only the concrete in compression is effective, and all of the tension is taken by the steel. The external moment from the applied loads is resisted by the internal force couple $Cz = Tz$. The behavior at this stage is almost identical to that of an ordinary reinforced concrete beam at overload. The main difference is that the very high strength steel used must be *prestrained* before loads are applied to the beam; otherwise, the high steel stresses would produce excessive concrete cracking and large beam deflections.

Each of the three viewpoints described—concrete stress control, equivalent loads, and reinforced concrete using prestrained steel—is useful in the analysis and design of prestressed concrete beams, and none of the three is sufficient in itself. Neither an elastic stress analysis nor an equivalent load analysis provides information about strength or safety margin. However, the stress analysis is helpful in predicting the extent of cracking, and the equivalent load analysis is often the best way to calculate deflections. Strength analysis is essential to evaluate safety against collapse, but it tells nothing about cracking or deflections of the beam under service conditions.

19.3 SOURCES OF PRESTRESS FORCE

Prestress can be applied to a concrete member in many ways. Perhaps the most obvious method of precompressing is to use jacks reacting against abutments, as shown in Fig. 19.4*a*. Such a scheme has been employed for large projects. Many variations are

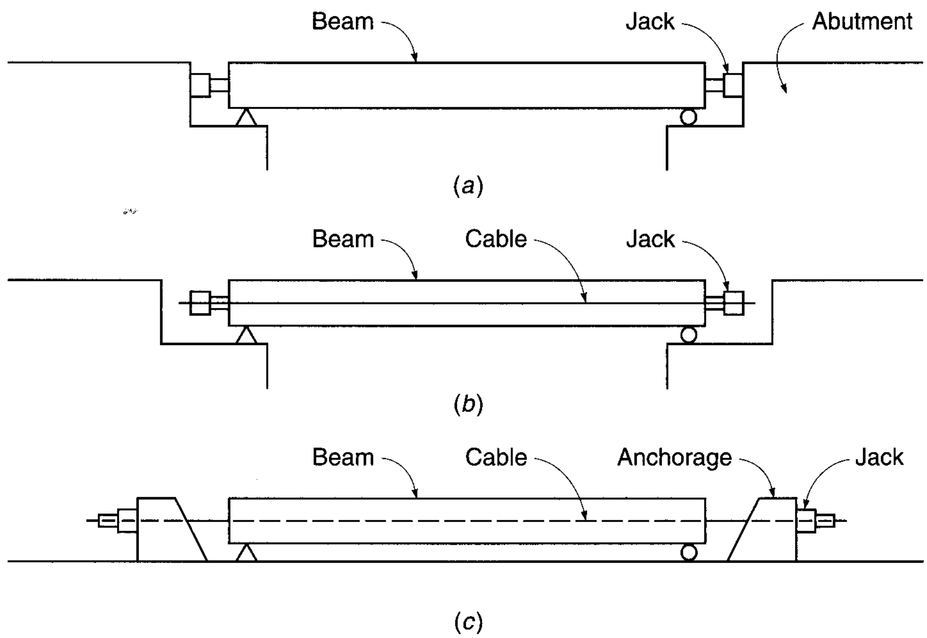

FIGURE 19.4
Prestressing methods: (*a*) post-tensioning by jacking against abutments; (*b*) post-tensioning with jacks reacting against beam; (*c*) pretensioning with tendon stressed between fixed external anchorages.

possible, including replacing the jacks with compression struts after the desired stress in the concrete is obtained or using inexpensive jacks that remain in place in the structure, in some cases with a cement grout used as the hydraulic fluid. The principal difficulty associated with such a system is that even a slight movement of the abutments will drastically reduce the prestress force.

In most cases, the same result is more conveniently obtained by tying the jack bases together with wires or cables, as shown in Fig. 19.4*b*. These wires or cables may be external, located on each side of the beam; more usually they are passed through a hollow conduit embedded in the concrete beam. Usually, one end of the prestressing tendon is anchored, and all of the force is applied at the other end. After reaching the desired prestress force, the tendon is wedged against the concrete and the jacking equipment is removed for reuse. In this type of prestressing, the entire system is self-contained and is independent of relative displacement of the supports.

Another method of prestressing that is widely used is illustrated by Fig. 19.4*c*. The prestressing strands are tensioned between massive abutments in a casting yard prior to placing the concrete in the beam forms. The concrete is placed around the tensioned strands, and after the concrete has attained sufficient strength, the jacking pressure is released. This transfers the prestressing force to the concrete by bond and friction along the strands, chiefly at the outer ends.

It is essential, in all three cases shown in Fig. 19.4, that the beam be supported in such a way as to permit the member to shorten axially without restraint so that the prestressing force can be transferred to the concrete.

Other means for introducing the desired prestressing force have been attempted on an experimental basis. Thermal prestressing can be achieved by preheating the steel by electrical or other means. Anchored against the ends of the concrete beam while in the extended state, the steel cools and tends to contract. The prestress force is developed through the restrained contraction. The use of expanding cement in concrete members has been tried with varying success. The volumetric expansion, restrained by steel strands or by fixed abutments, produces the prestress force.

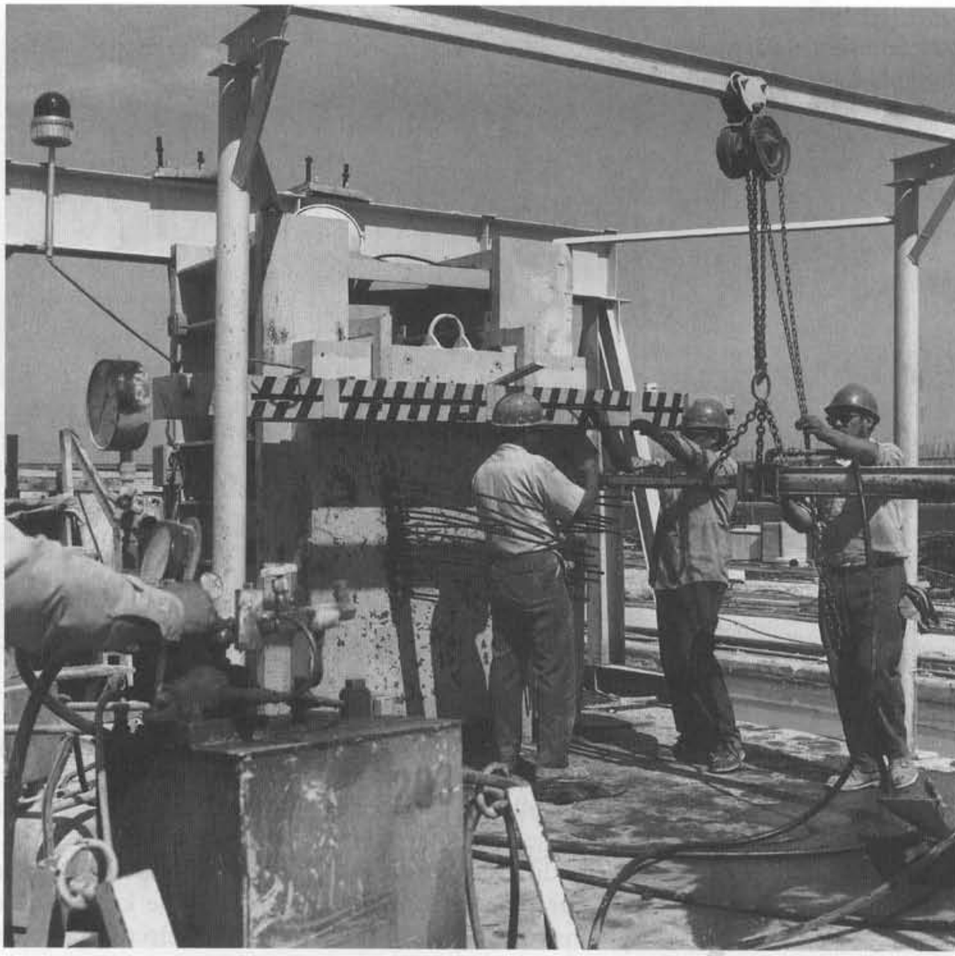

FIGURE 19.5
Massive strand jacking abutment at the end of a long pretensioning bed. (*Courtesy of Concrete Technology Corporation.*)

Most of the patented systems for applying prestress in current use are variations of those shown in Fig. 19.4*b* and *c*. Such systems can generally be classified as *pretensioning* or *post-tensioning* systems. In the case of pretensioning, the tendons are stressed before the concrete is placed, as in Fig. 19.4*c*. This system is well suited for mass production, since casting beds can be made several hundred feet long, the entire length cast at once, and individual beams fabricated to the desired length in a single casting. Figure 19.5 shows workers using a hydraulic jack to tension strands at the anchorage of a long pretensioning bed. Although each tendon is individually stressed in this case, large capacity jacks are often used to tension all strands simultaneously.

In post-tensioned construction, shown in Fig. 19.4*b*, the tendons are tensioned after the concrete is placed and has gained its strength. Usually, a hollow conduit or sleeve is provided in the beam, through which the tendon is passed. In some cases, tendons are placed in the interior of hollow box-section beams. The jacking force is usually applied against the ends of the hardened concrete, eliminating the need for massive abutments. In Fig. 19.6, six tendons, each consisting of many individual strands, are being post-tensioned sequentially using a portable hydraulic jack.

A large number of particular systems, steel elements, jacks, and anchorage fittings have been developed in this country and abroad, many of which differ from each other only in minor details (Refs. 19.1 to 19.8). As far as the designer of prestressed

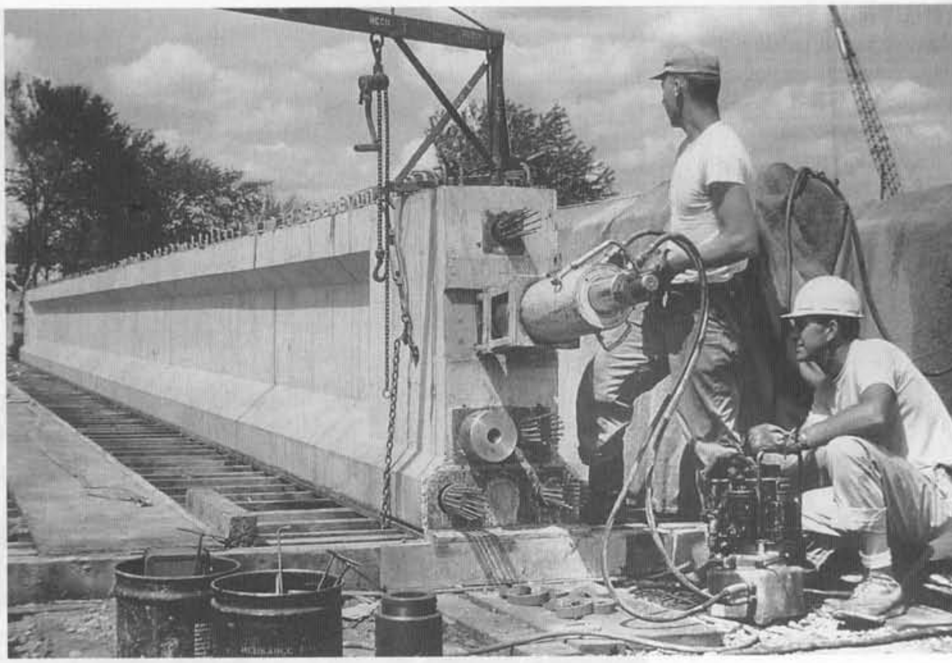

FIGURE 19.6
Post-tensioning a bridge girder using a portable jack to stress multistrand tendons. (*Courtesy of Concrete Technology Corporation.*)

concrete structures is concerned, it is unnecessary and perhaps even undesirable to specify in detail the technique that is to be followed and the equipment to be used. It is frequently best to specify only the magnitude and line of action of the prestress force. The contractor is then free, in bidding the work, to receive quotations from several different prestressing subcontractors, with resultant cost savings. It is evident, however, that the designer must have some knowledge of the details of the various systems contemplated for use, so that in selecting cross-sectional dimensions, any one of several systems can be accommodated.

19.4 PRESTRESSING STEELS

Early attempts at prestressing concrete were unsuccessful because steel with ordinary structural strength was used. The low prestress obtainable in such rods was quickly lost due to shrinkage and creep in the concrete.

Such changes in length of concrete have much less effect on prestress force if that force is obtained using highly stressed steel wires or cables. In Fig. 19.7*a*, a concrete member of length L is prestressed using steel bars with ordinary strength stressed to 24,000 psi. With $E_s = 29 \times 10^6$ psi, the unit strain ϵ_s required to produce the desired stress in the steel of 24,000 psi is

$$\epsilon_s = \frac{\Delta L}{L} = \frac{f_s}{E_s} = \frac{24{,}000}{29 \times 10^6} = 8.0 \times 10^{-4}$$

However, the long-term strain in the concrete due to shrinkage and creep alone, if the prestress force were maintained over a long period, would be on the order of 8.0×10^{-4} and would be sufficient to completely relieve the steel of all stress.

Alternatively, suppose that the beam is prestressed using high-strength steel stressed to 150,000 psi. The elastic modulus of steel does not vary greatly, and the

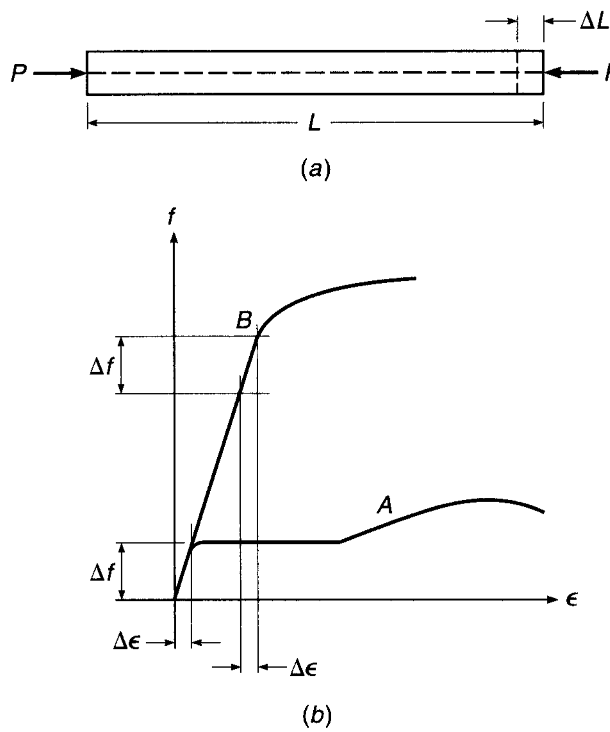

FIGURE 19.7
Loss of prestress due to concrete shrinkage and creep.

same value of 29×10^6 psi will be assumed here. Then in this case, the unit strain required to produce the desired stress in the steel is

$$\epsilon_s = \frac{150{,}000}{29 \times 10^6} = 51.7 \times 10^{-4}$$

If shrinkage and creep strain are the same as before, the net strain in the steel after these losses is

$$\epsilon_{s,\text{net}} = (51.7 - 8.0) \times 10^{-4} = 43.7 \times 10^{-4}$$

and the corresponding stress after losses is

$$f_s = \epsilon_{s,\text{net}} E_s = (43.7 \times 10^{-4})(29 \times 10^6) = 127{,}000 \text{ psi}$$

This represents a stress loss of about 15 percent, compared with 100 percent loss in the beam using ordinary steel. It is apparent that the amount of stress lost because of shrinkage and creep is independent of the original stress in the steel. Therefore, the higher the original stress, the lower the percentage loss. This is illustrated graphically by the stress-strain curves of Fig. 19.7*b*. Curve *A* is representative of ordinary reinforcing bars, with a yield stress of 60,000 psi, while curve *B* represents high tensile steel, with a tensile strength of 270,000 psi. The stress change Δf resulting from a certain change in strain $\Delta\epsilon$ is seen to have much less effect when high steel stress levels are attained. Prestressing of concrete is therefore practical only when steels of very high strength are used.

Prestressing steel is most commonly used in the form of individual wires, stranded cable (strands) made up of seven wires, and alloy-steel bars. The physical properties of these have been discussed in Section 2.16, and typical stress-strain curves appear in Fig. 2.16. Virtually all strands in use are low-relaxation (Section 2.16c).

TABLE 19.1
Maximum permissible stresses in prestressing steel

1. Due to tendon jacking force but not greater than the lesser of $0.80f_{pu}$ and the maximum value recommended by the manufacturer of the prestressing steel or anchorage devices	$0.94f_{py}$
2. Immediately after prestress transfer but not greater than $0.74f_{pu}$	$0.82f_{py}$
3. Post-tensioning tendons, at anchorage devices and couplers, immediately after tendon anchorage	$0.70f_{pu}$

The tensile stress permitted by ACI Code 18.5 in prestressing wires, strands, or bars is dependent upon the stage of loading. When the jacking force is first applied, a maximum stress of $0.80f_{pu}$ or $0.94f_{py}$ is allowed, whichever is smaller, where f_{pu} is the tensile strength of the steel and f_{py} is the yield strength. Immediately after transfer of prestress force to the concrete, the permissible stress is $0.74f_{pu}$ or $0.82f_{py}$, whichever is smaller (except at post-tensioning anchorages where the stress is limited to $0.70f_{pu}$). The justification for a higher allowable stress during the stretching operation is that the steel stress is known quite precisely at this stage. Hydraulic jacking pressure and total steel strain are quantities that are easily measured, and quality control specifications require correlation of load and deflection at jacking (Ref. 19.9). In addition, if an accidentally deficient tendon should break, it can be replaced; in effect, the tensioning operation is a performance test of the material. The lower values of allowable stress apply after elastic shortening of the concrete, frictional loss, and anchorage slip have taken place. The steel stress is further reduced during the life of the member due to shrinkage and creep in the concrete and relaxation in the steel. ACI allowable stresses in prestressing steels are summarized in Table 19.1.

The strength and other characteristics of prestressing wire, strands, and bars vary somewhat between manufacturers, as do methods of grouping tendons and anchoring them. Typical information is given for illustration in Table A.15 of Appendix A and in Refs. 19.1 to 19.8.

19.5 CONCRETE FOR PRESTRESSED CONSTRUCTION

Ordinarily, concrete of substantially higher compressive strength is used for prestressed structures than for those constructed of ordinary reinforced concrete. Most prestressed construction in the United States at present is designed for a compressive strength above 5000 psi. There are several reasons for this:

1. High-strength concrete normally has a higher modulus of elasticity (see Fig. 2.3). This means a reduction in initial elastic strain under application of prestress force and a reduction in creep strain, which is approximately proportional to elastic strain. This results in a reduction in loss of prestress.
2. In post-tensioned construction, high bearing stresses result at the ends of beams where the prestressing force is transferred from the tendons to anchorage fittings, which bear directly against the concrete. This problem can be met by increasing the size of the anchorage fitting or by increasing the bearing capacity of the concrete by increasing its compressive strength. The latter is usually more economical.
3. In pretensioned construction, where transfer by bond is customary, the use of high-strength concrete will permit the development of higher bond stresses.

TABLE 19.2
Permissible stresses in concrete in prestressed flexural members

Condition	Class U	Class T	Class C*
a. Extreme fiber stress in compression immediately after transfer (except as in b)	$0.60f'_{ci}$	$0.60f'_{ci}$	$0.60f'_{ci}$
b. Extreme fiber stress in compression at ends of simply supported members	$0.70f'_{ci}$	$0.70f'_{ci}$	$0.70f'_{ci}$
c. Extreme fiber stress in tension immediately after transfer (except as in d)	$3\sqrt{f'_{ci}}$	$3\sqrt{f'_{ci}}$	$3\sqrt{f'_{ci}}$
d. Extreme fiber stress in tension immediately after transfer at the end of simply supported members†	$6\sqrt{f'_{ci}}$	$6\sqrt{f'_{ci}}$	$6\sqrt{f'_{ci}}$
e. Extreme fiber stress in compression due to prestress plus sustained load	$0.45f'_c$	$0.45f'_c$	—
f. Extreme fiber stress in compression due to prestress plus total load	$0.60f'_c$	$0.60f'_c$	—
g. Extreme fiber stress in tension f_t in precompressed tensile zone under service load	$\leq 7.5\sqrt{f'_c}$	$>7.5\sqrt{f'_c}$ and $\leq 12\sqrt{f'_c}$	—

* There are no service stress requirements for Class C.

† When computed tensile stresses exceed these values, bonded auxiliary prestressed or nonprestressed reinforcement shall be provided in the tensile zone to resist the total tensile force in the concrete computed with the assumption of an uncracked section.

4. A substantial part of the prestressed construction in the United States is precast, with the concrete mixed, placed, and cured under carefully controlled conditions that facilitate obtaining higher strengths.

The strain characteristics of concrete under short-term and sustained loads assume an even greater importance in prestressed structures than in reinforced concrete structures because of the influence of strain on loss of prestress force. Strains due to stress, together with volume changes due to shrinkage and temperature changes, may have considerable influence on prestressed structures. In this connection, it is suggested that the reader review Sections 2.8 to 2.11, which discuss in some detail the compressive and tensile strengths of concrete under short-term and sustained loads and the changes in concrete volume that occur due to shrinkage and temperature change.

As for prestressing steels, the allowable stresses in the concrete, according to ACI Code 18.4, depend upon the stage of loading and the behavior expected of the member. ACI Code 18.3.3 defines three classifications of behavior, depending on the extreme fiber stress f_t at service load in the precompressed tensile zone. The three classifications are U, T, and C. Class U flexural members are assumed to behave as uncracked members. Class T members represent a transition between uncracked and cracked flexural members, while Class C members are assumed to behave as cracked flexural members. Permissible stresses for these three classifications are given in Table 19.2.

In Table 19.2, f'_{ci} is the compressive strength of the concrete at the time of initial prestress, and f'_c the specified compressive strength of the concrete. In parts e and f of Table 19.2, *sustained load* is any part of the service load that will be sustained for a sufficient period of time to cause significant time-dependent deflections, whereas *total load* refers to the total service load, a part of which may be transient or temporary live load. Thus, sustained load would include dead load and may or may not include service live load, depending on its duration. If the live load duration is short or intermittent, the higher limit of part f is permitted.

Two-way slabs are designated as Class U flexural members with f_t limited to values $\leq 6\sqrt{f'_c}$. Class C flexural members have no service level stress requirements but must satisfy strength and serviceability requirements. Service load stress calculations are computed based on uncracked section properties for Class U and T flexural members and on the cracked section properties for Class C members.

19.6 ELASTIC FLEXURAL ANALYSIS

It has been noted earlier in this text that the design of concrete structures may be based either on providing sufficient strength, which would be used fully only if the expected loads were increased by an overload factor, or on keeping material stresses within permissible limits when actual service loads act. In the case of ordinary reinforced concrete members, strength design is used. Members are proportioned on the basis of strength requirements and then checked for satisfactory service load behavior, notably with respect to deflection and cracking. The design is then modified if necessary.

Class C members are principally designed based on strength. Class U and T members, however, are proportioned so that stresses in the concrete and steel at actual service loads are within permissible limits. These limits are a fractional part of the actual capacities of the materials. There is some logic to this approach, since an important objective of prestressing is to improve the performance of members at service loads. Consequently, service load requirements often control the amount of prestress force used in Class U and Class T members. Design based on service loads may usually be carried out assuming elastic behavior of both the concrete and the steel, since stresses are relatively low in each.

Regardless of the starting point chosen for the design, a structural member must be satisfactory at all stages of its loading history. Accordingly, prestressed members proportioned on the basis of permissible stresses must also be checked to ensure that sufficient strength is provided should overloads occur, and deflection and cracking under service loads should be investigated. Consistent with most U.S. practice, in this text the design of prestressed concrete beams will start with a consideration of stress limits, after which strength and other properties will be checked.

It is convenient to think of prestressing forces as a system of external forces acting on a concrete member, which must be in equilibrium under the action of those forces. Figure 19.8*a* shows a simple-span prestressed beam with curved tendons, typical of many post-tensioned members. The portion of the beam to the left of a vertical cutting plane *x-x* is taken as a free body, with forces acting as shown in Fig. 19.8*b*. The force P at the left end is exerted on the concrete through the tendon anchorage, while the force P at the cutting plane *x-x* results from combined shear and normal stresses acting at the concrete surface at that location. The direction of P is tangent to the curve of the tendon at each location. Note the presence of the force N, acting on the concrete from the tendon, due to tendon curvature. This force will be distributed in some manner along the length of the tendon, the exact distribution depending upon the tendon profile. Its resultant and the direction in which the resultant acts can be found from the force diagram of Fig. 19.8*c*.

It is convenient when working with the prestressing force P to divide it into its components in the horizontal and vertical directions. The horizontal component (Fig. 19.8*d*) is $H = P \cos \theta$, and the vertical component is $V = H \tan \theta = P \sin \theta$, where θ is the angle of inclination of the tendon centroid at the particular section. Since the slope angle is normally quite small, the cosine of θ is very close to unity and it is sufficient for most calculations to take $H = P$.

The magnitude of the prestress force is not constant. The *jacking force* P_j is immediately reduced to what is termed the *initial prestress force* P_i because of elastic shortening of the concrete upon transfer, slip of the tendon as the force is transferred

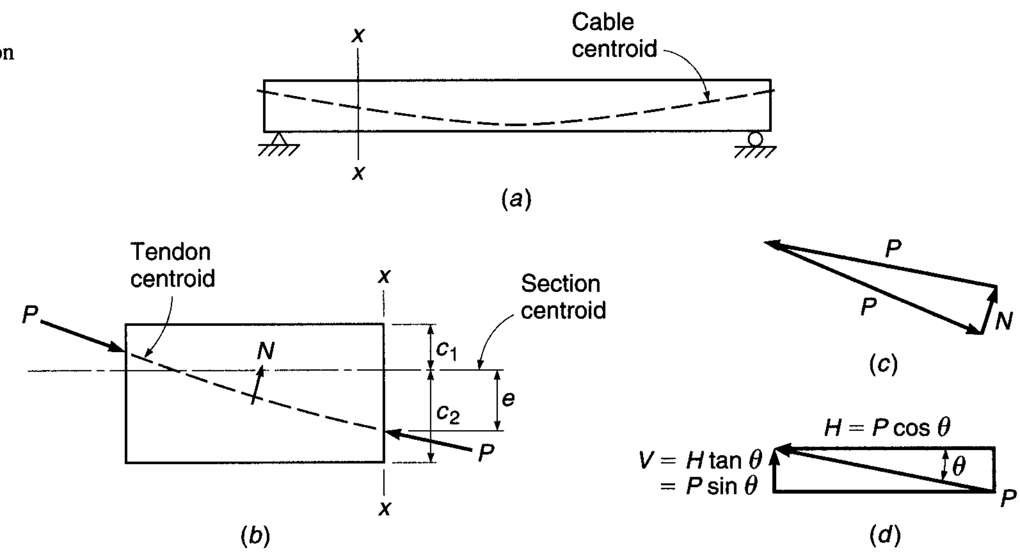

FIGURE 19.8
Prestressing forces acting on concrete.

from the jacks to the beam ends, and loss due to friction between the tendon and the concrete (post-tensioning) or between the tendon and cable alignment devices (pretensioning). There is a further reduction of force from P_i to the *effective prestress* P_e, occurring over a long period of time at a gradually decreasing rate, because of concrete creep under the sustained prestress force, concrete shrinkage, and relaxation of stress in the steel. Methods for predicting losses will be discussed in Section 19.13. Of primary interest to the designer are the initial prestress P_i immediately after transfer and the final or effective prestress P_e after all losses.

In developing elastic equations for flexural stress, the effects of prestress force, self-weight moment, and dead and live load moments are calculated separately, and the separate stresses are superimposed. When the initial prestress force P_i is applied with an eccentricity e below the centroid of the cross section with area A_c and top and bottom fiber distances c_1 and c_2, respectively, it causes the compressive stress $-P_i/A_c$ and the bending stresses $+P_iec_1/I_c$ and $-P_iec_2/I_c$ in the top and bottom fibers, respectively (compressive stresses are designated as negative, tensile stresses as positive), as shown in Fig. 19.9*a*. Then, at the top fiber, the stress is

$$f_1 = -\frac{P_i}{A_c} + \frac{P_iec_1}{I_c} = -\frac{P_i}{A_c}\left(1 - \frac{ec_1}{r^2}\right) \tag{19.1a}$$

and at the bottom fiber

$$f_2 = -\frac{P_i}{A_c} - \frac{P_iec_2}{I_c} = -\frac{P_i}{A_c}\left(1 + \frac{ec_2}{r^2}\right) \tag{19.1b}$$

where r is the radius of gyration of the concrete section. Normally, as the eccentric prestress force is applied, the beam deflects upward. The beam self-weight w_o then causes additional moment M_o to act, and the net top and bottom fiber stresses become

$$f_1 = -\frac{P_i}{A_c}\left(1 - \frac{ec_1}{r^2}\right) - \frac{M_oc_1}{I_c} \tag{19.2a}$$

$$f_2 = -\frac{P_i}{A_c}\left(1 + \frac{ec_2}{r^2}\right) + \frac{M_oc_2}{I_c} \tag{19.2b}$$

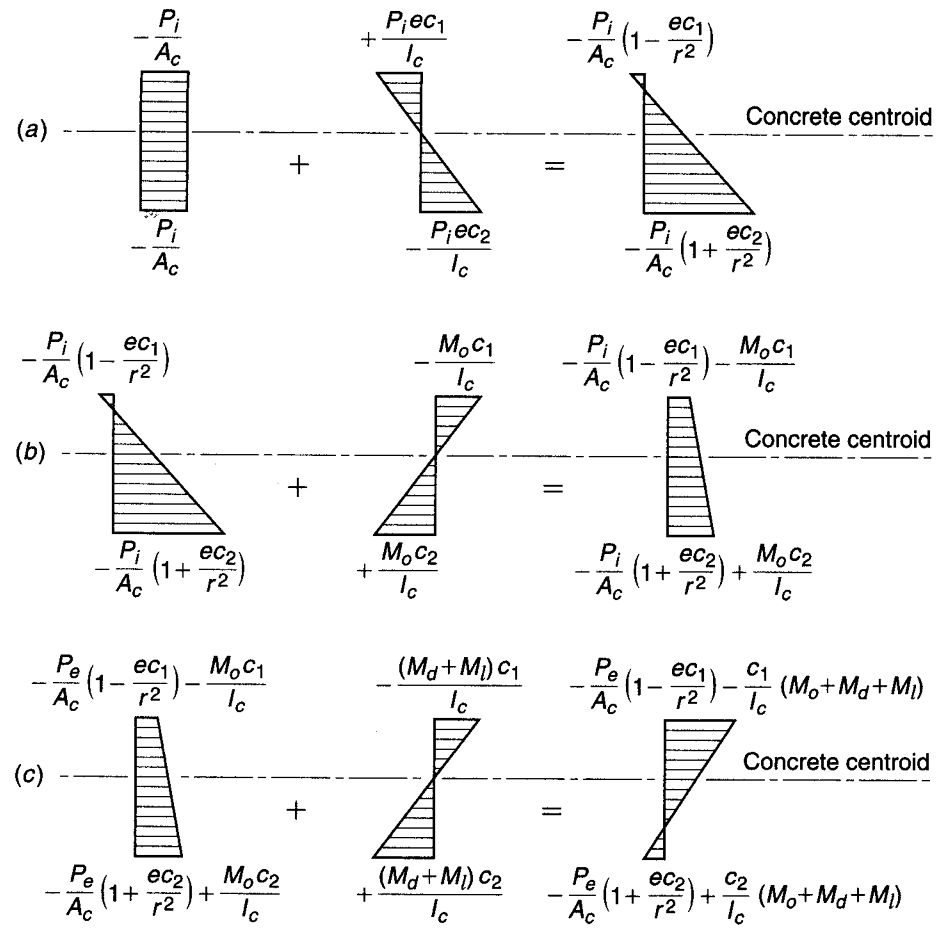

FIGURE 19.9
Concrete stress distributions in beams: (*a*) effect of prestress; (*b*) effect of prestress plus self-weight of beam; (*c*) effect of prestress, self-weight, and external dead and live service loads.

as shown in Fig. 19.9*b*. At this stage, time-dependent losses due to shrinkage, creep, and relaxation commence, and the prestressing force gradually decreases from P_i to P_e. It is usually acceptable to assume that all such losses occur prior to the application of service loads, since the concrete stresses at service loads will be critical after losses, not before. Accordingly, the stresses in the top and bottom fiber, with P_e and beam load acting, become

$$f_1 = -\frac{P_e}{A_c}\left(1 - \frac{ec_1}{r^2}\right) - \frac{M_o c_1}{I_c} \tag{19.3a}$$

$$f_2 = -\frac{P_e}{A_c}\left(1 + \frac{ec_2}{r^2}\right) + \frac{M_o c_2}{I_c} \tag{19.3b}$$

When full service loads (dead load in addition to self-weight of the beam, plus service live load) are applied, the stresses are

$$f_1 = -\frac{P_e}{A_c}\left(1 - \frac{ec_1}{r^2}\right) - \frac{(M_o + M_d + M_l)c_1}{I_c} \tag{19.4a}$$

$$f_2 = -\frac{P_e}{A_c}\left(1 + \frac{ec_2}{r^2}\right) + \frac{(M_o + M_d + M_l)c_2}{I_c} \tag{19.4b}$$

as shown in Fig. 19.9*c*.

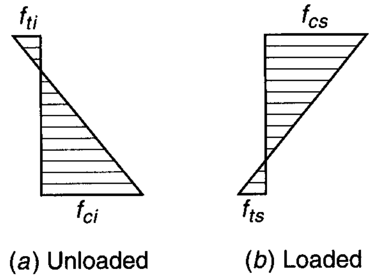

FIGURE 19.10
Stress limits: (*a*) unloaded beam, with initial prestress plus self-weight; (*b*) loaded beam, with effective prestress, self-weight, and full service load.

It is necessary, in reviewing the adequacy of a beam (or in designing a beam on the basis of permissible stresses), that the stresses in the extreme fibers remain within specified limits under any combination of loadings that can occur. Normally, the stresses at the section of maximum moment, in a properly designed beam, must stay within the limit states defined by the distributions shown in Fig. 19.10 as the beam passes from the unloaded stage (P_i plus self-weight) to the loaded stage (P_e plus full service loads). In the figure, f_{ci} and f_{ti} are the permissible compressive and tensile stresses, respectively, in the concrete immediately after transfer, and f_{cs} and f_{ts} are the permissible compressive and tensile stresses at service loads (see Table 19.2).

In calculating the section properties A_c, I_c, etc., to be used in the above equations, it is relevant that, in post-tensioned construction, the tendons are usually grouted in the conduits after tensioning. Before grouting, stresses should be based on the net section with holes deducted. After grouting, the transformed section should be used with holes considered filled with concrete and with the steel replaced with an equivalent area of concrete. However, it is satisfactory, unless the holes are quite large, to compute section properties on the basis of the gross concrete section. Similarly, while in pretensioned beams the properties of the transformed section should be used, it makes little difference if calculations are based on properties of the gross concrete section.†

It is useful to establish the location of the upper and lower *kern points* of a cross section. These are defined as the limiting points inside which the prestress force resultant may be applied without causing tension anywhere in the cross section. Their locations are obtained by writing the expression for the tensile fiber stress due to application of an eccentric prestress force acting alone and setting this expression equal to zero to solve for the required eccentricity. In Fig. 19.11, to locate the upper kern-point distance k_1 from the neutral axis, let the prestress force resultant P act at that point. Then the bottom fiber stress is

$$f_2 = -\frac{P}{A_c}\left(1 + \frac{ec_2}{r^2}\right) = 0$$

Thus, with

$$1 + \frac{ec_2}{r^2} = 0$$

one obtains the corresponding eccentricity

$$e = k_1 = -\frac{r^2}{c_2} \qquad (19.5a)$$

† ACI Code 18.2.6 contains the following provision: "In computing section properties prior to bonding of prestressing steel, the effect of loss of area due to open ducts shall be considered." It is noted in ACI Commentary 18.2.6 that "If the effect of the open duct area on design is deemed negligible, section properties may be based on total area. In post-tensioned members after grouting and in pretensioned members, section properties may be based on effective sections using transformed areas of bonded prestressing steel and nonprestressed gross sections, or net sections."

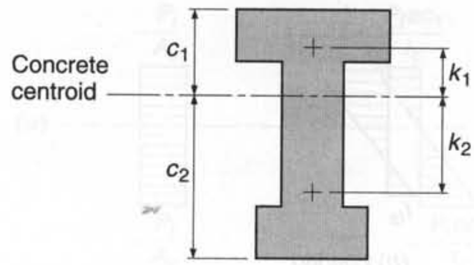

FIGURE 19.11
Location of kern points.

Similarly, the lower kern-point distance k_2 is

$$k_2 = \frac{r^2}{c_1} \tag{19.5b}$$

The region between these two limiting points is known as the *kern*, or in some cases the *core*, of the section.

EXAMPLE 19.1

Pretensioned I beam with constant eccentricity. A simply supported symmetrical I beam shown in cross section in Fig. 19.12*a* will be used on a 40 ft simple span. It has the following section properties

Moment of inertia: $I_c = 12{,}000 \text{ in}^4$
Concrete area: $A_c = 176 \text{ in}^2$
Radius of gyration: $r^2 = 68.2 \text{ in}^2$
Section modulus: $S = 1000 \text{ in}^3$
Self-weight: $w_o = 0.183$ kips/ft

and is to carry a superimposed dead plus live load (considered "sustained," not short-term) of 0.750 kips/ft in addition to its own weight. The beam will be pretensioned with multiple seven-wire strands with the centroid at a constant eccentricity of 7.91 in. The prestress force P_i immediately after transfer will be 158 kips; after time-dependent losses, the force will reduce to $P_e = 134$ kips. The specified compressive strength of the concrete $f'_c = 5000$ psi, and at the time of prestressing the strength will be $f'_{ci} = 3750$ psi. Calculate the concrete flexural stresses at the midspan section of the beam at the time of transfer, and after all losses with full service load in place. Compare with ACI allowable stresses for a Class U member.

SOLUTION. Stresses in the concrete along the length of the beam resulting from the initial prestress force of 158 kips may be found by Eqs. (19.1*a*) and (19.1*b*):

$$f_1 = -\frac{158{,}000}{176}\left(1 - \frac{7.91 \times 12}{68.2}\right) = +352 \text{ psi}$$

$$f_2 = -\frac{158{,}000}{176}\left(1 + \frac{7.91 \times 12}{68.2}\right) = -2147 \text{ psi}$$

The self-weight of the beam causes the immediate superposition of a moment at midspan of

$$M_o = 0.183 \times \frac{40^2}{8} = 36.6 \text{ ft-kips}$$

and corresponding stresses of $M_oc/I = 36{,}600 \times 12/1000 = 439$ psi, so that the net stresses at the top and bottom of the concrete section at midspan due to initial prestress and self-weight, from Eqs. (19.2*a*) and (19.2*b*), are

$$f_1 = +352 - 439 = -87 \text{ psi}$$

$$f_2 = -2147 + 439 = -1708 \text{ psi}$$

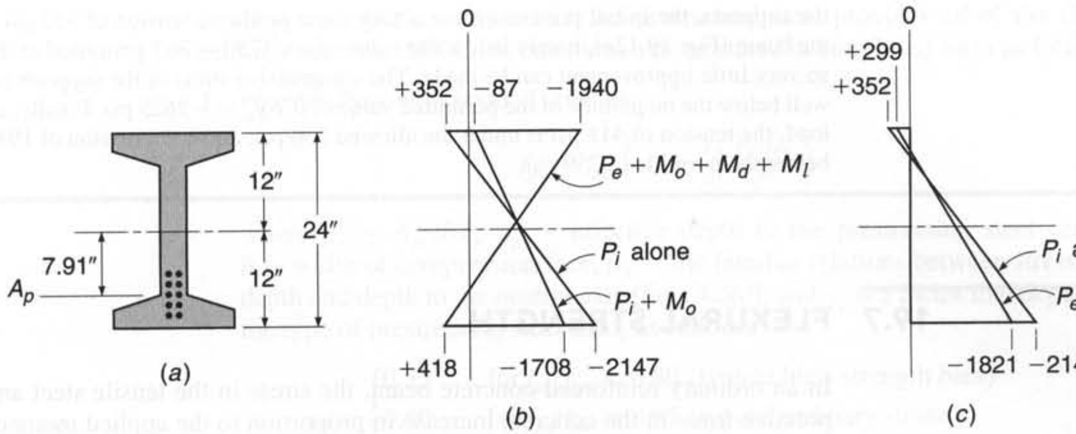

FIGURE 19.12
Pretensioned I beam. Design example: (*a*) cross section, (*b*) stresses at midspan (psi), (*c*) stresses at ends (psi).

After losses, the prestress force is reduced to 134 kips, and the concrete stresses at midspan due to that force plus self-weight are

$$f_1 = +352 \times \frac{134}{158} - 439 = 140 \text{ psi}$$

$$f_2 = -2147 \times \frac{134}{158} + 439 = -1382 \text{ psi}$$

and stresses at the end of the beam are

$$f_1 = +352\left(\frac{134}{158}\right) = 299$$

$$f_2 = -2147\left(\frac{134}{158}\right) = 1821$$

The superimposed load of 0.750 kip/ft produces a midspan moment of $M_d + M_l = 0.750 \times 40^2/8 = 150$ ft-kips and the corresponding stresses of $150{,}000 \times 12/1000 = 1800$ psi in compression and tension at the top and bottom of the beam, respectively. Thus, the service load stresses at the top and bottom faces at midspan are

$$f_1 = -140 - 1800 = -1940 \text{ psi}$$

$$f_2 = -1382 + 1800 = +418 \text{ psi}$$

Concrete stresses at midspan are shown in Fig. 19.12*b* and at the beam end in Fig. 19.12*c*. According to the ACI Code (see Table 19.2), the stresses permitted in the concrete are

$$\text{Tension at transfer: } f_{ti} = 3\sqrt{3750} = +184 \text{ psi}$$

$$\text{Compression at transfer: } f_{ci} = 0.60 \times 3750 = -2250 \text{ psi}$$

$$\text{Tension at service load: } f_{ts} = 7.5\sqrt{5000} = +530 \text{ psi}$$

$$\text{Compression at service load: } f_{cs} = 0.45 \times 5000 = -2250 \text{ psi}$$

At the initial stage, with prestress plus self-weight in place, the actual compressive stress of 1708 psi is well below the limit of 2250 psi, and no tension acts at the top, although 184 psi is allowed. While more prestress force or more eccentricity might be suggested to more fully utilize the section, to attempt to do so in this beam, with constant eccentricity, would violate limits at the support, where self-weight moment is zero. It is apparent that at the supports, the initial prestress force acting alone produces tension of 352 psi at the top of the beam (Fig. 19.12*c*), barely below the value of $6\sqrt{3750} = 367$ permitted at the beam end, so very little improvement can be made. The compressive stress at the supports is -2147 psi, well below the magnitude of the permitted value of $0.70f'_{ci} = -2625$ psi. Finally, at full service load, the tension of 418 psi is under the allowed 530 psi, and compression of 1940 psi is well below the permitted 2250 psi.

19.7 FLEXURAL STRENGTH

In an ordinary reinforced concrete beam, the stress in the tensile steel and the compressive force in the concrete increase in proportion to the applied moment up to and somewhat beyond service load, with the distance between the two internal stress resultants remaining essentially constant. In contrast to this behavior, in a prestressed beam, increased moment is resisted by a proportionate increase in the distance between the compressive and tensile resultant forces, the compressive resultant moving upward as the load is increased. The magnitude of the internal forces remains nearly constant up to, and usually somewhat beyond, service loads.

This situation changes drastically upon flexural tensile cracking of the prestressed beam. When the concrete cracks, there is a sudden increase in the stress in the steel as the tension that was formerly carried by the concrete is transferred to it. After cracking, the prestressed beam behaves essentially as an ordinary reinforced concrete beam. The compressive resultant cannot continue to move upward indefinitely, and increasing moment must be accompanied by a nearly proportionate increase in steel stress and compressive force. The strength of a prestressed beam can, therefore, be predicted by the same methods developed for ordinary reinforced concrete beams, with modifications to account for (a) the different shape of the stress-strain curve for prestressing steel, as compared with that for ordinary reinforcement, and (b) the tensile strain already present in the prestressing steel before the beam is loaded.

Highly accurate predictions of the flexural strength of prestressed beams can be made based on a *strain compatibility analysis* that accounts for these factors in a rational and explicit way (Ref. 19.1). For ordinary design purposes, certain approximate relationships have been derived. ACI Code 18.7 and the accompanying ACI Commentary 18.7 include approximate equations for flexural strength that will be summarized in the following paragraphs.

a. Stress in the Prestressed Steel at Flexural Failure

When a prestressed concrete beam fails in flexure, the prestressing steel is at a stress f_{ps} that is higher than the effective prestress f_{pe} but below the tensile strength f_{pu}. If the effective prestress $f_{pe} = P_e/A_{ps}$ is not less than $0.50f_{pu}$, ACI Code 18.7.2 permits use of certain approximate equations for f_{ps}. These equations appear quite complex as they are presented in the ACI Code, mainly because they are written in general form to account for differences in type of prestressing steel and to apply to beams in which nonprestressed bar reinforcement may be included in the flexural tension zone or the compression region or both. Separate equations are given for members with bonded tendons and unbonded tendons because, in the latter case, the increase in steel stress at the maximum moment section as the beam is overloaded is much less than if the steel were bonded throughout its length.

For the basic case, in which the prestressed steel provides all of the flexural reinforcement, the ACI Code equations can be stated in simplified form as follows:

1. For members with bonded tendons:

$$f_{ps} = f_{pu}\left(1 - \frac{\gamma_p}{\beta_1}\frac{\rho_p f_{pu}}{f_c'}\right) \tag{19.6}$$

where $\rho_p = A_{ps}/bd_p$, d_p = effective depth to the prestressing steel centroid, b = width of compression face, β_1 = the familiar relations between stress block depth and depth to the neutral axis [Eq. (3.26)], and γ_p is a factor that depends on the type of prestressing steel used, as follows:

$$\gamma_p = \begin{cases} 0.55 & \text{for } f_{py}/f_{pu} \geq 0.80 \text{ (typical high-strength bars)} \\ 0.40 & \text{for } f_{py}/f_{pu} \geq 0.85 \text{ (typical ordinary strand)} \\ 0.28 & \text{for } f_{py}/f_{pu} \geq 0.90 \text{ (typical low-relaxation strand)} \end{cases}$$

2. For members with unbonded tendons and with a span-depth ratio of 35 or less (this includes most beams),

$$f_{ps} = f_{pe} + 10{,}000 + \frac{f_c'}{100\rho_p} \tag{19.7}$$

but not greater than f_{py} and not greater than f_{pe} + 60,000 psi.

3. For members with unbonded tendons and with span-depth ratio greater than 35 (applying to many slabs),

$$f_{ps} = f_{pe} + 10{,}000 + \frac{f_c'}{300\rho_p} \tag{19.8}$$

but not greater than f_{py} and not greater than f_{pe} + 30,000 psi.

b. Nominal Flexural Strength and Design Strength

With the stress in the prestressed tensile steel when the member fails in flexure established by Eq. (19.6), (19.7), or (19.8), the nominal flexural strength can be calculated by methods and equations that correspond directly with those used for ordinary reinforced concrete beams. For rectangular cross sections, or flanged sections such as I or T beams in which the stress block depth is equal to or less than the average flange thickness, the nominal flexural strength is

$$M_n = A_{ps}f_{ps}\left(d_p - \frac{a}{2}\right) \tag{19.9}$$

where

$$a = \frac{A_{ps}f_{ps}}{0.85f_c'b} \tag{19.10}$$

Equations (19.9) and (19.10) can be combined as follows:

$$M_n = \rho_p f_{ps} b d_p^2\left(1 - 0.588\frac{\rho_p f_{ps}}{f_c'}\right) \tag{19.11}$$

In all cases, the *flexural design strength* is taken equal to ϕM_n, where ϕ is the strength reduction factor for flexure (see Section 19.7c).

If the stress block depth exceeds the average flange thickness, the method for calculating flexural strength is exactly analogous to that used for ordinary reinforced concrete I and T beams. The total prestressed tensile steel area is divided into two parts for computational purposes. The first part A_{pf}, acting at the stress f_{ps}, provides a tensile force to balance the compression in the overhanging parts of the flange. Thus,

$$A_{pf} = 0.85 \frac{f'_c}{f_{ps}}(b - b_w)h_f \tag{19.12}$$

The remaining prestressed steel area

$$A_{pw} = A_{ps} - A_{pf} \tag{19.13}$$

provides tension to balance the compression in the web. The total resisting moment is the sum of the contributions of the two force couples:

$$M_n = A_{pw}f_{ps}\left(d_p - \frac{a}{2}\right) + A_{pf}f_{ps}\left(d_p - \frac{h_f}{2}\right) \tag{19.14a}$$

or

$$M_n = A_{pw}f_{ps}\left(d_p - \frac{a}{2}\right) + 0.85f'_c(b - b_w)h_f\left(d_p - \frac{h_f}{2}\right) \tag{19.14b}$$

where

$$a = \frac{A_{pw}f_{ps}}{0.85f'_c b_w} \tag{19.15}$$

As before, the design strength is taken as ϕM_n, where ϕ is typically 0.90, as discussed in Section 19.7c.

If, after a prestressed beam is designed by elastic methods at service loads, it has inadequate strength to provide the required safety margin under factored load, nonprestressed reinforcement can be added on the tension side and will work in combination with the prestressing steel to provide the needed strength. Such nonprestressed steel, with area A_s, can be assumed to act at its yield stress f_y, to contribute a tension force at the nominal moment of $A_s f_y$. The reader should consult ACI Code 18.7 and ACI Commentary 18.7 for equations for prestressed steel stress at failure and for flexural strength, which are direct extensions of those given above.

c. Limits for Reinforcement

The ACI Code classifies prestressed concrete flexural members as tension-controlled or compression-controlled based on the net tensile strain ϵ_t in the same manner as done for ordinary reinforced concrete beams. Section 3.4d describes the strain distributions and the variation of strength reduction factors associated with limitations on the net tensile strain. Recall that the net tensile strain excludes strains due to creep, shrinkage, temperature, and effective prestress. To maintain a strength reduction factor ϕ of 0.90 and ensure that if flexural failure were to occur, it would be a ductile failure, a net tensile strain of at least 0.005 is required. Due to the complexity of computing net tensile strain in prestressed members, it is easier to perform the check using the c/d_t ratio. From Fig. 3.10a, this simplifies to

$$\frac{c}{d_t} \leq 0.375 \tag{19.16}$$

where d_t is the distance from the extreme compressive fiber to the extreme tensile steel. In many cases, d_t will be the same as d_p, the distance from the extreme compressive fiber to the centroid of the prestressed reinforcement. However, when supplemental nonprestressed steel is used or the prestressing strands are distributed through the depth of the section, d_t will be greater than d_p. If the prestressed beam does not meet the requirements of Eq. (19.16), it may no longer be considered as tension-controlled, and the strength reduction factor ϕ must be determined as shown in Fig. 3.9. If $c/d_t \geq 0.60$, corresponding to $\epsilon_t \leq 0.002$, the section is considered to be *overreinforced*, and alternative equations must be derived for computing the flexural strength (see Ref. 19.1).

It will be recalled that a *minimum tensile reinforcement ratio* is required for ordinary reinforced concrete beams, so that the beams will be safe from sudden failure upon the formation of flexural cracks. Because of the same concern, ACI Code 18.8.2 requires that the total tensile reinforcement in members with bonded prestressed reinforcement be adequate to support a factored load of at least 1.2 times the cracking load of the beam, calculated on the basis of a modulus of rupture of $7.5\sqrt{f_c'}$. A similar requirement is not placed on members with unbonded prestressed reinforcement. Unlike members with bonded reinforcement, which are subject to tendon failure when the concrete cracks and the tensile force in the concrete is suddenly transferred to the bonded steel, abrupt failure does not occur in beams with unbonded tendons because the reinforcement can undergo slip, which distributes the increased strain along the length of the tendon, lowering the magnitude of the increased stress in the tendon.

d. Minimum Bonded Reinforcement

To control cracking in beams and one-way prestressed slabs with *unbonded tendons*, some bonded reinforcement must be added in the form of nonprestressed reinforcing bars, uniformly distributed over the tension zone as close as permissible to the extreme tension fiber. According to ACI Code 18.9.2, the minimum amount of such reinforcement is

$$A_s = 0.004A_{ct} \tag{19.17}$$

where A_{ct} is the area of that part of the cross section between the flexural tension face and the centroid of the gross concrete cross section. ACI Code 18.9.3 provides exceptions for two-way slabs with very low tensile stresses.

EXAMPLE 19.2 **Flexural strength of pretensioned I beam.** The prestressed I beam shown in cross section in Fig. 19.13 is pretensioned using five low relaxation stress-relieved Grade 270 $\frac{1}{2}$ in. diameter strands, carrying effective prestress $f_{pe} = 160$ ksi. Concrete strength is $f_c' = 4000$ psi. Calculate the design strength of the beam.

SOLUTION. The effective prestress in the strands of 160 ksi is well above $0.50 \times 270 = 135$ ksi, confirming that the approximate ACI equations are applicable. The tensile reinforcement ratio is

$$\rho_p = \frac{0.765}{12 \times 17.19} = 0.0037$$

and the steel stress f_{ps} when the beam fails in flexure is found from Eq. (19.6) to be

$$f_{ps} = f_{pu}\left(1 - \frac{\gamma_p}{\beta_1}\frac{\rho_p f_{pu}}{f_c'}\right) = 270\left(1 - \frac{0.28}{0.85}\frac{0.0037 \times 270}{4}\right) = 248 \text{ ksi}$$

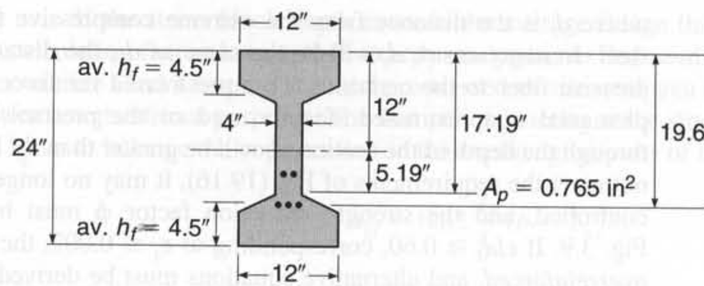

FIGURE 19.13
Post-tensioned beam of Example 19.2.

Next, it is necessary to check whether the stress block depth is greater or less than the average flange thickness of 4.5 in. On the assumption that it is not greater than the flange thickness, Eq. (19.10) is used:

$$a = \frac{A_p f_{ps}}{0.85 f_c' b} = \frac{0.765 \times 248}{0.85 \times 4 \times 12} = 4.65 \text{ in.}$$

It is concluded from this trial calculation that a actually exceeds h_f, so the trial calculation is not valid and equations for flanged members must be used. The steel that acts with the overhanging flanges is found from Eq. (19.12) to be

$$A_{pf} = \frac{0.85 \times 4(12 - 4)4.5}{248} = 0.494 \text{ in}^2$$

and from Eq. (19.13), the steel acting with the web is

$$A_{pw} = 0.765 - 0.494 = 0.271 \text{ in}^2$$

The actual stress block depth is now found from Eq. (19.15):

$$a = \frac{0.271 \times 248}{0.85 \times 4 \times 4} = 4.94 \text{ in.}$$

$$c = \frac{a}{\beta_1} = \frac{4.94}{0.85} = 5.81$$

A check should now be made to determine if the beam can be considered tension-controlled. As shown in Fig. 19.13, d_t = 19.64 in. From Eq. (19.16),

$$\frac{c}{d_t} = \frac{5.81}{17.19} = 0.338$$

This is less than 0.375 for $\epsilon_t \geq 0.005$, confirming that this can be considered to be a tension-controlled prestressed beam, and ϕ = 0.90. The nominal flexural strength, from Eq. (19.14*b*), is

$$\begin{aligned} M_n &= 0.271 \times 248(17.19 - 2.47) + 0.85 \times 4(12 - 4)4.5(17.19 - 2.25) \\ &= 2818 \text{ in-kips} = 235 \text{ ft-kips} \end{aligned}$$

and, finally, the design strength is ϕM_n = 211 ft-kips.

19.8 PARTIAL PRESTRESSING

Early in the development of prestressed concrete, the goal of prestressing was the complete elimination of concrete tensile stress at service load. This kind of design, in which the service load tensile stress limit f_{ts} = 0, is often referred to as *full prestressing*.

While full prestressing offers many advantages over nonprestressed construction, some problems can arise. Heavily prestressed beams, particularly those for which full live load is seldom in place, may have excessively large upward deflection, or camber, which will increase with time because of concrete creep under the eccentric prestress force. Fully prestressed beams may also have a tendency for severe longitudinal shortening, causing large restraint forces unless special provision is made to permit free movement at one end of each span. If shortening is permitted to occur freely, prestress losses due to elastic and creep deformation may be large. Furthermore, if heavily prestressed beams are overloaded to failure, they may fail in a sudden and brittle mode, with little warning before collapse.

Today there is general recognition of the advantages of *partial prestressing*, in which flexural tensile stress and some limited cracking are permitted under full service load. That full load may be infrequently applied. Typically, many beams carry only dead load much of the time, or dead load plus only part of the service live load. Under these conditions, a partially prestressed beam would normally not be subject to flexural tension, and cracks that form occasionally, when the full live load is in place, would close completely when that live load is removed. Controlled cracks prove no more objectionable in prestressed concrete structures than in reinforced concrete structures. With partial prestressing, excessive camber and troublesome axial shortening are avoided. Should overloading occur, there will be ample warning of distress, with extensive cracking and large deflections (Refs. 19.10 to 19.13).

Although the amount of prestressing steel may be reduced in partially prestressed beams compared with fully prestressed beams, a proper safety margin must still be maintained, and to achieve the necessary flexural strength, partially prestressed beams may require additional tensile reinforcement. In fact, partially prestressed beams are often defined as beams in which (1) flexural cracking is permitted at full service load and (2) the main flexural tension reinforcement includes both prestressed and nonprestressed steel. Analysis indicates, and tests confirm, that such nonprestressed steel is fully stressed to f_y at flexural failure.

The ACI Code does not specifically mention partial prestressing but does include the concept explicitly in the classification of flexural members. Class T flexural members require service level stress checks and have maximum allowable tensile stresses above the modulus of rupture. Class C flexural members do not require stress checks at service load but do require crack control checks (Section 19.18). The designations of Class T and Class C flexural members bring the ACI Code into closer agreement with European practice (Refs. 19.13 to 19.15).

The three classes of prestressed flexural members, U, T, and C, provide the designer with considerable flexibility in achieving economical designs. To attain the required strength, supplemental reinforcement in the form of nonprestressed ordinary steel or unstressed prestressing strand may be required. Reinforcing bars are less expensive than high-strength prestressing steel. Strand, however, at twice the cost of ordinary reinforcement, provides 3 times the strength. Labor costs for bar placement are generally similar to those for placing unstressed strand on site. Similarly, the addition of a small number of strands in a plant prestressing bed is often more economical than adding reinforcing bars. The designer may select the service level performance strategy best suited for the project. A criterion that includes no tensile stress under dead load and a tensile stress less than the modulus of rupture at the service live load is possible with Class U and T flexural members, while Class C members use prestressing primarily for deflection control.

The choice of a suitable degree of prestress is governed by a number of factors. These include the nature of the loading (for example, highway or railroad bridges, and storage warehouses), the ratio of live to dead load, the frequency of occurrence of the full service load, and the presence of a corrosive environment.

19.9 FLEXURAL DESIGN BASED ON CONCRETE STRESS LIMITS

As in reinforced concrete, problems in prestressed concrete can be separated generally as analysis problems or design problems. For the former, with the applied loads, the concrete cross section, steel area, and the amount and point of application of the prestress force known, Eqs. (19.1) to (19.4) permit the direct calculation of the resulting concrete stresses. The equations in Section 19.7 will predict the flexural strength. However, if the dimensions of a concrete section, the steel area and centroid location, and the amount of prestress are to be found—given the loads, limiting stresses, and required strength—the problem is complicated by the many interrelated variables.

There are at least three practical approaches to the flexural design of a prestressed concrete member. Some engineers prefer to assume a concrete section, calculate the required prestress force and eccentricities for what will probably be the controlling load stage, then check the stresses at all stages using the preceding equations, and finally check the flexural strength. The trial section is then revised if necessary. If a beam is to be chosen from a limited number of standard shapes, as is often the case for shorter spans and ordinary loads, this procedure is probably best. For longer spans or when customized shapes are used, a more efficient member may result by designing the cross section so that the specified concrete stress limits of Table 19.2 are closely matched. This cross section, close to "ideal" from the limit stress viewpoint, may then be modified to meet functional requirements (e.g., providing a broad top flange for a bridge deck) or to meet strength requirements, if necessary. Equations facilitating this approach will be developed in this section. A third method of design is based on load balancing, using the concept of equivalent loads (see Section 19.2b). A trial section is chosen, after which the prestress force and tendon profile are selected to provide uplift forces as to just balance a specified load. Modifications may then be made, if needed, to satisfy stress limits or strength requirements. This third approach will be developed in Section 19.12.

Notation is established pertaining to the allowable concrete stresses at limiting stages as follows:

f_{ci} = allowable compressive stress immediately after transfer

f_{ti} = allowable tensile stress immediately after transfer

f_{cs} = allowable compressive stress at service load, after all losses

f_{ts} = allowable tensile stress at service load, after all losses

The values of these limit stresses are normally set by specification (see Table 19.2).

a. Beams with Variable Eccentricity

For a typical Class U or T beam in which the tendon eccentricity is permitted to vary along the span, flexural stress distributions in the concrete at the maximum moment section are shown in Fig. 19.14*a*. The eccentric prestress force, having an initial value of P_i, produces the linear stress distribution (1). Because of the upward camber of the beam as that force is applied, the self-weight of the member is immediately introduced, the flexural stresses resulting from the moment M_o are superimposed, and the

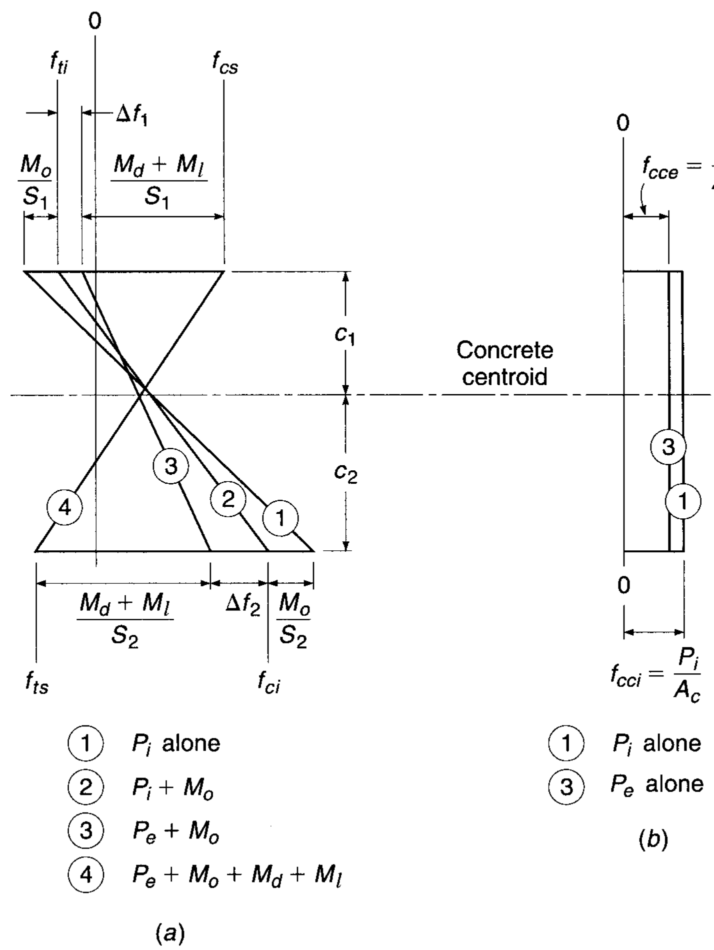

FIGURE 19.14
Flexural stress distributions for beams with variable eccentricity: (*a*) maximum moment section; (*b*) support section.

distribution (2) is the first that is actually attained. At this stage, the tension at the top surface is not to exceed f_{ti}, and the compression at the bottom surface is not to exceed f_{ci}, as shown in Fig. 19.14*a*.

It will be assumed that all the losses occur at this stage, and that the stress distribution changes to distribution (3). The losses produce a reduction of tension in the amount Δf_1 at the top surface and a reduction of compression in the amount Δf_2 at the bottom surface.

As the superimposed dead load moment M_d and the service live load moment M_l are introduced, the associated flexural stresses, when superimposed on stresses already present, produce distribution (4). At this stage, the tension at the bottom surface must not be greater than f_{ts}, and the compression at the top of the section must not exceed f_{cs} as shown.

The requirements for the sections moduli S_1 and S_2 with respect to the top and bottom surfaces, respectively, are

$$S_1 \geq \frac{M_d + M_l}{f_{1r}} \tag{a}$$

$$S_2 \geq \frac{M_d + M_l}{f_{2r}} \tag{b}$$

where the available stress ranges f_{1r} and f_{2r} at the top and bottom face can be calculated from the specified stress limits f_{ti}, f_{cs}, f_{ts}, and f_{ci}, once the stress changes Δf_1 and Δf_2, associated with prestress loss are known.

The effectiveness ratio R accounts for the loss of prestress and is defined as

$$R = \frac{P_e}{P_i} \tag{19.18}$$

Thus, the loss in prestress force is

$$P_i - P_e = (1 - R)P_i \tag{19.19}$$

The changes in stress at the top and bottom faces, Δf_1 and Δf_2, as losses occur, are equal to $(1 - R)$ times the corresponding stresses due to the initial prestress force P_i *acting alone*:

$$\Delta f_1 = (1 - R)\left(f_{ti} + \frac{M_o}{S_1}\right) \tag{c}$$

$$\Delta f_2 = (1 - R)\left(-f_{ci} + \frac{M_o}{S_2}\right) \tag{d}$$

where Δf_1 is a reduction of tension at the top surface and Δf_2 is a reduction of compression at the bottom surface.† Thus, the stress ranges available as the superimposed load moments $M_d + M_l$ are applied are

$$\begin{aligned} f_{1r} &= f_{ti} - \Delta f_1 - f_{cs} \\ &= Rf_{ti} - (1 - R)\frac{M_o}{S_1} - f_{cs} \end{aligned} \tag{e}$$

and

$$\begin{aligned} f_{2r} &= f_{ts} - f_{ci} - \Delta f_2 \\ &= f_{ts} - Rf_{ci} - (1 - R)\frac{M_o}{S_2} \end{aligned} \tag{f}$$

The minimum acceptable value of S_1 is thus established:

$$S_1 \geq \frac{M_d + M_l}{Rf_{ti} - (1 - R)M_o/S_1 - f_{cs}}$$

or

$$S_1 \geq \frac{(1 - R)M_o + M_d + M_l}{Rf_{ti} - f_{cs}} \tag{19.20}$$

Similarly, the minimum value of S_2 is

$$S_2 \geq \frac{(1 - R)M_o + M_d + M_l}{f_{ts} - Rf_{ci}} \tag{19.21}$$

† Note that the stress limits such as f_{ti} and other specific points along the stress axis are considered signed quantities, whereas stress changes such as M_o/S_1 and Δf_2 are taken as absolute values.

The cross section must be selected to provide at least these values of S_1 and S_2. Furthermore, since $I_c = S_1 c_1 = S_2 c_2$, the centroidal axis must be located such that

$$\frac{c_1}{c_2} = \frac{S_2}{S_1} \tag{g}$$

or in terms of the total section depth $h = c_1 + c_2$

$$\frac{c_1}{h} = \frac{S_2}{S_1 + S_2} \tag{19.22}$$

From Fig. 19.14a, the concrete centroidal stress under initial conditions f_{cci} is given by

$$f_{cci} = f_{ti} - \frac{c_1}{h}(f_{ti} - f_{ci}) \tag{19.23}$$

The initial prestress force is easily obtained by multiplying the value of the concrete centroidal stress by the concrete cross-sectional area A_c.

$$P_i = A_c f_{cci} \tag{19.24}$$

The eccentricity of the prestress force may be found by considering the flexural stresses that must be imparted by the bending moment $P_i e$. With reference to Fig. 19.14, the flexural stress at the top surface of the beam resulting from the eccentric prestress force alone is

$$\frac{P_i e}{S_1} = (f_{ti} - f_{cci}) + \frac{M_o}{S_1} \tag{h}$$

from which the required eccentricity is

$$e = (f_{ti} - f_{cci})\frac{S_1}{P_i} + \frac{M_o}{P_i} \tag{19.25}$$

Summarizing the design process to determine the best cross section and the required prestress force and eccentricity based on stress limitations: the required section moduli with respect to the top and bottom surfaces of the member are found from Eqs. (19.20) and (19.21) with the centroidal axis located using Eq. (19.22). Concrete dimensions are chosen to satisfy these requirements as nearly as possible. The concrete centroidal stress for this ideal section is given by Eq. (19.23), the desired initial prestress force by Eq. (19.24), and its eccentricity by Eq. (19.25).

In practical situations, very seldom will the concrete section chosen have exactly the required values of S_1 and S_2 as found by this method, nor will the concrete centroid be exactly at the theoretically ideal level. Rounding concrete dimensions upward, providing broad flanges for functional reasons, or using standardized cross-sectional shapes will result in a member whose section properties will exceed the minimum requirements. In such a case, the stresses in the concrete as the member passes from the unloaded stage to the full service load stage will stay within the allowable limits, but the limit stresses will not be obtained exactly. An infinite number of combinations of prestress force and eccentricity will satisfy the requirements. Usually, the design requiring the lowest value of prestress force, and the largest practical eccentricity, will be the most economical.

The total eccentricity in Eq. (19.25) includes the term M_o/P_i. As long as the beam is deep enough to allow this full eccentricity, the girder dead load moment is carried with no additional penalty in terms of prestress force, section, or stress range. This ability to carry the beam dead load "free" is a major contribution of variable eccentricity.

The stress distributions shown in Fig. 19.14*a*, on which the design equations are based, apply at the maximum moment section of the member. Elsewhere, M_o is less, and, consequently, the prestress eccentricity or the force must be reduced if the stress limits f_{ti} and f_{ci} are not to be exceeded. In many cases, tendon eccentricity is reduced to zero at the support sections, where all moments due to transverse load are zero. In this case, the stress distributions of Fig. 19.14*b* are obtained. The stress in the concrete is uniformly equal to the centroidal value f_{cci} under conditions of initial prestress and f_{cce} after losses.

EXAMPLE 19.3 **Design of beam with variable eccentricity tendons.** A post-tensioned prestressed concrete beam is to carry an intermittent live load of 1000 lb/ft and superimposed dead load of 500 lb/ft, in addition to its own weight, on a 40 ft simple span. Normal-density concrete will be used with design strength $f_c' = 6000$ psi. It is estimated that, at the time of transfer, the concrete will have attained 70 percent of f_c', or 4200 psi. Time-dependent losses may be assumed to be 15 percent of the initial prestress, giving an effectiveness ratio of 0.85. Determine the required concrete dimensions, magnitude of prestress force, and eccentricity of the steel centroid based on ACI stress limitations for a Class U beam, as given in Sections 19.4 and 19.5.

Solution. Referring to Table 19.2, the stress limits are

$$f_{ci} = -0.60 \times 4200 = -2520 \text{ psi}$$

$$f_{ti} = 3\sqrt{4200} = +194 \text{ psi}$$

$$f_{cs} = -0.60 \times 6000 = -3600 \text{ psi}$$

$$f_{ts} = 7.5\sqrt{6000} = +581 \text{ psi}$$

The self-weight of the girder will be estimated at 250 lb/ft. The service moments due to transverse loading are

$$M_o = \frac{1}{8} \times 0.250 \times 40^2 = 50 \text{ ft-kips}$$

$$M_d + M_l = \frac{1}{8} \times 1.500 \times 40^2 = 300 \text{ ft-kips}$$

The required section moduli with respect to the top and bottom surfaces of the concrete beam are found from Eqs. (19.20) and (19.21).

$$S_1 \geq \frac{(1-R)M_o + M_d + M_l}{Rf_{ti} - f_{cs}} = \frac{(0.15 \times 50 + 300)12{,}000}{0.85 \times 194 + 3600} = 980 \text{ in}^3$$

$$S_2 \geq \frac{(1-R)M_o + M_d + M_l}{f_{ts} - Rf_{ci}} = \frac{(0.15 \times 50 + 300)12{,}000}{581 + 0.85 \times 2520} = 1355 \text{ in}^3$$

The values obtained for S_1 and S_2 suggest that an asymmetrical section is most appropriate. However, a symmetrical section is selected for simplicity and to ensure sufficient compression area for flexural strength. The 28 in. deep I section shown in Fig. 19.15*a* will meet the requirements and has the following properties:

$$I_c = 19{,}904 \text{ in}^4$$

$$S = 1422 \text{ in}^3$$

$$A_c = 240 \text{ in}^2$$

$$r^2 = 82.9 \text{ in}^2$$

$$w_o = 250 \text{ lb/ft (as assumed)}$$

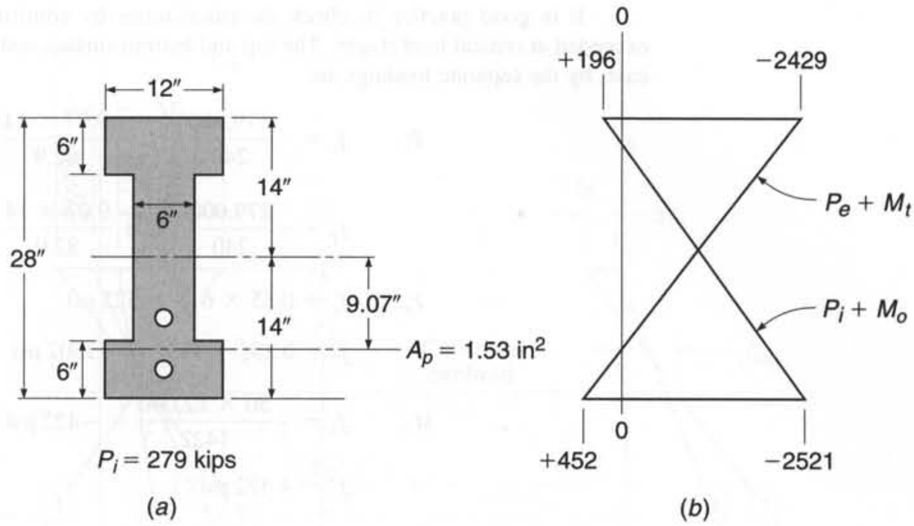

FIGURE 19.15
Design example of beam with variable eccentricity of tendons: (*a*) cross section dimensions; (*b*) concrete stresses at midspan (psi).

Next, the concrete centroidal stress is found from Eq. (19.23):

$$f_{cci} = f_{ti} - \frac{c_1}{h}(f_{ti} - f_{ci}) = 194 - \frac{1}{2}(195 + 2520) = -1163 \text{ psi}$$

and from Eq. (19.24) the initial prestress force is

$$P_i = A_c f_{cci} = 240 \times 1.163 = 279 \text{ kips}$$

From Eq. (19.25), the required tendon eccentricity at the maximum moment section of the beam is

$$e = (f_{ti} - f_{cci})\frac{S_1}{P_i} + \frac{M_o}{P_i} = (195 + 1163)\,\frac{1422}{279{,}000} + \frac{50 \times 12{,}000}{279{,}000}$$
$$= 9.07 \text{ in.}$$

Elsewhere along the span, the eccentricity will be reduced so that the concrete stress limits will not be violated.

The required initial prestress force of 279 kips will be provided using tendons consisting of $\frac{1}{2}$ in. diameter Grade 270 low-relaxation strands (see Section 2.16). The minimum tensile strength is $f_{pu} = 270$ ksi, and the yield strength may be taken as $f_{py} = 0.90 \times 270 = 243$ ksi. According to the ACI Code (see Section 19.4), the permissible stress in the strand immediately after transfer must not exceed $0.82 f_{py} = 199$ ksi or $0.74\, f_{pu} = 200$ ksi. The first criterion controls. The required area of prestressing steel is

$$A_{ps} = \frac{279}{199} = 1.40 \text{ in}^2$$

The cross-sectional area of one $\frac{1}{2}$ in. diameter strand is 0.153 in^2; hence, the number of strands required is

$$\text{Number of strands} = \frac{1.40}{0.153} = 9.2$$

Two five-strand tendons will be used, as shown in Fig. 19.15*a*, each stressed to 139.5 kips immediately following transfer.

It is good practice to check the calculations by confirming that stress limits are not exceeded at critical load stages. The top and bottom surface concrete stresses produced, in this case, by the separate loadings are

$$P_i: \quad f_1 = -\frac{279{,}000}{240}\left(1 - \frac{9.07 \times 14}{82.9}\right) = +618 \text{ psi}$$

$$f_2 = -\frac{279{,}000}{240}\left(1 + \frac{9.07 \times 14}{82.9}\right) = -2943 \text{ psi}$$

$$P_e: \quad f_1 = 0.85 \times 618 = 525 \text{ psi}$$

$$f_2 = 0.85(-2943) = -2502 \text{ psi}$$

$$M_o: \quad f_1 = -\frac{50 \times 12{,}000}{1422} = -422 \text{ psi}$$

$$f_2 = +422 \text{ psi}$$

$$M_d + M_l: \quad f_1 = -\frac{300 \times 12{,}000}{1422} = -2532 \text{ psi}$$

$$f_2 = +2532 \text{ psi}$$

Thus, when the initial prestress force of 279 kips is applied and the beam self-weight acts, the top and bottom stresses in the concrete at midspan are, respectively,

$$f_1 = +618 - 422 = +196 \text{ psi}$$

$$f_2 = -2943 + 422 = -2521 \text{ psi}$$

When the prestress force has decreased to its effective value of 237 kips and the full service load is applied, the concrete stresses are

$$f_1 = +525 - 422 - 2532 = -2429 \text{ psi}$$

$$f_2 = -2502 + 422 + 2532 = +452 \text{ psi}$$

These stress distributions are shown in Fig. 19.15*b*. Comparison with the specified limit stresses confirms that the design is satisfactory.

b. Beams with Constant Eccentricity

The design method presented in the previous section was based on stress conditions at the maximum moment section of a beam, with the maximum value of moment M_o resulting from the self-weight immediately being superimposed. If P_i and e were to be held constant along the span, as is often convenient in pretensioned prestressed construction, then the stress limits f_{ti} and f_{ci} would be exceeded elsewhere along the span, where M_o is less than its maximum value. To avoid this condition, the constant eccentricity must be less than that given by Eq. (19.25). Its maximum value is given by conditions at the support of a simple span, where M_o is zero.

Figure 19.16 shows the flexural stress distributions at the support and midspan sections for a beam with constant eccentricity. In this case, the stress limits f_{ti} and f_{ci} are not to be violated when the eccentric prestress moment acts alone, as at the supports. The stress changes Δf_1 and Δf_2 as losses occur are equal to $(1 - R)$ times the top and bottom surface stresses, respectively, due to initial prestress alone:

$$\Delta f_1 = (1 - R)(f_{ti}) \tag{a}$$

$$\Delta f_2 = (1 - R)(-f_{ci}) \tag{b}$$

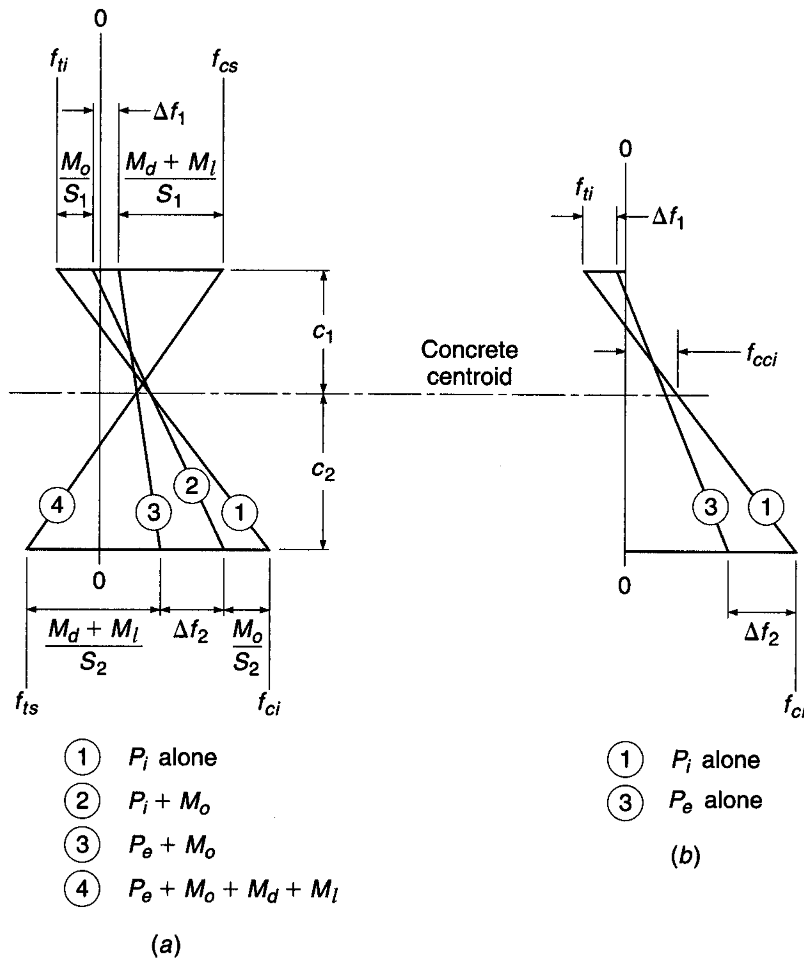

FIGURE 19.16
Flexural stress distributions for beam with constant eccentricity of tendons: (*a*) maximum moment section; (*b*) support section.

In this case, the available stress ranges between limit stresses must provide for the effect of M_o as well as M_d and M_l, as seen from Fig. 19.16*a*, and are

$$\begin{aligned} f_{1r} &= f_{ti} - \Delta f_1 - f_{cs} \\ &= Rf_{ti} - f_{cs} \end{aligned} \tag{c}$$

$$\begin{aligned} f_{2r} &= f_{ts} - f_{ci} - \Delta f_2 \\ &= f_{ts} - Rf_{ci} \end{aligned} \tag{d}$$

and the requirements on the section moduli are that

$$S_1 \geq \frac{M_o + M_d + M_l}{Rf_{ti} - f_{cs}} \tag{19.26}$$

$$S_2 \geq \frac{M_o + M_d + M_l}{f_{ts} - Rf_{ci}} \tag{19.27}$$

The concrete centroidal stress may be found by Eq. (19.23) and the initial prestress force by Eq. (19.24) as before. However, the expression for required eccentricity differs. In this case, referring to Fig. 19.16*b*,

$$\frac{P_i e}{S_1} = f_{ti} - f_{cci} \tag{e}$$

from which the required eccentricity is

$$e = (f_{ti} - f_{cci})\frac{S_1}{P_i} \tag{19.28}$$

A significant difference between beams with variable eccentricity and those with constant eccentricity will be noted by comparing Eqs. (19.20) and (19.21) with the corresponding Eqs. (19.26) and (19.27). In the first case, the section modulus requirement is governed mainly by the superimposed load moments M_d and M_l. Almost all of the self-weight is carried "free," that is, without increasing section modulus or prestress force, by the simple expedient of increasing the eccentricity along the span by the amount M_o/P_i. In the second case, the eccentricity is controlled by conditions at the supports, where M_o is zero, and the full moment M_o due to self-weight must be included in determining section moduli. Nevertheless, beams with constant eccentricity are often used for practical reasons.

EXAMPLE 19.4 **Design of beam with constant eccentricity tendons.** The beam in the preceding example is to be redesigned using straight tendons with constant eccentricity. All other design criteria are the same as before. At the supports, a temporary concrete tensile stress $f_{ti} = 6\sqrt{f'_{ci}} = 389$ psi and a compressive stress $f_{ci} = 0.7f'_{ci} = 2940$ psi are permitted.

Solution. Anticipating a somewhat less efficient beam, the dead load estimate will be increased to 270 lb/ft in this case. The resulting moment M_o is 54 ft-kips. The moment due to superimposed dead load and live load is 300 ft-kips as before.

Using Eqs. (19.26) and (19.27), the requirements for section moduli based on the midspan allowable stresses are

$$S_1 \geq \frac{M_o + M_d + M_l}{Rf_{ti} - f_{cs}} = \frac{(54 + 300)12{,}000}{0.85 \times 194 + 3600} = 1128 \text{ in}^3$$

$$S_2 \geq \frac{M_o + M_d + M_l}{f_{ts} - Rf_{ci}} = \frac{(54 + 300)12{,}000}{581 + 0.85 \times 2520} = 1560 \text{ in}^3$$

Once again, a symmetrical section will be chosen. Flange dimensions and web width will be kept unchanged compared with the previous example, but in this case a beam depth of 30.0 in. is required. The dimensions of the cross section are shown in Fig. 19.17a. The following properties are obtained:

$$I_c = 24{,}084 \text{ in}^4$$
$$S = 1606 \text{ in}^3$$
$$A_c = 252 \text{ in}^2$$
$$r^2 = 95.6 \text{ in}^2$$
$$w_o = 263 \text{ lb/ft (close to the assumed value)}$$

The concrete centroidal stress, from Eq. (19.23), is

$$f_{cci} = f_{ti} - \frac{c_1}{h}(f_{ti} - f_{ci}) = 194 - \frac{1}{2}(390 + 2520) = -1163 \text{ psi}$$

and from Eq. (19.24), the initial prestress force is

$$P_i = A_c f_{cci} = 252 \times 1.163 = 293 \text{ kips}$$

From Eq. (19.28), the required constant eccentricity is

$$e = (f_{ti} - f_{cci})\frac{S_1}{P_i} = (389 + 1163)\frac{1606}{293{,}000} = 8.51 \text{ in.}$$

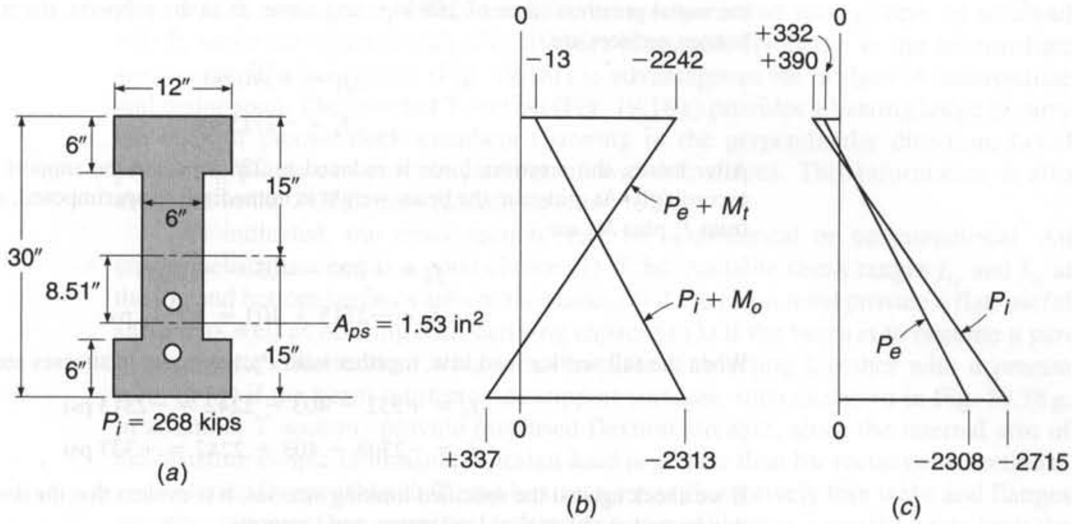

FIGURE 19.17
Design example of beam with constant eccentricity of tendons: (*a*) cross section dimensions; (*b*) stresses at midspan (psi); (*c*) stresses at supports (psi).

Again, two tendons will be used to provide the required prestress force, each composed of multiple $\frac{1}{2}$ in. diameter Grade 270 low-relaxation strands. With the maximum permissible stress in the stranded cable just after transfer of 199 ksi, the total required steel area is

$$A_{ps} = \frac{293}{199} = 1.47 \text{ in}^2$$

A total of 10 strands is required. Two identical five-strand tendons will be used as before, in this case being stressed to a total of 293 kips.

The calculations will be checked by verifying the concrete stresses at the top and bottom of the beam for the critical load stages. The component stress contributions are

$$P_i: \quad f_1 = -\frac{293{,}000}{252}\left(1 - \frac{8.51 \times 15.0}{95.6}\right) = +390 \text{ psi}$$

$$f_2 = -\frac{293{,}000}{252}\left(1 + \frac{8.51 \times 15.0}{95.6}\right) = -2715 \text{ psi}$$

$$P_e: \quad f_1 = 0.85 \times 390 = +332 \text{ psi}$$

$$f_2 = 0.85(-2715) = -2308 \text{ psi}$$

$$M_o: \quad f_1 = -\frac{54 \times 12{,}000}{1606} = -403 \text{ psi}$$

$$f_2 = +403 \text{ psi}$$

$$M_d + M_l: \quad f_1 = -\frac{300 \times 12{,}000}{1606} = -2242 \text{ psi}$$

$$f_2 = +2242 \text{ psi}$$

Superimposing the appropriate stress contributions, the stress distributions in the concrete at midspan and at the supports are obtained, as shown in Fig. 19.17*b* and *c*, respectively. When the initial prestress force of 268 kips acts alone, as at the supports, the stresses at the top and bottom surfaces are

$$f_1 = +390 \text{ psi}$$

$$f_2 = -2715 \text{ psi}$$

After losses, the prestress force is reduced to 228 kips and the support stresses are reduced accordingly. At midspan, the beam weight is immediately superimposed, and stresses resulting from P_i plus M_o are

$$f_1 = +390 - 403 = -13 \text{ psi}$$

$$f_2 = -2715 + 403 = -2312 \text{ psi}$$

When the full service load acts, together with P_e, the midspan stresses are

$$f_1 = +332 - 403 - 2242 = -2313 \text{ psi}$$

$$f_2 = -2308 + 403 + 2242 = +337 \text{ psi}$$

If we check against the specified limiting stresses, it is evident that the design is satisfactory in this respect at the critical load stages and locations.

19.10 SHAPE SELECTION

One of the special features of prestressed concrete design is the freedom to select cross-section proportions and dimensions to suit the special requirements of the job at hand. The member depth can be changed, the web thickness modified, and the flange widths and thicknesses varied independently to produce a beam with nearly ideal proportions for a given case.

Several common precast shapes are shown in Fig. 19.18. Some of these are standardized and mass-produced, employing reusable steel or fiberglass forms. Others are individually proportioned for large and important works. The double T (Fig. 19.18*a*) is probably the most widely used cross section in U.S. prestressed construction. A flat surface is provided, 4 to 12 ft wide. Slab thicknesses and web depths vary, depending upon requirements. Spans to 60 ft are not unusual. The single T (Fig. 19.18*b*) is more appropriate for longer spans, to 120 ft, and heavier loads. The I and bulb T sections

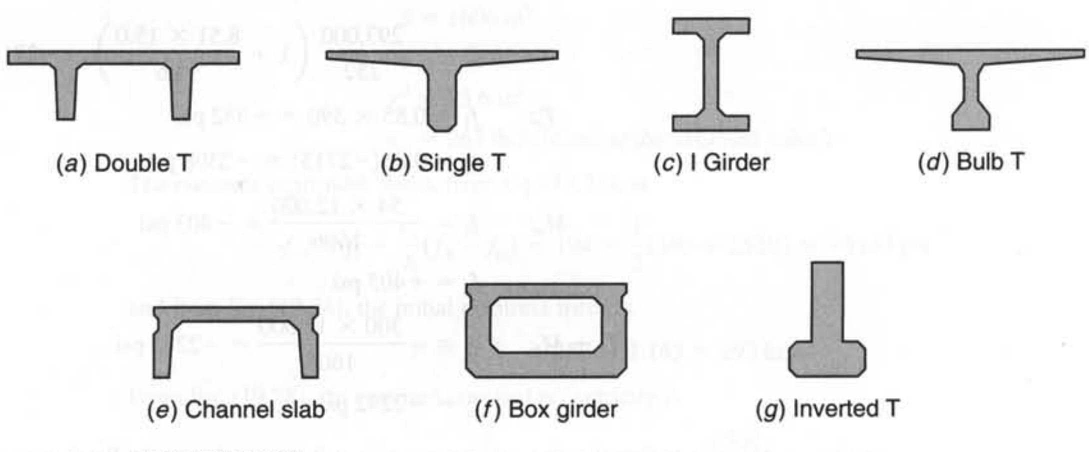

FIGURE 19.18
Typical beam cross sections.

(Fig. 19.18*c* and *d*) are widely used for bridge spans and roof girders up to about 140 ft, while the channel slab (Fig. 19.18*e*) is suitable for floors in the intermediate span range. The box girder (Fig. 19.18*f*) is advantageous for bridges of intermediate and major span. The inverted T section (Fig. 19.18*g*) provides a bearing ledge to carry the ends of precast deck members spanning in the perpendicular direction. Local precasting plants can provide catalogs of available shapes. This information is also available in the *PCI Design Handbook* (Ref. 19.8).

As indicated, the cross section may be symmetrical or unsymmetrical. An unsymmetrical section is a good choice (1) if the available stress ranges f_{1r} and f_{2r} at the top and bottom surfaces are not the same; (2) if the beam must provide a flat, useful surface as well as offering load-carrying capacity; (3) if the beam is to become a part of composite construction, with a cast-in-place slab acting together with a precast web; or (4) if the beam must provide support surfaces, such as shown in Fig. 19.18*g*. In addition, T sections provide increased flexural strength, since the internal arm of the resisting couple at maximum design load is greater than for rectangular sections.

Generally speaking, I, T, and box sections with relatively thin webs and flanges are more efficient than members with thicker parts. However, several factors limit the gain in efficiency that may be obtained in this way. These include the instability of very thin overhanging compression parts, the vulnerability of thin parts to breakage in handling (in the case of precast construction), and the practical difficulty of placing concrete in very thin elements. The designer must also recognize the need to provide adequate spacing and concrete protection for tendons and anchorages, the importance of construction depth limitations, and the need for lateral stability if the beam is not braced by other members against buckling (Ref. 19.16).

19.11 TENDON PROFILES

The equations developed in Section 19.9a for members with variable tendon eccentricity establish the requirements for section modulus, prestress force, and eccentricity at the maximum moment section of the member. Elsewhere along the span, the eccentricity of the steel must be reduced if the concrete stress limits for the unloaded stage are not to be exceeded. (Alternatively, the section must be increased, as demonstrated in Section 19.9b.) Conversely, there is a minimum eccentricity, or upper limit for the steel centroid, such that the limiting concrete stresses are not exceeded when the beam is in the full service load stage.

Limiting locations for the prestressing steel centroid at any point along the span can be established using Eqs. (19.2) and (19.4), which give the values of concrete stress at the top and bottom of the beam in the unloaded and service load stages, respectively. The stresses produced for those load stages should be compared with the limiting stresses applicable in a particular case, such as the ACI stress limits of Table 19.2. This permits a solution for tendon eccentricity e as a function of distance x along the span.

To indicate that both eccentricity e and moments M_o or M_t are functions of distance x from the support, they will be written as $e(x)$ and $M_o(x)$ or $M_t(x)$, respectively. In writing statements of inequality, it is convenient to designate tensile stress as larger than zero and compressive stress as smaller than zero. Thus, $+450 > -1350$, and $-600 > -1140$, for example.

Considering first the unloaded stage, the tensile stress at the top of the beam must not exceed f_{ti}. From Eq. (19.2*a*),

$$f_{ti} \geq -\frac{P_i}{A_c}\left[1 - \frac{e(x)c_1}{r^2}\right] - \frac{M_o(x)}{S_1} \tag{a}$$

Solving for the maximum eccentricity gives

$$e(x) \le \frac{f_{ti}S_1}{P_i} + \frac{S_1}{A_c} + \frac{M_o(x)}{P_i} \tag{19.29}$$

At the bottom of the unloaded beam, the stress must not exceed the limiting initial compression. From Eq. (19.2*b*),

$$f_{ci} \le -\frac{P_i}{A_c}\left[1 + \frac{e(x)c_2}{r^2}\right] + \frac{M_o(x)}{S_2} \tag{b}$$

Hence, the second lower limit for the steel centroid is

$$e(x) \le -\frac{f_{ci}S_2}{P_i} - \frac{S_2}{A_c} + \frac{M_o(x)}{P_i} \tag{19.30}$$

Now considering the member in the fully loaded stage, the upper limit values for the eccentricity may be found. From Eq. (19.4*a*),

$$f_{cs} \le -\frac{P_e}{A_c}\left[1 - \frac{e(x)c_1}{r^2}\right] - \frac{M_t(x)}{S_1} \tag{c}$$

from which

$$e(x) \ge \frac{f_{cs}S_1}{P_e} + \frac{S_1}{A_c} + \frac{M_t(x)}{P_e} \tag{19.31}$$

and using Eq. (19.4*b*)

$$f_{ts} \ge -\frac{P_e}{A_c}\left[1 + \frac{e(x)c_2}{r^2}\right] + \frac{M_t(x)}{S_2} \tag{d}$$

from which

$$e(x) \ge -\frac{f_{ts}S_2}{P_e} - \frac{S_2}{A_c} + \frac{M_t(x)}{P_e} \tag{19.32}$$

Using Eqs. (19.29) and (19.30), the lower limit of tendon eccentricity is established at successive points along the span. Then, using Eqs. (19.31) and (19.32), the corresponding upper limit is established. This upper limit may well be negative, indicating that the tendon centroid may be above the concrete centroid at that location.

It is often convenient to plot the envelope of acceptable tendon profiles, as done in Fig. 19.19, for a typical case in which both dead and live loads are uniformly distributed. Any tendon centroid falling completely within the shaded zone would be satisfactory from the point of view of concrete stress limits. It should be emphasized that it is only the tendon centroid that must be within the shaded zone; individual cables are often outside of it.

The tendon profile actually used is often a parabolic curve or a catenary in the case of post-tensioned beams. The duct containing the prestressing steel is draped to the desired shape and held in that position by wiring it to the transverse web reinforcement, after which the concrete may be placed. In pretensioned beams, *deflected tendons* are often used. The cables are held down at midspan, at the third points, or at the quarter points of the span and held up at the ends, so that a smooth curve is approximated to a greater or lesser degree.

In practical cases, it is often not necessary to make a centroid zone diagram, such as is shown in Fig. 19.19. By placing the centroid at its known location at midspan, at or

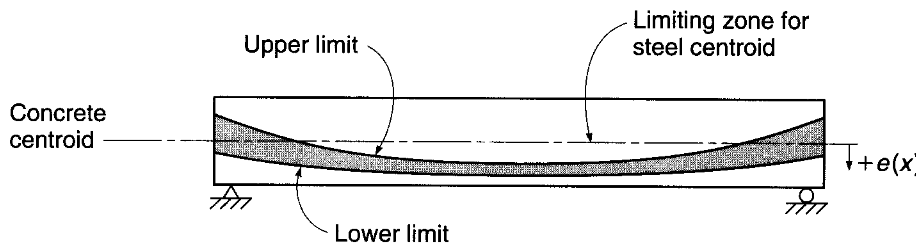

FIGURE 19.19
Typical limiting zone for centroid of prestressing steel.

close to the concrete centroid at the supports, and with a near-parabolic shape between those control points, satisfaction of the limiting stress requirements is ensured. With nonprismatic beams, beams in which a curved concrete centroidal axis is employed, or with continuous beams, diagrams such as Fig. 19.19 are a great aid.

19.12 FLEXURAL DESIGN BASED ON LOAD BALANCING

It was pointed out in Section 19.2b that the effect of a change in the alignment of a prestressing tendon in a beam is to produce a vertical force on the beam at that location. Prestressing a member with curved or deflected tendons thus has the effect of introducing a set of equivalent loads, and these may be treated just as any other loads in finding moments or deflections. Each particular tendon profile produces its own unique set of equivalent forces. Typical tendon profiles, with corresponding equivalent loads and moment diagrams, were illustrated in Fig. 19.2. Both Fig. 19.2 and Section 19.2b should be reviewed carefully.

The equivalent load concept offers an alternative approach to the determination of required prestress force and eccentricity. The prestress force and tendon profile can be established so that external loads that will act are exactly counteracted by the vertical forces resulting from prestressing. The net result, for that particular set of external loads, is that the beam is subjected only to axial compression and no bending moment. The selection of the load to be balanced is left to the judgment of the designer. Often the balanced load chosen is the sum of the self-weight and superimposed dead load.

The design approach described in this section was introduced in the United States by T. Y. Lin in 1963 and is known as the *load-balancing method.* The fundamentals will be illustrated in the context of the simply supported, uniformly loaded beam shown in Fig. 19.20*a*. The beam is to be designed for a balanced load consisting of its own weight w_o, the superimposed dead load w_d, and some fractional part of the live load, denoted by $k_b w_l$. Since the external load is uniformly distributed, it is reasonable to adopt a tendon having a parabolic shape. It is easily shown that a parabolic tendon will produce a uniformly distributed upward load equal to

$$w_p = \frac{8Py}{l^2} \tag{19.33}$$

where P = magnitude of prestress force
y = maximum sag of tendon measured with respect to the chord between its endpoints
l = span length

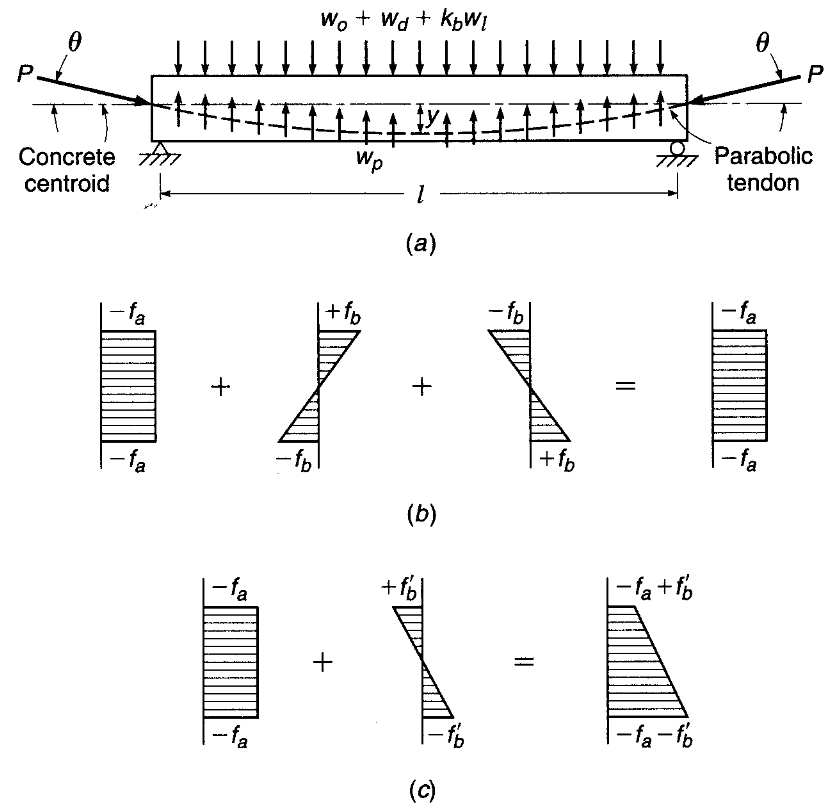

FIGURE 19.20
Load balancing for uniformly loaded beam: (*a*) external and equivalent loads; (*b*) concrete stresses resulting from axial and bending effects of prestress plus bending resulting from balanced external load; (*c*) concrete stresses resulting when load $k_b w_l$ is removed.

If the downward load exactly equals the upward load from the tendon, these two loads cancel and no bending stress is produced, as shown in Fig. 19.20*b*. The bending stresses due to prestress eccentricity are equal and opposite to the bending stresses resulting from the external load. The net resulting stress is uniform compression f_a equal to that produced by the axial force $P \cos \theta$. Excluding consideration of time-dependent effects, the beam would show no vertical deflection.

If the live load is removed or increased, then bending stresses and deflections will result because of the *unbalanced* portion of the load. Stresses resulting from this differential loading must be calculated and superimposed on the axial compression to obtain the net stresses for the unbalanced state. Referring to Fig. 19.20*c*, the bending stresses f_b' resulting from removal of the partial live loading are superimposed on the uniform compressive stress f_a, resulting from the combination of eccentric prestress force and full balanced load to produce the final stress distribution shown.

Loads other than uniformly distributed would lead naturally to the selection of other tendon configurations. For example, if the external load consisted of a single concentration at midspan, a deflected tendon such as that of Fig. 19.2*a* would be chosen, with maximum eccentricity at midspan, varying linearly to zero eccentricity at the supports. A third-point loading would lead the designer to select a tendon deflected at the third points. A uniformly loaded cantilever beam would best be stressed using a tendon in which the eccentricity varied parabolically, from zero at the free end to y at the fixed support, in which case the upward reaction of the tendon would be

$$w_p = \frac{2Py}{l^2} \tag{19.34}$$

It should be clear that, for simple spans designed by the load-balancing concept, it is necessary for the tendon to have zero eccentricity at the supports because the moment due to superimposed loads is zero there. Any tendon eccentricity would produce an unbalanced moment (in itself an equivalent load) equal to the horizontal component of the prestress force times its eccentricity. At the simply supported ends, the requirement of zero eccentricity must be retained.

In practice, the load-balancing method of design starts with selection of a trial beam cross section, based on experience and judgment. An appropriate span-depth ratio is often applied. The tendon profile is selected using the maximum available eccentricity, and the prestress force is calculated. The trial design may then be checked to ensure that concrete stresses are within the allowable limits should the live load be totally absent or fully in place, when bending stresses will be superimposed on the axial compressive stresses. There is no assurance that the section will be adequate for these load stages, or that adequate strength will be provided should the member be overloaded. Revision may be necessary.

It should further be observed that obtaining a uniform compressive concrete stress at the balanced load stage does not ensure that the member will have zero deflection at this stage. The reason is that the uniform stress distribution is made up of two parts: that from the eccentric prestress force and that from the external loads. The prestress force varies with time because of shrinkage, creep, and relaxation, changing the vertical deflection associated with the prestress force. Concurrently, the beam will experience creep deflection under the combined effects of the diminishing prestress force and the external loads, a part of which may be sustained and a part of which may be short-term. However, if load balancing is carried out based on the effective prestress force P_e plus self-weight and external dead load only, the result may be near-zero deflection for that combination.

The load-balancing method provides the engineer with a useful tool. For simple spans, it leads the designer to choose a sensible tendon profile and focuses attention very early on the matter of deflection. But the most important advantages become evident in the design of indeterminate prestressed members, including both continuous beams and two-way slabs. For such cases, at least for one unique loading, the member carries only axial compression but no bending. This greatly simplifies the analysis.

EXAMPLE 19.5 **Beam design initiating with load balancing.** A post-tensioned beam is to be designed to carry a uniformly distributed load over a 30 ft span, as shown in Fig. 19.21. In addition to its own weight, it must carry a dead load of 150 lb/ft and a service live load of 600 lb/ft. Concrete strength of 4000 psi will be attained at 28 days; at the time of transfer of the prestress force, the strength will be 3000 psi. Prestress loss may be assumed at 20 percent of P_i. On the basis that about one-quarter of the live load will be sustained over a substantial time period, k_b of 0.25 will be used in determining the balanced load.

Solution. On the basis of an arbitrarily chosen span-depth ratio of 18, a 20 in. deep, 10 in. wide trial section is selected. The calculated self-weight of the beam is 208 lb/ft, and the selected load to be balanced is

$$w_{\text{bal}} = w_o + w_d + k_b w_l = 208 + 150 + 150 = 508 \text{ lb/ft}$$

Based on a minimum concrete cover from the steel centroid to the bottom face of the beam of 4 in., the maximum eccentricity that can be used for the 20 in. trial section is 6 in. A parabolic tendon will be used to produce a uniformly distributed upward tendon load. To equilibrate the sustained downward loading, the prestress force P_e after losses, from Eq. (19.33), should be

$$P_e = \frac{w_{\text{bal}} l^2}{8y} = \frac{508 \times 900}{8 \times 0.5} = 114{,}000 \text{ lb}$$

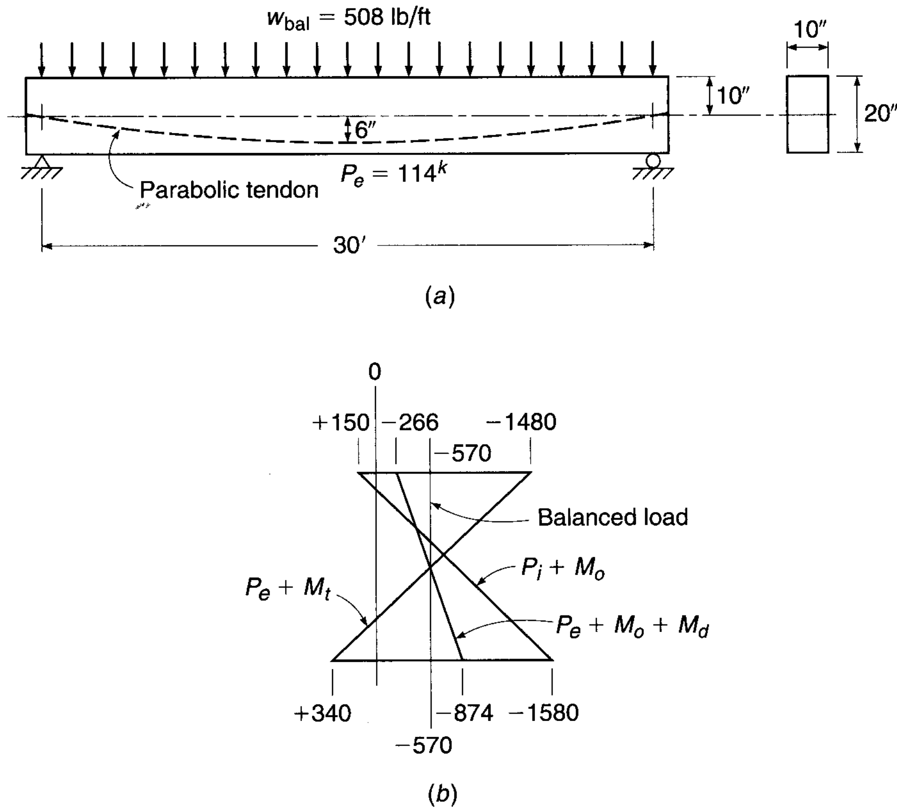

FIGURE 19.21 Example of design by load balancing: (*a*) beam profile and cross section; (*b*) flexural stresses at maximum moment section (psi).

and the corresponding initial prestress force is

$$P_i = \frac{P_e}{R} = \frac{114{,}000}{0.8} = 143{,}000 \text{ lb}$$

For the balanced load stage, the concrete will be subjected to a uniform compressive stress of

$$f_{\text{bal}} = \frac{114{,}000}{200} = -570 \text{ psi}$$

as shown in Fig. 19.21*b*. Should the partial live load of 150 lb/ft be removed, the stresses to be superimposed on f_{bal} result from a net *upward* load of 150 lb/ft. The section modulus for the trial beam is 667 in^3 and

$$M_{\text{unbal}} = 150 \times \frac{900}{8} = 16{,}900 \text{ ft-lb}$$

Hence, the unbalanced bending stresses at the top and bottom faces are

$$f_{\text{unbal}} = 16{,}900 \times \frac{12}{667} = 304 \text{ psi}$$

Thus, the net stresses are

$$f_1 = -570 + 304 = -266 \text{ psi}$$
$$f_2 = -570 - 304 = -874 \text{ psi}$$

Similarly, if the *full* live load should act, the stresses to be superimposed are those resulting from a net *downward* load of 450 lb/ft. The resulting stresses in the concrete at full service load are

$$f_1 = -570 - 910 = -1480 \text{ psi}$$
$$f_2 = -570 + 910 = +340 \text{ psi}$$

Stresses in the concrete with live load absent and live load fully in place are shown in Fig. 19.21*b*.

It is also necessary to investigate the stresses in the initial unloaded stage, when the member is subjected to P_i plus moment due to its own weight.

$$M_o = 208 \times \frac{900}{8} = 23{,}400 \text{ ft-lb}$$

Hence, in the initial stage:

$$f_1 = -\frac{143{,}000}{200}\left(1 - \frac{6 \times 10}{33.35}\right) - \frac{23{,}400 \times 12}{667} = +150 \text{ psi}$$

$$f_2 = -\frac{143{,}000}{200}\left(1 + \frac{6 \times 10}{33.35}\right) + \frac{23{,}400 \times 12}{667} = -1580 \text{ psi}$$

The stresses in the unloaded and full service load stages must be checked against these permitted by the ACI Code. With $f_c' = 4000$ psi and $f_{ci}' = 3000$ psi, the stresses permitted for a Class U member are

$$f_{ti} = +165 \text{ psi} \qquad f_{ts} = +474 \text{ psi}$$
$$f_{ci} = -1800 \text{ psi} \qquad f_{cs} = -2400 \text{ psi}$$

The actual stresses, shown in Fig. 19.21*b*, are within these limits and acceptably close, and no revision will be made in the trial 10 × 20 in. cross section on the basis of stress limits.

The flexural strength of the members must now be checked, to ensure that an adequate margin of safety against collapse has been provided. The required P_i of 143,000 lb will be provided using Grade 270 strand, with $f_{pu} = 270{,}000$ psi and $f_{py} = 243{,}000$ psi. Referring to Section 19.4, the initial stress immediately after transfer must not exceed 0.74 × 270,000 = 200,000 psi, or 0.82 × 243,000 = 199,000 psi, which controls in this case. Accordingly, the required area of tendon steel is

$$A_{ps} = 143{,}000/199{,}000 = 0.72 \text{ in}^2$$

This will be provided using five $\frac{1}{2}$ in. strands, giving an actual area of 0.765 in^2 (Table A.15). The resulting stresses at the initial and final stages are

$$f_{pi} = \frac{143{,}000}{0.765} = 187{,}000 \text{ psi}$$

$$f_{pe} = \frac{114{,}000}{0.765} = 149{,}000 \text{ psi}$$

Using the ACI approximate equation for steel stress at failure [see Eq. (19.6)], with ρ_p = 0.765/160 = 0.0048, and $\gamma_p = 0.40$ for the ordinary Grade 270 tendons, the stress f_{ps} is given by

$$\begin{aligned} f_{ps} &= f_{pu}\left(1 - \frac{\gamma_p}{\beta_1}\frac{\rho_p f_{pu}}{f_c'}\right) \\ &= 270\left(1 - \frac{0.40}{0.85}\frac{0.0048 \times 270}{4}\right) \\ &= 229 \text{ ksi} \end{aligned}$$

Then

$$\begin{aligned} a &= \frac{A_{ps} f_{ps}}{0.85 f_c' b} \\ &= \frac{0.765 \times 229}{0.85 \times 4 \times 10} = 5.15 \text{ in.} \end{aligned}$$

$$c = \frac{5.15}{0.85} = 6.06$$

$$\frac{c}{d_t} = \frac{6.06}{16} = 0.379$$

This exceeds $c/d_t = 0.375$, reducing ϕ to 0.89. The nominal flexural strength is

$$M_n = A_{ps}f_{ps}\left(d - \frac{a}{2}\right) = 0.765 \times 229{,}000\left(16 - \frac{5.15}{2}\right)\frac{1}{12}$$
$$= 196{,}000 \text{ ft-lb}$$

and the design strength with $\phi = 0.89$ is

$$\phi M_n = 0.89 \times 196{,}000 = 174{,}000 \text{ ft-lb}$$

It will be recalled that the ACI load factors with respect to dead and live loads are, respectively, 1.2 and 1.6. Calculating the factored load,

$$w_u = 1.2(208 + 150) + 1.6(600) = 1390 \text{ lb/ft}$$

$$M_u = \frac{1390(900)}{8} = 156{,}000 \text{ ft-lb}$$

Thus, $\phi M_n > M_u$, and the design is judged satisfactory.

19.13 LOSS OF PRESTRESS

As discussed in Section 19.6, the initial prestress force P_i immediately after transfer is less than the jacking force P_j because of elastic shortening of the concrete, slip at the anchorages, and frictional losses along the tendons. The force is reduced further, after a period of many months or even years, due to length changes resulting from shrinkage and creep of the concrete and relaxation of the highly stressed steel; eventually it attains its effective value P_e. In the preceding sections of this chapter, losses were accounted for, making use of an assumed effectiveness ratio $R = P_e/P_i$. Losses have no effect on the nominal strength of a member with bonded tendons, but overestimation or underestimation of losses may have a pronounced effect on service conditions including camber, deflection, and cracking.

The estimation of losses can be made on several different levels. Lump-sum losses, used in the early development of prestressed concrete, are now considered obsolete. Values of R based on detailed calculations and verified in field applications are used in design offices, as are tables of individual loss contributions. For cases where greater accuracy is required, it is necessary to estimate the separate losses, taking account of the conditions of member geometry, material properties, and construction methods that apply. Accuracy of loss estimation can be improved still further by accounting for the interdependence of time-dependent losses, using the summation of losses in a sequence of discrete time steps. These methods will be discussed briefly in the following paragraphs.

a. Lump-Sum Estimates of Losses

It was recognized very early in the development of prestressed concrete that there was a need for approximate expressions to be used to estimate prestress losses in design. Many thousands of successful prestressed structures have been built based on such estimates, and where member sizes, spans, materials, construction procedures, prestress forces, and environmental conditions are not out of the ordinary, this approach is satisfactory. For such conditions, the American Association of State Highway and Transportation Officials (AASHTO, Ref. 19.17) has recommended

TABLE 19.3
Estimate of prestress losses

Type of Beam Section	Level	Wires or Strands with f_{pu} = 235, 250, or 270 ksi[a]
Rectangular beams, solid slabs	Upper bound	33.0 ksi
	Average	30.0 ksi
Box girder	Upper bound	25.0 ksi
	Average	23.0 ksi
I girder	Average	$33.0[1 - 0.15(f_c' - 6.0)/6.0] + 6.0$
Single T, double T,	Upper bound	$39.0[1 - 0.15(f_c' - 6.0)/6.0] + 6.0$
hollow core and voided slab	Average	$39.0[1 - 0.15(f_c' - 6.0)/6.0] + 6.0$

[a] Values are for fully prestressed beams; reductions are allowed for partial prestress.
Losses due to friction are excluded. Friction losses should be computed according to Section 19.13b.
For low-relaxation strands, the values specified may be reduced by 4.0 ksi for box girders; 6.0 ksi for rectangular beams, solid slabs, and I girders; and 8.0 ksi for single T's, double T's, hollow core and voided slabs.

Source: Adapted from Ref. 19.17.

the values in Table 19.3 for preliminary design or for certain controlled precasting conditions. It should be noted that losses due to friction must be added to these values for post-tensioned members. These may be calculated separately by the equations of Section 19.13b below.

The AASHTO recommended losses of Table 19.3 include losses due to elastic shortening, creep, shrinkage, and relaxation (see Section 19.13b). Thus for comparison with R values for estimating losses, such as were employed for the preceding examples, which included only the time-dependent losses due to shrinkage, creep, and relaxation, elastic shortening losses should be estimated by the methods discussed in Section 19.13b and deducted from the total.

b. Estimate of Separate Losses

A separate estimate of individual losses is made for most designs and specifically required when using the ACI Code. Such an analysis is complicated by the interdependence of time-dependent losses. For example, the relaxation of stress in the tendons is affected by length changes due to creep of concrete. Rate of creep, in turn, is altered by change in tendon stress. In the following six subsections, losses are treated as if they occurred independently, although certain arbitrary adjustments are included to account for the interdependence of time-dependent losses. If greater refinement is necessary, a step-by-step approach like that mentioned in Section 19.13c may be used (see also Refs. 19.8, 19.18, and 19.19).

(1) Slip at the Anchorages As the load is transferred to the anchorage device in post-tensioned construction, a slight inward movement of the tendon will occur as the wedges seat themselves and as the anchorage itself deforms under stress. The amount of movement will vary greatly, depending on the type of anchorage and on construction techniques. The amount of movement due to seating and stress deformation associated with any particular type of anchorage is best established by test. Once this amount ΔL is determined, the stress loss is easily calculated from

$$\Delta f_{s,\text{slip}} = \frac{\Delta L}{L} E_s \qquad (19.35)$$

It is significant to note that the amount of slip is nearly independent of the cable length. For this reason, the stress loss will be large for short tendons and relatively small for long tendons. The practical consequence of this is that it is most difficult to post-tension short tendons with any degree of accuracy.

(2) Elastic Shortening of the Concrete In pretensioned members, as the tendon force is transferred from the fixed abutments to the concrete beam, elastic instantaneous compressive strain will take place in the concrete, tending to reduce the stress in the bonded prestressing steel. The steel stress loss is

$$\Delta f_{s,\text{elastic}} = E_s \frac{f_c}{E_c} = nf_c \tag{19.36}$$

where f_c is the concrete stress at the level of the steel centroid immediately after prestress is applied:

$$f_c = -\frac{P_i}{A_c}\left(1 + \frac{e^2}{r^2}\right) + \frac{M_o e}{I_c} \tag{19.37}$$

If the tendons are placed with significantly different effective depths, the stress loss in each should be calculated separately.

In computing f_c by Eq. (19.37), the prestress force used should be that after the losses being calculated have occurred. It is usually adequate to estimate this as about 10 percent less than P_j.

In post-tensioned members, if all of the strands are tensioned at one time, there will be no loss due to elastic shortening, because this shortening will occur as the jacking force is applied and before the prestressing force is measured. On the other hand, if various strands are tensioned sequentially, the stress loss in each strand will vary, being a maximum in the first strand tensioned and zero in the last strand. In most cases, it is sufficiently accurate to calculate the loss in the first strand and to apply one-half that value to all strands.

(3) Frictional Losses Losses due to friction, as the tendon is stressed in post-tensioned members, are usually separated for convenience into two parts: curvature friction and wobble friction. The first is due to intentional bends in the tendon profile as specified and the second to the unintentional variation of the tendon from its intended profile. It is apparent that even a "straight" tendon duct will have some unintentional misalignment so that wobble friction must always be considered in post-tensioned work. Usually, curvature friction must be considered as well. The force at the jacking end of the tendon P_o, required to produce the force P_x at any point x along the tendon, can be found from the expression

$$P_o = P_x e^{Kl_x + \mu\alpha} \tag{19.38a}$$

where e = base of natural logarithms
l_x = tendon length from jacking end to point x
α = angular change of tendon from jacking end to point x, rad
K = wobble friction coefficient, lb/lb per ft
μ = curvature friction coefficient

There has been much research on frictional losses in prestressed construction, particularly with regard to the values of K and μ. These vary appreciably, depending on construction methods and materials used. The values in Table 19.4, from ACI Commentary R18.6, may be used as a guide.

TABLE 19.4
Friction coefficients for post-tensioned tendons

Type of Tendon	Wobble Coefficient K, per ft	Curvature Coefficient μ
Grouted tendons in metal sheathing		
Wire tendons	0.0010–0.0015	0.15–0.25
High-strength bars	0.0001–0.0006	0.08–0.30
Seven-wire strand	0.0005–0.0020	0.15–0.25
Unbonded tendons		
Mastic-coated wire tendons	0.0010–0.0020	0.05–0.15
Mastic-coated seven-wire strand	0.0010–0.0020	0.05–0.15
Pregreased wire tendons	0.0003–0.0020	0.05–0.15
Pregreased seven-wire strand	0.0003–0.0020	0.05–0.15

If one accepts the approximation that the normal pressure on the duct causing the frictional force results from the undiminished initial tension all the way around the curve, the following simplified expression for loss in tension is obtained:

$$P_o = P_x(1 + Kl_x + \mu\alpha) \tag{19.38b}$$

where α is the angle between the tangents at the ends. The ACI Code permits the use of the simplified form, if the value of $Kl_x + \mu\alpha$ is not greater than 0.3.

The loss of prestress for the entire tendon length can be computed by segments, with each segment assumed to consist of either a circular arc or a length of tangent.

(4) Creep of Concrete Shortening of concrete under sustained load has been discussed in Section 2.8. It can be expressed in terms of the creep coefficient C_c. Creep shortening may be several times the initial elastic shortening, and it is evident that it will result in loss of prestress force. The stress loss can be calculated from

$$\Delta f_{s,\text{creep}} = C_c n f_c \tag{19.39}$$

Ultimate values of C_c for different concrete strengths for average conditions of humidity C_{cu} are given in Table 2.2.

In Eq. (19.39), the concrete stress f_c to be used is that at the level of the steel centroid, when the eccentric prestress force plus all sustained loads are acting. Equation (19.37) can be used, except that the moment M_o should be replaced by the moment due to *all* dead loads plus that due to any portion of the live load that may be considered sustained.

It should be noted that the prestress force causing creep is not constant but diminishes with the passage of time due to relaxation of the steel, shrinkage of the concrete, and length changes associated with creep itself. To account for this, it is recommended that the prestress force causing creep be assumed at 10 percent less than the initial value P_i.

(5) Shrinkage of Concrete It is apparent that a decrease in the length of a member due to shrinkage of the concrete will be just as detrimental as length changes due to stress, creep, or other causes. As discussed in Section 2.11, the shrinkage strain ϵ_{sh} may vary between about 0.0004 and 0.0008. A typical value of 0.0006 may be used in lieu of specific data. The steel stress loss resulting from shrinkage is

$$\Delta f_{s,\text{shrink}} = \epsilon_{sh} E_s \tag{19.40}$$

Only that part of the shrinkage that occurs after transfer of prestress force to the concrete need be considered. For pretensioned members, transfer commonly takes place just 18 hours after placing the concrete, and nearly all the shrinkage takes place after that time. However, post-tensioned members are seldom stressed at an age earlier than 7 days and often much later than that. About 15 percent of ultimate shrinkage may occur within 7 days, under typical conditions, and about 40 percent by the age of 28 days.

(6) Relaxation of Steel The phenomenon of relaxation, similar to creep, was discussed in Section 2.16c. Loss of stress due to relaxation will vary depending upon the stress in the steel, and may be estimated using Eqs. (2.11) and (2.12). To allow for the gradual reduction of steel stress resulting from the combined effects of creep, shrinkage, and relaxation, the relaxation calculation can be based on a prestress force 10 percent less than P_i.

It is interesting to observe that the largest part of the relaxation loss occurs shortly after the steel is stretched. For stresses of $0.80f_{pu}$ and higher, even a very short period of loading will produce substantial relaxation, and this in turn will reduce the relaxation that will occur later at a lower stress level. The relaxation rate can thus be artificially accelerated by temporary overtensioning. This technique is the basis for producing low-relaxation steel.

c. Loss Estimation by the Time-Step Method

The loss calculations of the preceding paragraphs recognized the interdependence of creep, shrinkage, and relaxation losses in an approximate way, by an arbitrary reduction of 10 percent of the initial prestress force P_i to obtain the force for which creep and relaxation losses were calculated. For cases requiring greater accuracy, losses can be calculated for discrete time steps over the period of interest. The prestress force causing losses during any time step is taken equal to the value at the end of the preceding time step, accounting for losses due to all causes up to that time. Accuracy can be improved to any desired degree by reducing the length and increasing the number of time steps.

A step-by-step method developed by the Committee on Prestress Losses of the Prestressed Concrete Institute uses only a small number of time steps and is adequate for ordinary cases (Ref. 19.18).

19.14 SHEAR, DIAGONAL TENSION, AND WEB REINFORCEMENT

In prestressed concrete beams at service load, there are two factors that greatly reduce the intensity of diagonal tensile stresses, compared with stresses that would exist if no prestress force were present. The first of these results from the combination of longitudinal compressive stress and shearing stress. An ordinary tensile reinforced concrete beam under load is shown in Fig. 19.22*a*. The stresses acting on a small element of the beam taken near the neutral axis and near the support are shown in (*b*). It is found by means of Mohr's circle of stress (*c*) that the principal stresses act at 45° to the axis of the beam (*d*) and are numerically equal to the shear stress intensity; thus

$$t_1 = t_2 = v \qquad (a)$$

FIGURE 19.22
Principal stress analysis for an ordinary reinforced concrete beam.

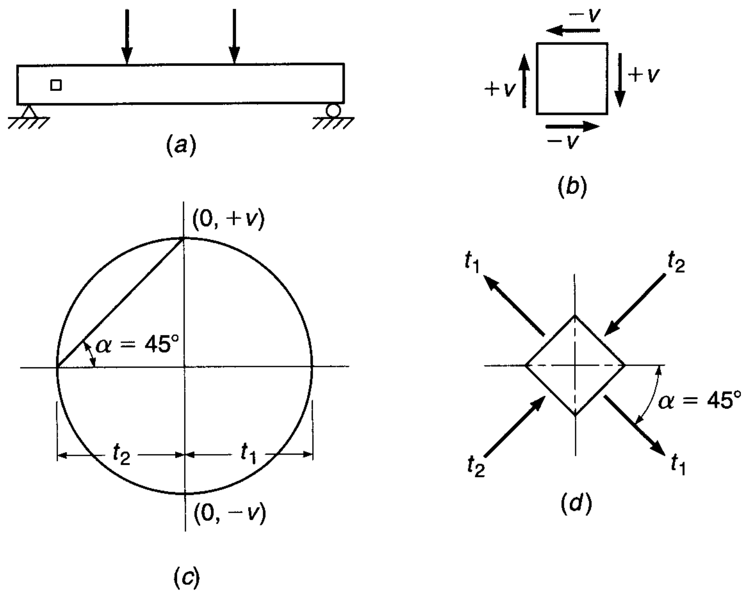

Now suppose that the same beam, with the same loads, is subjected to a precompression stress in the amount c, as shown in Fig. 19.23*a* and *b*. From Mohr's circle (Fig. 19.23*c*), the principal tensile stress is

$$t_1 = -\frac{c}{2} + \sqrt{v^2 + \left(\frac{c}{2}\right)^2} \tag{b}$$

and the direction of the principal tension with respect to the beam axis is

$$\tan 2\alpha = \frac{2v}{c} \tag{c}$$

as shown in Fig. 19.23*d*.

FIGURE 19.23
Principal stress analysis for a prestressed concrete beam.

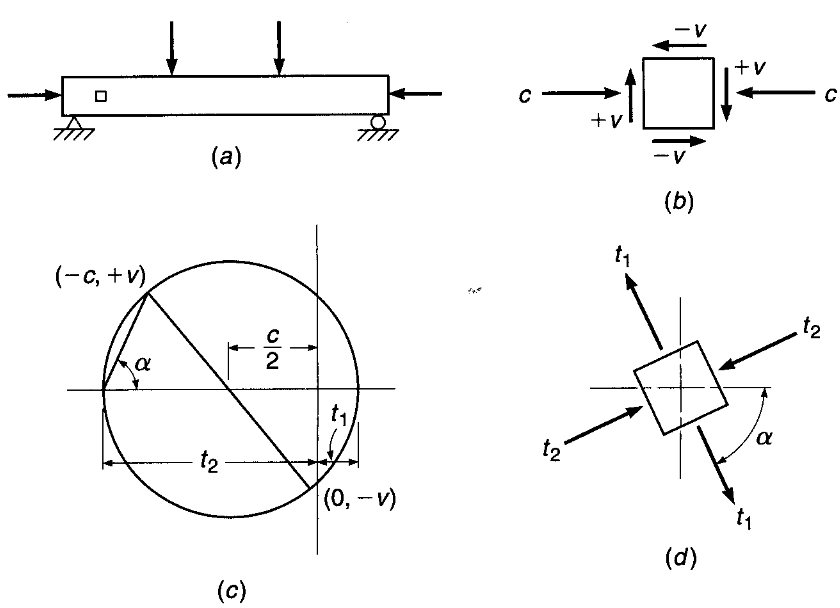

Comparison of Eq. (*a*) with Eq. (*b*) and Fig. 19.22*c* with Fig. 19.23*c* shows that, with the same shear stress intensity, the principal tension in the prestressed beam is much reduced.

The second factor working to reduce the intensity of the diagonal tension at service loads results from the slope of the tendons. Normally, this slope is such as to produce a shear due to the prestress force that is opposite in direction to the load-imposed shear. The magnitude of this *countershear* is $V_p = P_e \sin\theta$, where θ is the slope of the tendon at the section considered (see Fig. 19.8).

It is important to note, however, that in spite of these characteristics of prestressed beams at service loads, an investigation of diagonal tensile stresses at service loads does not ensure an adequate margin of safety against failure. In Fig. 19.23*c*, it is evident that a relatively small decrease in compressive stress and increase in shear stress, which may occur when the beam is overloaded, will produce a disproportionately large increase in the resulting principal tension. In addition to this effect, if the countershear of inclined tendons is used to reduce design shear, its contribution does not increase directly with load, but much more slowly (see Section 19.7). Consequently, a small increase in total shear may produce a large increase in the net shear for which the beam must be designed. For these two reasons, it is necessary to base design for diagonal tension in prestressed beams on conditions at factored load rather than at service load. The study of principal stresses in the uncracked prestressed beam is significant only in predicting the load at which the first diagonal crack forms.

At loads near failure, a prestressed beam is usually extensively cracked and behaves much like an ordinary reinforced concrete beam. Accordingly, many of the procedures and equations developed in Section 4.5 for the design of web reinforcement for nonprestressed beams can be applied to prestressed beams also. Shear design is based on the relation

$$V_u \leq \phi V_n \tag{19.41}$$

where V_u is the total shear force applied to the section at factored loads and V_n is the nominal shear strength, equal to the sum of the contributions of the concrete V_c and web reinforcement V_s:

$$V_n = V_c + V_s \tag{19.42}$$

The strength reduction factor ϕ is equal to 0.75 for shear.

In computing the factored load shear V_u, the first critical section is assumed to be at a distance $h/2$ from the face of a support, and sections located a distance less than $h/2$ are designed for the shear computed at $h/2$.

The shear force V_c resisted by the concrete after cracking has occurred is taken equal to the shear that causes the first diagonal crack. Two types of diagonal cracks have been observed in tests of prestressed concrete beams:

1. **Flexure-shear cracks,** occurring at nominal shear V_{ci}, start as nearly vertical flexural cracks at the tension face of the beam, then spread diagonally upward (under the influence of diagonal tension) toward the compression face. These are common in beams with a low value of prestress force.
2. **Web-shear cracks,** occurring at nominal shear V_{cw}, start in the web due to high diagonal tension, then spread diagonally both upward and downward. These are often found in beams with thin webs with high prestress force.

On the basis of extensive tests, it was established that the shear causing flexure shear cracking can be found using the expression

$$V_{ci} = 0.6\sqrt{f'_c}\,b_w d_p + V_{cr,o+d+l} \tag{a}$$

where $V_{cr,o+d+l}$ is the shear force, due to total load, at which the flexural crack forms at the section considered, and $0.6\sqrt{f'_c}b_w d_p$ represents an additional shear force required to transform the flexural crack into an inclined crack.

While self-weight is generally uniformly distributed, the superimposed dead and live loads may have any distribution. Consequently, it is convenient to separate the total shear into V_o caused by the beam self-weight (without load factor) and V_{cr}, the additional shear force, due to superimposed dead and live loads, corresponding to flexural cracking. Thus,

$$V_{ci} = 0.6\sqrt{f'_c}b_w d_p + V_o + V_{cr} \tag{b}$$

The shear V_{cr} due to superimposed loads can then be found conveniently from

$$V_{cr} = \frac{V_{d+l}}{M_{d+l}} M_{cre} \tag{c}$$

where V_{d+l}/M_{d+l}, the ratio of superimposed dead and live load shear to moment, remains constant as the load increases to the cracking load, and

$$M_{cre} = \frac{I_c}{y_t}\left(6\lambda\sqrt{f'_c} + f_{pe} - f_o\right) \tag{19.43}$$

where y_t = distance from concrete centroid to tension face
f_{pe} = compressive stress at tension face resulting from effective prestress force alone
f_o = stress due to beam self-weight (unfactored) at extreme fiber of section where tensile stress is caused by externally applied dead and live loads†

The first term inside the parentheses is a conservative estimate of the modulus of rupture. The bottom-fiber stress due to self-weight is subtracted here because self-weight is considered separately in Eq. (*b*). Thus, Eq. (*b*) becomes

$$V_{ci} = 0.6\lambda\sqrt{f'_c}b_w d_p + V_o + \frac{V_{d+l}}{M_{d+l}} M_{cre} \tag{19.44}$$

Tests indicate that V_{ci} need not be taken less than $1.7\lambda\sqrt{f'_c}b_w d_p$. The value of d_p need not be taken less than $0.80h$ for this and all other equations relating to shear, according to the ACI Code, unless specifically noted otherwise. Additionally, the values V_{d+l} and M_{d+l} should be computed for the load combination causing the maximum moment in the section. Because V_{d+l} is the incremental load above the beam self-weight, the ACI Code uses the notation $V_i M_{cre}/M_{max}$, noting that M_{cre} comes from Eq. (19.43).

The shear force causing web-shear cracking can be found from an exact principal stress calculation, in which the principal tensile stress is set equal to the direct tensile capacity of the concrete (conservatively taken equal to $4\lambda\sqrt{f'_c}$ according to the ACI Code). Alternatively, the ACI Code permits use of the approximate expression

$$V_{cw} = (3.5\lambda\sqrt{f'_c} + 0.3f_{pc})b_w d_p + V_p \tag{19.45}$$

in which f_{pc} is the compressive stress in the concrete, after losses, at the centroid of the concrete section (or at the junction of the web and the flange when the centroid lies in the flange) and V_p is the vertical component of the effective prestress force. In a pretensioned beam, the $0.3f_{pc}$ contribution to V_{cw} should be adjusted from zero at the beam end to its full value one transfer length (see Section 19.15b) in from the end of the beam.

† All stresses are used with absolute value here, consistent with ACI convention.

After V_{ci} and V_{cw} have been calculated, then V_c, the shear resistance provided by the concrete, is taken equal to the smaller of the two values.

Calculating M_{cre}, V_{ci}, and V_{cw} for a prestressed beam is a tedious matter because many of the parameters vary along the member axis. For hand calculations, the required quantities may be found at discrete intervals along the span, such as at $l/2$, $l/3$, $l/6$, and at $h/2$ from the support face, and stirrups spaced accordingly, or computer spreadsheets may be used.

To shorten the calculation required, the ACI Code includes, as a conservative alternative to the above procedure, an equation for finding the concrete shear resistance V_c directly:

$$V_c = \left(0.6\lambda\sqrt{f'_c} + 700\,\frac{V_u d_p}{M_u}\right)b_w d \tag{19.46}$$

in which M_u is the bending moment occurring simultaneously with shear force V_u, but $V_u d_p/M_u$ is not to be taken greater than 1.0, and d is the effective depth including prestressed and nonprestressed reinforcement. When this equation is used, V_c need not be taken less than $2\lambda\sqrt{f'_c}b_w d_p$ and must not be taken greater than $5\lambda\sqrt{f'_c}b_w d_p$. While Eq. (19.46) is temptingly easy to use and may be adequate for uniformly loaded members of minor importance, its use is apt to result in highly uneconomical designs for I beams with medium and long spans and for composite construction (Ref. 19.20).

When shear reinforcement perpendicular to the axis of the beam is used, its contribution to shear strength of a prestressed beam is

$$V_s = \frac{A_v f_{yt} d}{s} \tag{19.47}$$

the same as for a nonprestressed member. According to the ACI Code, the value of V_s must not be taken greater than $8\sqrt{f'_c}b_w d$.

The total nominal shear strength V_n is found by summing the contributions of the concrete and steel, as indicated by Eq. (19.42):

$$V_n = V_c + \frac{A_v f_{yt} d}{s} \tag{19.48}$$

Then, from Eq. (19.41),

$$V_u = \phi V_n = \phi(V_c + V_s)$$

from which

$$V_u = \phi\left(V_c + \frac{A_v f_{yt} d}{s}\right) \tag{19.49}$$

The required cross-sectional area of one stirrup A_v can be calculated by suitable transposition of Eq. (19.49).

$$A_v = \frac{(V_u - \phi V_c)s}{\phi f_{yt} d} \tag{19.50}$$

Normally, in practical design, the engineer will select a trial stirrup size, for which the required spacing is found. Thus, a more convenient form of the last equation is

$$s = \frac{\phi A_v f_{yt} d}{V_u - \phi V_c} \tag{19.51}$$

A minimum area of shear reinforcement is required in all prestressed concrete members where the total factored shear force is greater than one-half the design shear strength provided by the concrete ϕV_c. Exceptions are made for slabs and footings, concrete-joist floor construction, and certain very shallow beams, according to the ACI Code. The minimum area of shear reinforcement to be provided in all other cases is equal to the smaller of

$$A_v = 0.75\sqrt{f_c'}\,\frac{b_w s}{f_{yt}} \le 50\,\frac{b_w s}{f_{yt}} \tag{19.52}$$

and

$$A_v = \frac{A_{ps}}{80}\,\frac{f_{pu}}{f_{yt}}\,\frac{s}{d}\sqrt{\frac{d}{b_w}} \tag{19.53}$$

in which A_{ps} is the cross-sectional area of the prestressing steel, f_{pu} is the tensile strength of the prestressing steel, and all other terms are as defined above.

The ACI Code contains certain restrictions on the maximum spacing of web reinforcement to ensure that any potential diagonal crack will be crossed by at least a minimum amount of web steel. For prestressed members, this maximum spacing is not to exceed the smaller of $0.75h$ or 24 in. If the value V_s exceeds $4\sqrt{f_c'}\,b_w d_p$, these limits are reduced by one-half.

EXAMPLE 19.6

The unsymmetrical I beam shown in Fig. 19.24 carries an effective prestress force of 288 kips and supports a superimposed dead load of 345 lb/ft and service live load of 900 lb/ft, in addition to its own weight of 255 lb/ft, on a 50 ft simple span. At the maximum moment section, the effective depth to the main steel is 24.5 in. (eccentricity 11.4 in.). The strands are deflected upward starting 15 ft from the support, and eccentricity is reduced linearly to zero at the support. If concrete with $f_c' = 5000$ psi and stirrups with $f_{yt} = 60{,}000$ psi are used, and if the prestressed strands have strength $f_{pu} = 270$ ksi, what is the required stirrup spacing at a point 10 ft from the support?

Solution. For a cross section with the given dimensions, it is easily confirmed that $I_c = 24{,}200$ in^4, $A_c = 245$ in^2, and $r^2 = I_c/A_c = 99$ in^2. At a distance 10 ft from the support centerline, the tendon eccentricity is

$$e = 11.4 \times \frac{10}{15} = 7.6 \text{ in.}$$

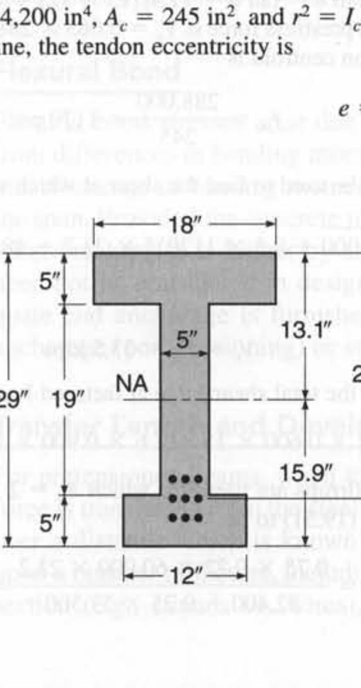

FIGURE 19.24
Post-tensioned beam in Example 19.6.

corresponding to an effective depth d from the compression face of 20.7 in. According to the ACI Code, the larger value of $d = 0.80 \times 29 = 23.2$ in. will be used. Calculation of V_{ci} is based on Eqs. (19.43) and (19.44). The bottom-fiber stress due to effective prestress acting alone is

$$f_{pe} = f_{2pe} = -\frac{P_e}{A_c}\left(1 + \frac{ec_2}{r^2}\right) = -\frac{288{,}000}{245}\left(1 + \frac{7.6 \times 15.9}{99}\right) = -2600 \text{ psi}$$

The moment and shear at the section due to beam load alone are, respectively,

$$M_{o,10} = \frac{w_o x}{2}(l - x) = 0.255 \times 5 \times 40 = 51 \text{ ft-kips}$$

$$V_{o,10} = w_o\left(\frac{l}{2} - x\right) = 0.255 \times 15 = 3.8 \text{ kips}$$

and the bottom-fiber stress due to this load is

$$f_{2o} = \frac{51 \times 12{,}000 \times 15.9}{24{,}200} = 402 \text{ psi}$$

Then, from Eq. (19.43),

$$M_{cre} = \frac{24{,}200(425 + 2600 - 402)}{15.9 \times 12} = 333{,}000 \text{ ft-lb}$$

The ratio of superimposed load shear to moment at the section is

$$\frac{V_{d+l}}{M_{d+l}} = \frac{l - 2x}{x(l - x)} = \frac{30}{400} = 0.075 \text{ ft}^{-1}$$

Equation (19.44) is then used to determine the shear force at which flexure-shear cracks can be expected to form.

$$V_{ci} = [0.6 \times 1\sqrt{5000}(5 \times 23.2) + 3800 + 0.075 \times 330{,}000] \times \frac{1}{1000} = 33.5 \text{ kips}$$

The lower limit of $1.7 \times 1\sqrt{5000}(5 \times 23.2)/1000 = 13.9$ kips does not control.

Calculation of V_{cw} is based on Eq. (19.45). The slope θ of the tendons at the section under consideration is such that $\sin\theta \approx \tan\theta = 11.4/(15 \times 12) = 0.063$. Consequently, the vertical component of the effective prestress force is $V_p = 0.063 \times 288 = 18.1$ kips. The concrete compressive stress at the section centroid is

$$f_{pc} = \frac{288{,}000}{245} = 1170 \text{ psi}$$

Equation (19.45) can now be used to find the shear at which web-shear cracks should occur.

$$V_{cw} = [(3.5 \times 1\sqrt{5000} + 0.3 \times 1170)5 \times 23.2 + 18{,}100] \times \frac{1}{1000} = 87.5 \text{ kips}$$

Thus, in the present case,

$$V_c = V_{ci} = 33.5 \text{ kips}$$

At the section considered, the total shear force at factored loads is

$$V_u = 1.2 \times 0.600 \times 15 + 1.6 \times 0.900 \times 15 = 32.4 \text{ kips}$$

When No. 3 (No. 10) U stirrups are used, for which $A_v = 2 \times 0.11 = 0.22 \text{ in}^2$, the required spacing is found from Eq. (19.51) to be

$$s = \frac{0.75 \times 0.22 \times 60{,}000 \times 23.2}{32{,}400 - 0.75 \times 33{,}500} = 32 \text{ in.}$$

Equation (19.53) is then applied to establish a maximum spacing criterion.

$$0.22 = \frac{1.75}{80} \times \frac{270}{60} \times \frac{s}{23.2}\sqrt{\frac{23.2}{5}} = 0.0091s$$

$$s = 24.1 \text{ in.}$$

The other criteria for maximum spacing, $\frac{3}{4} \times 29 = 22$ in. and 24 in., however, control here. Open U stirrups will be used, at a spacing of 22 in.

For comparison, the concrete shear will be calculated on the basis of Eq. (19.46). The ratio V_u/M_u is 0.075, and

$$V_c = \left(0.6 \times 1\sqrt{5000} + 700 \times \frac{0.075}{12} \times 23.2\right)(5 \times 23.2) \times \frac{1}{1000} = 16.7 \text{ kips}$$

The lower and upper limits, $2 \times 1\sqrt{5000}(5 \times 23.2)/1000 = 16.4$ kips and $5 \times 1\sqrt{5000}(5 \times 23.2)/1000 = 41.0$ kips, do not control. Thus, on the basis of V_c obtained from Eq. (19.46), the required spacing of No. 3 (No. 10) U stirrups is

$$s = \frac{0.75 \times 0.22 \times 60{,}000 \times 23.2}{32{,}400 - 0.75 \times 16{,}700} = 11.6 \text{ in.}$$

For the present case, an I-section beam of intermediate span, nearly 2 times the web steel is required at the location investigated if the alternative expression giving V_c directly is used.

19.15 BOND STRESS, TRANSFER LENGTH, AND DEVELOPMENT LENGTH

There are two separate sources of bond stress in prestressed concrete beams: (1) flexural bond, which exists in pretensioned construction between the tendons and the concrete and in grouted post-tensioned construction between the tendons and the grout, and between the conduit (if any) and concrete; and (2) prestress transfer bond, generally applicable to pretensioned members only.

a. Flexural Bond

Flexural bond stresses arise due to the change in tension along the tendon resulting from differences in bending moment at adjacent sections. They are proportional to the rate of change of bending moment, hence to the shear force, at a given location along the span. Provided the concrete member is uncracked, flexural bond stress is very low. After cracking, it is higher by an order of magnitude. However, flexural bond stress need not be considered in designing prestressed concrete beams, provided that adequate end anchorage is furnished for the tendon, in the form of either mechanical anchorage (post-tensioning) or strand embedment (pretensioning).

b. Transfer Length and Development Length

For pretensioned beams, when the external jacking force is released, the prestressing force is transferred from the steel to the concrete near the ends of the member by bond, over a distance which is known as the *transfer length*. The transfer length depends upon a number of factors, including the steel stress, the configuration of the steel cross section (e.g., strands vs. wires), the condition of the surface of the steel, and the suddenness with which the jacking force is released. Based on tests of seven-wire prestressing strand (Ref. 19.21), the effective prestress f_{pe} in the steel may be assumed to act at a transfer length from the end of the member equal to

$$l_t = \frac{f_{pe}}{3000} d_b \tag{a}$$

where l_t = transfer length, in.
d_b = nominal strand diameter, in.
f_{pe} = effective prestress, psi

The same tests indicate that the additional distance past the original transfer length necessary to develop the failure strength of the steel is closely represented by the expression

$$l_t' = \left(\frac{f_{ps} - f_{pe}}{1000}\right) d_b \tag{b}$$

where the quantity in parentheses is the stress increment above the effective prestress level, in psi units, to reach the calculated steel stress at failure f_{ps}. Thus the total development length at failure is

$$l_d = l_t + l_t' \tag{c}$$

or

$$l_d = \left(\frac{f_{ps} - \frac{2}{3} f_{pe}}{1000}\right) d_b \tag{19.54}$$

The ACI Code does not require that flexural bond stress be checked in either pretensioned or post-tensioned members, but for pretensioned strand it is required that the full development length, given by Eq. (19.54), be provided beyond the critical bending section. Investigation may be limited to those cross sections nearest each end of the member that are required to develop their full flexural strength under the specified factored load.

The development length of prestressing strand affects both shear and flexural strength at the end of pretensioned beams. The prestress component of the concrete shear contribution in Eq. (19.45) is usually considered to vary linearly from zero at the beam end to its full value of $0.3f_{pc}$ at the end of the transfer length l_t, according to ACI Commentary 12.9; and the flexural strength reduction factor $\phi = 0.75$ from the end of the member to the end of the transfer length and then varies linearly from 0.75 to 0.9 from the end of the transfer length to the end of the development length l_d, according to ACI Code 9.3.2.7. These reductions are especially relevant if concentrated loads are applied between the beam end and the end of the development length.

19.16 ANCHORAGE ZONE DESIGN

In prestressed concrete beams, the prestressing force is introduced as a load concentration acting over a relatively small fraction of the total member depth. For post-tensioned beams with mechanical anchorage, the load is applied at the end face, while for pretensioned beams it is introduced somewhat more gradually over the transfer length. In either case, the compressive stress distribution in the concrete becomes linear, conforming to that dictated by the overall eccentricity of the applied forces, only after a distance from the end roughly equal to the depth of the beam.

FIGURE 19.25
Contours of equal vertical stress. (*Adapted from Ref. 19.16.*)

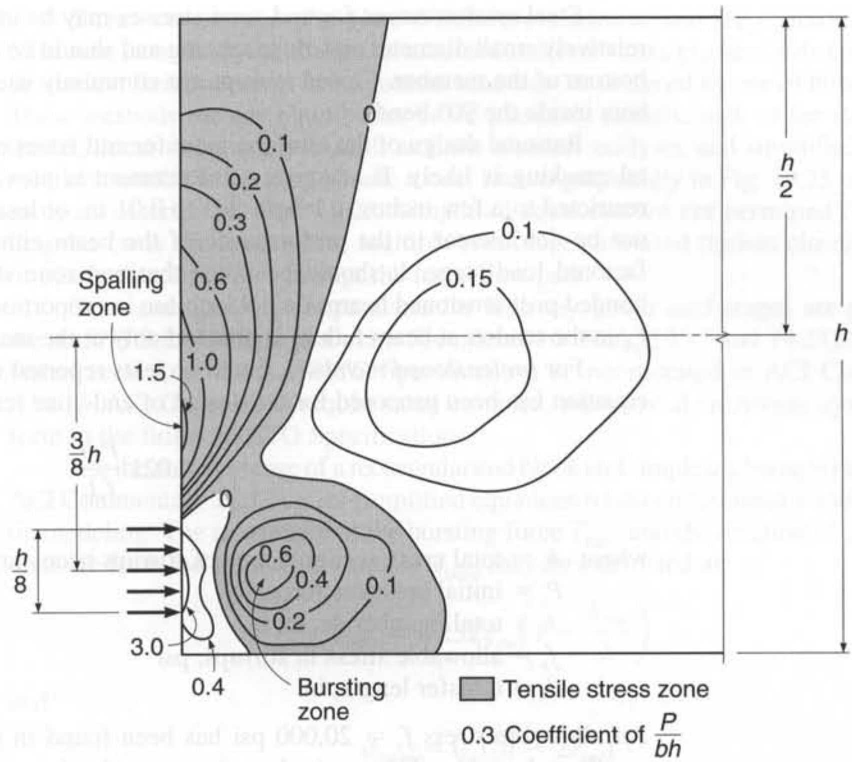

This transition of longitudinal compressive stress, from concentrated to linearly distributed, produces transverse (vertical) tensile stresses that may lead to longitudinal cracking of the member. The pattern and magnitude of the concrete stresses depend on the location and distribution of the concentrated forces applied by the tendons. Numerous studies have been made using the methods of classical elasticity, photoelasticity, and finite element analysis, and typical results are given in Fig. 19.25. Here the beam is loaded uniformly over a height equal to $h/8$ at an eccentricity of $3h/8$. Contour lines are drawn through points of equal vertical tension, with coefficients expressing the ratio of vertical stress to average longitudinal compression. Typically, there are high *bursting stresses* along the axis of the load a short distance inside the end zone and high *spalling stresses* at the loaded face.

In many post-tensioned prestressed I beams, solid end blocks are provided, as shown in Fig. 19.26. While these are often necessary to accommodate end-anchorage hardware and supplemental reinforcement, they are of little use in reducing transverse tension or avoiding cracking.

FIGURE 19.26
Post-tensioned I beam with rectangular end block.

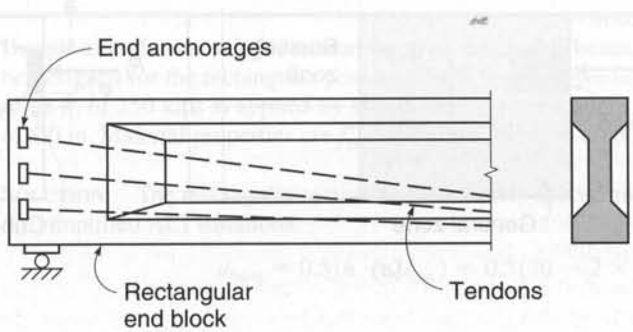

Steel reinforcement for end-zone stresses may be in the form of vertical bars of relatively small diameter and close spacing and should be well anchored at the top and bottom of the member. Closed stirrups are commonly used, with auxiliary horizontal bars inside the 90° bends.

Rational design of the reinforcement for end zones must recognize that horizontal cracking is likely. If adequate reinforcement is provided, so that the cracks are restricted to a few inches in length and to 0.01 in. or less in width, these cracks will not be detrimental to the performance of the beam either at service load or at the factored load stage. It should be noted that end-zone stresses in pretensioned and bonded post-tensioned beams do not increase in proportion to loads. The failure stress f_{ps} in the tendon at beam failure is attained only at the maximum moment section.

For *pretensioned members*, based on tests reported in Ref. 19.22, a very simple equation has been proposed for the design of end-zone reinforcement:

$$A_t = 0.021\,\frac{P_i h}{f_s l_t} \tag{19.55}$$

where A_t = total cross-sectional area of stirrups necessary, in^2
P_i = initial prestress force, lb
h = total member depth, in.
f_s = allowable stress in stirrups, psi
l_t = transfer length, in.

An allowable stress f_s = 20,000 psi has been found in tests to produce acceptably small crack widths. The required reinforcement having total area A_t should be distributed over a length equal to $h/5$ measured from the end face of the beam, and for most efficient crack control the first stirrup should be placed as close to the end face as practical. It is recommended in Ref. 19.22 that vertical reinforcement according to Eq. (19.55) be provided for *all* pretensioned members, unless tests or experience indicates that cracking does not occur at service or overload stages.

For post-tensioned members, the end region is divided into two zones, local and general, as shown in Fig. 19.27*a*. The *local zone* is a rectangular prism immediately surrounding the anchorage device and any confining reinforcement around the device. The *general zone* consists of a region that is approximately one structural depth h from the end of the beam and includes the local zone. For internal anchors, such as used in slabs, the general zone extends a distance h ahead of and behind the anchorage hardware. Stresses in the local zone are determined based on tests. The post-tensioning supplier specifies the reinforcement details for the local zone.

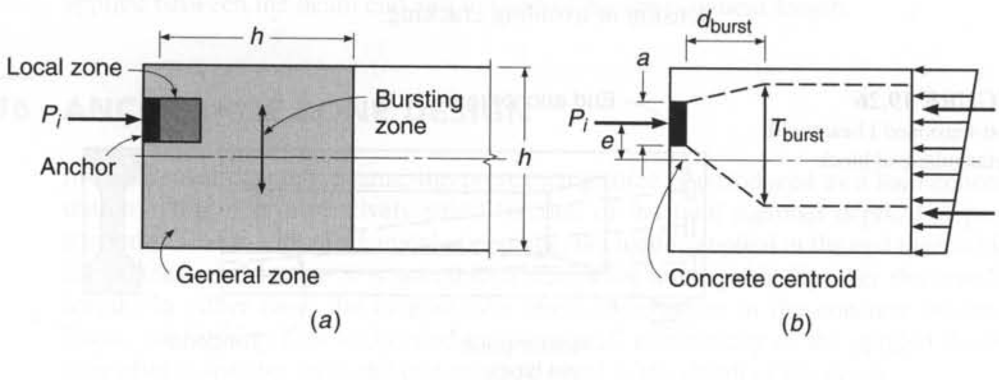

FIGURE 19.27
Post-tensioned end block: (*a*) local and general zone; (*b*) strut-and-tie model.

Stress variations in the general zone are nonlinear and are characterized by a transition from the local zone to an assumed uniform stress gradient a distance h from the anchor. Reinforcement in the general zone may be designed by one of three methods. These methods include equilibrium-based plasticity models, such as the strut-and-tie model, linear stress analysis such as finite element analysis, and simplified elasticity solutions similar to the photoelastic model shown graphically in Fig. 19.25 or elasticity analyses described in Ref. 19.23. Simplified equations are not permitted for nonrectangular cross sections, where multiple anchorages are used (unless closely spaced), or where discontinuities disrupt the force flow path.

Strut-and-tie design approaches for highway girder anchorages are detailed in the *AASHTO LRFD Bridge Design Specifications* (Refs. 19.17 and 19.23). An abbreviated version of the AASHTO Specifications is incorporated in ACI Commentary R18.13. ACI Code 18.15 requires that complex, multistrand anchorage systems conform to the full AASHTO Specifications.

For the common case of a rectangular end block and simple anchorage (Fig. 19.27*b*), ACI Commentary 18.13 offers simplified equations based on test results and strut-and-tie modeling. The magnitude of the bursting force T_{burst} and the location of its centroid distance from the front of the anchor d_{burst} may be calculated as

$$T_{\text{burst}} = 0.25\Sigma P_{pu}\left(1 - \frac{h_{\text{anc}}}{h}\right) \tag{19.56}$$

and

$$d_{\text{burst}} = 0.5(h - 2e_{\text{anc}}) \tag{19.57}$$

where ΣP_{pu} = sum of total factored post-tensioning force
e_{anc} = absolute value of eccentricity of anchorage device to centroid of concrete section
h = depth of cross section
h_{anc} = depth of anchorage device

The use of the factored post-tensioning force P_{pu} recognizes that the tendon force is acting as a load. Hence, the maximum jacking stress $0.80f_{pu}$ is multiplied by a load factor of 1.2 to calculate P_{pu}.

$$P_{pu} = 1.2(0.80f_{pu})A_{ps} = 0.96f_{pu}A_{ps} \tag{19.58}$$

Transverse reinforcement with total area $A_s = T_{\text{burst}}/\phi f_y$ is added in a region that is centered on the location d_{burst} to carry the bursting force.

In cases where the simplified equations do not apply, a strut-and-tie model (Chapter 10) or finite element analysis may be required to design the bursting zone.

EXAMPLE 19.7 **Design of end-zone reinforcement for post-tensioned beam.** End-zone reinforcement is to be designed for the rectangular post-tensioned beam shown in Fig. 19.28. The initial prestress force P_i of 250 kips is applied by two closely spaced tendons having a combined eccentricity of 8.0 in. Material properties are f'_{ci} = 4250 psi and f_y = 60,000 psi.

Solution. The rectangular section and the closely spaced anchorage devices allow the use of the simplified ACI equations.

$$d_{\text{burst}} = 0.5(h - 2e_{\text{anc}}) = 0.5(30 - 2 \times 8) = 7 \text{ in.}$$

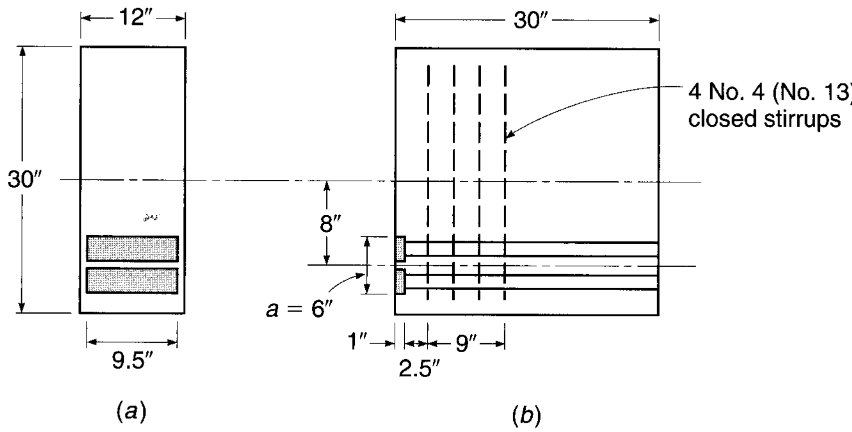

FIGURE 19.28
Design of post-tensioned anchor zone: (*a*) section at end anchors; (*b*) end zone reinforcement.

The initial prestressing force is 250 kips, which corresponds to a tendon stress level of $0.82f_{py}$. The maximum jacking stress level in the tendons is $0.94f_{py}$, or $0.80f_{pu}$. In this example, only the initial prestress is provided. Hence, the factored tendon force is calculated as

$$P_{pu} = 1.2\left(\frac{0.94}{0.82}\right)250 = 344 \text{ kips}$$

for which

$$T_{\text{burst}} = 0.25\Sigma P_{pu}\left(1 - \frac{h_{\text{anc}}}{h}\right) = 0.25 \times 344\left(1 - \frac{6}{30}\right) = 68.8 \text{ kips}$$

The area of steel needed to resist T_{burst} is

$$A_s = \frac{T_{\text{burst}}}{\phi f_y} = \frac{68.8}{0.85 \times 60} = 1.35 \text{ in}^2$$

Using No. 4 (No. 13) closed stirrups with an area of 2×0.20 in^2 gives

$$n = \frac{1.35}{2 \times 0.20} = 3.4 \text{ stirrups}$$

Four No. 4 (No. 13) closed stirrups will be used. The first stirrup will be placed $2\frac{1}{2}$ in. from the anchor plate, and the other three stirrups will be placed 3 in. on center, as shown in Fig. 19.28*b*, centering the stirrups a distance d_{burst} from the anchor plate. The closed stirrups ensure that anchorage requirements are satisfied. Details of the reinforcement in the local zone are not shown.

19.17 DEFLECTION

Deflection of the slender, relatively flexible beams that are made possible by prestressing must be predicted with care. Many members, satisfactory in all other respects, have proved to be unserviceable because of excessive deformation. In some cases, the absolute amount of deflection is excessive. Often, it is the differential deformation between adjacent members (e.g., precast roof-deck units) that causes problems. More often than not, any difficulties that occur are associated with upward deflection due to the sustained prestress load. Such difficulties are easily avoided by proper consideration in design.

When the prestress force is first applied, a beam will normally camber upward. With the passage of time, concrete shrinkage and creep will cause a gradual reduction of prestress force. In spite of this, the upward deflection usually will increase, due to the differential creep, affecting the highly stressed bottom fibers more than the top. With the application of superimposed dead and live loads, this upward deflection will be partially or completely overcome, and zero or downward deflection obtained. Clearly, in computing deformation, careful attention must be paid to both the age of the concrete at the time of load application and the duration of the loading.

The prediction of deflection can be approached at any of several levels of accuracy, depending upon the nature and importance of the work. In some cases, it is sufficient to place limitations on the span-depth ratio, based on past experience. Generally, deflections must be calculated. (Calculation is required for *all* prestressed members, according to ACI Code 9.5.4.) The approximate method described here will be found sufficiently accurate for most purposes. In special circumstances, where it is important to obtain the best possible information on deflection at all important load stages, such as for long-span bridges, the only satisfactory approach is to use a summation procedure based on incremental deflection at discrete time steps, as described in Refs. 19.1, 19.8, 19.24, and 19.25. In this way, the time-dependent changes in prestress force, material properties, and loading can be accounted for to the desired degree of accuracy.

Normally, the deflections of primary interest are those at the initial stage, when the beam is acted upon by the initial prestress force P_i and its own weight, and one or more combinations of load in service, when the prestress force is reduced by losses to the effective value P_e. Deflections are modified by creep under the sustained prestress force and due to all other sustained loads.

The short-term deflection Δ_{pi} due to the initial prestress force P_i can be found based on the variation of prestress moment along the span, making use of moment-area principles and superposition. For statically determinate beams, the ordinates of the moment diagram resulting from the eccentric prestress force are directly proportional to the eccentricity of the steel centroid line with respect to the concrete centroid. For indeterminate beams, eccentricity should be measured to the thrust line rather than to the steel centroid (see Ref. 19.1). In either case, the effect of prestress can also be regarded in terms of equivalent loads and deflections found using familiar deflection equations.

The downward deflection Δ_o due to girder self-weight, which is usually uniformly distributed, is easily found by conventional means. Thus, the net deflection obtained immediately upon prestressing is

$$\Delta = -\Delta_{pi} + \Delta_o \tag{19.59}$$

where the negative sign indicates upward displacement.

Long-term deflections due to prestress occur as that force is gradually reducing from P_i to P_e. This can be accounted for in an approximate way by assuming that creep occurs under a constant prestress force equal to the average of the initial and final values. Corresponding to this assumption, the total deflection resulting from prestress alone is

$$\Delta = -\Delta_{pe} - \frac{\Delta_{pi} + \Delta_{pe}}{2} C_c \tag{19.60}$$

where

$$\Delta_{pe} = \Delta_{pi} \frac{P_e}{P_i}$$

TABLE 19.5
Deflection and crack width requirements for prestressed concrete members

	Class		
Condition	**U**	**T**	**C**
Assumed behavior	Uncracked	Transition between cracked and uncracked	Cracked
Deflection calculation basis	Gross section	Cracked section—bilinear behavior	Cracked section—bilinear behavior

and C_c is set equal to the ultimate creep coefficient C_u for the concrete (see Table 2.1).

The long-term deflection due to self-weight is also increased by creep and can be obtained by applying the creep coefficient directly to the instantaneous value. Thus, the total member deflection, after losses and creep deflections, when effective prestress and self-weight act, is

$$\Delta = -\Delta_{pe} - \frac{\Delta_{pi} + \Delta_{pe}}{2} C_c + \Delta_o(1 + C_c) \tag{19.61}$$

The deflection due to superimposed loads can now be added, with the creep coefficient introduced to account for the long-term effect of the sustained loads, to obtain the net deflection at full service loading:

$$\Delta = -\Delta_{pe} - \frac{\Delta_{pi} + \Delta_{pe}}{2} C_c + (\Delta_o + \Delta_d)(1 + C_c) + \Delta_l \tag{19.62}$$

where Δ_d and Δ_l are the immediate deflections due to superimposed dead and live loads, respectively.

The selection of section properties for the calculation of deflections is dependent upon the cracking in the section. Table 19.5 defines the appropriate section properties and deflection calculation methodology for Class U, T, and C members (Refs. 19.1, 19.23, and 19.24). Bilinear behavior in Table 19.5 implies that deflections based on loads up to the cracking moment are based on the gross section, and deflections on loads greater than the cracking load are based on the effective cracked section properties (Ref. 19.8).

EXAMPLE 19.8 The 40 ft simply supported T beam shown in Fig. 19.29 is prestressed with a force of 314 kips, using a parabolic tendon with an eccentricity of 3 in. above the concrete centroid at the supports and 7.9 in. below the centroid at midspan. After time-dependent losses have occurred, this prestress is reduced to 267 kips. In addition to its own weight of 330 lb/ft, the girder must carry a short-term superimposed live load of 900 lb/ft. Estimate the deflection at all critical stages of loading. The creep coefficient $C_c = 2.0$, $E_c = 4 \times 10^6$ psi, and modulus of rupture = 530 psi.

Solution. It is easily confirmed that the stress in the bottom fiber when the beam carries the maximum load to be considered is 80 psi compression, meeting the requirements for a Class U

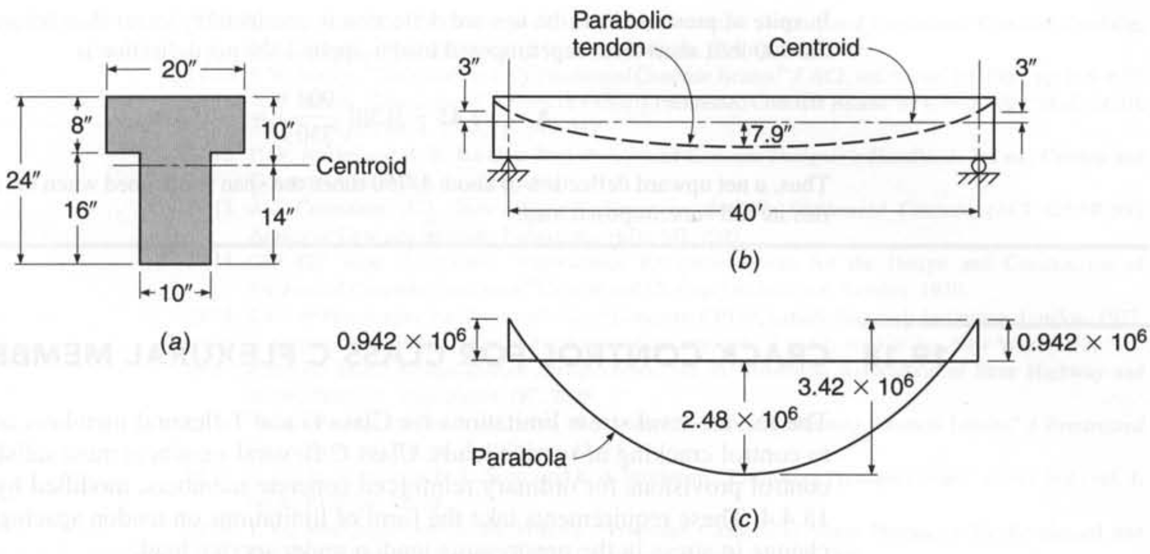

FIGURE 19.29
T beam of Example 19.8: (*a*) cross section; (*b*) tendon profile; (*c*) moment from initial prestressing force (in-lb).

member. All deflection calculations can, therefore, be based on the moment of inertia of the gross concrete section $I_c = 15{,}800$ in^4. It is convenient to calculate the deflection due to prestress and that due to girder load separately, superimposing the results later. For the eccentricities of the tendon profile shown in Fig. 19.29*b*, the application of $P_i = 314$ kips causes the moments shown in Fig. 19.29*c*. Applying the second moment-area theorem by taking moments of the M/EI diagram between midspan and the support, about the support, produces the vertical displacement between those two points as follows:

$$\Delta_{pi} = \frac{-(3.42 \times 10^6 \times 240 \times \frac{2}{3} \times 240 \times \frac{5}{8}) + (0.942 \times 10^6 \times 240 \times 120)}{4 \times 10^6 \times 15{,}800} = -0.87 \text{ in.}$$

the minus sign indicating upward deflection due to initial prestress alone. The downward deflection due to the self-weight of the girder is calculated by the well-known equation

$$\Delta_o = \frac{5wl^4}{384EI} = \frac{5 \times 330 \times 40^4 \times 12^4}{384 \times 12 \times 4 \times 10^6 \times 15{,}800} = +0.30 \text{ in.}$$

When these two results are superimposed, the net upward deflection when initial prestress and girder load act together is

$$-\Delta_{pi} + \Delta_o = -0.87 + 0.30 = -0.57 \text{ in.}$$

Shrinkage and creep of the concrete cause a gradual reduction of prestress force from $P_i =$ 314 kips to $P_e = 267$ kips and reduce the bending moment due to prestress proportionately. Concrete creep, however, acts to increase both the upward deflection component due to the prestress force and the downward deflection component due to the girder load. The net deflection after these changes take place is found using Eq. (19.60), with $\Delta_{pe} = -0.87 \times 267/314 =$ -0.74 in.:

$$\Delta = -0.74 - \frac{0.87 + 0.74}{2} \times 2.0 + 0.30(1 + 2.0)$$

$$= -0.74 - 1.61 + 0.90 = -1.45 \text{ in.}$$

In spite of prestress loss, the upward deflection is considerably larger than before. Finally, as the 900 lb/ft short-term superimposed load is applied, the net deflection is

$$\Delta = -1.45 + 0.30\left(\frac{900}{330}\right) = -0.63 \text{ in.}$$

Thus, a net upward deflection of about 1/750 times the span is obtained when the member carries its full superimposed load.

19.18 CRACK CONTROL FOR CLASS C FLEXURAL MEMBERS

The service level stress limitations for Class U and T flexural members are sufficient to control cracking at service loads. Class C flexural members must satisfy the crack control provisions for ordinary reinforced concrete members, modified by ACI Code 18.4.4. These requirements take the form of limitations on tendon spacing and on the change in stress in the prestressing tendon under service load.

For Class C prestressed flexural members not subjected to fatigue or aggressive exposure, the spacing of bonded reinforcement nearest the extreme tension face may not exceed that given for nonprestressed concrete in Section 6.3. Aggressive conditions occur where the tendons may be exposed to chemical attack and include seawater and corrosive industrial environments. In these situations, the designer should increase the concrete cover or reduce the tensile stresses, based on professional judgment, commensurate with the exposure risk.

The spacing requirements for reinforcement in Class C members may be satisfied by using nonprestressed bonded tendons. The spacing between bonded tendons, however, may not exceed two-thirds of the maximum spacing for nonprestressed reinforcement given in Eq. (6.3). When both conventional reinforcement and bonded tendons are used to meet the spacing requirements, the spacing between a tendon and a bar may not exceed five-sixths of that permitted in Eq. (6.3). When applying Eq. (6.3), Δf_{ps} is substituted for f_s, where Δf_{ps} is the difference between the tendon stress at service loads based on a cracked section and the decompression stress f_{dc}, which is equal to the stress in the tendon when concrete stress at the level of the tendon is zero. ACI Code 18.4.4 permits f_{dc} to be taken as the effective prestress f_{pe}. The magnitude of Δf_{ps} is limited to a maximum of 36 ksi. When Δf_{ps} is less than 20 ksi, the reduced spacing requirements need not be applied. If the effective depth of the member exceeds 36 in., additional skin reinforcement along the sides of the member web, as described in Section 6.3, is required to prevent excessive surface crack widths above the main flexural reinforcement.

REFERENCES

19.1. A. H. Nilson, *Design of Prestressed Concrete*, 2nd ed., John Wiley, New York, 1987.
19.2. A. E. Naaman, *Prestressed Concrete Analysis and Design: Fundamentals*, 2nd ed., TechnoPress 3000, Ann Arbor, Michigan, 2004.
19.3. T. Y. Lin and N. H. Burns, *Design of Prestressed Concrete Structures*, 3rd ed., John Wiley, New York, 1981.
19.4. J. R. Libby, *Modern Prestressed Concrete*, 3rd ed., Van Nostrand Reinhold, New York, 1984.
19.5. E. G. Nawy, *Prestressed Concrete*, 5th ed., Prentice-Hall, Englewood Cliffs, NJ, 2005.
19.6. M. P. Collins and D. Mitchell, *Prestressed Concrete Structures*, Prentice-Hall, Englewood Cliffs, NJ, 1991.
19.7. *Post-Tensioning Manual*, 6th ed., Post-Tensioning Institute, Phoenix, AZ, 2006.
19.8. *PCI Design Handbook*, 6th ed., Precast/Prestressed Concrete Institute, Chicago, IL, 2004.

19.9. *Quality Control for Plants and Production of Structural Precast and Prestressed Concrete Products*, MNL 116-99, Precast/Prestressed Concrete Institute, Chicago, IL, 1999.
19.10. P. W. Abeles, "Design of Partially Prestressed Concrete Beams," *J. ACI*, vol. 64, no. 10, 1967, pp. 669–677.
19.11. A. H. Nilson, "Discussion of 'Design of Partially Prestressed Concrete Beams' by P. W. Abeles" (Ref. 19.10), *J. ACI*, vol. 65, no. 4, 1968, pp. 345–347.
19.12. P. W. Abeles and B. K. Bardhan-Roy, *Prestressed Concrete Designer's Handbook*, 3rd ed., Cement and Concrete Association, London, 1981.
19.13. ACI Committee 423, *State-of-the-Art Report on Partially Prestressed Concrete* (ACI 423.5R-99), American Concrete Institute, Farmington Hills, MI, 1999.
19.14. CEB-FIP Joint Committee, "International Recommendations for the Design and Construction of Prestressed Concrete Structures," Cement and Concrete Association, London, 1970.
19.15. *Code of Practice for the Structural Use of Concrete*, CP110, British Standards Institution, London, 1972.
19.16. Y. Guyon, *Limit State Design of Prestressed Concrete*, vols. 1 and 2, John Wiley, New York, 1972.
19.17. *AASHTO LRFD Bridge Design Specifications*, 4th ed., American Association of State Highway and Bridge Officials, Washington, DC, 2008.
19.18. PCI Committee on Prestress Losses, "Recommendations for Estimating Prestress Losses," *J. Prestressed Concr. Inst.*, vol. 20, no. 4, 1975, pp. 43–75.
19.19. P. Zia, H. K. Preston, N. L. Scott, and E. B. Workman, "Estimating Prestress Losses," *Concr. Intl.*, vol. 1, no. 6, 1979, pp. 32–38.
19.20. J. G. MacGregor and J. M. Hanson, "Proposed Changes in Shear Provisions for Reinforced and Prestressed Concrete Beams," *J. ACI*, vol. 66, no. 4, 1969, pp. 276–288.
19.21. N. W. Hanson and P. W. Kaar, "Flexural Bond Tests of Pretensioned Prestressed Beams," *J. ACI*, vol. 30, no. 7, 1959, pp. 783–802.
19.22. W. T. Marshall and A. H. Mattock, "Control of Horizontal Cracking in the Ends of Pretensioned Prestressed Concrete Girders," *J. Prestressed Concr. Inst.*, vol. 5, no. 5, 1962, pp. 56–74.
19.23. J. E. Breen, O. Burdet, C. Roberts, D. Sanders, G. Wollman, and B. Falconer, "Anchorage Zone Reinforcement for Post-Tension Concrete Girders," NCHRP Report 356, Transportation Research Board, National Academy Press, Washington, DC, 1994.
19.24. ACI Committee 435, "Deflection of Prestressed Concrete Members," *J. ACI*, vol. 60, no. 12, 1963, pp. 1697–1728.
19.25. D. E. Branson, *Deformation of Concrete Structures*, McGraw-Hill, New York, 1977.

PROBLEMS

19.1. A rectangular concrete beam with width $b = 11$ in. and total depth $h = 28$ in. is post-tensioned using a single parabolic tendon with an eccentricity of 7.8 in. at midspan and 0 in. at the simple supports. The initial prestress force $P_i = 334$ kips, and the effectiveness ratio $R = 0.84$. The member is to carry superimposed dead and live loads of 300 and 1000 lb/ft, respectively, uniformly distributed over the 40 ft span. Specified concrete strength $f'_c = 5000$ psi, and at the time of transfer $f'_{ci} = 4000$ psi. Determine the flexural stress distributions in the concrete at midspan (*a*) for initial conditions before application of superimposed load and (*b*) at full service load. Compare with the ACI limit stresses for Class U members.

19.2. A pretensioned prestressed beam has a rectangular cross section of 6 in. width and 20 in. total depth. It is built using normal-density concrete with a specified strength $f'_c = 4000$ psi and a strength at transfer of $f'_{ci} = 3000$ psi. Stress limits are as follows: $f_{ti} = 165$ psi, $f_{ci} = -1800$ psi, $f_{ts} = 475$ psi, and $f_{cs} = -1800$ psi. The effectiveness ratio R may be assumed equal to 0.80. For these conditions, find the initial prestress force P_i and eccentricity e to maximize the superimposed load moment $M_d + M_l$ that can be carried without exceeding the stress limits. What uniformly distributed load can be carried on a 30 ft simple span? What tendon profile would you recommend?

19.3. A pretensioned beam is to carry a superimposed dead load of 600 lb/ft and service live load of 1200 lb/ft on a 55 ft simple span. A symmetrical I section with $b = 0.5h$ will be used. Flange thickness $h_f = 0.2h$ and web width $b_w = 0.4b$.

The member will be prestressed using Grade 270 strands. Time-dependent losses are estimated at 20 percent of P_i. Normal-density concrete will be used, with $f'_c = 5000$ psi and $f'_{ci} = 3000$ psi.

(*a*) Using straight strands, find the required concrete dimensions, prestress force, and eccentricity. Select an appropriate number and size of tendons, and show by sketch their placement in the section.

(*b*) Revise the design of part (*a*) using tendons harped at the third points of the span, with eccentricity reduced to zero at the supports.

(*c*) Comment on your results. In both cases, ACI stress limits are to be applied. You may assume that deflections are not critical and that the beam is Class T at full service load.

19.4. The hollow core section shown in Fig. P19.4 is prestressed with four $\frac{1}{2}$ in. diameter, 270 ksi low-relaxation strands and is simply supported on masonry walls with a span length of 20 ft, center to center of the supports. In addition to its self-weight, the section carries a superimposed live load of 225 psf. Material properties are $f'_c = 5000$ psi and $f'_{ci} = 3500$ psi. Determine (*a*) if service load stresses in the section are suitable for a Class U flexural member using $R = 0.82$ and (*b*) if the section has sufficient capacity for the specified loads.

FIGURE P19.4

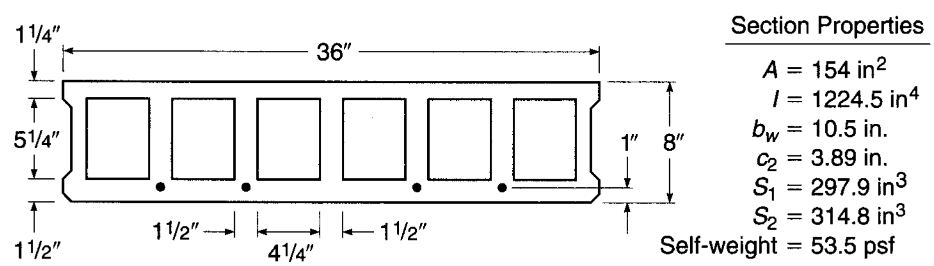

19.5. For the beam in Problem 19.4, make a detailed computation of the losses in the prestressing force. Compare your results to the assumed value of $R = 0.82$.

19.6. Establish the required spacing of No. 3 (No. 10) stirrups at a beam cross section subject to factored load shear V_u of 35.55 kips and moment M_u of 474 ft-kips. Web width $b_w = 5$ in., effective depth $d = 24$ in., and total depth $h = 30$ in. The concrete shear contribution may be based on the approximate relationship of Eq. (19.46). Use $f_y = 60{,}000$ psi for stirrup steel, and take $f'_c = 5000$ psi.

19.7. A symmetrical prestressed I beam having total depth 48 in., flange width 24 in., flange thickness 9.6 in., and web thickness 9.6 in. is to span 70 ft. It is post-tensioned using 18 Grade 270 $\frac{1}{2}$ in. diameter low-relaxation strands in a single tendon having a parabolic profile, with $e = 18$ in. at midspan and 0 in. at the supports. (The curve can be approximated by a circular arc for loss calculations.) The jacking force $P_j = 618$ kips. Calculate losses due to slip, elastic shortening, friction, creep, shrinkage, and relaxation. Express your results in tabular form both numerically and as percentages of initial prestress P_i. Creep effects may be assumed to occur under the combination of prestress force plus self-weight. The beam is prestressed when the concrete is aged 7 days. Anchorage slip = 0.25 in., coefficient of strand friction = 0.20, coefficient of wobble friction = 0.0010, creep coefficient = 2.35. Member properties are as follows: $A_c = 737$ in², $I_c = 192{,}000$ in⁴, $c_1 = c_2 = 24$ in., $f'_c = 5000$ psi, $E_c = 4{,}000{,}000$ psi, $E_s = 27{,}000{,}000$ psi, $w_c = 150$ pcf, and $C_c = 2.65$.

19.8. The concrete T beam shown in Fig. P19.8 is post-tensioned at an initial force $P_i = 229$ kips, which reduces after 1 year to an effective value $P_e = 183$ kips. In addition to its own weight, the beam will carry a superimposed short-term live load of 21.5 kips at midspan. Using the approximate method described in Section 19.17, find (*a*) the initial deflection of the unloaded girder and (*b*) the deflection at the age of 1 year of the loaded girder. The following data are given: $A_c = 450$ in^2, $c_1 = 8$ in., $I_c = 24{,}600$ in^4, $E_c = 3{,}500{,}000$ psi, $C_c = 2.5$.

FIGURE P19.8

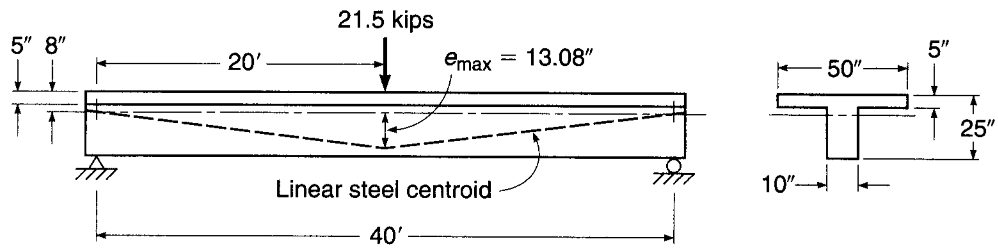

20 Seismic Design

20.1 INTRODUCTION

Earthquakes result from the sudden movement of tectonic plates in the earth's crust. The movement takes place at fault lines, and the energy released is transmitted through the earth in the form of waves that cause ground motion many miles from the epicenter. Regions adjacent to active fault lines are the most prone to experience earthquakes. The map in Fig. 20.1 shows the *maximum considered ground motion* for the contiguous 48 states. The mapped values, expressed as a percent of gravity, represent the expected peak acceleration of a single-degree-of-freedom system with a 0.2 sec period and 5 percent of critical damping. Known as the *0.2 sec spectral response acceleration* S_s (subscript *s* for *short* period), it is used, along with the 1.0 sec spectral response acceleration S_1 (mapped in a similar manner), to establish the loading criteria for seismic design. Accelerations S_s and S_1 are based on historical records and local geology. For most of the country, they represent earthquake ground motion with a "likelihood of exceedance of 2 percent in 50 years," a value that is equivalent to a return period of about 2500 years (Ref. 20.1).

As experienced by structures, earthquakes consist of random horizontal and vertical movements of the earth's surface. As the ground moves, inertia tends to keep structures in place (Fig. 20.2), resulting in the imposition of displacements and forces that can have catastrophic results. The purpose of seismic design is to proportion structures so that they can withstand the displacements and the forces induced by the ground motion.

Historically in North America, seismic design has emphasized the effects of horizontal ground motion because the horizontal components of an earthquake usually exceed the vertical component and because structures are usually much stiffer and stronger in response to vertical loads than they are in response to horizontal loads. Experience has shown that the horizontal components are the most destructive. For structural design, the intensity of an earthquake is usually described in terms of the peak ground acceleration as a fraction of the acceleration of gravity, i.e., $0.1g$, $0.2g$, or $0.3g$. Although peak acceleration is an important design parameter, the frequency characteristics and duration of an earthquake are also important; the closer the frequency of the earthquake motion is to the natural frequency of a structure and the longer the duration of the earthquake, the greater the potential for damage.

Based on elastic behavior, structures subjected to a major earthquake would be required to undergo large displacements. However, North American practice (Ref. 20.2) requires that structures be designed for only a fraction of the forces associated with those displacements. The relatively low design forces are justified by the observations that buildings designed for low forces have behaved satisfactorily and that structures

FIGURE 20.1
Map showing maximum considered earthquake ground motion, 0.2 sec spectral response acceleration (5 percent of critical damping), for the contiguous United States. (*United States Geological Survey.*)

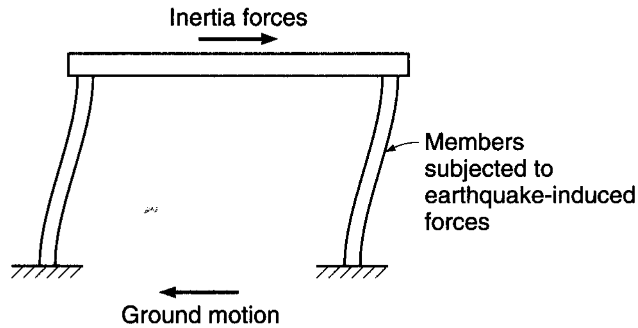

FIGURE 20.2
Structure subjected to ground motion.

dissipate significant energy as the materials yield and behave inelastically. This nonlinear behavior, however, usually translates into increased displacements, which may require significant ductility and result in major nonstructural damage. Displacements may also be of such a magnitude that the strength of the structure is affected by stability considerations, such as discussed for slender columns in Chapter 9.

Designers of structures that may be subjected to earthquakes, therefore, are faced with a choice: (1) providing adequate stiffness and strength to limit the response of structures to the elastic range or (2) providing lower-strength structures, with presumably lower initial costs, that have the ability to withstand large inelastic deformations while maintaining their load-carrying capability.

20.2 STRUCTURAL RESPONSE

The safety of a structure subjected to seismic loading rests on the designer's understanding of the response of the structure to ground motion. For many years, the goal of earthquake design in North America has been to construct buildings that will withstand *moderate earthquakes without damage and severe earthquakes without collapse*. Building codes have undergone regular modification as major earthquakes have exposed weaknesses in existing design criteria.

Design for earthquakes differs from design for gravity and wind loads in the relatively greater sensitivity of earthquake-induced forces to the geometry of the structure. Without careful design, forces and displacements can be concentrated in portions of a structure that are not capable of providing adequate strength or ductility. Steps to strengthen a member for one type of loading may actually increase the forces in the member and change the mode of failure from ductile to brittle.

a. Structural Considerations

The closer the frequency of the ground motion is to one of the natural frequencies of a structure, the greater the likelihood of the structure experiencing resonance, resulting in an increase in both displacement and damage. Therefore, earthquake response depends strongly on the geometric properties of a structure, especially height. Tall buildings respond more strongly to long-period (low-frequency) ground motion, while short buildings respond more strongly to short-period (high-frequency) ground motion. Figure 20.3 shows the shapes for the principal modes of vibration of a three-story frame structure. The relative contribution of each mode to the lateral displacement of the structure depends on the frequency characteristics of the ground motion. The first mode (Fig. 20.3*a*) usually provides the greatest contribution to lateral displacement.

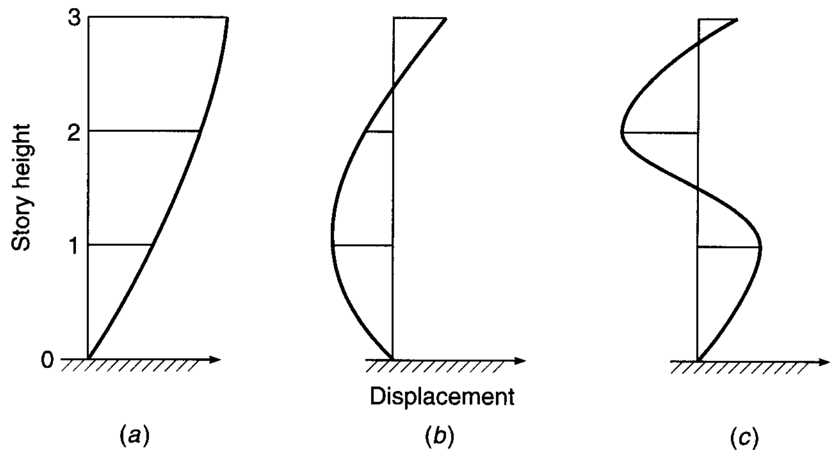

FIGURE 20.3
Modal shapes for a three-story building: (*a*) first mode; (*b*) second mode; (*c*) third mode. (*Adapted from Ref. 20.3.*)

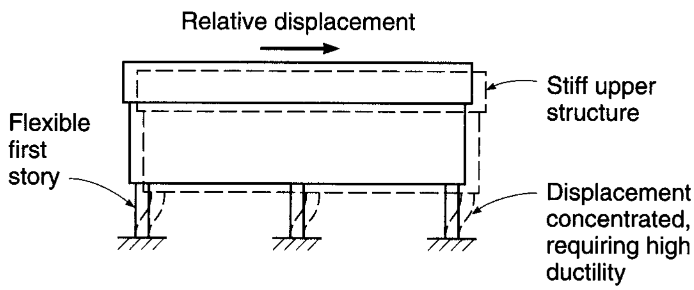

FIGURE 20.4
Soft first story supporting a stiff upper structure.

The taller a structure, the more susceptible it is to the effects of higher modes of vibration, which are generally additive to the effects of the lower modes and tend to have the greatest influence on the upper stories. Under any circumstances, the longer the duration of an earthquake, the greater the potential for damage.

The configuration of a structure also has a major effect on its response to an earthquake. Structures with a discontinuity in stiffness or geometry can be subjected to undesirably high displacements or forces. For example, the discontinuance of shear walls, infill walls, or even cladding at a particular story level, such as shown in Fig. 20.4, will have the result of concentrating the displacement in the open, or "soft," story. The high displacement will, in turn, require a large amount of ductility if the structure is not to fail. Such a design is not recommended, and the stiffening members should be continued to the foundation. The problems associated with a soft story are illustrated in Fig. 20.5, which shows the Olive View Hospital following the 1971 San Fernando earthquake. The high ductility "demand" could not be satisfied by the column at the right, with low amounts of transverse reinforcement. Even the columns at center, with significant transverse reinforcement, performed poorly because the transverse reinforcement was not continued into the joint, resulting in the formation of hinges at the column ends. Figure 20.6 illustrates structures with vertical geometric and plan irregularities, which result in torsion induced by ground motion.

Within a structure, stiffer members tend to pick up a greater portion of the load. When a frame is combined with a shear wall, this can have the positive effect of reducing the displacements of the structure and decreasing both structural and non-structural damage. However, when the effects of higher stiffness members, such as masonry infill walls, are not considered in the design, unexpected and often undesirable results can occur.

FIGURE 20.5
Damage to soft story columns in the Olive View Hospital as a result of the 1971 San Fernando earthquake. (*Photograph by James L. Stratta. Courtesy of the Federal Emergency Management Agency.*)

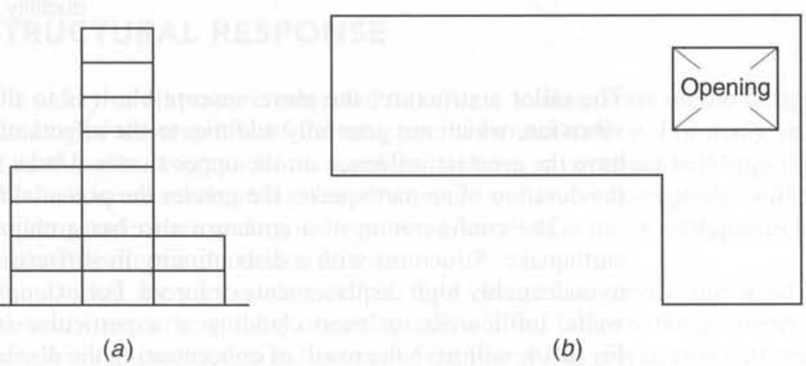

FIGURE 20.6
Structures with (*a*) vertical geometric and (*b*) plan irregularities. (*Adapted from Ref. 20.3.*)

Finally, any discussion of structural considerations would be incomplete without emphasizing the need to provide adequate separation between structures. Lateral displacements can result in structures coming in contact during an earthquake, resulting in major damage due to hammering, as shown in Fig. 20.7. Spacing requirements to ensure that adjacent structures do not come into contact as the result of earthquake-induced motion are specified in Ref. 20.2.

b. Member Considerations

Members designed for seismic loading must perform in a ductile fashion and dissipate energy in a manner that does not compromise the strength of the structure. Both the overall design and the structural details must be considered to meet this goal.

FIGURE 20.7
Damage caused by hammering for buildings with inadequate separation in the 1985 Mexico City earthquake. (*Photograph by Jack Moehle.*)

The principal method of ensuring ductility in members subject to shear and bending is to provide confinement for the concrete. This is accomplished through the use of closed *hoops* or spiral reinforcement, which enclose the core of beams and columns. Specific criteria are discussed in Sections 20.4, 20.5, and 20.6. When confinement is provided, beams and columns can undergo nonlinear cyclic bending while maintaining their flexural strength and without deteriorating due to diagonal tension cracking. The formation of *ductile hinges* allows reinforced concrete frames to dissipate energy.

Successful seismic design of frames requires that the structures be proportioned so that hinges occur at locations that least compromise strength. For a frame undergoing lateral displacement, such as shown in Fig. 20.8*a*, the flexural capacity of the members at a joint (Fig. 20.8*b*) should be such that the columns are stronger than the beams. In this way, hinges will form in the beams rather than the columns, minimizing the portion of the structure affected by nonlinear behavior and maintaining the overall vertical load capacity. For these reasons, the "weak beam–strong column" approach is used to design reinforced concrete frames subject to seismic loading.

When hinges form in a beam, or in extreme cases within a column, the moments at the end of the member, which are governed by flexural strength, determine the shear

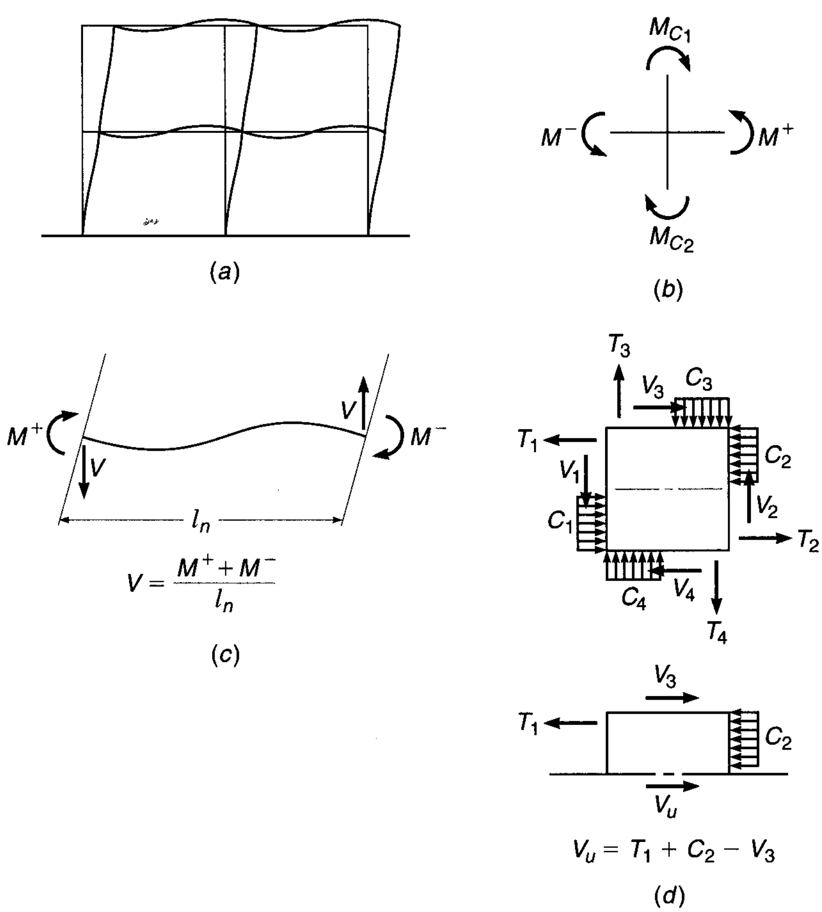

FIGURE 20.8
Frame subjected to lateral loading: (*a*) deflected shape; (*b*) moments acting on beam-column joint; (*c*) deflected shape and forces acting on a beam; (*d*) forces acting on faces of a joint due to lateral load.

that must be carried, as illustrated in Fig. 20.8*c*. The shear V corresponding to a flexural failure at both ends of a beam or column is

$$V = \frac{M^+ + M^-}{l_n} \tag{20.1}$$

where M^+ and M^- = flexural capacities at the ends of the member
l_n = clear span between supports

The member must be checked for adequacy under the shear V in addition to shear resulting from dead and live gravity loads. Transverse reinforcement is added, as required. For members with inadequate shear capacity, the response will be dominated by the formation of diagonal cracks, rather than ductile hinges, resulting in a substantial reduction in the energy dissipation capacity of the member.

If short members are used in a frame, the members may be unintentionally strong in flexure compared to their shear capacity. An example would be columns in a structure with deep spandrel beams or with "nonstructural" walls with openings that expose a portion of the columns to the full lateral load. As a result, the exposed region, called a *captive column*, responds by undergoing a shear failure, as shown in Fig. 20.9.

The lateral displacement of a frame places beam-column joints under high shear stresses because of the change from positive to negative bending in the flexural members from one side of the joint to the other, as shown in Fig. 20.8*d*. The joint must

FIGURE 20.9
Shear failure in a captive column without adequate transverse reinforcement.
(*Photograph by Jack Moehle.*)

be able to withstand the high shear stresses and allow for a change in bar stress from tension to compression between the faces of the joint. Such a transfer of shear and bond is often made difficult by congestion of reinforcement through the joint. Thus, designers must ensure that joints not only have adequate strength but are also constructable. Two-way systems without beams are especially vulnerable because of low ductility at the slab-column intersection.

Additional discussion of seismic design can be found in Refs. 20.3 to 20.7.

20.3 SEISMIC LOADING CRITERIA

In the United States, the design criteria for earthquake loading are based on design procedures developed by the Building Seismic Safety Council (Ref. 20.1) and incorporated in *Minimum Design Loads for Buildings and Other Structures* (ASCE/SEI 7) (Ref. 20.2). The values of the spectral response accelerations S_s and S_1 are obtained from detailed maps produced by the United States Geological Survey† (e.g., Fig. 20.1) and included in ASCE/SEI 7. The values of S_s and S_1 are used to determine the spectral response accelerations S_{DS} and S_{D1} that are used in design.

$$S_{DS} = \frac{2}{3} F_a S_s \tag{20.2}$$

$$S_{D1} = \frac{2}{3} F_v S_1 \tag{20.3}$$

† A full set of maps is available at the United States Geological Survey website.

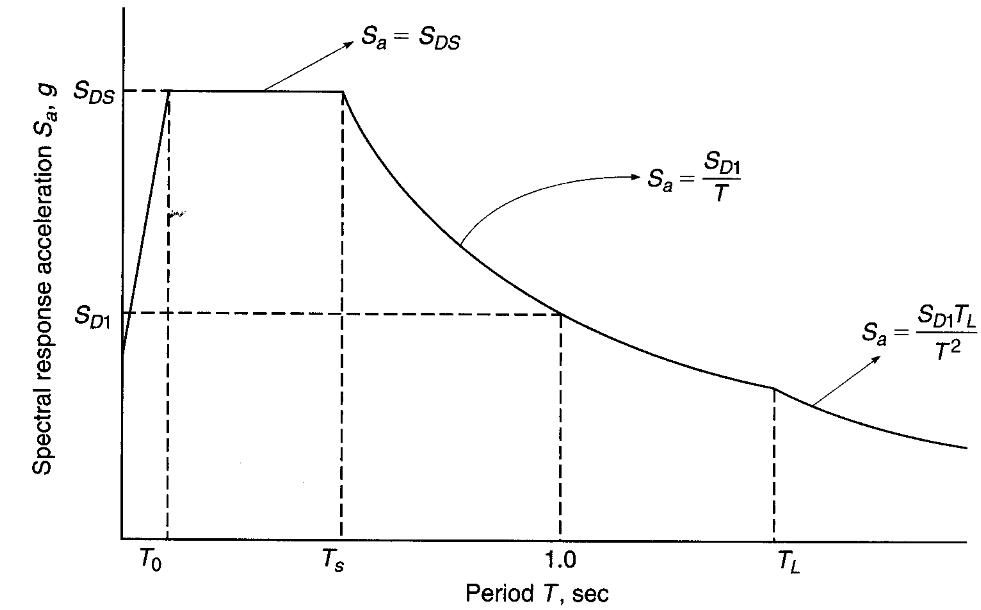

FIGURE 20.10
Design response spectrum.
(*Adapted from Ref. 20.2.*)

where F_a and F_v are site coefficients that range from 0.8 to 0.25 and from 0.8 to 0.35, respectively, as a function of the geotechnical properties of the building site and the values of S_s and S_1, respectively. Higher values of F_a and F_v are possible for some sites. The coefficients F_a and F_v increase in magnitude as site conditions change from hard rock to thick, soft clays and (for softer foundations) as the values of S_s and S_1 decrease.

Both S_{DS} and S_{D1} are used to construct the design response spectrum shown in Fig. 20.10, which relates the spectral response acceleration S_a, used to calculate the earthquake force, to the fundamental period of the structure T. In the spectrum, $T_0 = 0.2S_{D1}/S_{DS}$, $T_S = S_{D1}/S_{DS}$, and T_L is the site-specific *long-period transition period,* which, like S_s and S_1, is obtained from maps provided by the U.S. Geological Survey.

Structures are assigned to one of six *Seismic Design Categories* (SDCs) A through F as a function of (1) structure occupancy and use and (2) the values of S_{DS} and S_{D1}. Requirements for seismic design and detailing are minimal for SDCs A and B but become progressively more rigorous for SDCs C through F.

As presented in Table 1.2, earthquake loading is included in two combinations of factored load.

$$U = 1.2D + 1.0E + 1.0L + 0.2S \tag{20.4}$$

$$U = 0.9D + 1.0E + 1.6H \tag{20.5}$$

where D = dead load
E = earthquake load
H = weight or pressure from soil
L = live load
S = snow load

For SDC A, the earthquake load E is a horizontal load equal to 1 percent of the dead load D assigned to each floor. For SDCs B through F, the values of the earthquake load E used in Eqs. (20.4) and (20.5) are, respectively,

$$E = \rho Q_E + 0.2S_{DS}D \tag{20.6a}$$

$$E = \rho Q_E - 0.2S_{DS}D \tag{20.6b}$$

where Q_E = effect of horizontal seismic forces
ρ = reliability factor

The factor ρ is taken as 1.0 for structures assigned to SDCs B and C and as 1.3 for structures assigned to SDCs D though F, except for structures meeting specific criteria described in Ref. 20.2, in which case ρ may be taken as 1.0.

Combining Eq. (20.4) with Eq. (20.6*a*) and Eq. (20.5) with Eq. (20.6*b*) gives

$$U = (1.2 + 0.2S_{DS})D + \rho Q_E + 1.0L + 0.2S \tag{20.7}$$

$$U = (0.9 - 0.2S_{DS})D + \rho Q_E + 1.6H \tag{20.8}$$

Equations (20.4) and (20.6*a*) are used when dead load adds to the effects of horizontal ground motion, while Eqs. (20.5) and (20.6*b*) are used when dead load counteracts the effects of horizontal ground motion. Thus, the total load factor for dead load is greater than 1.2 in Eq. (20.7) and less than 0.9 in Eq. (20.8).

ASCE/SEI 7 specifies six procedures (if SDC A is included) for determining the horizontal earthquake load Q_E. These procedures include three progressively more detailed methods that represent earthquake loading through the use of equivalent static lateral loads, *modal response spectrum analysis, linear time-history analysis,* and *nonlinear time-history analysis.* The method selected depends on the seismic design category. All but the most basic reinforced concrete structures in Seismic Design Categories B through F must be designed using *equivalent lateral force analysis* (the most detailed of the three equivalent static lateral load procedures), modal response analysis, or time-history analysis. These procedures are discussed next.

a. Equivalent Lateral Force Procedure

According to ASCE/SEI 7 (Ref. 20.2), equivalent lateral force analysis may be applied to all structures with S_{DS} less than $0.33g$ and S_{D1} less than $0.133g$, as well as structures subjected to much higher design spectral response accelerations, if the structures meet certain requirements. More sophisticated dynamic analysis procedures must be used otherwise.

The equivalent lateral force procedure provides for the calculation of the total lateral force, defined as the design base shear V, which is then distributed over the height of the building. The design base shear V is calculated for a given direction of loading according to the equation

$$V = C_s W \tag{20.9}$$

where W is the total dead load plus applicable portions of other loads and

$$C_s = \frac{S_{DS}}{R/I} \tag{20.10}$$

which need not be greater than

$$C_s = \frac{S_{D1}}{T(R/I)} \qquad \text{for } T \le T_L \tag{20.11}$$

or

$$C_s = \frac{S_{D1}T_L}{T^2(R/I)} \qquad \text{for } T > T_L \tag{20.12}$$

but may not be less than

$$C_s = 0.44IS_{DS} \ge 0.01 \tag{20.13}$$

or where $S_1 \geq 0.6g$,

$$C_s = \frac{0.5S_1}{R/I} \tag{20.14}$$

where R = response modification factor (depends on structural system). Values of R for most reinforced concrete structures range from 4 to 8, based on ability of structural system to sustain earthquake loading and to dissipate energy
I = occupancy important factor = 1.0, 1.25, or 1.5, depending upon the occupancy and use of structure
T = fundamental period of structure

According to ASCE/SEI 7, the period T can be calculated based on an analysis that accounts for the structural properties and deformational characteristics of the elements within the structure. Approximate methods may also be used in which the fundamental period of the structure may be calculated as

$$T = C_t h_n^x \tag{20.15}$$

where h_n = height above the base to the highest level of structure, ft
C_t = 0.016 for reinforced concrete moment-resisting frames in which frames resist 100 percent of required seismic force and are not enclosed or adjoined by more rigid components that will prevent frame from deflecting when subjected to seismic forces, and 0.020 for all other reinforced concrete buildings
x = 0.90 for $C_t = 0.016$ and 0.75 for $C_t = 0.020$

Alternately, for structures not exceeding 12 stories in height, in which the lateral-force-resisting system consists of a moment-resisting frame and the story height is at least 10 ft,

$$T = 0.1N \tag{20.16}$$

where N = number of stories.

For shear wall structures, ASCE/SEI 7 permits T to be approximated as

$$T = \frac{0.0019}{\sqrt{C_w}} h_n \tag{20.17}$$

where

$$C_w = \frac{100}{A_B} \sum_{i=1}^{n} \left(\frac{h_n}{h_i}\right)^2 \frac{A_i}{1 + 0.83(h_i/D_i)^2} \tag{20.18}$$

where A_B = base area of structure, ft^2
A_i = area of shear wall, ft^2
D_i = length of shear wall i, ft
n = number of shear walls in building that are effective in resisting lateral forces in direction under consideration

The total base shear V is distributed over the height of the structure in accordance with Eq. (20.19).

$$F_x = \frac{w_x h_x^k}{\sum_{i=1}^{n} w_i k_i^k} V \tag{20.19}$$

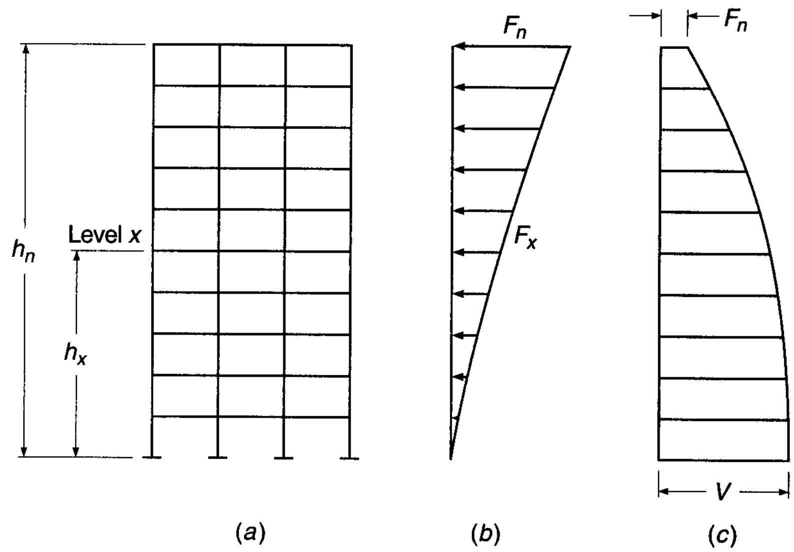

FIGURE 20.11
Forces based on ASCE/SEI 7 (Ref. 20.2) equivalent lateral force procedure: (*a*) structure; (*b*) distribution of lateral forces over height; (*c*) story shears.

where F_x = lateral seismic force induced at level x
w_x, w_i = portion of W at level x and level i, respectively
h_x, h_i = height to level x and level i, respectively
k = exponent related to structural period, = 1 for $T \leq 0.5$ sec and = 2 for $T \geq 2.5$ sec. For $0.5 < T < 2.5$, k is determined by linear interpolation or set to a value of 2

The design shear at any story V_x equals the sum of the forces F_x at and above that story. For a 10-story building with a uniform mass distribution over the height and $T = 1.0$ sec, the lateral forces and story shears are distributed as shown in Fig. 20.11.

At each level, V_x is distributed in proportion to the stiffness of the elements in the vertical lateral-force-resisting system. To account for unintentional building irregularities that may cause a horizontal torsional moment, a minimum 5 percent eccentricity must be applied if the vertical lateral-force-resisting systems are connected by a floor system that is rigid in its own plane.

In addition to the criteria just described, ASCE/SEI 7 includes criteria to account for overturning effects and provides limits on story drift. P-Δ effects must be considered (as discussed in Chapter 9), and the effects of upward loads must be accounted for in the design of horizontal cantilever components and prestressed members.

b. Dynamic Lateral Force Procedures

ASCE/SEI 7 includes dynamic lateral force procedures that involve the use of (1) response spectra, which provide the earthquake-induced forces as a function of the natural periods of the structure, or (2) time-history analyses of the structural response based on a series of ground motion acceleration histories that are representative of ground motion expected at the site. Both procedures require the development of a mathematical model of the structure to represent the spatial distribution of mass and stiffness. Response spectra, such as shown in Fig. 20.10, are used to calculate peak forces for a "sufficient number of nodes to obtain the combined modal mass participation of at least 90 percent of the actual mass in each of two orthogonal directions"

(Ref. 20.2). Since these forces do not always act in the same direction, as shown in Fig. 20.3, the peak forces are averaged statistically, in most cases using the square root of the sum of the squares to obtain equivalent static lateral forces for use in design. In cases where the periods in the translational and torsional modes are closely spaced and result in significant cross correlation of the modes, the *complete quadratic combination* method is used (Ref. 20.8). When time-history analyses, which may include a linear or nonlinear representation of the structure, are used, design forces are obtained directly from the analyses. Both modal response spectrum and time-history procedures provide more realistic representations of the seismically induced forces in a structure than do equivalent lateral force analyses. The details of these methods are presented in Refs. 20.1 and 20.2.

20.4 ACI PROVISIONS FOR EARTHQUAKE-RESISTANT STRUCTURES

Criteria for seismic design are contained in Earthquake-Resistant Structures, Chapter 21 of the ACI Code (Ref. 20.9). The principal goal of the provisions is to ensure adequate toughness under inelastic displacement reversals brought on by earthquake loading. The provisions accomplish this goal by requiring the designer to provide for concrete confinement and inelastic rotation capacity. The provisions apply to frames, walls, coupling beams, diaphragms, and trusses in structures assigned to Seismic Design Categories D, E, and F, and to frames, including two-way slab systems, and precast walls in structures assigned to Seismic Design Category C. Structural systems in SDCs D, E, and F are referred to as *special,* while systems in SDC C are referred to as *intermediate.*

The requirements for frame structures assigned to SDC B, described as *ordinary moment frames,* are limited. Beams must have at least two longitudinal bars that are continuous along both the top and bottom faces of the beam and developed at the face of the supports; and columns with a clear height less than or equal to 5 times the column dimension in the direction of bending must be designed for shear, as required for intermediate frames (described in Section 20.8). There are no special requirements in ACI Code Chapter 20 for structures assigned to SDC A.

The ACI provisions are based on many of the observations made earlier in this chapter. The effect of nonstructural elements on overall structural response must be considered, as must the response of the nonstructural elements themselves. Structural elements that are not specifically proportioned to carry earthquake loads must also be considered.

The load factors used for earthquake loads are given in Eqs. (20.4) and (20.5). The strength reduction factors used for seismic design are the same as those used for nonseismic design (Table 1.3), with the additional requirements that $\phi = 0.60$ for shear, if the nominal shear capacity of a member is less than the shear based on the nominal flexural strength [see Eq. (20.1)], and $\phi = 0.85$ for shear in joints and diagonally reinforced coupling beams.

To ensure adequate ductility and toughness under inelastic rotation, ACI Code 21.1.4 sets a minimum concrete strength of 3000 psi. For lightweight aggregate concrete, an *upper limit* of 5000 psi is placed on concrete strength; this limit is based on a lack of experimental evidence for higher-strength lightweight concretes.

Under ACI Code 21.1.5, reinforcing steel must meet ASTM A706 (see Table 2.4). ASTM A706 specifies a Grade 60 steel with a maximum yield strength of 78 ksi and

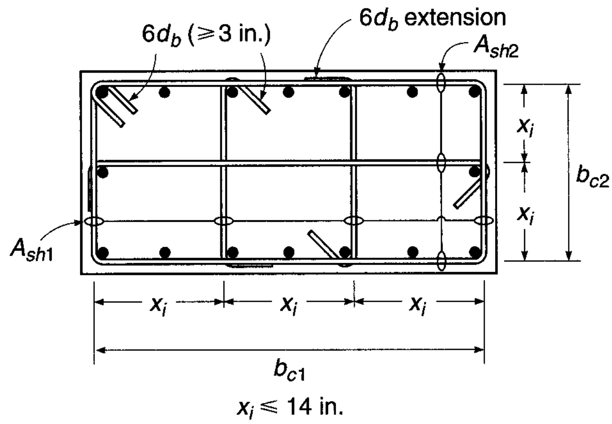

FIGURE 20.12
Example of transverse reinforcement in columns; consecutive crossties engaging the same longitudinal bars must have 90° hooks on opposite sides of columns. (*Adapted from Ref. 20.9.*)

a minimum tensile strength equal to 80 ksi. The actual tensile strength must be at least 1.25 times the actual yield strength. In addition to reinforcement manufactured under ASTM A706, the Code allows the use of Grades 40 and 60 reinforcement meeting the requirements of ASTM A615, provided that the actual yield strength does not exceed the specified yield by more than 18 ksi and that the actual tensile strength exceeds the actual yield strength by at least 25 percent. The upper limits on yield strength are used to limit the maximum moment capacity of the section because of the dependency of the earthquake-induced shear on the moment capacity [Eq. (20.1)]. The minimum ratio of tensile strength to yield strength helps provide adequate inelastic rotation capacity. Evidence reported in Ref. 20.10 indicates that an increase in the ratio of the ultimate moment to the yield moment results in an increase in the nonlinear deformation capacity of flexural members.

Confinement for concrete is provided by transverse reinforcement consisting of stirrups, hoops, and crossties. To ensure adequate anchorage, a *seismic hook* [with a bend not less than 135° and a 6 bar diameter (but not less than 3 in.) extension that engages the longitudinal reinforcement and projects into the interior of the stirrup or hoop] is used on stirrups, hoops, and crossties. *Hoops*, shown in Figs. 7.11*a*, *c–e* and 20.12, are closed ties that can be made up of several reinforcing elements, each having seismic hooks at both ends, or continuously wound ties with seismic hooks at both ends. A *crosstie* (see Fig. 20.12) is a continuous reinforcing bar with a seismic hook at one end and a hook with not less than a 90° bend and at least a 6 bar diameter extension at the other end. The hooks on crossties must engage peripheral longitudinal reinforcing bars.

In the following sections, ACI requirements for frames, walls, diaphragms, and trusses subject to seismic loading are discussed. Sections 20.5 and 20.6 describe the general design and detailing criteria for members in structures assigned to SDCs D, E, and F. Specific shear strength requirements are presented in Section 20.7. Section 20.8 describes requirements for frame structures assigned to SDC C.

20.5 ACI PROVISIONS FOR SPECIAL MOMENT FRAMES

ACI Code Chapter 21 addresses four member types in frame structures, termed *special moment frames*, subject to high seismic risk: flexural members, members subjected to bending and axial load, joints, and members not proportioned to resist earthquake forces. Two-way slabs without beams are prohibited as lateral-load-resisting systems in structures assigned to SDCs D, E, and F.

a. Flexural Members

Flexural members are defined by ACI Code 21.5.1 as structural members that resist earthquake-induced forces but have a factored axial compressive load P_u that does not exceed $A_g f_c'/10$, where A_g is the gross area of the cross section. The members must have a clear span-to-effective-depth ratio of at least 4 and a width b_w not less than $0.3h$ or 10 in. The width b_w may not be wider than the support width c_2 plus a distance on either side of the support equal to the smaller of the width of the supporting member c_2 or 0.75 times the dimension of the supporting member in the direction of the span c_1, as shown in Fig. 20.13. The minimum clear span-to-depth ratio helps ensure that flexural rather than shear strength dominates member behavior under inelastic load reversals. Minimum web dimensions help provide adequate confinement for the concrete, whereas the width relative to the support (typically a column) is limited to provide adequate moment transfer between beams and columns.

In accordance with ACI Code 21.5.2, both top and bottom minimum flexural steel is required. $A_{s,\min}$ should not be less than given by Eq. (3.41) but need not be greater than four-thirds of that required by analysis, with a minimum of two reinforcing bars, top and bottom, throughout the member. In addition, the positive moment capacity at the face of columns must be at least one-half of the negative moment strength at the same location, and neither positive nor negative moment strength at any section in a member may be less than one-fourth of the maximum moment strength at either end of the member. These criteria are designed to provide for ductile behavior throughout the member, although the minimum of two reinforcing bars on the top and bottom is based principally on construction requirements. A maximum reinforcement ratio of 0.025 is set to limit problems with steel congestion and to ensure adequate member size for carrying shear that is governed by the flexural capacity of the member [Eq. (20.1)].

To obtain ductile performance, the location of lap splices is limited. They may not be used within joints, within twice the member depth from the face of a joint, or where analysis indicates that flexural yielding is caused by inelastic lateral displacements of the frame. Lap splices must be enclosed by hoops or spirals with a maximum spacing of one-fourth of the effective depth or 4 in. Welded and mechanical connections may be used, provided that they are not used within a distance equal to twice the member depth from the face of a column or beam or sections where yielding of the reinforcement is likely to occur due to inelastic displacements under lateral load, in accordance with ACI Code 21.1.6 and 21.1.7.

Transverse reinforcement is required throughout flexural members in frames resisting earthquake-induced forces. According to ACI Code 21.5.3, transverse reinforcement in the form of hoops must be used over a length equal to twice the member depth measured from the face of the supporting member toward midspan, at both ends of the flexural member, and over lengths equal to twice the member depth on both sides of a section where flexural yielding is likely to occur in connection with inelastic lateral displacements of the frame. The first hoop must be located not more than 2 in. from the face of the supporting member, and the maximum spacing of the hoops must not exceed one-fourth of the effective depth, 8 times the diameter of the smallest longitudinal bar, 24 times the diameter of the hoop bars, or 12 in.

FIGURE 20.13
Maximum effective width of wide beam and required transverse reinforcement.
(*Adapted from Ref. 20.9.*)

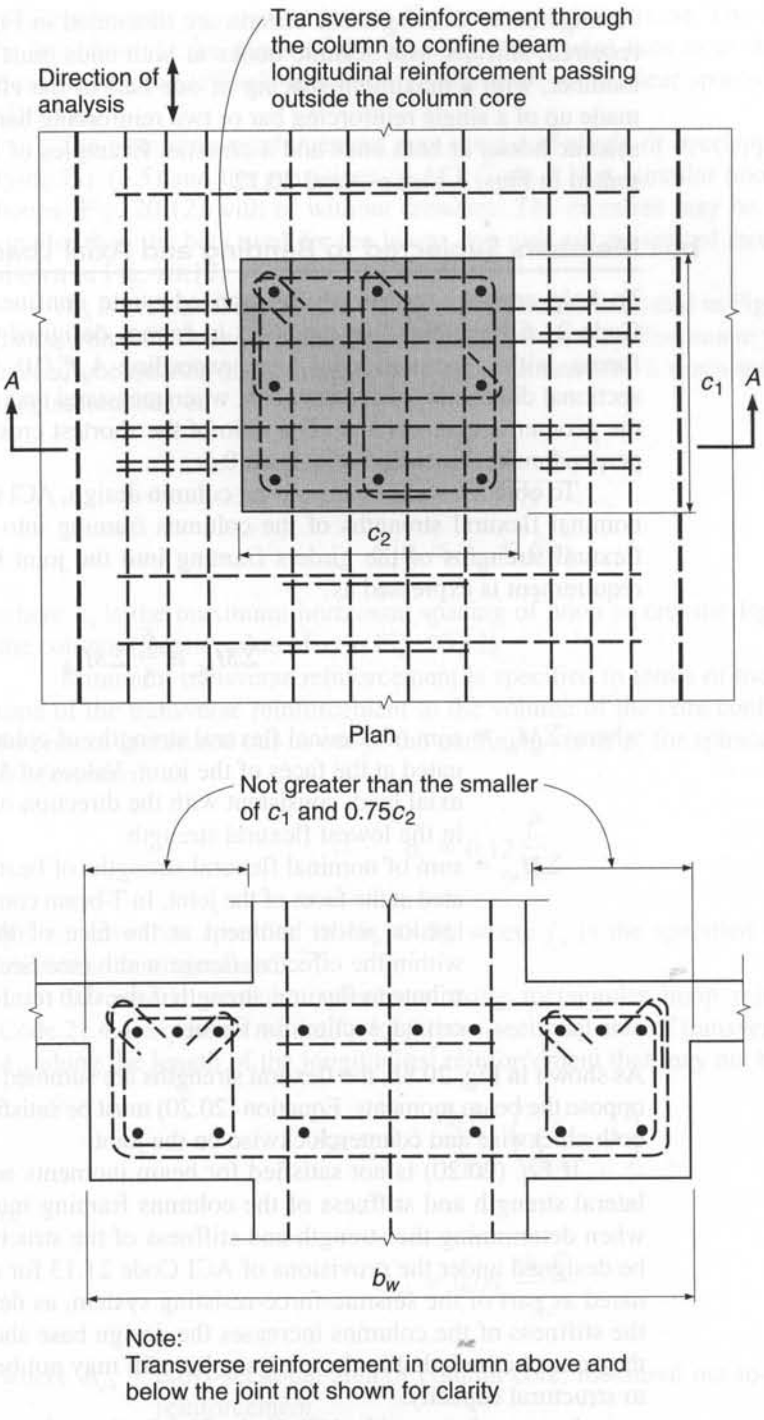

To provide adequate support for longitudinal bars on the perimeter of a flexural member when the bars are placed in compression due to inelastic rotation, ACI Code 21.5.3 requires that hoops be arranged so that every corner and alternate longitudinal bar is provided lateral support by ties, in accordance with ACI Code 7.10.5.3.

Arrangements meeting these criteria are illustrated in Fig. 8.3. Where hoops are not required, stirrups with seismic hooks at both ends must be provided throughout the member, with a maximum spacing of one-half of the effective depth. Hoops can be made up of a single reinforcing bar or two reinforcing bars consisting of a stirrup with seismic hooks at both ends and a crosstie. Examples of hoop reinforcement are presented in Figs. 7.11*a*, *c–e* and 20.12.

b. Members Subjected to Bending and Axial Load

To help ensure constructability and adequate confinement of the concrete, ACI Code 21.6.1 requires that members in frames designed to resist earthquake-induced forces, with a factored axial force exceeding $A_g f_c'/10$, have (1) a minimum cross-sectional dimension of at least 12 in. when measured on a straight line passing through the geometric centroid and (2) a ratio of the shortest cross-sectional dimension to the perpendicular dimension of at least 0.4.

To obtain a weak beam–strong column design, ACI Code 21.6.2 requires that the nominal flexural strengths of the columns framing into a joint exceed the nominal flexural strengths of the girders framing into the joint by at least 20 percent. This requirement is expressed as

$$\Sigma M_{nc} \geq \frac{6}{5}\,\Sigma M_{nb} \tag{20.20}$$

where ΣM_{nc} = sum of nominal flexural strengths of columns framing into joint, evaluated at the faces of the joint. Values of M_{nc} are based on the factored axial load, consistent with the direction of the lateral forces, resulting in the lowest flexural strength

ΣM_{nb} = sum of nominal flexural strengths of beams framing into joint, evaluated at the faces of the joint. In T-beam construction, where the slab is in tension under moment at the face of the joint, slab reinforcement within the effective flange width (see Section 3.8) is assumed to contribute to flexural strength if the slab reinforcement is developed at the critical section for flexure

As shown in Fig. 20.8*b*, the flexural strengths are summed so that the column moments oppose the beam moments. Equation (20.20) must be satisfied for beam moments acting both clockwise and counterclockwise on the joint.

If Eq. (20.20) is not satisfied for beam moments acting in both directions, the lateral strength and stiffness of the columns framing into the joint must be ignored when determining the strength and stiffness of the structures, and the columns must be designed under the provisions of ACI Code 21.13 for members that are not designated as part of the seismic-force-resisting system, as described in Section 20.5d. If the stiffness of the columns increases the design base shear or the effects of torsion, they must be included in the analysis, but still may not be considered as contributing to structural capacity.

In accordance with ACI Code 21.6.3, the column reinforcement ratio based on the gross section ρ_g must meet the requirement: $0.01 \leq \rho_g \leq 0.06$. Welded splices and mechanical connections in columns must satisfy the same requirements specified for flexural members, whereas lapped splices must be designed for tension and are permitted only within the center half of columns.

ACI Code 21.6.4 specifies the use of minimum transverse reinforcement over length l_o from each joint face and on both sides of any section where flexural yielding is likely because of inelastic lateral displacement of the frame. The length l_o may not be less than (1) the depth of the member at the joint face or at the section where flexural yielding is likely to occur, (2) one-sixth of the clear span of the member, or (3) 18 in.

The transverse reinforcement may consist of single or overlapping spirals satisfying Eq. (8.5) and the provisions of ACI Code 7.10.4, circular hoops, or rectilinear hoops (Fig. 20.12) with or without crossties. The crossties may be the same size or smaller than the bars used for the hoops and may not be spaced more than 14 in., as shown in Fig. 20.12.

A_{sh} is evaluated in both the 1 and 2 directions, as indicated in Fig. 20.12. In accordance with ACI Code 21.6.4, the spacing of transverse reinforcement within l_o may not exceed one-quarter of the minimum member dimension, 6 times the diameter of the longitudinal bar, or

$$s_o = 4 + \frac{14 - h_x}{3} \tag{20.21a}$$

$$4 \text{ in.} \leq s_o \leq 6 \text{ in.} \tag{20.21b}$$

where h_x is the maximum horizontal spacing of hoop or crosstie legs on all faces of the column (largest value of x_i in Fig. 20.12).

Minimum transverse reinforcement is specified in terms of the ratio of the volume of the transverse reinforcement to the volume of the core confined by the reinforcement (measured out-to-out of the confining steel) ρ_s for spirals or circular hoop reinforcement as

$$\rho_s = 0.12 \frac{f_c'}{f_{yt}} \tag{20.22}$$

but not less than specified in Eq. (8.5), where f_{yt} is the specified yield strength of transverse reinforcement.

To provide similar confinement using rectangular hoop reinforcement, ACI Code 21.4.4 requires a minimum total cross-sectional area of transverse reinforcement A_{sh} along the length of the longitudinal reinforcement that may not be less than

$$A_{sh} = 0.3 \frac{s b_c f_c'}{f_{yt}} \left(\frac{A_g}{A_{ch}} - 1 \right) \tag{20.23}$$

or

$$A_{sh} = 0.09 \frac{s b_c f_c'}{f_{yt}} \tag{20.24}$$

where A_{ch} = cross-sectional area of column core, measured out-to-out of transverse reinforcement

s = spacing of transverse reinforcement

b_c = cross-sectional dimension of column core, measured to outside edges of transverse reinforcement composing A_{sh}

For regions outside of l_o, when the minimum transverse reinforcement defined above is not provided, the spacing of spiral or hoop reinforcement may not exceed 6 times the diameter of the longitudinal column bars or 6 in.

To account for the major ductility demands that are placed on columns that support rigid members (see Figs. 20.4 and 20.5), the Code specifies that, for such columns, the minimum transverse reinforcement requirements must be satisfied throughout the *full column height* and that the transverse reinforcement must extend into the discontinued stiff member for at least the development length of the largest longitudinal reinforcement for walls and at least 12 in. into foundations.

If the concrete cover outside the confining transverse reinforcement is greater than 4 in., the Code requires the addition of transverse reinforcement with a cover of 4 in. or less to limit the potential hazard caused by spalling of the concrete shell away from the column.

EXAMPLE 20.1

Relative flexural strengths of members at a joint and minimum transverse column reinforcement. The exterior joint shown in Fig. 20.14 is part of a reinforced concrete frame designed to resist earthquake loads. A 6 in. slab, not shown, is reinforced with No. 5 (No. 16) bars spaced 10 in. center to center at the same level as the flexural steel in the beams. The member section dimensions and reinforcement are as shown. The frame story height is 12 ft. Material strengths are $f_c' = 4000$ psi and $f_y = 60{,}000$ psi. The maximum factored axial load on the upper column framing into the joint is 2210 kips, and the maximum factored axial load on the lower column is 2306 kips. Determine if the nominal flexural strengths of the columns exceed

FIGURE 20.14
Exterior beam-column joint for Examples 20.1 and 20.2: (*a*) plan view; (*b*) cross section through spandrel beam; (*c*) cross section through normal beam. Note that confining reinforcement is not shown, except for column hoops and crossties in (*a*).

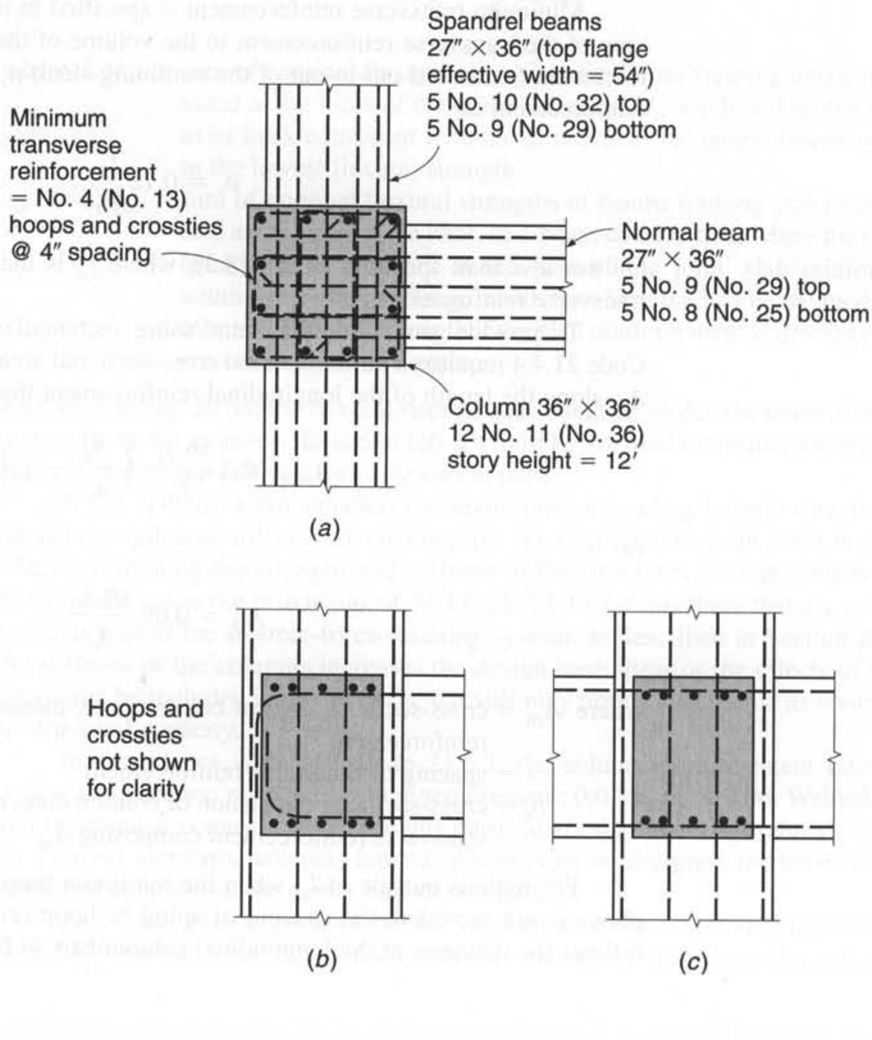

those of the beams by at least 20 percent, as required by Eq. (20.20), and determine the minimum transverse reinforcement required over the length l_o in the columns.

Solution. Checking the relative flexural strengths in the frame of the spandrel beams will be sufficient, since this is clearly the controlling case for the joint. In addition, because the beam reinforcement is the same on both sides of the joint, a single comparison will suffice for both clockwise and counterclockwise beam moments.

The negative nominal flexural strength of the beam at the joint is governed by the top steel, which consists of five No. 10 (No. 32) bars in the beams plus four No. 5 (No. 16) bars in the slab within the effective width of the top flange, $A_s = 6.35 + 1.24 = 7.59$ in^2. The yield force in the steel is

$$A_s f_y = 7.59 \times 60 = 455 \text{ kips}$$

The effective depth is $d = 36.0 - 1.5 - 0.5 - 1.27/2 = 33.4$ in., and with stress block depth $a = 455/(0.85 \times 4 \times 27) = 4.96$ in., the nominal moment is

$$M_{nb} = \frac{455}{12}\left(33.4 - \frac{4.96}{2}\right) = 1172 \text{ ft-kips}$$

The positive nominal flexural strength of the beam at the joint is determined by the bottom steel, five No. 9 (No. 29) bars, $A_s = 5.00$ in^2. The yield force in the steel is

$$A_s f_y = 5.00 \times 60 = 300 \text{ kips}$$

The effective depth is $d = 36.0 - 1.5 - 0.5 - 1.128/2 = 33.4$ in., and with stress block depth $a = 300/(0.85 \times 4 \times 54) = 1.63$ in., the nominal moment is

$$M_{nb} = \frac{300}{12}\left(33.4 - \frac{1.63}{2}\right) = 815 \text{ ft-kips}$$

The minimum nominal flexural strengths of the columns in this example depend on the maximum factored axial loads, which are 2210 and 2306 kips for the upper and lower columns, respectively. For the 36 × 36 in. columns, this gives

$$\frac{P_u}{f_c' A_g} = \frac{2210}{4 \times 1296} = 0.426 \qquad \text{upper column}$$

$$\frac{P_u}{f_c' A_g} = \frac{2306}{4 \times 1296} = 0.445 \qquad \text{lower column}$$

With total reinforcement of 12 No. 11 (No. 36) bars, $A_{st} = 18.72$ in^2 and the reinforcement ratio $\rho_g = 18.72/1296 = 0.0144$. Using cover to the center of the bars of 3 in., $\gamma = (36 - 6)/36 = 0.83$, Graphs A.7 and A.8 in Appendix A are appropriate for determining the flexural capacity.

For the upper column,

$$R_n = \frac{M_{nc}}{f_c' A_g h} = 0.167$$

$$M_{nc} = 0.167 \times 4 \times 1296 \times \frac{36}{12} = 2597 \text{ ft-kips}$$

For the lower column,

$$R_n = \frac{M_{nc}}{f_c' A_g h} = 0.164$$

$$M_{nc} = 0.164 \times 4 \times 1296 \times \frac{36}{12} = 2550 \text{ ft-kips}$$

Checking the relative flexural capacities,

$$\Sigma M_{nc} = 2597 + 2550 = 5147 \text{ ft-kips}$$

$$\Sigma M_{nb} = 1172 + 815 = 1987 \text{ ft-kips}$$

By inspection, $\Sigma M_{nc} \geq \frac{6}{5}\,\Sigma M_{nb}$.

Minimum transverse reinforcement is required over a length l_o on either side of the joint. According to ACI Code 21.6.4, l_o is the greater of (1) the depth $h = 36$ in., (2) one-sixth of the clear span $= (12 \times 12 - 36)/6 = 18$ in., or (3) 18 in. Since every corner and alternate longitudinal bar must have lateral support and because the spacing of crossties and legs of hoops is limited to a maximum of 14 in. within the plane of the transverse reinforcement, the scheme shown in Fig. 20.14*a* will be used, giving a maximum spacing of slightly less than 12.5 in. The maximum spacing of transverse reinforcement s is limited to the smaller of one-quarter of the minimum member dimension $= 36/4 = 9$ in., 6 times the diameter of the longitudinal bar, $6 \times 1.41 = 8.46$ in., or

$$s_o = 4 + \frac{14 - 12.5}{3} = 4.5 \text{ in.}$$

with 4 in. $\leq s_o \leq$ 6 in. A 4 in. spacing will be used.

Using No. 4 (No. 13) bars, the cross-sectional dimension of the column core, measured to the outside edges of the confining steel, is $b_c = 33$ in., and the cross-sectional area of column core, also measured to the outside edges of the confining steel, is $A_{ch} = 33 \times 33 = 1089 \text{ in}^2$.

For $f_{yt} = 60$ ksi, the total area of transverse reinforcement with the 4 in. spacing is the larger of Eqs. (20.23) and (20.24).

$$A_{sh} = 0.3\,\frac{4 \times 33 \times 4}{60}\left(\frac{1296}{1089} - 1\right) = 0.50 \text{ in}^2$$

$$A_{sh} = 0.09\,\frac{4 \times 33 \times 4}{60} = 0.79 \text{ in}^2$$

The requirement for 0.79 in^2 is satisfied by four No. 4 (No. 13) bar legs.

c. Joints and Development of Reinforcement

The design of beam-column joints is discussed in Section 11.2. The forces acting on a joint subjected to lateral loads are illustrated in Fig. 11.4. The factored shear acting on a joint is

$$\begin{aligned} V_u &= T_1 + C_2 - V_{col} \\ &= T_1 + T_2 - V_{col} \end{aligned} \tag{20.25}$$

where T_1 = tensile force in negative moment beam steel on one side of a joint
T_2 = tensile force in positive moment beam steel on one side of a joint
C_2 = compressive force counteracting T_2
V_{col} = shear in the column at top and bottom faces of the joint corresponding to the net moment in the joint and points of inflection at midheight of columns (see Fig. 11.5)

For seismic design, the forces T_1 and T_2 ($= C_2$) must be based on a stress in the flexural tension reinforcement of $1.25f_y$. In accordance with ACI Code 21.7.4, the nominal shear capacity of a joint depends on the degree of confinement provided by members framing into the joint.

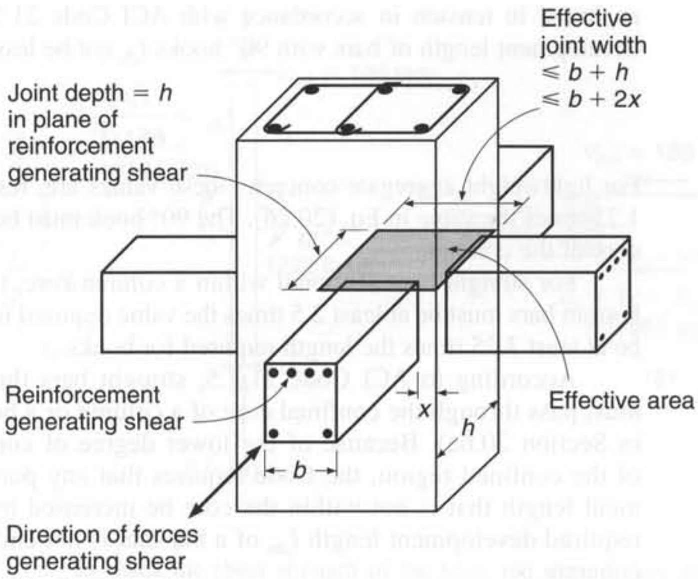

FIGURE 20.15
Effective area of joint A_j, which must be considered separately for forces in each direction of framing. Note that the joint illustrated does not meet conditions necessary to be considered as confined because the forming members do not cover at least $\frac{3}{4}$ of each joint face. (*Adapted from Ref. 20.9.*)

For joints confined on all four faces	$20\sqrt{f'_c}\,A_j$
For joints confined on three faces or two opposite faces	$15\sqrt{f'_c}\,A_j$
For others	$12\sqrt{f'_c}\,A_j$

where A_j is the effective cross-sectional area of the joint in a plane parallel to the plane of reinforcement generating shear in the joint. The joint depth is the overall depth of the column. For beams framing into a support of larger width, the effective width of the joint is the smaller of (1) beam width plus joint depth or (2) twice the smaller perpendicular distance from the longitudinal axis of the beam to the column side. The effective area of a joint is illustrated in Fig. 20.15. The nominal shear strength for lightweight aggregate concrete is limited to three-quarters of the values given above.

To provide adequate confinement within a joint, the transverse reinforcement used in columns must be continued through the joint, in accordance with ACI Code 21.5.2. This reinforcement may be reduced by one-half within the depth of the shallowest framing member, and the spacing of spirals or hoops may be increased to 6 in., if beams or girders frame into all four sides of the joint and the flexural members cover at least three-fourths of the column width.

For joints where the beam is wider than the column, transverse reinforcement, as required for columns (ACI Code 21.5.3), must be provided to confine the flexural steel in the beam, as shown in Fig. 20.13, unless confinement is provided by a transverse flexural member.

To provide adequate development of beam reinforcement passing through a joint, ACI Code 21.7.2 requires that the column dimension parallel to the beam reinforcement be at least 20 times the diameter of the largest longitudinal bar for normalweight concrete and 26 times the bar diameter for lightweight concrete. For beam longitudinal reinforcement that is terminated within a column, both hooked and straight reinforcement must be extended to the far face of the column core. The use of headed deformed reinforcement is not addressed. The reinforcement must be anchored in compression as described in Section 5.8 (ACI Code Chapter 12) and anchored in tension in accordance with ACI Code 21.7.5, which requires that the development length of bars with 90° hooks l_{dh} not be less than $8d_b$, 6 in., or

$$l_{dh} = \frac{f_y d_b}{65\sqrt{f'_c}} \tag{20.26}$$

For lightweight aggregate concrete, these values are, respectively, $10d_b$, 7.5 in., and 1.25 times the value in Eq. (20.26). The 90° hook must be located within the confined core of the column.

For straight bars anchored within a column core, the development length l_d of bottom bars must be at least 2.5 times the value required for hooks; l_d for top bars must be at least 3.25 times the length required for hooks.

According to ACI Code 21.7.5, straight bars that are terminated at a joint must pass through the confined core of a column or a boundary element (discussed in Section 20.6a). Because of the lower degree of confinement provided outside of the confined region, the Code requires that any portion of the straight embedment length that is not within the core be increased by a factor of 1.6. Thus, the required development length l_{dm} of a bar that is not entirely embedded in confined concrete is

$$l_{dm} = 1.6(l_d - l_{dc}) + l_{dc} \tag{20.27a}$$

$$l_{dm} = 1.6l_d - 0.6l_{dc} \tag{20.27b}$$

where l_d = required development length for a straight bar embedded in confined concrete

l_{dc} = length embedded in confined concrete

EXAMPLE 20.2 **Design of exterior joint.** Design the joint shown in Fig. 20.14.

Solution. As discussed in Chapter 11, a joint must be detailed so that the beam and column bars do not interfere with each other and so that placement and consolidation of the concrete are practical. Bar placement is shown in Fig. 20.14.

Development of the spandrel beam flexural steel within the joint is checked based on the requirement that the column dimension be at least 20 times the bar diameter of the largest bars. This requirement is met for the No. 10 (No. 32) bars used as top reinforcement.

$$20 \times 1.27 = 25.4 \text{ in.} < 36 \text{ in.}$$

The flexural steel in the normal beam must be anchored within the core of the column based on Eq. (20.26), but not less than $8d_b$ or 6 in. For the No. 9 (No. 29) top bars, Eq. (20.26) controls

$$l_{dh} = \frac{60{,}000 \times 1.128}{65\sqrt{4000}} = 16.5 \text{ in.}$$

The same holds true for the No. 8 (No. 25) bottom bars, which must also be anchored in tension (ACI Code 12.11.2) because lateral loading will subject the beam to both positive and negative bending moments at the exterior joint.

$$l_{dh} = \frac{60{,}000 \times 1.0}{65\sqrt{4000}} = 14.6 \text{ in.}$$

Since $3.25l_{dh}$ is not available for the top bars and $2.5l_{dh}$ is not available for the bottom bars, all flexural steel from the normal beam must be anchored using hooks, not straight reinforcement, extended to the far face of the column core, as shown in Fig. 20.14*b*.

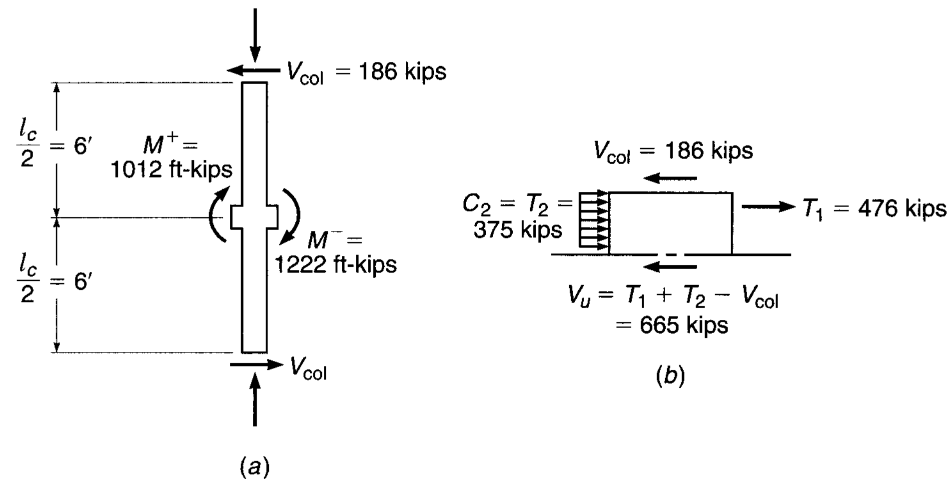

FIGURE 20.16
Free-body diagrams in plane of spandrel beam for Example 20.2: (*a*) column and joint region; (*b*) forces acting on joint due to lateral load.

To check the shear strength of the joint, the shear forces acting on the joint must be calculated based on a stress of $1.25f_y$ in the flexural reinforcement. By inspection, shear in the plane of the spandrel beam will control.

The tensile force in the negative steel is

$$T_1 = 1.25 \times 6.35 \times 60 = 476 \text{ kips}$$

For an effective depth of 33.4 in. (Example 20.1) and a depth of stress block $a = 476/(0.85 \times 4 \times 27) = 5.19$ in., the moment due to negative bending is

$$M^- = \frac{476}{12}\left(33.4 - \frac{5.19}{2}\right) = 1222 \text{ ft-kips}$$

For positive bending on the other side of the column,

$$T_2 = 1.25 \times 5.00 \times 60 = 375 \text{ kips}$$

$$a = \frac{375}{0.85 \times 4 \times 54} = 2.04 \text{ in.}$$

$$M^+ = \frac{375}{12}\left(33.4 - \frac{2.04}{2}\right) = 1012 \text{ ft-kips}$$

The column shear corresponding to the sum of the moments M^+ and M^- and based on the free body of the column between assumed midheight inflection points, as shown in Fig. 20.16*a*, is $V_{col} = (1222 + 1012)/12 = 186$ kips. The shear forces acting on the joint are shown in Fig. 20.16*b*, and the factored joint shear is

$$V_u = T_1 + T_2 - V_{col} = 476 + 375 - 186 = 665 \text{ kips}$$

For a joint confined on three faces with an effective cross-sectional area $A_j = 36 \times 36 = 1296 \text{ in}^2$, the nominal and design capacities of the joint are

$$V_n = 15\sqrt{f'_c}A_j = \frac{15\sqrt{4000} \times 1296}{1000} = 1229 \text{ kips}$$

$$\phi V_n = 0.85 \times 1229 = 1045 \text{ kips}$$

Since $\phi V_n > V_u$, the joint is satisfactory for shear.

Because the joint is not confined on all four sides, the transverse reinforcement in the column must be continued, unchanged, through the joint.

d. Members Not Designated as Part of Seismic-Force-Resisting System

Frame members in structures assigned to SDCs D, E, and F that are assumed not to contribute to the structure's ability to carry earthquake forces must still be able to support the factored gravity loads [see Eqs. (20.4) and (20.5)] for which they are designed as the structures undergo lateral displacement. To provide adequate strength and ductility, ACI Code 21.13.2 requires that these members be designed based on moments corresponding to the design displacement, which ACI Commentary 21.13 suggests should be based on models that will provide a conservatively large estimate of displacement. In this case, ACI Code 21.13.3 permits the load factor for live load L to be reduced to 0.5, except for garages, places of public assembly, and areas where $L > 100$ psf.

When the induced moments and shears, combined with the factored gravity moments and shears (see Table 1.2), do not exceed the design capacity of a frame member, ACI Code 21.13.3 requires that members with factored gravity axial forces below $A_g f_c'/10$ contain minimum longitudinal top and bottom reinforcement as provided in Eq. (3.41), a reinforcement ratio not greater than 0.025, and at least two continuous bars top and bottom. In addition, stirrups are required with a maximum spacing of $d/2$ throughout.

For members with factored gravity axial forces exceeding $A_g f_c'/10$, the longitudinal reinforcement must meet the requirements for columns proportioned for earthquake loads, and the transverse reinforcement must consist of hoops and crossties, as used in columns designed for seismic loading (as required by ACI Code 21.6.4.2). The maximum longitudinal spacing of the transverse reinforcement s_o may not be more than 6 times the diameter of the smallest longitudinal bar or 6 in. throughout the column height. In addition, the transverse reinforcement must carry shear induced by inelastic rotation at the ends of the member, as required by ACI Code 21.6.5 (discussed in Section 20.7). Members with factored gravity axial forces exceeding 35 percent of the axial capacity without eccentricity $0.35P_o$ must be designed with transverse reinforcement equal to at least one-half of that specified in ACI Code 21.6.4.4 [see Eqs. (20.21) through (20.24)].

If the induced moments or shears under the design lateral displacements exceed the design moment or shear strengths, or if such a calculation is not made, ACI Code 21.13.4 requires that the members meet the material criteria for concrete and steel in ACI Code 21.1.4 and 21.1.5 (see Section 20.4), along with criteria for mechanical and welded splices (ACI Code 21.1.6 and 21.1.7.1, respectively). For frame members with factored gravity axial loads below $A_g f_c'/10$, the minimum reinforcement criteria specified in ACI Code 21.5.2 must be met, along with the requirement that the shear capacity of the member be adequate to carry forces induced by flexural yielding under the criteria of ACI Code 21.5.4 [see Fig. 20.18 and Eq. (20.30) in Section 20.7]. In addition, stirrups may not be spaced at greater than $d/2$ throughout the length of the member. For members with factored gravity axial forces exceeding $A_g f_c'/10$, the longitudinal reinforcement ratio ρ_g must be within the range 0.01 to 0.06, and all requirements for transverse reinforcement and shear capacity specified for columns designed for earthquake-induced lateral loading must be satisfied. In addition, the transverse column reinforcement must be continued within the joints, as required by ACI Code 21.7.3.1 (see Section 20.5c) for frames in structures assigned to SDCs D, E, and F.

To reduce the potential for a punching shear failure for slab-column connections in two-way slabs without beams, ACI Code 12.13.6 requires that stirrups or headed studs satisfying the requirements of ACI Code 11.11.3 or 11.11.5, respectively (see Section 13.10), and providing V_s of at least $3.5\sqrt{f'_c}b_o d$ extend at least 4 times the slab thickness away from the face of the support, unless either (1) the requirements of ACI Code 11.11.7 are satisfied using the factored shear due to gravity load V_{ug} and the induced moment transferred between the slab and column under the design displacement, as described in Section 13.11, or (2) the design story drift ratio (relative lateral displacement under design load from the top to the bottom of a story divided by the height of the story) does not exceed the larger of 0.005 and $[0.035 - 0.05(V_{ug}/\phi V_c)]$. The design story drift ratio is equal to the larger of the design story drift ratios of the stories above and below the slab-column connection. V_c is defined by Eqs. (13.11*a*) through (13.11*c*), and V_{ug} is the factored shear force on the slab critical section for two-way action for the load combination $1.2D + 1.0L + 0.2S$. The load factor on the live load L may be reduced to 0.5, except for garages, places of public assembly, and cases in which L exceeds 100 lb/ft^2.

20.6 ACI PROVISIONS FOR SPECIAL STRUCTURAL WALLS, COUPLING BEAMS, DIAPHRAGMS, AND TRUSSES

ACI Code Chapter 21 includes requirements for stiff structural systems and members that carry earthquake forces or distribute earthquake forces between portions of structures that carry earthquake forces. Structural walls, coupling beams, diaphragms, trusses, struts, ties, chords, and collector elements are in this category. The general requirements for these members are presented in this section. The requirements for shear design are presented in Section 20.7c.

a. Structural Walls

To ensure adequate ductility, ACI Code 21.9.2 requires that structural walls have minimum shear reinforcement ratios in both the longitudinal and transverse directions ρ_l and ρ_t of 0.0025 and a maximum reinforcement spacing of 18 in. If the factored shear force assigned to a wall exceeds $2A_{cv}\lambda\sqrt{f'_c}$, where A_{cv} is the net area of the concrete section bounded by the web thickness and the length of the section in the direction of the factored shear force, at least two curtains of reinforcement must be used. If, however, the factored shear is not greater than $A_{cv}\lambda\sqrt{f'_c}$, the minimum reinforcement criteria of ACI Code 14.3 govern.

Boundary elements are added along the edges of structural walls and diaphragms to increase strength and ductility. The elements include added longitudinal and transverse reinforcement and may lie entirely within the thickness of the wall or may require a larger cross section, as shown in Fig. 20.17. Under certain conditions, openings must be bordered by boundary elements. For walls that are continuous from the base of the structure to the top of a wall, compression zones must be reinforced with

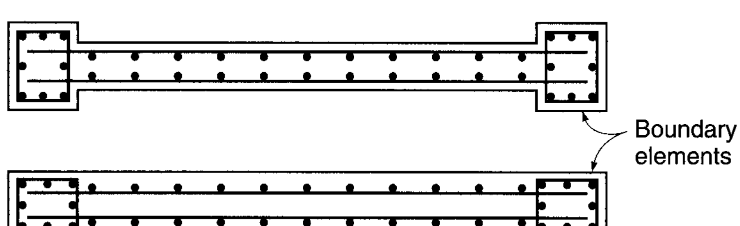

FIGURE 20.17
Cross sections of structural walls with boundary elements.

special boundary elements when the depth to the neutral axis c exceeds the value given in Eq. (20.28).

$$c \geq \frac{l_w}{600(\delta_u/h_w)} \tag{20.28}$$

where l_w and h_w are the length and width of the wall, respectively, and δ_u is the design displacement. In Eq. (20.28), δ_u/h_w is not taken greater than 0.007. When special boundary elements are required based on Eq. (20.28), the reinforcement in the boundary element must be extended vertically from the critical section a distance equal to the greater of l_w or $M_u/4V_u$.

Structural walls are also required to have boundary elements at boundaries and around openings where the maximum extreme fiber compressive stress under factored loads exceeds $0.2f'_c$. Stresses are calculated based on a linear elastic model using the gross cross section [$\sigma = (P/A) \pm (My/I)$]. The boundary elements may be discontinued once the calculated compressive stress drops below $0.15f'_c$. The confinement provided by the boundary element increases both the ductility of the wall and its ability to carry repeated cycles of loading. When required, the boundary element must extend horizontally from the extreme compressive fiber a distance not less than $c - 0.1l_w$ or $c/2$, whichever is greater, where c is the largest neutral axis depth calculated for the factored load and nominal moment capacity consistent with the displacement δ_u. When flanged sections are used, the boundary element is defined based on the effective flange width and extends at least 12 in. into the web. Transverse reinforcement within the boundary element must meet the requirements for columns in ACI Code 21.6.2 through 21.6.4 (discussed in Section 20.5b), but need not meet the requirements in Eq. (20.23), and the spacing limit for transverse reinforcement of one-quarter of the minimum member dimension in columns [described prior to Eq. (20.21) and specified in ACI Code 21.6.4.3(a)] is changed to one-third of the least dimension of the boundary element. The transverse reinforcement within a boundary element must extend into the support a distance equal to at least the development length of the largest longitudinal reinforcement, except where the boundary element terminates at a footing or mat, in which case the transverse reinforcement must extend at least 12 in. into the foundation. Horizontal reinforcement in the wall web must be anchored within the confined core of the boundary element, a requirement that usually requires standard 90° hooks or mechanical anchorage.

When boundary elements are not required and when the longitudinal reinforcement ratio in the wall boundary is greater than $400/f_y$, the transverse reinforcement at the boundary must consist of hoops or spirals at the wall boundary with crossties or legs that are not spaced more than 14 in. on center extending into the wall a distance of $c - 0.1l_w$ or $c/2$, whichever is greater, at a spacing of not greater than 8 in. The transverse reinforcement in such cases must be anchored with a standard hook around the edge reinforcement, or the edge reinforcement must be enclosed in U stirrups of the same size and spacing as the transverse reinforcement. This requirement need not be met if the maximum shear force is less than $A_{cv}\lambda\sqrt{f'_c}$.

b. Coupling Beams

Coupling beams connect structural walls, as shown in Fig. 20.18*a*. Under lateral loading, they can increase the stiffness of the structure and dissipate energy. Deeper coupling beams can be subjected to significant shear, which is carried effectively by diagonal reinforcement. According to ACI Code 21.9.7, coupling beams with clear span-to-total-depth ratios l_n/h of 4 or greater may be designed using the criteria for flexural members described in Section 20.5a. In this case, however, the limitations

FIGURE 20.18
Coupled shear walls and coupling beam. (*Parts b and c adapted from Ref. 20.9.*)

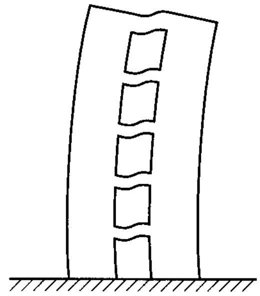

(*a*) Coupled shear walls

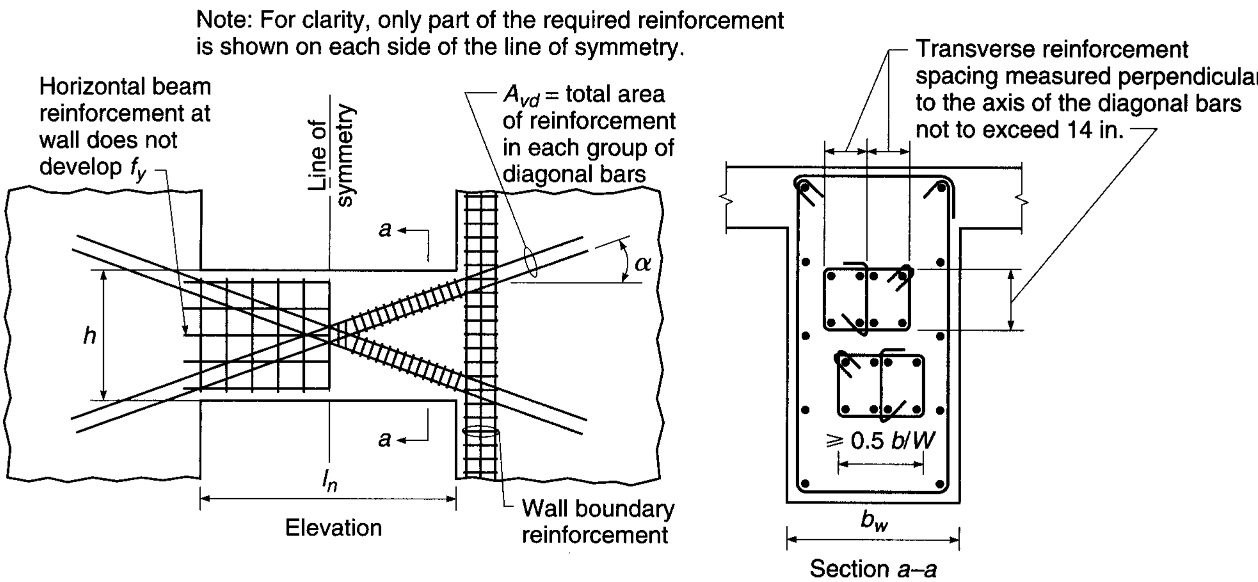

(*b*) Coupling beam with confinement of individual diagonals

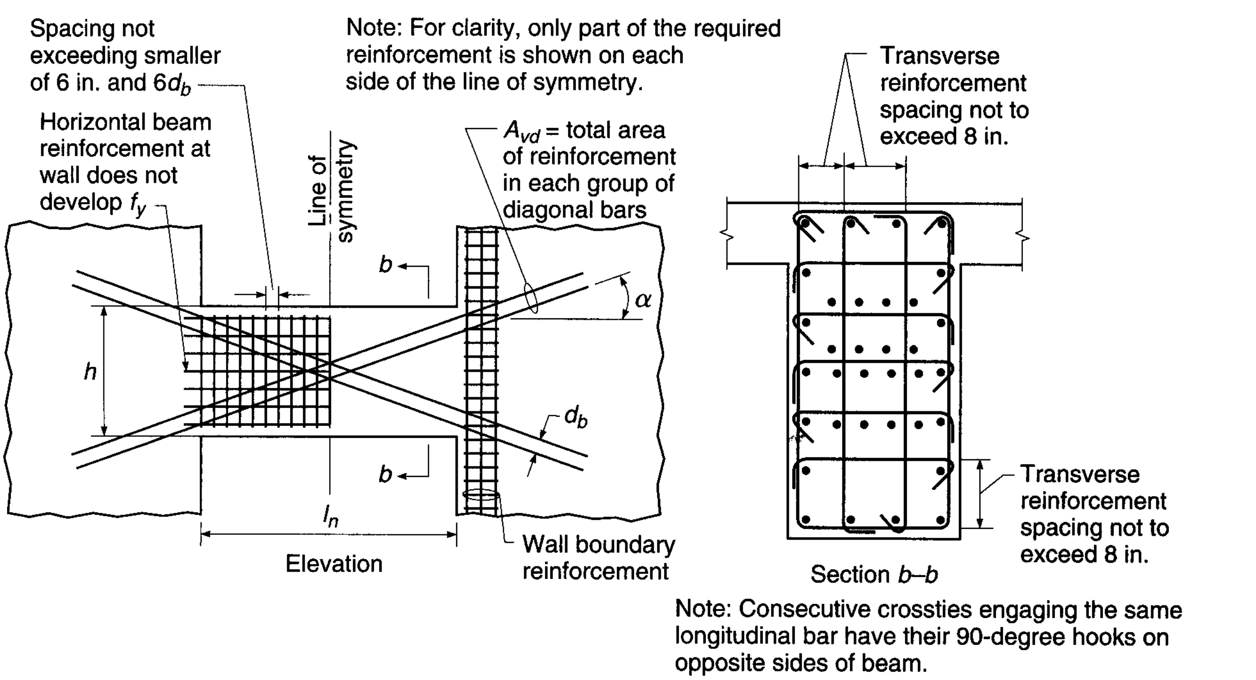

(*c*) Coupling beam with full confinement of diagonally reinforced concrete beam section on width-to-depth ratio and total width for flexural members need not be applied if it can be shown by analysis that the beam has adequate lateral stability. Coupling beams with l_n/h less than 2 and a factored shear $V_u > 4\lambda\sqrt{f'_c}A_{cw}$, where A_{cw} is the concrete area resisting shear, must be reinforced with two intersecting groups of diagonal reinforcement, as shown in Fig. 20.18*b* and *c*, unless it can be shown that the loss of stiffness and strength in the beams will not impair the vertical load-carrying capacity of the structure, egress from the structure, or the integrity of nonstructural components and their connections to the structure. Coupling beams with $2 \le l_n/h < 4$ may be designed using the criteria for flexural members or may be reinforced using two intersecting groups of diagonally placed bars that are symmetrical about the midspan. Such reinforcement is not effective unless it is placed at a steep angle (Refs. 20.11 and 20.12) and thus is not permitted for coupling beams with $l_n/h \ge 4$. The criteria for shear reinforcement in coupling beams are discussed in Section 20.7c.

c. Structural Diaphragms

Floors and roofs serve as structural diaphragms in buildings. In addition to supporting vertical dead, live, and snow loads, they connect and transfer lateral forces between the members in the vertical lateral-force-resisting system and support other building elements, such as partitions, that may resist horizontal forces but do not act as part of the vertical lateral-force-resisting system. Floor and roof slabs that act as diaphragms may be monolithic with the other horizontal elements in the structures or may include a topping slab. ACI Code 21.11.6 requires that concrete slabs and composite topping slabs designed as structural diaphragms to transmit earthquake forces be at least 2 in. thick. Topping slabs placed over precast floor or roof elements that do not rely on composite action must be at least $2\frac{1}{2}$ in. thick.

d. Collector and Structural Truss Elements

To provide adequate confinement and ductility, collector elements, which act in tension or compression to transmit seismic forces between structural diaphragms and vertical load-carrying elements, with compressive stresses greater than $0.2f'_c$ must meet the same transverse reinforcement requirements as boundary elements in seismic-load-resisting frames, but over the full length of the elements. The special transverse reinforcement may be discontinued at a section where the calculated compressive stress is less than $0.15f'_c$ in accordance with ACI Code 21.11.7.5. Transverse reinforcement is also required for truss elements with compressive stresses greater than $0.2f'_c$, but in contrast with collector elements, must be continued over the full length of the element. For trusses, the requirements for columns in ACI Code 21.6.4.2 through 21.6.4.4 and 21.6.4.7 are used, as described in Section 20.5b. Compressive stresses in collector and truss elements are calculated for the factored forces using a linear elastic model and the gross section properties of the elements. Continuous reinforcement in stiff structural systems must be anchored and spliced to develop f_y in tension.

20.7 ACI PROVISIONS FOR SHEAR STRENGTH

a. Beams

A prime concern in the design of seismically loaded structures is the shear induced in members due to nonlinear behavior in flexure [Eq. (20.1)]. As discussed in Section 20.2, increasing the flexural strength of beams and columns may increase the shear in these

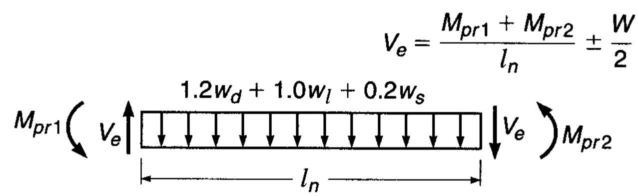

FIGURE 20.19
Forces considered in the shear design of flexural members subjected to seismic loading. $W/2$ is the shear corresponding to gravity loads based on $1.2D + 1.0L + 0.2S$.

members if the structure is subjected to severe lateral loading. As a result, the ACI Code requires that beams and columns in frames that are part of the seismic-force-resisting system (including some members that are not designed to carry lateral loads) be designed for the combined effects of factored gravity load and shear induced by the formation of plastic hinges at the ends of the members.

For members with axial loads less than $A_g f'_c/10$, ACI Code 21.5.4 requires that the design shear force V_e be based on the factored tributary gravity load along the span plus shear induced by moments of opposite sign corresponding to the *probable flexural strength* M_{pr}. Loading corresponding to this case is shown in Fig. 20.19. The probable flexural strength M_{pr} is based on the reinforcing steel achieving a stress of $1.25f_y$.

$$M_{pr} = 1.25A_s f_y \left(d - \frac{a}{2}\right) \tag{20.29a}$$

where

$$a = \frac{1.25f_y A_s}{0.85f'_c b} \tag{20.29b}$$

The shear V_e is given by

$$V_e = \frac{M_{pr1} + M_{pr2}}{l_n} \pm \frac{w_u l_n}{2} \tag{20.30}$$

where M_{pr1} and M_{pr2} = probable moment strengths at two ends of member when moments are acting in the same sense
l_n = length of member between faces of supports
w_u = factored uniform gravity load based on $1.2D + 1.0L + 0.2S$

Equation (20.30) should be evaluated separately for moments at both ends acting in the clockwise and then counterclockwise directions.

To provide adequate ductility and concrete confinement, the transverse reinforcement over a length equal to twice the member depth from the face of the support, at both ends of the flexural member, must be designed based on a concrete shear capacity $V_c = 0$, when the earthquake-induced shear force in Eq. (20.30) $(M_{pr1} + M_{pr2})/l_n$ is one-half or more of the maximum required shear strength within that length and the factored axial compressive force in the member, including earthquake effects, is below $A_g f'_c/20$.

EXAMPLE 20.3 **Beam shear design.** An 18 in. wide by 24 in. deep reinforced concrete beam spans between two interior columns in a building frame designed for a region of high seismic risk. The clear span is 24 ft, and the reinforcement at the face of the support consists of four No. 10 (No. 32) top bars and four No. 8 (No. 25) bottom bars. The effective depth is 21.4 in. for both top and bottom steel. The maximum factored shear $w_u l_n/2 = (1.2w_d + 1.0w_l)l_n/2 = 32$ kips at each

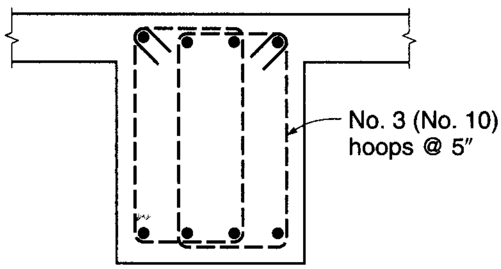

FIGURE 20.20
Configuration of hoop reinforcement for beam in Example 20.3.

end of the beam. Materials strengths are $f_c' = 5000$ psi and $f_y = 60{,}000$ psi. Design the shear reinforcement for the regions adjacent to the column faces.

Solution. The probable moment strengths M_{pr} are based on a steel stress of $1.25f_y$. For negative bending, the area of steel is $A_s = 5.08$ in^2 at both ends of the beam, the stress block depth is $a = 1.25 \times 5.08 \times 60/(0.85 \times 5 \times 18) = 4.98$ in., and the probable strength is

$$M_{prl} = \frac{1.25 \times 5.08 \times 60}{12}\left(21.4 - \frac{4.98}{2}\right) = 600 \text{ ft-kips}$$

For positive bending, the area of steel is $A_s = 3.16$ in^2, the effective width is 90 in., the stress block depth $a = 1.25 \times 3.16 \times 60/(0.85 \times 5 \times 90) = 0.62$ in., and the probable strength is

$$M_{pr2} = \frac{1.25 \times 3.16 \times 60}{12}\left(21.4 - \frac{0.62}{2}\right) = 417 \text{ ft-kips}$$

As given in the problem statement, the effect of factored gravity loads $w_u l_n/2 = (1.2w_d + 1.0w_l)l_n/2 = 32$ kips giving a design shear force at each end of the beam, according to Eq. (20.30), of

$$V_e = \frac{600 + 417}{24} + 32 = 42 + 32 = 74 \text{ kips}$$

Since the earthquake-induced force, 42 kips, is greater than one-half of the maximum required shear strength, the transverse hoop reinforcement must be designed to resist the full value of V_e (i.e., $\phi V_s \geq V_e$) over a length $2h = 48$ in. from the face of the column, in accordance with ACI Code 21.3.3. The maximum spacing of the hoops s is based on the smaller of $d/4 = 5.4$ in., $8d_b$ for the smallest longitudinal bars $= 8$ in., or $24d_b$ for the hoop bars [assumed to be No. 3 (No. 10) bars] $= 9$ in., or 12 in. A spacing $s = 5$ in. will be used.

The area of shear reinforcement within a distance s is

$$A_v = \frac{(V_e/\phi)s}{f_{yt}d} = \frac{(74/0.75)5}{60 \times 21.4} = 0.38 \text{ in}^2$$

Providing support for corner and alternate longitudinal bars, in accordance with ACI Code 21.5.3, leads to the use of overlapping hoop reinforcement, shown in Fig. 20.20, and a total area of transverse steel $A_v = 0.44$ in^2.

The first hoop is placed 2 in. from the face of the column. The other hoops are spaced at 5 in. within 48 in. from each column face. Transverse reinforcement for the balance of the beam is calculated based on the value of V_e at that location and a nonzero concrete contribution V_c. The stirrups must have seismic hooks and a maximum spacing of $d/2$.

b. Columns

In accordance with ACI Code 21.6.5, shear provisions similar to those used for beams to account for the formation of inelastic hinges must also be applied to members with

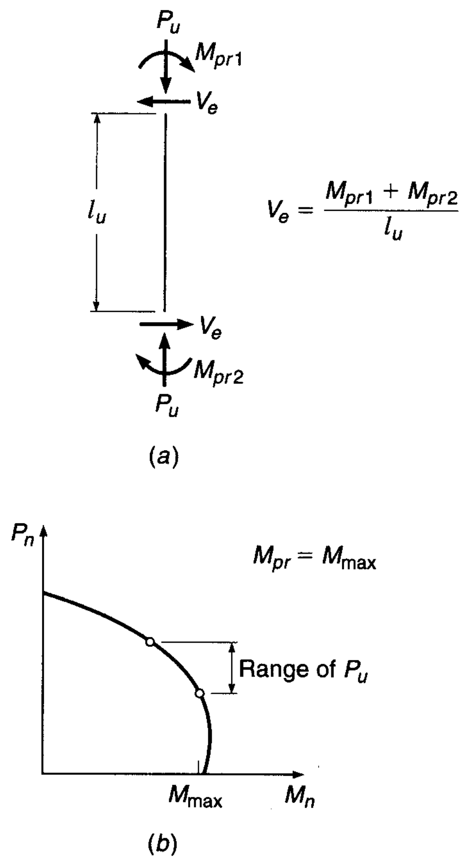

FIGURE 20.21
(*a*) Forces considered in the shear design of columns subjected to seismic loading. (*b*) Column interaction diagram used to determine maximum probable moment strengths. Note that M_{pr} for columns is usually governed by M_{pr} of the girders framing into a joint, rather than M_{max}.

axial loads greater than $A_g f'_c/10$. In this case, the loading is illustrated in Fig. 20.21*a*, and the factored shear is

$$V_e = \frac{M_{pr1} + M_{pr2}}{l_u} \tag{20.31}$$

where l_u is the clear distance between beams, and M_{pr1} and M_{pr2} are based on a steel tensile strength of $1.25f_y$.

In Eq. (20.31), M_{pr1} and M_{pr2} are the maximum probable moment strengths for the range of factored axial loads to which the column will be subjected, as shown in Fig. 20.21*b*; V_e, however, need not be greater than a value based on M_{pr} for the transverse members framing into the joint. For most frames, the latter will control. Of course, V_e may not be less than that obtained from the analysis of the structure under factored loads.

The ACI Code requires that the transverse reinforcement in a column over a length l_o (the greater of the depth of the member at the joint face, one-sixth of the clear span, or 18 in.) from each joint face be proportioned to resist shear based on a concrete shear capacity $V_c = 0$ when (1) the earthquake-induced shear force is one-half or more of the maximum required shear strength within those lengths and (2) the factored axial compressive force, including earthquake effects, is less than $A_g f'_c/20$.

c. Walls, Coupling Beams, Diaphragms, and Trusses

According to ACI Code 21.9.3 and 21.11.9, the factored shear force V_u for walls, coupling beams, diaphragms, and trusses must be obtained from analysis based on the factored (including earthquake) loads.

In accordance with ACI Code 21.9.4, the nominal shear strength V_n of structural walls and diaphragms is taken as

$$V_n = A_{cv}(\alpha_c \lambda \sqrt{f'_c} + \rho_t f_y) \tag{20.32}$$

where A_{cv} = gross area of concrete section bounded by the web thickness and length of the section in the direction of shear force
ρ_t = ratio of distributed shear reinforcement on a plane perpendicular to the plane of A_{cv}
α_c = 3.0 for $h_w/l_w \leq 1.5$, = 2.0 for $h_w/l_w \geq 2.0$, and varies linearly for intermediate values of h_w/l_w

The values of h_w and l_w used to calculate α_c are the height and length, respectively, of the entire wall or diaphragm or segments of the wall or diaphragm. l_w is measured in the direction of the shear force. In applying Eq. (20.32), the ratio h_w/l_w is the larger of the ratios for the entire member or the segment of the member being considered. The use of α_c greater than 2.0 is based on the higher shear strength observed for walls with low aspect ratios.

As described in Section 20.6, ACI Code 21.9.2 requires that walls and diaphragms contain distributed shear reinforcement in two orthogonal directions in the plane of the member. For $h_w/l_w \leq 2.0$, the reinforcement ratio for steel crossing the plane of A_{cv}, ρ_l, must at least equal ρ_t. The nominal shear strength of all wall piers (vertical regions of a wall separated by openings) that together carry the lateral force is limited to a maximum value of $8A_{cv}\sqrt{f'_c}$, with no individual pier assumed to carry greater than $10A_{cw}\sqrt{f'_c}$, where A_{cv} is the total cross-sectional area and A_{cw} is the cross-sectional area of an individual pier. The nominal shear strength of horizontal wall segments (regions of a wall bounded by openings above and below) and coupling beams is limited to $10A_{cw}\sqrt{f'_c}$.

For coupling beams reinforced with two intersecting groups of diagonally placed bars symmetrical about the midspan (Fig. 20.18*b*), each group of the diagonally placed bars must consist of at least four bars provided in two or more layers and embedded into the wall not less than 1.25 times the development length required for f_y in tension. The nominal strength provided by the diagonal bars is given by

$$V_n = 2A_{vd} f_y \sin \alpha \leq 10\sqrt{f'_c} A_{cw} \tag{20.33}$$

where A_{vd} = total area of longitudinal reinforcement in an individual diagonal
A_{cw} = area of concrete section resisting shear
α = angle between diagonal reinforcement and longitudinal axis of coupling beam

The upper limit in Eq. (20.33) is a safe upper bound based on the experimental observation that coupling beams remain ductile at shear forces exceeding this value (Ref. 20.12).

ACI Code 21.9.7 allows two options for providing confinement for coupling beams. In the first, shown in Fig. 20.18*b*, each group of diagonal bars must be enclosed by transverse reinforcement having out-to-out dimensions not smaller than $0.5b_w$ in the direction parallel to b_w and $0.2b_w$ along the other sides (i.e., perpendicular to b_w). The transverse reinforcement must consist of hoops satisfying Eqs. (20.23) and (20.24), with a spacing measured parallel to the diagonal bars satisfying Eq. (20.21), but not exceeding 6 times the diameter of the diagonal bars, and have spacing of crossties or legs of hoops measured perpendicular to the diagonal bars not exceeding 14 in. When computing A_g for use in Eqs. (8.5) and (21.23), the concrete cover required by ACI Code 7.7 (see Section 3.6a) is assumed on all four sides of each group of diagonal bars. The transverse reinforcement must be continued through the intersection of the diagonal bars. Additional longitudinal and transverse reinforcement must be distributed around the beam perimeter with a total area in each direction not less than $0.002b_w s$ and spacing not greater than 12 in.

For the second option, shown in Fig. 20.18*c*, ACI Code 21.9.7 allows hoops to be provided for the entire beam cross section satisfying Eqs. (20.23) and (20.24) and extra confining transverse reinforcement, as required by ACI Code 21.6.4.7 when the cover exceeds 4 in., with longitudinal spacing not exceeding the smaller of 6 in. and 6 times the diameter of the diagonal bars, and with spacing of crossties or legs of hoops both vertically and horizontally in the plane of the beam cross section not exceeding 8 in. Each crosstie and each hoop leg must engage a longitudinal bar of equal or larger diameter.

According to ACI Code 21.11.9, the maximum nominal shear strength of diaphragms is

$$V_n = A_{cv}(2\lambda\sqrt{f'_c} + \rho_t f_y) \leq 8A_{cv}\sqrt{f'_c} \tag{20.34}$$

where A_{cv} is the gross area of the concrete bounded by the diaphragm thickness and length of the diaphragm in the direction of the shear force. Web reinforcement in the diaphragm is distributed uniformly in both directions.

20.8 ACI PROVISIONS FOR INTERMEDIATE MOMENT FRAMES

ACI Code 21.3 governs the design of frames in structures assigned to SDC C. The requirements include specified loading and detailing requirements. Unlike structures assigned to SDCs D, E, and F, two-way slab systems without beams are allowed to serve as lateral-load-resisting systems. Walls, diaphragms, and trusses in regions of moderate seismic risk are designed using the main part of the Code.

ACI Code 21.3.3 offers two options for the shear design of frame members. The first option is similar to that illustrated in Figs. 20.19 and 20.21 and Eqs. (20.30) and (20.31), with the exception that the probable strengths M_{pr} are replaced by the nominal strengths M_n. For beams, f_y is substituted for $1.25f_y$ in Eq. (20.29). For columns, the moments used at the top and bottom of the column [Fig. 20.21 and Eq. (20.31)] are based on the capacity of the column alone (not considering the moment capacity of the beams framing into the joints) under the factored axial load P_u that results in the maximum nominal moment capacity.

As an alternative to designing for shear induced by the formation of hinges at the ends of the members, ACI Code 21.3.3 allows shear design to be based on load combinations that include an earthquake effect that is twice that required by the governing building code. Thus, Eq. (20.4) becomes

$$U = 1.2D + 2.0E + 1.0L + 0.2S \tag{20.35}$$

For beams and columns, the Code prescribes detailing requirements that are not as stringent as those used in regions of high seismic risk, but that provide greater confinement and increased ductility compared to those used in structures not designed for earthquake loading. For beams, the positive-moment strength at the face of a joint must be at least one-third of the negative-moment strength at the joint, in accordance with ACI Code 21.3.4. Both the positive and negative-moment strength along the full length of a beam must be at least one-fifth of the maximum moment strength at the face of either joint. Hoops are required at both ends of beams over a length equal to twice the member depth; the first hoop must be placed within 2 in. of the face of the support, and the maximum spacing in this region may not exceed one-fourth of the effective depth, 8 times the diameter of the smallest longitudinal bar, 24 times the stirrup diameter, or 12 in. The maximum stirrup spacing elsewhere in beams is one-half of the effective depth.

For columns, within length l_o from the joint face, the tie spacing s_o may not exceed 8 times the diameter of the smallest longitudinal bar, 24 times the diameter of the tie bar, one-half of the smallest cross-sectional dimension of the column, or 12 in. The length l_o must be greater than one-sixth of the column clear span, the maximum cross-sectional dimension of the member, or 18 in. The first tie must be located not more than $s_o/2$ from the joint face. Outside of l_o, the spacing of the transverse reinforcement must not exceed $d/2$ or 24 in. and must satisfy the requirements specified by ACI Code 7.10 for transverse reinforcement in columns. In accordance with ACI Code 21.3.5 and 11.10, lateral joint reinforcement with an area as specified in Eq. (4.13) must be provided within the column for a depth not less than the depth of the deepest flexural member framing into the joint.

Like columns in special moment frames, columns in intermediate moment frames must be designed to provide for ductile behavior when supporting discontinuous stiff members, such as walls. Columns in intermediate moment frames must contain transverse reinforcement with spacing s_o over the full height beneath the level at which the discontinuity occurs if the portion of factored axial compressive force in the columns related to earthquake effects exceeds $A_g f_c'/10$. This transverse reinforcement must extend above and below the columns into the discontinued stiff member for at least the development length of the largest longitudinal reinforcement for walls and at least 12 in. into foundations.

For two-way slabs without beams, ACI Code 21.3.6 requires design for earthquake effects using Eqs. (20.4) and (20.5). Under these loading conditions, the reinforcement provided to resist the unbalanced moment transferred between the slab and the column M_s (M_u in Section 13.11) must be placed within the column strip. Reinforcement to resist the fraction of the unbalanced moment M_s defined by Eq. (13.16*a*), $M_{ub} = \gamma_f M_u = \gamma_f M_s$, but not less than one-half of the reinforcement in the column strip at the support, must be concentrated near the column. This reinforcement is placed within an effective slab width located between lines $1.5h$ on either side of the column or column capital, where h is the total thickness of the slab or drop panel.

To ensure ductile behavior throughout two-way slabs without beams, at least one-quarter of the top reinforcement at the support in column strips must be continuous throughout the span, as must bottom reinforcement equal to at least one-third of the top reinforcement at the support in column strips. A minimum of one-half of all bottom reinforcement at midspan in both column and middle strips must be continuous and develop its yield strength at the face of the support. For discontinuous edges of the slab, both the top and bottom reinforcement must be developed at the face of the support. Finally, at critical sections for two-way shear at columns (Section 13.10a), V_u may not exceed $0.4\phi V_c$. The latter provision may be waived if the requirements of ACI Code 21.13.6 for slab-column connections in members not designated as part of the seismic-force-resisting system are met (see Section 20.5b).

REFERENCES

20.1 *2003 NEHRP Recommended Provisions for Seismic Regulations for New Buildings and Other Structures*, Part 1—Provisions, Part 2—Commentary, Building Seismic Safety Council, Washington, DC, 2003.

20.2 *Minimum Design Loads for Buildings and Other Structures*, ASCE/SEI 7-05, American Society of Civil Engineers, Reston, VA, 2005.

20.3 S. K. Ghosh, A. W. Domel, Jr., and D. A. Fanella, *Design of Concrete Buildings for Earthquake and Wind Forces*, 2nd ed., Portland Cement Association, Skokie, IL, and International Conference of Building Officials, Whittier, CA, 1995.

20.4 W.-F. Chen and C. Scrawthorn, eds., *Earthquake Engineering Handbook*, CRC Press, Boca Raton, FL, 2003.

20.5 T. Paulay and M. J. N. Priestly, *Seismic Design of Reinforced Concrete and Masonry Buildings*, John Wiley & Sons, Inc., New York, 1992.

20.6 G. G. Penelis and A. J. Kappos, *Earthquake-Resistant Concrete Structures*, E & FN Spon, New York, 1997.

20.7 *Concrete Structures in Earthquake Regions: Design & Analysis*, E. Booth, ed., Longman Scientific & Technical, Harlow, England, 1994.

20.8 *Seismic Analyisis of Safety-Related Nuclear Structures*, SEI/ASCE 4-98, American Society of Civil Engineers, Reston, VA, 2000.

20.9 *Building Code Requirements for Structural Concrete*, (ACI 318-08) *and Commentary*, American Concrete Institute, Farmington Hills, MI, 2008.

20.10 ACI Committee 352, *Recommendations for Design of Beam-Column Joints in Monolithic Reinforced Concrete Structures*, ACI 352R-02, American Concrete Institute, Farmington Hills, MI, 2008.

20.11 T. Paulay and J. R. Binney, "Diagonally Reinforced Coupling Beams of Shear Walls," in *Shear in Reinforced Concrete*, SP-42, American Concrete Institute, Detroit, MI, 1974, pp. 579–798.

20.12 G. B. Barney, K. N. Shiu, B. G. Rabbat, A. E. Fiorato, H. G. Russell, and W. G. Corley, *Behavior of Coupling Beams under Load Reversals* (RD068.01), Portland Cement Association, Skokie, IL, 1980.

PROBLEMS

20.1. An interior column joint in a reinforced concrete frame structure assigned to SDC D consists of 28 in. wide by 20 in. deep beams and 36 in. wide by 20 in. deep girders framing into a 28 × 28 in. column. The slab thickness is 5 in., and the effective overhanging flange width on either side of the web of the flexural members is 40 in. Girder reinforcement at the joint consists of five No. 10 (No. 32) top bars and five No. 8 (No. 25) bottom bars. Beam reinforcement consists of four No. 10 (No. 32) top bars and four No. 8 (No. 25) bottom bars. As the flexural steel crosses the joint, the top and bottom girder bars rest on the respective top and bottom beam bars. Column reinforcement consists of 12 No. 9 (No. 29) bars evenly spaced around the perimeter of the column, similar to the placement shown in Fig. 20.14. Clear cover on the outermost main flexural and column longitudinal reinforcement is 2 in. Assume No. 4 (No. 13) stirrups and ties. For earthquake loading, the maximum factored axial load on the upper column framing into the joint is 1098 kips, and the maximum factored axial load on the lower column is 1160 kips. For a frame story height of 13 ft, determine if the nominal flexural strengths of the columns exceed those of the beams and girders by at least 20 percent, and determine the minimum transverse reinforcement required in the columns adjacent to the beams. Use $f_c' = 4000$ psi and $f_y = 60{,}000$ psi.

20.2. Design the joint and the transverse column reinforcement for the members described in Problem 20.1. The factored shears due to earthquake load are 29 kips in the upper column and 31 kips in the lower column. Minimum factored axial loads are 21 and 25 kips below the forces specified in Problem 20.1 for the upper and lower columns, respectively.

20.3. In Example 20.1, the columns are spaced 28 ft on center in the direction of the spandrel beams. The total dead load on the spandrel beam (including self-weight) is 2 kips/ft and the total live load is 0.93 kips/ft. Design the spandrel beam transverse reinforcement for a building subject to high seismic risk.

20.4. Repeat Problem 20.3 for an intermediate frame.

20.5. An interior column joint in a reinforced concrete frame structure assigned to SDC E consists of 20 in. wide by 28 in. deep beams and girders framing into 26×26 in. columns. The slab thickness is 4 in., and the effective overhanging flange width on either side of the web of the flexural members is 32 in. Girder and beam reinforcement at the joint consists of four No. 10 (No. 32) top bars and four No. 9 (No. 29) bottom bars. As the flexural steel crosses the joint, the top and bottom girder bars are outside the respective top and bottom beam bars. Column reinforcement consists of eight No. 14 (No. 43) bars evenly spaced around the perimeter of the column, similar to the placement shown in Fig. 11.10. Clear cover on the outermost main flexural and column longitudinal reinforcement is 2 in. Assume No. 4 (No. 13) stirrups and ties. For earthquake loading, the maximum factored axial load on the upper column framing into the joint is 1100 kips, and the maximum factored axial load on the lower column is 1230 kips. The story height is 12 ft, and the columns are spaced 24 ft on center in the direction of the girders. Use $f_c' = 4000$ psi and $f_y = 60{,}000$ psi.

(*a*) Determine if the nominal flexural strengths of the columns exceed those of the beams and girders by at least 20 percent, and determine the minimum transverse reinforcement required in the columns adjacent to the beams.

(*b*) The total dead load on the girder (including self-weight) is 2.8 kips/ft, and the total live load is 1.3 kips/ft. Design the girder transverse reinforcement.

APPENDIX

A Design Aids

TABLE A.1
Designations, diameters, areas, and weights of standard bars

Bar No. Inch-Pound[a]	Bar No. SI[b]	Diameter, in.	Cross-Sectional Area, in^2	Nominal Weight, lb/ft
3	10	$\frac{3}{8} = 0.375$	0.11	0.376
4	13	$\frac{1}{2} = 0.500$	0.20	0.668
5	16	$\frac{5}{8} = 0.625$	0.31	1.043
6	19	$\frac{3}{4} = 0.750$	0.44	1.502
7	22	$\frac{7}{8} = 0.875$	0.60	2.044
8	25	$1 = 1.000$	0.79	2.670
9	29	$1\frac{1}{8} = 1.128^c$	1.00	3.400
10	32	$1\frac{1}{4} = 1.270^c$	1.27	4.303
11	36	$1\frac{3}{8} = 1.410^c$	1.56	5.313
14	43	$1\frac{3}{4} = 1.693^c$	2.25	7.650
18	57	$2\frac{1}{4} = 2.257^c$	4.00	13.600

[a]Based on the number of eighths of an inch included in the nominal diameter of the bars. The nominal diameter of a deformed bar is equivalent to the diameter of a plain bar having the same weight per foot as the deformed bar.

[b]Bar number approximates the number of millimeters included in the nominal diameter of the bar. Bars are marked with this designation.

[c]Approximate to nearest $\frac{1}{8}$ in.

TABLE A.2
Areas of groups of standard bars, in^2

Bar No. Inch-Pound	Bar No. SI	Number of Bars 1	2	3	4	5	6	7	8	9	10	11	12
4	13	0.20	0.40	0.60	0.80	1.00	1.20	1.40	1.60	1.80	2.00	2.20	2.40
5	16	0.31	0.62	0.93	1.24	1.55	1.86	2.17	2.48	2.79	3.10	3.41	3.72
6	19	0.44	0.88	1.32	1.76	2.20	2.64	3.08	3.52	3.96	4.40	4.84	5.28
7	22	0.60	1.20	1.80	2.40	3.00	3.60	4.20	4.80	5.40	6.00	6.60	7.20
8	25	0.79	1.58	2.37	3.16	3.95	4.74	5.53	6.32	7.11	7.90	8.69	9.48
9	29	1.00	2.00	3.00	4.00	5.00	6.00	7.00	8.00	9.00	10.00	11.00	12.00
10	32	1.27	2.54	3.81	5.08	6.35	7.62	8.89	10.16	11.43	12.70	13.97	15.24
11	36	1.56	3.12	4.68	6.24	7.80	9.36	10.92	12.48	14.04	15.60	17.16	18.72
14	43	2.25	4.50	6.75	9.00	11.25	13.50	15.75	18.00	20.25	22.50	24.75	27.00
18	57	4.00	8.00	12.00	16.00	20.00	24.00	28.00	32.00	36.00	40.00	44.00	48.00

TABLE A.3
Areas of bars in slabs, in^2/ft

Spacing, in.	Bar No. Inch-Pound: 3 / SI: 10	4 / 13	5 / 16	6 / 19	7 / 22	8 / 25	9 / 29	10 / 32	11 / 36
3	0.44	0.78	1.23	1.77	2.40	3.14	4.00	5.06	6.25
$3\frac{1}{2}$	0.38	0.67	1.05	1.51	2.06	2.69	3.43	4.34	5.36
4	0.33	0.59	0.92	1.32	1.80	2.36	3.00	3.80	4.68
$4\frac{1}{2}$	0.29	0.52	0.82	1.18	1.60	2.09	2.67	3.37	4.17
5	0.26	0.47	0.74	1.06	1.44	1.88	2.40	3.04	3.75
$5\frac{1}{2}$	0.24	0.43	0.67	0.96	1.31	1.71	2.18	2.76	3.41
6	0.22	0.39	0.61	0.88	1.20	1.57	2.00	2.53	3.12
$6\frac{1}{2}$	0.20	0.36	0.57	0.82	1.11	1.45	1.85	2.34	2.89
7	0.19	0.34	0.53	0.76	1.03	1.35	1.71	2.17	2.68
$7\frac{1}{2}$	0.18	0.31	0.49	0.71	0.96	1.26	1.60	2.02	2.50
8	0.17	0.29	0.46	0.66	0.90	1.18	1.50	1.89	2.34
9	0.15	0.26	0.41	0.59	0.80	1.05	1.33	1.69	2.08
10	0.13	0.24	0.37	0.53	0.72	0.94	1.20	1.52	1.87
12	0.11	0.20	0.31	0.44	0.60	0.78	1.00	1.27	1.56

TABLE A.4
Limiting steel reinforcement ratios for tension-controlled members

f_y, psi	f'_c, psi	β_1	$\rho_{0.005}$[a] $\epsilon_t = 0.005$[b]	ρ_{max}[a] $\epsilon_t = 0.004$[c]	$\rho_{min} = \frac{200}{f_y}$	$\rho_{min} = \frac{3\sqrt{f'_c}}{f_y}$
40,000	3000	0.85	0.0203	0.0232	0.0050	0.0041
	4000	0.85	0.0271	0.0310	0.0050	0.0047
	5000	0.80	0.0319	0.0364	0.0050	0.0053
	6000	0.75	0.0359	0.0410	0.0050	0.0058
	7000	0.70	0.0390	0.0446	0.0050	0.0063
	8000	0.65	0.0414	0.0474	0.0050	0.0067
	9000	0.65	0.0466	0.0533	0.0050	0.0071
50,000	3000	0.85	0.0163	0.0186	0.0040	0.0033
	4000	0.85	0.0217	0.0248	0.0040	0.0038
	5000	0.80	0.0255	0.0291	0.0040	0.0042
	6000	0.75	0.0287	0.0328	0.0040	0.0046
	7000	0.70	0.0312	0.0357	0.0040	0.0050
	8000	0.65	0.0332	0.0379	0.0040	0.0054
	9000	0.65	0.0373	0.0426	0.0040	0.0057
60,000	3000	0.85	0.0135	0.0155	0.0033	0.0027
	4000	0.85	0.0181	0.0206	0.0033	0.0032
	5000	0.80	0.0213	0.0243	0.0033	0.0035
	6000	0.75	0.0239	0.0273	0.0033	0.0039
	7000	0.70	0.0260	0.0298	0.0033	0.0042
	8000	0.65	0.0276	0.0316	0.0033	0.0045
	9000	0.65	0.0311	0.0355	0.0033	0.0047
75,000	3000	0.85	0.0108	0.0124	0.0027	0.0022
	4000	0.85	0.0145	0.0165	0.0027	0.0025
	5000	0.80	0.0170	0.0194	0.0027	0.0028
	6000	0.75	0.0191	0.0219	0.0027	0.0031
	7000	0.70	0.0208	0.0238	0.0027	0.0033
	8000	0.65	0.0221	0.0253	0.0027	0.0036
	9000	0.65	0.0249	0.0284	0.0027	0.0038

[a] $\rho = 0.85\beta_1 \frac{f'_c}{f_y} \frac{0.003}{0.003 + \epsilon_t}$

[b] $\frac{c}{d_t} = 0.375, \frac{a}{d_t} = 0.375\beta_1$

[c] $\frac{c}{d_t} = 0.429, \frac{a}{d_t} = 0.429\beta_1$

TABLE A.5a
Flexural resistance factor: $R = \rho f_y\left(1 - 0.588\,\dfrac{\rho f_y}{f'_c}\right)$ psi

	f_y = 40,000 psi				f_y = 60,000 psi			
	f'_c, psi				f'_c, psi			
ρ	3000	4000	5000	6000	3000	4000	5000	6000
0.0005	20	20	20	20	30	30	30	30
0.0010	40	40	40	40	59	59	60	60
0.0015	59	59	60	60	88	89	89	89
0.0020	79	79	79	79	117	118	118	119
0.0025	98	99	99	99	146	147	147	148
0.0030	117	118	118	119	174	175	176	177
0.0035	136	137	138	138	201	204	205	206
0.0040	155	156	157	157	229	232	233	234
0.0045	174	175	176	177	256	259	261	263
0.0050	192	194	195	196	282	287	289	291
0.0055	211	213	214	215	309	314	317	319
0.0060	229	232	233	234	335	341	345	347
0.0065	247	250	252	253	360	368	372	375
0.0070	265	268	271	272	385	394	399	403
0.0075	282	287	289	291	410	420	426	430
0.0080	300	305	308	310	435	446	453	457
0.0085	317	323	326	329	459	472	479	485
0.0090	335	341	345	347	483	497	506	511
0.0095	352	359	363	366	506	522	532	538
0.0100	369	376	381	384	529	547	558	565
0.0105	385	394	399	403	552	572	583	591
0.0110	402	412	417	421	575	596	609	617
0.0115	419	429	435	439	597	620	634	643
0.0120	435	446	453	457	618	644	659	669
0.0125	451	463	471	476	640	667	684	695
0.0130	467	480	488	494	661	691	708	720
0.0135	483	497	506	511	681	714	733	746
0.0140	499	514	523	529	702	736	757	771
0.0145	514	531	540	547	722	759	781	796
0.0150	529	547	558	565	741	781	805	821
0.0155	545	563	575	582	760	803	828	845
0.0160	560	580	592	600		825	852	870
0.0165	575	596	609	617		846	875	894
0.0170	589	612	626	635		867	898	918
0.0175	604	628	642	652		888	920	942
0.0180	618	644	659	669		909	943	966
0.0185	633	660	676	686		929	965	989
0.0190	647	675	692	703		949	987	1013
0.0195	661	691	708	720		969	1009	1036
0.0200	675	706	725	737		988	1031	1059

TABLE A.5b
Flexural resistance factor: $R = \rho f_y\left(1 - 0.588\,\frac{\rho f_y}{f'_c}\right)$ psi

	f_y = 40,000 psi				f_y = 60,000 psi			
	f'_c, psi				f'_c, psi			
ρ	3000	4000	5000	6000	3000	4000	5000	6000
0.003	117	118	118	119	174	175	176	177
0.004	155	156	157	157	229	232	233	234
0.005	192	194	195	196	282	287	289	291
0.006	229	232	233	234	335	341	345	347
0.007	265	268	271	272	385	394	399	403
0.008	300	305	308	310	435	446	453	457
0.009	335	341	345	347	483	497	506	511
0.010	369	376	381	384	529	547	558	565
0.011	402	412	417	421	575	596	609	617
0.012	435	446	453	457	618	644	659	669
0.013	467	480	488	494	661	691	708	720
0.014	499	514	523	529	702	736	757	771
0.015	529	547	558	565	741	781	805	821
0.016	560	580	592	600	779	825	852	870
0.017	589	612	626	635		867	898	918
0.018	618	644	659	669		909	943	966
0.019	647	675	692	703		949	987	1013
0.020	675	706	725	737		988	1031	1059
0.021	702	736	757	771			1073	1104
0.022	728	766	789	804			1115	1149
0.023	754	796	820	837			1156	1193
0.024		825	852	870			1196	1237
0.025		853	882	902				1280
0.026		881	913	934				1322
0.027		909	943	966				1363
0.028		936	972	997				
0.029		962	1002	1028				
0.030		988	1031	1059				
0.031		1014	1059	1089				
0.032			1087	1119				
0.033			1115	1149				
0.034			1142	1179				
0.035			1170	1208				
0.036			1196	1237				
0.037				1265				
0.038				1294				
0.039				1322				
0.040				1349				
0.041				1376				

TABLE A.6
Parameters k and j for elastic, cracked section beam analysis, where $k = \sqrt{2\rho n + (\rho n)^2} - \rho n$; $j = 1 - \frac{1}{3}k$

	$n = 7$		$n = 8$		$n = 9$		$n = 10$	
ρ	k	j	k	j	k	j	k	j
0.0010	0.112	0.963	0.119	0.960	0.125	0.958	0.132	0.956
0.0020	0.154	0.949	0.164	0.945	0.173	0.942	0.180	0.940
0.0030	0.185	0.938	0.196	0.935	0.207	0.931	0.217	0.928
0.0040	0.210	0.930	0.223	0.926	0.235	0.922	0.246	0.918
0.0050	0.232	0.923	0.246	0.918	0.258	0.914	0.270	0.910
0.0054	0.240	0.920	0.254	0.915	0.267	0.911	0.279	0.907
0.0058	0.247	0.918	0.262	0.913	0.275	0.908	0.287	0.904
0.0062	0.254	0.915	0.269	0.910	0.283	0.906	0.296	0.901
0.0066	0.261	0.913	0.276	0.908	0.290	0.903	0.303	0.899
0.0070	0.268	0.911	0.283	0.906	0.298	0.901	0.311	0.896
0.0072	0.271	0.910	0.287	0.904	0.301	0.900	0.314	0.895
0.0074	0.274	0.909	0.290	0.903	0.304	0.899	0.318	0.894
0.0076	0.277	0.908	0.293	0.902	0.308	0.897	0.321	0.893
0.0078	0.280	0.907	0.296	0.901	0.311	0.896	0.325	0.892
0.0080	0.283	0.906	0.299	0.900	0.314	0.895	0.328	0.891
0.0082	0.286	0.905	0.303	0.899	0.317	0.894	0.331	0.890
0.0084	0.289	0.904	0.306	0.898	0.321	0.893	0.334	0.889
0.0086	0.292	0.903	0.308	0.897	0.324	0.892	0.338	0.887
0.0088	0.295	0.902	0.311	0.896	0.327	0.891	0.341	0.886
0.0090	0.298	0.901	0.314	0.895	0.330	0.890	0.344	0.885
0.0092	0.300	0.900	0.317	0.894	0.332	0.889	0.347	0.884
0.0094	0.303	0.899	0.320	0.893	0.335	0.888	0.350	0.883
0.0096	0.306	0.898	0.323	0.892	0.338	0.887	0.353	0.882
0.0098	0.308	0.897	0.325	0.892	0.341	0.886	0.355	0.882
0.0100	0.311	0.896	0.328	0.891	0.344	0.885	0.358	0.881
0.0104	0.316	0.895	0.333	0.889	0.349	0.884	0.364	0.879
0.0108	0.321	0.893	0.338	0.887	0.354	0.882	0.369	0.877
0.0112	0.325	0.892	0.343	0.886	0.359	0.880	0.374	0.875
0.0116	0.330	0.890	0.348	0.884	0.364	0.879	0.379	0.874
0.0120	0.334	0.889	0.353	0.882	0.369	0.877	0.384	0.872
0.0124	0.339	0.887	0.357	0.881	0.374	0.875	0.389	0.870
0.0128	0.343	0.886	0.362	0.879	0.378	0.874	0.394	0.867
0.0132	0.347	0.884	0.366	0.878	0.383	0.872	0.398	0.867
0.0136	0.351	0.883	0.370	0.877	0.387	0.871	0.403	0.866
0.0140	0.355	0.882	0.374	0.875	0.392	0.869	0.407	0.864
0.0144	0.359	0.880	0.378	0.874	0.396	0.868	0.412	0.863
0.0148	0.363	0.879	0.382	0.873	0.400	0.867	0.416	0.861
0.0152	0.367	0.878	0.386	0.871	0.404	0.865	0.420	0.860
0.0156	0.371	0.876	0.390	0.870	0.408	0.864	0.424	0.859
0.0160	0.374	0.875	0.394	0.869	0.412	0.863	0.428	0.857
0.0170	0.383	0.872	0.403	0.867	0.421	0.860	0.437	0.854
0.0180	0.392	0.869	0.412	0.863	0.430	0.857	0.446	0.851
0.0190	0.400	0.867	0.420	0.860	0.438	0.854	0.455	0.848
0.0200	0.407	0.864	0.428	0.857	0.446	0.851	0.463	0.846

TABLE A.7
Maximum number of bars as a single layer in beam stems

$\frac{3}{4}$ in. Maximum Size Aggregate, No. 4 (No. 13) Stirrups[a]

Bar No. Inch-Pound	Bar No. SI	Beam Width b_w, in. 8	10	12	14	16	18	20	22	24	26	28	30
5	16	2	4	5	6	7	8	10	11	12	13	15	16
6	19	2	3	4	6	7	8	9	10	11	12	14	15
7	22	2	3	4	5	6	7	8	9	10	11	12	13
8	25	2	3	4	5	6	7	8	9	10	11	12	13
9	29	1	2	3	4	5	6	7	8	9	9	10	11
10	32	1	2	3	4	5	6	6	7	8	9	10	10
11	36	1	2	3	3	4	5	5	6	7	8	8	9
14	43	1	2	2	3	3	4	5	5	6	6	7	8
18	57	1	1	2	2	3	3	4	4	4	5	5	6

1 in. Maximum Size Aggregate, No. 4 (No. 13) Stirrups[a]

Bar No. Inch-Pound	Bar No. SI	Beam Width b_w, in. 8	10	12	14	16	18	20	22	24	26	28	30
5	16	2	3	4	5	6	7	8	9	10	11	12	13
6	19	2	3	4	5	6	7	8	9	9	10	11	12
7	22	1	2	3	4	5	6	7	8	9	10	10	11
8	25	1	2	3	4	5	6	7	7	8	9	10	11
9	29	1	2	3	4	5	6	7	7	8	9	9	10
10	32	1	2	3	4	5	6	6	7	7	8	9	10

[a]Minimum concrete cover assumed to be $1\frac{1}{2}$ in. to the No. 4 (No. 13) stirrup.

Source: Adapted from Ref. 3.8. Used by permission of American Concrete Institute.

TABLE A.8
Minimum number of bars as a single layer in beam stems governed by crack control requirements of the ACI Code

(*a*) 2 in. clear cover, sides and bottom

Bar No.		Minimum Number of Bars as a Single Layer of a Beam Stem														
		Beam Stem Width b_w, in.														
Inch-Pound	SI	8	10	12	14	16	18	20	22	24	26	28	30	32	34	36
3–14	10–43	1	1	2	2	3	3	3	3	3	4	4	4	4	4	5
18	57	1	1	2	2	2	3	3	3	3	3	4	4	4	4	4

(*b*) $1\frac{1}{2}$ in. clear cover, sides and bottom

Bar No.		Minimum Number of Bars as a Single Layer of a Beam Stem														
		Beam Stem Width b_w, in.														
Inch-Pound	SI	8	10	12	14	16	18	20	22	24	26	28	30	32	34	36
3–4	10–13	1	1	2	2	3	3	3	3	3	4	4	4	4	4	4
5–14	16–43	1	1	2	2	3	3	3	3	3	3	4	4	4	4	4
18	57	1	1	2	2	2	3	3	3	3	3	4	4	4	4	4

TABLE A.9
Design strength ϕM_n for slab sections 12 in. wide, ft-kips; $f_y = 60$ ksi; $\phi M_n = \phi \rho f_y b d^2(1 - 0.59\rho f_y/f'_c)$

		Effective Depth *d*, in.												
f'_c, psi	ρ	3.0	3.5	4.0	4.5	5.0	5.5	6.0	6.5	7.0	8.0	9.0	10.0	12.0
3000	0.002	0.9	1.3	1.7	2.1	2.6	3.2	3.8	4.5	5.2	6.7	8.5	10.5	15.2
	0.003	1.4	1.9	2.5	3.2	3.9	4.7	5.6	6.6	7.7	10.0	12.7	15.6	22.5
	0.004	1.9	2.5	3.3	4.2	5.1	6.2	7.4	8.7	10.1	13.2	16.7	20.6	29.6
	0.005	2.3	3.1	4.1	5.1	6.4	7.7	9.1	10.7	12.4	16.3	20.6	25.4	36.6
	0.006	2.7	3.7	4.8	6.1	7.5	9.1	10.8	12.7	14.8	19.3	24.4	30.1	43.4
	0.007	3.1	4.2	5.5	7.0	8.7	10.5	12.5	14.7	17.0	22.2	28.1	34.7	49.9
	0.008	3.5	4.8	6.3	7.9	9.8	11.8	14.1	16.5	19.2	25.0	31.7	39.1	56.3
	0.009	3.9	5.3	7.0	8.8	10.9	13.1	15.6	18.4	21.3	27.8	35.2	43.4	62.6
	0.010	4.3	5.8	7.6	9.6	11.9	14.4	17.1	20.1	23.3	30.5	38.6	47.6	68.6
	0.011	4.7	6.3	8.3	10.5	12.9	15.6	18.6	21.8	25.3	33.1	41.9	51.7	74.4
4000	0.002	1.0	1.3	1.7	2.1	2.7	3.2	3.8	4.5	5.2	6.8	8.6	10.6	15.3
	0.003	1.4	1.9	2.5	3.2	3.9	4.8	5.7	6.7	7.7	10.1	12.8	15.8	22.7
	0.004	1.9	2.6	3.3	4.2	5.2	6.3	7.5	8.8	10.2	13.3	16.9	20.8	30.0
	0.005	2.3	3.2	4.1	5.2	6.5	7.8	9.3	10.9	12.6	16.5	20.9	25.8	37.2
	0.006	2.8	3.8	4.9	6.2	7.7	9.3	11.0	13.0	15.0	19.6	24.9	30.7	44.2
	0.007	3.2	4.3	5.7	7.2	8.9	10.7	12.8	15.0	17.4	22.7	28.7	35.5	51.1
	0.008	3.6	4.9	6.4	8.1	10.0	12.1	14.5	17.0	19.7	25.7	32.5	40.1	57.8
	0.009	4.0	5.5	7.2	9.1	11.2	13.5	16.1	18.9	21.9	28.6	36.2	44.7	64.4
	0.010	4.4	6.0	7.9	10.0	12.3	14.9	17.7	20.8	24.1	31.5	39.9	49.2	70.9
	0.011	4.8	6.6	8.6	10.9	13.4	16.2	19.3	22.7	26.3	34.3	43.4	53.6	77.2
	0.012	5.2	7.1	9.3	11.7	14.5	17.5	20.9	24.5	28.4	37.1	46.9	57.9	83.4
	0.013	5.6	7.6	9.9	12.6	15.5	18.8	22.4	26.2	30.4	39.8	50.3	62.1	89.5
	0.014	6.0	8.1	10.6	13.4	16.6	20.0	23.8	28.0	32.5	42.4	53.6	66.2	95.4
	0.015	6.3	8.6	11.2	14.2	17.6	21.2	25.3	29.7	34.4	45.0	56.9	70.2	101.2
5000	0.002	1.0	1.3	1.7	2.2	2.7	3.2	3.8	4.5	5.2	6.8	8.6	10.6	15.3
	0.003	1.4	1.9	2.5	3.2	4.0	4.8	5.7	6.7	7.8	10.1	12.8	15.9	22.8
	0.004	1.9	2.6	3.4	4.3	5.2	6.3	7.6	8.9	10.3	13.4	17.0	21.0	30.2
	0.005	2.3	3.2	4.2	5.3	6.5	7.9	9.4	11.0	12.8	16.7	21.1	26.0	37.5
	0.006	2.8	3.8	5.0	6.3	7.8	9.4	11.2	13.1	15.2	19.9	25.1	31.0	44.7
	0.007	3.2	4.4	5.7	7.3	9.0	10.9	12.9	15.2	17.6	23.0	29.1	35.9	51.7
	0.008	3.7	5.0	6.5	8.3	10.2	12.3	14.7	17.2	20.0	26.1	33.0	40.8	58.7
	0.009	4.1	5.6	7.3	9.2	11.4	13.8	16.4	19.2	22.3	29.1	36.9	45.5	65.5
	0.010	4.5	6.1	8.0	10.2	12.5	15.2	18.1	21.2	24.6	32.1	40.6	50.2	72.3
	0.011	4.9	6.7	8.8	11.1	13.7	16.6	19.7	23.1	26.8	35.1	44.4	54.8	78.9
	0.012	5.3	7.3	9.5	12.0	14.8	17.9	21.3	25.1	29.1	37.9	48.0	59.3	85.4
	0.013	5.7	7.8	10.2	12.9	15.9	19.3	22.9	26.9	31.2	40.8	51.6	63.7	91.8
	0.014	6.1	8.3	10.9	13.8	17.0	20.6	24.5	28.8	33.4	43.6	55.2	68.1	98.1
	0.015	6.5	8.9	11.6	14.7	18.1	21.9	26.1	30.6	35.5	46.3	58.6	72.4	104.3
	0.016	6.9	9.4	12.3	15.5	19.2	23.2	27.6	32.4	37.5	49.0	62.1	76.6	110.3
	0.017	7.3	9.9	12.9	16.4	20.2	24.4	29.1	34.1	39.6	51.7	65.4	80.8	116.3

TABLE A.10
Simplified tension development length in bar diameters l_d/d_b for uncoated bars and normalweight concrete

		No. 6 (No. 19) and Smaller[a]			No. 7 (No. 22) and Larger		
		f'_c, psi			f'_c, psi		
	f_y, ksi	4000	5000	6000	4000	5000	6000
(1) Bottom bars							
Spacing, cover and ties as per Case *a* or *b*	40	25	23	21	32	28	26
	50	32	28	26	40	35	32
	60	38	34	31	47	42	39
Other cases	40	38	34	31	47	42	39
	50	47	42	39	59	53	48
	60	57	51	46	71	64	58
(2) Top bars							
Spacing, cover and ties as per Case *a* or *b*	40	33	29	27	41	37	34
	50	41	37	34	51	46	42
	60	49	44	40	62	55	50
Other cases	40	49	44	40	62	55	50
	50	62	55	50	77	69	63
	60	74	66	60	92	83	76

Case *a*: Clear spacing of bars being developed or spliced $\geq d_b$, clear cover $\geq d_b$, and stirrups or ties throughout l_d not less than the Code minimum.

Case *b*: Clear spacing of bars being developed or spliced $\geq 2d_b$, and clear cover not less than d_b.

[a]ACI Committee 408 recommends that the values indicated for bar sizes No. 7 (No. 22) and larger be used for all bar sizes.

TABLE A.11

Development length in compression, in., for normalweight concrete

l_{dc} = greater of $(0.02f_y/\sqrt{f'_c})d_b$ or $0.0003f_yd_b$ (Minimum length 8 in. in all cases.)

Bar No.			f'_c, psi							
			3000		4000		5000		6000	
Inch-Pound	SI	f_y, ksi	Basic l_{db}	Confined	Basic l_{db}	Confined	Basic l_{db}	Confined	Basic l_{db}	Confined
3	10	40	8	8	8	8	8	8	8	8
		50	8	8	8	8	8	8	8	8
		60	8	8	8	8	8	8	8	8
4	13	40	8	8	8	8	8	8	8	8
		50	9	8	8	8	8	8	8	8
		60	11	8	9	8	9	8	9	8
5	16	40	9	8	8	8	8	8	8	8
		50	11	9	10	8	9	8	9	8
		60	14	10	12	9	11	8	11	8
6	19	40	11	8	9	8	9	8	9	8
		50	14	10	12	9	11	8	11	8
		60	16	12	14	11	14	10	14	10
7	22	40	13	10	11	8	11	8	11	8
		50	16	12	14	10	13	10	13	10
		60	19	14	17	12	16	12	16	12
8	25	40	15	11	13	9	12	9	12	9
		50	18	14	16	12	15	11	15	11
		60	22	16	19	14	18	14	18	14
9	29	40	16	12	14	11	14	10	14	10
		50	21	15	18	13	17	13	17	13
		60	25	19	21	16	20	15	20	15
10	32	40	19	14	16	12	15	11	15	11
		50	23	17	20	15	19	14	19	14
		60	28	21	24	18	23	17	23	17
11	36	40	21	15	18	13	17	13	17	13
		50	26	19	22	17	21	16	21	16
		60	31	23	27	20	25	19	25	19
14	43	40	25	19	21	16	20	15	20	15
		50	31	23	27	20	25	19	25	19
		60	37	28	32	24	30	23	30	23
18	57	40	33	25	29	21	27	20	27	20
		50	41	31	36	27	34	25	34	25
		60	49	37	43	32	41	30	41	30

TABLE A.12
Common stock styles of welded wire reinforcement (WWR)

Steel Designation[a]	Steel Area, in^2/ft Longitudinal	Steel Area, in^2/ft Transverse	Weight (Approximate), lb per 100 ft^2
Rolls			
6 × 6-W1.4 × W1.4	0.028	0.028	19
6 × 6-W2.0 × W2.0	0.040	0.040	27
6 × 6-W2.9 × W2.9	0.058	0.058	39
6 × 6-W4.0 × W4.0	0.080	0.080	54
4 × 4-W1.4 × W1.4	0.042	0.042	29
4 × 4-W2.0 × W2.0	0.060	0.060	41
4 × 4-W2.9 × W2.9	0.087	0.087	59
4 × 4-W4.0 × W4.0	0.120	0.120	82
Sheets			
6 × 6-W2.9 × W2.9	0.058	0.058	39
6 × 6-W4.0 × W4.0	0.080	0.080	54
6 × 6-W5.5 × W5.5	0.110	0.110	75
4 × 4-W4.0 × W4.0	0.120	0.120	82

[a]The designation W indicates smooth wire; WWR is also available as deformed wire, designated with a D.

TABLE A.13A

Coefficients for slabs with variable moment of inertia[a]

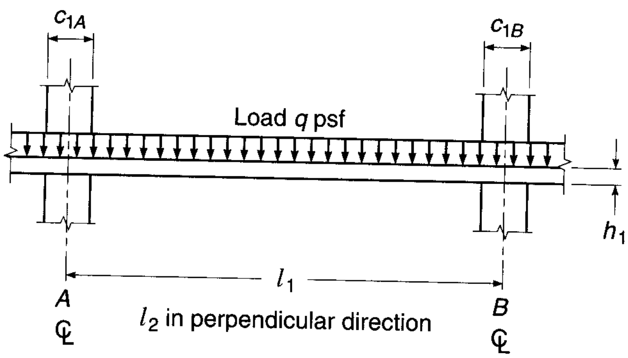

Column Dimension		Uniform Load FEM = Coeff. $(ql_2l_1^2)$		Stiffness Factor[b]		Carryover Factor	
c_{1A}/l_1	c_{1B}/l_1	M_{AB}	M_{BA}	k_{AB}	k_{BA}	COF_{AB}	COF_{BA}
0.00	0.00	0.083	0.083	4.00	4.00	0.500	0.500
	0.05	0.083	0.084	4.01	4.04	0.504	0.500
	0.10	0.082	0.086	4.03	4.15	0.513	0.499
	0.15	0.081	0.089	4.07	4.32	0.528	0.498
	0.20	0.079	0.093	4.12	4.56	0.548	0.495
	0.25	0.077	0.097	4.18	4.88	0.573	0.491
0.05	0.05	0.084	0.084	4.05	4.05	0.503	0.503
	0.10	0.083	0.086	4.07	4.15	0.513	0.503
	0.15	0.081	0.089	4.11	4.33	0.528	0.501
	0.20	0.080	0.092	4.16	4.58	0.548	0.499
	0.25	0.078	0.096	4.22	4.89	0.573	0.494
0.10	0.10	0.085	0.085	4.18	4.18	0.513	0.513
	0.15	0.083	0.088	4.22	4.36	0.528	0.511
	0.20	0.082	0.091	4.27	4.61	0.548	0.508
	0.25	0.080	0.095	4.34	4.93	0.573	0.504
0.15	0.15	0.086	0.086	4.40	4.40	0.526	0.526
	0.20	0.084	0.090	4.46	4.65	0.546	0.523
	0.25	0.083	0.094	4.53	4.98	0.571	0.519
0.20	0.20	0.088	0.088	4.72	4.72	0.543	0.543
	0.25	0.086	0.092	4.79	5.05	0.568	0.539
0.25	0.25	0.090	0.090	5.14	5.14	0.563	0.563

[a]Applicable when $c_1/l_1 = c_2/l_2$. For other relationships between these ratios, the constants will be slightly in error.
[b]Stiffness is $K_{AB} = k_{AB}E(l_2h_1^3/12l_1)$ and $K_{BA} = k_{BA}E(l_2h_1^3/12l_1)$.

TABLE A.13B
Coefficients for slabs with variable moment of inertia[a]

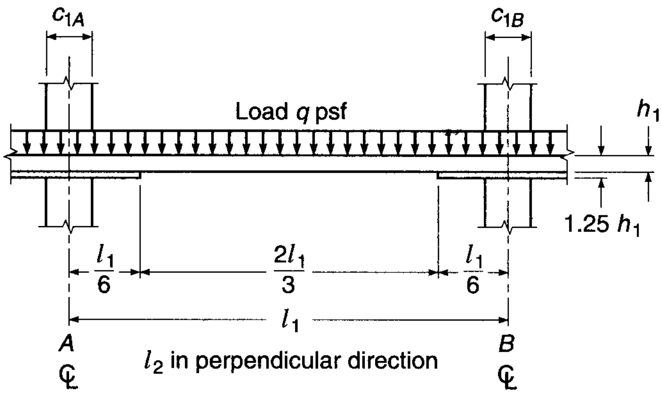

Column Dimension		Uniform Load FEM = Coeff.$(ql_2l_1^2)$		Stiffness Factor[b]		Carryover Factor	
c_{1A}/l_1	c_{1B}/l_1	M_{AB}	M_{BA}	k_{AB}	k_{BA}	COF_{AB}	COF_{BA}
0.00	0.00	0.088	0.088	4.78	4.78	0.541	0.541
	0.05	0.087	0.089	4.80	4.82	0.545	0.541
	0.10	0.087	0.090	4.83	4.94	0.553	0.541
	0.15	0.085	0.093	4.87	5.12	0.567	0.540
	0.20	0.084	0.096	4.93	5.36	0.585	0.537
	0.25	0.082	0.100	5.00	5.68	0.606	0.534
0.05	0.05	0.088	0.088	4.84	4.84	0.545	0.545
	0.10	0.087	0.090	4.87	4.95	0.553	0.544
	0.15	0.085	0.093	4.91	5.13	0.567	0.543
	0.20	0.084	0.096	4.97	5.38	0.584	0.541
	0.25	0.082	0.100	5.05	5.70	0.606	0.537
0.10	0.10	0.089	0.089	4.98	4.98	0.553	0.553
	0.15	0.088	0.092	5.03	5.16	0.566	0.551
	0.20	0.086	0.094	5.09	5.42	0.584	0.549
	0.25	0.084	0.099	5.17	5.74	0.606	0.546
0.15	0.15	0.090	0.090	5.22	5.22	0.565	0.565
	0.20	0.089	0.094	5.28	5.47	0.583	0.563
	0.25	0.087	0.097	5.37	5.80	0.604	0.559
0.20	0.20	0.092	0.092	5.55	5.55	0.580	0.580
	0.25	0.090	0.096	5.64	5.88	0.602	0.577
0.25	0.25	0.094	0.094	5.98	5.98	0.598	0.598

[a] Applicable when $c_1/l_1 = c_2/l_2$. For other relationships between these ratios, the constants will be slightly in error.
[b] Stiffness is $K_{AB} = k_{AB}E(l_2h_1^3/12l_1)$ and $K_{BA} = k_{BA}E(l_2h_1^3/12l_1)$.

TABLE A.13C
Stiffness factors for columns with variable moment of inertia[a]

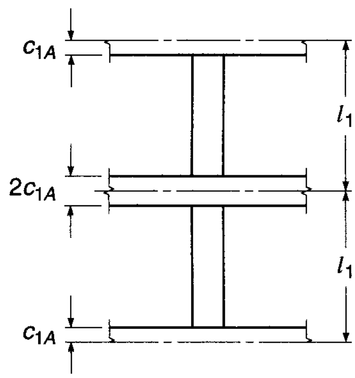

Slab Half-depth c_{1A}/l_1	Stiffness Factor k_{AB}	Slab Half-depth c_{1A}/l_1	Stiffness Factor k_{AB}
0.00	4.00	0.14	9.43
0.02	4.43	0.16	11.01
0.04	4.94	0.18	13.01
0.06	5.54	0.20	15.56
0.08	6.25	0.22	18.87
0.10	7.11	0.24	23.26
0.12	8.15		

[a]Adapted from S. H. Simmonds and J. Misic, "Design Factors for the Equivalent Frame Method," *J. ACI,* vol. 68, no. 11, 1971, pp. 825–831.

TABLE A.14
Size and pitch of spirals, ACI Code

		f'_c, psi		
Diameter of Column, in.	Out to Out of Spiral, in.	3000	4000	5000
f_y = 40,000 psi				
14, 15	11, 12	$\frac{3}{8}$–$1\frac{3}{4}$	$\frac{1}{2}$–$2\frac{1}{2}$	$\frac{1}{2}$–$1\frac{3}{4}$
16	13	$\frac{3}{8}$–$1\frac{3}{4}$	$\frac{1}{2}$–$2\frac{1}{2}$	$\frac{1}{2}$–2
17–19	14–16	$\frac{3}{8}$–$1\frac{3}{4}$	$\frac{1}{2}$–$2\frac{1}{2}$	$\frac{1}{2}$–2
20–23	17–20	$\frac{3}{8}$–$1\frac{3}{4}$	$\frac{1}{2}$–$2\frac{1}{2}$	$\frac{1}{2}$–2
24–30	21–27	$\frac{3}{8}$–2	$\frac{1}{2}$–$2\frac{1}{2}$	$\frac{1}{2}$–2
f_y = 60,000 psi				
14, 15	11, 12	$\frac{3}{8}$–$2\frac{3}{4}$	$\frac{3}{8}$–2	$\frac{1}{2}$–$2\frac{3}{4}$
16–23	13–20	$\frac{3}{8}$–$2\frac{3}{4}$	$\frac{3}{8}$–2	$\frac{1}{2}$–3
24–29	21–26	$\frac{3}{8}$–3	$\frac{3}{8}$–$2\frac{1}{4}$	$\frac{1}{2}$–3
30	27	$\frac{3}{8}$–3	$\frac{3}{8}$–$2\frac{1}{4}$	$\frac{1}{2}$–$3\frac{1}{4}$

TABLE A.15
Properties of prestressing steels

Seven-Wire Strand, f_{pu} = 270 ksi

Nominal Diameter (in.)	Area, in²	Weight, plf	$0.7f_{pu}A_{ps}$, kips	$0.75f_{pu}A_{ps}$, kips	$0.8f_{pu}A_{ps}$, kips	$f_{pu}A_{ps}$, kips
0.375	0.085	0.29	16.1	17.3	18.4	23.0
0.438	0.115	0.39	21.7	23.3	24.8	31.0
0.500	0.153	0.52	28.9	31.0	33.0	41.3
0.520	0.167	0.57	31.5	33.8	36.0	45.0
0.563	0.192	0.65	36.2	38.8	41.4	51.7
0.600	0.217	0.74	41.0	44.0	46.9	58.6
0.700	0.294	1.00	55.6	59.6	63.5	79.4

Prestressing Wire

Diameter	Area, in²	Weight, plf	f_{pu}, ksi	$0.7f_{pu}A_{ps}$, kips	$0.8f_{pu}A_{ps}$, kips	$f_{pu}A_{ps}$, kips
0.192	0.0290	0.098	250	5.07	5.80	7.25
0.196	0.0302	0.100	250	5.28	6.04	7.55
0.250	0.0491	0.170	240	8.25	9.43	11.78
0.276	0.0598	0.200	235	9.84	11.24	14.05

Deformed Prestressing Bars

Nominal Diameter (in.)	Area, in²	Weight, plf	f_{pu}, ksi	$0.7f_{pu}A_{ps}$, kips	$0.8f_{pu}A_{ps}$, kips	$f_{pu}A_{ps}$, kips
$\frac{5}{8}$	0.28	0.98	157	30.5	34.8	43.5
1	0.85	3.01	150	89.3	102.0	127.5
1	0.85	3.01	160	95.2	108.8	136.0
$1\frac{1}{4}$	1.25	4.39	150	131.3	150.0	187.5
$1\frac{1}{4}$	1.25	4.39	160	140.0	160.0	200.0
$1\frac{3}{8}$	1.58	5.56	150	165.9	159.6	237.0
$1\frac{3}{4}$	2.58	9.10	150	270.9	309.6	387.0
$2\frac{1}{2}$	5.16	18.20	150	541.8	619.2	774.0

GRAPH A.1*a*
Moment capacity of rectangular sections.

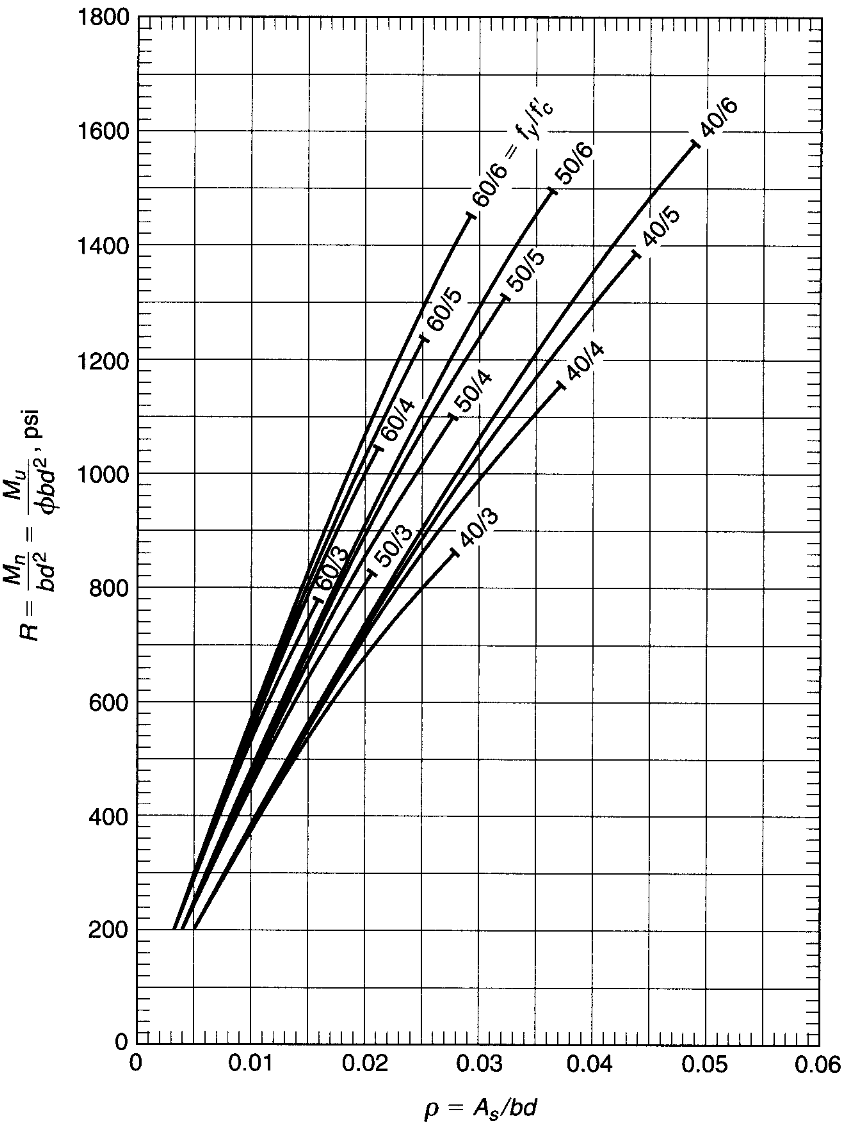

GRAPH A.1*b*
Moment capacity of rectangular sections.

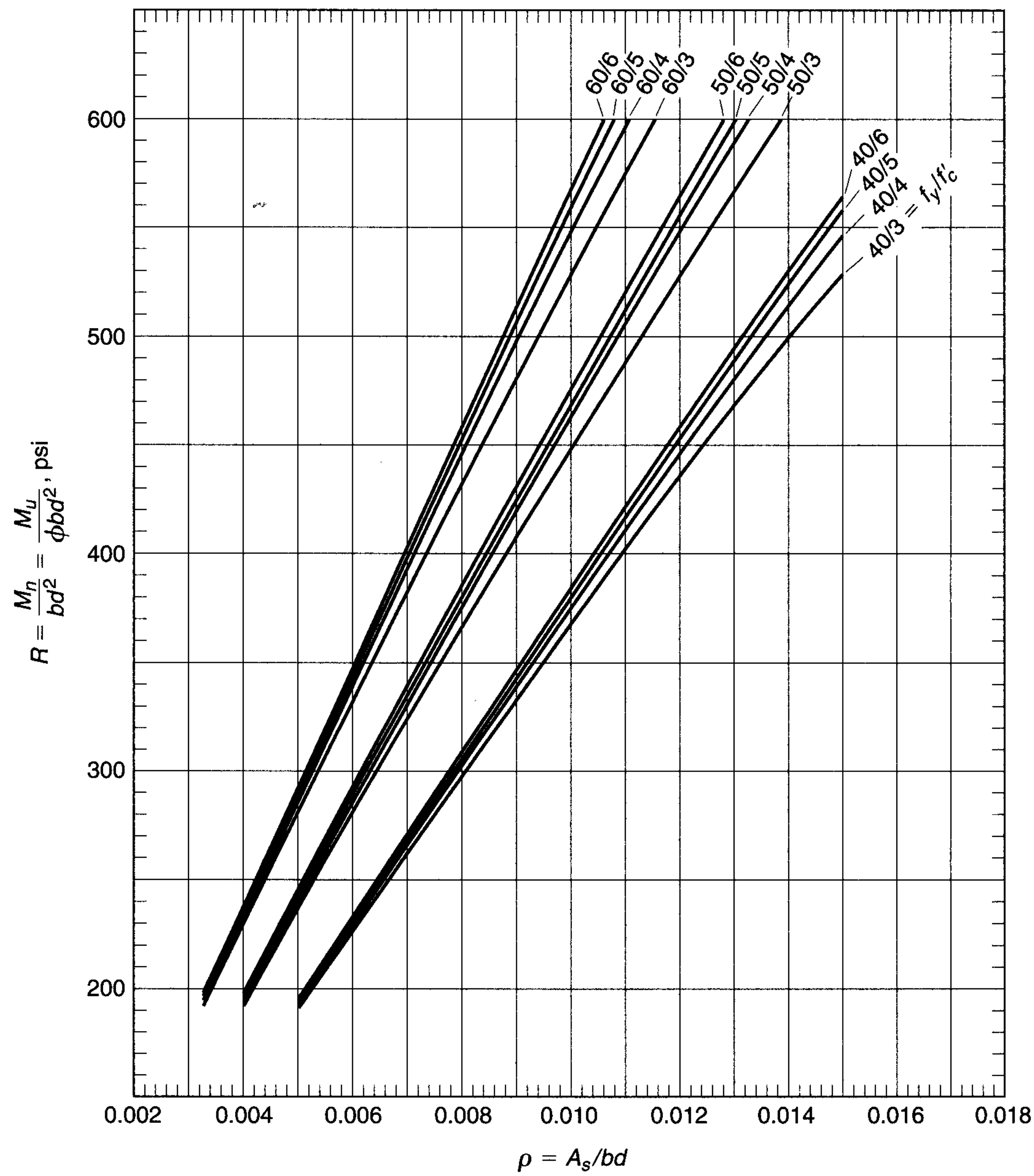

GRAPH A.2
Location of points where bars can be bent up or cut off for simply supported beams uniformly loaded.

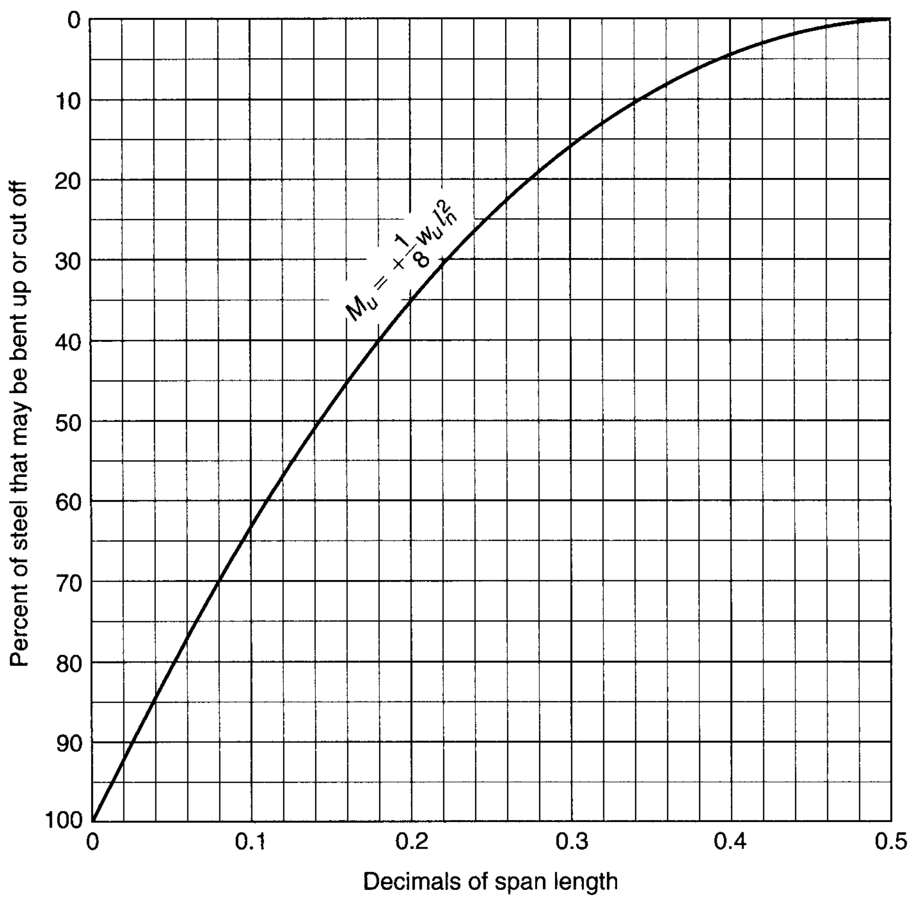

GRAPH A.3
Approximate locations of points where bars can be bent up or down or cut off for continuous beams uniformly loaded and built integrally with their supports according to the coefficients in the ACI Code.

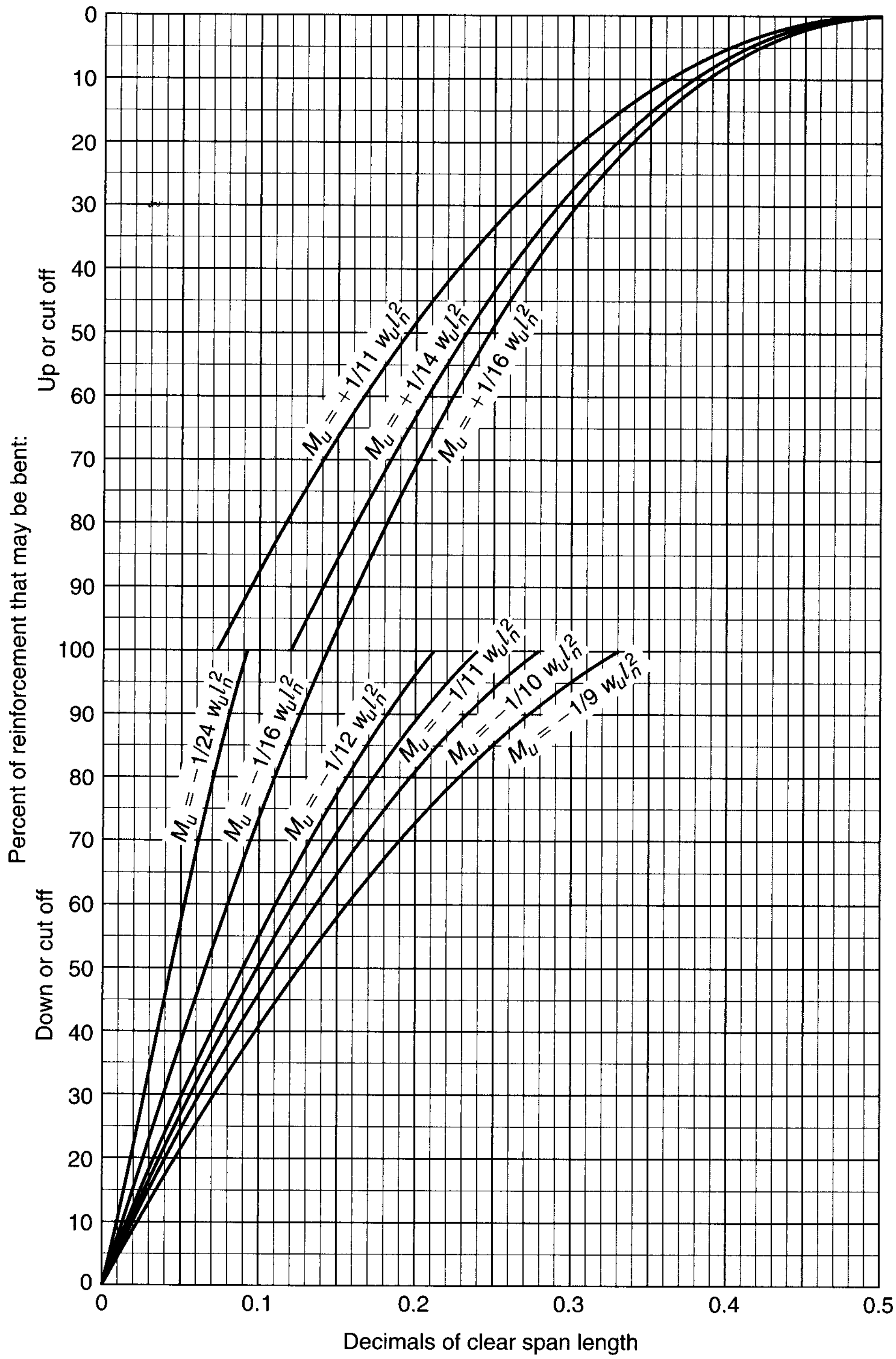

GRAPH A.4
Interpolation charts for lateral distribution of slab moments.

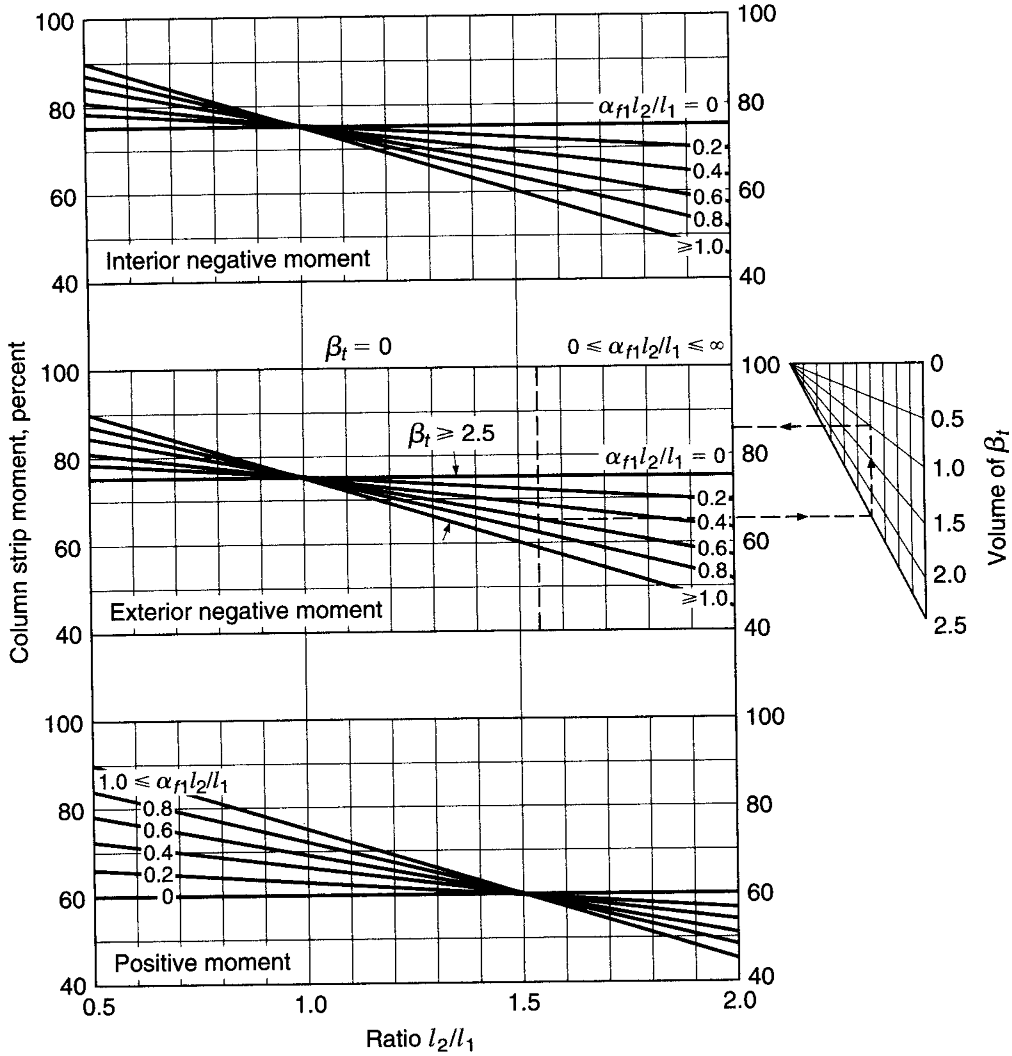

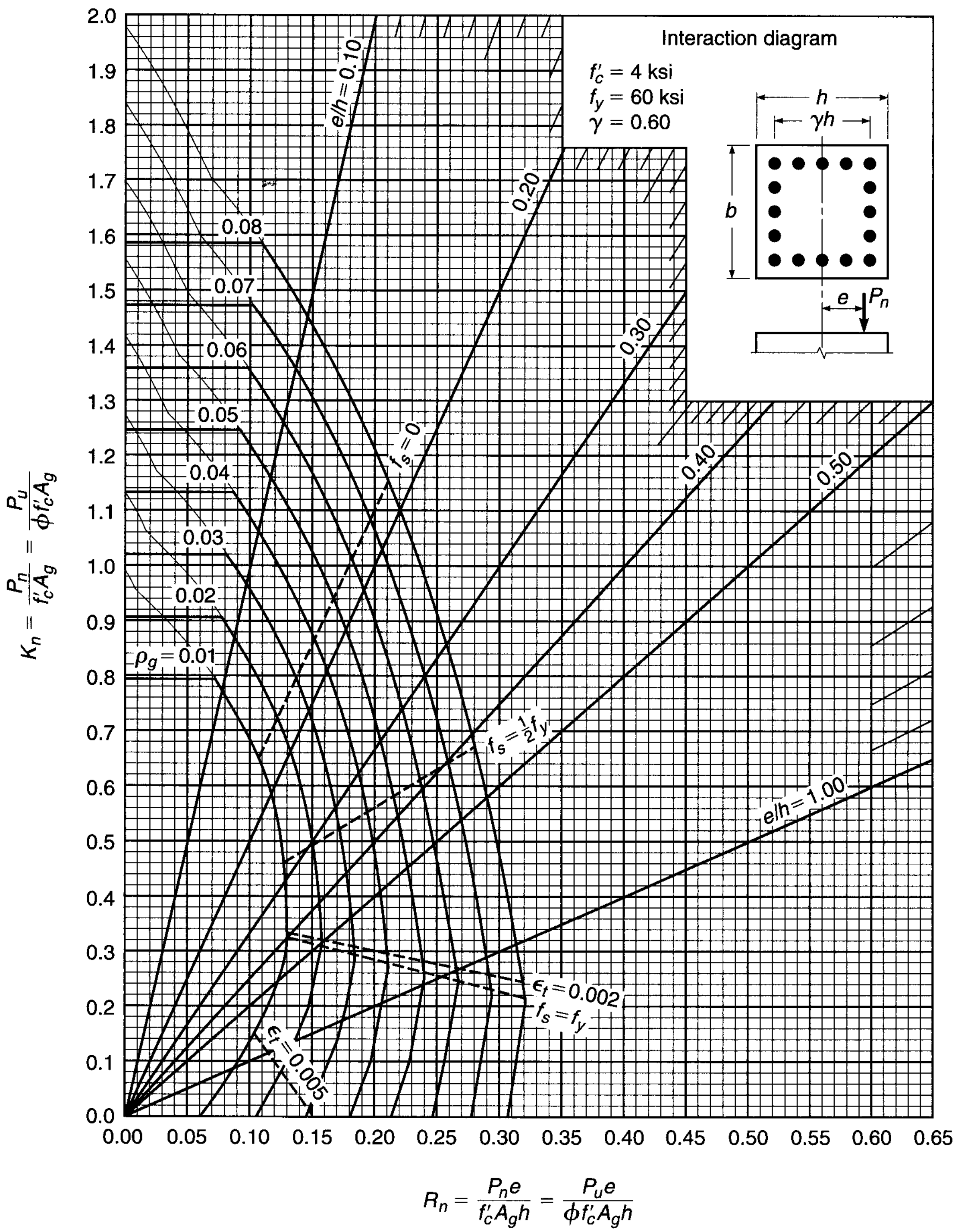

GRAPH A.5

Column strength interaction diagram for rectangular section with bars on four faces and $\gamma = 0.60$.

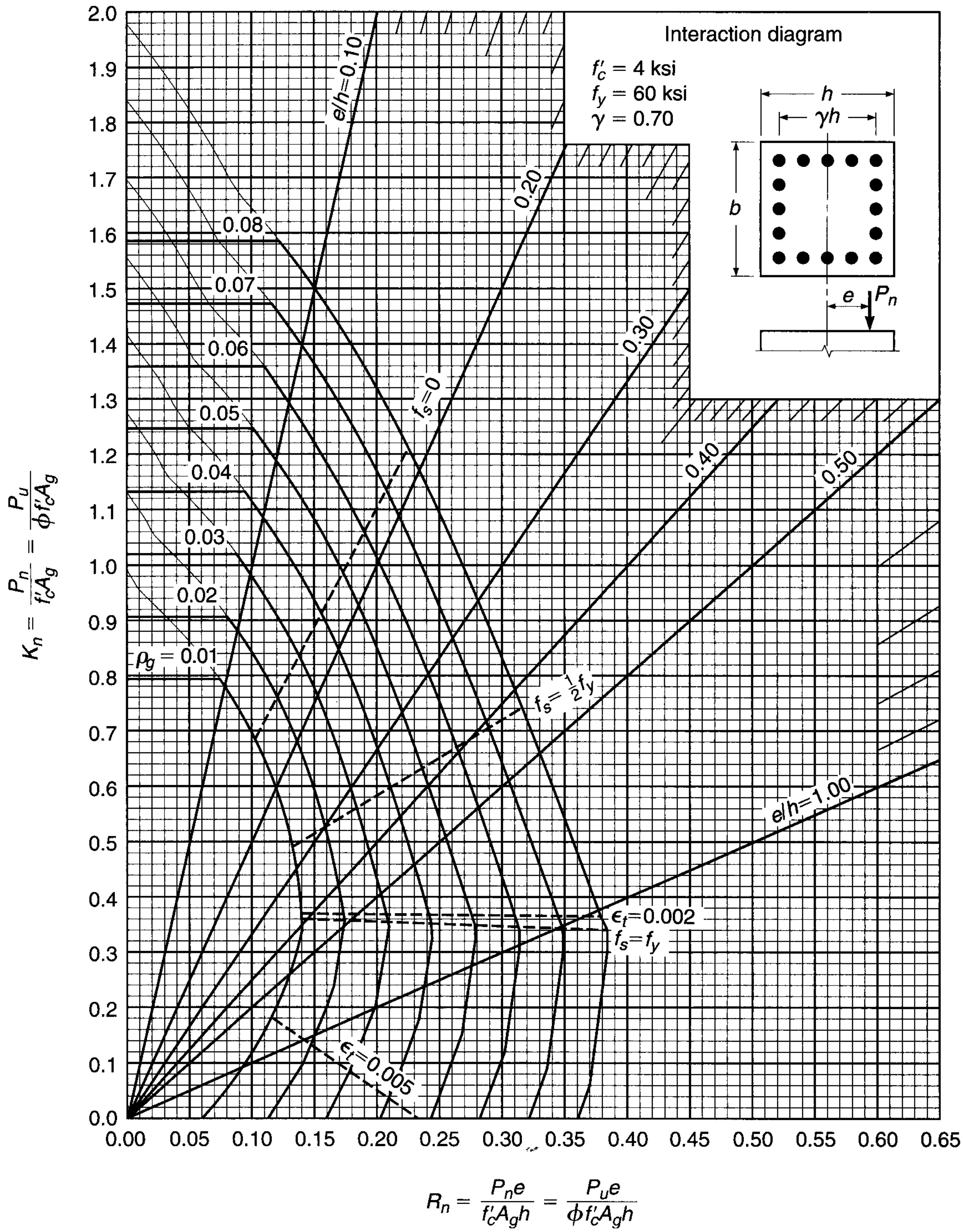

GRAPH A.6
Column strength interaction diagram for rectangular section with bars on four faces and $\gamma = 0.70$.

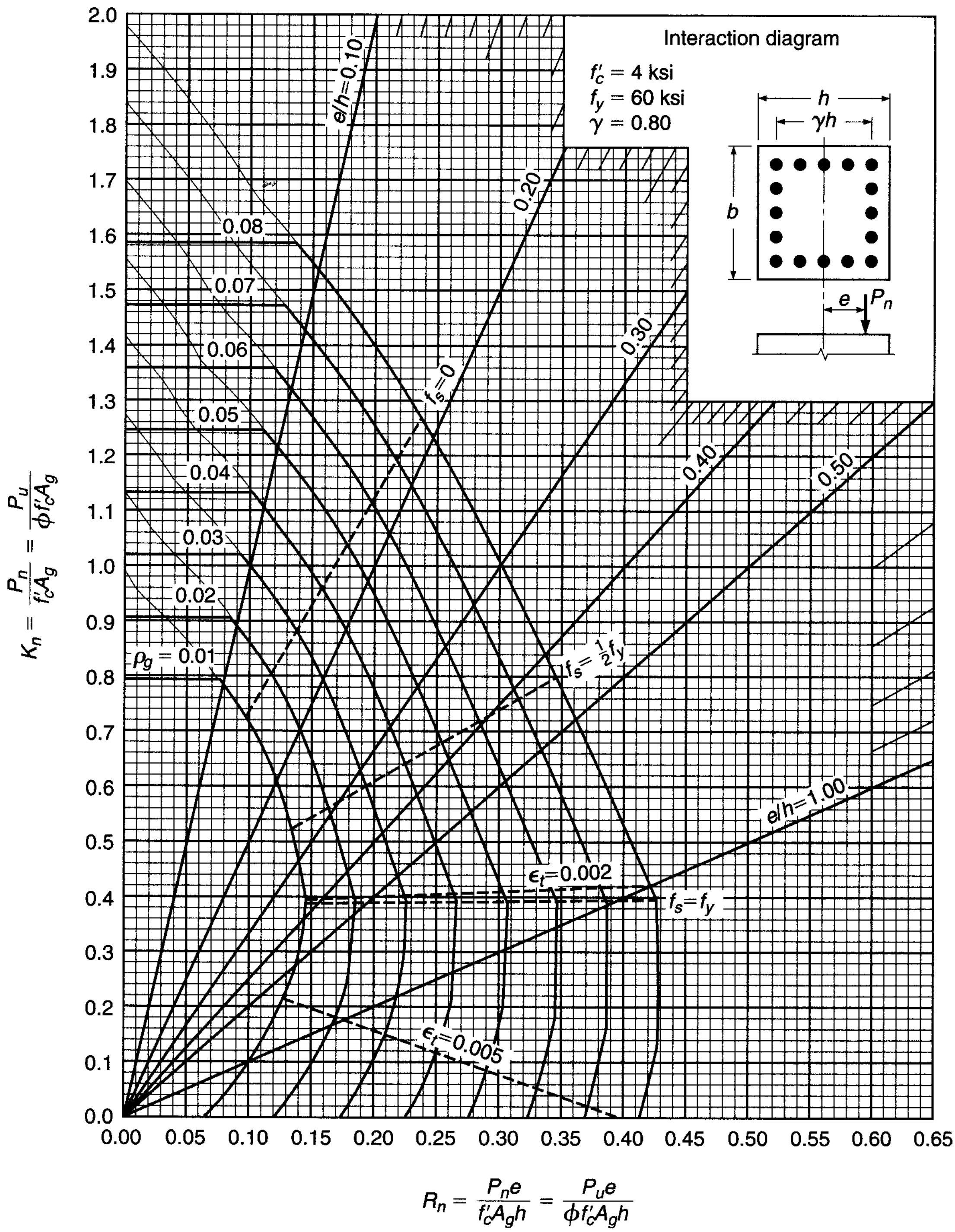

GRAPH A.7
Column strength interaction diagram for rectangular section with bars on four faces and $\gamma = 0.80$.

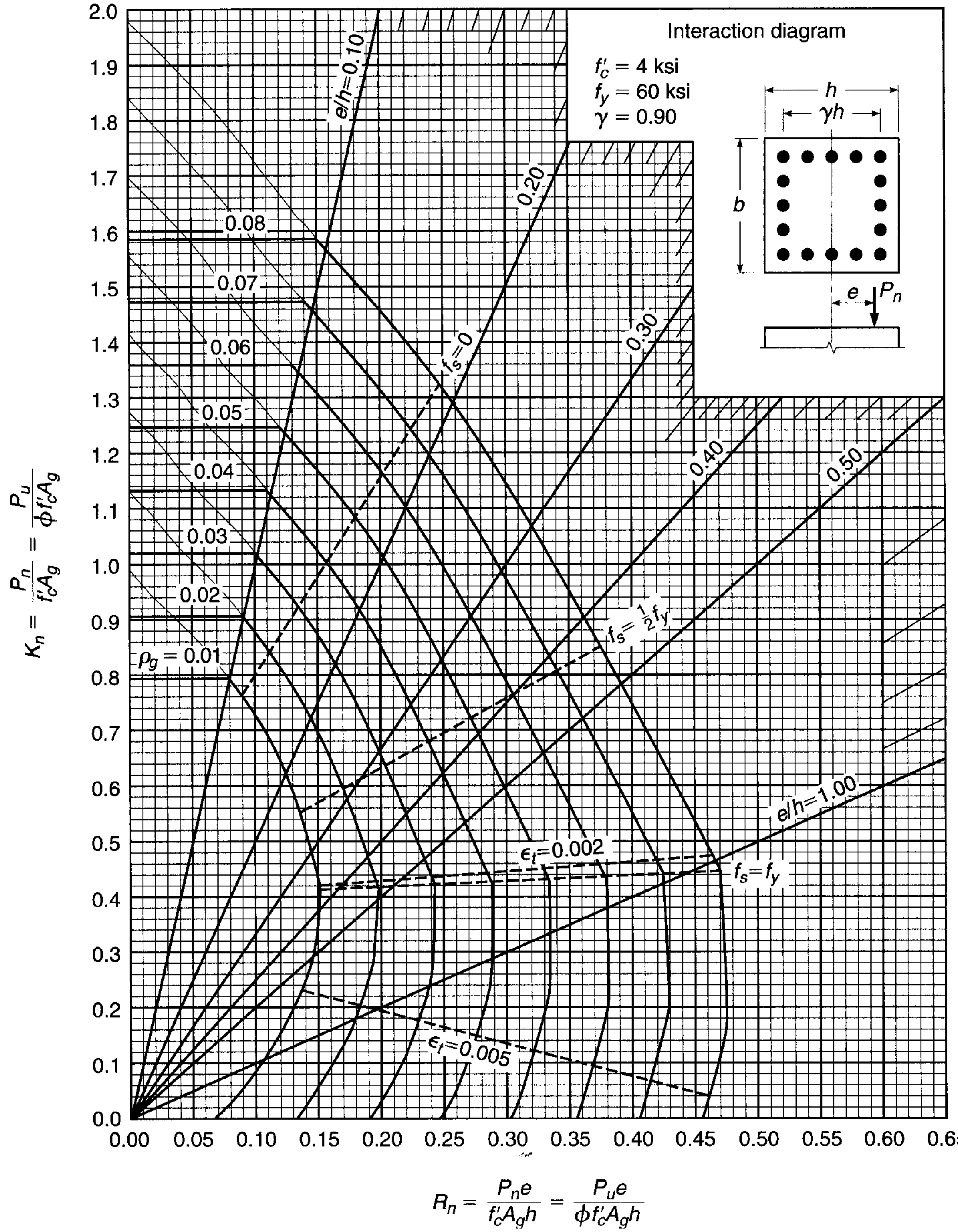

GRAPH A.8

Column strength interaction diagram for rectangular section with bars on four faces and γ = 0.90.

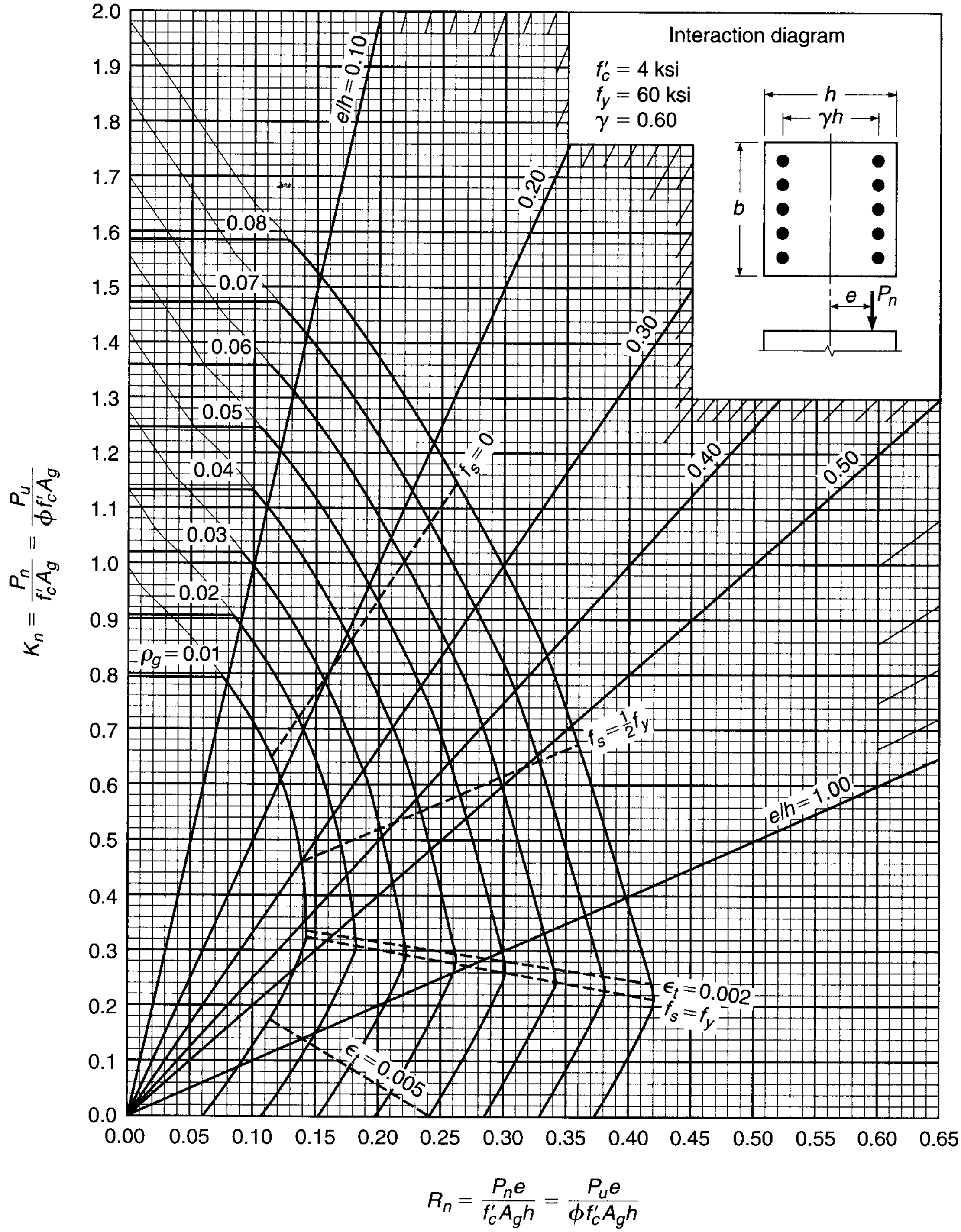

GRAPH A.9

Column strength interaction diagram for rectangular section with bars on end faces and $\gamma = 0.60$.

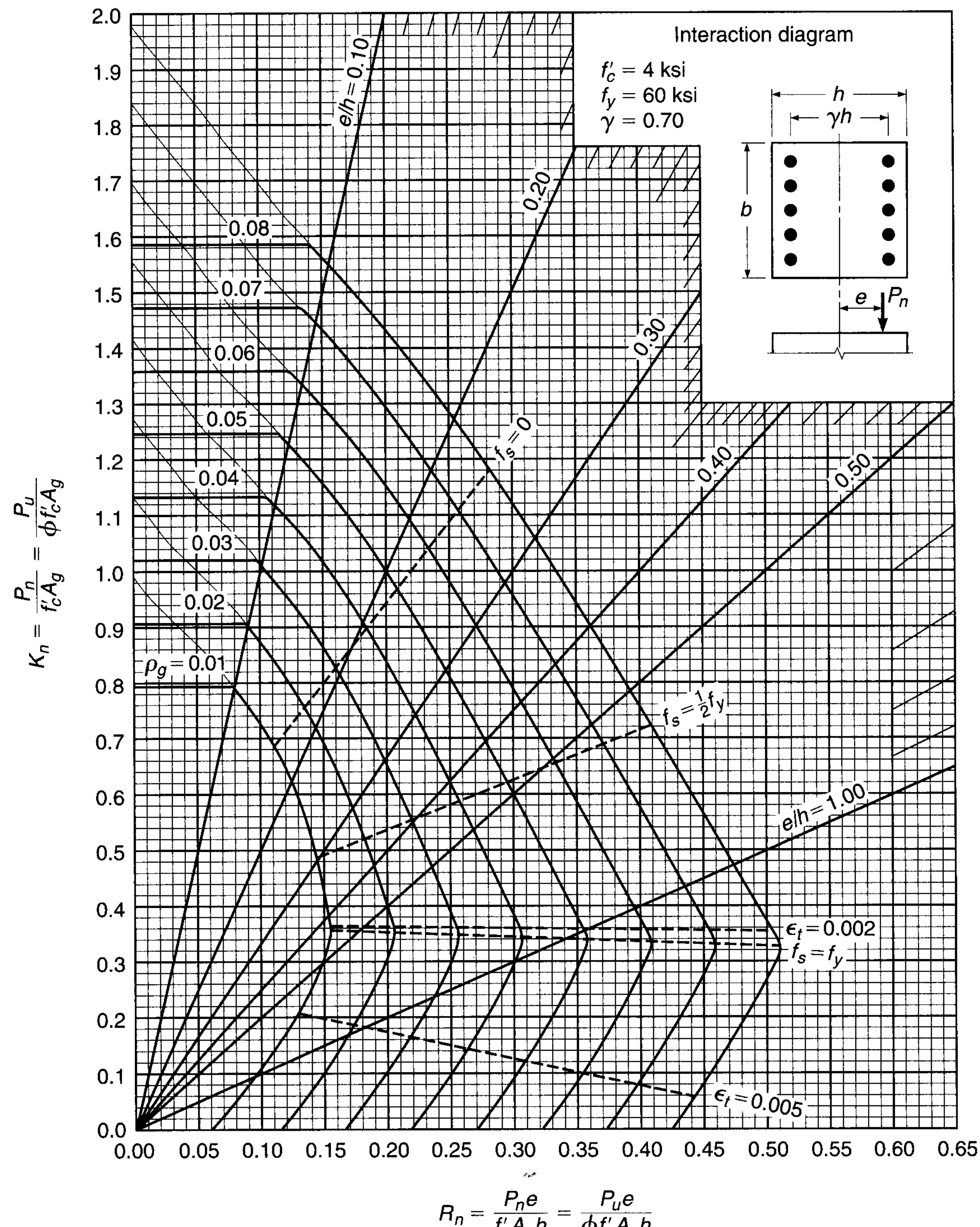

GRAPH A.10
Column strength interaction diagram for rectangular section with bars on end faces and γ = 0.70.

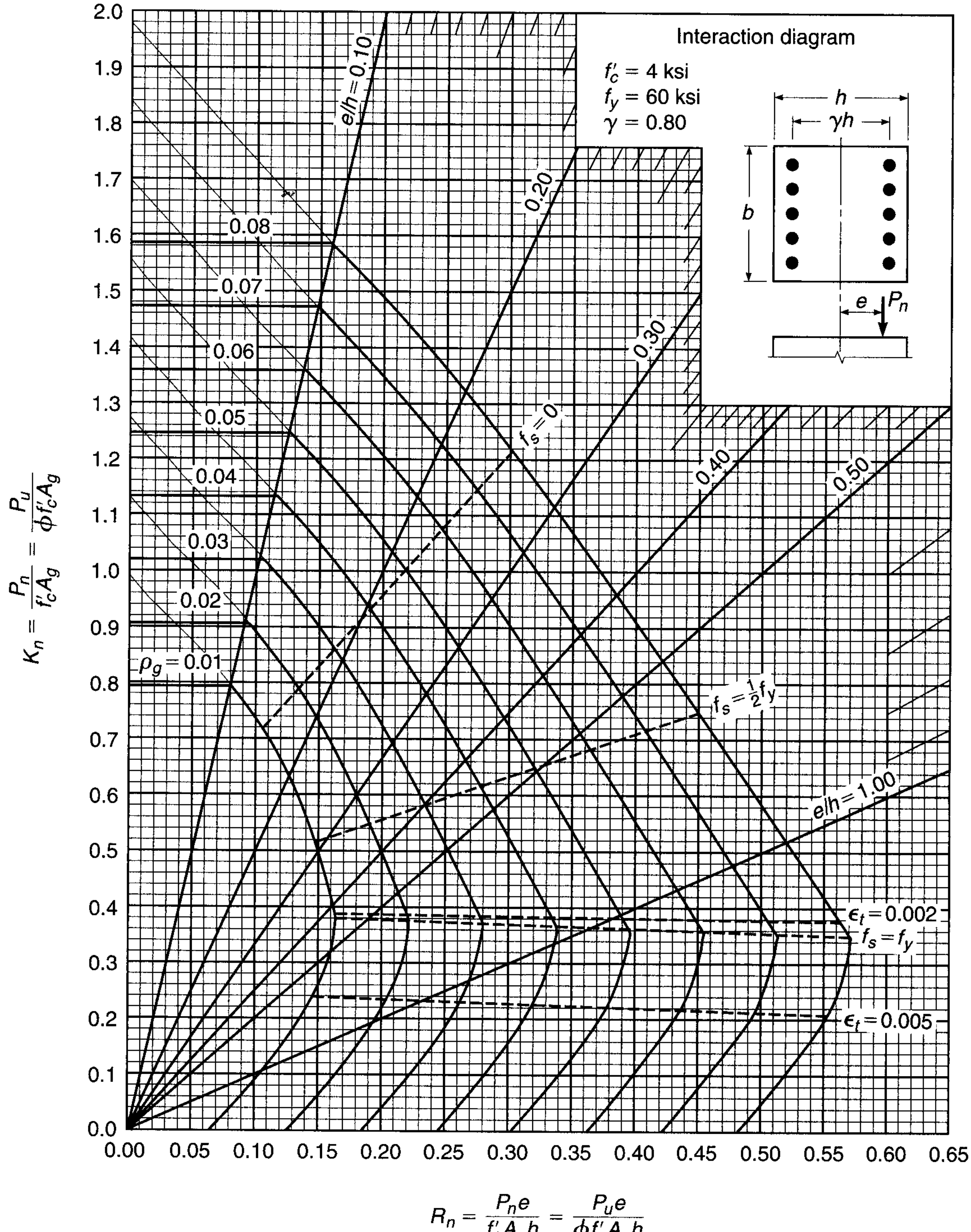

GRAPH A.11
Column strength interaction diagram for rectangular section with bars on end faces and γ = 0.80.

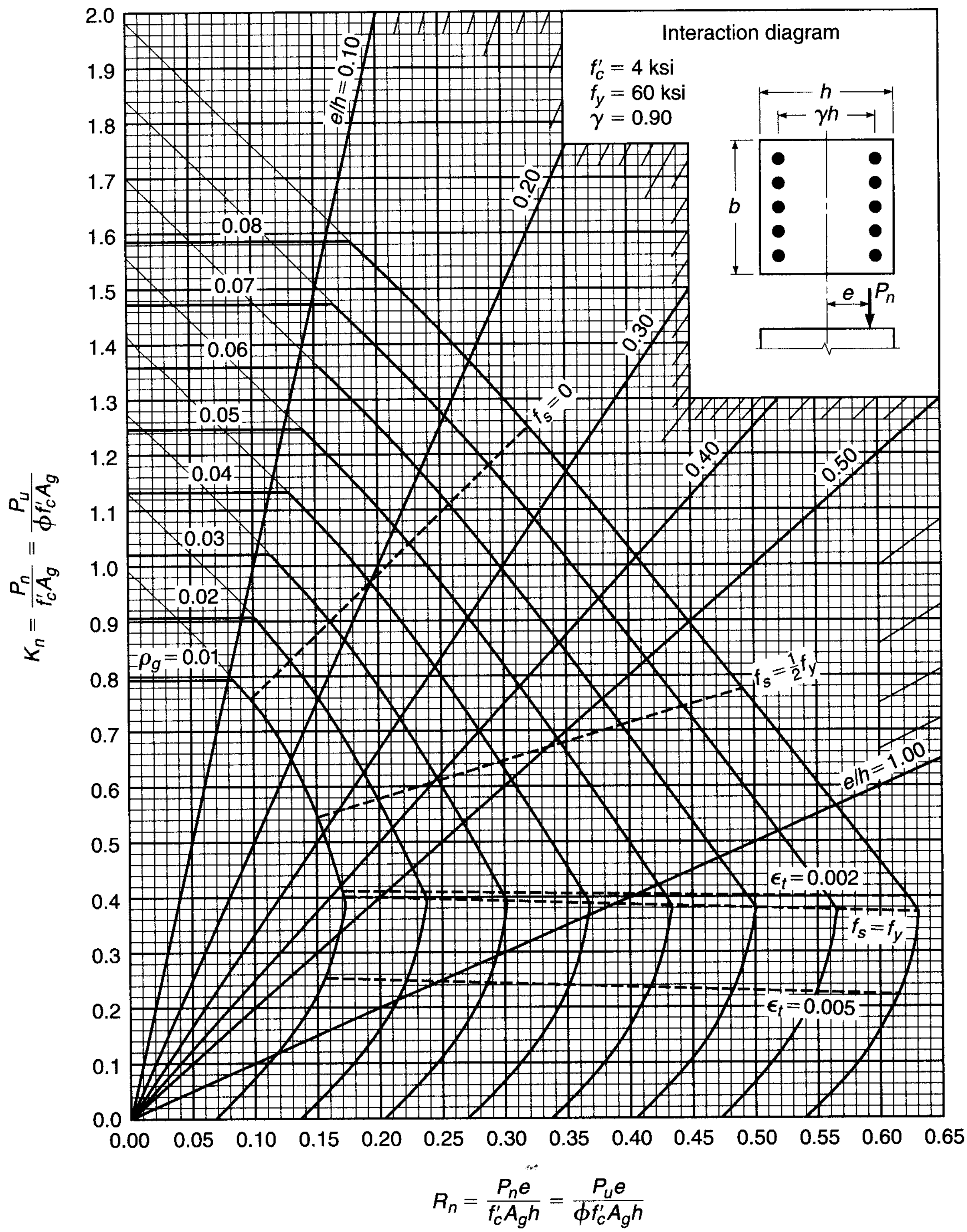

GRAPH A.12
Column strength interaction diagram for rectangular section with bars on end faces and $\gamma = 0.90$.

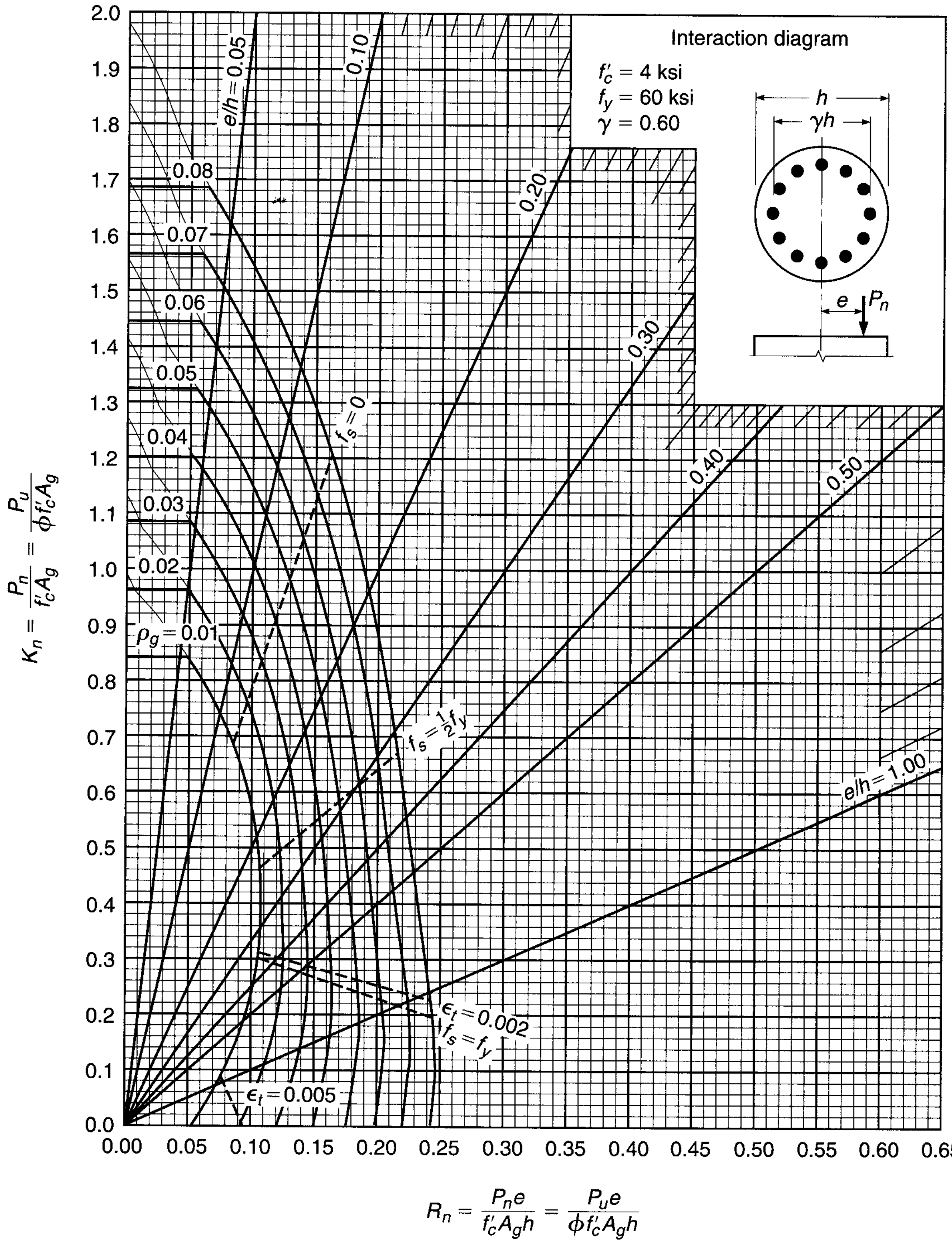

GRAPH A.13

Column strength interaction diagram for circular section with $\gamma = 0.60$.

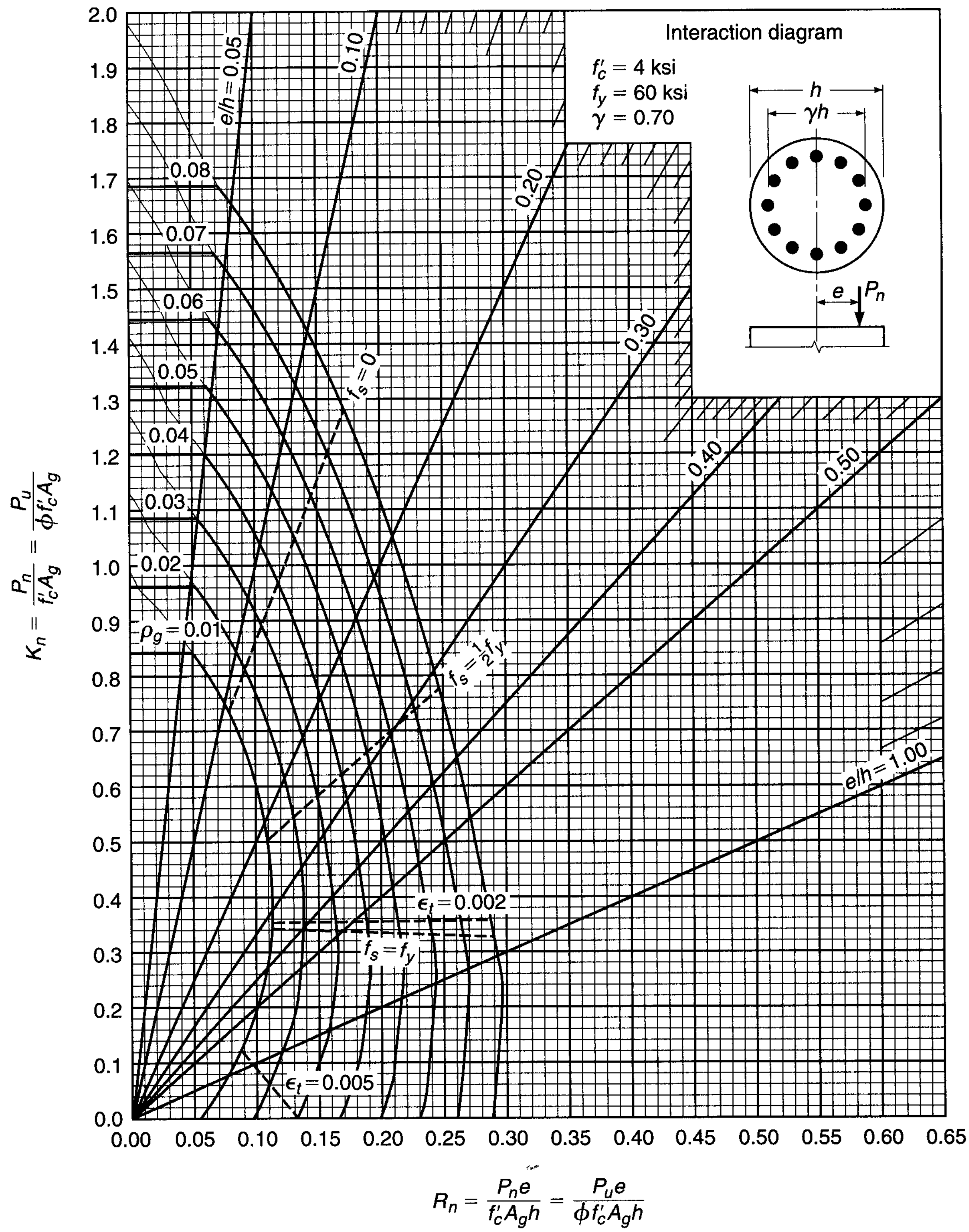

GRAPH A.14
Column strength interaction diagram for circular section with γ = 0.70.

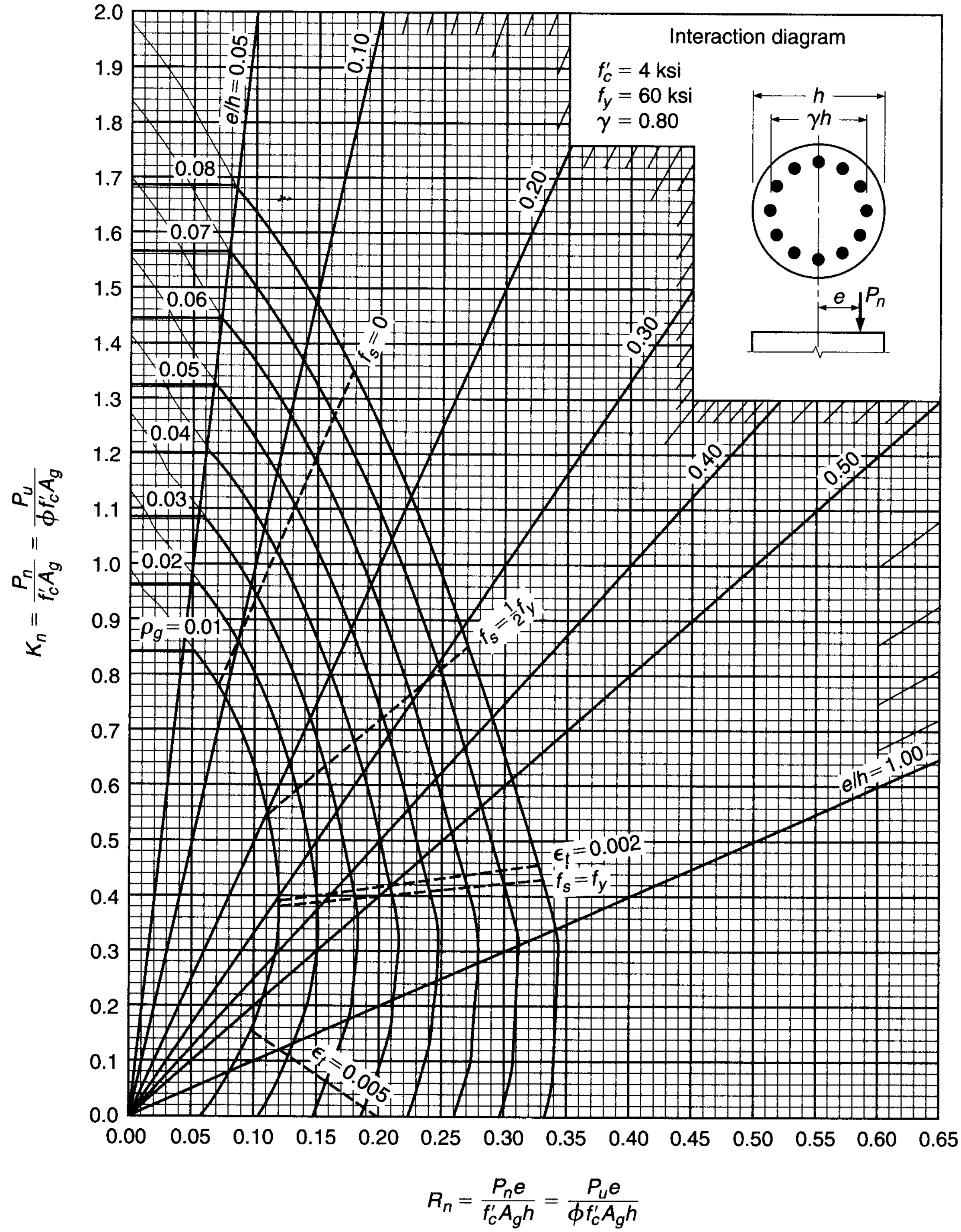

GRAPH A.15

Column strength interaction diagram for circular section with γ = 0.80.

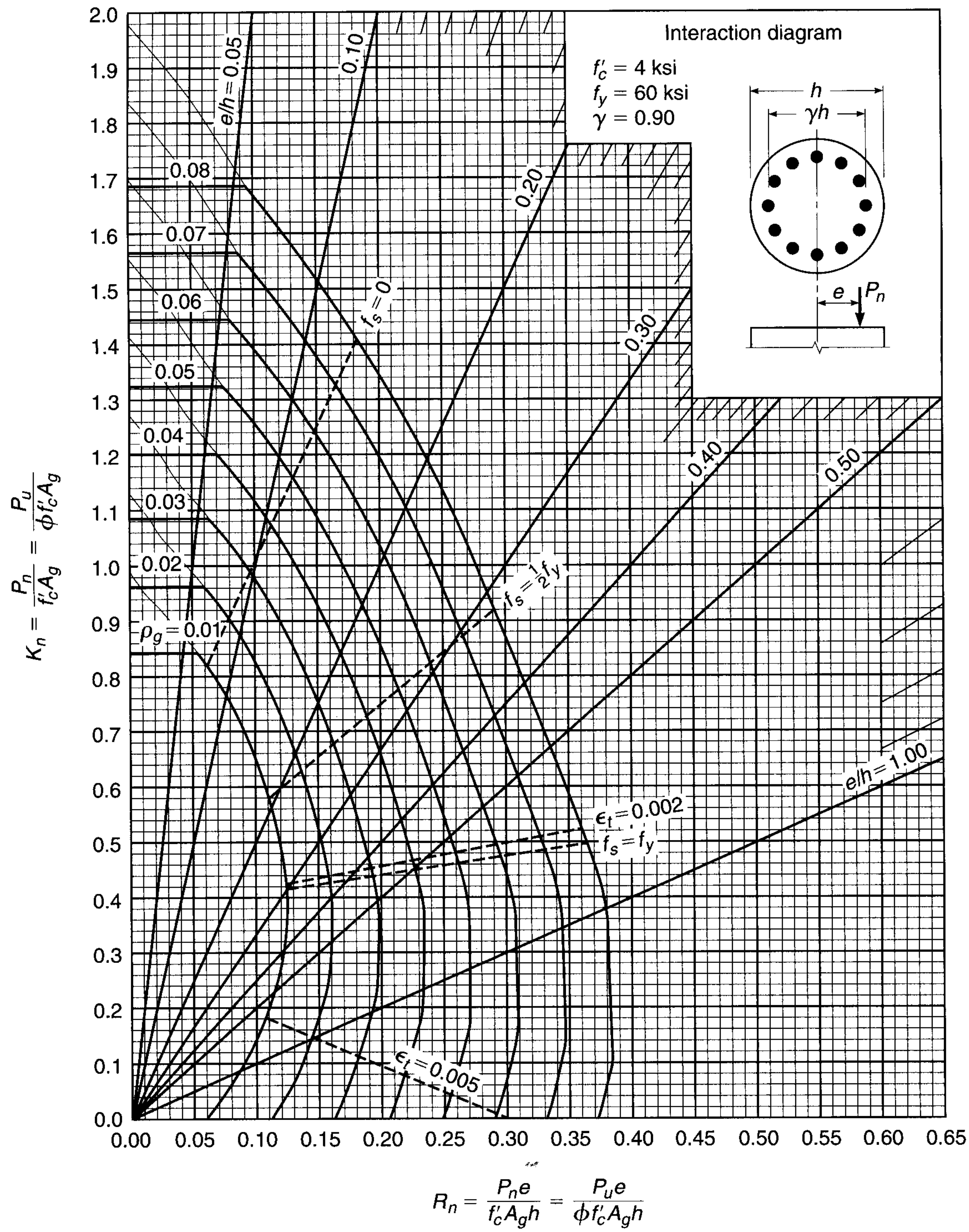

GRAPH A.16
Column strength interaction diagram for circular section with $\gamma = 0.90$.

APPENDIX

B SI Conversion Factors: Inch-Pound Units to SI Units

Overall Geometry	
Spans	1 ft = 0.3048 m
Displacements	1 in. = 25.4 mm
Surface area	1 ft^2 = 0.0929 m^2
Volume	1 ft^3 = 0.0283 m^3
	1 yd^3 = 0.765 m^3
Structural Properties	
Cross-sectional dimensions	1 in. = 25.4 mm
Area	1 in^2 = 645.2 mm^2
Section modulus	1 in^3 = 16.39 $\times$ 10^3 mm^3
Moment of inertia	1 in^4 = 0.4162 $\times$ 10^6 mm^4
Material Properties	
Density	1 lb/ft^3 = 16.03 kg/m^3
Modulus and stress	1 lb/in^2 = 0.006895 MPa
	1 kip/in^2 = 6.895 MPa
Loadings	
Concentrated loads	1 lb = 4.448 N
	1 kip = 4.448 kN
Density	1 lb/ft^3 = 0.1571 kN/m^3
Linear loads	1 kip/ft = 14.59 kN/m
Surface loads	1 lb/ft^2 = 0.0479 kN/m^2
	1 kip/ft^2 = 47.9 kN/m^2
Stress and Moments	
Stress	1 lb/in^2 = 0.006895 MPa
	1 kip/in^2 = 6.895 MPa
Moment or torque	1 ft-lb = 1.356 N-m
	1 ft-kip = 1.356 kN-m

Index

J

K

L

M

N

O

P

Q

R

S

T

U

V

W

Y

Z

The fourteenth edition of the classic text, ***Design of Concrete Structures,*** is completely revised using the newly released 2008 American Concrete Institute (ACI) Code. This new edition has the same dual objectives as the previous editions: first to establish a firm understanding of the behavior of structural concrete, then to develop proficiency in the methods used in current design practice.

Design of Concrete Structures covers the behavior and design aspects of concrete and provides updated examples and homework problems. New material on slender columns, seismic design, anchorage using headed deformed bars, and reinforcing slabs for shear using headed studs has been added. The notation has been thoroughly updated to match changes in the ACI Code.

The text also presents the basic mechanics of structural concrete and methods for the design of individual members for bending, shear, torsion, and axial force, and provides detail on the various types of structural systems applications, including an extensive presentation of slabs, footings, foundations, and retaining walls.

NOTABLE FEATURES INCLUDE:

- Coverage updated to match ACI 318-08.
- Expanded presentation and enhanced example problems in Chapter 3 on Flexural Analysis and Design.
- New homework problem sets.
- Updated modified compression theory method of shear design from the AASHTO *LRFD Bridge Design Specifications* and modified shear friction design procedures from the ACI Code added to Chapter 4.
- Expanded coverage on bond and development of reinforcement using headed deformed bars in Chapter 5.
- Slender column design requirements revised and updated in Chapter 9.
- Guidance on preliminary design and guidelines for proportioning members in Chapter 12.
- Updated design procedures for prestressed concrete in Chapter 19.
- Expanded description of loading criteria and description of new design requirements for seismic design in Chapter 20.
- Text features applications that reflect the authors' practical experience.

For Professors, the Instructor's Solutions Manual is available online at www.mhhe.com/concrete

The McGraw-Hill Companies

Mc Graw Hill Higher Education

ISBN 978-0-07-329349-3
MHID 0-07-329349-0

90000

EAN

9 780073 293493

www.mhhe.com